Chemistry of *s*-block metal coordination polymers: Synthesis, reactivity characteristics, spectroscopic and structural investigations

A Thesis submitted to Goa University for the Award of the
Degree of
DOCTOR OF PHILOSOPHY
in
(Chemistry)

By

(Santosh Yeso Shetgaonkar)

Research Guide

(Prof. B. R. Srinivasan)

Goa University
Taleigao Goa 403 206, India
(2013)

EXAMINED BY
S.K. Das 21/10/2013

All corrections are incorporated in them.

Prof. B. R. Srinivasan
Department of Chemistry
GOA UNIVERSITY
Goa 403206 INDIA

DECLARATION

I hereby declared that the work incorporated in the thesis entitled " Chemistry of *s*-block metal coordination polymers: Synthesis, reactivity characteristics, spectroscopic and structural investigations " is the result of investigation carried out by me under the guidance of Prof. B. R. Srinivasan and Prof. S. G. Tilve Department of Chemistry, Goa University and it has not previously formed basis for any other titles.

In keeping with the general practice of reporting scientific observations, due acknowledgement has been made wherever the work described is based on the findings of other investigators.

Shetgaonkar

Santosh Y. Shetgaonkar
Research Scholar,
Department of Chemistry,
Goa University, 403206

April 2012

Goa University
Taleigao Plateau,
Goa - 403206

CERTIFICATE

Certified that the work incorporated in the thesis entitled "Chemistry of *s*-block metal coordination polymers: Synthesis, reactivity characteristics, spectroscopic and structural investigations" submitted by **Mr. Santosh Y. Shetgaonkar**, was carried out by the candidate under our supervision and the same has not been submitted elsewhere for the award of a degree.

Prof. B. R. Srinivasan
Department of Chemistry
Goa University, 403206

Prof. S. G. Tilve
Department of Chemistry
Goa University, 403206

April 2012

ACKNOWLEDGEMENT

It gives me immense pleasure to express my deep sense of gratitude to all the people who have directly or indirectly helped me in various capacities in the successful completion of the thesis.

First and foremost, I would like to thank my respectable advisors Prof. B. R. Srinivasan and Prof. S. G. Tilve (Head, Department of Chemistry, Goa University) for making my time at Goa University enjoyable, productive and beneficial. I also thank them for their valuable guidance, innovative ideas, generous support and encouragement through out my Ph. D. work.

I offer my sincere thanks to the Vice-chancellor of Goa University for allowing me to work in the institute. I am very much thankful to Prof. A. V. Salker (Ex-Head), Prof. J. B. Fernandes (Ex-Head and Ex-Dean), Dr. V. S. M. Verenkar (Subject expert) and Prof. K. S. Rane (Ex-Dean) for providing all the necessary facilities to carry out my research work.

I am also thankful to Prof. V. P. Kamat, Prof. S. P. Kamat, Dr. V. S. Nadkarni, Dr. R. N. Shirsat, Dr. Sunder Dhuri and Dr. N. N. Ghosh (BITS, Goa) for their encouragement and useful advises.

I am obliged to Prof. W. Bensch and Prof. C. Nather, Institute of Anorganische Chemie, Universitat of Kiel, Kiel Germany for recording and solving the crystal structures of compounds and for their knowledgeable suggestions. I thank Dr. Ragahavhai and Prof. S. K. Das, University of Hyderabad, for recording and solving the crystal structure of compounds. My sincere thanks are due to the authorities of Goa University, for providing all the necessary facilities. I gratefully acknowledged authorities of Syngenta India Ltd. for allowing me to pursue my Ph. D.

My special thanks to Dr. Prashant Potnis, Dr. Deepnandan Dubhashi, Mr. Brijnandan Mishra, Dr. Rachel Stenson and Dr. Pascal Bugnon (Syngenta India Ltd.) for their moral support and necessary help during my entire Ph. D. course.

I am thankful to Dr. J. V. Sawant, Dr. Sarvesh Sawant, Dr. Ashish Naik for helpful discussions during my research work and for being patient with me throughout my tenure. I would like to thank all the teaching and non-teaching staff from Chemistry Department, Goa University. I also acknowledge the Librarian and the staff members of Library, Goa University for their constant help.

I am at loss of words to thank all my friends for their help and support during the entire period of my thesis work. Notably among these are Prakash, Satish, Rupesh, Mahesh, Vijay, Vinod, Rajesh, Rohan, Umesh, Ratan, Chinmaya, Prachi, Sonia, Reshma, Priyanka, Lactina, Hari, Sandesh, Kashinath, Shrikant, Rajashree, Kiran, Puzy, Sifali, Siddhali, Jose, Savia, Sulaksha, Divya, Supriya, Savita, Durga and Videsh. Their untiring company, suggestions and constant encouragement always boosted my morale enabling me to give my investigation the present shape and making my stay enjoyable over here.

I also thank Manav Saxena, Bhanudas Naik, Sabeta Kohli for their support in recording and interpreting data related to luminescence, X-ray powder diffractograms, single crystal data and surface area measurements. I am greatly thankful to my friends and colleagues from Syngenta India Ltd. and Syngenta bioscience Pvt. Ltd., especially Vivek, Sarah, Krupa, Kiran, Amit, Somanath, Abhilash, Digant, Vinayak, Shridhar, Rajasi, Kishore, Chetan, Jagdish, Deepa, Milind, Abhijit, Arvind, Manoj, Kawar, Gayatri, Shrikant, Subodh, Sudhakar, Geetali, Rashmi, Gauri, Snehalata, Eddie Silva, Manjunath, Vikrant and Quality control department for their all time support.

I am greatly indebted to my parents and family members for morale support, encouragement, valuable suggestions, great affection and selfless sacrifice. Without their constant support and inspiration, it would have been impossible for me to be where I am at present.

I close with thanks to almighty for the showers of blessing during the hours of trial.

Mr. Santosh Y. Shetgaonkar

Dedicated
to my
beloved
Parents

TABLE OF CONTENTS

LIST OF ABBREVIATIONS

2-MeIm	2-methylimidazole
2-nbaH	2-nitrobenzoic acid
5-niphth	5-nitroisophthalate
2-ap	2-aminopyridine
4-nbaH	4-nitrobenzoic acid
Å	Angstrom unit, 10^{-10} m
AR	Analytical Reagent
IR	Infrared spectroscopy
BDC	Benzenedicarboxylate
BenzIm	Benzimidazole
Bpy	Bipyridine
H_3btc	1,3,5-benzenetricarboxylic acid
2-ca-4nba	2-carbamoyl-4-nitrobenzoate
L_2 or 2-Clphac	2-chlorophenylacetic acid
L_1 or 4-OMephac	Para-methoxyphenylacetic acid
L or 4-phac	Phenylacetic acid
3-nphth	3-nitrophthalate
pyr	Pyrazole
LMCT	Ligand-to-metal charge transfer
cm^{-1}	Wave number
dmf	N,N-dimethylformamide
DMSO	Dimethylsulphoxide
dmp	3,5-dimethylpyrazole
MLCT	Metal-to-ligand charge transfer
nmf	N-methylformamide
DSC	Differential Scanning Calorimetry
DTA	Differential Thermal Analysis
hip	Hippurate
$HCONH_2$	Formamide
K/min	Kelvin/minute
Im	Imidazole
nm	Nanometer, 10^{-9} m
N-MeIm	N-methylimidazole
NMR	Nuclear Magnetic Resonance
XRD	X-ray diffractometry
Py	Pyridine
pyr	Pyrazole
TG	Thermogravimetry
υ	Frequency

Name of the candidate: **Mr. SANTOSH YESO SHETGAONKAR**

Guiding teacher: **Prof. B. R. SRINIVASAN**

Co Guide: **Prof. S. G. TILVE**

Institution: **DEPARTMENT OF CHEMISTRY**
GOA UNIVERSITY

Title of Ph.D. thesis: **Chemistry of *s*-block metal coordination polymers: Synthesis, reactivity characteristics, spectroscopic and structural investigations**

Synopsis submitted to

DEPARTMENT OF CHEMISTRY
GOA UNIVERSITY
GOA 403 206 INDIA

October 2011

Chemistry of *s*-block metal coordination polymers: Synthesis, reactivity characteristics, spectroscopic and structural investigations

In recent years coordination polymers (CPs) also known as metal organic frameworks have attracted much attention because of their topology and applications in catalysis, adsorption (gas storage), separation and luminescence [1-6]. The term CP is derived from organic polymers and defined [7] as "the term given in inorganic chemistry to a metal coordination compound where a ligand bridges between metal centers, where each metal centre binds to more than one ligand to create an infinite array of metal centers". A fundamental problem of comparing CPs with organic polymers is that the organic polymers by definition are macromolecules made up of monomers or oligomers associated through covalent bonds with defined molecular weights. In contrast, coordination polymers are comprised of metal-organic units linked together at least in one dimension to form an infinite array through extended covalent or coordinate interactions [1-4].

The formation of an infinite array of metal ions bridged by organic linkers can be visualized as follows. The building blocks (metal ions, organic ligands, solvent molecules, or neutral ligands) interact through coordination interactions and weak forces such as hydrogen bonds, π-π stacking or vander Waals interactions in solution giving some small molecular units or monomers, and then a self assembly processes leading to the formation of coordination polymers of different dimensionalities (Scheme 1) [8].

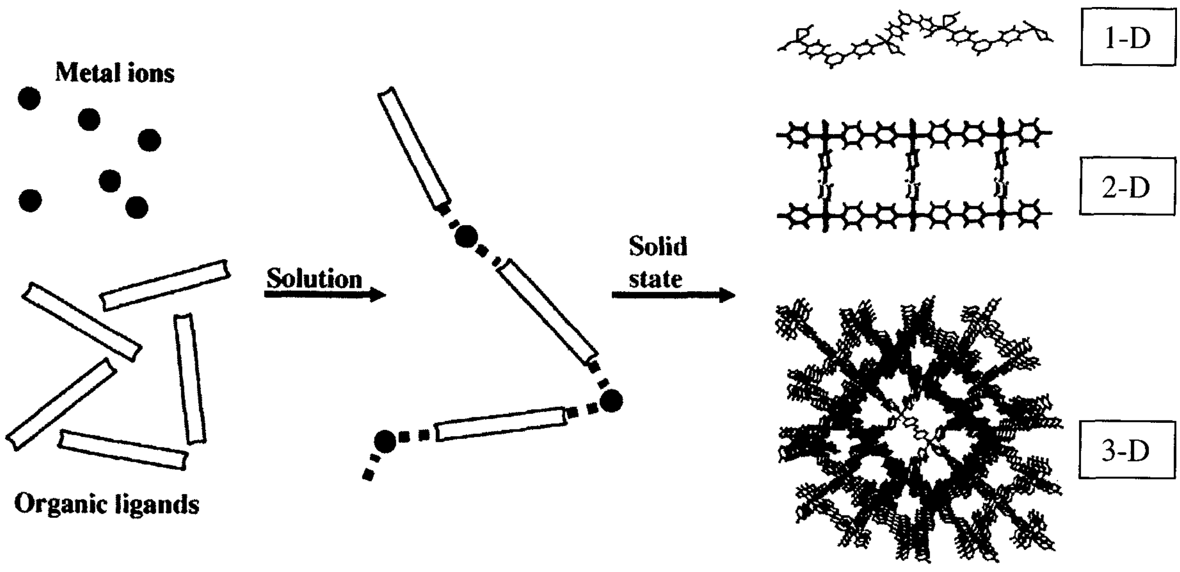

Scheme 1 - Formation of coordination polymers.

Organic ligands which are ditopic like 4,4′-bipyridine, terephthalic acid etc, or tritopic like trimesic acid, etc can be employed as linkers to create an infinite array of metal centres. The formation of chains (one dimensional) or layers (two dimensional) or framework (three dimensional) depends on both the steric requirements of the metal ion employed as well as the nature of the binding mode of the bridging ligand employed for the formation of coordination polymers. An extensive chemistry of coordination polymers based on transition metals has been developed in the last two decades [1-5]. In contrast, the coordination chemistry of group 1 and 2 metal compounds with organic ligands is a relatively less explored area. The reluctance in using alkali metal or alkaline earth cations as building blocks for coordination polymer can be attributed to their unpredictable coordination numbers and geometries as no ligand field stabilization effects govern their bonding. Although, the closed shell *s*-block metal cations lack useful properties like magnestism or variable oxidation states, alkali and alkaline-earth metals are preferred to transition or lanthanide metal ions because many of the *s*-block cations have the advantage of being non-toxic, cheap and soluble in aqueous media. Current interest in the coordination chemistry of *s*-block elements can be evidenced by several recent reports [9-18]. Different ligands and polymer types of the *s*-block compounds have been reviewed by Fromm [19]. For the oxophilic *s*-block metals, carboxylic acids are useful linkers for the construction of coordination polymers as the metal can be linked into an extended chain with the aid of bridging binding modes of the carboxylate ligand.

In this research the reaction of *s*-block metal especially alkaline earths have been investigated with aromatic carboxylic acids in the presence of N- or O- donor (Scheme 2) and the results of this work are described in the thesis entitled, "Chemistry of *s*-block metal coordination polymers: Synthesis, reactivity characteristics, spectroscopic and structural investigations". The details of experimental work and methods of synthesis of different compounds are given in Schemes 3-8.

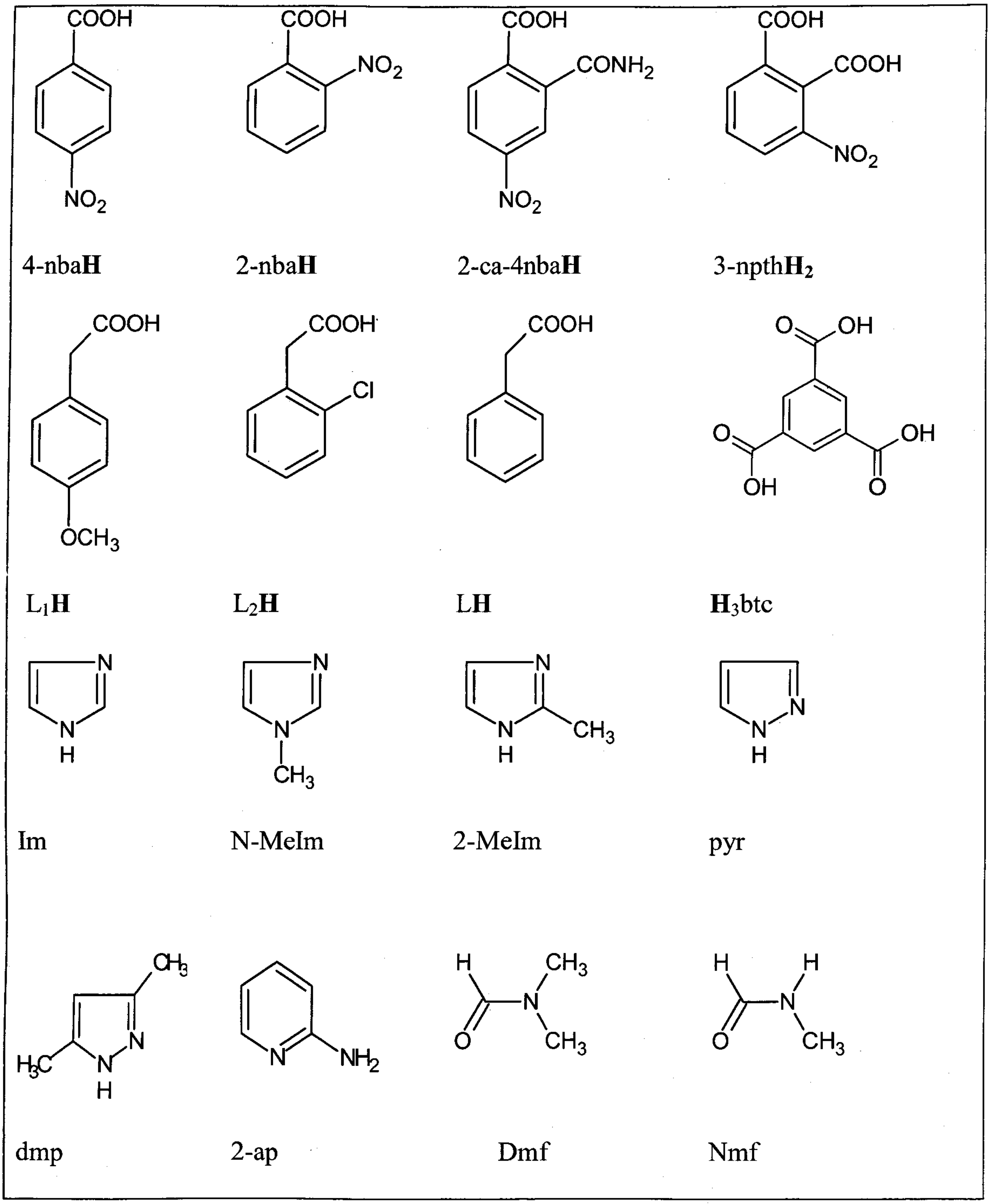

Scheme 2- Nomenclature of carboxylic acids and N-donor and O-donor ligands relevant to this study

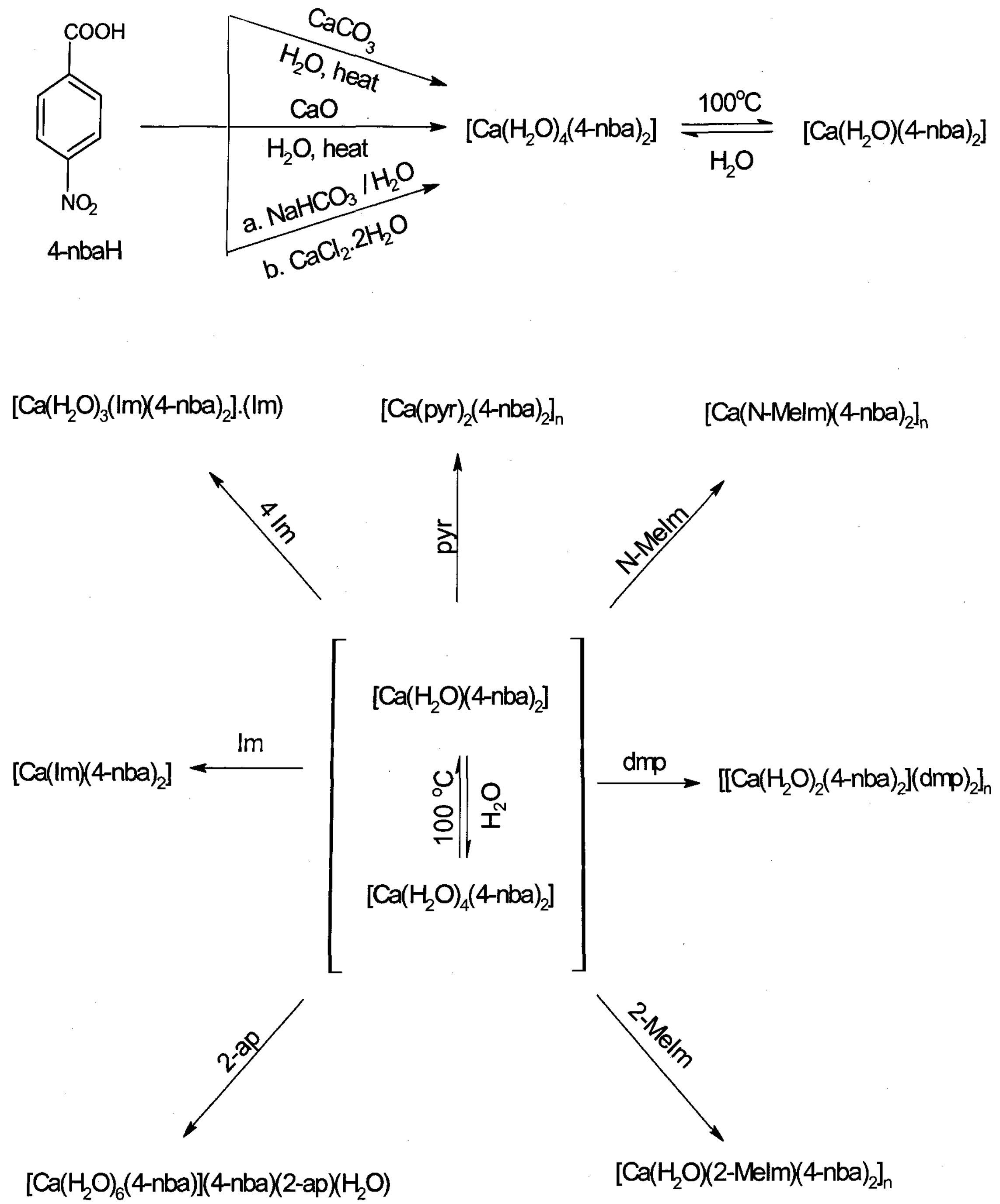

Scheme 3- Synthesis of monomeric $[Ca(H_2O)_4(4\text{-nba})_2]$ compound and its reactivity with neutral N-donor ligands

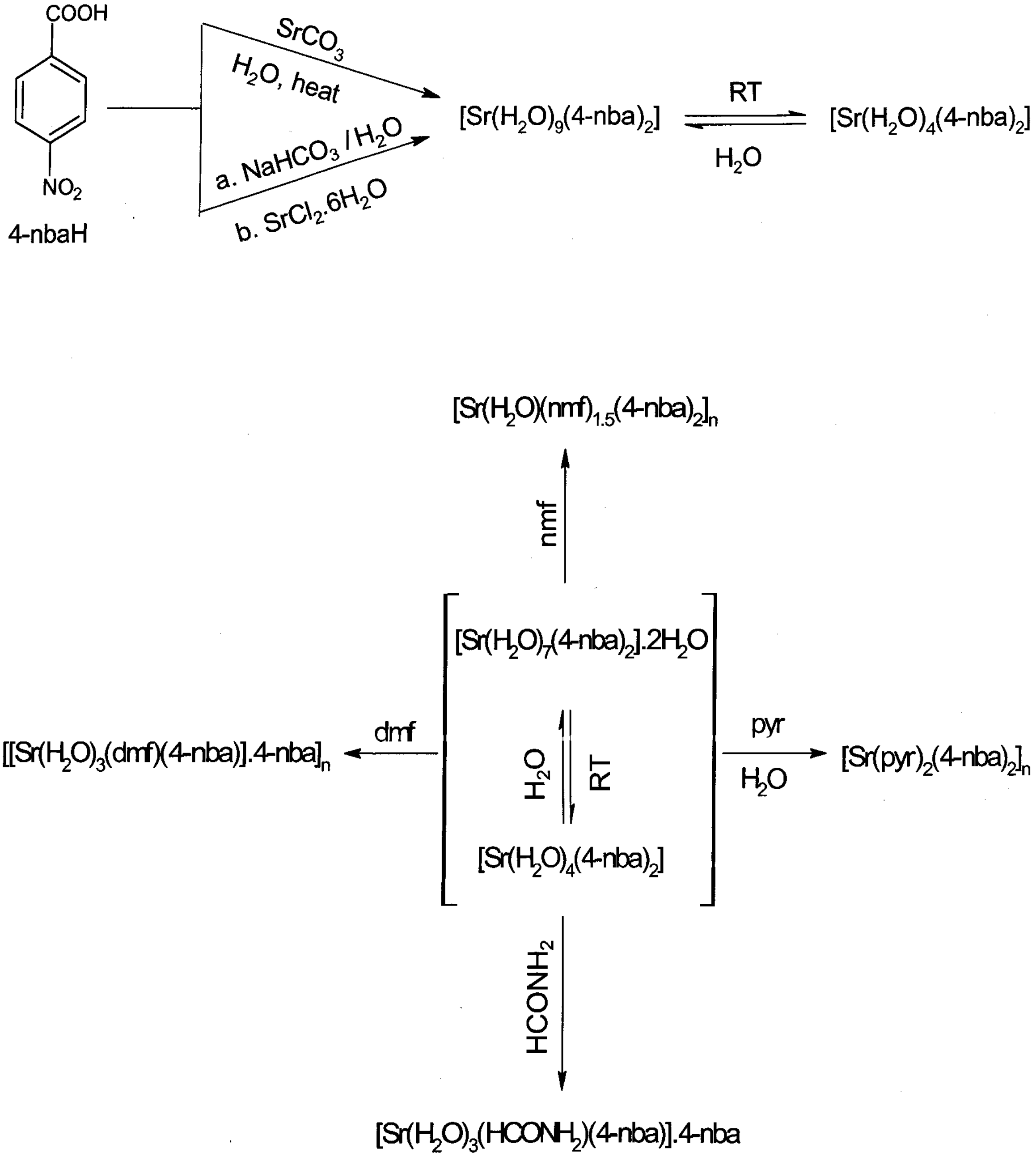

Scheme 4- Synthesis of monomeric $[Sr(H_2O)_9(4\text{-nba})_2]$ compound and its reactivity with neutral N-donor and O-donor ligands

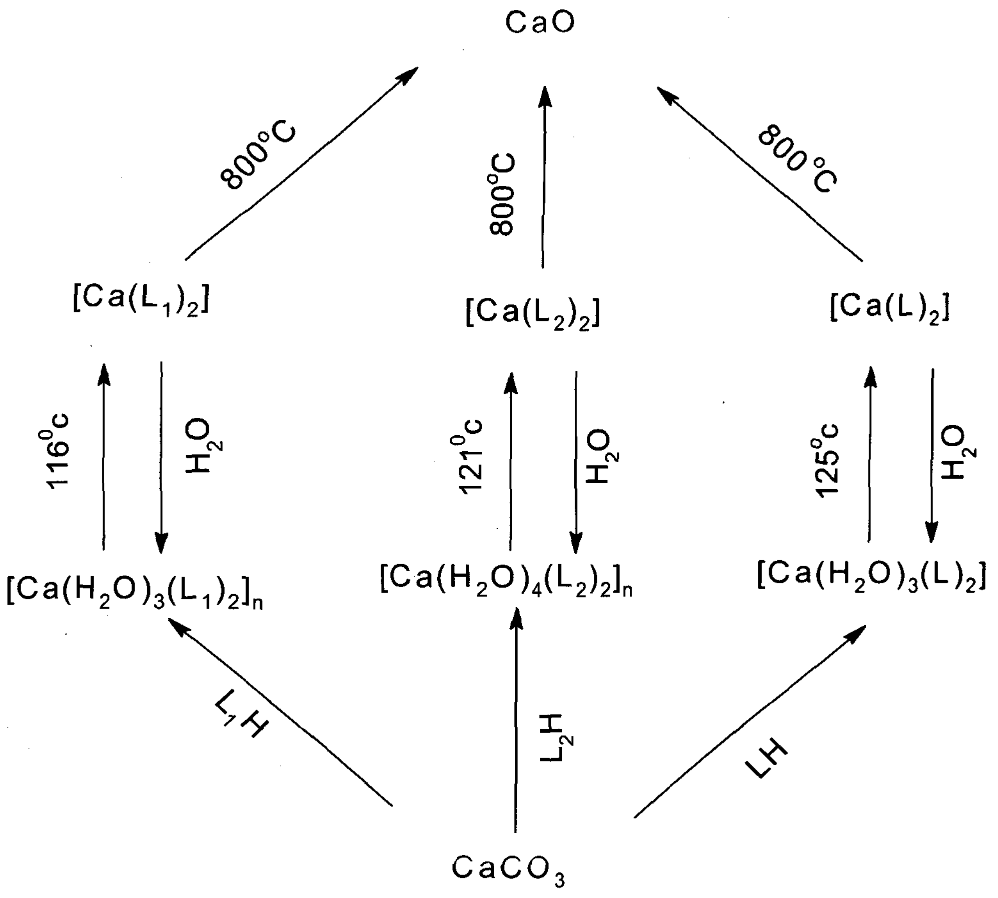

Scheme 5 - Synthesis of calcium phenyl acetates and its transformations

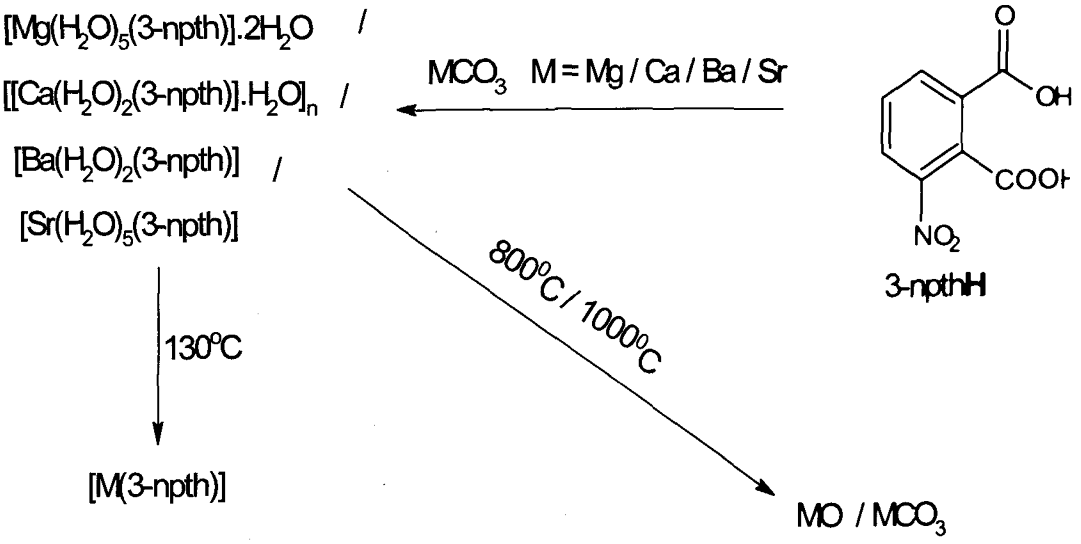

Scheme 6 - Synthesis of alkaline earth 3nitrophthalate

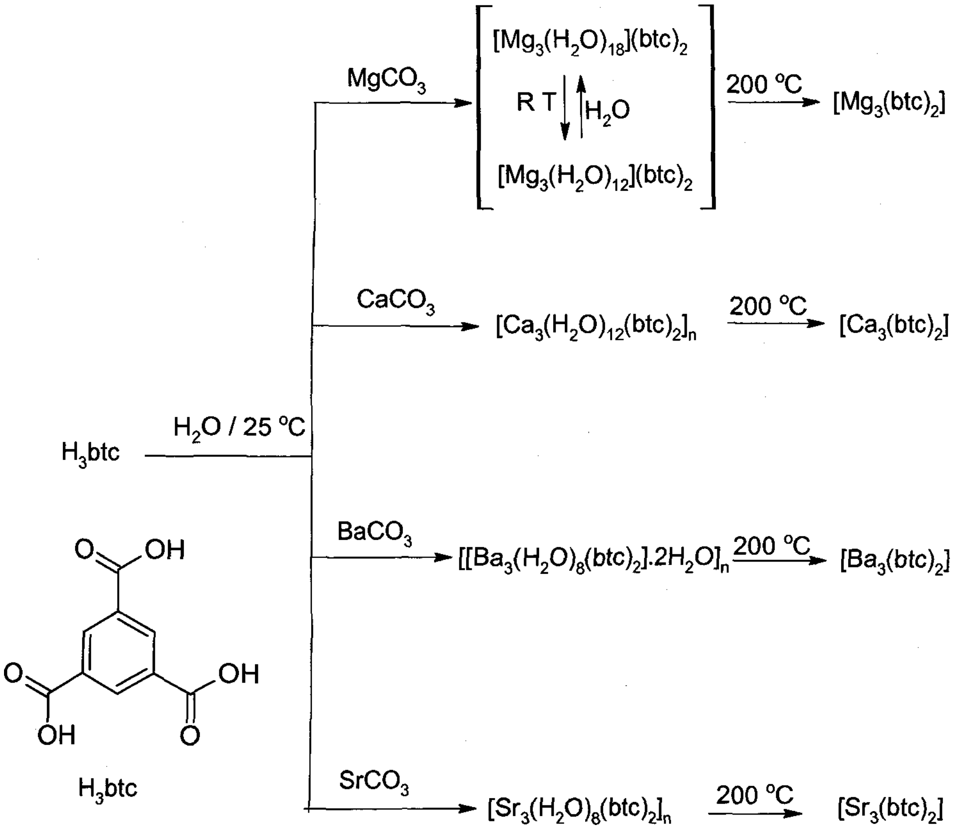

Scheme 7- Synthesis of alkaline earth metal carboxylate using H_3btc under ambient conditions

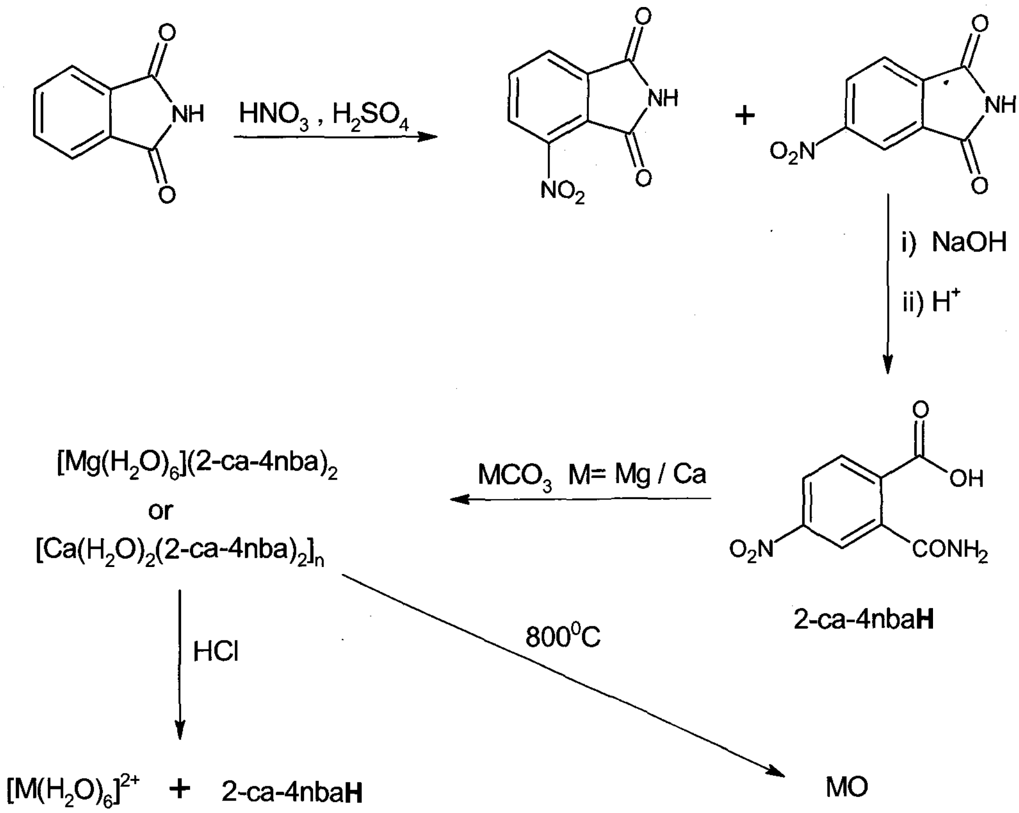

Scheme 8 - Synthesis of 2-ca-4-nbaH and its reaction with calcium and magnesium carbonate

The compounds prepared in this work have been characterized by a variety of methods. The composition of the different compounds was arrived at based on elemental analysis, isothermal weight loss studies, and estimation of insoluble aromatic acid and the residue of thermal decomposition. UV-visible spectra of the *s*-block compounds described in this work are nearly similar to that of the free acid indicating that the absorption bands are due to the intramolecular charge transfer of the aromatic acid. Several compounds were investigated for their emission characteristics and in some cases for example $[Ca(H_2O)_2(4\text{-nba})_2].(dmp)_2$ an enhancement of the fluorescence emission was observed [Fig. 1]. The luminescent property can be attributed to ligand centered orbital transitions since similar emissions are also observed for the free ligands. Infrared spectroscopy have been extensively employed to study the nature of compounds prepared and the characteristic absorption signals for the presensce of water, nitro functionality, N-donor, amide group etc. have been observed and appropriate assignments made. Although infrared spectral data provide useful information for the presence of the carboxylate groups, the exact nature of the binding mode cannot be inferred based only on infrared data. However infrared spectral data do provide evidence for the formation of new compounds [Fig. 2].

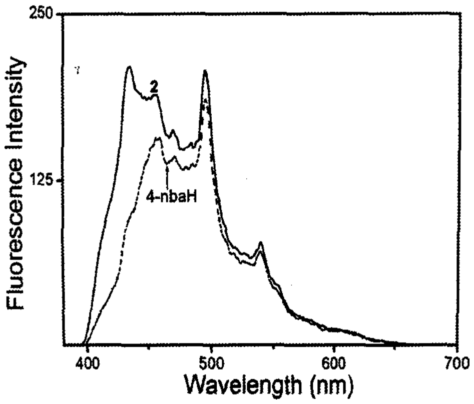

Fig 1. Fluorescence spectra of 4-nbaH and $[Ca(H_2O)_2(4\text{-nba})_2].(dmp)_2]_n$ **2**

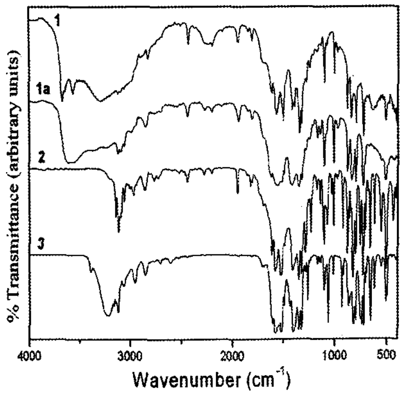

Fig 2. IR spectral comparison of [Ca(H2O)4(4-nba)2] 1, [Ca(H2O)(4-nba)2] 1a,[Ca(N-MeIm)(4-nba)2]n 2, [Ca(im)(4-nba)2] 3

In addition infrared spectra have been used to prove that some of the compounds can be dehydrated to form anhydrous compounds [Fig. 3]. The crystalline nature of the compounds prepared in this study has been inferred based on the powder diffraction studies and this technique has been used to show the formation of phase pure compounds [Fig. 4].

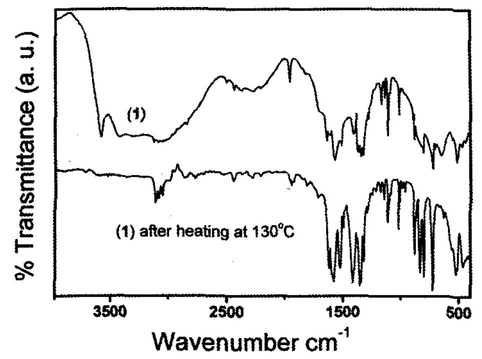

Fig-3: Infrared spectra of $[(H_2O)_4Li_2(\mu\text{-}H_2O)_2](4\text{-nba})_2$ (1) and (1) after heating at 130 °C.

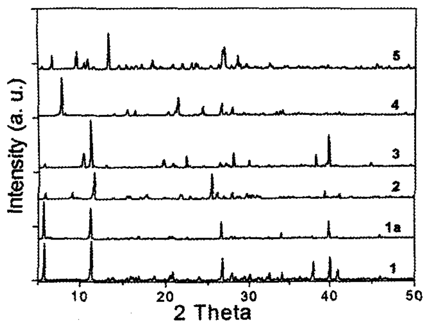

Fig-4: X-ray powder pattern of $[Sr(4\text{-nba})(H_2O)_7](4\text{-nba}).2H_2O$ **1**, $[Sr(4\text{-nba})_2(H_2O)_4]$ **1a**, $[Sr(4\text{-nba})(DMF)(H_2O)_3](4\text{-nba})$ **2**, $[Sr(H_2O)(4\text{-nba})_2(NMF)_{1.5}]$ **3** $[Sr(4\text{-nba})_2(pyr)_2]$ **4** and $[Sr(4\text{-nba})_2(HCONH_2)(H_2O)_3]$ **5**

All the compounds have been characterized by thermal methods. The carboxylates of the lighter metals magnesium and calcium decompose to form the oxide while the heavier metal (Sr and Ba) carboxylates decompose to form the corresponding metal carbonates. The thermal pattern show endothermic events for loss of neutral molecules like water or N-donor ligands at temperatures below 200°C while the carboxylate decomposition is observed at higher temperatures around 400°C as exothermic processes. Several compounds prepared in this work have been characterized by single crystal X-ray diffraction method. The central Mg^{II} ion in $[Mg(H_2O)_5(3\text{-npth})]\cdot 2H_2O$ and $[Mg(H_2O)_4(2\text{-nba})_2]$ .contains a monodentate carboxylate unit bonded to the Mg^{II} ion [Fig. 5-6]. The crystal structure of $[Mg(H_2O)_6](2\text{-ca-4nba})_2$ consists of an octahedral hexaaquamagnesium (II) cation and a free uncoordinated 2-ca-4nba anion [Fig. 7]. The cation and the anion are involved in three varieties of H-bonding interactions, resulting in a supramolecular bilayer of 2-ca-4nba anions sandwiched between layers of $[Mg(H_2O)_6]^{2+}$ cations. The structures of one dimensional mixed ligand coordination polymers formed based on 4-nba are shown in [Fig. 8-11]. The crystal structures and packing diagrams of coordination polymers based on 2-nba, 3-nhpth, 2-ca-4nba are shown in Figures [12-16].

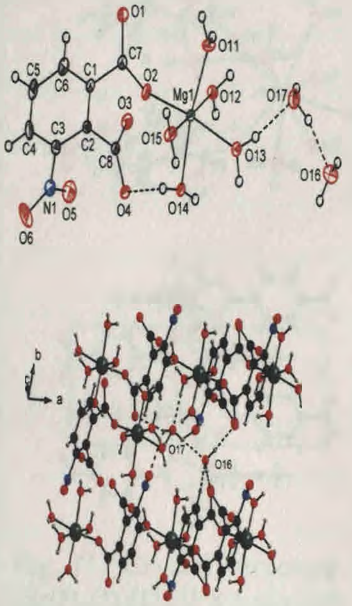

Fig 5: Coordination sphere of the metal ion in $[Mg(H_2O)_5(3\text{-npth})]\cdot 2H_2O$ (top) and hydrogen bonding situation around water dimmer (bottom)

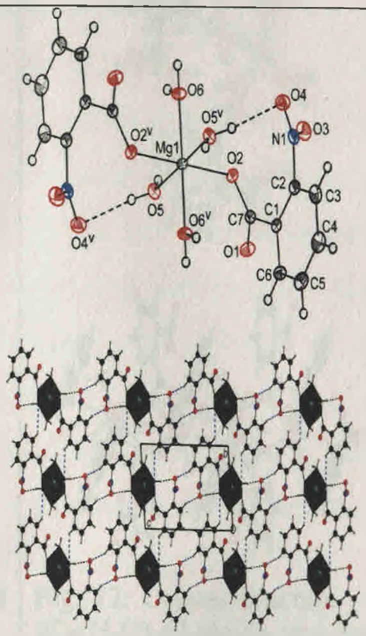

Fig 6: Coordination sphere of the metal ion in $[Mg(H_2O)_4(2\text{-nba})_2]$ (top) and packing diagram (bottom)

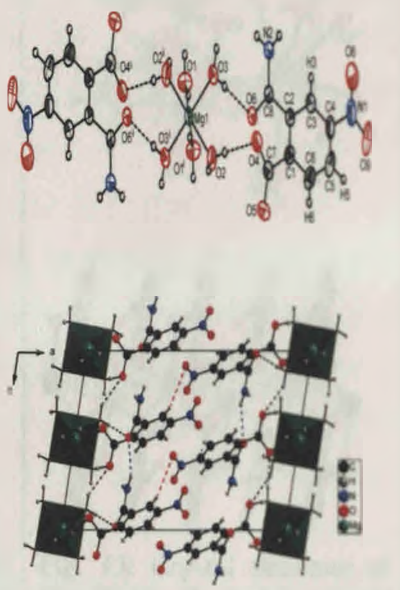

Fig 7: Crystal structure (top) and Crystallographic packing of $[Mg(H_2O)_6](2\text{-ca-4nba})_2$ viewed along *b* axis (bottom)

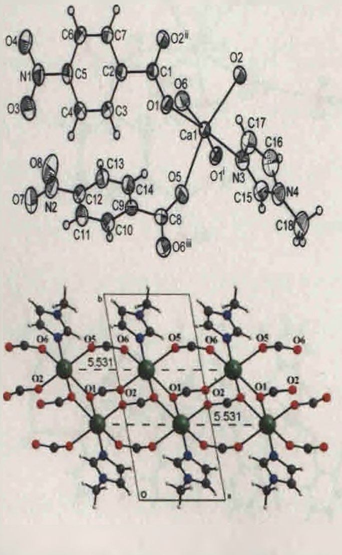

Fig 8: Crystal structure (top) and A view of the bridging bidentate coordinationof 4-nba through O5 and O6 leading to 1-D chain $[Ca(N\text{-}MeIm)(4\text{-nba})_2]_n$ (below)

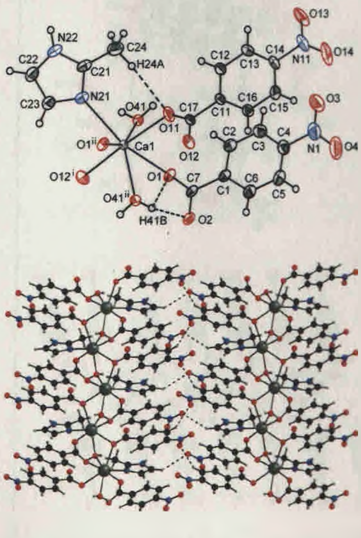

Fig 9: Crystal structure (top) and two polymeric chains of $[Ca(H_2O)(2\text{-MeIm})(4\text{-nba})_2]_n$ in ab crytallographic plane are linked by weak C-H-O bonds shown in broken lines (below)

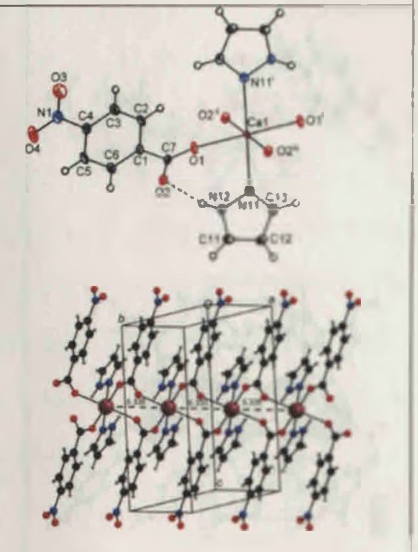

Fig 10: Crystal structure (top) and A portion of the 1D chain extending along a axis of $[Ca(pyr)_2(4\text{-nba})_2]_n$ polymer (below)

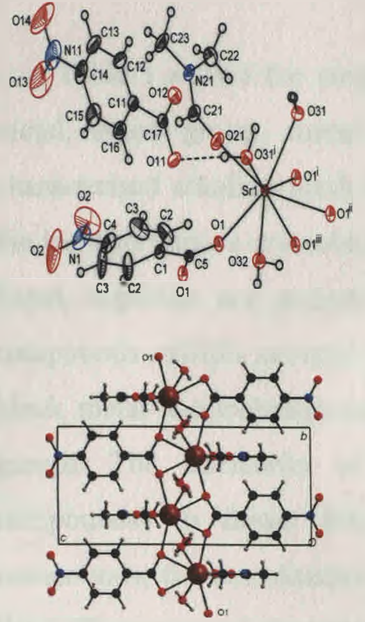

Fig 11: Crystal structure of $[Sr(H_2O)_3(DMF)(4\text{-}nba)](4\text{-}nba)$ showing the atom labeling scheme (top) and the 1-D chain showing terminal and bridging ligands around Sr(II) (bottom)

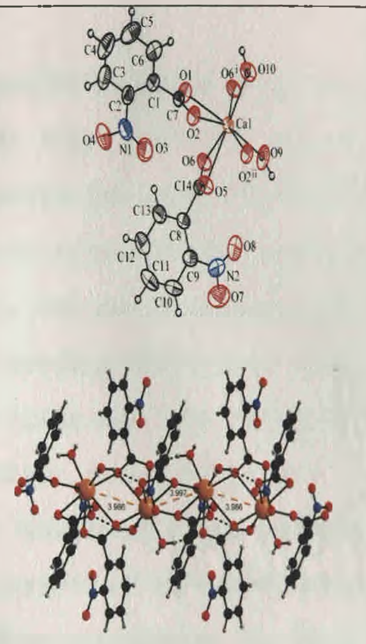

Fig. 12: Crystal structure of $[Ca(H_2O)_2(2\text{-}nba)_2]_n$ (top) and a 1-D chain formed due to linkage of tricyclic dicalcium-bis(2-nitrobenzoate) unit formed by a pair of $\mu_2\text{-}\eta^2{:}\eta^1$ 2-nba ligands between two Ca(II) ions (botom).

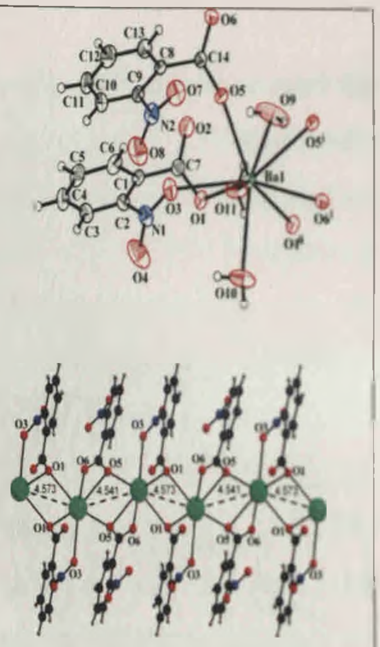

Fig. 13: Crystal structure of $[Ba(H_2O)_3(2\text{-}nba)_2]_n$ (top) and a 1-D chain (bottom)

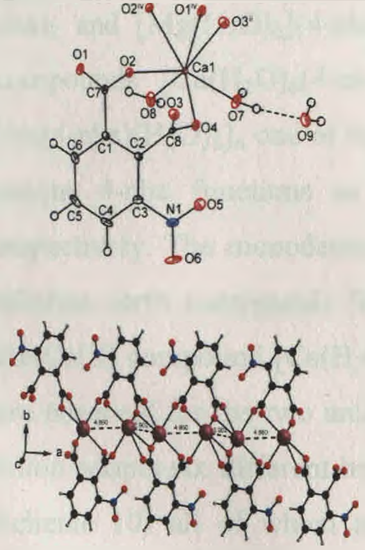

Fig 14: Crystal structure (top) and a part of the infinite chain extending along *a* axis in $[[Ca(H_2O)_2(3\text{-}npth)]\cdot H_2O]_n$ with alternating Ca···Ca distances of 4.860 and. 3.902 Å (bottom)

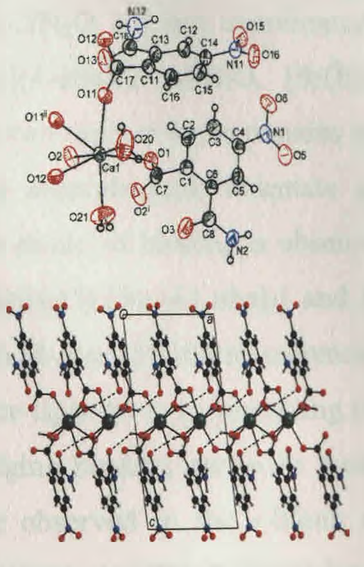

Fig 15: Crystal structure of $[Ca(H_2O)_2(2\text{-}ca\text{-}4nba)_2]_n$ (top) and view along *b* axis showing a part of the one dimensional chain extending along *a* axis due to the bridging binding modes of the unique 2-ca-4nba ligands (bottom)

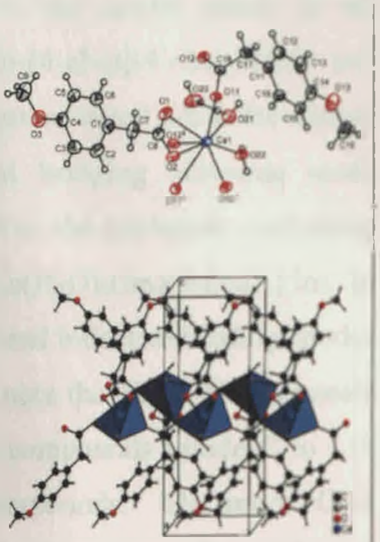

Fig. 16: Crystal structure of $[Ca(H_2O)_2(L_1)_2]\cdot H_2O$ (top) Crystallographic packings showing eight coordinate Ca(II) ion (bottom).

Table 1 shows the comparative structural features (coordination sphere around the metal, space group, metal to water ratio and type of interactions) of structurally characterised alkaline-earth metalcarboxylates. All the compounds in Table 1 excepting the last two entries crystallize in centrosymmetric space groups. Of the thirty compounds listed, eighteen are polymers, ten are monomers and the rest are dimers. All the compounds exhibit several H-bonding interactions. All the structurally characterized *s*-block metal 4-nitrobenzoates (entry no. 1 to 19) crystallize in centrosymmetric space groups. The nuclearity of these 4-nba compounds ranges from monomer (seven compounds) to dimer (two compounds) and polymer (ten compounds). In these compounds, the coordination number of the central metal varies from four to nine, with the Li(I) compound showing four coordination. The Na(I) and the Mg(II) compounds are six coordinated while the Sr and Ba compounds exhibit eight and nine coordination respectively. Coordination numbers ranging from six to eight are observed in the Ca(II) compounds. In addition to functioning as charge balancing anions for the *s*-block metal in all these compounds, 4-nba is bonded to the central metal as a monodentate or bidentate or as a bridging (μ-) ligand (Scheme 10). The 4-nba anions in $[(H_2O)_4Li_2(\mu\text{-}H_2O)_2](4\text{-nba})_2$ and $[Mg(H_2O)_6](4\text{-nba})_2.2H_2O$ are not coordinated to the central metal. In the compounds $[Ca(H_2O)_6(4\text{-nba})](4\text{-nba})(2\text{-ap})\cdot H_2O$, $[Sr(H_2O)_7(4\text{-nba})](4\text{-nba}).2H_2O$ and $[Na(4\text{-nba})(H_2O)_3]_n$ one of the two unique 4-nba remains uncoordinated while the second unique 4-nba functions as a monodentate, bidentate and bridging bidentate mode respectively. The monodentate mode of binding is observed in the imidazole containing alkaline earth compounds $[Mg(H_2O)_2(Im)_2(4\text{-nba})_2]$ and $[Ca(H_2O)_3(Im)(4\text{-nba})_2]\cdot Im$. In the Ca(II) compound $[Ca(H_2O)_4(4\text{-nba})_2]$ both monodentate and bidentate binding modes are observed for the two unique ligands. It is interesting to note that the 4-nitrobenzoate anion adopts six different bridging binding modes in these compounds (mode C to I in Scheme 10) all of which are observed in the *s*-block compounds. The mode G is observed for the first time in $[[Sr(4\text{-nba})(DMF)(H_2O)_3](4\text{-nba})]_n$ polymer. Four of these (Mode C to mode F) are μ_2-bridging type while mode G-I are μ_3-bridging in nature. The bridging binding modes F and I involving the binding of the central metal to the oxygen atom of the nitro group are observed only in the alkali metal compounds $[Na(4\text{-nba})(H_2O)_3]_n$ and $[KH(4\text{-nba})]_n$. The bonding of the oxygen of the nitro group to *s*-block elements is a known structural feature observed in other *s*-block compounds. The μ_2-binding modes C and F are symmetrical bridging bidentate in nature but differ in that in mode C the two carboxylate oxygens bridge between two metals while the oxygen atoms of the nitro group are the binding sites in mode F as observed in the $[Na(4\text{-nba})(H_2O)_3]_n$ compound. The symmetrical μ_2-bridging mode C is observed in the mixed ligand dimeric compound $[Mg(H_2O)(L^1)_2(4\text{-nba})_2]_2$ and in four other coordination polymers. An asymmetric μ_2-bridging binding mode involving a single oxygen (mode D) and μ_2-bridging tridentate coordination mode (mode E) are observed in the Ca(II) coordination polymers. A list of publications based on the present thesis is given at the end.

Table 1 - Comparative structural features of structurally characterised alkaline-earth metalcarboxylates

Compound	C.S.	S. G.	M:H_2O	Nuclearity	H-bonding
$[(H_2O)_4Li_2(\mu\text{-}H_2O)_2](4\text{-nba})_2$	$\{LiO_4\}$	$P2_1/c$	1.3	dimer	O-H···O, C-H···O
$[Na(4\text{-nba})(H_2O)_3]_n$	$\{NaO_6\}$	$P\bar{1}$	1:3	monomer	O-H···O, C-H···O
$[KH(4\text{-nba})]_n$	$\{KO_6\}$	$P\bar{1}$	1:0	polymer	O-H···O, N-H···O, C-H···O
$[Mg(H_2O)_6](4\text{-nba})_2\cdot 2H_2O$	$\{MgO_6\}$	$P\bar{1}$	1:6	monomer	O-H···O
$[Mg(H_2O)_2(Im)_2(4\text{-nba})_2]$	$\{MgO_4N_2\}$	$P\bar{1}$	1:2	monomer	O-H···O, N-H···O
$[Mg(H_2O)(N\text{-}MeIm)_2(4\text{-}nba)_2]_2$	$\{MgO_4N_2\}$	$P\bar{1}$	1:1	dimer	O-H···O
$[Ca(H_2O)_4(4\text{-nba})_2]_n$	$\{CaO_7\}$	$P2_1/c$	1:7	monomer	O-H···O, C-H···O
$[Ca(H_2O)_3(Im)(4\text{-nba})_2]\cdot Im$	$\{CaO_5N\}$	$P2_1/c$	1:3	monomer	O-H···O, N-H···O, O-H···N
$[Ca(H_2O)_6(4\text{-nba})](4\text{-nba})(2\text{-}ap)\cdot H_2O$	$\{CaO_7\}$	$P\bar{1}$	1:6	monomer	O-H···N, C-H···O, N-H···O
$[Ca(N\text{-}MeIm)(4\text{-nba})_2]_n$	$\{CaO_5N\}$	$P\bar{1}$	1:0	polymer	C-H···O
$[Ca(H_2O)(2\text{-}MeIm)(4\text{-nba})_2]_n$	$\{CaO_6N\}$	$P2_1/n$	1:1	polymer	O-H···O, N-H···O, C-H···O
$[Ca(pyr)_2(4\text{-nba})_2]_n$	$\{CaO_4N_2\}$	$P\bar{1}$	1:0	polymer	N-H···O, C-H···O
$[[Ca(H_2O)_2(4\text{-nba})_2](dmp)_2]_n$	$\{CaO_8\}$	$P\bar{1}$	1:2	polymer	O-H···O, N-H···O, O-H···N, C-H···O
$[Sr(H_2O)_7(4\text{-nba})](4\text{-}nba)\cdot 2H_2O$	$\{SrO_9\}$	$P2_1/c$	1:5	monomer	O-H···O, C-H···O
$[[Sr(4\text{-nba})(DMF)(H_2O)_3](4\text{-}nba)]_n$	$\{SrO_8\}$	$P2_{1/m}$	1:3	polymer	O-H···N, C-H···O, N-H···O
$[Sr(H_2O)(4\text{-nba})_2(NMF)_{1.5}]_n$	$\{SrO_8\}$	$C2/c$	1:1	polymer	O-H···N, C-H···O, N-

					H···O
$[Sr(pyr)_2(4\text{-}nba)_2]_n$	$\{SrO_6N_2\}$	*C2/c*	1:0	polymer	O-H···N, C-H···O, N-H···O
$[Sr(H_2O)_3(4\text{-}nba)_2(HCONH_2)]_n$	$\{SrO_8\}$	$P2_{1/m}$	1:3	polymer	O-H···N, C-H···O, N-H···O
$[Ba(H_2O)_5(4\text{-}nba)_2]_n$	$\{BaO_9\}$	$P2_1/c$	1:3	polymer	O-H···O, C-H···O
$[Mg(H_2O)_6](2\text{-}ca\text{-}4nba)_2$	$\{MgO_6\}$	$P2_1/c$	1:6	monomer	O-H···O, N-H···O, C-H···O
$[Ca(H_2O)_2(2\text{-}ca\text{-}4nba)_2]_n$	$\{CaO_7\}$	$P\bar{1}$	1:2	polymer	O-H···O, N-H···O, C-H···O
$[Mg(H_2O)_4(2\text{-}nba)_2]$	$\{MgO_6\}$	$P\bar{1}$	1:4	monomer	O-H···O, C-H···O
$[Ca(H_2O)_2(2\text{-}nba)_2]_n$	$\{CaO_8\}$	$P\bar{1}$	1:2	polymer	O-H···O, C-H···O
$[Ba(H_2O)_3(2\text{-}nba)_2]_n$	$\{BaO_9\}$	$P\bar{1}$	1:2	polymer	O-H···O, C-H···O
$[Mg(H_2O)_5(3\text{-}npth)]\cdot 2H_2O$	$\{MgO_6\}$	$P\bar{1}$	1:5	monomer	O-H···O
$[[Ca(H_2O)_2(3\text{-}npth)]\cdot H_2O]_n$	$\{CaO_7\}$	$P2_1/c$	1:2	polymer	O-H···O
$[Ca_3(btc)_2(H_2O)_{12}]_n$	$\{CaO_7\}$, $\{CaO_8\}$	C2/C	1:4	polymer	O-H···O, C-H···O
$[[Ba_3(btc)_2(H_2O)_8].2H_2O]_n$	$\{BaO_9\}$	$P2_{1/c}$	1:2.75	polymer	O-H···O, C-H···O
$[[Ca(H_2O)_2(L_1)_2]\cdot H_2O]_n$	$\{CaO_8\}$	$P2_1$	1:2	polymer	O-H···O, C-H···O
$[[Ca(H_2O)_2(L_2)_2]\cdot 2H_2O]_n$	$\{CaO_8\}$	$P2_1$	1:2	polymer	O-H···O, C-H···O

Abbreviations used: C.S. = coordination sphere of central metal; S.G. = space group; ligand abbreviations are as per **Scheme 2**

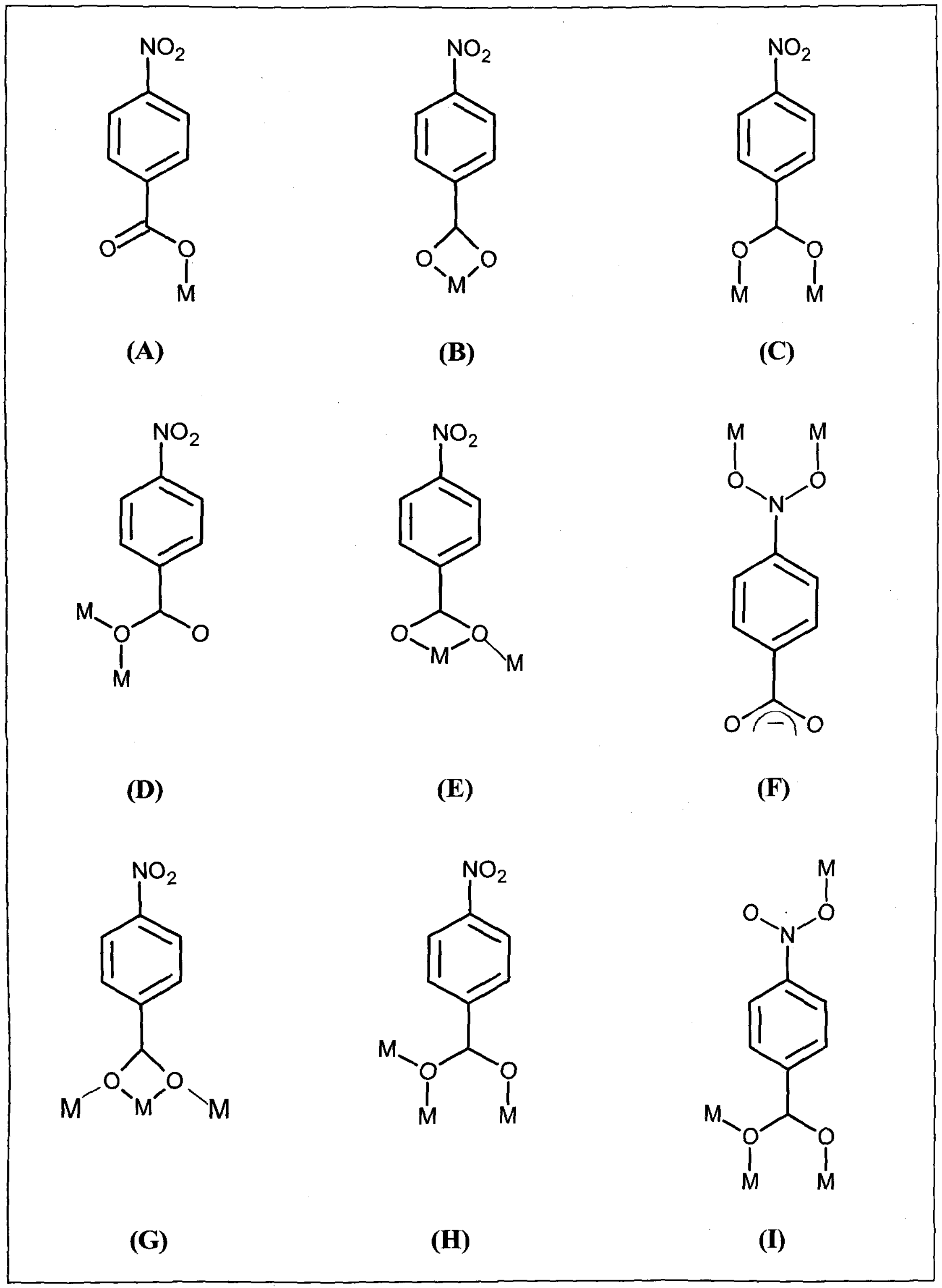

(A) (B) (C)

(D) (E) (F)

(G) (H) (I)

Scheme 10 – Structurally characterized binding modes of 4-nba**H**

SELECTED REFERENCES

[1] S. R. Batten, S.M. Neville, D. R. Turner, Coordination Polymers: Design, Analysis and Application, RSC Publishing, Cambridge UK (2009).

[2] C. Janiak, J. K. Vieth, New J. Chem., **34** (2010) 2366

[3] R. Robson, J. Chem. Soc. Dalton Trans., (2008) 5113

[4] K. Biradha, A. Ramanan, J. J. Vittal, Cryst. Growth Des., **9** (2009) 2969

[5] M. D. Allendorf, C. A. Bauer, R. K. Bhakta, R. J. T. Houk, Chem. Soc. Rev. **38** (2009) 1330

[6] D. Britt, D. Tranchemontagne, O. M. Yaghi, Proc. Natl. Acad. Sci. **105** (2008) 11623

[7] Coordination polymers: In Wikipedia, The Free Encyclopedia. http://en.wikipedia.org/wiki/Coordination_polymers

[8] A. Y. Robin, K.M. Fromm, Coord. Chem. Rev. **250** (2006) 2127

[9] S. Chen, S. Hoffmann, Y. Prots, J-T. Zhao, R. Kniep Z. Anorg. Allg. Chem., **636**, (2010) 1710

[10] P.C. Dietzel, R. Blom, H. Fjellvag, Z. Anorg. Allg. Chem., **635**, (2009) 1953

[11] Z. Guo, G. Li, L. Zhou, S. Su, Y. Lei, S. Dang, H. Zhang, Inorg. Chem., **48**, (2009) 8069

[12] L. N. Appelhans, M. Kosa, A.V. Radha, P. Simoncic, A. Navrotsky, M. Parrinello, A. K. Cheetham, J. Am. Chem. Soc. **131**, (2009) 15375

[13] D. T. Tran, D. Chu, A. J. Oliver, S. R. J. Oliver, Inorg. Chem. Commun., **12**, (2009) 351

[14] C.A. Williams, A.J. Blake, C. Wilson, P. Hubberstey, M. Schroder, Cryst. Growth Des., **8**, (2008) 911

[15] M. C. Das, S. K. Ghosh, E. C. Sanudo, P. K. Bharadwaj, Dalton Trans (2009) 1644

[16] B. M. Borah, S. K. Dey, G. Das, Cryst. Growth Des., **11**, (2011) 2773

[17] R. Murugavel, R. Korah, Inorg. Chem., **46** (2007) 11048

[18] C. N. Morrison, A. K. Powell, G. E. Kostakis, Cryst. Growth Des., **11** (2011) 3653

[19] K. M. Fromm, Coord. Chem. Rev. **252** (2008) 856

Chapter 1

CHAPTER 1

INTRODUCTION

In recent years coordination polymers (CPs) also known as metal-organic frameworks (MOFs) have attracted much attention because of their topology and applications in catalysis, adsorption (gas storage), separation and luminescence [1-9]. The term CP is derived from organic polymers and defined [9] as "the term given in inorganic chemistry to a metal coordination compound where a ligand bridges between metal centers, where each metal centre binds to more than one ligand to create an infinite array of metal centers". The well known organic polymers for example polyethylene by definition are macromolecules made up of monomers or oligomers associated through covalent bonds with defined molecular weights. In contrast, coordination polymers are made up of metal-organic units linked together at least in one dimension to form an infinite array through extended covalent or coordinate interactions [10-11]. The term metal-organicframework (MOF) is also used by several research groups to designate solids which exhibit extended network structures. In view of such different terminologies in existence, the IUPAC division of Inorganic Chemistry has initiated a project on coordination polymers and metal-organic frameworks: Terminology and nomenclature guidelines [12]

Wikipedia defines MOFs as crystalline compounds consisting of metal ions or clusters coordinated to rigid organic molecules to form one-, two-, or three-dimensional structures that can be porous. This definition seems to be very specific for crystallinity and dimensionality, the latter is restricted to only extended interactions through covalent and coordinate bonds and not to other nonbonding interactions. It is to be noted that, porosity is only an additional feature and is not particular to the definition. Inorganic chemists use the term CPs, while solid state chemist tend to prefer the term MOF [13]. The term coordination polymer very broadly encompasses all the extended structures based on metal ions linked into an infinite chain, sheet or three dimensional architectures by bridging ligands, usually containing carbon atoms [14].

A framework structure is defined in solid state science as a crystalline structure in which there are strong inter atomic bonds which are not confined to a single plane, in contrast to a layer structure. Based on such a definition, even the layered structure such as clays may not qualify as "framework structures". In a recent perspective article on the pros and cons of using these terminologies (CP or MOF) Biradha *et al* have proposed to describe one dimensional and two dimensional extended structures as coordination polymers (CPs) and three dimensional structures as metal organic frameworks [15].

The formation of an infinite array of metal ions bridged by organic linkers can be visualized as follows. The building blocks (metal ions, organic ligands, solvent molecules, or neutral ligands) interact through coordination interactions and weak forces such as hydrogen bonds, π-π stacking or Van der Waals interactions in solution giving some small molecular units or monomers, and then a self assembly processes leading to the formation of coordination polymers of different dimensionalities (Scheme 1) [16].

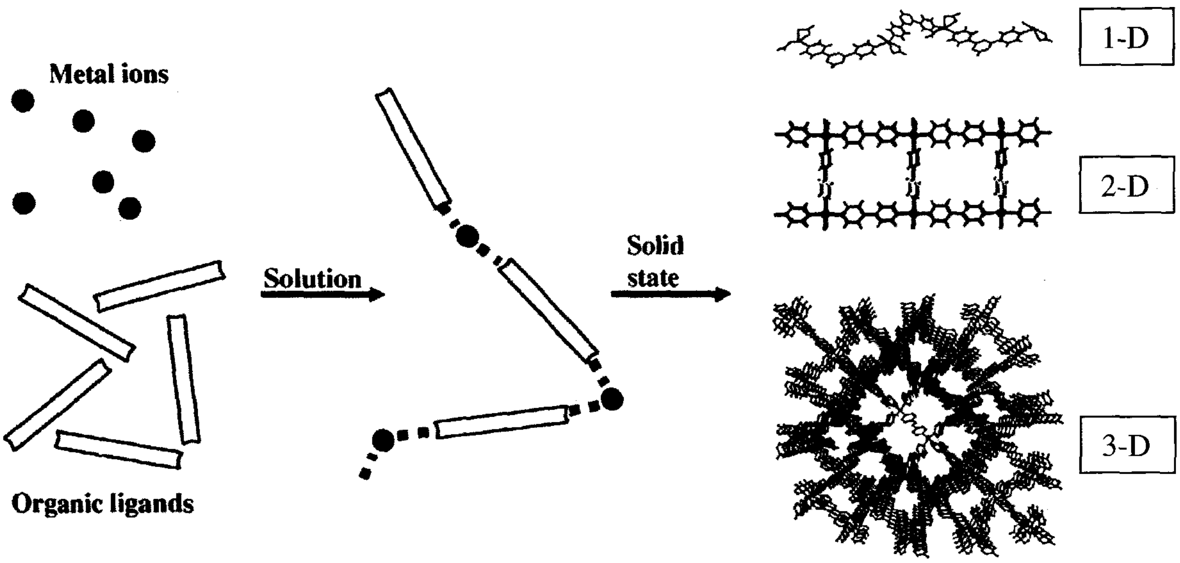

Scheme 1 - Formation of coordination polymers

Organic ligands which are ditopic like 4,4′-bipyridine, terephthalic acid etc, or tritopic like trimesic acid, etc can be employed as linkers to create an infinite array of metal centers. The formation of chains (one dimensional) or layers (two dimensional) or framework (three dimensional) depends on both the steric requirements of the metal ion employed as well as the nature of the binding mode of the bridging ligand employed for the formation of coordination polymers [17-18]. An extensive chemistry of coordination polymers based on transition metals has been developed in last two decades. In contrast, the coordination chemistry of group 1 and 2 metal compounds with organic ligands is a relatively less explored area. The reluctance in using alkali metal or alkaline earth cations as building blocks for coordination polymer can be attributed to their unpredictable coordination numbers and geometries as no ligand field stabilization effects govern their bonding. Although, the closed shell *s*-block metal cations lack useful properties like magnetism or variable oxidation states, alkali and alkaline-earth metals are preferred to transition or lanthanide metal ions because many of the *s*-block cations have the advantage of being non-toxic, cheap and soluble in aqueous media.

Current interest in the coordination chemistry of *s*-block elements can be evidenced by several recent reports and the field has been reviewed [16-27]. With no crystal field stabilization energy requirement in *s*-block complexes and the ability of heavier *s*-block elements to adopt higher coordination number leads to extended structures of different dimensionalities. The size of the *s*-block metal ion varies (Table 1) and it has been observed that the heavier *s*-block metal ions like K, Rb, Cs (in alkali group) and Ca, Sr, Ba (in alkaline-earth family) prefer higher coordination numbers (8 to 10) in most known compounds, while the lighter metals like Li or Be prefer a coordination number of 4. The oxophilic nature of the metals can also be evidenced from the average M-O (M = Metal) distance listed in Table 2. For the oxophilic *s*-block metals, carboxylic acids are useful linkers for the construction of coordination polymers as the metal can be linked into an extended chain with the aid of bridging binding modes of the carboxylate ligand. The dimensionality of the network depends on the reaction conditions used and the nature of carboxylic acid used [28].

Table 1- Properties of alkali and alkaline-earth metal cations [29]

Alkali/alkaline earth metal	Atomic radius (Å)	Ionic radius (Å)	Ionization energy ($kjmol^{-1}$)	Electronegativity (Pauling)
Li	1.52	0.76	52.01	1.0
Na	1.86	1.02	495.7	0.9
K	2.27	1.38	418.6	0.8
Rb	2.48	1.52	402.9	0.8
Cs	2.65	1.67	375.6	0.7
Be	1.12	0.31	1757	1.5
Mg	1.60	0.72	1450	1.2
Ca	1.97	1.0	1145	1.0
Sr	2.15	1.18	1064	1.0
Ba	2.22	1.35	965	0.9

Table 2- Average bond distance variation in *s*-block metal carboxylate networks [a]

Metal-O carboxylate	distance (Å)	Metal-O carboxylate	distance (Å)
Li-O	1.976 (0.09)	Be-O	1.636 (0.005)
Na-O	2.431 (0.004)	Mg-O	2.066 (0.02)
K-O	2.802 (0.006)	Ca-O	2.428 (0.006)
Rb-O	2.997(0.016)	Sr-O	2.622(0.006)
Cs-O	3.185 (0.015)	Ba-O	2.816 (0.005)

[a] Cambridge crystallography Database (CSD)

Using different monocarboxylic acids several extended networks of *s*-block metals have been characterized. The most commonly used organic linkers are aromatic carboxylic acids due to their structural rigidity and bonding interactions between the oxophilic metal centers and the carboxylate oxygen atoms. Aromatic carboxylic acids containing substituents like $-NH_2$, $-CH_3$, $-CONH_2$, $-NO_2$, etc are useful linkers for metal ions. The positioning of these groups can be altered with respect to the carboxylate functionality. The introduction of additional groups affects the acidity of the carboxylic acid, which is useful from a synthetic point of view of metal carboxylates. In addition, the substituents can participate in secondary interactions, which can influence product formation. The dicarboxylic acids like 1,2-benzenedicarboxylic acid, 1,3-benzenedicarboxylic acid, 1,4-benzenedicarboxylic acid or terephthalic acid have been widely employed as linker in *s*-block metal coordination polymers. The 4-nitrobenzoic acid used in our study is isoelectronic with respect to terephthalic acid. Although $-NO_2$ group is not electron donating the oxophilic nature of *s*-block metal may sometime result in bonding of oxygen of $-NO_2$ group with *s*-block metal and it is worth investigating this phenomenon (Chart 1). It is to be noted that, the carboxylate ligand is a good choice in view of its documented versatile ligational behavior towards metal ions (Chart 2) [30-31]. In addition to functioning as a simple anion (free uncoordinated group) for charge balance in many metal compounds, the carboxylate group can bind to metals as a monodentate ligand or as a bidentate ligand binding to a single metal or alternatively as a bridging bidentate ligand coordinating to two or more metals. The bridging binding modes are the ones which can link the metal ions into an extended structure.

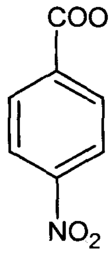

4-nitrobenzoic acid

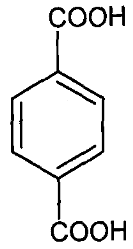

Terephthalic acid

Chart 1

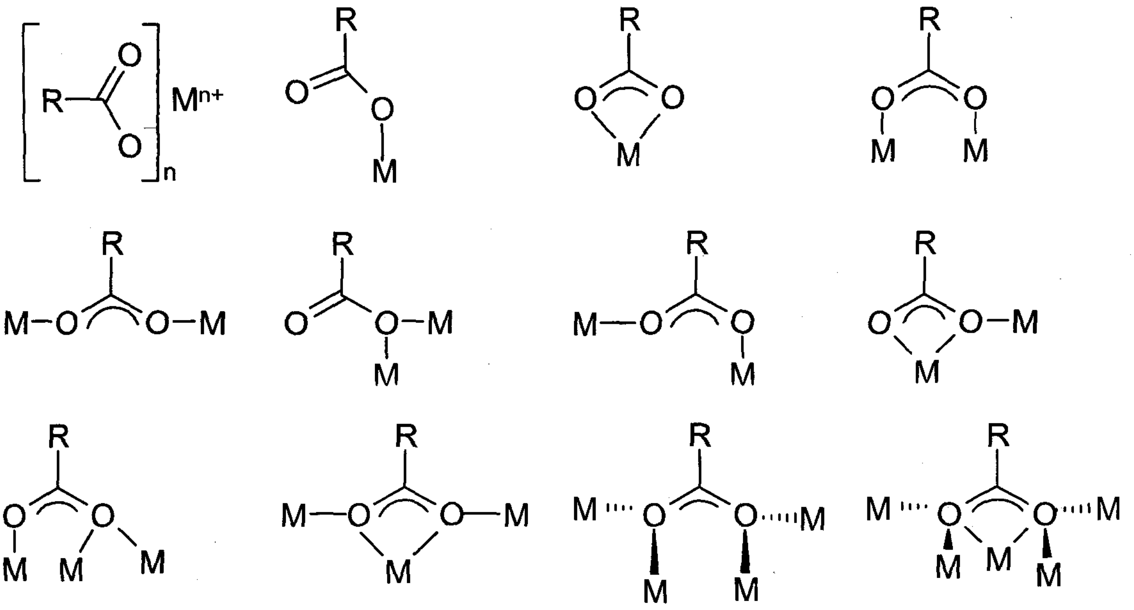

Chart 2 - Different binding modes of carboxylate ligand

1.1. Synthesis of *s*-block metal carboxylates

Many synthetic strategies for obtaining metal carboxylates / coordination polymers are well documented [16-28]. Improvement of synthesis is essential in order to get good quality single crystals suitable for X-ray measurement. It is to be noted that by using the same starting materials different products can be obtained by changing the reaction conditions. The synthesis of metal carboxylates / CPs is straitforward, using well soluble metal salts (metal chlorides, metal nitrates, sulfates, acetates etc.) or insoluble metal carbonates / hydroxides as the source for the metal component. The organic ingredients, which are mono-, di-, tri-, and tetracarboxylic acids are supplied in solvent like water or dmf (dimethylformamide) in presence of suitable base. After combination of these inorganic and organic components under stirring, metal carboxylates are formed by self assembly at temperatures varying from room temperature to temperatures above the boiling point of solvent (solvothermal reaction). For the preparation of coordination polymers different synthetic methodologies have been developed. These include the direct reaction of basic metal sources like metal carbonate or metal hydroxide with the carboxylic acid in water under ambient conditions, reaction of aqueous metal chloride or metal nitrate with the carboxylic acid in the presence of a mild base, the hydrothermal reaction of metal sources with carboxylic acids in autoclaves under autogeneous pressures [16-171]. While reviewing the synthetic methods of *s*-block coordination compounds, Fromm has mentioned that microwave and solid state synthesis are scarce for the preparation of alkaline-earth metal-organic frameworks unlike the solution methods of synthesis or hydrothermal method which have been more widely used [16-17]. Different types of reaction are summarized below (Scheme 2).

$$MCO_3 / M(OH)_2 / MO \;+\; R\text{-}COOH \xrightarrow{\text{RT / heat}} [M(H_2O/\text{solvent})_x(R\text{-}COO)_2]_n \qquad \text{Eq. 1}$$

$$RCOOH \;+\; NaOH / NaHCO_3 / Na_2CO_3 \xrightarrow{H_2O} R\text{-}COONa \qquad \text{Eq. 2}$$

$$MCl_2 / M(NO_3)_2 / M(Oac)_2 \;+\; R\text{-}COONa \xrightarrow{H_2O\text{ / Solvent}} [M(H_2O/\text{solvent})_x(R\text{-}COO)_2]_n \qquad \text{Eq. 3}$$

$$M(\text{source}) \;+\; \text{Base} \;+\; R\text{-}COOH \xrightarrow[\text{diffusion}]{\text{membrane}} [M(H_2O/\text{solvent})_x(R\text{-}COO)_2]_n \qquad \text{Eq. 4}$$

$$M(\text{source}) \;+\; \text{Org/Inorg base} \;+\; R\text{-}COOH \xrightarrow[\text{Solvothermal}]{120\text{-}200^{\circ}C} [M(H_2O/\text{solvent})_x(R\text{-}COO)_2]_n \qquad \text{Eq. 5}$$

R = alkyl or aryl group M = alkali or alkaline earth metal

Scheme 2 - General synthesis of metal carboxylates

In addition, metal sources can be combined with carboxylic acid in other non-conventional ways as described below for product formation.

a) Saturation method –

In this method the reactants / reagents are mixed in required proportions based on molar quantities in particular solvent based on solubility of the reactants as well as final products. Molecular recognition permits the construction of products following pre-determined rules. This technique needs convenient conditions:

- Crystals grow in saturated solutions. Ideal concentration is achieved by slow evaporation of the mother liquor.
- Solubility increases with temperature and crystals can appear during cooling step, which can be well-controlled as far as speed of cooling and final temperature are concerned. This method has been widely used in our study.

b) Diffusion method -

This method is preferred to get single crystal suitable for X-ray diffraction analysis instead of non- or poly-crystalline products, especially if the products are poorly soluble. The principle of this method is to slowly bring into contact the different species.

c) Hydrothermal / Solvothermal method-

The temperature range is usually 120-260°C inside a closed vessal (autoclave) under autogeneous pressure. Under this condition the reduced viscosity of water enhances the diffusion process and thus extraction of solids and crystal growth from solution is favoured. As the difference of solubility between organic and inorganic components in the same solvent is often a barrier in the formation of single crystals, hydrothermal experiments can be a good alternative as solubilities of starting material can be increased. This crystallization technique is a non-equilibrium synthesis and may lead to metastable products. This can be influenced mainly by the cooling speed at the end of the reaction.

d) Microwave and ultrasonic method -

These methods are based on the improvement of solubilities in order to better react involved species and crystallize the products. This method is relatively a less explored area.

e) Mechanochemical or Solvent-free synthesis -

Co-grinding of two or more crystalline materials under solvent-free conditions generates new co-crystal phases of an inclusion complex or adduct. The heat generated in the mechanochemical process may induce local melting or metastable eutectic phase at the interface between different crystals or loss of neutral molecules from the original crystal lattice therby creating valence for incorporation of new ligands in the original crystal lattice. The phenomenon of crystallization in the solid state is interesting as the molecules in crystals which are bound to the original crystal lattice with fixed conformation, orientation and location have to be freed from the original lattice and diffuse and rearrange themselves together with foreign molecules to form a new structures of 1-D, 2-D or 3-D periodicity, in the solid state.

Thus metal carboxylates of different dimensionalities can be prepared by varying the nature of reactants and synthetic conditions. A survey of the literature reveals a synthetic chemistry of alkaline-earth metal carboxylates as evidenced by compound synthesis by different methods which are summarized in Table 3.

i) Mg forms compounds containing $[Mg(H_2O)_6]^{2+}$ cations in many compounds when reaction are performed under ambient conditions, while Ca, Sr and Ba forms one dimensional polymers even with monocarboxylic acids.

ii) Use of di-, tri-, tetra- carboxylic acids and solvothermal conditions result in the formation of compounds having higher dimensionality.

iii) The number of coordinated water molecules in the heavier alkaline earths are fewer as compared to that in Mg.

Table 3- Synthesis of alkaline-earth metal carboxylates

Compound	**Metal source / base / others**	**Conditions**	**Acid**	**Ref.**
Magnesium carboxylates				
$[Mg(H_2O)_6](4\text{-nba})_2$	$MgCO_3/MgCl_2.6H_2O/ NaHCO_3$	H_2O / 100°C	4-nba**H**	133
$[Mg(H_2O)_6](C_7H_4NO_5)_2$	$MgCl_2.6H_2O$ / NaOH	H_2O / 25°C	$C_7H_5NO_5$	132
$[Mg(H_2O)_6](2\text{-ca-4nba})_2$	$MgCO_3/MgCl_2.6H_2O/ NaHCO_3$	H_2O / 100°C	2-ca-4nba**H**	170
$[Mg_3(H_2O)_{18}](BTC)_2$	$MgCO_3/MgCl_2.6H_2O/ NaHCO_3$	H_2O / 25°C	$\mathbf{H_3}BTC$	This work
$[Mg(H_2O)_6](2\text{-aba})_2{\cdot}2H_2O$	$MgCl_2.6H_2O$ / KOH	H_2O / 25°C	2-aba**H**	134
$[Mg(H_2O)_6](4\text{-aba})_2{\cdot}2H_2O$	$MgCl_2.6H_2O/NH_4OH$	H_2O / 25°C	4-aba**H**	39
$[Mg(H_2O)_2(hip)_2].2H_2O]$	$MgCl_2.6H_2O/NH_4OH$	MeOH / H_2O / reflux	hip**H**	122
$[Mg(H_2O)_4(Sa)_2]$	$MgCl_2.6H_2O/NH_4OH$	MeOH / H_2O/ reflux	Sa-**H**	139
$[Mg(H_2O)_6](optp)_2$	$Mg(Oac)_2$	H_2O/ 100°C / 72 hrs / Solvothermal	**H**optp	148
$[Mg(H_2O)_4](2\text{-nba})_2$	$MgCO_3$ /$MgCl_2.6H_2O$ / $NaHCO_3$	H_2O / 100°C	2-nba**H**	120
$[Mg(H_2O)_4(C_7H_3NO_5)]$	$Mg(OH)_2.6H_2O$	H_2O / acetone / reflux	$C_7H_5NO_5$	132
$[Mg(H_2O)_6](\mathbf{H_2}PMA)$	$Mg(OH)_2.6H_2O/ MgCO_3$	H_2O / 100°C / 18 hrs	$\mathbf{H_4}PMA$	135
$[Mg(H_2O)_6](C_8H_5O_4)_2$	MgO	H_2O/25°C	$C_8H_6O_4$	136
$[Mg(H_2O)_6](Nic)_2{\cdot}4H_2O$	$[Mg(H_2O)_4](Nic)_2$	H_2O/Recryst/25°C	-	44
$[Mg_2(H_2O)_7(TTF)_2(EtOH)] {\cdot}4H_2O$	$Mg(NO_3)_2.6H_2O$ / NaOH	EtOH/H_2O/dmf/25°C	$\mathbf{H_2}TTF$	123
$[Mg(H_2O)_5(3\text{-npth})].2H_2O$	$MgCO_3/MgCl_2.6H_2O/ NaHCO_3$	H_2O/100°C	3-npth$\mathbf{H_2}$	120
$[Mg(H_2O)(N\text{-MeIm})_2(\eta^1\text{-}4\text{-nba})(\mu_2\text{-}\eta^1{:}\eta^1\text{-}4\text{-nba})]_2$	$MgCO_3/MgCl_2.6H_2O/ NaHCO_3$	H_2O/N-MeIm/100°C	4-nba**H**	133
$[Mg(H_2O)_4].(C_4H_4O_4)_2$	$Mg(OH)_2.6H_2O$	MeOH/H_2O/25°C	$C_4H_5O_4$	92

$[Mg_2(H_2O)(Oac)_4(Im)_4]$	$Mg(Oac)_2.4H_2O$	Im/H_2O/25°C	-	137
$[Mg_2(H_2O)(Oac)_4(Bzim)_4]$	$Mg(Oac)_2.4H_2O$	Bzim/H_2O/25°C	-	137
$[Mg(H_2O)_4(d,l\text{-}aspH)_2]$	$Mg(OH)_2.6H_2O$	H_2O/100°C/12 hrs	d,l-asp$\mathbf{H}_2$	138
$[Mg_2(H_2O)_4(BTEC)]\cdot 2H_2O$	$Mg(NO_3)_2.6H_2O$/ BPP	H_2O/180°C/0.5 hrs /Microwave-solvo.	$\mathbf{H}_4$BTEC	131
$[Mg_2(H_2O)_6(BTEC)]$	$Mg(NO_3)_2.6H_2O$/ BPP	H_2O/150°C/0.5 hrs/ Microwave-solvo.	$\mathbf{H}_4$BTEC	131
$[Mg_2(H_2O)_8(BTEC)]$	$Mg(NO_3)_2.6H_2O$/ BPP	H_2O/150°C/0.5 hrs/ microwave-solvo.	$\mathbf{H}_4$BTEC	131
$[Mg(H_2O)_4(C_{11}H_7O_3)_2]$	$MgCl_2.6H_2O$ / NaOH	H_2O/160°C/ 3 days / solvothermal	$C_{11}H_7O_3\mathbf{H}_2$	140
$[Mg(H_2O)_2(C_8H_9N_2O_4)].3.5H_2O$	$Mg(OAc)_2$	H_2O/160°C/ 2 days / solvothermal	$C_8H_9N_2O_4H_2$	141
$[Mg(H_2O)_2(C_6H_5N_2O_4)]$	$Mg(NO_3)_2.6H_2O$	Solvothermal	$C_6H_7N_2O_4$	142
$[Mg(H_2O)_4(C_{12}H_8N_2)].(C_8H_5Cl_2O_2)_2$	$MgCl_2.6H_2O$ / NaOH	H_2O / 25°C / 1,10-phen	$C_8H_5Cl_2O_2\mathbf{H}$	143
$[Mg(H_2O)_4(dmf)_2].ndc$	$Mg(NO_3)_2.6H_2O$	dmf/H_2O/110°C/ solvothermal	2,6- $\mathbf{H}_2$ndc	144
$[Mg_3(dmf)_4(ndc)_3]_n$	$Mg(NO_3)_2.6H_2O$	dmf /110°C/solvothermal	2,6-$\mathbf{H}_2$ndc	144
$[Mg_3(dif)_4(ndc)_3]_n$	$Mg(NO_3)_2.6H_2O$	dif/110°C/solvothermal	2,6-$\mathbf{H}_2$ndc	145
$[Mg_3(dmf)_2(ndc)_3(CH_3OH)(H_2O)](dmf)$	$Mg(NO_3)_2.6H_2O$	dmf/MeOH/110°C/solvothermal	2,6- $\mathbf{H}_2$ndc	145
$[Mg_3(def)_4(ndc)_3]_n$	$Mg(NO_3)_2.6H_2O$	def/110°C/solvothermal	2,6-$\mathbf{H}_2$ndc	146
$[Mg_3(H_2O)_4(BPT)_2]_n$	$Mg(NO_3)_2.6H_2O$	dmf/H_2O/120°C/48 hrs/solvothermal	$\mathbf{H}_3$BPT	147
$[Mg(H_2O)_6](optp)_2$	$Mg(Oac)_2$	H_2O/100°C	optp$\mathbf{H}$	148
$[[Mg_3(dmf)_3(3,5\text{-}PDC)_3]\cdot dmf]_n$	$Mg(NO_3)_2.6H_2O$	dmf/100°C/5days/solvothermal	$\mathbf{H}_2$PDC	149
$[Mg(H_2O)_2(3,5\text{-}PDC)]_n$	$Mg(NO_3)_2.6H_2O$	EtOH/100°C/5days/solvothermal	$\mathbf{H}_2$PDC	149
$[[Mg(H_2O)(3,5\text{-}PDC)].2H_2O]_n$	$Mg(NO_3)_2.6H_2O$	dmf/etOH/100°C/5days/ solvothermal	$\mathbf{H}_2$PDC	149
$[[Mg_4(H_2O)_2(dmf)_2(3,5\text{-}PDC)_4].2dmf.4.5H_2O]_n$	$Mg(NO_3)_2.6H_2O$	dmf/etOH/100°C/5days/ solvothermal	$\mathbf{H}_2$PDC	149
$[Mg_3(ptc)_2.8H_2O)]_n$	$Mg(NO_3)_2$	H_2O/140°C/72hrs/solvothermal	$\mathbf{H}_3$ptc	76
$[[Mg(ptc).0.5[Mg(H_2O)_6].H_2O]]_n$	$Mg(NO_3)_2$	H_2O/140°C/72hrs/solvothermal	$\mathbf{H}_3$ptc	76
$[Mg_{12}(btc)_8(H_2O)_{18}(dioxane)_6]_n$	$Mg(NO_3)_2$	dioxane/110/72 hrs	$\mathbf{H}_3$btc	174
$[Mg(\mathbf{H}_{1.5}btc)_{2/3}(btc)_{1/3}(DMA)_2(DMA)_{1/3}]_n$	$Mg(NO_3)_2$	DMA/90°c/hydrothermal	$\mathbf{H}_3$btc	173
$[Mg(1,3\text{-}bdc)(EtOH)]_n$	$Mg(NO_3)_2$	EtOH/100°C/120hrs/solvothermal	1,3-bdc$\mathbf{H}_2$	27
$[Mg_4(1,3\text{-}bdc)_3(HCOO)_2(dmf)_2]_n$	$Mg(NO_3)_2$	dmf/180°C/120hrs/solvothermal	1,3-bdc$\mathbf{H}_2$	27
Calcium carboxylates				
$[Ca(pyr)_2(4\text{-}nba)_2]_n$	$CaCO_3/CaCl_2.2H_2O$	H_2O /100°C/pyr	4-nba$\mathbf{H}$	120
$[Ca(H_2dhtp)]$	$Ca(NO_3)_2.4H_2O/NaHCO_3$	H_2O/120°C/24hrs/solvothermal	H_4dhtp	110
$[Ca(C_5H_3N_2O_2)_2]_n$	$CaCl_2.2H_2O$/NaOH	H_2O/reflux/3hrs	2-CNpy	113
$[Ca(l\text{-}tartarate)]_n$	$Ca(Oac)_2$	H_2O/125°C/solvothermal	L-tartaric-$\mathbf{H}$	118
$[Ca(m\text{-}tartarate)]_n$	$Ca(Oac)_2$	H_2O/125°C/solvothermal	m-tartaric-$\mathbf{H}$	118
$[Ca(dmf)_2(TTF)]_n$	$Ca(NO_3)_2.4H_2O$/	dmf/H_2O/ solvothermal	$\mathbf{H}_2$TTF	123

	$NaHCO_3$			
$[Ca_2(OH)_2(ndc)]_n$	$Ca(OH)_2$	H_2O/HNO_3/ 180°C/ solvothermal	2,6-ndc-$\mathbf{H}_2$	53
$[Ca(NH_2.NH.CO_2)_2]_n$	$Ca(OH)_2$	H_2O/25°C	NH_2-$NHCO_2\mathbf{H}$	37
$[Ca(C_3H_3O_4)_2]_n$	$Ca(OH)_2$	H_2O/157°C/72hrs/solvothermal	Malonic-**H**	56
[Ca(N-MeIm)(4-nba)$_2$]$_n$	$CaCO_3/CaCl_2.2H_2O/NaHCO_3$	H_2O/100°C/N-MeIm	4-nba**H**	24
[Ca(μ-dmf)(μ-DADC)]$_n$	$Ca(NO_3)_2.4H_2O$	Dmf/150°C/5days/solvothermal	H_2DADC	73
$[Ca(Sa)_2(Phen)]_n$	$[Ca(Sa)_2(H_2O)_2]$	Recryst./H_2O/MeOH/ 25°C	-	49
$[Ca(C_5H_3O_3)_2]_n$	CaO	H_2O/100°C	Furoic-**H**	64
$[Ca(C_{10}H_9O_4)_2]_n$	$CaBr_2$/KOH	H_2O/25°C	Benz-malonic-**H**	93
[Ca(μ-dmf)(μ-NDC)]$_n$	$Ca(NO_3)_2.4H_2O$	Dmf/140°C/5days/solvothermal	$\mathbf{H}_2$NDC	73
[Ca(μ-def)(μ-TPDC)]$_n$	$Ca(NO_3)_2.4H_2O$	Dmf/125°C/5days/solvothermal	$\mathbf{H}_2$TPDC	73
[Ca$_{1.5}$(def)(μ-BDC)$_{1.5}$]$_n$	$Ca(NO_3)_2.4H_2O$	def/125°C/4days/solvothermal	$\mathbf{H}_2$BDC	73
[α-Ca(HCOO)$_2$]$_n$	$CaCO_3$	H_2O/25°C	HCOO**H**	80
$[Ca_3(C_{57}H_{102}N_9O_{18})_6]_n.3CH_3CN$	$CaCl_2.2H_2O$	H_2O/25°C	$C_{57}H_{102}N_9O_{18}\mathbf{H}_2$	94
$[Ca(C_8H_4O_4)]_n.H_2O$	$CaCO_3$	H_2O / 100°C	$C_8H_4O_4H_2$	83
$[[Ca(NH_2\text{-}NHCO_2)_2].H_2O]_n$	$Ca(OH)_2$	H_2O/25°C	NH_2-$NHCO_2\mathbf{H}$	37
$(C_3H_7N_6)_4[Ca(C_7H_3NO_4)_3].6H_2O$	$Ca(NO_3)_2.4H_2O$	H_2O/25°C	2,6-pydc$\mathbf{H}_2$	115
[Ca(H$_2$O)(dnSa)]$_n$	$CaCl_2.2H_2O$/NaOH	H_2O/25°C	dnSa-**H**	38
$[Ca(H_2O)(C_{10}H_8O_6)]_n$	$CaCl_2.2H_2O/Et_3N$	H_2O / dmf /25°C	$C_{10}H_8O_6\mathbf{H}_2$	59
[Ca(H$_2$O)(Hpdc)]$_n$	$CaCl_2$ /$Ca(OH)_2$ / Et_3N/ pH = 9	H_2O/150°C/72hrs/solvothermal	$\mathbf{H}_3$pdc	48
[[Ca(H$_2$O)(ptaH)].6H$_2$O]$_n$	$Ca(NO_3)_2.4H_2O$/pyridin	H_2O/25°C	pta$\mathbf{H}_3$	75
[Ca(H$_2$O)(val)$_2$]$_n$	$Ca(OH)_2$	H_2O/100°C	Val-**H**	22
$[Ca_2(H_2O)(A_3Br).4H_2O]_n$	$CaCO_3$	H_2O/25°C	$A_3Br\mathbf{H}_2$	60
[Ca(H$_2$O)(gly)$_2$]$_n$	$Ca(OH)_2$	H_2O/100°C	Gly-**H**	22
$[Ca(H_2O)((O_2C)_2C_6H_3CO_2H)]_n$	$Ca(OH)_2$	H_2O/180°C/24hrs/solvothermal	1,2,4-$\mathbf{H}_3$btc	23
[Ca(H$_2$O)(tda)]$_n$	$CaCl_2$	H_2O/25°C	tda$\mathbf{H}_2$	58
[[Ca$_2$(H$_2$O)$_2$(TTF)$_2$(EtOH)].MeOH]$_n$	$Ca(NO_3)_2.4H_2O/NaHCO_3$	EtOH/H_2O/solvothermal	$\mathbf{H}_2$TTF	123
$[Ca(H_2O)(C_3H_2O_4)]_n.H_2O$	$CaCO_3$	H_2O/25°C	malonic**H**	87
[Ca(H$_2$O)(Oac)$_2$]$_n$	Reccryst. from Calcium acetate	10% EtOH / H_2O	-	102
[Ca(H$_2$O)(bpdc)]$_n$	$Ca(NO_3)_2.4H_2O$/KOH	H_2O/180°C/24hrs/solvothermal	$\mathbf{H}_2$bpdc	53
[Ca(H$_2$O)(DMF)(benz)$_2$]$_n$	$CaCl_2.2H_2O$/KOH	Dmf/H_2O/25°C	benz**H**	40
$[Ca(H_2O)(C_4H_5O_2)_2]_n$	$CaCO_3$	H_2O/25°C	$C_4H_5O_2\mathbf{H}$	90
[Ca(H$_2$O)(4-nba)$_2$(2-MeIm)]$_n$	$CaCO_3/CaCl_2.2H_2O/NaHCO_3$	H_2O/100°C/2-MeIm	4-nba**H**	26
[Ca(H$_2$O)$_{1.5}$(DPA)]$_2$	$Ca(NO_3)_2.4H_2O$/ $NaHCO_3$	H_2O/100°C	DPA$\mathbf{H}_2$	105
[[Ca(H$_2$O)$_2$(3-npth)].H$_2$O]$_n$	$CaCO_3/CaCl_2.2H_2O$/Na	H_2O/100°C	3-npth$\mathbf{H}_2$	120

	HCO$_3$			
[Ca(H$_2$O)$_2$(C$_3$H$_2$O$_4$)]$_n$	CaCl$_2$.2H$_2$O	Silica/diffusion	malonic**H**	79
[Ca(H$_2$O)$_2$HN(CH$_2$COO)$_3$]$_n$	CaCO$_3$	H$_2$O/25°C	**H**$_3$N(CH$_2$COO)$_3$	85
[Ca(H$_2$O)$_2$(2-ca-4nba)$_2$]$_n$	CaCO$_3$/CaCl$_2$.2H$_2$O/NaHCO$_3$	H$_2$O/100°C	2-ca-4nba**H**	117
[Ca(H$_2$O)$_2$(C$_3$H$_2$O$_4$)]$_n$.2H$_2$O	CaO	H$_2$O/25°C	malonic**H**$_2$	96
[Ca(H$_2$O)$_2$(todd)]	Ca(OH)$_2$	H$_2$O/25°C	**H**$_2$todd	101
[Ca(H$_2$O)$_2$(C$_8$H$_5$O$_3$)$_2$]$_n$	CaCO$_3$	H$_2$O/25°C	C$_8$H$_5$O$_3$**H**	45
[Ca(H$_2$O)$_2$(C$_4$H$_4$O$_5$)$_2$]$_n$	CaCl$_2$.2H$_2$O	Silica/diffusion	malic**H**	68
[Ca(H$_2$O)$_2$(C$_7$H$_3$O$_2$F$_2$)$_2$]$_n$	CaCO$_3$	H$_2$O/100°C	C$_7$H$_3$O$_2$F$_2$**H**	106
[Ca(H$_2$O)$_2$(DTBB)(C$_2$H$_5$OH)$_{0.5}$]$_n$	CaCl$_2$.2H$_2$O/NH$_4$OH	H$_2$O/EtOH /25°C	**H**$_2$DTBB	129
[Ca$_2$(H$_2$O)$_2$(Oac)$_3$(NO$_3$)]$_n$	Ca(Oac)$_2$/Ca(NO$_3$)$_2$.4H$_2$O	H$_2$O/25°C	-	41
[Ca(H$_2$O)$_2$(4-aba)$_2$]$_n$	CaCl$_2$.2H$_2$O/NH$_4$OH	H$_2$O/25°C	4-aba**H**	39
[Ca(H$_2$O)$_2$(L-Asp)]$_n$	CaCO$_3$	H$_2$O/25°C	L-Asp**H**	109
[Ca(H$_2$O)$_2$(3-aba)$_2$]$_n$	CaCl$_2$.2H$_2$O/NH$_4$OH	H$_2$O/80°C	3-aba**H**	42
[Ca(H$_2$O)$_2$(4-CNbenz)$_2$]$_n$	Ca(ClO$_4$)$_2$.6H$_2$O	H$_2$O/ButOH/120°C/10hrs/solvothermal	4-Cnbenz**H**	20
[Ca(H$_2$O)$_2$(2-OPA)$_2$]$_n$	Ca(NO$_3$)$_2$.4H$_2$O/NaOH	H$_2$O/25°C	2-OPA**H**	46
[Ca$_2$(H$_2$O)$_2$(C$_{14}$H$_4$O$_8$)]$_n$	CaCO$_3$/Ca(OH)$_2$	H$_2$O/150°C/24hrs/solvothermal	Ntc-dianhydride	57
[Ca(H$_2$O)$_2$(HBTC)]$_n$	Ca(Oac)$_2$	H$_2$O/180°C/10hrs/solvothermal	**H**$_3$BTC	70
[Ca(H$_2$O)$_2$(C$_7$H$_2$O$_6$)$_2$].N$_2$H$_6$	CaSO$_4$	H$_2$O/25°C	C$_7$H$_2$O$_6$**H**	65
[Ca$_{1.5}$(H$_2$O)$_2$(ptc)]$_n$	Ca(NO$_3$)$_2$.4H$_2$O	H$_2$O/180°C/96hrs/solvothermal	ptc**H**$_3$	76
[Ca(H$_2$O)$_2$(CMA)$_2$]	Ca(NO$_3$)$_2$.4H$_2$O/NaOH	H$_2$O/25°C	CMA**H**	108
[Ca(H$_2$O)$_2$(2-nba)$_2$]$_n$	CaCO$_3$/CaCl$_2$.2H$_2$O/NaHCO$_3$	H$_2$O/100°C	2-nba**H**	25
[Ca(H$_2$O)$_2$(C$_4$H$_2$O$_4$)]$_n$	CaCO$_3$	H$_2$O/25°C	Fumaric**H**	89
[Ca(H$_2$O)$_2$(L$_1$)$_2$]	Ca(Oac)$_2$/KOH	H$_2$O/25°C	L$_1$**H**	67
[Ca(H$_2$O)$_2$(H$_2$dhtp)]	Ca(NO$_3$)$_2$.4H$_2$O/TBAOH	H$_2$O/120°C/24hrs/solvothermal	**H**$_4$dhtp	110
[Ca(H$_2$O)$_2$(C$_6$H$_3$ClNO$_2$)$_2$]$_n$	CaCl$_2$.2H$_2$O	MeOH/H$_2$O/reflux	2-Cl-nic**H**$_2$	112
[Ca(H$_2$O)$_2$(C$_8$H$_9$N$_2$O$_4$)$_2$]$_n$	CaCl$_2$	H$_2$O/160°C/72hrs/solvothermal	C$_8$H$_9$N$_2$O$_4$**H**	114
[Ca(H$_2$O)$_2$(C$_8$H$_9$NO$_6$)].H$_2$O	CaCO$_3$	H$_2$O/25°C	3-nphth**H**$_2$	116
[[Ca(H$_2$O)$_2$(L-OMe)$_2$].H$_2$O]$_n$	CaCO$_3$/CaCl$_2$.2H$_2$O/NaHCO$_3$	H$_2$O/100°C	L$_1$**H**	119
[[Ca(H$_2$O)$_2$(L-Cl)$_2$].2H$_2$O]$_n$	CaCO$_3$/CaCl$_2$.2H$_2$O/NaHCO$_3$	H$_2$O/100°C	L$_2$**H**	119
[Ca(H$_2$O)$_2$(4-nba)$_2$].(dmp)$_2$]$_n$	CaCO$_3$/CaCl$_2$.2H$_2$O/NaHCO$_3$	H$_2$O/dmp /100°C	4-nba**H**	121
[Ca(H$_2$O)$_2$(hip)$_2$].H$_2$O]$_n$	CaCl$_2$.2H$_2$O /NH$_4$OH	MeOH/H$_2$O/reflux	hip**H**$_2$	122
[[Ca(H$_2$O)$_2$(C$_8$H$_5$Cl$_2$O$_3$)$_2$].H$_2$O]$_n$	CaCl$_2$.2H$_2$O /KOH	H$_2$O/160°C/72hrs/solvothermal	C$_8$H$_5$Cl$_2$O$_3$ (Oac)	91
[Ca(H$_2$O)$_2$(C$_4$H$_4$O$_4$)].H$_2$O]$_n$	CaCO$_3$	H$_2$O/25°C	Succcinic**H**$_2$	55
[Ca(H$_2$O)$_2$(C$_5$H$_7$NO$_4$)]$_n$.H$_2$O	CaBr$_2$	H$_2$O/25°C	Glutamic**H**	81
[[Ca(H$_2$O)$_2$(PY-Thr)$_2$].2H$_2$O]$_n$	CaCl$_2$.2H$_2$O	H$_2$O/25°C	PY-Thr**H**	50

$[Ca(H_2O)_2(C_5H_8NO_4)_2]_n.2H_2O$	$[Ca(H_2O)_2(C_5H_7NO_4)]_n.H_2O$	Recrystallization	-	82
$[Ca_3(H_2O)_2(C_4H_4O_4)_3]_n.2H_2O$	$Ca(OH)_2$	H_2O/25°C	Methyl-malonic**H**	92
$[Ca(H_2O)_2(C_9H_8NO_4)_2].2.5H_2O]_n$	$CaCl_2.2H_2O$	$C_9H_8NO_4\mathbf{Na}$	-	51
$[[Ca(H_2O)_2(Nic)_2].3H_2O]_n$	$CaCl_2.6H_2O/NaHCO_3$	H_2O/25°C	Nic**H**	44
$[Ca(H_2O)_2(C_{84}H_{126}O_{16})(L_2)_2].L_2(H_2O)_4$	$Ca(Oac)_2$	Diffusion	$C_{84}H_{126}O_{16}\mathbf{H}$	72
$[[Ca(H_2O)_2(1,3\text{-}bdc)]_{2.5}.4H_2O]_n$	$Ca(OH)_2$	Hydrothermal	1,4-CN-benzene	21
$[[Ca_5(H_2O)_9(1,3\text{-}bdc)_5].8H_2O]_n$	$CaCO_3$	H_2O/100°C	1,3-bdc$\mathbf{H}_2$	35
$[Ca_2(H_2O)_5(C_{30}H_{32}O_{24}N_{12})].3H_2O]_n$	$CaCO_3$	H_2O/100°C	$\mathbf{H}_4$TTHA	62
$[[Ca(H_2O)_3(4\text{-}fba)](4\text{-}fba)]_n$	$CaCl_2.6H_2O/KOH$	H_2O/25°C	4-fba**H**	32
$[Ca(H_2O)_3(benz)_2]_n$	$CaCl_2.6H_2O/KOH$	H_2O/25°C	benz**H**	33
$[Ca(H_2O)_3(C_6H_6O_7)]_n$	$CaCl_2.6H_2O/NaOH$	-	Citric$\mathbf{H}_2$	103
$[Ca(H_2O)_3(C_8H_4O_4)]_n$	$Ca(Oac)_2$ / KOH	Diffusion / 24 hrs	1,4-bdc$\mathbf{H}_2$	104
$[Ca(H_2O)_3(DPA)]_2$	$CaCl_2.2H_2O/NaOH$	H_2O/100°C	DPA$\mathbf{H}_2$	105
$[Ca(H_2O)_3(CaEDTA)].4H_2O]_n$	$Ca(Oac)_2$ / TMAOH	H_2O/25°C	$\mathbf{H}_4$EDTA	98
$[Ca(H_2O)_3(C_9H_{11}N_6O_5)_2]_n$	$CaCl_2.6H_2O$	-	$C_9H_{11}N_6O_5K$	52
$[[Ca(H_2O)]_2(L)(\mu\text{-}H_2O)]_n$	$Ca(OH)_2$	H_2O/MeOH/25°C	**HL**	36
$[Ca(H_2O)_3(leu)_2]_n$	$Ca(OH)_2$	H_2O/100°C	Leu-**H**	22
$[Ca(H_2O)_3(5\text{-}OH\text{-}BDC)]_n.H_2O$	$CaCl_2.2H_2O/NaOH$	H_2O/25°C	5-OH-BDC-$\mathbf{H}_2$	61
$[Ca(H_2O)_3(2\text{-}aba)_2]_n$	$CaCl_2.2H_2O$ /NH_4OH	MeOH/ H_2O /reflux	2-aba**H**	47
$[Ca(H_2O)_3(bpdc)]_n$	$CaCl_2.2H_2O/KOH$	H_2O/180°C/24hrs/solvothermal	$\mathbf{H}_2$bpdc	53
$[Ca(H_2O)_3(edoda)]_2$	$CaCl_2.2H_2O/NaOH$	H_2O/25°C	$\mathbf{H}_2$edoda	84
$[[Ca(H_2O)_3(C_2H_5NO_2)_2].I_2]_n$	CaI_2	H_2O/25°C	glycine**H**	111
$[Ca(H_2O)_3(Im)(\eta^1\text{-}4\text{-}nba)_2]\cdot Im$	$CaCO_3/CaCl_2.2H_2O/NaHCO_3$	H_2O/Im /100°C	4-nba**H**	175
$[CaCl_2(Hgly)(H_2O)_3]_n$	$CaCl_2$	Diffusion	**H**gly	124
$[[Ca(H_2O)_4][Ca(L^1)(H_2O)_2]_2.7H_2O]_n$	$Ca(OH)_2$	H_2O/25°C	$\mathbf{H}_3L^1$	43
$[Ca(H_2O)_4(1,4\text{-}bdc)]_n$	$CaCO_3$	Solvothermal	1,4-bdc$\mathbf{H}_2$	34
$[Ca(H_2O)_4(\eta^1\text{-}4\text{-}nba)(\eta^2\text{-}4\text{-}nba)]$	$CaCO_3/CaCl_2.2H_2O/CaO$	H_2O/100°C	4-nba**H**	63
$[Ca_3(H_2O)_4(Sa)_6(4\text{-}bpy)_2]_n$	$CaCO_3$	4-bpy/ H_2O/100°C	Sa-**H**	49
$[Ca(H_2O)_4(Tartarate)]_n$	-	Isolated from rat kidney stone	-	77
$[Ca(H_2O)_4Br(C_{12}H_{21}O_{12})]$	$CaBr_2$	H_2O/25°C	Lactobionic**H**	95
$[Ca(H_2O)_4(L\text{-}Asp)]_n$	$CaCO_3$	H_2O/25°C	L-Asp-**H**	109
$[Ca(H_2O)_4(C_8H_6N_2O_6)]_n$	$CaCl_2$ / LiOH	H_2O/25°C	$C_8H_6N_2O_6H_2$	66
$[Ca(H_2O)_4(C_4H_4O_6)]_n$	$CaCl_2.2H_2O$	Gel diffusion	Tartaric-**H**	78
$[[Ca(H_2O)_4(Hpdc)].2H_2O]_n$	$CaCl_2$/ pH = 2.5	H_2O/150°C/72hrs/solvothermal	$\mathbf{H}_3$pdc	48
$[Ca_2(H_2O)_7(C_{12}H_2O_{12}).2H_2O]_n$	$CaCl_2.2H_2O$	H_2O/25°C	Mellitic$\mathbf{H}_2$	86
$[Ca_3(H_2O)_8(BTA)_2]_n.3H_2O$	$CaCO_3$	H_2O/25°C	$\mathbf{H}_3$BTA	71
$[Ca_3(H_2O)_{12}(BTC)_2]_n$	$Ca(Oac)_2/Et_3N$	H_2O/25°C	$\mathbf{H}_3$BTC	69

$[Ca(H_2O)_4(H_2L^1)][(H_2L^1)].4H_2O$	$Ca(OH)_2$	H_2O/100°C	$\mathbf{H}_3L^1$	43
$[[Ca(H_2O)_4(AIP)_2](H_2O)]_n$	$Ca(OH)_2$	H_2O/100°C	5-AIP**H**	19
$[[Ca(H_2O)_4(Hpdc)].H_2O]_n$	$CaCl_2$ /Et_3N pH = 5	H_2O/150°C/72hrs/solvothermal	$\mathbf{H}_3$pdc	48
$[Ca(H_2O)_5(C_9H_7O_4)_2]_n$	$CaCl_2.2H_2O$/KOH	H_2O/25°C	$C_9H_7O_4\mathbf{H}$	88
$[Ca(H_2O)_5(O(CH_2CO_2)_2)_2].H_2O$	$CaCl_2$/TMAOH	H_2O/25°C	$O(CH_2CO_2\mathbf{H})_2$	99
$[Ca(H_2O)_6$(PY-Valinato)$_2]_n$	$CaCl_2.2H_2O$	H_2O/25°C	PY-valin**H**	50
$[Ca_2(H_2O)_6(C_5H_3O_2N_2)_2]$	$Ca(Oac)_2$	H_2O/100°C	$C_5H_3O_2N_2\mathbf{H}$	54
$[Ca(H_2O)_6(C_{16}H_{12}O_4)]_n.H_2O$	$Ca(OH)_2$	H_2O/25°C	$C_{16}H_{12}O_4\mathbf{H}$	107
[Ca(dl-tartarate)$(H_2O)_4]_n$	$Ca(Oac)_2$	H_2O/ 200°C/ solvothermal	dl-tartaric$\mathbf{H}_2$	118
$[Ca(H_2O)(dmf)(BDC)]_n$	$Ca(NO_3)_2.4H_2O$	H_2O/dmf/150°C/48hrs/solvothermal	$\mathbf{H}_2$BDC	125
$[Ca(dmf)(ABDC)]_n$	$Ca(NO_3)_2.4H_2O$	H_2O/dmf/EtOH/90°C/48hrs/solvothermal	$\mathbf{H}_2$ABDC	125
$[[Ca_3(H_2O)_2(dmf)_2(BTC)_2].3H_2O]_n$	$Ca(NO_3)_2.4H_2O$	H_2O/dmf/90°C/48hrs/solvothermal	$\mathbf{H}_3$BTC	125
$[Ca(H_2dhtp)(dmf)]$	$Ca(NO_3)_2.4H_2O$	H_2O/dmf/EtOH/120°C/20 min/microwave-solvothermal	$\mathbf{H}_4$dhtp	125
$[Ca(H_2dhtp)(dmf)_2]$	$Ca(NO_3)_2.4H_2O$	H_2O/dmf/EtOH/90°C/48hrs/solvothermal	$\mathbf{H}_4$dhtp	125
$[Ca(H_2O)_2(H_2dhtp)_2]$	$Ca(NO_3)_2.4H_2O$	H_2O/dmf/EtOH/120°C/48hrs/solvothermal	$\mathbf{H}_4$dhtp	125
$[[Ca(PDC)(H_2O)_{1.5}]_n$	$Ca(OH)_2$	H_2O/dmf/HNO_3/180°C/72hrs/solvothermal	2,6-PDC$\mathbf{H}_2$	126
$[[Ca(PDC)(H_2O)_2]_n$	$Ca(OH)_2$	H_2O/dmf/HNO_3/180°C/72hrs/solvothermal	2,6-PDC$\mathbf{H}_2$	126
$[Ca(H_2O)_2(Sa)_2]_n$	$CaCl_2.2H_2O$ /NH_4OH	MeOH/H_2O/reflux	Sa-**H**	139
$[Ca(H_2O)_6$(PY-glycinato)$_2]_n$	$CaCl_2.2H_2O$	H_2O/25°C	TMA(Py-glycinate)	50
$[Ca(H_2O)_4(Hbtc)]_n$	$CaCl_2.2H_2O$ /Na_2CO_3	H_2O/25°C	$\mathbf{H}_3$btc	127
$[Ca(TbbA)(H_2O)_3].H_2O$	$Ca(NO_3)_2.4H_2O$ /K_2CO_3	H_2O/25°C	H_2TbbA	128
$[Ca(H_2O)_6$(4-nba)(2-ap)](4-nba)(2-ap)	$CaCO_3/CaCl_2.2H_2O$ or $[Ca(H_2O)_4$(4-nba)$_2]$	H_2O /100°C/2-ap	4-nba**H**	130
$[[(H_2O)_6Ca$(3,5-Hpdc)$Ca(H_2O)_3$(3,5-Hpdc)$_2$](3,5-Hpdc) .$2H_2O$]	CaO	H_2O /100°C	3,5-$\mathbf{H}_2$pdc	171
Strontium Compound				
$[Sr_2(H_2O)_7$(4-nba)].(4-nba).H_2O	$SrCO_3/SrCl_2.6H_2O/NaHCO_3$	H_2O/100°C	4-nba**H**	177
$[Sr(H_2O)_3$(4-nba)(dmf)].(4nba)	$SrCO_3/SrCl_2.6H_2O/NaHCO_3$	H_2O/dmf/100°C	4-nba**H**	This work
$[Sr(H_2O)$(4-nba)$_2(nmf)_{1.5}]$	$SrCO_3/SrCl_2.6H_2O/NaHCO_3$	H_2O/nmf/100°C	4-nba**H**	This work
[Sr(4-nba)$_2(pyr)_2]$	$SrCO_3/SrCl_2.6H_2O/NaHCO_3$	H_2O/pyr/100°C	4-nba**H**	This work
$[Sr(H_2O)_3$(4-nba)$_2(HCONH_2)]$	$SrCO_3/SrCl_2.6H_2O/NaHCO_3$	$H_2O/HCONH_2$/100°C	4-nba**H**	This work
$[Sr(H_2O)_4$(2-nba)$_2]$	$SrCO_3/SrCl_2.6H_2O/NaHCO_3$	H_2O/100°C	2-nba**H**	This work

$[Sr(2\text{-ca-4-nba})_2]$	$SrCO_3/SrCl_2.6H_2O/NaHCO_3$	H_2O/100°C	2-ca-4-nba**H**	This work
$[Sr(H_2O)(3\text{-npth})]_n$	$SrCO_3/SrCl_2.6H_2O/NaHCO_3$	H_2O/100°C	3-npth**H**	This work
$[Sr_2(H_2O)_4(2,3\text{-DHB})_2].3H_2O$	$SrCO_3$/ $Sr(Oac)_2$	H_2O/50°C/30min	2,3-DHB**H**	166
$[Sr(H_2O)_4(2,4\text{-DHB})_2].H_2O$	$SrCO_3$/ $Sr(Oac)_2$	H_2O/50°C/30min	2,4-DHB**H**	166
$[Sr(H_2O)_2(3,5\text{-DHB})_2].4H_2O$	$SrCO_3$	H_2O/50°C/30min	3,5-DHB**H**	166
$[Sr(H_2O)_2(2,6\text{-DHB})_2].0.5H_2O$	$SrCO_3$	H_2O/50°C/30min	2,6-DHB**H**	166
$[Sr(H_2O)_3(Oac)(2,4\text{-DHB})_2].0.5H_2O$	$SrCO_3$/ $Sr(Oac)_2$	H_2O/50°C/30min	2,4-DHB**H**/ Oac**H**	166
$[Sr(H_2O)_4(C_7H_7N_2O_4)_2]$	$SrCO_3$	H_2O/25°C	$C_7H_7N_2O_4\mathbf{H}_2$	167
$[Sr_3(H_2O)_4(BTC)_2]_n$	$Sr(Oac)_2.0.5H_2O$	H_2O/150°C/72hrs/solvothermal	$\mathbf{H}_3$BTC	168
$[Sr(dmf)(\mu\text{-BDC})]_n$	$Sr(NO_3)_2$	Dmf/130°C/5days/solvothermal	$\mathbf{H}_2$BDC	73
$[Sr(def)(H_2O)_2(\mu\text{-BDC})]_n$	$Sr(NO_3)_2$	def/130°C/5days/solvothermal	$\mathbf{H}_2$BDC	73
$[Sr(\mu\text{-dmf})(\mu\text{-NDC})]_n$	$Sr(NO_3)_2$	Dmf/140°C/5days/solvothermal	$\mathbf{H}_2$NDC	73
$[Sr(\mu\text{-def})(\mu\text{-TPDC})]_n$	$Sr(NO_3)_2$	def/125°C/5days/solvothermal	$\mathbf{H}_2$TPDC	73
$[Sr(\mu\text{-def})(\mu\text{-PDC})]_n$	$Sr(NO_3)_2$	def/130°C/5days/solvothermal	$\mathbf{H}_2$PDC	73
$[Sr(\mu\text{-dmf})(\mu\text{-DADC})]_n$	$Sr(NO_3)_2$	Dmf/150°C/5days/solvothermal	$\mathbf{H}_2$DADC	73
$[Sr(H_2O)_3(H_3pdc)(H_2pdc)_2]_2.2(H_3pdc). 4H_2O$	$Sr(ClO_4)_2$/ pH = 2.5	H_2O/150°C/72hrs/solvothermal	$\mathbf{H}_3$pdc	48
$[Sr(H_2O)(Hpdc)]$	$SrCl_2.6H_2O$ /Et_3N /pH = 9	H_2O/150°C/72hrs/solvothermal	$\mathbf{H}_3$pdc	48
$[Sr_2(Sa)_4(Phen)_4]_n$	$SrCl_2.6H_2O/NH_4OH$/Phen	H_2O/25°C	Sa**H**	49
$[[Sr_2(Sa)_2](4\text{-bpy})_{1.5}(H_2O)]_n$	$SrCO_3$/4-bpy	H_2O/MeOH/Reflux	Sa**H**	49
$[[Sr(H_2O)_6(PY\text{-Thr})_2]$	$SrCl_2.6H_2O$	H_2O/25°C	PY-Thr**H**	50
$[Sr(H_2O)_7(PY\text{-glycilglycinato})_2]$	$Sr(OH)_2$/TMACl	H_2O /25°C	Py-glycilgly**H**	50
$[Sr(tda)]_n$	$SrCl_2$	H_2O/25°C	tda$\mathbf{H}_2$	58
$[Sr(l\text{-tartarate})]_n$	$Sr(Oac)_2$	H_2O/125-200°C/ solvothermal	L-tartaric-**H**	118
$[Sr(m\text{-tartarate})]_n$	$Sr(Oac)_2$	H_2O/125-200°C/ solvothermal	m-tartaric-**H**	118
$[Sr(dl\text{-tartarate})]_n$	$Sr(Oac)_2$	H_2O/125-200°C / solvothermal	dl-tartaric$\mathbf{H}_2$	118
$[Sr(A_3Br)]_n$	$SrCO_3$	H_2O/25°C	$A_3Br\mathbf{H}_2$	60
$[Sr(H_2O)_2(Sa)_2]_n$	$SrCl_2.6H_2O$ /NH_4OH	MeOH/H_2O/reflux	Sa-**H**	139
$[Sr(H_2O) (H_2dhtp)]_n$	$Sr(Oac)_2$	H_2O/THF/120°C/24hrs/solvothermal	$\mathbf{H}_4$dhtp	110
$[[Sr(H_2O)_3(ptaH)].6H_2O]_n$	$Sr(NO_3)_2.4H_2O$/pyridin	H_2O/ THF/25°C	pta$\mathbf{H}_3$	75
$[Sr(H_2O)_2(hip)_2].H_2O]$	$SrCl_2.6H_2O$ /NH_4OH	MeOH/H_2O/reflux	hip$\mathbf{H}_2$	122
$[[Sr(2\text{-aba})_2(H_2O)_2].H_2O]_n$	$SrCl_2.2H_2O$ /NH_4OH	MeOH/H_2O/reflux	2-aba**H**	47
$[Sr(H_2O)_2(DTBB)(C_2H_5O$	$SrCl_2.2H_2O/NH_4OH$	H_2O/EtOH /25°C	$\mathbf{H}_2$DTBB	129

H)$_{0.5}$]$_n$				
$[Sr(H_2O)_6(5\text{-}NO_2\text{-}bdc)]_n$	$SrCl_2.2H_2O/NaOH$	H_2O /25°C	5-NO_2-bdc$\mathbf{H}_2$	159
$[Sr_{1.5}(ptc).5H_2O]_n$	$Sr(NO_3)_2$	H_2O/180°C/solvothermal	$\mathbf{H}_3$ptc	76
$[Sr(btc\mathbf{H})(H_2O)_2]_n$	$Sr(Oac)_2$	180	$\mathbf{H}_3$btc	172
$[Sr(H_2O)_4(C_8H_6N_2O_6)]_n$	$Sr(NO_3)2$ / LiOH	H_2O/25°C	$C_8H_6N_2O_6\mathbf{H}_2$	66
$[Sr(H_2O)(C_{10}H_8O_6)]_n$	$SrCl_2.2H_2O/Et_3N$	H_2O / dmf /25°C	$C_{10}H_8O_6\mathbf{H}_2$	59
Barium Compounds				
$[\{Ba_2(DTBB)_2(H_2O)_2\}0.5\ H_2O]_n$	$BaCl_2.2H_2O/NH_4OH$	H_2O/EtOH /25°C	$\mathbf{H}_2$DTBB	129
$[Ba(C_6H_4(COO)_2)]_n$	-	-	1,4-bdc$\mathbf{H}_2$	153
$[Ba(Hbpdc)_2(H_2O)_2]_n$	$Ba(OH)_2.8H_2O$	H_2O/100°C	$\mathbf{H}_2$bpdc	151
$[Ba_9(CH_3COO)_{14}(ClO_4)_4]_n$	$Ba(Oac)_2$ +$Ba(ClO_4)_2$	Recrystallised	-	152
$[Ba(2\text{-}aba)_2(H_2O)_2]_n$	$BaCl_2.2H_2O$ /NH_4OH	MeOH/ H_2O/reflux	2-aba$\mathbf{H}$	47
$[Ba(C_7H_5O_2S)_2(H_2O)_4]_n$	$BaCl_2.2H_2O/KOH$	-	$\mathbf{H}C_7H_5O_2S$	150
$[Ba(C_8H_5O_3)_2(H_2O)_2]_n$	$BaCO_3$	H_2O/ EtOH/reflux		154
$[[Ba(PY\text{-}met)_2(H_2O)_4].3H_2O]_n$	$BaCl_2.2H_2O/KOH$	H_2O/25°C	PY-met$\mathbf{H}$	50
$[[Ba(H_2O)_3(2\text{-}nba)_2]_2]_n$	$BaCO_3/BaCl_2.2H_2O/NaHCO_3$	H_2O/100°C	2-nba$\mathbf{H}$	165
$[Ba(C_5H_4O_4)_2(H_2O)_4]_n$	$BaCO_3$	H_2O/25°C	Mesoconic$\mathbf{H}$	155
$[Ba(1,3\text{-}BDOA)(H_2O)_2]_n$	$BaCl_2.2H_2O$/pyridine	H_2O/120°C/5days/solvothermal	1,3-BDOA$\mathbf{H}$	156
$[Ba(C_{10}H_{12}N_5O_6)_2(H_2O)_6]_n$	$BaCl_2.2H_2O$	H_2O/25°C	glutamic$\mathbf{H}$	157
$[Ba(mal)(malH_2)]$	$BaCO_3$	H_2O/25°C	mal$\mathbf{H}_2$	164
$[Ba(H_2PMA)(H_2O)_5]_n$	$BaBr_2.2H_2O$	Diffusion	$\mathbf{H}_4$PMA	135
$[Ba(H_2O)_5(4\text{-}nba)_2]_n$	$BaCO_3/BaCl_2.2H_2O/NaHCO_3$	H_2O/100°C	4-nba$\mathbf{H}$	169
$[[Ba(H_2IDC)_2(H_2O)_4].2H_2O]_n$	$BaCl_2.2H_2O$	H_2O/150°C/solvothermal	$\mathbf{H}_3$IDC	158
$[[Ba(PY\text{-}glycinato)_2(H_2O)_5].H_2O]_n$	$BaCl_2.2H_2O$	H_2O/25°C	TMA(PY-glycinate)	50
$[[Ba(PY\text{-}serinato)_2(H_2O)_4].3H_2O]_n$	$BaCl_2.2H_2O/KOH$	H_2O/25°C	PY-serin$\mathbf{H}$	50
$[[Ba(PY\text{-}glycilglycinato)_2(H_2O)_2]_n$	$Ba(OH)_2$	H_2O/25°C	PY-glcyl gly$\mathbf{H}$	50
$[Ba(\mu\text{-}dmf)(\mu\text{-}NDC)]_n$	$BaCl_2.2H_2O$	DMF/100°C/5days/solvothermal	$\mathbf{H}_2$NDC	73
$[Ba(H_2O)_4(H_2pdc)_2].2H_2O$	$BaCl_2$ / pH = 3	H_2O/150°C/72hrs/solvothermal	$\mathbf{H}_3$pdc	48
$[Ba(H_2O)(Hpdc)_2]$	$BaCl_2$ /Et_3N / pH = 9	H_2O/150°C/72hrs/solvothermal	$\mathbf{H}_3$pdc	48
$[Ba(Sa)_2(Phen)_2]_n$	$BaCl_2.2H_2O/NH_4OH$/Phen	H_2O/25°C	Sa$\mathbf{H}$	49
$[[Ba(Sa)_2(H_2O)_3](4\text{-}bpy)_{1.5}(H_2O)]_n$	$BaCO_3$/4-bpy	H_2O/MeOH/Reflux	Sa$\mathbf{H}$	49
$[Ba_3(H_2O)_8(BTA)_2]_n.3H_2O$	$BaCO_3$	H_2O/25°C	$\mathbf{H}_3$BTA	71
$[Ba(l\text{-}tartarate)]_n$	$Ba(Oac)_2$	H_2O/125-200°C/solvothermal	L-tartaric-$\mathbf{H}$	118
$[Ba(m\text{-}tartarate)]_n$	$Ba(Oac)_2$	H_2O/125-200°C/solvothermal	m-tartaric-$\mathbf{H}$	118
$[Ba(dl\text{-}tartarate)]_n$	$Ba(Oac)_2$	H_2O/Solvothermal/125-200°C	dl-tartaric$\mathbf{H}_2$	118
$[Ba(A_3Br)]_n$	BaO	H_2O/25°C	$A_3Br\mathbf{H}_2$	60
$[Ba(H_2O)_2(Sa)_2]_n$	$Ba(Oac)_2/NH_4OH$	MeOH/H_2O/reflux	Sa-$\mathbf{H}$	139
$[[Ba(H_2O)_3(ptaH)].6H_2O]_n$	$Ba(NO_3)_2.4H_2O$/pyridin	H_2O/ THF/25°C	pta$\mathbf{H}_3$	75

$[Ba(H_2O)_2(hip)_2]$	$BaCl_2.2H_2O$ /NH_4OH	MeOH/H_2O/reflux	hip$\mathbf{H}_2$	122
$[Ba_3(H_2O)_8(BTC)_2].2H_2O]_n$	$BaCO_3/BaCl_2.2H_2O/NaHCO_3$	H_2O/25°C	$\mathbf{H}_3$BTC	This work
$[Ba(H_2O)_6(5\text{-}NO_2\text{-}bdc)]_n$	$BaCl_2.2H_2O/NaOH$	H_2O /25°C	5-NO_2-bdc$\mathbf{H}_2$	159
$[Ba(C_8H_5NO_5)(H_2O)_5]_n$		H_2O/25°C	$C_8H_5NO_5\mathbf{H}_2$	160
$[Ba(C_7H_3NO_4)(H_2O)_3]_n$	$Ba(NO_3)_2.4H_2O$	H_2O/25°C	$C_7H_3NO_4\mathbf{H}_2$	161
$[[Ba(C_7H_2N_2O_7)(H_2O)_2].H_2O]_n$	$Ba(NO_3)_2.4H_2O$	H_2O/25°C	$C_7H_2N_2O_7\mathbf{H}_2$	162
$[Ba(C_7H_5O_7)_2(C_{12}H_8N_2)_2(H_2O)_2]_n$	$BaCl_2$/NaOH/1,10-phenanthroline	H_2O/EtOH/Reflux	**3-(OH)-**benz**H**	163
$[[Ba(ptc)(H_2O)][Ba(ptc\mathbf{H}_2)(H_2O)]]_n$	$Ba(NO_3)_2$	H2O/180°C / 96 h / solvothermal	ptc$\mathbf{H}_3$	76
$[Ba(btc\mathbf{H})(H_2O)_2]_n$	$Ba(OAc)_2$	180°c/solvothermal	btc$\mathbf{H}_3$	172
$[Ba(H_2O)_3(5\text{-}OH\text{-}BDC)]_n$	$BaCl_2.2H_2O/NaOH$	H_2O/25°C	5-OH-BDC-$\mathbf{H}_2$	61
$[Ba(H_2O)(C_{10}H_8O_6)]_n$	$BaCl_2.2H_2O/Et_3N$	H_2O / dmf /25°C	$C_{10}H_8O_6\mathbf{H}_2$	59

Abbreviations used: 4-nba**H** = 4-nitrobenzoic acid; 2-ca-4nba**H** = 2-carbamoyl-4-nitrobenzoic acid; 2-aba**H** = 2-aminobenzoic acid; 4-aba**H** = 4-aminobenzoic acid; $C_8H_6O_4$ = phthalic acid; $C_7H_5NO_5$ = 3-hydroxy-4-nitrobenzoic acid; $\mathbf{H}_4$PMA = benzene-1,2,4,5-tetracarboxylic acid; nic = nicotinic acid; $\mathbf{H}_2$TTF = tetrathiafulvenebicarboxylic acid; $C_4H_5O_4$ = methylmalonic acid; Oac = acetate; Im = imidazole; Bzim = benzimidazole; d,l-asp$\mathbf{H}_2$ = d,l-aspartic acid; BPP = 4,4′-trimethylenedipyridine; $\mathbf{H}_4$BTEC = 1,2,4,5-benzenetetracarboxylic acid; hip**H** = hippuric acid Sa**H** = salicylic acid; $C_{11}H_8O_3$ = 1-hydroxynaphthoic acid; $C_8H_{10}N_2O_4$ = 1-H-2-propyl-imidazole-4,5-dicarboxylic acid; $C_6H_7N_2O_4$ = 2-methyl-1H-imidazole-4,5-dicarboxylic acid; $C_8H_6Cl_2O_2$ = 2,4-dichlorophenylacetic acid; 2,6-$\mathbf{H}_2$ndc = 2,6-naphthalenedicarboxylic acid; dmf = dimethylformamide; dif = diisopropylformamide; def = diethylforamide; $\mathbf{H}_3$BPT = biphenyl-,3,4′,5-tricarboxylate; **H**optp = 1-oxopyridinium-2-thiopropionic acid; 3-npth$\mathbf{H}_2$ = 3-nitrophthalate; PDC = 3,5-pyridinedicarboxylate; DMA = dimethylacetamide; pyr = pyrazole; $\mathbf{H}_2$dhtp = 2,5-dihydroxyterephalic acid, $C_5H_3N_2O_2$ = 2-CNpy = 2-cyanopyrimidine; $NH_2.NH.(CO_2)_2$ = Hydrazine carboxylate; $C_3H_3O_4$ = Malonate; N-MeIm = 1-Methylimidazole; DADC = 5,10-dihydroanthracene-2,7-dicarboxylate; Phen = 1, 10-phenanthroline; $C_5H_3O_3$ = 2-Furancarboxylate; $C_{10}H_9O_4$ = Benzylmalonate; $\mathbf{H}_2$TPDC = 4,5,9,10-Tetrahydropyrene-2,7-dicarboxylic acid; 1,4-bdcH_2 =Benzene-1,4-dicarboxylic acid; HCOO = Formate; $C_{57}H_{102}N_9O_{18}$ = t-butyl-Glycyl-N-isobutylglycine-N-isobutylglycine; $C_7H_3NO_4$ = 2,6-pydc$\mathbf{H}_2$ = pyridine-2,6-dicarboxylic acid, $C_6H_3ClNO_2$ =2-Cl-nic$\mathbf{H}_2$ = 2-chloronicotinic acid, $C_8H_9N_2O_4\mathbf{H}$ = 4-carboxy-2-propyl-1H-imidazole-5-carboxylic acid; dnSa = 3,5-dinitrosalicylato; $C_{10}H_8O_6$ = benzene 1,4 dioxylacetate; $\mathbf{H}_2$pdc=3,5-Pyrazoledicarboxylate; ptaH = tris-{2-(4-carboxyphenoxy)ethyl}-amine; val = rac-valinate; A_3Br = 1, 3-biscarboxyethylimidazolium bromide; gly = glycinate; $(O_2C)_2C_6H_3CO_2H$ = 1,2,4-benzenetricarboxylate or trimellitate; tda$\mathbf{H}_2$ = $S(CH_2COOH)_2$; bpdc = 4,4′-biphenyldicarboxylate; benz = benzoate; $C_4H_5O_2$ = 3-butenoate; 2-MeIm = 2-methylimidazole; DPA = DPA$\mathbf{H}_2$ = dipicolinic acid; $N(CH_2COO)_3$ = nitrilotriacetate; $C_3H_2O_4$ = malate; todd = 3,6,9-trioxaundecanedioate; $C_8H_5O_3$ = 2-formylbenzoate; $C_4H_4O_5$ = Malate; $C_7H_3O_2F_2$ = 2,6-difluorobenzoate; DTBB = 2,2′-dithiobis(benzoate); NO_3 = nitrate; L-Asp = L-aspartate; 3-aba = 3-aminobenzoate; 4-CNbenz = 4-cyanobenzoate; 2-OPA = 2-oxo-1,2-dihydropyridine-1-acetate; $C_{14}H_4O_8$ = 1,4,5,8-naphthalenetetracarboxylate; BTC = 1,3,5-benzene tricarboxylate; $C_7H_2O_6$ = chelidonic acid; $\mathbf{H}_3$ptc = pyridine-2,4,6-tricarboxylic acid; CMA = 9,10-dihydro-9-oxo-10-acridineacetate; 2-nba = 2-nitrobenzoate; $C_4H_2O_4$ = Fumarate; L_1 = $C_{34}H_{46}N_4O_8$ = 2,6-bis(2,2-dimethylpropionylamino)benzoate; $C_8H_9NO_6$ = 3-nitrophthalate; L-Ome = P-methoxyphenylacetate; L-Cl = 2-Chloro-phenylacetate; dmp = 3,5-dimethylpyrazole; $C_8H_5Cl_2O_3$ = (2,4-dichlorophenoxy)acetate; $C_5H_7NO_4$ = L-Glutamate; PY = N-(6-amino-3,4-dihydro-3-methyl-5-nitroso-4-oxopyrimidin-2-yl); Thr = Threonate; $C_5H_8NO_4$ = L-Glutamate; $C_4H_4O_4$ = methylmalate; $C_9H_8NO_4$ = 2-(pyridinium-1-yl)butanedioate; Nic = 3-carboxypyridine; L_2 = DMSO; $C_{84}H_{126}O_{16}$ = 5,11,17,23-tetracarboxy-4,6,10,12,16,18,22,24-octa-O-methyl-2,8,14,20-tetra(n-undecyl)resorc[4]arene; 1,3-bdc = 1,3-benzenedicarboxylate; $C_{30}H_{32}O_{24}N_{12}$ =

1,3,5-Triazine-2,4,6-triaminehexaacetate; 4-fba = 4-fluorobenzoate; $C_6H_6O_7$ = citrate; EDTA = Ethylenediaminetetraacetate; $C_9H_{11}N_6O_5$ = Bis[N-(6-amino-3,4-dihydro-3-methyl-5-nitroso-4-oxopyrimidine-2-yl) glycylglycinate; L = 4-(2-nitrophenyl)-3,6-dioxaoctane dioate; leu = rac-leucinate; 5-OH-BDC = 5-hydroxyisophthalate; $C_2H_5NO_2$ = Glycine**H**, Hgly = H-glycinate, edoda = ethylenedioxydiacetate; L^1 = 2,2′,2″-Nitrilotribenzoate; 1,4-bdc = 1,4-benzene dicarboxylate; 4-bpy = 4-4' bipyridine; $C_4H_4O_6$ = Tartrate; $C_{12}H_{21}O_{12}$ = Lactobionic acid; $C_8H_6N_2O_6$ = 3,6-Dioxo-2,5-diazabicyclo[2.2.2.]octane-1,4-dicarboxylate; $C_{12}H_2O_{12}$ = Benzene hexacarboxylic acid; $\mathbf{H}_3$BTA = 1,3,5-benzenetriaceticacid; AIP = 5-Aminoisopthalate; $C_9H_7O_4$ = Homophthalate; $O(CH_2CO_2)_2$ = Oxydiacetate; $C_5H_3O_2N_2$ = Pyridazine-3-carboxylate; $C_{16}H_{12}O_4$ = meso-2,3-diphenylsuccinate; ABDC = 2-aminobenzene-1,4-dicarboxylate; $C_5H_3N(CO_2)_2$ = 2,6-pyridinedicarboxylate(PDC), H_2pdc = pyridine-3,5-dicarboxylic acid; nmf = N-methyl formamide; $HCONH_2$ = formamide; 2-ap = 2amino pyridine; 3,5-Hpdc = pyridine-3,5-dicarboxylic acid; 2,3-DHB**H** = 2,3-dihydroxybenzoic acid; 2,4-DHB**H** = 2,4-dihydroxybenzoic acid; 3,5-DHB**H** = 3,5-dihydroxybenzoic acid; 2,6-DHB**H** = 2,6-dihydroxybenzoic acid; $C_7H_7N_2O_4\mathbf{H}_2$ = 1,3-bis(carboxymethyl)imidazoldicarboxylic acid; 5-NO_2-bdc = 5-nitroisophthalate; $(C_6H_4(COO)_2)]$ = terephthalate; Hbpdc = 2′carboxybiphenyl-2-carboxylate; $(C_7H_5O_2S)$ = thiosalicylate; $(C_8H_5O_3)$ = 2-formylbenzoate; met = monoanion of methionine; $C_5H_4O_4$ = mesaconate anion; (1,3-BDOA) = m-phenylenedioxyacetate; $(C_{10}H_{12}N_5O_6)$ = N-4-amino-1,6-dihydro-1-methyl-5-nitroso-6-oxopyrimidin-2-yl)-(S)-glutamato; H_2IDC = 1H-imidazole-4,5-dicarboxylatomonoanion; $C_8H_5NO_5$ = 5-carboxylato-2-oxidopyridinium-1-acetato; $C_7H_3NO_4$ = Pyridine-3,5-dicarboxylate; $C_7H_2N_2O_7$ = dnSa = 3,5-dinitrosalicylato; $C_7H_5O_7$ = 3-hydroxybenzoate; $C_{12}H_8N_2$ = 1,10-phenanthroline.

1.2. Structural features of *s*-block metal carboxylates

The bonding interaction of *s*-block metal centers with carboxylate oxygen atom is mainly ionic in nature due to large differences in electronegativity, which provide little room for prediction and control over coordination geometry. The mutual orientation of the functional groups plays a bigger role in determining the coordination nature of the metal center within the network. In small molecular weight compounds, many of which are normally crystallized from aqueous media, the affinity of Mg(II) for water can be evidenced by the structural characterization of many compounds which contain the octahedral $[Mg(H_2O)_6]^{2+}$ ion [131-140] (Table 4). Unlike Mg^{+2} which adopts hexacoordination in most of its compounds, Ca(II) is more flexible. The structural flexibility of Ca(II) ion can be evidenced by the observation of coordination numbers ranging from six to eight in many compounds with eight coordination being mostly preferred [24, 25,26, 32-125].

In a pioneering study of the crystal structures of fifty four calcium-carboxylates, Einspahr and Bugg [192] reported that the Ca ion in all calcium-carboxylates lies near the plane of the carboxylate group and usually binds to several carboxylate groups. The most commonly observed number of carboxylates bound to each Ca was three and the carboxylate groups so bound may be crystallographically independent or symmetry related. It was also noted that the carboxylate groups coordinate to more than one Ca ion the most common number being two Ca ions. Based on the metal ion binding by amino acids Schmidbaur *et al* [193] has shown that for the coordinatively non-discriminative large alkaline earth metals strontium and barium a very high coordination number nine is preferred.

1.3. Spectroscopic and thermal studies of *s*-block metal carboxylates:

The carboxylate anions do not exhibit any carbonyl absorption at about 1700 cm^{-1} but show absorption bands with assymetric stretching at υ_{as}(-COO) at 1650-1510 (s) cm^{-1} and a symmetric stretching vibration at around υ_{ss}(-COO) = 1440-1280 (m) cm^{-1} [194]. Chelation and symmetric bridging, shifts both υ(-COO) frequencies in the same direction. Such seperations are significantly less than the ionic values and are considered as indicative of chelating and bridging carboxylate group [194]. Since most of the alkaline earth metal carboxylates are prepared under aqueous condition and contain coordinated or lattice water the υ_{-OH} absorption is observed as a broad and strong signal at around 3600 cm^{-1}. The presence of large number of absorptions in the mid-IR region is characteristic of presence of organic moiety. The presence of other functional groups on the ligand shows characteristic peak in defined IR range [194, 195]. Based on IR data alone, the structure especially the carboxylate binding mode cannot be predicted.

In conjugation with the other spectroscopic techniques like NMR, electronic absorption techniques have been used considerably to understand the exact nature of the interactions of carboxylate ion with metal ions in solution and solid state. Morgant and co-workers [132] have shown how absorption bands centred at around 211, 276 and 353 nm of 3-hydroxybenzoic acid varies in solution with change in pH with isobastic point at 199, 235 and 318 nm. Alkaline earth metals do not show any absorption in the UV-vis region of the spectrum because of a closed shell electronic configuration. In view of this the observed strong bands in UV-vis spectrum are due to the intraligand charge transfer transition of aromatic carboxylates both in solution and solid state. The luminescent studies of alkaline earth carboxylates are of considerable importance since the divalent cations Mg and Ca are the most abundant in living cells and play important roles in cellular processes [19].

Thermogravimetry is one of the most important technique, used to determine the presence of water / solvent or organic matrices present in the crystal lattice as well as to predict the thermal stability of the compounds under study in combination with DSC or DTA. The intermediate and the final decomposition pattern along with residue formation may sometimes help to predict the final decomposition product of metal carboxylates of alkaline earth metals. Magnesium and calcium carboxylates forms the corresponding oxide above 600°C while the carboxylates of Sr and Ba form the metal carbonates as residue.

1.4. Applications of *s*-block metal carboxylates:

Interesting physical and chemical properties of MOFs make them promising candidates in applications of porous materials, drug storage and delivery, sensors and luminescent materials, Non linear optical properties, conductivity, magnestism; however these areas have not been explored as broadly as gas storage and gas separation application in the literature. In a recent review, Janiak [2] has reviewed several different applications of MOFs (Figure 1).

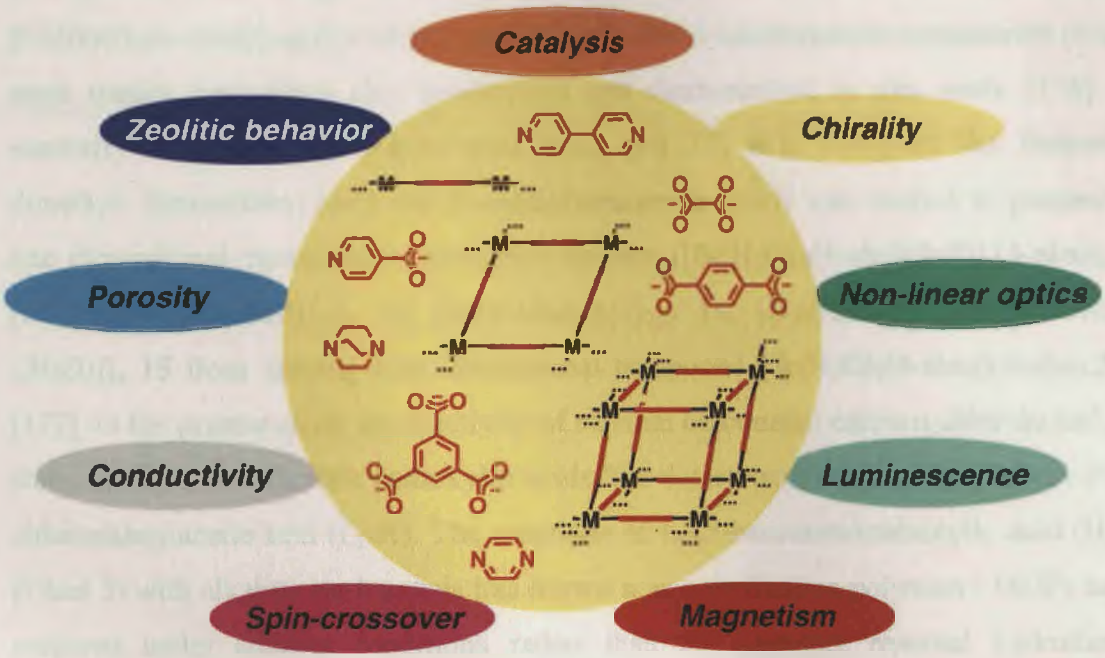

Figure 1- Schematic presentation of application-oriented properties of MOFs(1D-3D structures) with prototypical linkers in clockwise order: 4,4′-bipyridine, oxalate, benzene-1,4-dicarboxylate(terethalate), pyrazine, benzene-1,3,5-tricarboxylate (trimesate), 1,4-diaza-bicyclo[2.2.2]octane, isonicotinate.

1.5. Scope of present work

In this research the reaction of *s*-block metal especially alkaline earths have been investigated with aromatic carboxylic acids in the presence of N- or O- donor (Chart 3) and the results of this work are described in this thesis entitled, "Chemistry of *s*-block metal coordination polymers: Synthesis, reactivity characteristics, spectroscopic and structural investigations". In the present study we have investigated the reaction of alkali and alkaline earth metal carbonates or chlorides with aromatic nitrocarboxylic acids like 2-nitrobenzoic acid (2-nbaH) [25,165,120], 4-nitrobenzoic acid (4-nbaH), 2-carbamoyl-4-nitrobenzoic acid (2-ca-4nbaH) [117,170], 3-nitrophthalic acid (3-nphtH) [120] in aqueous media (Chart 3). The reaction of $[Ca(H_2O)_4(4\text{-nba})_2]$ **1** [63] with N-donor ligands, show how a zero dimensional compound, can be transformed into mixed ligand Ca(II) coordination polymers containing less or no water as evidenced by the characterization of $[Ca(N\text{-MeIm})(4\text{-nba})_2]_n$ **2** [24], $[Ca(Im)(4\text{-nba})_2]$ **3** [24], $[Ca(H_2O)(2\text{-MeIm})(4\text{-nba})_2]_n$ **4** [26], $[Ca(pyr)_2(4\text{-nba})_2]_n$ **5** [120], $[Ca(H_2O)_2(4\text{-nba})_2](dmp)_2]_n$ **6** [121] (Im = imidazole; N-MeIm = N-methylimidazole; 2-MeIm = 2-methylimidazole; pyr = pyrazole, dmp = 3,5-dimethylpyrazole) compounds (Chart 3). The reaction of compound **1** with 2-ap (2-aminopyridine) resulted in the formation of a water rich compound $[Ca(H_2O)_6(4\text{-nba})(2\text{-ap})](4\text{-nba})(2\text{-ap})]$ **7** [130]. The 4-nitrobenzoate compounds of alkali earth metals have been also synthesized and characterized in this study [176]. The reactivity of $[Sr(H_2O)_7(4\text{-nba})](4\text{-nba}).2H_2O$ **11** [177] with O-donors like formamide, dimethyl- formamide (dmf) and N-methylformamide (nmf) was studied to prepare few one dimensional coordination polymers namely $[[Sr(H_2O)_3(4\text{-nba})(dmf)].(4\text{-nba})]_n$ **12**, $[Sr(H_2O)(4\text{-nba})_2(nmf)_{1.5}]_n$ **13**, $[Sr(4\text{-nba})_2(pyr)_2]_n$ **14**, $[[Sr(H_2O)_2(4\text{-nba})_2(HCONH_2)]\text{-}.(H_2O)]]_n$ **15** from starting zero dimensional compound $[Sr(H_2O)_7(4\text{-nba})](4\text{-nba}).2H_2O$ [177]. In the present study the reactivity of calcium carbonate / calcium chloride has been studied with a few flexible carboxylic acids like 4-methoxyphenylacetic acid (L_1-H), 2-chlorophenylacetic acid (L_2-H). The reactions of 1,3,5-benzenetricarboxylic acid (H_3btc) (Chart 3) with alkaline earth metals has shown how coordination polymers / MOFs can be prepared under ambient conditions rather than the literature reported hydrothermal methods.

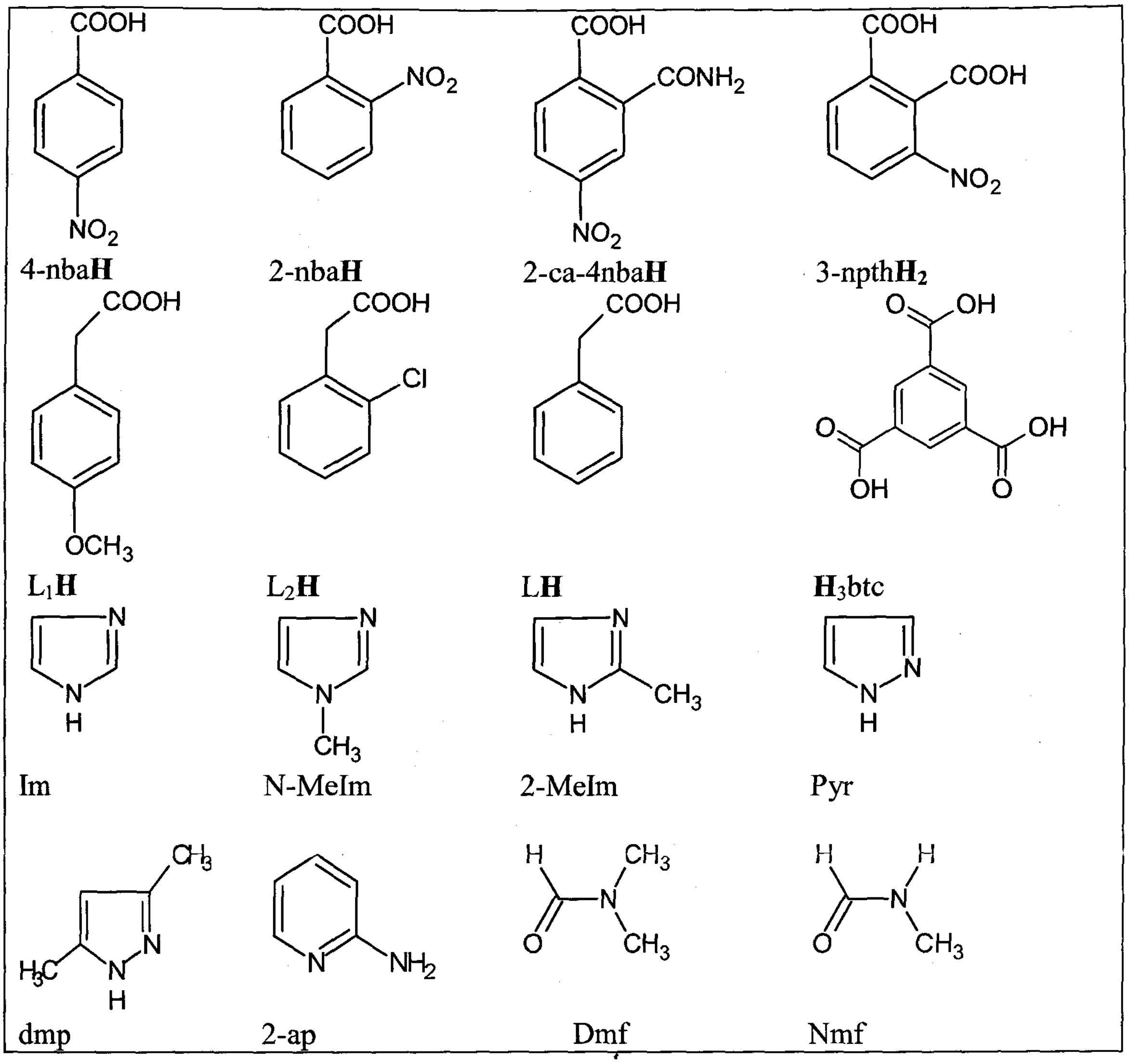

4-nba**H** 2-nba**H** 2-ca-4nba**H** 3-npth$\mathbf{H}_2$

L_1**H** L_2**H** L**H** $\mathbf{H}_3$btc

Im N-MeIm 2-MeIm Pyr

dmp 2-ap Dmf Nmf

Chart 3 - Nomenclature of carboxylic acids and N-donor and O-donor ligands relevant to this study

Chapter 2

EXPERIMENTAL DETAILS

GENERAL CONSIDERATIONS:

All the chemicals used in this study were of reagent grade and were used as received. The starting materials and reaction products are air stable and hence were prepared under normal laboratory conditions without any special precautions. Distilled water was used as a solvent in almost all the reactions. Infrared (IR) spectra were recorded on a Shimadzu (IR prestige -21) FT-IR spectrometer in the range 4000-400 cm^{-1}. Samples for IR spectra were diluted with solid KBr and the signals referenced to polystyrene bands. UV-visible diffuse-reflectance spectra were obtained using a Shimadzu UV-2450 double beam spectrophotometer. $BaSO_4$ powder was used as reference (100% reflectance). Absorption data were calculated from the reflectance data using the Kubelka–Munk function ($a / S = (1-R)^2 / 2R$ where a is the absorption coefficient, R the reflectance and S the scattering coefficient). The electronic spectra were recorded in methanol or water using matched quartz cells on Shimadzu UV-2450 double beam spectrophotometer. TG-DSC measurements were done in Al_2O_3 crucibles on a STA-409PC simultaneous thermal analyzer from Netzsch in flowing air. A heating rate of 10 K min^{-1} was employed for all measurements. Metal analyses were performed titrimetrically following standard procedures [205]. The pH of the solution were determined using short range pH paper as well as electronic pH meter (Model PHAN, lab India). ^{1}H NMR spectra of the synthesized samples were recorded (in DMSO-d_6 or D_2O as solvent) on a Bruker 400 MHz instrument. Thermal decomposition studies were performed in an electric furnace equipped with a temperature controller. BET surface areas were measured using micromeritics surface area and porosimetry analyzer (Tristar 3000, Norcross, GA) and N_2 gas as adsorbate. X-ray powder pattern were recorded on a Rigaku Miniflex II powder diffractometer using Cu-K_α radiation with Ni-filter. Luminescence spectra of the solid samples were recorded at RT using a Perkin Elmer LS 55 Luminescence spectrophotometer. CHN analyses of synthesized compounds were done using Elementar vario micro cube CHN analyser in department of chemistry, Goa University.

Modified method for the rapid synthesis of [Ca(H_2O)$_4$(4-nba)$_2$] 1

A modified method involving less reaction time is described for the rapid and bulk synthesis of the earlier reported [Ca(H_2O)$_4$(4-nba)$_2$] [63].

Method 1

The 4-nbaH (3.34 g, 20 mmol) was taken in water (20 mL) and the slurry was warmed on a water bath to expel dissolved CO_2. A freshly prepared sample of CaO obtained by heating commercial $CaCO_3$ (1 g, 10 mmol) in a muffle furnace at 800°C for ~30 min, was added to the above slurry. The reaction mixture was stirred well for ~10 min, resulting in the immediate formation of a microcrystalline product. The reaction mixture was cooled to room temperature, filtered and the product was washed well with water, followed by ether and dried. The infrared spectrum and thermal properties of the product were identical to that of the reported compound. (Yield 3.9 g, 87.6%) [63].

Method 2

Calcium carbonate (1.0 g, 10 mmol) and 4-nbaH (3.34 g, 20 mmol) was taken in water (20 ml). The slurry was poured in a Teflon vial and sealed from top. The vial was then placed in the programmed microwave oven and subjected to microwave conditions for 20 minutes at 150 °c under autonomous pressure. The vial was then cooled to 40-50 °c and pressure was released. The hot solution was filtered and kept aside for crystallization. Fine blocks of compound **1** that separated after 1 hr were filtered, washed with cold water, ether and air dried. The Infrared spectrum and thermal properties of the product were identical to that of the reported compound as above. (Yield 4.0 g, 90 %) [63]

Analytical data: Calc. for $C_{14}H_{16}CaN_2O_{12}$ (444.24) **1**: Ca, 9.02; 4-nbaH, 74.77; C, 38.07; H, 3.66; N, 6.34; CaO, 12.59. Found: Ca, 8.90; 4-nbaH, 73.98, C, 37.84; H, 3.7; N, 6.28; CaO, 11.68

IR (KBr) data: 3666(s), 3561(s), 3512-2570(br), 2247(w), 2208(w), 1955(w), 1817(w), 1614(s), 1568(s), 1504(m), 1414(s), 1391(s), 1342(s), 1321(m), 1280(m), 1250(s), 1105(s), 1009(w), 881(s), 845(s), 799(s), 725(s), 642(w), 513(s) cm^{-1}.

DTA (in °C) : 104 (endo), 419 (exo), 477 (exo), 558 (exo).

Preparation of [Ca(H_2O)(4-nba)$_2$] 1a

A powdered sample of **1** (0.444 g) was heated on a steam bath for ~30 minutes. The heat-treated sample was kept in a dessicator and allowed to cool to room temperature and weighed to obtain **1a**. The observed decrease in weight (12.15%) corresponds to the removal of three moles of water. The yield was quantitative. The compound is insoluble in MeOH, CH_3CN etc.

Analytical data: Calc. for $C_{14}H_{10}CaN_2O_9$ (390.42) **1a**: Ca, 10.25; 4-nbaH, 85.68; CaO, 14.35. Found: Ca, 10.01; 4-nbaH, 84.8, CaO, 14.0

IR (KBr) data: 3611-3100 (br), 3113(s), 2849(w), 1944(w), 1813(w), 1612(s), 1558(s), 1524(m), 1493(sh), 1414(s), 1346(s), 1319(s), 1171(m), 1142(m), 1107(s), 1015(s), 980(s), 880(s), 839(s), 799(s), 725(s), 511(s) cm^{-1}.

DSC (in °C) : 260 (exo), 410 (exo), 477 (exo) 558 (exo).

Preparation of [Ca(N-MeIm)(4-nba)$_2$]$_n$ 2

Method 1

N-Methylimidazole (0.082 g, 1 mmol) was added into a freshly prepared sample of **1a** and the reaction mixture was kept in a dessicator for ~30 min. The reaction mixture was washed with ether and dried to obtain **2**. Alternatively **2** can also be prepared by directly heating a mixture of a finely powdered sample of **1** (0.45 g, 1 mmol) and N-MeIm (0.082 g, 1 mmol) in a steam bath for ~30 min. The hot reaction mixture was cooled, washed well with ether and dried in air. (Yield 0.45 g, 98%).

Method 2

A powdered sample of **1** (1.78 g, 4 mmol) was heated with N-MeIm (1.4 ml, 17 mmol) on a steam bath for ~1 h to obtain a light yellow solid. To this hot mass distilled water (~8 ml) was added and the mixture reheated to obtain a pale yellow solution. The hot solution was quickly filtered and kept aside for crystallization. Fine colourless blocks of crystals suitable for X-ray study, which separated were washed with ether (5ml) and dried in air. (Yield: 1.82 g, 60%). The use of reduced amounts of N-MeIm in the thermal reaction or excess water for recrystallisation results in the formation of the tetraaqua compound **1** in accordance with its hydration characteristics (*vide infra*). The infrared spectrum and the DSC thermogram of this product is identical with that of the product obtained in the thermal reaction.

Analytical data: Calc. for $C_{18}CaH_{14}N_4O_8$ (454.43) **2**: Ca, 8.8; 4-nbaH, 73.11; CaO, 12.34; C, 47.53; H, 3.0; N, 12.32, Found: Ca, 8.8; 4-nbaH, 73, CaO, 12.2; C, 47.6; H, 3.03; N, 11.81 %.

IR (KBr) data: 3121(s), 2967(s), 2855(w), 1614(s), 1584(s), 1520(m), 1402(s), 1375(s), 1344(s), 1321(s), 1279(s), 1230(m), 1107(s), 1014(s), 1082(m), 934(s), 878(s), 822(s), 800(s), 752(s), 727(s), 667(s), 621(s), 559(s), 509(s) cm^{-1}.

UV-Vis 274 nm (23775 L. mol^{-1}. cm^{-1})

^{1}H NMR (DMDO-d_6) δ (in ppm): 3.63 (s, 3H); 6.86 (s, 1H); 7.09 (s, 1H); 7.55 (s, 1H); 8.16 (m, 4H)

DSC (in °C): 188 (endo), 412 (exo), 558 (exo)

Preparation of $[Ca(Im)(4\text{-}nba)_2]$ 3

Imidazole (0.068 g, 1 mmol) was added into a freshly prepared sample of **1a** and the reaction mixture was kept in a dessicator for ~30 min. The reaction mixture was washed with ether and dried to obtain **3**. Alternatively **3** can also be prepared by directly heating a mixture of a finely powdered sample of **1** (0.45 g, 1 mmol) and Im (0.068 g, 1 mmol) in a steam bath for ~30 min. The hot reaction mixture was cooled, washed well with ether and dried in air. Yield: (quantitative).

Anaytical data: Calc. for $C_{17}CaH_{12}N_4O_8$ **3**: Ca, 9.08; 4-nbaH, 75.88; CaO, 12.73; C, 46.31; H, 2.72; N, 12.71, Found: Ca, 8.9; 4-nbaH, 74.28; CaO, 12.3; C, 45.95; H, 3.13; N, 10.94.

IR (KBr) data: 3381(s), 3223(s), 3061(w), 2941(w), 1604(w), 1570(s), 1516(s), 1490(m), 1402 (s), 1348(s), 1321(s), 1261(s), 1171(m), 1142(m), 1107(s), 1066 (s), 1014(s), 935 (s), 918 (s), 860 (s), 825(s), 802(s), 752(s), 740(s), 723 (s), 659(s), 617(s), 497(s), 511(s) cm^{-1}.

^{1}H NMR (DMDO-d_6) δ (in ppm): 7.00 (s, 1H); 7.63 (s, 1H); 8.13 (m, 4H).

DSC (in °C): 198 (endo), 415 (exo), 547 (exo)

Rehydration of compound 2 and 3

A powdered sample of **2** (200 mg) was suspended in water (~5 ml) and the reaction mixture was left undisturbed overnight. The reaction mixture was filtered and the residue was washed with alcohol followed by ether and dried to obtain **1** in quantitative yields. The formation of **1** is evidenced by its characteristic IR spectrum and DSC thermogram. Alternatively **2** can be transformed to **1** by suspending an amount (200 mg) of **2** in water (5 ml) and heating the solution till dissolution of the entire solid. The hot solution is cooled to obtain **1** in quantitative yield. The equilibration of a powdered sample of **3** over water vapour resulted in the formation of the starting compound **1** in quantitative yield in about a day as evidenced by its characteristic IR spectrum and DSC thermogram.

Preparation of $[Ca(H_2O)(2\text{-MeIm})(4\text{-nba})_2]_n$ 4

A powdered sample of compound **1** (0.444 g, 1 mmol) was mixed well with 2-methylimidazole (2-MeIm) (0.082 g, 1 mmol) and the solid mixture was heated on a steam bath for ~30 min. The hot reaction mixture was cooled, washed well with ether and dried in air to obtain compound **4** as a yellow powder in quantitative yield. Crystals suitable for structure determination were prepared by recrystallizing the powdered sample from hot water (~10 ml) containing 2-MeIm (0.246 g, 3 mmol). The crystalline needles of **4** were washed with cold water followed by alcohol and then dried in air. The infrared spectrum and the DSC thermogram of the crystalline product are identical with that of the yellow powder. **4** can also be prepared by first heating a powdered sample of **1** on a steam bath for ~20 min to obtain the monohydrate $[Ca(H_2O)(4\text{-nba})_2]$. The N-donor ligand 2-MeIm was mixed with this freshly prepared monohydrate and left at 100°C for 15 min to obtain **4**. (Yield 0.46 g, 98%)

Analytical data: Calc. for $CaC_{18}H_{16}N_4O_9$ (472.43) **4**: Ca, 8.48; 4-nbaH, 70.75; CaO, 11.87; C 45.76; H 3.41; N 11.86. Found: Ca, 8.48; 4-nbaH, 70.30, CaO, 11.87; C, 45.73; H, 3.63; N, 11.8%.

IR (KBr) data: 3536 ($\upsilon_{O\text{-}H}$), 3264 ($\upsilon_{N\text{-}H}$), 3117, 2204, 1944, 1622, 1591, 1570, 1514, 1487, 1412, 1346, 1323, 1280, 1169, 1148, 1103, 1011, 997, 876, 854, 827, 795, 787, 752, 721, 673, 600, 517, 440 cm^{-1}.

^1H NMR (DMDO-d_6) δ (in ppm): 2.25 (s, 3H); 6.83 (d, 2H); 7.14 (d, 2H); 8.14 (q, 2H); 11.52 (s, H)

DSC (in °C): 172 (endo) 410 (exo) 559 (exo)

UV-Vis (Diffused reflectance): 251, 330 nm

Preparation of $[Ca(pyr)_2(4\text{-nba})_2]$ 5

A powdered sample of $[Ca(H_2O)_4(4\text{-nba})_2]$ (0.444 g, 1 mmol) was heated on a steam bath for ~20 min to obtain the monohydrate $[Ca(H_2O)(4\text{-nba})_2]$. To this, powdered pyrazole (pyr) (0.136 g, 2 mmol) was added and the solid mixture was cooled in a dessicator and washed well with ether and dried in air to obtain compound **5** as a fine powder in near quantitative yield. Crystals suitable for structure determination were prepared by recrystallizing the powdered sample (0.480 g) from hot water (~5 mL) containing pyrazole (0.136 g, 2 mmol). The crystals were washed with cold water followed by ether and air dried to obtain 0.390 g of **5**. The IR spectrum and the DTA thermogram of the crystalline product are identical with that of the powder. (Yield 0.40 g, 80%)

Analytical data: Calc. for $CaC_{20}H_{16}N_6O_8$ (508.47) **5**; 4-nbaH, 65.74; CaO 11.03. Found 4-nbaH, 65.02; CaO 11.08 %.

IR (KBr) data: 3180 (υ_{NH}), 3148, 3119, 2997, 2877, 1614, 1572 υ_{as}(-COO), 1512 υ_{as}(-NO_2), 1489, 1396 υ_{ss}(-COO), 1346 υ_{ss}(-NO_2), 1319, 1334, 1105, 1064, 1039, 1013, 939, 878, 826, 800, 772, 725, 611, 557, 511, 444 cm^{-1}.

UV- Vis (diffuse reflectance): 254, 317 nm

DTA (in ^{o}C): 232 (endo), 421 (exo), 481 (exo), 575 (exo).

Preparation of $[Ca(H_2O)_2(4\text{-nba})_2].2(dmp)$ 6

Method 1

A powdered sample of $[Ca(H_2O)_4(4\text{-nba})_2]$ **1** (0.444 g, 1 mmol) was heated on steam bath for 15 minutes and then mixed with 3,5-dimethylpyrazole (dmp) (0.193 g, 2 mmol). The resulting mixture was dissolved in water (~5 ml) and then allowed to crystallize at room temperature. The colorless needle shaped crystals obtained in 2 hrs were washed with cold water, and then with ether and air dried. Alternatively compound **6** can be also prepared by directly mixing $[Ca(H_2O)_4(4\text{-nba})_2]$ (0.444 g, 1 mmol) and 3,5-dimethylpyrazole (dmp) (0.193 g, 2 mmol) in water (5 ml) and then allowing it to crystallize at room temperature. However X-ray quality crystals were prepared by using 4 mmol of 3,5-dimethylpyrazole (0.385 g). Isolated crystals by both the methods gave same yield and identical infrared and thermal data. (Yield 0.48 g, 80%)

Method 2

$[Ca(H_2O)_4(4\text{-nba})_2]$ was first generated in-situ by reaction of 4-nitrobenzoic acid (1.67 g, 1 mmol) with calcium carbonate (0.5 g, 0.5 mmol) in water (25 ml) on steam bath. To the hot solution, 3,5-dimethylpyrazole (1.92 g, 4mmol) was added and resulting reaction mixture was filtered and kept aside for crystallization. The colorless crystals obtained after one day were isolated as described above. All the analytical data obtained was identical to the product obtained using two mmols of 3,5-dimethylpyrazole. (Yield 2.1 g, 70%)

Analytical data: Calc. For $CaC_{24}H_{28}N_6O_{10}$ (600.60) **6**; C, 48.0; H, 4.70; N, 13.99; 4-nbaH 55.65; CaO, 9.34; Found; C, 46.92; H, 4.54; N, 13.75; 4-nbaH, 54.84; CaO, 9.2 %.

IR (KBr) data: 3600(br, υ_{OH}), 3387, 3269(υ_{NH}), 3148, 3105, 1614, 1568 υ_{as}(-COO), 1514 υ_{as}(-NO_2), 1416υ_{ss}(-COO), 1342 υ_{ss}(-NO_2), 1317, 1288, 1151, 1105, 1015, 974, 878, 843, 797, 726, 694, 660, 592, 511 cm^{-1}.

UV- Vis (diffuse reflectance): 245, 320 nm

DTA (in °C): 110 (endo), 236 (exo), 411 (exo), 545 (exo).

Preparation of [Ca(H_2O)$_6$(4-nba)](4-nba)(2-ap)·H_2O 7

A mixture of [Ca(H_2O)$_4$(4-nba)$_2$] **1** (0.445 g, 1 mmol) and 2-aminopyridine (0.366 g, 4 mmol) was taken in water (~8 mL) and the reaction mixture was heated on a steam bath to obtain a clear yellow solution. The clear reaction mixture was left aside for crystallization. The pale yellow crystalline blocks suitable for structure determination which separated after ~3 h were isolated by filtration, washed with a little ice cold water followed by ether and air dried. The use of stoichiometric amount of 2-ap (1 mmol) also resulted in the formation of a microcrystalline product which analyzed satisfactorily. The use of 4-ap instead of 2-ap in the above reaction under identical conditions resulted in the formation of the starting material **1**. (Yield 0.46 g, 77 %).

Analytical data: Calc. For [Ca(H_2O)$_6$(4-nba)](4-nba)(2-ap)·H_2O **7**: $CaC_{19}H_{28}N_4O_{15}$ (592.52); Ca, 6.76; C, 38.51; H 4.76; N 9.46; CaO, 9.46: Found: Ca 6.21; C 38.13; H 4.21; N 8.74; CaO, 9.69 %

IR (KBr) data: 3475 (υ_{OH}), 3443, 3379 (υ_{NH}), 3347, 3217, 1678, 1620, 1572 υ_{as}(-COO), 1518 υ_{as}(-NO_2), 1445, 1422 υ_{ss}(-COO), 1341 υ_{ss}(-NO_2), 1319, 1258, 1155, 1105, 1044, 988, 876, 839, 797, 779, 771, 727, 623, 557, 515 cm^{-1}.

DTA (in °C) : 117 (endo), 238 (endo), 421 (endo), 534 (exo).

UV-Vis (λ_{max} in water) = 297 nm.

^{1}HNMR (DMSO-d_6) δ (in ppm): 5.85 (s, 2H), 6.41 (m, 1H), 6.40 (m,1H), 7.34 (m, 1H), 7.88 (d, 1H), 8.11 (d, 2H), 8.20 (d, 2H).

Preparation of [Ca(2-ap)(4-nba)$_2$] 7a

A finely powdered solid mixture of [Ca(H_2O)$_4$(4-nba)$_2$] **1** (0.445 g, 1 mmol) and 2-aminopyridine (0.094 g, 1 mmol) was heated over a steam bath at 100 °C for 15-20 min., until the entire powder turned light yellow. The mixture was washed with ether and dried under vacuo. The observed weight loss of the product indicated the loss of four molecules of water resulting in the formation of an anhydrous compound **7a**. Alternatively **7a** can be also prepared by first heating **1** at 100 °C for 15 min. and then adding 2-ap, followed by washing with ether and drying under vacuo. The use of 4-aminopyridine (4-ap) in the above reaction instead of 2-ap resulted in the formation of the monohydrate [Ca(H_2O)(4-nba)$_2$]. (Yield 0.458 g, 98 %).

Analytical data: Calc. for [Ca(2-ap)(4-nba)$_2$] **7a**: $CaC_{19}H_{14}N_4O_8$: (466.41): CaO 12.02; Found: CaO 12.50 %.

IR (KBr) data: 3458 (υ_{NH}), 3345 (υ_{NH}), 3082, 1620, 1566 υ_{as}(-COO), 1518 υ_{as}(-NO_2), 1487, 1440, 1416 υ_s(-COO), 1346 υ_s(-NO_2), 1317, 1153, 1107, 1014, 878, 841, 799, 775, 725, 513 cm^{-1}.

Preparation of [(H_2O)$_4$$Li_2$(μ-$H_2O$)$_2$](4-nba)$_2$ 8 and [Na(4-nba)(H_2O)$_3$] 9

A mixture of 4-nitrobenzoic acid (3.340 g, 20 mmol) and lithium carbonate (0.739 g, 10 mmol) in water (50 mL) was heated on a water bath till all the 4-nitrobenzoic acid dissolved completely to give a clear solution. The hot reaction mixture was filtered and left aside for crystallization. Pale yellow crystalline blocks of **9** that separated were filtered, washed with ether and dried in air. (Yield: 3.1 g, 68 %). Use of sodium carbonate (1.06 g, 10 mmol) instead of lithium carbonate in the above reaction resulted in the formation of **9**. (Yield: 3.6g, 70%).

Analytical data: Calc. for $Li_2C_{14}H_{20}N_2O_{14}$ (454.20) **8**: 4-nbaH, 73.59; C, 37.02, H, 4.44; N, 6.17. Found: 4-nbaH, 73.03; C, 36.52; H, 3.82; N, 6.03 %.

IR (KBr) data: 3582, 3400-2800 (br) 1641, 1566 υ_{as}(-COO), 1512 υ_{as}(-NO_2), 1408 υ_s(-COO), 1369, 1344 υ_s(-NO_2), 1323, 1161, 1105, 1011, 802, 723, 648, 517 cm^{-1}.

DTA (in °C): 105 (endo), 389 (exo)

UV–Vis (in H_2O): 299 nm.

Analytical data: Calc. for $NaC_7H_{10}NO_7$ (243.15) **9**: 4-nbaH, 68.73; C, 34.58; H, 4.15; N, 5.76. Found: 4-nbaH, 68.39; C, 34.32; H, 4.11; N, 5.87 %.

IR (KBr) data: 3578, 3500-2800 (br) 1678, 1572 υ_{as}(-COO), 1514 υ_{as}(-NO_2), 1393 υ_s(-COO), 1350 υ_s(-NO_2), 1319, 1107, 1011, 833, 804, 723, 511 cm^{-1}.

DTA (in °C): 105 (endo), 368 (exo)

UV–Vis (in H_2O): 299 nm

Synthesis of [K(4-nba)(H_2O)$_2$] 10

A mixture of 4-nitrobenzoic acid (3.340 g, 20 mmol) and potassium carbonate (1.38 g, 10 mmol) in water (50 mL) was heated on a water bath till all the 4-nitrobenzoic acid dissolved completely to give a clear solution. The hot reaction mixture was filtered and left aside for crystallization. Pale yellow crystalline blocks of **10** that separated were filtered, washed with ether and dried in air. (Yield 3.0 g, 62 %).

Analytical data: Calc. for $KC_7H_8NO_6$ (241.24) **10**: 4-nbaH, 69.27; C, 34.85, H, 3.34; N, 5.81; K_2CO_3, 28.6; Found: 4-nbaH, 68.58; C, 32.3; H, 3.89; N, 5.70; K_2CO_3, 26.8 %.

IR (KBr) data: 3600-2800 (br), 1612, 1564 υ_{as}(-COO), 1530 υ_{as}(-NO_2), 1402 υ_s(-COO), 1348 υ_s(-NO_2), 1321, 1105, 1012, 885, 827, 804, 726, 556, 511 cm^{-1}.

DSC (in °C): 90 (endo), 281 (endo), 349(exo), 432(exo), 573(exo)

UV–Vis (in H_2O): 299 nm.

Synthesis of [Li(4-nba)] 8a, [Na(4-nba)] 9a and [K(4-nba)] 10a

A powdered sample of **8** (0.454 g), **9** (0.50 g) and **10** (0.50 g) was heated at 130°C for 30 min. This resulted in the formation of the anhydrous compound **8a** (0.346 g), **9a** (0.3 g) and **10a** (0.31 g) respectively. The observed mass losses of (10 %), (10.2 %) and (14.5%) are in agreement with the expected value (8.81 %) for **8** (11.1%) for **9** and (14.93%) for **10**, for the loss of three moles of water in **8** and **9** and two moles of water in **10** respectively.

Analytical data: Calc. for $Li_2C_{14}H_{20}N_2O_{14}$ (454.20) **8a**: 4-nbaH, 73.59; Found: 4-nbaH, 73.03 %

IR (KBr) data: 3115, 1618, 1566 υ_{as}(-COO), 1518 υ_{as}(-NO_2), 1417 υ_s(-COO), 1354 υ_s(-NO_2), 1319, 1107, 1014, 875, 837, 802, 725, 518 cm^{-1}.

Analytical data: Calc. for $NaC_7H_{10}NO_7$ (243.15) **9a**: 4-nbaH, 68.73 Found: 4-nbaH, 68.39 %

IR (KBr) data: 3111, 1618, 1585 υ_{as}(-COO), 1521 υ_{as}(-NO_2), 1406 υ_s(-COO), 1352 υ_s(-NO_2), 1317, 1105, 1016, 877, 833, 798, 725, 505 cm^{-1}.

Analytical data: Calc. for $KC_7H_8NO_6$ (241.24) **10a**: 4-nbaH, 69.27; Found: 4-nbaH, 68.58 %

IR (KBr) data: 1612, 1564 υ_{as}(-COO), 1530 υ_{as}(-NO_2), 1402 υ_s(-COO), 1348 υ_s(-NO_2), 1321, 1105, 1012, 885, 827, 804, 726, 556, 511 cm^{-1}.

Synthesis of [Sr(4-nba)(H_2O)$_7$](4-nba).2H_2O 11

The 4-nitrobenzoic acid (3.34 g, 20 mmol) was taken in water (100 ml) and heated over steam bath, To the hot solution, $SrCO_3$ (1.47 g, 10 mmol) was added slowly and continued heating until all the effervescence due to CO_2 liberation stopped completely. The hot reaction mixture was filtered and resulting clear solution was kept aside for crystallization. The colourless flakes that crystallized after four days were filtered washed with ether and air dried. Alternatively this can be also prepared by reaction of sodium salt of 4-nitrobenzoic acid generated *in-situ* by reaction 4-nitrobenzoic acid (3.34 g, 20 mmol) with sodium bicarbonate (1.68 g, 20 mmol) in water (90 ml) and using $SrCl_2.6H_2O$ (2.66 g, 10 mmol dissolved in 10 ml of water) as strontium source. Product was isolated as described above. (Yield 4.5 g, 78%)

Analytical data: Calc. for $[Sr(4\text{-nba})(H_2O)_7](4\text{-nba}).2H_2O$ **11** ($C_{14}H_{26}SrN_2O_{17}$) (581.98); $SrCO_3$, 25.37; C, 28.89; H, 4.50; N, 4.81 Found: $SrCO_3$, 23.69; C, 29.73; H, 2.01; N, 4.89 %.

IR (KBr) data: 3603-3100(br υ_{O-H}), 1946, 1620, 1564 υ_{as}(-COO), 1520 $\upsilon_{as}(-NO_2)$, 1412υ_{ss}(-COO), 1343$\upsilon_{ss}(-NO_2)$, 1319, 1107, 1013, 880, 835, 799, 725, 511 cm^{-1}.

DTA (in °C): 115(endo), 424(exo), 534(exo). Residue = 25.29%

Transformation of $[Sr(H_2O)_7(4\text{-nba})](4\text{-nba}).2H_2O$ 11 to intermediate $[Sr(H_2O)_4(4\text{-nba})_2]$ 11a

Compound $[Sr(H_2O)_7(4\text{-nba})](4\text{-nba}).2H_2O$ **11** (0.581 g, 1 mmol) when exposed to air overnight at room temperature shows a weight of 0.491 g accounting for weight loss of 15.56% for loss of 5 moles of water to form a intermediate stable compound $[Sr(H_2O)_4(4\text{-nba})_2]$ **11a**. This compound when heated at 120°C for 1 hr results in the formation of dehydrated $[Sr(4\text{-nba})_2]$ with loss of remaining 4 water and total water loss of 28.12% as expected.

Analytical data: Calc. for $[Sr(H_2O)_4(4\text{-nba})_2]$ $C_{14}H_{12}SrN_2O_{12}$ (487.87) **11a**: $SrCO_3$ 30.26; C, 34.47; H, 2.48; N, 5.74; Found: $SrCO_3$, 29.44; C, 34.2; H, 2.49; N, 5.70 %.

IR (KBr) data: 3632 (br υ_{O-H}), 3559, 3530, 3400, 3111, 3082, 1942, 1618, 1564 υ_{as}(-COO), 1512 $\upsilon_{as}(-NO_2)$, 1412υ_{ss}(-COO), 1350 $\upsilon_{ss}(-NO_2)$, 1319, 1167, 1136, 1105, 1012, 878, 831, 799, 723, 513 cm^{-1}.

DTA (in °C): 104(endo), 156(endo), 429(exo), 556(exo). Residue = 30.56

Synthesis of $[Sr(H_2O)_3(4\text{-nba})(dmf)](4\text{-nba})$ 12

Method 1

The 4-nitrobenzoic acid (3.34 g, 20 mmol) was dissolved in mixture of solvent (20 ml water / 20 ml methanol / 50 ml dimethylformamide) at room temperature and few drops of triethylamine were added to get a clear solution. To this mixture $SrCl_2.6H_2O$ (2.66 g, 10 mmol, dissolved in 10 ml of water) solution was added and resulting solution was filtered and kept aside for crystallization. Fine needle shaped crystals of [Sr(4-nba)(dmf)$(H_2O)_3$](4-nba) **12** were isolated after four days, washed with cold water followed by ether and air dried. (Yield 3.8 g, 69%).

Method 2

Compound **12** can also be prepared by first isolating [Sr(4-nba)$(H_2O)_7$](4-nba).$2H_2O$ **11** (0.581 g, 1 mmol) by reported method and then dissolving compound **11** in dimethylformamide (5 ml) at room temperature and then allowing it to crystallize. Fine blocks of [Sr(4-nba)(dmf)$(H_2O)_3$](4-nba) **12** were isolated next day washed with cold water and then with ether and air dried. (Yield 0.35 g, 64%)

Method 3

Alternatively the above compound can also be prepared by heating **11** on a steam bath for 15 minutes to get intermediate [Sr$(H_2O)_4$(4-nba)$_2$] followed by addition of dmf (5 ml) to get a clear solution. Fine blocks of [Sr$(H_2O)_3$(4-nba)(dmf)](4-nba) **12** were isolated next day washed with cold water and then with ether and air dried (Yield 3.55 g, 65%).

Analytical data: Calc. for [$SrC_{17}H_{21}N_3O_{12}$] (546.99) **12**: $SrCO_3$, 26.99; C 37.33; H 3.87; N 7.68, Found: $SrCO_3$, 26.75; C, 35.98; H, 3.66; N, 7.28 %.

IR (KBr) data: 3604-3302 (br, υ_{O-H}), 1933, 1665 υ_{CO}(amide), 1613, 1562 υ_{as}(-COO), 1512 υ_{as}($-NO_2$), 1414 υ_{ss}(-COO), 1393, 1348 υ_{ss}($-NO_2$), 1317, 1254, 1105, 1013, 880, 827, 798, 725, 665, 563, 511 cm^{-1}.

DTA (in °C): 113(endo), 435(exo), 525(exo). Residue, 26%

Preparation of [Sr(H_2O)(4-nba)$_2$(nmf)$_{1.5}$] 13

Method 1

Compound **13** was prepared by above described method 1 using N-methylformamide (nmf) instead of dimethylformamide (dmf). The 4-nitrobenzoic acid (1.67 g, 1 mmol) was dissolved in mixture of solvent (10 ml water/10 ml methanol/25 ml N-methylformamide) at room temperature and few drops of triethylamine were added to get a clear solution. To this mixture $SrCl_2.6H_2O$ (1.33 g, 0.5 mmol dissolved in 5 ml of water) solution was added and resulting solution was filtered and kept aside for crystallization. Fine blocks of [Sr(H_2O)(4-nba)(nmf)$_{1.5}$](4-nba) **13** were isolated after seven days, washed with cold water followed by ether and air dried. (Yield 1.8 g, 69%)

Method 2

[Sr$(H_2O)_7$(4-nba)](4-nba).$2H_2O$ **11** (0.581 g, 1 mmol) was dissolved in N-methylformamide (5 ml) at room temperature and then allowed to crystallize. Fine blocks of [Sr(H_2O)(4-nba)$_2$(nmf)$_{1.5}$] **13** were isolated next day washed with cold water and then with ether and air dried. (Yield 0.34 g, 64%)

Method 3

Alternatively the above compound can be also prepared by heating freshly prepared compound **11** on steam bath for 15 minutes to get intermediate [Sr(H_2O)$_4$(4-nba)$_2$] **11a** followed by addition of nmf (5 ml) to get a clear solution. The above procedure was repeated to isolate the product. (Yield 0.345 g, 65%)

Analytical data: Calc. for [$SrC_{17}H_{17.5}N_{3.5}O_{10.5}$] (526.47) **13**: $SrCO_3$ 27.97; C, 38.78; H, 3.35; N, 9.31 Found: $SrCO_3$, 26.65; C, 36.55; H, 2.83 N, 8.26 %.

IR (KBr) data: 3600 (br $\upsilon_{O\text{-}H}$), 3408 $\upsilon_{N\text{-}H}$, 3113, 1678 υ_{CO}(amide), 1624, 1562 υ_{as}(-COO), 1524 υ_{as}(-NO_2), 1406 υ_{ss}(-COO), 1348 υ_{ss}(-NO_2), 1319, 1107, 1013, 879, 837, 800, 725, 625, 509 cm^{-1}.

DTA (in °C): 109(endo), 430(exo), 536(exo). Residue, 27.68%

Preparation of [Sr(4-nba)$_2$(Pyr)$_2$] 14

Method 1

[Sr(H_2O)$_7$(4-nba)](4-nba).2H_2O **11** was generated *in-situ* by reacting 4-nitrobenzoic acid (0.334 g, 2 mmol) with $SrCO_3$ (0.147 g, 1 mmol) in water (10 ml) on steam bath until no effervescence due to CO_2 evolution were observed, To the hot filtered solution, pyrazole (0.272 g, 4 mmol) was added and kept aside for crystallization. Fine needles of [Sr(4-nba)$_2$(pyr)$_2$] **14** that separated out next day were washed with cold water and then with ether and air dried (Yield 0.35 g, 63%)

Method 2

[Sr(H_2O)$_7$(4-nba)](4-nba).2H_2O **11** (0.581 g, 1 mmol) or [Sr(H_2O)$_4$(4-nba)$_2$] **11a** (0.488 g, 1 mmol) was mixed with pyrazole (0.272 g, 4 mmol) and dissolved in water (10 ml) on a steam bath, the clear solution obtained was then allowed to crystallize. Fine needles of [Sr(4-nba)$_2$(pyr)$_2$] **14** that separated out next day were washed with cold water and then with ether and air dried. (Yield 0.42 g, 79%)

Method 3

Alternatively this compound can be also prepared thermally by heating freshly prepared compound (0.581 g, 1 mmol) **11** on steam bath for 15 minutes to get intermediate [Sr(H_2O)$_4$(4-nba)$_2$] followed by addition of pyrazole (0.272 g, 4 mmol) to get compound **14**. The crude product was washed with ether and air dried. (Yield 0.32 g, 59%)

Analytical data: Calc. for [$SrC_{20}H_{16}N_6O_8$] (556.0) **14**: $SrCO_3$ 26.55; C, 43.20; H, 2.90; N, 15.12 Found: $SrCO_3$, 24.80; C, 41.50; H, 2.73 N, 14.45 %.

IR (KBr) data: 3354 (s, υ_{N-H}), 3103, 3076, 2974, 2843, 1957, 1612, 1562 (s, υ_{as}(-COO), 1512 (s, υ_{as}(-NO_2), 1462 (s), 1398 (s, υ_{ss}(-COO), 1346(m, υ_{ss}(-NO_2), 1317(s), 1250(m), 1132(s), 1018(s), 1033(s), 931(s), 885(s), 835(s), 800(m), 760(s), 733(s), 609(s), 509(s), 433(w) cm^{-1}.

DTA (in °C): 236(endo), 403(exo), 565(exo). Residue, 25.2%.

Preparation of [$Sr(H_2O)_3(4\text{-}nba)_2(HCONH_2)$] 15

Method 1

[$Sr(4\text{-}nba)(H_2O)_7$](4-nba).$2H_2O$ **11** was first generated *in-situ* by reacting 4-nitrobenzoic acid (1.67 g, 10 mmol) with $SrCO_3$ (1.47 g, 10 mmol) in water (25 ml) on steam bath. To hot mixture formamide (10 ml) was added and resulting solution was filtered and kept aside for crystallization. Fine needle shaped crystals of [$Sr(H_2O)_3(4\text{-}nba)_2(HCONH_2)$] **15** were isolated after four days, washed with cold water followed by ether and air dried. (Yield 1.42 g, 50 %)

Method 2

Compound **15** can also be prepared by first isolating [$Sr(4\text{-}nba)(H_2O)_7$](4-nba).$2H_2O$ **11** (0.581 g, 1 mmol) by earlier reported method and then dissolving compound **11** in mixture of formamide and water (5 ml each) on steam bath. This results in formation of [$Sr(H_2O)_3(4\text{-}nba)_2(HCONH_2)$] **15** as fine needle shaped crystals after 1-2 hour. Isolated product is washed with cold water and then with ether and air dried. (Yield 0.28 g, 50 %)

Analytical data: Calc. for [$SrC_{15}H_{13}N_3O_{12}$] (514.90) **15**: $SrCO_3$, 28.64; C, 34.99; H, 2.54; N, 8.16 Found: $SrCO_3$, 26.15; C, 33.89; H, 2.66; N, 9.31.

IR data: 3600-3500 (br, υ_{O-H}), 3402 (υ_{N-H}), 3246, 3113, 3086, 2907, 2843, 2783, 2700, 2446, 2286, 2207, 1942, 1811, 1689 υ_{CO}(amide), 1605, 1562 υ_{as}(-COO), 1514 υ_{as}(-NO_2), 1400 υ_{ss}(-COO), 1348 υ_{ss}(-NO_2), 1317, 1107, 1057, 1018, 874, 833, 798, 725, 606, 509 cm^{-1}

DTA (in °C): 165(endo), 415(exo), 531(exo). Residue, 26.52 %

Synthesis of Nitrophthalamic acid (2-Ca-4-nbaH)

Nitration of phthalimide by a literature method [203] afforded a mixture of the isomeric 3- and 4-nitrophthalimide. After separation from the soluble 3-nitro isomer (minor product), the insoluble 4-nitrophthalimide (10 g, 0.052 mol) was taken in water (50 mL) containing NaOH (2.08 g, 0.052 mol) at room temperature and stirred for 15 min to obtain a clear brown solution. To this, dilute HCl was added in drops (*p*H = 4-5) resulting in the separation of the crude product. The solid was filtered and washed well with water till free of chloride and recrystallized from alcohol to obtain 2-ca-4nba**H** (Yield 8 g, 50 %) (M. pt. 144- 145 °C)

IR (KBr) data: 3396, 3268, 3219, 3116, 3093, 2872, 2778, 2596, 2480, 1725 υ_{as}(-COO), 1667 υ_{CO}(amide), 1611, 1572 υ_{as}(-NO_2) 1502, 1485, 1441, 1380, 1354 υ_s(-NO_2), 1306, 1267, 1246, 1120, 1068, 977, 910, 861, 807, 777, 737, 685, 643, 620, 547, 429 cm^{-1}.

^{1}H NMR (DMSO-d_6) δ (in ppm): 7.64 (d, *J* = 8.4 Hz, H3), 8.20 (dd, *J* = 2.4 Hz, *J* = 8.4 Hz, H5), 8.36 (d, *J* = 2.4 Hz, H6), 8.94 (br s, *J* = 2.4, -N-H). For assignment, the numbering for H-atom is same as the crystallographic labeling.

UV-vis: λ_{max} = 293 nm (ε = 5210 $L.mol^{-1}.cm^{-1}$);

Preparation of [Mg(H_2O)$_6$(2-ca-4nba)$_2$] 16

Compound (**1**) (2.14 g, 10 mmol) was taken in water (50 mL) and heated on a steam bath till most of the solid dissolved. To the hot reaction mixture, $MgCO_3$ (0.42 g, 5 mmol) was added slowly resulting in brisk effervescence. The heating was continued till effervescence ceased completely to obtain a clear pale yellow solution. The hot reaction mixture was filtered and kept undisturbed at room temperature. Pale yellow crystalline blocks that separated out after 5 days were filtered, washed with ice cold water, followed by ether and dried in air. (Yield 1.92 g, 69.5 %).

Analytical data: Calc. for $C_{16}H_{22}N_4MgO_{16}$ (550.67): Mg, 4.41; MgO, 7.32; C, 34.90; H, 4.03; N, 10.17. Found: Mg, 4.33; MgO, 7.21; C, 34.53; H, 4.02; N, 9.57%.

IR (KBr) data: 3568-3215 (br, υ_{OH}), 1680 υ_{as}(-COO), 1643 υ_{CO}(amide), 1612, 1566 υ_{as}(-NO_2), 1516, 1487, 1427, 1395, 1350 υ_s(-NO_2), 1305, 1262, 1149, 1131, 1077, 923, 866, 816, 736, 649, 571, 505 cm^{-1}.

^{1}H NMR (DMSO-d_6) δ (in ppm) 7.65 (d, *J* = 8.4 Hz, H3), 8.20 (dd, *J* = 2.4 Hz, *J* = 8.4 Hz, H5), 8.4 (d, *J* = 2.4 Hz, H6), 9.1 (br s, -N-H);

DSC (in °C): 94 (endo), 136 (endo), 245 (endo), 433 (exo), 545 (exo).

UV-vis: 293 nm (ε = 15035 L $mol^{-1}cm^{-1}$)

Preparation of [Ca(H_2O)$_2$(2-ca-4nba)$_2$] 17

A mixture of 2-carbamoyl-4-nitrobenzoic acid (0.420 g, 2 mmol) and $CaCO_3$ was taken in water (25 mL) and heated on a steam bath for ~2 h till the effervescence ceased completely to obtain a clear pale yellow solution. The hot reaction mixture was filtered and kept undisturbed at room temperature. Pale yellow crystalline blocks of **17** that separated after several days were filtered, washed with a little ice cold water, followed by ether and dried in air, (Yield 0.32 g, 64%). Alternatively compound **17** can also be prepared by reacting 2-ca-4nbaH (0.420 g, 2 mmol) with Na_2CO_3 (0.106 g, 1 mmol) at room temperature in water (25 mL) to obtain the Na salt. To the clear solution thus obtained $CaCl_2.2H_2O$ (0.147 g, 1 mmol) was added. The reaction mixture was filtered and kept aside for crystallization. The product was isolated as above. (Yield 0.36 g, 75 %).

Analytical data: Calc. for $CaC_{16}H_{14}N_4O_{12}$, M = 494.39 (**17**): C, 38.87; H, 2.85; N, 11.33; CaO, 11.32. Found: C, 38.47; H, 2.79; N, 11.03; CaO, 11.1 %.

IR (KBr) data: 3613, 3464, 3358, 3115, 3082, 2843, 2787, 2467, 2251, 2102, 1942, 1827, 1680, 1605, 1574, 1512, 1487, 1416, 1379, 1358, 1273, 1163, 1149, 1113, 1070, 974, 914, 858, 849, 833, 795, 787, 746, 692, 642, 584, 569, 488, 447 cm^{-1}.

UV-Vis (Diffused reflectance): 305 nm

DTA data (in °C): 152 (endo), 297 (endo), 440 (exo), 557 (exo)

Preparation of $[Sr(2\text{-}ca\text{-}4nba)_2]$ 18

A mixture of 2-carbamoyl-4-nitrobenzoic acid (0.420 g, 2 mmol) and $SrCO_3$ (0.147 g, 1 mmol) was taken in water (50 mL) and heated on a steam bath for ~2 h till the effervescence ceased completely to obtain a clear pale yellow solution. The hot reaction mixture was filtered and kept undisturbed at room temperature. Pale yellow precipitate of **18** that separated after 1-2 hrs was filtered, washed with a little ice cold water, followed by ether and dried in air, (Yield 0.40 g, 79 %).

Analytical data: Calc. for $SrC_{16}H_{10}N_4O_{10}$ (505.89) (**18**): C, 37.99; H, 1.99; N, 11.07; $SrCO_3$, 29.18; Found: C, 37.0; H, 1.8; N, 11.0; $SrCO_3$, 29.0 %.

IR data (in cm^{-1}): 2843, 2787, 2467, 2251, 2102, 1942, 1827, 1680, 1605, 1574, 1512, 1487, 1416, 1379, 1358, 1273, 1163, 1149, 1113, 1070, 974, 914, 858, 849, 833, 795, 787, 746, 692, 642, 584, 569, 488, 447.

UV-Vis (Diffused reflectance): 305 nm

DTA data (in °C): 136 (endo), 441 (exo),

Preparation of $[Ba(2\text{-}ca\text{-}4nba)_2]$ 19

A mixture of 2-carbamoyl-4-nitrobenzoic acid (0.420 g, 2 mmol) and freshly prepared $BaCO_3$ (0.244 g $BaCl_2.2H_2O$ and 0.106 g Na_2CO_3 in water) was taken in water (50 mL) and heated on a steam bath for ~2 h till the effervescence ceased completely. A pale yellow precipitate of **19** that separated immediately was filtered, washed with a little ice cold water, followed by ether and dried in air. (Yield 0.40 g, 72 %).

Analytical data: Calc. for $BaC_{16}H_{10}N_4O_{10}$ (555.60) (**19**): C, 34.59; H, 1.81; N, 10.08; $BaCO_3$, 35.51. Found: C, 34.0; H, 1.51; N, 10.01; $BaCO_3$, 35.0 %.

IR data: 2787, 2467, 2251, 2102, 1942, 1827, 1680, 1605, 1574, 1512, 1487, 1416, 1379, 1358, 1273, 1163, 1149, 1113, 1070, 974, 914, 858, 849, 833, 795, 787, 746, 692, 642, 584, 569, 488, 447 cm^{-1}.

UV-Vis (Diffused reflectance): 305 nm

DTA data (in °C): 152 (endo), 297 (endo), 440 (exo), 557 (exo)

Synthesis of $[Mg(H_2O)_4(2\text{-nba})_2]$ 20

Method 1

2-nbaH (1.67 g, 20 mmol) was weighed and dissolved in 50 ml of water, to this $MgCO_3$ (0.42 g, 10 mmol) was added slowly at room temperature, strong effervescence were observed, the resulting solution was then heated over steam bath for 30 minutes to ensure completion of the reaction. The yellow solution was filtered and kept aside for crystallization. Pale yellow colored crystals obtained were filtered, washed with cold water and then with alcohol, ether and air dried. (Yield, 1.5 g, 70 %).

Method 2

2-nbaH (1.67 g, 10 mmol) was weighed and dissolved in 50 ml of water, to this $NaHCO_3$ (0.84 g, 10 mmol) was added slowly at room temperature, strong effervescence were observed, to the clear solution $MgCl_2.6H_2O$ (1.04 g, 5 mmol) was added and the resulting yellow solution was filtered and kept aside for crystallization. Pale yellow colored crystals obtained were filtered, washed with cold water and then with alcohol, ether and air dried. (Yield 1.72 g, 79 %).

Method 3

2-nbaH (1.67 g, 10 mmol) was dissolved in 50 ml of water and to this Na_2CO_3 (0.53 g, 5 mmol) was added, to the clear solution obtained $MgCl_2.6H_2O$ (1.04 g, 5 mmol) was then added and the resulting pale yellow colored solution was filtered and kept aside for crystallization. Colorless crystals that separated were filtered, washed with cold water then with alcohol, ether and air dried. (Yield 1.80, 84 %)

Analytical data; Calc. for $C_{14}H_{16}MgN_2O_{12}$ (428.60): C, 39.23; H, 3.76; N 6.54; MgO 9.40%. Found: C, 39.57; H, 3.87; N, 6.74; MgO, 9.56 %.

IR (KBr) data: 3647, 3572 (υ_{OH}), 3155, 3110, 2879, 1681, 1646, 1591, 1572 υ_{as}(-COO), 1523 υ_{as}(-NO_2), 1483, 1445, 1423 υ_s(-COO), 1388, 1366, 1352 υ_s(-NO_2), 1308, 1273, 1165, 1145, 1081, 1042, 998, 964, 895, 868, 847, 816, 783, 747, 702, 649, 591, 556, 424 cm^{-1}.

UV- Vis (λ_{max} in H_2O) = 264 nm.

DSC (in °C): 89 (endo), 231 (endo), 336 (exo), 457 (exo).

Preparation of [Mg(2-nba)$_2$] 20a

Compound **20** (0.857 g, 2 mmol) when heated in temperature controlled oven for 30 minutes yielded a dehydrated compound **20a**. The final weight of the product obtained corresponds to loss of 4 moles of water.

Analytical data Calc. for $C_{14}H_8MgN_2O_8$ (356.53): MgO, 11.30; Found: MgO, 11.19.

IR (KBr) data- 3088(s), 3044(m), 2956(m), 2916(m), 2862(s), 2824(m), 2784(m), 1592(s), 1568(s), 1556(s), 1520(s), 1479(s), 1437(s), 1415(s), 1402(s) 1338(s), 1309(s), 1261(s), 1142(s), 1075(s), 1040(s), 967(s), 864(s), 837(s), 781(s), 7549(s), 700(s), 648(s), 536(s), 428(s) cm^{-1}.

DSC (°C) 231(endo), 334(exo), 458(exo).

Rehydration study

Compound [Mg(2-nba)$_2$] **20a** (0.357 g, 1 mmol) when exposed to water vapor showed a increase in weight to (0.429 g) yielding compound **20** as expected for absorption of 4 moles of water. This was further confirmed by the infrared spectrum which was identical to that of the starting material.

Preparation of [Ca(H_2O)$_2$(2-nba)$_2$] 21

A mixture of calcium carbonate (1.0 g, 10 mmol) and 2-nitrobenzoic acid (2-nbaH) (3.34 g, 20 mmol) was taken in water (50 ml) and heated on a steam bath. The insoluble $CaCO_3$ slowly started dissolving accompanied with brisk effervescence. The heating of the reaction mixture was stopped when there was no more evolution of CO_2. At this stage, the reaction mixture was almost clear. The hot pale yellow solution was filtered and left undisturbed for 9-10 days. The colorless crystalline blocks that separated were filtered, washed thoroughly with ether and dried. (Yield 3.42 g, 84%). The crystals obtained in this method were suitable for X-ray studies. Compound **21** can be also prepared using $CaCl_2$ as the Ca source. The sodium salt of 2-nba was first generated *in situ* by reacting 2-

nbaH (1.67 g, 10 mmol) with $NaHCO_3$ (0.84 g, 10 mmol) in water. Into this, an aqueous solution of $CaCl_2$ (0.555 g, 5 mmol) was added and the reaction mixture was filtered and left aside for crystallization. The crystals that separated after a few days were isolated in 71% yield. The IR spectrum and the DSC thermogram of the product obtained in this method were identical to that of the product obtained using $CaCO_3$ as the Ca source. (Yield 2.85 g, 71 %).

Analytical data: Calc. for $C_{14}H_{12}CaN_2O_{10}$ (408.34): Ca, 9.82; C, 41.18; H, 2.96; N 6.86; 2-nbaH, 81.86; CaO, 13.73. Found: Ca, 9.80; C, 41.10; H, 2.98; N, 6.58; 2-nbaH, 80.35; CaO, 13.70 %.

IR (in cm^{-1}): 3649, 3591, 3350, 3078, 2864, 2425, 2000, 1967, 1859, 1626, 1568, 1526, 1485, 1423, 1350, 1306, 1265, 1144, 1076, 968, 870, 851, 795, 789, 746, 702, 650, 430.

UV-Vis in water (in nm): 250, 350

DSC (°C): 144 (endo), 322 (exo), 354 (exo), 545 (exo); Residual mass 14.3%.

Preparation of $[Ca(2\text{-}nba)_2]$ 21a

A powdered sample of **21** (0.325 g) was heated at 150°C for 15 min. This resulted in the formation of the anhydrous compound **21a**. The observed mass loss of 8.80% is in agreement with the expected value (8.81 %) for the loss of two moles of water.

Analytical data: Calc. for $C_{14}H_8CaN_2O_8$ (372.34): Ca, 10.76; C, 45.17; H, 2.17; N 7.52; 2-nbaH, 89.78; CaO, 15.06. Found: Ca, 10.5; C, 44.53; H, 2.1; N, 7.40; 2-nbaH, 88.15; CaO, 14.80 %.

IR (in cm^{-1}): 3074, 2866, 1585, 1566, 1524, 1517, 1485, 1415, 1350, 1308, 1265, 1153, 1078, 961, 864, 847, 785, 737, 700, 648, 432

DSC (°C): 322 (exo), 354 (exo), 545 (exo); Residual mass 14.3 %.

Rehydration studies

The anhydrous compound **21a** was prepared from **21** as mentioned above. Equilibration of a powdered sample of **21a** over water vapor resulted in the formation of the starting material **21** in near quantitative yield in about a day. The IR spectrum and the DSC thermogram of the rehydrated compound are identical to that of **21**.

Synthesis of [Sr(H_2O)$_4$(2-nba)$_2$] 22

Method 1

2-Nitrobenzoic acid (2-nbaH) (1.67 g, 10 mmol) was weighed and dissolved in water (50 ml), to this $SrCO_3$ (0.738 g, 5 mmol) was added slowly at room temperature, strong effervescence were observed, the resulting solution was then heated over steam bath for 30 minutes to ensure completion of the reaction. The yellow solution was filtered and kept aside for crystallization. Pale yellow colored crystals obtained were filtered, washed with cold water and then with alcohol, ether and air dried. (Yield 1.78 g, 73 %).

Method 2

2-nitrobenzoic acid (2-nbaH) (1.67 g, 10 mmol) was weighed and dissolved in 50 ml of water, to this $NaHCO_3$ (0.84 g, 10 mmol) was added slowly at room temperature, strong effervescence were observed, to the clear solution $SrCl_2.6H_2O$ (1.33 g, 5 mmol) was added and the resulting yellow solution was filtered and kept aside for crystallization. Pale yellow colored crystals obtained were filtered, washed with cold water and then with alcohol, ether and air dried. (Yield 1.85 g, 74 %).

Analytical data: Calc. for $C_{14}H_{16}SrN_2O_{12}$ (491.90): C, 34.18; H, 3.28; N, 5.69; 2-nbaH, 89.78; $SrCO_3$, 30.01; Found: C, 33.14; H, 4.10; N, 5.60; 2-nbaH, 88.0; $SrCO_3$, 31.10%.

IR (KBr) data- 3559(s), 3362(br), 1995(m), 1955(m), 1922(m), 1848(m), 1642(s), 1603(s), 1525(s), 1476(s), 1441(s), 1476(s), 1397(s), 1344(s) 1314(s), 1266(s), 1143(s), 1097(s), 957(s), 864(s), 790(s), 742(s), 703(s), 644(s), 507(s) cm^{-1}.

DSC (°C): 72 (endo), 116 (endo), 180 (exo), 266 (endo), 320 (exo), 351 (exo), 416 (exo).

Uv- vis λmax = 264 nm, Solid state λmax = 258 nm.

Preparation of [Sr(2-nba)$_2$] 22a

A powdered sample of **22** (0.491 g) was heated at 120°C for 15 min., This resulted in the formation of the anhydrous compound **22a**. The observed mass loss of 14.56 % is in agreement with the expected value (14.66 %) for the loss of four moles of water.

Analytical data: Calc. for $C_{14}H_8SrN_2O_8$ (419.84): C, 40.05; H, 1.92; N 6.67; $SrCO_3$, 35.16: Found: C, 40.05; H, 1.92; N, 6.6; $SrCO_3$, 34.80%.

IR data- 3112(s), 3083(m), 3039(m), 2990(s), 2907(s), 2750(s), 1843(s), 1593(s), 1568(s), 1531(s), 1486(s), 1394(s), 1377(s), 1307(s), 1270(s), 1167(s), 1151(s), 1080(s), 1040(m), 974(s), 869(s), 840(s), 776(s), 737(s), 702(s), 648(s), 585(s), 536(s), 434(s) cm^{-1}.

Tg-DSC- 189(exo), 271(endo), 332(exo), 358(exo), 451(exo), 498(exo).

Rehydration study

Compound **22a** (0.419 g, 1 mmol) when exposed to water vapor showed weight increase of (0.491 g) indicating the formation of compound **22** as expected for absorption of 4 moles of water. This was further confirmed by the infrared spectrum which was identical to that of the starting material.

Preparation of $[[Ba(H_2O)_3]_2(\mu_2\text{-2-nba-O,O,O-NO}_2)_2(\mu_2\text{-2-nba-O,O,O'})_2]_n$ 23

A mixture of barium carbonate (1.98 g, 10 mmol) and 2-nitrobenzoic acid (2-nbaH) (3.34 g, 20 mmol) was taken in water (50 ml) and heated on a steam bath. The insoluble $BaCO_3$ slowly started dissolving accompanied with brisk effervescence. The heating of the reaction mixture was stopped when there was no more evolution of CO_2. At this stage, the reaction mixture was almost clear. The hot solution was filtered and left undisturbed for 7-8 days. The colourless crystalline blocks that separated were filtered, washed thoroughly with ether and dried. (Yield: 4.430 g, 85 %). The crystals obtained in this method were suitable for X-ray studies. The compound **23** can also be prepared starting from $BaCl_2$ as the Ba source. The sodium salt of 2-nba was first generated *in situ* by reacting 2-nbaH (1.67 g, 10 mmol) with $NaHCO_3$ (0.84 g, 10 mmol) in water. Into this, an aqueous solution of $BaCl_2.4H_2O$ (1.221 g, 5 mmol) was added and the reaction mixture was filtered and left aside for crystallization. The crystals that separated after a few days were obtained in 81 % yield. The IR spectrum and the DSC thermogram of the product obtained in this method were identical to that of the product obtained using $BaCO_3$ as the Ba source. (Yield: 2.1 g, 81 %).

Analytical data: Calc. for $C_{14}H_{14}BaN_2O_{11}$ (523.61): Ba, 26.33; 2-nbaH, 63.83; C, 32.46; H, 2.7; N 5.41 Found: Ba, 25.50; 2-nbaH, 62.99; C, 31.53; H, 2.49; N 4.91%.

IR (KBr) data: 3730-2922(br), 2833(w), 2525(w), 1815(w), 1594(s), 1566(s), 1552(s), 1537(m), 1523(s), 1512(s), 1504(m), 1478(s), 1440(s), 1404(s), 1393(s), 1347(s), 1308(s), 1265(w), 1248(w), 1144(w), 1076(w), 1037(w), 1013(w), 863(m), 841(s), 786(s), 735(s), 702(s), 679(w), 630(m), 513(s), 428(s) cm^{-1}.

UV-Vis: 274 nm (ε =14000 $L.mol^{-1}.cm^{-1}$)

DSC (in ^{o}C): 88 (endo), 230 (endo), 277 (endo), 338 (exo), 444 (exo)

Preparation of barium bis(2-nitrobenzoate)$[Ba(2\text{-nba})_2]$ 23a

A powdered sample of **23** (0.350 g) was heated on a steam bath for 15 min. This resulted in the formation of the anhydrous compound **23a**. The observed mass loss of 10.5 % is in good agreement with the expected value (10.32 %) for the loss of three moles of water.

IR (KBr) data: 3086(w), 3068(w), 3032(w), 2852(w), 1593(s), 1568(s), 1554(s), 1530(s), 1520(s), 1477(m), 1437(s), 1415(s), 1404(s), 1341(s), 1310(s), 1261(s), 1142(s), 1074(s), 1039(w), 964(w), 862(s), 837(s), 775(s), 780(s), 754(s), 702(s), 648(s), 534(w), 630(m), 432(s) cm^{-1}.

DSC (in ^{o}C): 231 (endo), 272 (endo), 336 (exo), 450 (exo).

Rehydration studies

The anhydrous compound **23a** was prepared from **23** as mentioned above. Equilibration of a powdered sample of **23a** over water vapour resulted in the formation of the starting material **23** in near quantitative yield in about a day. The IR spectra and DSC thermogram of the rehydrated compound is identical to that of **23**.

Preparation of $[Cs_2(H_2O)_2(3\text{-nphth})]_n$ 24

A mixture of cesium carbonate (0.325 g, 10 mmol) and 3-nitrophthalic acid (3-nphtH$_2$) (0.210 g, 10 mmol) was taken in water (25 mL) at room temperature. The reaction was accompanied by strong effervescence. The solution obtained was warmed slightly, filtered and left undisturbed for 9-10 days to obtain colorless crystalline blocks of **24**. The product was filtered, washed thoroughly with ether and air dried. The fine blocks obtained in this method were suitable for X-ray studies. (Yield 0.357g, 75 %)

Analytical data: Calc. for $C_8H_3Cs_2NO_6$ (474.92); C, 20.20; H, 0.64; N, 2.95; Cs_2CO_3, 68.60 Found: C, 18.8; H, 1.5; N, 2.7; Cs_2CO_3, 68.56 %.

IR data: 1656, 1606, 1574 υ_{as}(-COO), 1523 υ_{as}(-NO_2), 1460 υ_{s}(-COO), 1346υ_{s}(-NO_2), 785, 750, 709 cm^{-1}.

DTA (in ^{o}C) : 104 (endo), 480 (exo).

UV- Vis (diffuse reflectance) = 288 nm.

Preparation of $[[Ca(H_2O)_2(3\text{-npth})]\cdot H_2O]_n$ 25 and $[Mg(H_2O)_5(3\text{-npth})]\cdot 2H_2O$ 26

A mixture of calcium or magnesium carbonate (1.0 or 0.84 g, 10 mmol) and 3-nitrophthalic acid (3-nptH$_2$) (2.10 g, 10 mmol) was taken in water (50 mL) and heated on a steam bath. The insoluble metal carbonate slowly started dissolving accompanied with brisk effervescence. Heating was stopped when there was no more evolution of CO_2. At this stage, the reaction mixture was almost clear. The hot solution was filtered and left undisturbed for 9-10 days to obtain colorless crystalline blocks of **26** (Mg) or **25** (Ca) in about 70 % yield. The product was filtered, washed thoroughly with ether and dried. The crystals obtained in this method were suitable for X-ray studies. (Yield **26** (Mg) 2.59 g, 70%; Yield, **25** (Ca), 2.12 g, 70 %)

Analytical data: Calc. for $C_8H_{17}MgNO_{13}$ (372.34) (**26**); C, 26.73; H, 4.77; N, 3.90; MgO, 11.13%. Found: C, 26.89; H, 4.61; N, 3.80; MgO, 12.15

IR (KBr) data: 3558 (υ_{OH}), 3500-3200, 1680, 1568 υ_{as}(-COO), 1537 υ_{as}(-NO_2), 1462, 1379 υ_s(-COO), 1348 υ_s(-NO_2), 1310, 1275, 1153, 1072, 914, 843, 779, 758, 704, 548, 397 cm^{-1}.

DTA (in °C): 125 (endo), 212 (endo), 412 (exo), 568 (exo).

UV-Vis (λ_{max} in H_2O) = 288 nm.

Analytical data: Calc. for $C_8H_9CaNO_9$ (303.24) (**25**); C, 31.69; H, 2.99; N, 4.64; CaO 18.49%. Found: C, 31.72; H, 2.94; N, 4.49; CaO, 19.0 %.

IR (KBr) data: 3604 υ(-OH), 3500-3281, 1651, 1605, 1574 υ_{as}(-COO), 1535 υ_{as}(-NO_2), 1469, 1418 υ_s(-COO), 1387, 1348 υ_s(-NO_2),, 1310, 1275, 1161, 1071, 934, 843, 791, 779, 721, 688, 567 cm^{-1}.

DTA (in °C) : 125 (endo), 428 (exo), 443 (exo).

UV-Vis (diffuse reflectance) = 288 nm.

Preparation of [Ca(3-npth)]$_n$ 25a and [Mg(3-npth)] 26a

A powdered sample of **26** (0.372 g) or **25** (0.303 g) was heated in temperature controlled oven at 130°c for 30 min. This resulted in the formation of the anhydrous compound **26a** or **25a**. The observed mass loss of 33.5 % for **26** and 16.9 % for **25** is in good agreement with the expected value 33.87 % for formation of **26a** and 17.8 for formation of **25a** resulting in the loss of seven and three moles of water in compound **26** and **25** respectively.

Analytical data: Calcd for $C_8H_3MgNO_6$ (233.42) **26a**: MgO 33.87; Found: MgO, 33.5 %.

IR (KBr) data: 3044, 2956, 2916, 2862, 2824, 2784, 1592, 1568 υ_{as}(-COO), 1556, 1520 υ_{as}(-NO_2), 1479, 1437, 1415, 1402 υ_s(-COO), 1338 υ_s(-NO_2), 1309, 1261, 1142, 1075, 1040, 967, 864, 837, 781(s), 754, 700, 648, 536, 428 cm^{-1}.

DTA(in °C) : 412(exo), 568(exo).

Analytical data: Calcd for $C_8H_3CaNO_6$ (249.19) **25a**: CaO, 22.50; Found CaO, 22.01 %

IR (KBr) data: 3045, 1651, 1605, 1574 υ_{as}(-COO), 1535 υ_{as}(-NO_2), 1469, 1418 υ_s(-COO), 1387, 1348 υ_s(-NO_2), 1310, 1275, 1161, 1071, 934, 843, 791, 779, 721, 688, 567 cm^{-1}

DTA(in °C) : 425(exo), 507(exo)

Preparation of [Sr(3-nphth)] 27

A mixture of strontium carbonate (1.47 g, 10 mmol) and 3-nitrophthalic acid (3-nphtH$_2$) (2.10 g, 10 mmol) was taken in water (50 mL) and heated on a steam bath. The insoluble metal carbonate slowly started dissolving accompanied with brisk effervescence. Heating was stopped when there was no more evolution of CO$_2$. The precipitated compound was filtered washed with cold water and then with ether and air dried. (Yield 1.89 g, 64%)

Analytical data: Calc. for $C_8H_3SrNO_6$ (296.73): C, 32.38; H, 1.02; N, 4.72; $SrCO_3$, 49.54. Found: C, 31.0; H, 1.04; N, 4.7; $SrCO_3$, 47.0 %.

IR (KBr) data: 1630, 1575 υ_{as}(-COO), 1547 υ_{as}(-NO$_2$), 1530, 1470, 1410 υ_{ss}(-COO), 1350 υ_{ss}(-NO$_2$), 1161, 1071, 924, 822, 785, 750, 708, 557, 447 cm^{-1}.

DSC (^{o}C): 441 (exo); Residual mass = 47%

UV-Vis (diffuse reflectance) - 288 nm.

Preparation of [Ba(3-nphth)] 28

A mixture of freshly prepared barium carbonate (1.98 g, 10 mmol) and 3-nitrophthalic acid (3-nphtH$_2$) (2.10 g, 10 mmol) was taken in water (50 mL) and heated on a steam bath. The insoluble metal carbonate slowly started dissolving accompanied with brisk effervescence and simultaneous precipitation of compound **28**. Heating was stopped when there was no more evolution of CO$_2$. The colorless compound that separated out was filtered washed with cold water and then with ether and air dried. The product was microcrystalline hence crystals were not suitable for X-ray studies. (Yield 2.47 g, 68%)

Analytical data: Calc. For $C_8H_3BaNO_6$ (346.44): C, 27.74; H, 0.87; N, 4.04; $BaCO_3$, 56.89 Found: C, 28.0; H, 0.88; N, 4.12; $BaCO_3$, 55.28.

IR (KBr): 1620, 1583 υ_{as}(-COO), 1555, 1524 υ_{as}(-NO$_2$), 1456, 1400 υ_{ss}(-COO), 1367, 1342 υ_{ss}(-NO$_2$), 1199, 1157, 1068, 920, 824, 789, 754, 716, 689, 563, 544, 413 cm^{-1}.

DSC (^{o}C): 468 (exo); Residual mass = 61.2

UV- Vis (λ_{max} in H$_2$O) = 288 nm.

Synthesis of [Mg$_3$(H$_2$O)$_{18}$(btc)$_2$] 29

Method 1

1,3,5-benzenetricarboxylic acid (H$_3$btc) (0.42 g, 2 mmol) was dissolved in 50 ml of water and to the clear solution magnesium carbonate (0.252 g, 3 mmol) was added slowly under stirring at room temperature. Strong effervescence was observed during addition of MgCO$_3$. The resulting solution was filtered and kept aside for crystallization. Colorless crystals of $[Mg_3(btc)_2(H_2O)_{18}]$ suitable for X-ray studies were isolated after one week. The crystals isolated were washed with cold water followed by ether and then air dried. (Yield 0.52 g, 74 %)

Method 2

Compound **29** can be also prepared by using magnesium chloride as magnesium source. The trisodium salt of 1,3,5-benzenetricarboxylic acid was prepared by reaction of 1,3,5-benzenetricarboxylic acid (H_3btc) (0.42 g, 2 mmol) with sodium carbonate (0.318 g, 3 mmol) in water (50 ml) at room temperature. To clear solution $MgCl_2.6H_2O$ (0.606 g, 3 mmol) was added under stirring and the resulting clear solution was filtered and kept aside for crystallization. The colorless crystals of $[Mg_3(H_2O)_{18}(btc)_2]$ obtained after ten days were washed with water followed by ether and air dried. (Yield 0.5 g, 71%)

Analytical data: Calc. for $Mg_3C_{18}H_{42}O_{30}$ (811.42) (1): MgO, 14.89; Found: MgO, 14.71.

IR (KBr) data: 3600-3000 (br, υ_{O-H}), 1688 (s), 1607 (s), 1549 (s, υ_{as}(-COO)), 1524 (s), 1480(s), 1433 (s, υ_{ss}(-COO), 1366(s), 1109(s), 760(s), 717(s) cm^{-1}.

DSC data (in °C): 100 (endo), 180 (endo)

UV-Vis (Diffused reflectance): 330 nm

Transformation of $[Mg_3(H_2O)_{18}(btc)_2]$ to $[Mg_3(H_2O)_{12}(btc)_2]$ compound at room temperature

A freshly prepared $[Mg_3(H_2O)_{18}(btc)_2]$ (0.81 g, 1 mmol) compound when exposed to air at room temperature results in the formation of $[Mg_3(H_2O)_{12}(btc)_2]$ (0.70 g, 1 mmol) compound with mass loss of 13.0 % accounting for the expected value of 13.31 % for loss of all the 6 moles of water. This was also confirmed based on the TG-DTA curve observed for the freshly prepared sample.

Analytical data: Calc. for $Mg_3C_{18}H_{30}O_{24}$ (703.33): Mg, 10.37; MgO, 17.19; C, 30.74; H, 4.30; Found: Mg, 10.40; MgO, 17.02; C, 31.35; H, 4.45%.

IR (KBr) data: 3600-3000 (br, υ_{O-H}), 1659(s), 1605 (s), 1518 (s, υ_{as}(-COO)), 1431(s, υ_{ss}(-COO), 1384(s), 1369(s), 1107(s), 970(s), 760(s), 758(s), 710(s), 565(s), 467(s), 397(s) cm^{-1}.

DSC (in °C): 178 (endo), 210 (endo), 599 (exo), 676 (exo). Residue, 25.64%

Preparation of $[Mg_3(btc)_2]$ 29a

However on further heating of $[Mg_3(H_2O)_{12}(btc)_2]$ at 200°C in temperature controlled oven for 5 hr resulted in formation of anhydrous compound $[Mg_3(btc)_2]$ accounting for further loss of remaining 12 moles of water i.e. 28.2 % (expected 30.73 %). However infrared spectrum of the dehydrated sample shows small peak due to rapid absorption of moisture while recording the spectra.

Analytical data: Calc. for $Mg_3C_{18}H_6O_{12}$ (487.15) : MgO, 24.63; Found: MgO, 22.

IR (KBr) data: 3076 (m), 1610 (s), 1562 (s, υ_{as}(-COO)), 1443(s, υ_{ss}(-COO), 1400 (s), 1369 (s), 1221 (s), 1119 (s), 932 (s), 768 (s), 719 (s), 577 (s), 471 (s) cm^{-1}.

DSC (in °C): 601 (exo), 676 (exo). Residue, 27%

Synthesis of $[Ca_3(H_2O)_{12}(btc)_2]$ 30

Method 1

1,3,5-benzenetricarboxylic acid (H_3btc) (0.42 g, 2 mmol) was dissolved in 50 ml of water and to this calcium carbonate (0.30 g, 3 mmol) was added slowly at room temperature. Strong effervescence was observed during addition which ceased completely when all the $CaCO_3$ was added. The resulting solution was filtered and kept aside for crystallization. Fine colorless crystals of $[Ca_3(H_2O)_{12}(btc)_2]$ **30** that separated after 1 hour were isolated and washed with excess of cold water, alcohol followed by ether and then air dried. (Yield, 0.634 g, 86 %)

Method 2

Alternatively this can be also prepared by using calcium chloride as calcium source. The trisodium salt of the acid was prepared by reaction of 1,3,5-benzenetricarboxylic acid (H_3btc) (0.42 g, 2 mmol) with sodium carbonate (0.318 g, 3 mmol) in water (50 ml) at room temperature. To the clear solution $CaCl_2.2H_2O$ (0.441 g, 3 mmol) was added and the resulting solution so obtained was filtered and kept aside for crystallization. Colorless blocks of **30** that separated immediately were filtered and washed with water, alcohol followed by ether and air dried. (Yield, 0.68 g, 91%)

Method 3

The trisodium salt of the acid was prepared by reaction of 1,3,5-benzenetricarboxylic acid (H_3btc) (0.42 g, 2 mmol) with sodium carbonate (0.318 g, 3 mmol) in water (50 ml). To the clear solution calcium acetate (0.475 g, 3 mmol) was added. After 1hr fine colorless crystals of $[Ca_3(H_2O)_{12}(btc)_2]$ **30** were obtained. The isolated needle shaped crystals were washed with excess of cold water and alcohol followed by ether and then air dried. The yield obtained in this method was higher than that obtained using method 1 or 2. (Yield, 0.66, 88 %)

Analytical data: Calc. for $Ca_3C_{18}H_{30}O_{24}$ (750.65) (**30**): Ca, 16.02; CaO, 22.41; C, 28.80; H, 4.03; Found: Ca, 15.80; CaO, 21.93; C, 30.87; H, 5.22 %.

IR (KBr) data: 3600-3000 (br, $\upsilon_{O\text{-}H}$), 1692 (s), 1607(s), 1549 (s, υ_{as}(-COO)), 1445 (s), 1433 (s, υ_{ss}(-COO), 1390(s), 1271(s), 1250(s), 1207(s), 1111(s), 930(s), 856(s), 795(s), 762(s), 729(s), 687(s), 529(s) cm^{-1}.

DSC data (in °C): 131(endo), 593(exo), 610(exo). Residue = 22.29 %.

DTA data (in °C): 146(endo), 558(exo), 627 (exo). Residue = 28 %

UV-Vis (Diffused reflectance): 281 nm.

Preparation of [Ca_3(btc)$_2$] 30a

A [$Ca_3(H_2O)_{12}$(btc)$_2$] (0.750 g 1 mmol) compound when heated at 200°C in a temperature controlled oven for 5 hrs results in the formation of [Ca_3(btc)$_2$] (0.539 g, 1 mmol) compound with mass loss of 28.65 % accounting to the expected value of 28.79 % for loss of all the twelve moles of water. This was also confirmed based on the TG-DTA curve observed for the dehydrated sample. However the infrared spectrum of dehydrated sample shows a small water band due to rapid absorption of moisture during recording.

Analytical data: Calc. for $Ca_3C_{18}H_6O_{12}$ (534.47) (**30a**): CaO, 37.03; Found: CaO, 37.15%

IR (KBr) data: 3057 (m), 2983-2486(br), 1705(m), 1607(s), 1555 (s, υ_{as}-COO), 1433 (s, υ_{ss}-COO), 1368 (s), 1109 (s), 984 (s), 772 (s), 710 (s), 532 (s), 460 (m) cm^{-1}.

DSC data (in °C): 593(exo), 610(exo). Residue = 32.58 %.

DTA data (in °C): 558(exo), 649 (exo). Residue = 38 %

Synthesis of [$Sr_3(H_2O)_8$(btc)$_2$] 31

Method 1

1,3,5-benzenetricarboxylic acid (H_3btc) (0.42 g, 2 mmol) was dissolved in water (50 ml) and to this strontium carbonate (0.443 g, 3 mmol) was added slowly under stirring at ambient temperature. Strong effervescence were observed during addition of $SrCO_3$ to H_3btc solution followed by immediate precipitation of [$Sr_3(H_2O)_8$(btc)$_2$] **31** as fine crystals. The resulting precipitate was filtered as first crop while the filtrate gave colorless crystals of [$Sr_3(H_2O)_8$(btc)$_2$] after 4 days suitable for X-ray studies. The crops were washed with excess of cold water and alcohol followed by ether and then air dried. The total weight of the product (Yield 0.72 g, 87 %)

Method 2

Alternatively this can be also prepared by using strontium chloride as strontium source. The trisodium salt of the acid was prepared by reaction of 1,3,5-benzenetricarboxylic acid (0.42 g, 2 mmol) with sodium carbonate (0.318 g, 3 mmol) in water (50 ml). To the clear solution $SrCl_2.6H_2O$ (0.80 g, 3 mmol) was added and the resulting solution so obtained was filtered and kept aside for crystallization. Colorless precipitate obtained was filtered and washed with cold water alcohol and then with ether and air dried. The filtrate yielded crystals suitable for X-ray crystallography. (Yield 0.68 g, 83 %)

Analytical data: Calc. for $Sr_3C_{18}H_{22}O_{20}$ (821.22) (**31**): $SrCO_3$, 53.93; C, 26.33; H, 2.70; Found: $SrCO_3$, 52.1; C, 26.39; H, 2.46 %.

IR (KBr) data: 3600-3000 (υ_{O-H}), 1697 (s), 1611 (s), 1542 (s, υ_{as}-COO), 1436 (s, υ_{ss}-COO), 1371(s), 1285(s), 1198 (s), 1110 (s), 899 (s), 756 (s), 724 (s), 692 (s), 525 (s) cm^{-1}.

DTA data (in °C): 172 (endo), 210 (endo), 525 (exo), 662 (exo). Residue = 53 %.

UV-Vis (Diffused reflectance): 330 nm.

Preparation of $[Sr_3(btc)_2]$ 31a

A $[Sr_3(H_2O)_8(btc)_2]$ (0.822 g, 1 mmol) compound when heated to 200°C in a temperature controlled oven results in the formation of $[Sr_3(btc)_2]$ **31a** (0.678 g, 1 mmol) compound with mass loss of 17.57 % accounting for the expected loss of 17.54 % for eight moles of water. This was also confirmed based on the TG-DTA curve observed for the dehydrated sample. However the infrared spectrum of the dehydrated sample showed water peak due to rapid absorption of moisture.

Analytical data: Calc. for $Sr_3C_{18}H_6O_{12}$ (677.09) (**31a**): $SrCO_3$, 65.41; Found: $SrCO_3$, 65.01 %.

IR (KBr) data: 3076 (m), 1547 (s, υ_{as}(-COO)), 1440 (s, υ_{ss}(-COO)), 1393 (s), 1368 (s), 1207 (s), 1109 (s), 932 (s), 858 (m), 766 (s), 723 (m), 523 (s) cm^{-1}.

DTA data (in °C): 525(exo), 662(exo). Residue = 64%.

Synthesis of $[Ba_3(H_2O)_8(btc)_2].2H_2O$ 32

Method 1

1,3,5-benzenetricarboxylic acid (H_3btc) (0.42 g, 2 mmol) was dissolved in water (50 ml) and to this freshly prepared barium carbonate (0.59 g, 3 mmol) was added slowly under stirring at room temperature. Strong effervescence was observed during addition of $BaCO_3$ followed by simultaneous precipitation of $[Ba_3(H_2O)_8(btc)_2].2H_2O$ **32** as fine crystals. The fine crystals separated imidiately were filtered washed with cold water, alcohol then with ether. While the filtrate gave colorless crystals of $[Ba_3(H_2O)_8(btc)_2].2H_2O$ suitable for X-ray studies. The crystals isolated were washed with excess of water, alcohol followed by ether and then air dried. (Yield 0.78 g, 78 %)

Method 2

Alternatively this can also be prepared by using barium chloride as barium source. The trisodium salt of acid was prepared by reaction of 1,3,5-benzenetricarboxylic acid (H_3btc) (0.42 g, 2 mmol) with sodium carbonate (0.318 g, 3 mmol) in water (50 ml) under ambient conditions. To the clear solution $BaCl_2.2H_2O$ (0.733 g, 3 mmol) was added and the resulting solution obtained was filtered and kept aside for crystallization. Fine colorless needles that separated after one hour were filtered and washed with water, alcohol and then with ether and air dried. (Yield 0.80 g, 80 %)

Method 3

Trisodium salt of acid was prepared by reaction of 1,3,5-benzenetricarboxylic acid (H_3btc) (0.42 g, 2 mmol) with sodium carbonate (0.318 g, 3 mmol) in water (50 ml) to this barium acetate (0.765 g, 3 mmol) was added under normal laboratory conditions. Fine crystals of $[Ba_3(H_2O)_8(btc)_2].2H_2O$ **32** that separated after one hour were filtered and washed with water, alcohol and then with ether and air dried. However the yield obtained in this method are higher than that obtained using method 1 or 2. (Yield 0.924 g, 92 %)

Analytical data: Calc. for $Ba_3C_{18}H_{26}O_{22}$ *(1006.37)* (**32**): Ba, 40.94; $BaCO_3$, 58.83; C, 21.48; H, 2.60; Found: Ba, 40; $BaCO_3$, 58.12; C, 21.45; H, 2.64 %.

IR (KBr) data: 3600-3000 (υ_{O-H}), 1697(s), 1614(s), 1549 (s, υ_{as}(-COO)), 1433 (s, υ_{ss}(-COO), 1378 (s), 1284(s), 1197(s), 1110(s), 899(s), 792(s), 754(s), 723(s), 692(s), 667(s), 520(s) cm^{-1}.

DSC data (in °C): 100 (endo), 139 (endo), 190 (endo), 570 (exo), Residue, 58.13.

DSC data (in °C): 102(endo), 131(endo), 183(endo), 540(exo). Residue, 55 %.

DTA data (in °C): 148 (endo), 525 (exo), 593 (exo).

UV-Vis (Diffused reflectance): 281 nm.

Preparation of $[Ba_3(btc)_2]$ 32a

$[Ba_3(H_2O)_{10}(btc)_2]$ (1 g, 1 mmol) compound when heated to 200°C in a temperature controlled oven for 5 hrs results in the formation of $[Ba_3(btc)_2]$ (0.820 g, 1 mmol) compound with mass loss of 17.57 % against the expected value of 17.90 % for loss of all the ten moles of water. This was also confirmed based on TG-DTA curve observed for the dehydrated sample. However the infrared spectrum of the dehydrated sample shows presence of moisture due to rapid absorption of moisture during recording.

Analytical data: Calc. for $Ba_3C_{18}H_6O_{12}$ (826.21) (**32a**): $BaCO_3$, 71.65; Found: $BaCO_3$, 72 %.

IR data: 3347(bs), 1603(s), 1543(s, υ_{as}(-COO)), 1433(s, υ_{ss}(-COO)), 1368(s), 1207(s), 1107(s), 932(s), 818(s), 768(s), 721(s), 518(m) cm^{-1}.

DTA data (in °C): 525 (exo), 593(exo).

UV-Vis (Diffused reflectance): 281 nm.

Preparation of $[Ca(H_2O)_2(L_1)_2]\cdot H_2O$ 33, $[Ca(H_2O)_2(L_2)_2]\cdot 2H_2O$ 34

To a slurry of $CaCO_3$ (0.500 g, 5 mmol) in water (50 mL) was added L_1-H (1.66 g, 10 mmol) and the reaction mixture was heated on a water bath. The insoluble $CaCO_3$ slowly started dissolving accompanied by brisk effervescence. Heating was stopped when effervescence ceased completely resulting in the formation of an almost clear solution. The hot reaction mixture was filtered and left undisturbed for 6-7 days to obtain colorless crystalline needles of **33** in 84 % yield, which were filtered, washed with water followed by ether and dried in air. Use of L_2-H (1.7 g, 10 mmol) in the above reaction instead of L_1-H resulted in the formation of **34** in 70 % yields. (Yield 33, 1.7 g, 84 % and Yield 34, 1.57 g, 70 %)

Anaytical data: Calc. for $CaC_{18}H_{24}O_9$ (424.46) **33**: Ca, 9.44, C, 50.93, H, 5.70, CaO, 13.19 Found: Ca, 9.4; C, 50.92; H, 5.79; CaO, 13.28%.

IR (KBr) data: 3610 υ(-OH), 3427, 3001, 2961, 2928, 2838, 2050, 1612, 1567 υ_{as}(-COO), 1546, 1512, 1444, 1416, 1401 υ_s(-COO), 1287, 1250 υ_{as}(-COC-), 1201, 1177, 1153, 1105, 1036, 950, 926, 824, 790, 736, 696, 627, 600, 543 cm^{-1}.

DTA (in °C): 116 (endo), 375 (exo) 492 (exo).

Analytical data Calc. for $CaC_{16}H_{20}Cl_2O_8$ (451.31) **34**: Ca, 8.88; C, 42.58; H, 4.47; CaO, 12.42; Found: Ca, 8.5; C, 42.5; H, 4.40; CaO, 12.3.

IR (KBr) data: 3636 υ(-OH), 3326, 3062, 1618, 1556 υ_{as}(-COO), 1500, 1452, 1431, 1402 υ_s(-COO), 1292, 1146, 1076, 1031, 939, 842, 733, 706, 695, 659 cm^{-1}.

DTA (in °C) : 121 (endo), 318 (exo), 588 (exo).

Prepartion of [Ca(L_1)$_2$] 33a, [Ca(L_2)$_2$] 34a rehydration studies

An amount of a powdered sample (0.500 g) of **33** or **34** was heated at 130 °C for 15 min. The observed mass losses of 12.65 % (for **33**) and 15.57 % (for **34**) are in good agreement with the expected value for the formation of the anhydrous compounds [Ca(L_1)$_2$] **33a** or [Ca(L_2)$_2$] **34a**.

Analytical data: Calc. for $CaC_{18}H_{18}O_6$ (370.41) **33a**; CaO, 15.14; Found; CaO, 15.02%.

IR (KBr) data - 3000, 2953, 2934, 2910, 2833, 1551 υ_{as}(-COO), 1512, 1429, 1406 υ_s(-COO), 1300, 1279, 1248, 1177, 1105, 1036, 947, 818, 799, 729, 696 cm^{-1}.

Analytical data: Calc. for $CaC_{16}H_{12}Cl_2O_4$ (379.25) **34a**: CaO, 14.79. Found; CaO, 14.63%

IR (KBr) data; 3066, 1566, 1556 υ_{as}(-COO), 1474, 1425, 1396 υ_s(-COO), 1302, 1269, 1177, 1122, 1053, 1040, 934, 843, 743, 687, 619, 577 cm^{-1}.

Preparation of [Ca(H_2O)$_2$(L)$_2$]·H_2O 35

Phenylacetic acid (LH) (1.36 g, 10 mmol) and $CaCO_3$ (0.5 g, 5 mmol) was taken in beaker containing water (50 ml) and heated over steam bath until clear solution was obtained, filtered and kept aside for crystallization. Alternatively **35** can be also prepared by using $CaCl_2$ as calcium source. The sodium salt of acid was first generated in-situ by reacting LH (1.36 g, 10 mmol) with $NaHCO_3$ (0.84 g, 10 mmol) in water (50 ml). This solution was filtered into the aqueous solution of calcium chloride dihydrate (0.74 g, 5 mmol). (Yield 1.6 g, 85 %).

Analytical data: Calc. for $CaC_{16}H_{20}O_7$ (364.40) **35**: Ca, 11; C, 52.74; H, 5.53; CaO, 15.39; Found: Ca, 11.0; C, 52.62; H, 5.44; CaO, 15.35.

IR (KBr) data: 3600 υ(-OH), 3063, 1954, 1881, 1808, 1618, 1545 υ_{as}(-COO), 1495, 1452, 1427, 1402 υ_s(-COO), 1293, 1177, 1153, 1076, 939, 842, 733, 706, 695, 659 cm^{-1}.

DSC (°C): 125 (endo), 521 (exo).

Preparation of [Ca(L)$_2$] 35a

Compound **35a** is prepared by heating compound **35** at 130°C for 15 minutes. The observed mass loss of 14.67 % is in good agreement for expected value of 14.82 %.

Analytical data: Calc. for $CaC_{16}H_{14}O_4$ (310.36) **35a**: Ca, 12.91; C, 61.92; H, 4.55; CaO, 18.07; Found; CaO, 17.81 %

IR (KBr) data: 3084, 3061, 3028, 1554 υ_{as}(-COO), 1495, 1421, 1402 υ_{ss}(-COO), 1288, 1163, 1074, 1029, 945, 729, 706, 696, 620, 656 cm^{-1}.

DSC data (°C): 513 (exo).

Preparation $[Ba(H_2O)_4(L_2)_2]_n$ 36

2-Chlorophenylacetic acid (L_2H) (3.4 g, 2 mmol) was taken in water (50 ml) and heated over steam bath to this freshly prepared barium carbonate (1.97 g, 1 mmol) was added slowly under stirring. Strong effervescence was observed during addition of $BaCO_3$ to the solution. Reaction was stopped when all the acid dissolved and efferevescence ceased completely. The fine crystals that separated after 10 days were filtered washed with cold water, alcohol then with ether and air dried. (Yield 3.0 g, 60 %).

Analytical data: Calc. for $BaC_{16}H_{26}O_{11}Cl_2$ (602.60) (**36**): $BaCO_3$, 32.74; C, 31.89; H, 4.35; Found: $BaCO_3$, 31.70; C, 31.2; H, 4.30 %.

IR (KBr) data: 3634-3279 (br, υ-OH), 1593, 1572, 1549 (s, $υ_{as}$-COO), 1445, 1392 (s, $υ_{ss}$-COO), 1365, 1288, 1267, 1159, 1125, 935, 746 (s), 679, 646, 515 cm^{-1}.

DTA data (in °C): 126 (endo), 510 (exo)

Preparation $[Mg(H_2O)_6(5\text{-niphth})]$ 37

5-nitroisophthalic acid (5-niphthH) (0.422 g, 20 mmol) was taken in a beaker containing 50 ml of water and heated over steam bath. To the hot solution $MgCO_3$ (0.168 g, 20 mmol) was added slowly under stiring, strong efferevescence were observed during addition which ceased completely after 1 hrs of heating. The hot reaction mixture was filtered and the clear solution obtained was kept aside for crystallization. Colourless crystals isolated after several days were filtered, washed with cold water and then with ether and air dried. (Yield = 0.35 g, 57 %)

Analytical data: Calc. for $MgC_8H_{13}NO_{11}$ (323.49) (**37**): Mg, 7.51; MgO, 12.45; C, 29.70; H, 4.05; N, 4.33 Found: Mg, 7.5; MgO, 12.46; C, 29.01; H, 4.02, N, 4.31%.

IR (KBr) data: 3634-3099 (br, υ-OH), 1641, 1602, 1556 (s, $υ_{as}$-COO), 1524 (s, $υ_{as}NO_2$), 1454, 1369 (s, $υ_{ss}$-COO), 1350 (s, $υ_{as}NO_2$), 1093, 929, 795, 737, 716 , 627, 390 cm^{-1}.

DTA data (in °C): 184 (endo), 483 (exo), 566 (exo)

Preparation $[Ca(H_2O)_4(5\text{-niphth})]$ 38

5-nitroisophthalic acid (0.422 g, 20 mmol) was taken in a beaker containing 50 ml of water and heated over steam bath. To the hot solution $CaCO_3$ (0.20 g, 20 mmol) was added slowly under stiring, strong efferevescence were observed during addition which ceased completely after 1 hrs of heating. The hot reaction mixture was filtered and the clear solution obtained was kept aside for crystallization. Colourless crystals isolated after several days were filtered, washed with cold water and then with ether and air dried. (Yield = 0.30 g, 46 %)

Analytical data: Calc. for $CaC_8H_{11}O_{10}N$ (321.25) (**38**): Ca, 12.48; CaO, 17.45; C, 29.91; H, 3.45; N, 4.36 Found: Ca, 12.40; CaO, 18.08; C, 29.9; H, 2.9; N, 4.3 %.

IR data: 3600-3096 (br, υ-OH), 1674, 1631, 1606, 1572 (s, υ_{as}-COO), 1535 (s, $\upsilon_{as}NO_2$), 1448, 1388 (s, υ_{ss}-COO), 1346 (s, $\upsilon_{as}NO_2$), 1205, 1088, 924, 789, 733, 532, 507 cm^{-1}.

DTA data (in °C): 149 (endo), 452(exo), 550 (exo)

Preparation $[Mg(H_2O)_6(hip)_2]$ 39

Hippuric acid (0.90 g, 5 mmol) was taken in a beaker containing 25 ml of water and to this $NaHCO_3$ (0.42 g, 5 mmol) was added slowly under stiring and warmed slightly. To the hot reaction mixture $MgNO_3.6H_2O$ (0.64 g, 2.5 mmol) was added and the clear solution obtained was kept aside for crystallization. Colourless crystals isolated after several days were filtered, washed with cold water and then with ether and air dried. (Yield = 0.62 g, 64 %)

Analytical data: Calc. for $MgC_{18}H_{28}N_2O_{12}$ (488.73) (**39**): Mg, 4.97; MgO, 8.24; C, 44.24; H, 5.77; N, 5.73 Found: Mg, 4.9; MgO, 8.19; C, 44.2; H, 5.67, N, 5.77 %.

IR (KBr) data: 3600-3100 (br, υ-OH), 1632, 1602 (s, υ_{as}-CONH), 1577, 1550 (s, υ_{as}-COO), 1489, 1433, 1406 (s, υ_{ss}-COO), 1256, 1186, 1076, 1007, 926, 725, 689 cm^{-1}.

DTA data (in °C): 105 (endo), 421 (exo).

Preparation $[Sr(hip)_2(H_2O)_4]$ 40

Hippuric acid (0.90 g, 5 mmol) was taken in a beaker containing 25 ml of water and to this $NaHCO_3$ (0.42 g, 5 mmol) was added slowly under stiring and warmed slightly. To the hot reaction mixture $SrCl_2.6H_2O$ (0.665 g, 2.5 mmol) was added and the clear solution obtained was kept aside for crystallization. Colourless plate like crystals isolated after several days were filtered, washed with cold water and then with ether and air dried. (Yield = 0.72 g, 69 %)

Analytical data: Calc. for $SrC_{18}H_{24}N_2O_{10}$ (516.01) (**40**): $SrCO_3$, 28.61; C, 41.90; H, 4.69; N, 5.43 Found: $SrCO_3$, 28.69; C, 42.2; H, 5.10, N, 5.41 %.

IR (KBr) data: 3600-3203 (br, υ-OH), 1643 (s, υ_{as}-CONH), 1574 (s, υ_{as}-COO), 1553, 1489, 1437, 1408 (s, υ_{ss}-COO), 1306, 1254, 1185, 1167, 1074, 1011, 1005, 926, 840, 729, 686, 561 cm^{-1}.

DTA data (in °C): 130 (endo), 539 (exo)

Chapter 3

CHAPTER - 3

Results and discussions

This chapter describes the synthetic aspects, reactivity characteristics, spectral, thermal and structural aspects of the synthesized metal carboxylate complexes. The synthesized complexes were studied by a variety of chemical and analytical techniques and the results of these investigations are described. The characterization techniques which include various elemental analysis (C, H, N), Infrared (IR), ^{1}H NMR, UV-Vis spectroscopy, Thermogravimetry, Differential scanning calorimetry (DSC), DTA (Differential thermal analysis), BET Surface area, X-ray diffraction.

3.1 Synthetic Aspects and reactivity characteristics

Metal carboxylates can be prepared by reacting the corresponding alkali or alkaline earth metal carbonate with aromatic (mono, di, tri) carboxylic acids.

The general reaction for the formation of the complexes can be represented as below.

$$M_2CO_3 + 2\,ArCOOH \xrightarrow[\Delta]{H_2O} 2\,[M(H_2O)_x(ArCOO)] \qquad \text{Eq. 3.1}$$

Where M = Li, Na, K, Rb, Cs

$$MCO_3 + 2\,ArCOOH \xrightarrow[\Delta]{H_2O} [M(H_2O)_x(ArCOO)_2] \qquad \text{Eq. 3.2}$$

Where M = Mg, Ca, Sr, Ba

The use of an carbonate is advantageous for synthesis of metal carboxylates as slight excess of insoluble carbonate can be used to ensure complete consumption of the carboxylic acid and the excess of unreacted metal carbonate can be easily filtered off.

The use of freshly prepared metal carbonates instead of commercial carbonate reduces the duration of reaction appreciably. In this methodology, the metal carbonate generated *in-situ* is directly reacted with carboxylic acid. The general reaction can be written as follows. This strategy was employed for synthesis of Ba compounds.

$$MCl_2.xH_2O + Na_2CO_3 \xrightarrow{H_2O} MCO_3 + 2\,NaCl \qquad \text{Eq. 3.3}$$

$$MCO_3 + 2\,ArCOOH \xrightarrow[\Delta]{H_2O} [M(H_2O)_x(ArCOO)_2] \qquad \text{Eq. 3.4}$$

Where M = Mg, Ca, Sr, Ba

In addition metal chlorides were reacted with *in-situ* generated sodium salt of aromatic acid. In this method the reactions were performed at room temperature, the chloride ions remain in solution as highly soluble NaCl and the less soluble carboxylate crystallizes out in good yields and the product of formation can be represented as follows.

$$MCl_2.xH_2O + 2\,[ArCOOH + NaHCO_3] \xrightarrow{H_2O} [M(H_2O)_x(ArCOO)_2] + 2NaCl \qquad \text{Eq. 3.5}$$

Where M = Mg, Ca, Sr, Ba

The list of compounds prepared and properties like appearance and obtained yields are summarized in Table 1.

Table 1 - Physical properties and yields of synthesized *s*-block metal carboxylates

Sr. No.	Compound	Appearance	Yield in %
1	$[Ca(H_2O)_4(4\text{-}nba)_2]$ **1**	Colorless crystals	90
2	$[Ca(4\text{-}nba)_2(N\text{-}MeIm)]_n$ **2**	Colorless crystals	98
3	$[Ca(4\text{-}nba)_2(Im)]_n$**3**	Colorless powder	98
4	$[Ca(H_2O)(4\text{-}nba)_2(2\text{-}MeIm)]_n$**4**	Pale yellow crystals	98
5	$[Ca(4\text{-}nba)_2(pyr)_2]_n$ **5**	Colorless crystals	80
6	$[[Ca(H_2O)_2(4\text{-}nba)_2].(dmp)_2]_n$ **6**	Colorless crystals	80
7	$[Ca(H_2O)_6(4\text{-}nba)(2\text{-}ap)](4\text{-}nba)(2\text{-}ap)$ **7**	Pale yellow crystals	77
8	$[(H_2O)_4Li_2(\mu\text{-}H_2O)_2](4\text{-}nba)_2$ **8**	Colorless powder	68
9	$[Na(4\text{-}nba)(H_2O)_3]_n$ **9**	Colorless crystals	70
10	$[K(4\text{-}nba)(H_2O)_2]$ **10**	Colorless crystals	62
11	$[Sr(H_2O)_7(4\text{-}nba)](4\text{-}nba).2H_2O$ **11**	Colorless crystals	78
12	$[[Sr(H_2O)_3(4\text{-}nba)(dmf)].(4\text{-}nba)]_n$ **12**	Colorless crystals	69
13	$[Sr(H_2O)(4\text{-}nba)_2(nmf)_{1.5}]_n$ **13**	Colorless crystals	69
14	$[Sr(4\text{-}nba)_2(pyr)_2]_n$ **14**	Colorless crystals	79
15	$[Sr(H_2O)_3(4\text{-}nba)_2(HCONH_2)]_n$ **15**	Colorless crystals	50
16	$[Mg(H_2O)_6(2\text{-}ca\text{-}4\text{-}nba)_2]$ **16**	Yellow crystals	70
17	$[Ca(H_2O)_2(2\text{-}ca\text{-}4\text{-}nba)_2]_n$ **17**	Yellow crystals	75
18	$[Ba(H_2O)_2(2\text{-}ca\text{-}4\text{-}nba)_2]$ **18**	Yellow powder	72
19	$[Sr(2\text{-}ca\text{-}4\text{-}nba)_2]$ **19**	Yellow powder	79
20	$[Mg(H_2O)_4(2\text{-}nba)_2]$ **20**	Pale yellow crystals	70
21	$[Ca(H_2O)_2(2\text{-}nba)_2]_n$ **21**	Pale yellow crystals	71
22	$[Ba(H_2O)_3(2\text{-}nba)_2]_n$ **22**	Pale yellow crystals	81
23	$[Sr(H_2O)_4(2\text{-}nba)_2]$ **23**	Pale yellow crystals	73
24	$[Cs_2(H_2O)_5(3\text{-}npth)]$ **24**	Colorless crystals	70

25	$[Mg(H_2O)_5(3\text{-npth})].2H_2O$ **25**	Colorless crystals	70
26	$[[Ca(H_2O)_2(3\text{-npth})].H_2O]_n$ **26**	Colorless crystals	70
27	$[Ba(3\text{-npth})]_n$ **27**	Colorless powder	68
28	$[Sr(3\text{-npth})]_n$ **28**	Colorless powder	64
29	$[Mg_3(H_2O)_{18}(btc)_2]$ **29**	Colorless crystals	74
30	$[Ca_3(H_2O)_{12}(btc)_2]_n$ **30**	Colorless crystals	86
31	$[Sr_3(H_2O)_8(btc)_2]_n$ **31**	Colorless powder	87
32	$[[Ba_3(H_2O)_8(btc)_2].2H_2O]_n$ **32**	Colorless crystals	78
33	$[Ca(H_2O)_2(4\text{-OMephac})_2].H_2O$ **33**	Colorless crystals	84
34	$[[Ca(H_2O)_2(2\text{-Clphac})_2].2H_2O]_n$ **34**	Colorless crystals	70
35	$[Ca(H_2O)_3(phac)_2].H_2O$ **35**	Colorless crystals	85
36	$[Ba(H_2O)_2(2\text{-Clphac})_2]_n$ **36**	Colorless crystals	60
37	$[Mg(H_2O)_6(5\text{-niphth})]$ **37**	Colorless crystals	57
38	$[Ca(H_2O)_4(5\text{-niphth})]$ **38**	Colorless crystals	46
39	$[Mg(hippurate)_2(H_2O)_6]$ **39**	Colorless crystals	64
40	$[Sr(hippurate)_2(H_2O)_4]$ **40**	Colorless crystals	69

All compounds synthesized were stable in air, Heating of the above compounds at temperatures > 100°C results in the formation of its anhydrous phases in quantitative yields.

3.2 Reactivity studies of synthesized compounds

3.2.1 Synthetic and reactivity aspects of $[Ca(H_2O)_4(4\text{-nba})_2]$ 1

Metal carboxylates can be prepared by direct reaction of freshly prepared metal oxide with carboxylic acid. Based on this principle we have developed a facile method for the synthesis of $[Ca(H_2O)_4(4\text{-nba})_2]$ **1**. This method involves direct reaction of a slurry of 4-nbaH in water with freshly prepared CaO (Scheme 1). Use of CaO affords the synthesis of **1** in high yields in a very short time period, unlike the earlier reported method [63] using $CaCO_3$ where the reaction of commercial $CaCO_3$ with aqueous 4-nbaH as well as crystallization of **1** required longer time duration. Thermal behaviour of **1** (Scheme 1) to form $[Ca(H_2O)(4\text{-nba})_2]$ **1a** with loss of three moles of water (weight loss = 12.16%) on heating at 100°C, serves as a sensitive and useful method for the convenient identification of **1**. Reaction of 4-nbaH with $CaCO_3$ under microwave conditions also resulted in the formation of compound **1** in 90 % yield in about 20 minutes. The infrared and thermal data of isolated compound by this method was found to be identical to that of **1** and showed similar properties.

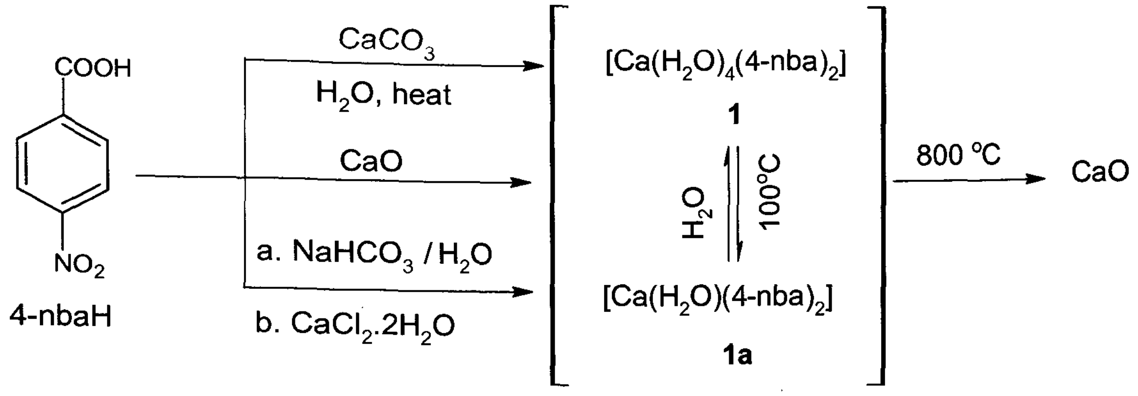

Scheme 1- Modified method for synthesis of $[Ca(H_2O)_4(4\text{-nba})_2]$ **1** using $CaCO_3$/CaO/microwave technique.

Heating of a solid sample of the tetrahydrate $[Ca(H_2O)_4(4\text{-nba})_2]$ **1** at 100°C resulted in the loss of three moles of water leading to the formation of a monohydrate $[Ca(H_2O)(4\text{-nba})_2]$ **1a** (Scheme 1). On exposure to moisture the monohydrate rapidly transforms into the seven coordinated starting material **1**. This property of compound **1** was investigated and new mixed ligand compounds $[Ca(4\text{-nba})_2(N\text{-MeIm})]_n$ **2**, $[Ca(4\text{-nba})_2(Im)]_n$ **3**, $[Ca(H_2O)(4\text{-nba})_2(2\text{-MeIm})]_n$ **4**, $[Ca(4\text{-nba})_2(pyr)_2]_n$ **5**, $[[Ca(H_2O)_2(4\text{-nba})_2].(dmp)_2]_n$ **6**, $[Ca(H_2O)_6(4\text{-nba})(2\text{-ap})](4\text{-nba})(2\text{-ap})$ **7** were synthesized. The reaction of N-MeIm or Im with the monohydrate **1a** results in the displacement of water by the N-donor ligands and the formation of anhydrous mixed ligand compounds **2** or **3** having molar composition of Ca:4-nba:N-MeIm(Im) 1:2:1 (Scheme 2). The use of excess N-MeIm or Im in the thermal reaction did not result in the formation of new products containing additional N-donor ligands. The anhydrous mixed ligand compounds **2** or **3** can also be synthesized in a single step by directly heating a mixture of powdered sample of **1** and N-MeIm in a 1:1 mole ratio. The solid state reaction of an intimate mixture of the tetraaqua compound **1** and 2-methylimidazole (2-MeIm) at 100°C resulted in the formation of the mixed ligand Ca(II) compound $[Ca(H_2O)(2\text{-MeIm})(4\text{-nba})_2]$ **4** in quantitative yield (Scheme 2). The use of excess 2-MeIm in the thermal reaction did not result in the formation of new products containing additional N-donor ligands. Also the reaction of 2-MeIm with **1a** at 100°C afforded the new compound **4**, which is insoluble in all common solvents like water, CH_3CN, CH_2Cl_2, etc. Crystals of **2** and **4** suitable for structure determination were prepared by heating a mixture of **1** and excess N-MeIm or 2-MeIm at 100°C followed by recrystallisation from minimum quantity of water. Similar attempts to prepare compound **3** in crystalline form suitable for X-ray structure determination by solution method always resulted in the formation of the known monomeric compound $[Ca(H_2O)_3(Im)(\eta^1\text{-}4\text{-}$

nba)$_2$]·Im [175]. Compounds **2**, **3** and **4** are relatively stable compared to the moisture sensitive monohydrate **1a**.

The reaction of the monohydrate **1a** with pyrazole (pyr) afforded the anhydrous compound **5** in good yield. Crystals suitable for X-ray structure were prepared by recrystallizing from an aqueous solution in the presence of excess pyrazole. The mixed ligand compound **5** could also be prepared by a direct reaction of an intimate mixture of [Ca(H$_2$O)$_4$(4-nba)$_2$] **1** with pyr (Scheme 2). It is interesting to note that the use of pyrazole which is a positional isomer of Im has resulted in the formation of an anhydrous compound with a Ca:N-donor ligand (pyr) in a 1:2 ratio. The reaction of compound **1** with an excess of 3,5-dimethylpyrazole results in the formation of a new Ca(II) coordination polymer **6**. Analytical data of **5** indicates Ca:4-nba:pyr in 1:2:2 ratio while **6** shows the presence of Ca:4-nba:dmp:water in a 1:2:2:2 ratio.

The aminopyridines are both water and organic soluble and hence, were employed for the formation of new compounds in this study by reaction with [Ca(H$_2$O)$_4$(4-nba)$_2$] **1** in the solid state or in aqueous solution. Reaction of a solid 1:1 mixture of **1** and 2-aminopyridine at 100°C resulted in the formation of the anhydrous compound [Ca(2-ap)(4-nba)$_2$] **7-a** in near quantitative yields (Scheme 2). The presence of free or unreacted 2-ap can be easily ruled out as no free 2-ap was recovered on washing of compound **7-a** with ether. Alternatively, **7-a** was prepared by first heating **1** at 100°C for 15 min to form the reactive monohydrate [Ca(H$_2$O)(4-nba)$_2$] and then adding 2-ap. However under identical conditions, reaction of 4-ap with [Ca(H$_2$O)$_4$(4-nba)$_2$] resulted in the formation of [Ca(H$_2$O)(4-nba)$_2$] and unreacted 4-ap which could be separated from the monohydrate by washing with ether in which 4-ap dissolves while the monohydrate remains insoluble. The reaction of [Ca(H$_2$O)$_4$(4-nba)$_2$] **1** was investigated in aqueous solution in the presence of excess 2-ap and 4-ap (Ca:aminopyridine = 1:4). With 4-ap, only the starting material [Ca(H$_2$O)$_4$(4-nba)$_2$] could be recovered as evidenced by the IR spectrum and weight loss study of the product at 100°C. Interestingly, the aqueous reaction of **1** with 2-ap resulted in the formation of a crystalline material **7** which is quite different from that of the product of the solid state reaction, namely, **7-a**. The different nature of **7-a** and **7** can be readily evidenced from the spectral, analytical and thermal data. The crystalline material **7** exhibits a weight loss of 16.2% at 100 °C indicating that it was not the starting material **1**. Further, the large weight loss is indicative of the probable presence of more water in **7** than in **1**. Analytical data of **7** reveals a Ca:4-nba:2-ap:water in 1:2:1:7 ratio. The presence of seven moles of water in **7** can be accounted for by six coordinated water molecules and a lattice water based on the single crystal data (vide infra). Compound **7** can be fully dehydrated by heating at 120°C leading to the formation of **7-a**, while **7-a** can be converted to **7** on exposure to moisture under controlled conditions. Both **7-a** and **7** can be converted to **1** by stirring in excess water (Scheme 2). The thermal reaction of **1** was investigated with other N-donor ligands like pyridine (pKa 5.1), benzimidazole (pKa 5.4) and 4-picoline (pKa 6.02). However from these reactions no new product containing N-donor ligand could be obtained. In all these cases the product obtained consisted of a mixture of $[Ca(H_2O)(4\text{-nba})_2]$ and unreacted N-donor ligand. The unreacted ligand could be quantitatively recovered by washing the mixture with ether. The non-incorporation of N-donor ligand can be attributed to the less basic nature of benzimidazole and the pyridine ligands as compared to N-MeIm (pKa 7.1) or 2-MeIm (pKa 7.75). Pyrolysis of all **1-7** compounds as well as intermediates resulted in the formation of binary oxide, while reaction with dilute HCl results in decomposition leading to the quantitative formation of insoluble 4-nbaH which can be filtered and weighed. The composition of all the compounds was arrived at based on elemental analysis, 4-nbaH content obtained by acidification and CaO formed on pyrolysis and weight loss studies. It is to be noted that, all the compounds **1-7** can be transformed to **1** by suspending them in water overnight or alternatively by heating respective compounds in water (Scheme 2).

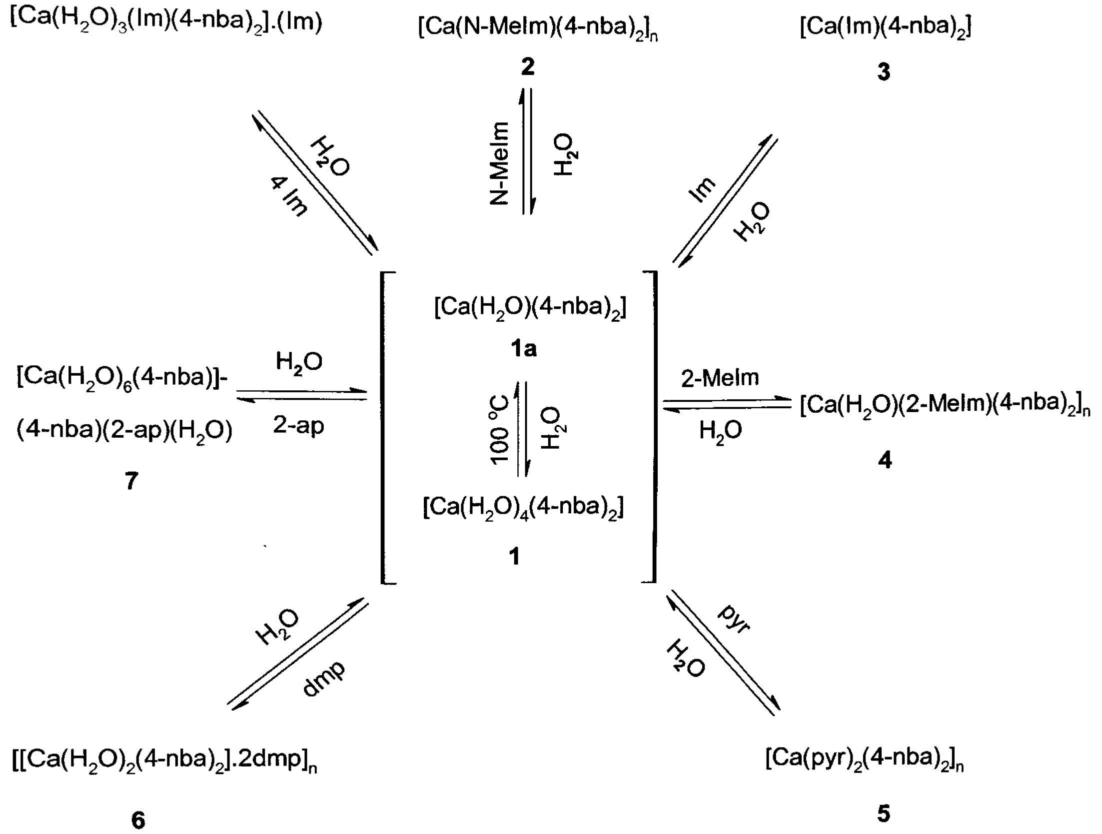

Scheme 2 - Reactions of $[Ca(H_2O)_4(4\text{-nba})_2]$ **1** with N-donor ligands

3.3.2- Synthetic aspects of $[(H_2O)_4Li_2(\mu\text{-}H_2O)_2](4\text{-nba})_2$ 8, $[Na(4\text{-nba})(H_2O)_3]$ 9 and $[K(4\text{-nba})(H_2O)_2]$ 10

The insoluble acid 4-nbaH was dissolved by heating with an aqueous alkali metal carbonate M_2CO_3 (M = Li or Na and K) solution to afford in good yields the alkali metal 4-nitrobenzoates $[(H_2O)_4Li_2(\mu\text{-}H_2O)_2](4\text{-nba})_2$ **8**, $[Na(4\text{-nba})(H_2O)_3]$ **9** and $[K(4\text{-nba})(H_2O)_2]$ **10** (Eq. 3.1). The unit cell parameters of a trihydrate of Li(I) charge balanced by 4-nba, with no details on compound synthesis, were reported by Prabhakar *et al* [201]. More recently the synthesis of anhydrous [M(4-nba)] (M = Li or Na) by an aqueous reaction of MOH with 4-nbaH followed by removal of solvent under reduced pressure, has been reported by Regulska *et al* [202]. For synthesis of compound **9**, $NaHCO_3$ can also be used instead of Na_2CO_3. Compounds **8**, **9** and **10** which were isolated from a neutral reaction mixture are freely water soluble but unstable in acidic medium. On reaction with dilute HCl compounds **8**, **9** and **10** decomposes forming quantitatively 4-nbaH, the insoluble nature of which provides a convenient method for the gravimetric analysis of **8**, **9** and **10**. The composition of **8**, **9** and **10** was arrived at based on elemental analysis, and the 4-nbaH content obtained by acidification. Analytical data of **8**, **9** reveals the presence of three moles of water per mole of alkali metal while compound **9** contains two moles of water. The presence of water in all the three compounds was also confirmed based on their characteristic infrared spectra in the O-H region and weight loss studies on heating at 130°C. Presence of three moles of water in **8**, **9** and two moles in **10** is evidenced by mass loss of 24.0% (in **8**), 21.98% (in **9**) and 14.92% (in **10**) respectively.

3.2.3 - Reactivity studies of $[Sr(H_2O)_7(4\text{-nba})].2H_2O.(4\text{-nba})$ 11

The reaction of 4-nitrobenzoic acid with $SrCO_3$ or $SrCl_2.6H_2O$ results in the formation of zero dimensional compound $[Sr(H_2O)_7(4\text{-nba})](4\text{-nba}).2H_2O$ **11** as reported earlier $[Sr(H_2O)_7(4\text{-nba})](4\text{-nba}).2H_2O$ [177]. Unlike the monomeric $[Ca(H_2O)_4(4\text{-nba})_2]$ **1** which results in formation of monohydrate at 100°C, the monomeric $[Sr(4\text{-nba})(H_2O)_7](4\text{-nba}).2H_2O$ **11** losses 5 moles of water under ambient conditions overnight leading to the formation of intermediate tetrahydrate compound mainly $[Sr(H_2O)_4(4\text{-nba})_2]$ **11a**. This unusual property of compound **11** has been thoroughly investigated and its reactivity with some of the O-donor and N-donor compounds was studied (Scheme 3). The compound **11** or its tetrahydrate **11a** when reacted with O-donor ligands like dimethylformamide (dmf), N-methylformamide (nmf) or formamide at 100°C results in the formation of a new coordination polymer mainly $[Sr(4\text{-nba})(dmf)(H_2O)_3](4\text{-nba})$ **12**, $[Sr(H_2O)(4\text{-nba})_2(nmf)_{1.5}]$ **13**, and $[Sr(H_2O)_3(4\text{-nba})_2(HCONH_2)]$ **15** while its reaction with N-donor ligand like pyrazole (pyr) results in formation of $[Sr(4\text{-nba})_2(pyr)_2]$ **14** coordination polymer. However when **11** or **11a** is heated at 130°C for 30 minutes it results in the formation of the anhydrous compound $[Sr(4\text{-nba})_2]$. Both **11a** and anhydrous $[Sr(4\text{-nba})_2]$ phase get reversibly hydrated to the starting compound **11** on exposure to water vapour. Further the freshly prepared compound **11** or **11a** when dissolved in excess of O-donor solvents like N,N-dimethylformamide (dmf) or N-methylformamide (nmf) or formamide at room temperature results in the formation of new compounds $[Sr(H_2O)_3(4\text{-nba})(dmf)](4\text{-nba})$ **12**, $[Sr(H_2O)(4\text{-nba})_2(nmf)_{1.5}]$ **13**, and $[Sr(H_2O)_3(4\text{-nba})_2(HCONH_2)]$ **15** respectively. Compound **12**, **13** and **15** can be also prepared by reaction of 4-nbaH with $SrCl_2.6H_2O$ in presence of mixture of solvent (water/dmf) for compound **12** and (water/nmf) for **13** and (water/$HCONH_2$) for compound **15** with a mild base like triethylamine. However reaction of **11** or **11a** with neutral N-donor ligand like pyrazole resulted in the formation of a anhydrous Sr(II) coordination polymer $[Sr(4\text{-nba})_2(pyr)_2]$ **14** as shown in (Scheme 3). A comparison of the X-ray powder pattern of starting material **11** or **11a** with the products namely **12**, **13**, **14** and **15** revealed the formation of a new crystalline phase. Thermal and analytical data provide additional evidence for the formation of compounds **12, 13, 14** or **15**. Pyrolysis of compounds **11-15** leads to the formation of $SrCO_3$ as the final product, while the reaction with dilute HCl results in decomposition leading to the quantitative formation of insoluble 4-nbaH, which was filtered and weighed as described earlier [200]. The composition of all the compounds was arrived based on the elemental analysis, 4-nbaH content obtained by acidification and formation of $SrCO_3$ on pyrolysis and weight loss studies. Compounds **12-15** when heated in excess of water get transformed to starting compound **11**. Analytical data indicates the presence of Sr:4-nba: (dmf/nmf/pyr/$HCONH_2$):water in a 1:2:1:1 ratio in compounds **12** and **15** while **13** indicates 1:2:1.5:1 and **14** shows 1:2:2:0 respectively.

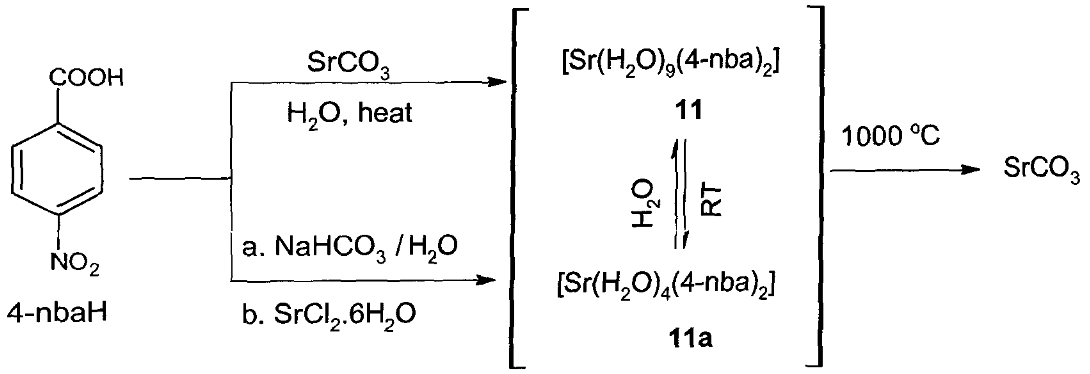

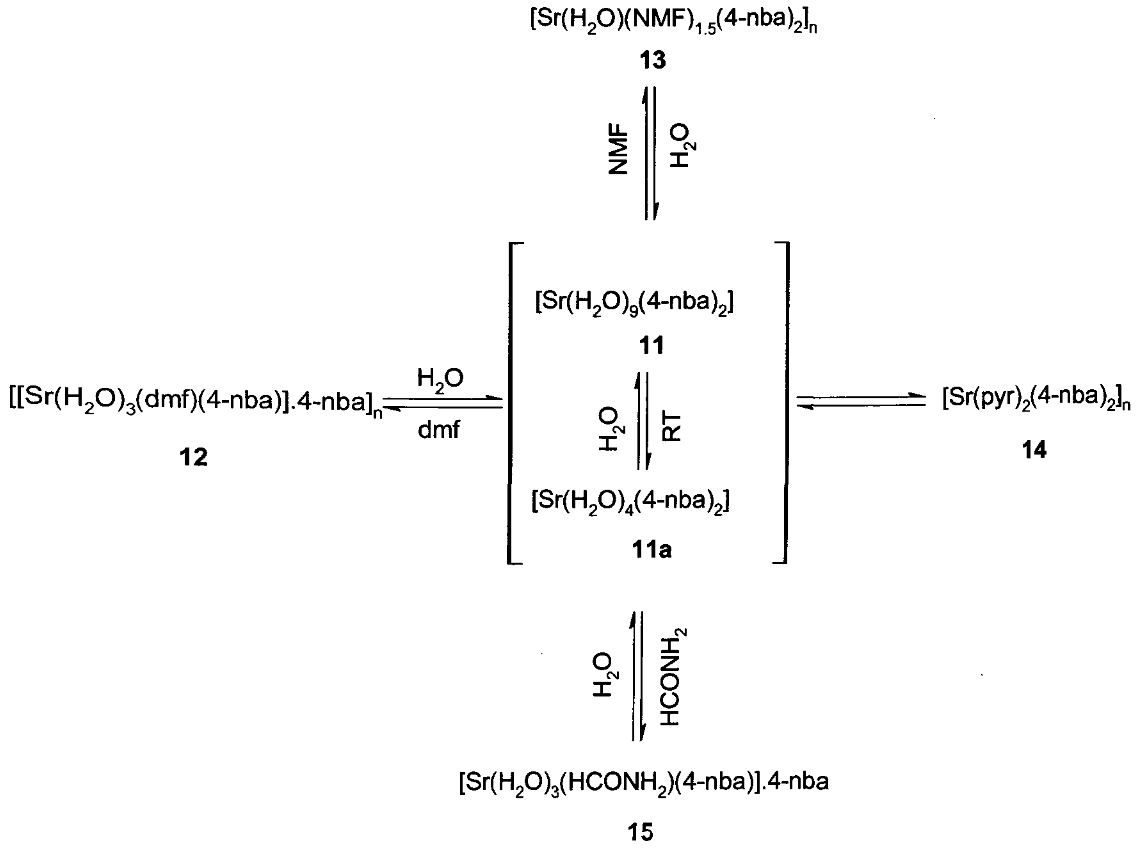

Scheme 3- Preparation of $[Sr(H_2O)_7(4\text{-nba})](4\text{-nba}).2H_2O$ **11** and its reactivity with O- and N- donor ligands

3.2.4- Synthetic aspects of $[Mg(H_2O)_6](2\text{-ca-4nba})_2$ 16, $[Ca(H_2O)_2(2\text{-ca-4-nba})_2]_n$ 17, $[Sr(2\text{-ca-4nba})_2]_n$ 18 and $[Ba(2\text{-ca-4nba})_2]_n$ 19

Nitration of phthalimide resulted in the formation of a mixture of isomeric 3- and 4-nitrophthalimides containing the insoluble 4-nitrophthalimide as the major product, which on alkaline hydrolysis followed by acidification afforded the amide substituted acid 2-ca-4nba**H** (Scheme 4), whose identity was confirmed from spectral data. Aqueous reaction of MCO_3 (M = Mg in **16** or **Ca** in **17**) with 2-ca-4nbaH in a 1:2 ratio followed by crystallization resulted in the formation of X-ray quality blocks of $[Mg(H_2O)_6](2\text{-ca-4nba})_2$ **16** and $[Ca(H_2O)_2(2\text{-ca-4-nba})_2]_n$ **17** respectively.

Compound **16** and **17** were also prepared by the reaction of aqueous solution of MCl_2 (M = Mg or Ca) with the Na-salt of 2-ca-4nba**H**. Our synthetic methodology is very similar to the one employed for the synthesis of several Mg(II) carboxylates (Table 2) wherein $MgCO_3$ or $Mg(OH)_2$ is reacted with the carboxylic acid or alternatively the water soluble $MgCl_2$ is reacted with the Na or K salt of the acid generated *in situ* by use of NaOH, KOH or $NaHCO_3$ [132,133,134,139, 135-141]. In all reactions, a Mg(II) carboxylate product containing a minimum of six moles of water per Mg(II) is obtained. However, with 3-hydroxy-4-nitrobenzoic acid a compound having Mg:H_2O in a 1:4 ratio has been reported using $Mg(OH)_2$ as Mg source [132]. Coordination polymers having one or two moles of water per Mg or no water, are obtained under hydrothermal conditions [131-149]. $MgNO_3$ in presence of base like NH_4OH has been used as Mg source during hydrothermal synthesis [131-149]. Reaction of **16** and **17** with dilute HCl, results in the quantitative formation of the free acid 2-ca-4nbaH. Both compounds were formulated based on elemental analysis and the mass loss leading to the formation of MO (M = Mg or Ca) on pyrolysis. Compounds $[Sr(2\text{-ca-4nba})_2]_n$ **18** and $[Ba(2\text{-ca-4nba})_2]_n$ **19** were similarly prepared by carbonate as well as metal chloride route using above strategy having Sr or Ba:2-ca-4nba**H** in a 1:2 ratio. Reaction of **18** and **19** with dilute HCl, results in the quantitative formation of the free acid 2-ca-4nba**H**. Compound **18** and **19** were formulated based on elemental analysis and the mass loss leading to the formation of MCO_3 on pyrolysis.

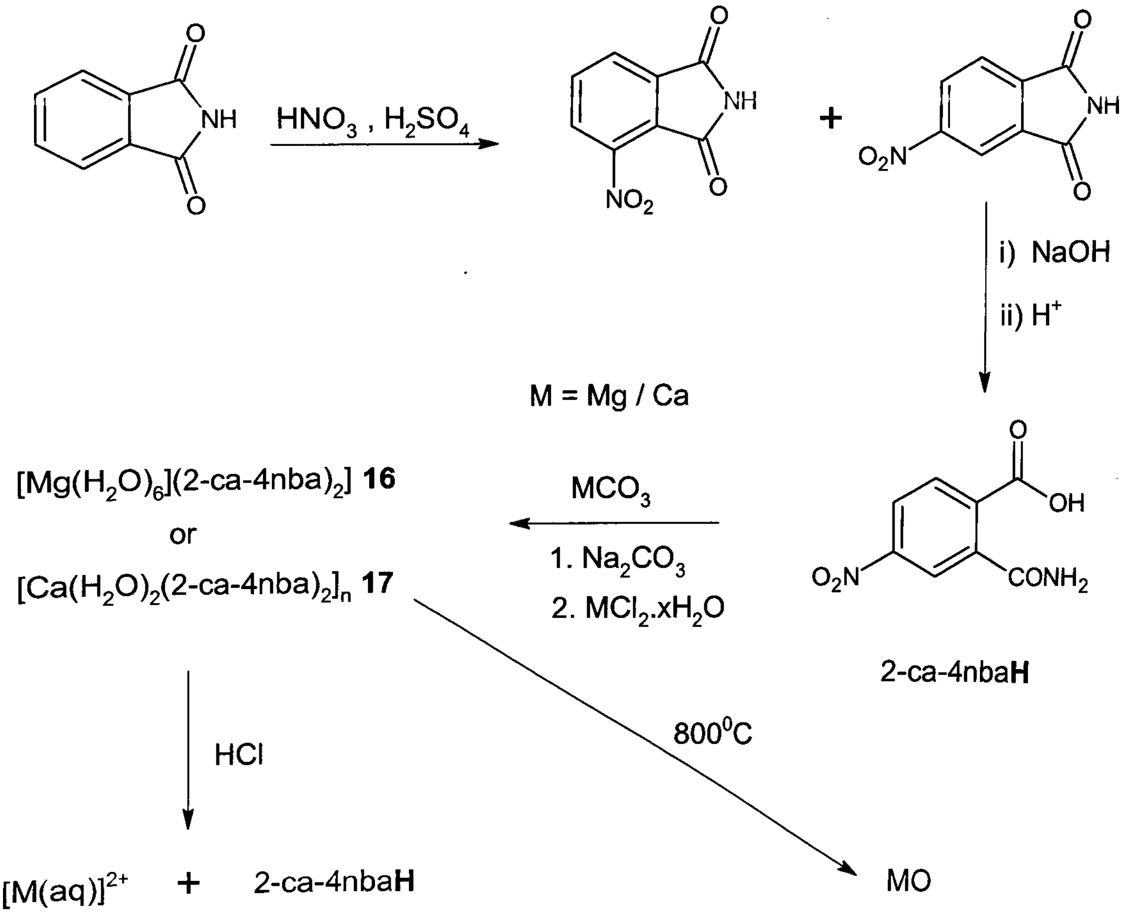

Scheme 4 - Preparation of 2-ca-4nbaH and its reaction with $MgCO_3$ and $CaCO_3$

Table 2 – Synthesis[a] and structural aspects[b] of some Mg(II) carboxylates

Compound	Mg source	Base	Space group	Secondary interaction	Ref
$[Mg(H_2O)_6](2\text{-ca-4nba})_2$	$MgCO_3$ $MgCl_2$	---- $NaHCO_3$	$P2_1/c$	O-H···O, N-H···O, C-H···O	170
$[Mg(H_2O)_6](2\text{-aba})_2\cdot 2H_2O$	$MgCl_2$	KOH	$P2_1/c$	O-H···O, N-H···O	134
$[Mg(H_2O)_6](4\text{-aba})_2\cdot 2H_2O$	$MgCl_2$	NH_4OH	$Pbca$	O-H···O, N-H···O	39
$[Mg(H_2O)_6](4\text{-nba})_2\cdot 2H_2O$	$MgCO_3$	----	$P\bar{1}$	O-H···O	133
$[Mg(H_2O)_6](C_7H_4NO_5)_2$	$MgCl_2$	NaOH	$P\bar{1}$	O-H···O	132
$[Mg(H_2O)_4(C_7H_3NO_5)]^d$	$Mg(OH)_2$	---	$P\bar{1}$	O-H···O	132
$[Mg(H_2O)_6](H_2PMA)_2$	$MgCO_3$	----	$P2/m$	O-H···O	135
$[Mg(H_2O)_5(3\text{-npth})].2H_2O$	$MgCO_3$ $MgCl_2$	$NaHCO_3$	$P\bar{1}$	O-H···O	120
$[Mg_3(H_2O)_{18}](BTC)_2$	$MgCO_3/MgCl_2$	$NaHCO_3$	-	-	
$[Mg(H_2O)_6](C_8H_5O_4)_2$	MgO	----	$P\bar{1}$	O-H···O	136
$[Mg(H_2O)_6](Nic)_2\cdot 4H_2O$	$[Mg(H_2O)_4](Nic)_2$	Recryst	$P2_1/a$	O-H···O	44
$[Mg_2(H_2O)_7(TTF)_2(EtOH)]\cdot 4H_2O$	$Mg(NO_3)_2$	NaOH/EtOH	$Pna2_1$	O-H···O	123
$[Mg(H_2O)_4].(C_4H_4O_4)$	$Mg(OH)_2$	----	$Pnma$	O-H···O	92
$[Mg_2(H_2O)(Oac)_4(Im)_4]$	$Mg(Oac)_2$	Im	$Aba2$	O-H···O	137
$[Mg_2(H_2O)(Oac)_4(Bzim)_4]$	$Mg(Oac)_2$	Bzim	$Aba2$	O-H···O	137
$[Mg(H_2O)_4(d,l\text{-aspH})_2]$	$Mg(OH)_2$	----	$P2_1/c$	O-H···O	138
$[Mg(H_2O)_2(hip)_2].2H_2O]$	$MgCl_2$	NH_4OH			122
$[Mg(H_2O)_4(Sa)_2]$	$MgCl_2$	NH_4OH	$P2_1/n$	O-H···O	139
$[Mg(H_2O)_4(C_{11}H_7O_3)_2]$	Recrystallized at RT	-	$P2_1/n$	O-H···O	140
$[Mg(H_2O)_2(C_8H_9N_2O_4)].3.5\ H_2O$	Recrystallized at RT	-	$P\bar{1}$	O-H···O, N-H···O	141
$[Mg_2(H_2O)_4(BTEC)]\cdot 2H_2O$	$Mg(NO_3)_2.6H_2O$/ BPP	H_2O/180°C	$P\bar{1}$	O-H···O	131
$[Mg_2(H_2O)_6(BTEC)]$	$Mg(NO_3)_2.6H_2O$/ BPP	H_2O/150°C	$P\bar{1}$	O-H···O	131
$[Mg_2(H_2O)_8(BTEC)]$	$Mg(NO_3)_2$	BPP/150°C	$P2_1/n$	O-H···O	131
$[Mg(H_2O)_2(C_6H_5N_2O_4)]$	$Mg(NO_3)_2$	Solvo	$P\bar{1}$	O-H···O, N-H···O	142
$[Mg(H_2O)_4(C_{12}H_8N_2)].(C_8H_5Cl_2O_2)_2$	Recrystallized at RT	-	$C2/c$	O-H···O	143
$[Mg(H_2O)_4(dmf)_2].ndc$	$Mg(NO_3)_2$	dmf/110°C	$P2_1/c$	O-H···O,	144
$[Mg_3(dmf)_4(ndc)_3]_n$	$Mg(NO_3)_2$	dmf/110°C	$C2/c$	-	144
$[Mg_3(dif)_4(ndc)_3]_n$	$Mg(NO_3)_2$	dif/110°C	$P2_1/n$	-	145
$[Mg_3(dmf)_2(ndc)_3(CH_3OH)(H_2O)](dmf)$	$Mg(NO_3)_2$	dmf/MeOH/110°C	$P\bar{1}$	O-H···O	145
$[Mg_3(def)_4(ndc)_3]_n$	$Mg(NO_3)_2$	def/110°C	$C2/c$	-	146
$[Mg_3(H_2O)_4(BPT)_2]_n$	$Mg(NO_3)_2$	dmf/120°C	$R3^-$	O-H···O	147
$[Mg(H_2O)_6](optp)_2$	$Mg(Oac)_2$	H_2O/100°C	$P\bar{1}$	O-H···O	148
$[[Mg_3(dmf)_3(3,5\text{-PDC})_3]\cdot dmf]_n$	$Mg(NO_3)_2$	dmf/100°C	$P2_1/n$	N-H···O	149
$[Mg(H_2O)_2(3,5\text{-PDC})]_n$	$Mg(NO_3)_2$	EtOH/100°C	$C2/c$	O-H···O, N-H···O	149

$[[Mg(H_2O)(3,5\text{-}PDC)].2H_2O]_n$	$Mg(NO_3)_2$	H_2O/100°C	$P6_122$	O-H···O, N-H···O	149
$[[Mg_4(H_2O)_2(dmf)_2(3,5\text{-}PDC)_4].2dmf.4.5H_2O]_n$	$Mg(NO_3)_2$	dmf/H_2O/100 °C	$P2_1/c$	O-H···O, N-H···O	149

a - In a typical synthesis $MgCO_3$ or $Mg(OH)_2$ is reacted with the acid in aqueous medium. Alternatively $MgCl_2$ can be reacted with the acid in the presence of a base.

b- All compounds listed in Table are six coordinated and contain a $\{MgO_6\}$ octahedron with Mg(II) situated on an inversion centre.

d. ($C_7H_3NO_5$) functions as a bidentate ligand binding through a phenolate O and a nitro O.

Abbreviations: 2-aba = 2-aminobenzoic acid; 4-aba = 4-aminobenzoic acid; 4-nba = 4-nitrobenzoic acid; $C_7H_4NO_5$ = 3-hydroxy-4-nitrobenzoic acid; **H_4PMA** = benzene-1,2,4,5-Tetracarboxylic acid; 3-npth = 3-nitrophthalic acid; 2-ca-4nba = 2-carbamoyl-4-nitrobenzoic acid; $C_8H_6O_4$ = phthalic acid; nic = nicotinic acid; TTF = tetrathiafulvenedicarboxylic acid; $C_4H_5O_4$ = methylmalonic acid; Oac = acetic acid; Im = imidazole; Bzim = benzimidazole; d,l-asp = d,l-aspartic acid; BPP = 4,4′-trimethylenedipyridine; BTEC = 1,2,4,5-benzenetetracarboxylic acid; hip = hippuric acid; Sa = salicylicylic acid; $C_{11}H_8O_3$ = 1-hydroxynaphthoic acid; $C_8H_{10}N_2O_4$ = 1-H-2-propyl-imidazole-4,5-dicarboxylic acid; $C_6H_7N_2O_4$ = 2-methyl-1H-imidazole-4,5-dicarboxylic acid; $C_8H_6Cl_2O_2$ = 2,4-dichlorophenylacetic acid; 2,6-H_2ndc = 2,6-naphthalenedicarboxylic acid; dmf = dimethylformamide; dif = diisopropylformamide; def = diethylformamide; BPT = biphenyl-,3,4′,5-tricarboxylic acid; optp = 1-oxopyridinium-2-thiopropionic acid; PDC = 3,5- pyridinedicarboxylate

3.2.5- Synthetic aspects of Alkaline earth 2-nitrobenzoates of Mg, Ca, Ba and Sr

The alkaline earth 2-nitrobenzoate compounds **20-23** were prepared by reaction of metal carbonates with 2-nitrobenzoic acid in a 1:2 mole ratio. The compounds **20-23** could be also prepared by reacting aqueous solution of MCl_2 with *in-situ* generated sodium salt of 2-nbaH (Scheme 5). The composition of compounds **20-23** was arrived at based on elemental analysis, 2-nbaH content obtained by acidification and MO/MCO_3 formed on pyrolysis and weight loss studies. All four compounds **20-23** could be dehydrated to the anhydrous $[M(2\text{-}nba)_2]$ by heating above 100°C (Scheme 5). The temperature for the dehydration reaction was chosen based on the thermal properties (*vide infra*) of respective hydrates. Equilibriation of the anhydrous compounds **20a-23a** in an atmosphere of water vapor resulted in the regeneration of compounds **20-23**. This was confirmed by a comparison of the IR spectrum and the TG-DSC thermogram of the rehydrated products with that of starting compounds **20-23**. The hydrated and dehydrated compounds **20**, **20a** and **21**, **21a** decomposed to MO (Mg or Ca) by heating in a furnace at 800°C while compounds **22**, **22a** and **23**, **23a** formed respective MCO_3 (M = Sr, Ba) at 1000°C as shown in scheme below (Scheme 5).

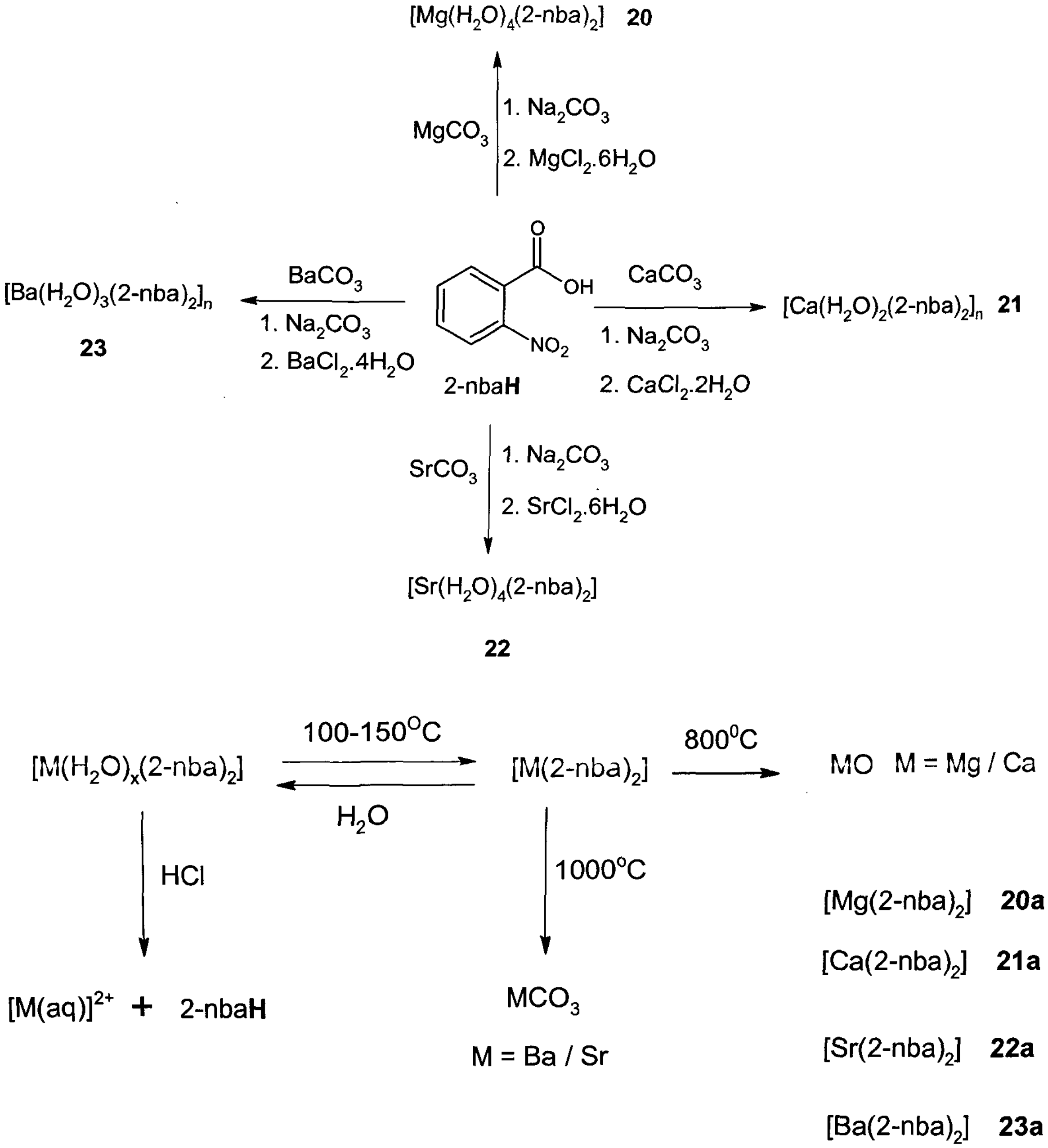

Scheme 5 – Preparation of alkaline earth 2-nitrobenzoates (top) and reversible hydration (bottom)

3.2.6- Synthesis of [$Cs_2(H_2O)_2$(3-npth)] 24, [[$Ca(H_2O)_2$(3-npth)].H_2O]$_n$ 25, [$Mg(H_2O)_5$(3-npth)].$2H_2O$ 26, [Ba(3-npth)]$_n$ 27, [Sr(3-npth)] 28.

The compounds **24-28** were prepared by reaction of metal carbonate with the corresponding nitrocarboxylic acid in 1:1 ratio (Scheme 6). Compounds **24** to **28** could also be prepared by reacting an aqueous solution of MCl_2 (M = Ca or Mg) with *in situ* generated sodium salt of the 3-nitrocarboxylic acid while compounds **27** and **28** were found to be anhydrous. The M:H_2O ratio in **24** is 1:1 while it is 1:3 and 1:7 in **25** and **26** respectively. From crystal structure, it is evident that **26** contain five coordinated and two lattice water molecules while **25** contains two crystal and one lattice water. In contrast, the central Mg(II) in **26** contain a mondentate carboxylate bonded to Mg(II). The composition of the synthesized compounds **24** to **26** were determined based on the analytical data and the metal oxide formed by heating in a furnace at 800°C while that of **24**, **27** and **28** were formulated based on metal carbonate obtained after heatig to 1000°C.

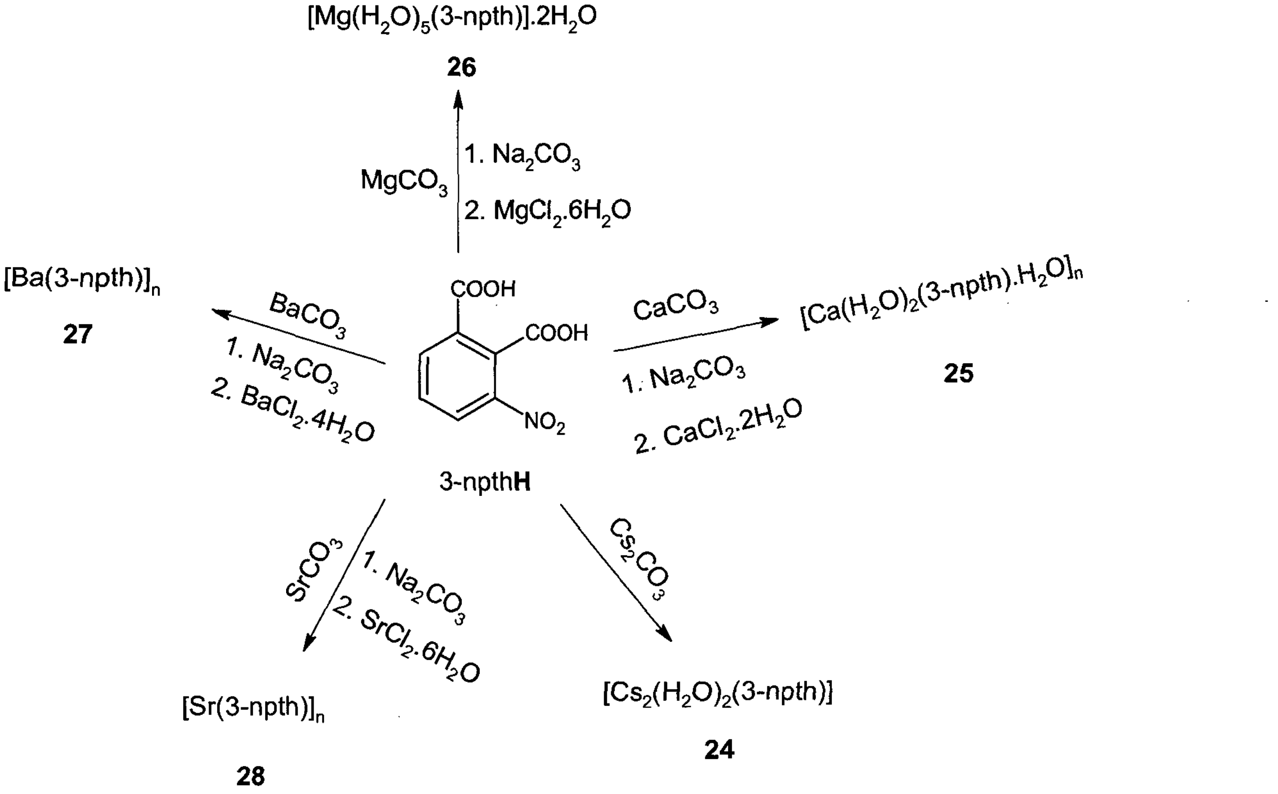

Scheme 6 – Preparation of alkaline earth 3-nitrophthalates

3.2.7- Synthetic aspects of 1,3,5-benzenetricarboxylic acid with alkaline earth metals and preparation of compounds 29, 30, 31, 32

Usually 3-D polymers are prepared by reaction of di or tricarboxylic acid with metal carbonate or metal salt under hydrothermal conditions involving high temperature and autonomous pressures. In the current study, compounds **29-32** were prepared under ambient conditions. Compounds **29-31** were prepared by direct reaction of MCO_3 (M= Mg, Ca, Sr) with H_3btc while compound **32** was prepared by reaction of freshly prepared

$BaCO_3$. $BaCO_3$ was first generated *in-situ* by reaction of $BaCl_2.2H_2O$ with Na_2CO_3 and then reacted with 1,3,5-benzenetricarboxylic acid at room temperature, resulting in immediate precipitation of compound **32** as fine needles. Alternatively compounds **29-32** can be also prepared by first generating *in-situ* sodium salt of H_3btc and then reacting with MCl_2 as metal sources. The yields obtained in the chloride as well as acetate methods were comparatively higher as compared to that of carbonate method under ambient conditions (Scheme 7).

There are ninteen coordination polymers of alkaline earth metals reported in literature having benzene-tricarboxylate group as ligand. Out of this, nine are 3-D polymers, seven are 2-D and remaining three compounds are 1-D polymers. Synthesis of 3-D polymers involves hydrothermal conditions entry no. 1-8 [Table 3] and except in entry no. 9 where we have reported soft synthesis utilizing ambient conditions. However 2-D or 1-D polymeric compounds are prepared both under ambient as well as hydrothermal conditions. Out of the four compounds **29-32** prepared in this series, two compounds mainly calcium compound $[Ca_3(btc)_2(H_2O)_{12}]_n$ 30 has been structurally characterized and is found to be a 2-D polymer as reported earlier [69] while compound $[[Ba_3(btc)_2(H_2O)_8].2H_2O]_n$ **32** is a 3-D polymer.

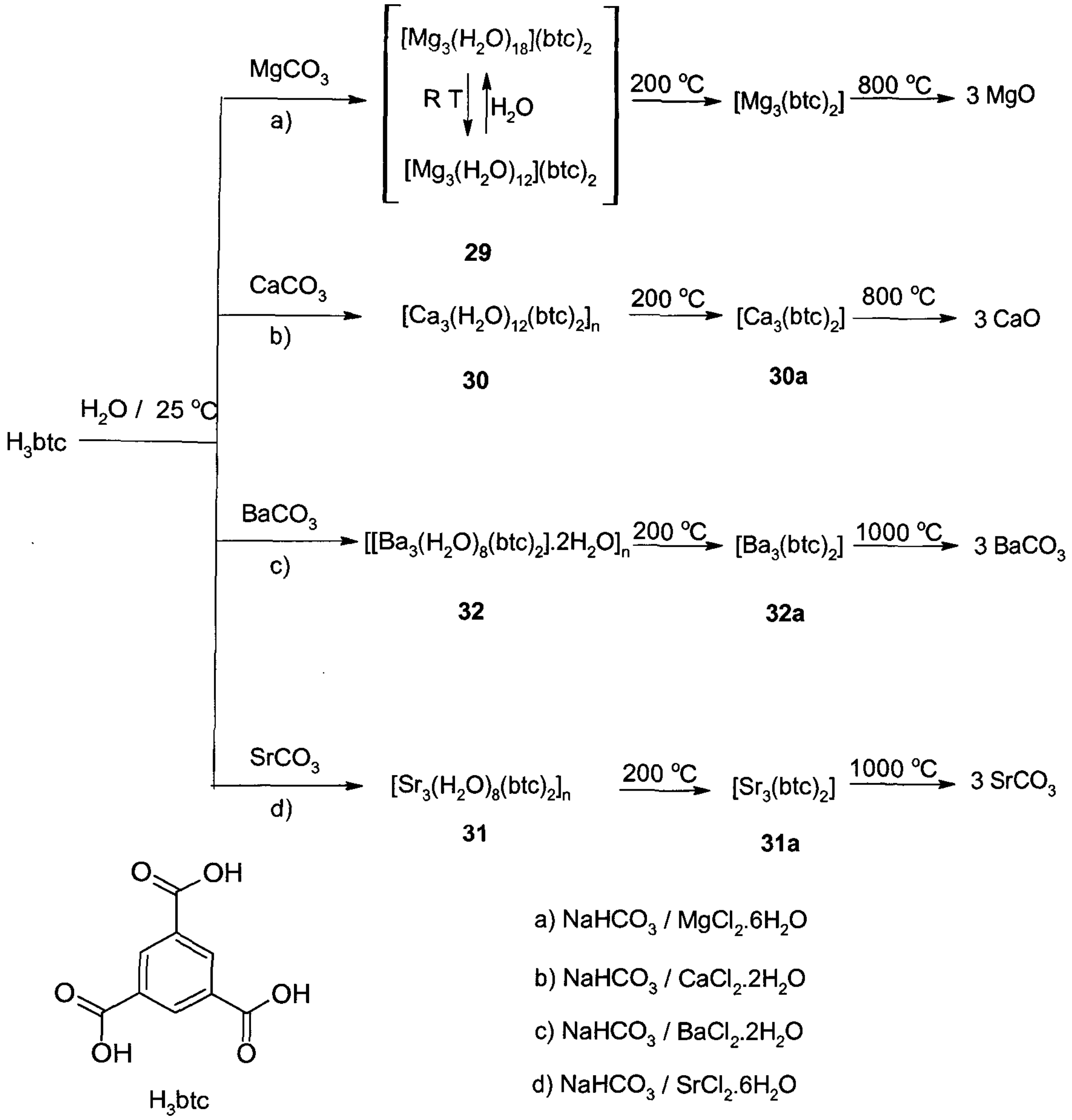

Scheme 7- Synthesis of coordination polymers using 1,3,5-benzenetricarboxylic acid as ligand.

Table 3 - Synthesis of alkaline-earth compounds based on btc

Compound	Metal source	Temp. (^oC)	C. N.	D	Ref.
$[[Ca(btc\mathbf{H})(H_2O)].H_2O]_n$	$Ca(OAc)_2$	180	8	3-D	70
$[Sr_3(btc)_2(H_2O)_4]_n$	$Sr(Oac)_2$	150	$7,9,9^a$	3-D	168
$[Sr(btc\mathbf{H})(H_2O)_2]_n$	$Sr(Oac)_2$	180	9	3-D	172
$[Ba(btc\mathbf{H})(H_2O)_2]_n$	$Ba(OAc)_2$	180	9	3-D	172
$[[Ba(ptc)(H_2O)][Ba(ptc\mathbf{H}_2)(H_2O)]]_n$	$Ba(NO_3)_2$	180	$8,10^b$	3-D	76
$[Ca_{1.5}(ptc).2H_2O]_n$	$CaNO_3$	180	6,7	3-D	76
$[Sr_{1.5}(ptc).5H_2O]_n$	$SrNO_3$	180	9	3-D	76
$[Mg_{12}(btc)_8(H_2O)_{18}(dioxane)_6]_n$	$MgNO_3$	110	6	3-D	174
$[[Ba_3(btc)_2(H_2O)_8].2H_2O]_n$	$BaCO_3$	RT	$8,10^b$	3-D	This work
$[Ca_3(btc)_2(H_2O)_{12}]_n$	$Ca(OAc)_2$	RT	$7,8^b$	2-D	69
$[Ba(\mathbf{H}_2PMA)_2(H_2O)_5]_n$	$BaBr_2$	RT	9	2-D	135
$[Ca(1,2,4\text{-}btc\mathbf{H})(H_2O)]_n$	$Ca(OH)_2$	180	8	2-D	23
$[Ca(btc\mathbf{H})(H_2O)_4]_n$	$CaCl_2$	RT	7	2-D	127
$[Ca_3(bta)_2(H_2O)_8].3H_2O]_n$	$CaCO_3$	RT	7	2-D	71
$[Ba_3(bta)_2(H_2O)_8]_n$	$BaCO_3$	RT	8	2-D	71
$[Mg(\mathbf{H}_{1.5}btc)_{2/3}(btc)_{1/3}$ $(DMA)_2(DMA)_{1/3}]_n$	$MgNO_3$	90	6	2-D	173
$[Ca_3(btc)_2(H_2O)_2(dmf)_2].3H_2O]_n$	$CaNO_3$	90	$7,8^a$	1-D	125
$[Mg_3(ptc)_2.8H_2O)]_n$	$Mg(NO_3)_2$	140	6	1-D	76
$[[Mg(ptc).0.5[Mg(H_2O)_6].H_2O]]_n$	$Mg(NO_3)_2$	140	7	1-D	76

Abbreviations: Temp. = reaction temperature; C. N. = coordination number; D = Dimensionality; $\mathbf{H}_3btc$ = benzene-1,3,5-tricarboxylic acid; OAc = acetate; $\mathbf{H}_3ptc$ = pyridine -2,4,6-tricarboxylic acid; H_4PMA = pyromellitic acid; 1,2,4-btc**H** = benzene-1,2,4-tricarboxylic acid; bta = benzene-1,3,5-triacetic acid; dmf = dimethylformamide; DMA = dimethylacetamide

3.2.8- Reaction of phenylacetic acid $[[Ca(H_2O)_2(4\text{-}OMephac)_2].H_2O]_n$ 33 $[[Ca(H_2O)_2(2\text{-}Clphac)_2].2H_2O]_n$ 34 $[Ca(H_2O)_3(phac)_2]$ 35 and $[Ba(H_2O)_2(2\text{-}Clphac)_2]$ 36

The methodology employed for the synthesis of compounds **34-36** is as described earlier. Thus, the aqueous reaction of $CaCO_3$ with the substituted phenylacetic acid L_1-H, L_2-H (or L-H) resulted in the formation of the title compounds **33**, **34**, **35** and **36** in good yield (Scheme 8). Compounds **33**, **34**, **35** and **36** were also prepared in a two step reaction. In the first step the sodium salt of L_1-**H**, L_2-**H** or L-**H** were generated *in situ* by reaction of the acids with $NaHCO_3$. In the second step the aqueous solution of Na-salt was reacted with $CaCl_2$ and the title compounds were then crystallized from the reaction mixture. All the three compounds can be dehydrated to the corresponding anhydrous compounds **33a**, **34a** and **35a** by heating at 130°C. On reaction with dilute HCl, all compounds (**33, 33a, 34, 34a** and **35, 35a)** decompose resulting in the separation of the insoluble L_1-**H** or L_2-**H or** L-**H**. Analytical and thermal data shows that, compounds **33-34** which are differently hydrated contain Ca: carboxylate in a 1:2 mole ratio. The reaction of L_2-H with freshly prepared $BaCO_3$ resulted in the formation of $[Ba(H_2O)_2(2\text{-}Clphac)_2]$ **36**. Similar strategy was involved for synthesis of compound **37-40** (Scheme 9). Schem for the preparation of compounds **36-40** is shown below (Scheme 9). The metal content as oxide or carbonate of synthesized compounds after decomposing in furnace at 800-1000 °C is tabulated in Table 4. The calculated and found carboxylic acid content (as 4-nba**H**, 2-ca-4nba**H** or 2-nba**H**) after acidification of compounds containg 4-nba or 2nba or 2-ca-4nba as ligand is also tabulated in Table 4. The Table 5 gives the details about the found and calculated CHN values of compounds prepared in the present study.

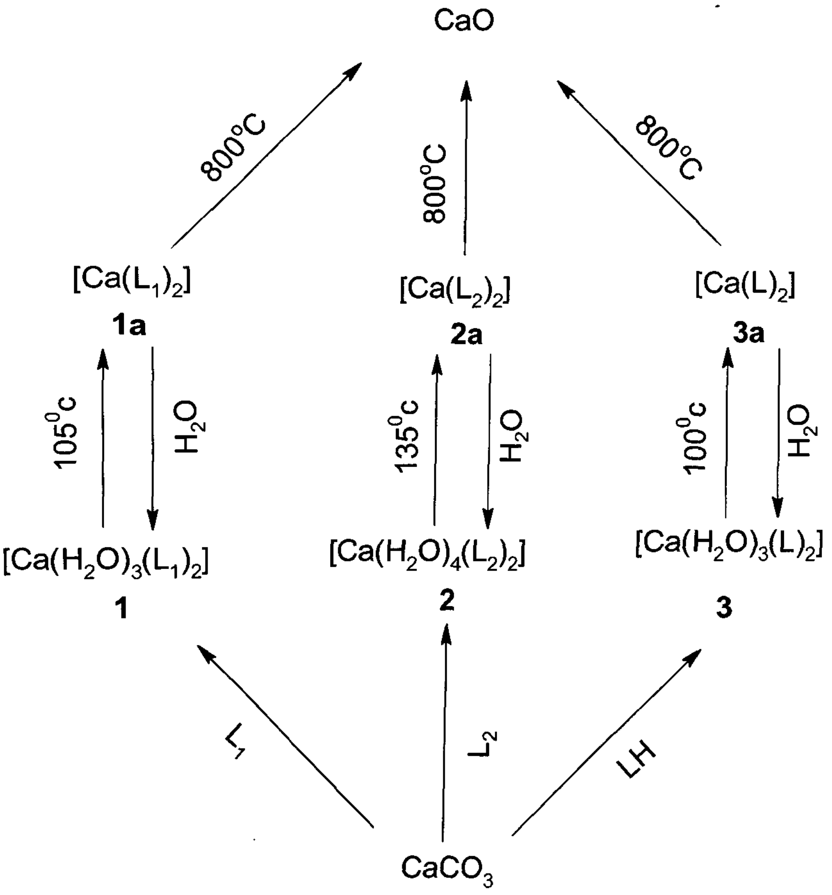

Scheme 8- Synthesis of $[[Ca(H_2O)_2(4\text{-}OMephac)_2].H_2O]_n$ **33** $[[Ca(H_2O)_2(2\text{-}Clphac)_2].2H_2O]_n$ **34** $[Ca(H_2O)_3(phac)_2]$ **35**

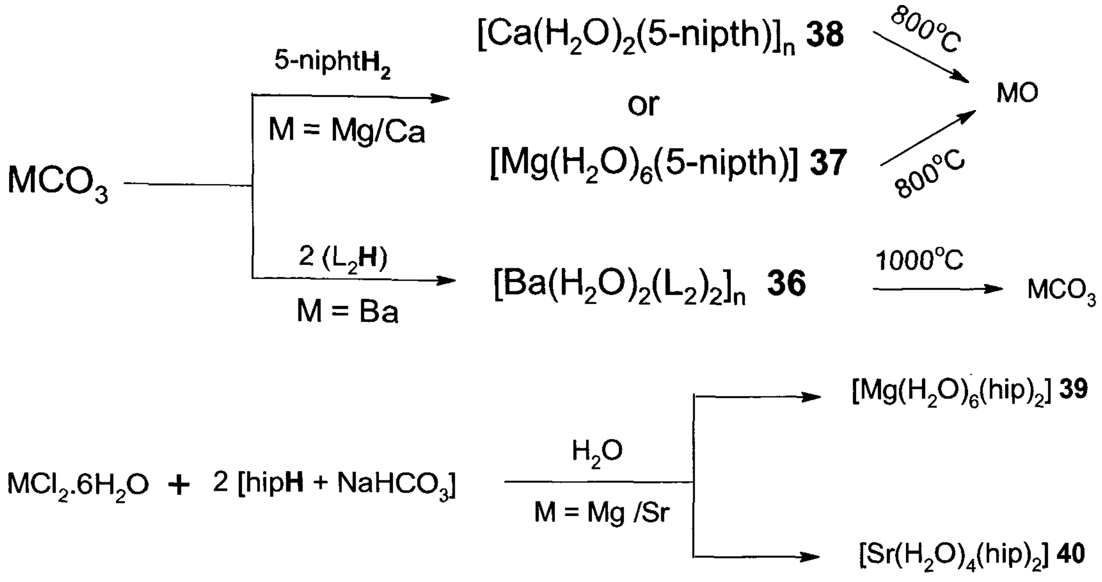

Scheme 9- Synthetic scheme showing the methods used for preparation of compounds **36-40**.

Table 4 - Metal oxide / metal carbonate, 4-nbaH and 2nbaH content.

Compound	Metal content as oxide or carbonate		Carboxylic acid	
	Observed	Expected	Observed	Expected
$[Ca(H_2O)_4(4\text{-nba})_2]$ **1**	11.68	12.59	73.98	74.77
$[Ca(4\text{-nba})_2(N\text{-MeIm})]_n$ **2**	12.20	12.34	73.0	73.11
$[Ca(4\text{-nba})_2(Im)]_n$**3**	12.73	12.3	74.28	75.88
$[Ca(H_2O)(4\text{-nba})_2(2\text{-MeIm})]_n$ **4**	11.87	11.87	70.30	70.75
$[Ca(4\text{-nba})_2(pyr)_2]_n$ **5**	11.03	11.08	65.02	65.74
$[[Ca(H_2O)_2(4\text{-nba})_2].(dmp)_2]_n$ **6**	9.2	9.34	54.84	55.65
$[Ca(H_2O)_6(4\text{-nba})(2\text{-ap})](4\text{-nba})(2\text{-ap})$ **7**	9.69	9.46	59.1	56.41
$[(H_2O)_4Li_2(\mu\text{-}H_2O)_2](4\text{-nba})_2$ **8**	-	-	73.03	73.59
$[Na(4\text{-nba})(H_2O)_3]_n$ **9**	-	-	68.39	68.73
$[K(4\text{-nba})(H_2O)_2]$ **10**	-	-	68.58	69.27
$[Sr(H_2O)_7(4\text{-nba})](4\text{-nba}).2H_2O$ **11**	23.69	25.37	57.1	57.43
$[[Sr(H_2O)_3(4\text{-nba})(dmf)].(4\text{-nba})]_n$ **12**	26.75	26.99	60.12	61.11
$[Sr(H_2O)(4\text{-nba})_2(nmf)_{1.5}]_n$ **13**	26.65	27.97	62.02	63.49
$[Sr(4\text{-nba})_2(pyr)_2]_n$ **14**	24.80	26.55	59.0	59.27
$[Sr(H_2O)_3(4\text{-nba})_2(HCONH_2)]_n$ **15**	26.15	28.64	62.13	64.91
$[Mg(H_2O)_6(2\text{-ca-4-nba})_2]$ **16**	7.21	7.32	-	-
$[Ca(H_2O)_2(2\text{-ca-4-nba})_2]_n$ **17**	11.1	11.32	-	-
$[Ba(H_2O)_2(2\text{-ca-4-nba})_2]$ **18**	35.0	35.51	-	-
$[Sr(2\text{-ca-4-nba})_2]$ **19**	29.0	29.18	-	-
$[Mg(H_2O)_4(2\text{-nba})_2]$ **20**	9.56	9.4	-	-
$[Ca(H_2O)_2(2\text{-nba})_2]_n$ **21**	13.70	13.73	80.35	81.86
$[Ba(H_2O)_3(2\text{-nba})_2]_n$ **22**	-	-	62.99	63.83

[Sr(H$_2$O)$_4$(2-nba)$_2$] **23**	31.10	30.01	88.0	89.78
[Cs$_2$(H$_2$O)$_2$(3-npth)] **24**	63.56	63.76	-	-
[Mg(H$_2$O)$_5$(3-npth)].2H$_2$O **25**	12.15	11.13	-	-
[[Ca(H$_2$O)$_2$(3-npth)].H$_2$O]$_n$ **26**	19.0	18.49	-	-
[Ba(3-npth)]$_n$ **27**	55.28	56.89	-	-
[Sr(3-npth)]$_n$ **28**	47	49.54	-	-
[Mg$_3$(H$_2$O)$_{18}$(btc)$_2$] **29**	14.71	14.89	-	-
[Ca$_3$(H$_2$O)$_{12}$(btc)$_2$]$_n$ **30**	21.93	22.41	-	-
[Sr$_3$(H$_2$O)$_8$(btc)$_2$]$_n$ **31**	52.1	53.93	-	-
[[Ba$_3$(H$_2$O)$_8$(btc)$_2$].2H$_2$O]$_n$ **32**	58.12	58.83	-	-
[Ca(H$_2$O)$_2$(4-OMephac)$_2$].H$_2$O **33**	13.28	13.19	-	-
[[Ca(H$_2$O)$_2$(2-Clphac)$_2$].2H$_2$O]$_n$ **34**	12.3	12.42	-	-
[Ca(H$_2$O)$_3$(phac)$_2$].H$_2$O **35**	15.35	15.39	-	-
[Ba(H$_2$O)$_2$(2-Clphac)$_2$]$_n$ **36**	38.2	38.5	-	-
[Mg(H$_2$O)$_6$(5-niphth)] **37**	12.46	12.45	-	-
[Ca(H$_2$O)$_4$(5-niphth)] **38**	18.08	17.45	-	-
[Mg(hippurate)$_2$(H$_2$O)$_6$] **39**	8.19	8.24	-	-
[Sr(hippurate)$_2$(H$_2$O)$_4$] **40**	28.69	28.61	-	-

Table 5- C, H, N analytical data of synthesized compounds

Compound	Molecular Formula (MW)	N		C		H	
		Found	Calcd	Found	Calcd	Found	Calcd
[Ca(H$_2$O)$_4$(4-nba)$_2$]	$C_{14}H_{16}CaN_2O_{12}$ (444.24)	6.28	6.34	37.84	38.07	3.7	3.66
[Ca(N-MeIm)(4-nba)$_2$]$_n$	$C_{18}H_{14}CaN_4O_8$ (454.43)	11.81	12.32	47.6	47.53	3.03	3.0
[Ca(Im)(4-nba)$_2$]	$C_{17}H_{12}CaN_4O_8$ (440.38)	10.94	12.72	45.95	46.37	2.72	2.75
[Ca(H$_2$O)(2-MeIm)(4-nba)$_2$]$_n$	$C_{18}H_{16}CaN_4O_9$ (472.43)	11.80	11.86	45.73	45.76	3.63	3.41
[Ca(pyr)$_2$(4-nba)$_2$]	$C_{20}H_{16}CaN_6O_8$ (454.43)	16.44	16.53	46.81	47.24	3.05	3.17
[Ca(H$_2$O)$_2$(4-nba)$_2$].2(dmp)	$CaC_{24}H_{28}N_6O_{10}$ (600.60)	13.75	13.99	46.92	48.0	4.54	4.70
[Ca(H$_2$O)$_6$(4-nba)](4-nba)(2-ap)·H$_2$O	$CaC_{19}H_{28}N_4O_{15}$ (592.52)	8.74	9.46	38.13	38.51	4.21	4.76
[Ca(4-nba)$_2$(2-ap)]	$CaC_{19}H_{14}N_4O_8$ (466.41)	-	12.01	-	48.93	-	3.03
[(H$_2$O)$_4$Li$_2$(4-nba)(μ-H$_2$O)$_2$](4-nba)	$Li_2C_{14}H_{20}N_2O_{14}$ (454.20)	6.03	6.17	36.52	37.02	3.82	4.44
[Na(4-nba)(H$_2$O)$_3$]	$NaC_7H_{10}NO_7$ (243.15)	5.87	5.76	34.32	34.58	4.11	4.15
[K(4-nba)(H$_2$O)$_2$]	$KC_7H_{10}NO_7$ (259.26)	5.70	5.81	32.3	34.85	3.89	3.34
[Sr(4-nba)(H$_2$O)$_7$](4-nba).2H$_2$O	$C_{14}H_{26}SrN_2O_{17}$ (581.98)	4.89	4.81	29.73	28.89	2.05	4.50
[Sr(4-nba)$_2$(H$_2$O)$_4$]	$C_{14}H_{12}SrN_2O_{12}$ (487.87)	5.70	5.74	34.2	34.47	2.49	2.48
[Sr(4-nba)(dmf)]	$C_{17}H_{21}SrN_3O_{12}$	7.16	7.68	35.89	37.33	3.54	3.87

$(H_2O)_3]$.(4-nba)	(546.98)						
$[Sr(H_2O)(4$-nba$)_2(nmf)_{1.5}]$	$C_{34}H_{35}Sr_2N_7O_{21}$ (526.46)	8.26	9.31	36.55	38.78	2.83	3.04
$[Sr(H_2O)_3(4$-nba$)_2(form)]$	$C_{15}H_{13}SrN_3O_{12}$ (514.90)	9.31	8.16	33.89	34.99	2.66	2.54
[Sr(4-nba$)_2(pyr)_3]$	$C_{20}H_{16}SrN_6O_8$ (556.01)	14.45	15.12	41.50	43.20	2.73	2.90
$[Mg(H_2O)_6$(2-ca-4nba$)_2]$	$C_{16}H_{22}MgN_4O_{16}$ (550.67)	9.57	10.17	34.53	34.90	4.02	4.03
$[Ca(H_2O)_2$(2-ca-4nba$)_2]$	$C_{16}H_{14}CaN_4O_{12}$ (494.39)	11.03	11.33	38.47	38.87	2.79	2.85
[Sr(2-ca-4-nba$)_2]$	$C_{16}H_{10}SrN_4O_{10}$ (505.89)	11.03	11.07	37	37.99	1.8	1.99
[Ba(2-ca-4-nba$)_2]$	$C_{16}H_{10}BaN_4O_{10}$ (555.60)	10.01	10.08	34.0	34.59	1.51	1.81
[Mg(2-nba$)_2(H_2O)_4]$	$C_{14}H_{16}MgN_2O_{12}$ (428.60)	6.74	6.54	39.57	39.23	3.87	3.76
$[Ca(H_2O)_2$(2-nba$)_2]$	$C_{14}H_{12}CaN_2O_{10}$ (408.34)	6.58	6.86	41.10	41.18	2.98	2.96
[Sr(2-nba$)_2(H_2O)_4]$	$C_{14}H_{16}SrN_2O_{12}$ (491.90)	5.60	5.96	34.18	33.14	4.0	3.28
[Ba(2-nba$)_2(H_2O)_3]$	$C_{14}H_{14}BaN_2O_{11}$ (523.61)	4.91	5.41	31.53	32.46	2.49	2.7
$[Cs_2(H_2O)_2$(3-npth)]	$C_8H_3CsNO_6$ (474.92)	2.7	2.95	18.8	20.20	1.5	0.64
$[[Ca(H_2O)_2$(3-npth)]$\cdot H_2O]_n$	$C_8H_9CaNO_9$ (303.24)	4.49	4.64	31.72	31.69	2.94	2.99
$[Mg(H_2O)_5$(3-npth)]$\cdot 2H_2O$	$C_8H_{17}MgNO_{13}$ (372.34)	3.80	3.90	26.89	26.73	4.61	4.77
[Sr(3-npth)$]_n$	$C_8H_3SrNO_6$ (296.73)	4.7	4.72	31.0	32.38	1.04	1.02
[Ba(3-npth)$]_n$	$C_8H_3BaNO_6$ (346.44)	4.12	4.04	28.0	27.74	0.88	0.87
$[Mg_3(btc)_2(H_2O)_{18}]$	$Mg_3C_{18}H_{42}O_{30}$ (811.42)	-	-	-	26.64	-	5.22
$[Mg_3(btc)_2(H_2O)_{12}]$	$Mg_3C_{18}H_{30}O_{24}$ (703.33)	-	-	31.35	30.74	4.45	4.3
$[Ca_3(btc)_2(H_2O)_{12}]$	$Ca_3C_{18}H_{30}O_{24}$ (750.65)	-	-	30.86	28.80	5.22	4.03
$[Sr_3(btc)_2(H_2O)_8]$	$Sr_3C_{18}H_{22}O_{20}$ (821.22)	-	-	26.65	26.33	2.46	2.7
$[Ba_3(btc)_2(H_2O)_8].2H_2O$	$Ba_3C_{18}H_{26}O_{22}$ (1006.37)	-	-	21.45	21.48	2.64	2.6
$[Ca(H_2O)_2(L_1)_2]\cdot H_2O$	$CaC_{18}H_{24}O_9$ (424.46)	-	-	50.92	50.93	5.79	5.70
$[Ca(H_2O)_2(L_2)_2]\cdot 2H_2O$	$CaC_{16}H_{20}Cl_2O_8$ (451.31)	-	-	42.5	42.58	4.40	4.47
$[Ca(L)_2(H_2O)_3]$	$CaC_{16}H_{20}O_7$ (364.40)	-	-	52.61	52.74	5.43	5.53
$[Ba(H_2O)_5$(2-Clphac$)_2]_n$	$BaC_{16}H_{26}O_{11}Cl_2$	-	-	31.2	31.89	4.3	4.35

	(602.60)						
[$Mg(H_2O)_6$(5-niphth)]	$C_8H_{13}MgNO_{11}$ (323.49)	4.31	4.33	29.0	29.7	4.02	4.05
[$Ca(H_2O)_4$(5-niphth)]	$C_8H_{11}CaNO_{10}$ (321.25)	4.3	4.36	29.9	29.9	2.9	3.45
[Mg(hip)$_2$(H_2O)$_6$]	$C_{18}H_{28}MgN_2O_{12}$ (488.73)	5.77	5.73	44.2	44.24	5.77	5.73
[Sr(hip)$_2$(H_2O)$_4$]	$C_{18}H_{24}SrN_2O_{10}$ (516.01)	5.41	5.43	42.2	41.9	5.41	5.43

3.3- Spectral Investigations

3.3.1- Infrared spectroscopy

The metal carboxylate complexes prepared in this work were studied using infrared spectroscopy. The infrared spectra of the samples were recorded on an IR Prestige -21 Fourier transform (SHIMADZU) (4000-400 cm^{-1}) infrared (IR) spectrometer as KBr diluted palletes and the signals were referenced to polystyrene bands. The complexes prepared exhibit several sharp signals in the mid IR region, many of which are also observed in the free carboxylic acid clearly indicating the presence of the organic moiety in the synthesized complexes. The mixed ligand complexes prepared in this work showed additional bands in the mid-IR region which further confirmed the incorporation of N or O-donor into the metal carboxylate complex. Further, The presence of water (O-H signal) in the metal carboxylate complexes prepared was confirmed based on the presence of strong and broad absorption signal in 3600-3000 cm^{-1} region. The presence of water was further quantified based on the isothermal weight loss studies (*vide infra*). The infrared stretching frequencies of the functional groups were assigned based on the known literature data from standard textbooks [194-195]. The carboxylate (O=C=O) group in the complexes showed two strong signals due to asymmetric stretching in the region 1650-1500 cm^{-1} and symmetric stretching was observed in the region 1400-1350 cm^{-1}. The asymmetric and symmetric stretching of nitro group (O=N=O) was observed as strong bands in the region 1500-1570 cm^{-1} and 1300-1350 cm^{-1} respectively. The signals due to N-H and amide (CO) group were seen in the range 3300-3100 cm^{-1} and 1660-1680 cm^{-1} respectively. A comparative table showing the infrared stretching frequencies of functional groups present in synthesized compounds is shown below (Table 6).

Table 6- Infrared data showing tentative assignments for synthesized compounds

Compound	Stretching frequency in cm^{-1}		O=C=O stretching frequency in cm^{-1}		NO_2 stretching frequency in cm^{-1}		$CONH_2$ stretch frequency in cm^{-1}
	O-H	N-H	asy	Sym	asy	sym	
$[Ca(H_2O)_4(4\text{-}nba)_2]$	3666-3100	-	1568	1391	1504	1342	-
$[Ca(H_2O)(4\text{-}nba)_2]$	3611-3100	-	1558	1414	1524	1346	-
$[Ca(N\text{-}MeIm)(4\text{-}nba)_2]_n$	-	-	1584	1402	1520	1375	-
$[Ca(Im)(4\text{-}nba)_2]$	-	3381	1570	1402	1516	1348	-
$[Ca(H_2O)(2\text{-}MeIm)(4\text{-}nba)_2]_n$	3536	3264	1591	1412	1514	1346	-
$[Ca(pyr)_2(4\text{-}nba)_2]$	-	3180	1572	1396	1512	1346	-
$[Ca(H_2O)_2(4\text{-}nba)_2].2(dmp)$	3600	3269	1568	1416	1514	1342	-
$[Ca(H_2O)_6(4\text{-}nba)](4\text{-}nba)(2\text{-}ap)\cdot H_2O$	3475	3379	1572	1422	1518	1341	-
$[Ca(4\text{-}nba)_2(2\text{-}ap)]$	-	3458, 3345	1566	1416	1518	1346	-
$[(H_2O)_4Li_2(4\text{-}nba)(\mu\text{-}H_2O)_2](4\text{-}nba)$	3582	-	1566	1408	1512	1344	
$[Na(4\text{-}nba)(H_2O)_3]$	3578	-	1572	1393	1514	1350	
$[K(4\text{-}nba)(H_2O)_2]$	3578	-	1564	1402	1530	1348	
$[Sr(4\text{-}nba)(H_2O)_7](4\text{-}nba).2H_2O$	3603	-	1564	1412	1520	1343	-
$[Sr(4\text{-}nba)_2(H_2O)_4]$	3632-3300	-	1564	1412	1512	1350	-
$[Sr(4\text{-}nba)(DMF)(H_2O)_3].(4\text{-}nba)$	3604	-	1562	1414	1512	1348	1665
$[Sr_2(H_2O)_2(4\text{-}nba)_4(NMF)_3]$	3600	3408	1562	1406	1524	1348	1678
$[Sr(H_2O)_3(4\text{-}nba)_2(form)_3]$	3600-3300	3402	1562	1400	1514	1348	1689
$[Sr(4\text{-}nba)_2(pyr)_3]$	-	3354	1562	1398	1512	1346	-
$[Mg(H_2O)_6(2\text{-}ca\text{-}4nba)_2]$	3568-3215	-	1643	1427	1566	1350	1680
$[Ca(H_2O)_2(2\text{-}ca\text{-}4nba)_2]$	3613-3464	-	1605	1416	1574	1358	1680
$[Mg(2\text{-}nba)_2(H_2O)_4]$	3647-3572	-	1572	1423	1523	1352	-
$[Mg(2\text{-}nba)_2]$	-	-	1568	1402	1520	1338	-
$[Ca(H_2O)_2(2\text{-}nba)_2]$	3649	-	1568	1423	1526	1350	-
$[Ca(2\text{-}nba)_2]$	-	-	1566	1415	1524	1350	-
$[Sr(2\text{-}nba)_2(H_2O)_4]$	3539-3362	-	1603	1397	1525	1344	-
$[Sr(2\text{-}nba)_2]$	-	-	1568	1394	1531	1377	-
$[Ba(2\text{-}nba)_2(H_2O)_3]$	3700-2900	-	1566	1404	1523	1347	-
$[Ba(2\text{-}nba)_2]$	-	-	1568	1404	1520	1341	-
$[Cs_2(3\text{-}npth)]_n$	-	-	1574	1460	1523	1346	-
$[[Ca(H_2O)_2(3\text{-}$	3604-	-	1574	1418	1535	1348	-

$npth)]\cdot H_2O]_n$	3500						
$[Mg(H_2O)_5(3\text{-}npth)]\cdot 2H_2O$	3600-3558	-	1568	1379	1537	1348	-
$[Sr(3\text{-}npth)]$	-	-	1575	1410	1547	1350	-
$[Ba(3\text{-}npth)]$	-	-	1583	1400	1524	1342	-
$[Mg_3(btc)_2(H_2O)_{18}]$	3600-3000	-	1688	1433	-	-	-
$[Mg_3(btc)_2(H_2O)_{12}]$	3600-3000	-	1659	1431	-	-	-
$[Ca_3(btc)_2(H_2O)_{12}]$	3600-3000	-	1607	1433	-	-	-
$[Ca_3(btc)_2]$	-	-	1555	1433	-	-	-
$[Sr_3(btc)_2(H_2O)_8]$	3600-3000	-	1611	1436	-	-	-
$[Ba_3(btc)_2(H_2O)_8].2H_2O$	3600-3000	-	1614	1433	-	-	-
$[Ca(H_2O)_2(L_1)_2]\cdot H_2O$	3610	-	1567	1401	-	-	-
$[Ca(L_1)_2]$	-	-	1551	1406	-	-	-
$[Ca(H_2O)_2(L_2)_2]\cdot 2H_2O$	3636	-	1556	1402	-	-	-
$[Ca(L_2)_2]$	-	-	1556	1396	-	-	-
$[Ca(L)_2(H_2O)]$	3600	-	1545	1402	-	-	-
$[Ca(L)_2]$	-	-	1554	1402	-	-	-
$[Ba(H_2O)_2(2\text{-}Clphac)_2]_n$	3600-3279	-	1549	1392	-	-	-
$[Mg(H_2O)_6(5\text{-}niphth)]$	3634-3099	-	1556	1369	1514	1350	-
$[Ca(H_2O)_4(5\text{-}niphth)]$	3600-3096	-	1572	1388	1535	1346	-
$[Mg(hip)_2(H_2O)_6]$	3600-3100	1602	1550	1406	-	-	-
$[Sr(hip)_2(H_2O)_4]$	3600-3200	1643	1574	1408	-	-	-

The presence of water in **1a** is evidenced by the strong and broad absorption around 3500 cm^{-1} in its infrared spectrum assignable to O-H vibration. It is to be noted that the profile of the O-H signal of compound **1a** is quite different as compared to that of the tetrahydrate compound **1**. In addition, the IR signals of the nitro and carboxylate functionalities, which occur between 1300 to 1650 cm^{-1} are broadened in **1a** as compared to the spectrum of **1** (Figure 1). The formation of the anhydrous compounds **2** or **3** is evidenced by their IR spectra, which are devoid of the signals for O-H vibrations of water and is further confirmed by the appearance of additional bands due to the incorporation of the N-donor ligand in its mid IR spectrum (Figure 1). The presence of water in **4** is inferred from the strong signal in its infrared spectrum at 3536 cm^{-1}. The signal at 3264 cm^{-1} can be assigned to the υ_{N-H} (2-MeIm) vibration (Figure 2) of the N-donor ligand. It is to be noted that the profile of the infrared spectra in the region 3500 to 2800 cm^{-1} of compound **4** is quite different as compared to that of the tetraaqua compound **1** or the monohydrate [Ca(H_2O)(4-nba)$_2$] **1a**. Compound **4** exhibits several signals in the mid IR region indicating the presence of the organic moieties. The strong signals at 1514 and 1346 cm^{-1} can be assigned to the asymmetric and symmetric stretching vibrations of the –NO_2 group of 4-nba while the bands at 1591 and 1570 cm^{-1} are assignable to the asymmetric vibration of the carboxylate group. The signal at 1411 cm^{-1} is assigned for the symmetric vibration of the –COO group.

The IR spectrum of **5** and **6** exhibits several sharp bands in the mid-infrared region, indicating the presence of the organic moieties. A comparison of the IR spectra of **5** and **6** with that of [Ca(H_2O)$_4$(4-nba)$_2$] **1** reveals changes in profile of the spectra in the 3000-3500 cm^{-1} region and the 1600-1300 cm^{-1} region due to the differently hydrated nature of **1** and **6** (Figure 3). Compound **5** shows no absorption in 3600-3500 cm^{-1} region indicating absence of water. In both the compounds **5** and **6** the symmetric and asymmetric stretching vibrations of the carboxylate are observed at 1568 and 1416 cm^{-1}, while those of the nitro group are observed at around 1514 and 1342 cm^{-1} respectively. In addition to a change in profile of the IR spectrum of **7** as compared to that of [Ca(H_2O)$_4$(4-nba)$_2$] **1** in the 3000-3500 cm^{-1} region, additional signals are observed in the spectrum of **7** at 1258, 1155, 1044, 988, 876, 779 cm^{-1} indicating the presence of 2-ap in **7**. A broad and strong absorption in the O-H and N-H region of the IR spectrum with signals centered around 3475 cm^{-1} and 3345 cm^{-1} may be assigned for the O-H and N-H stretching vibrations of water and amine of 2-ap respectively in **7**. The symmetric and asymmetric stretching vibrations of carboxylate are observed at 1572 and 1421 cm^{-1} respectively, while those of the nitro group are observed at around 1517 and 1341 cm^{-1} respectively (Figure 4). Although the IR spectrum of all the compounds exhibits absorptions due to the vibrations of the carboxylate and nitro groups, no definite conclusions can be drawn on the exact nature of the binding of the 4-nba ligand based only on infrared data.

The presence of 4-nba in compounds **8**, **9** and **10** can be confirmed based on the several signals in the mid IR region. It is interesting to note that the infrared spectra of all the three compounds are nearly similar excepting for a change in the profile of the spectra in the 3500-3000 cm^{-1} region (Figure 5). The broad signal in this region assignable for the $\upsilon_{O\text{-}H}$ vibration disappears in the spectra of samples obtained on heating **8** and **9** at 130°C (Figure 6). The values of the symmetric (υ_s) and asymmetric (υ_{as}) stretching vibrations of the carboxylate and the nitro groups are in the expected range for compounds **8-9**.

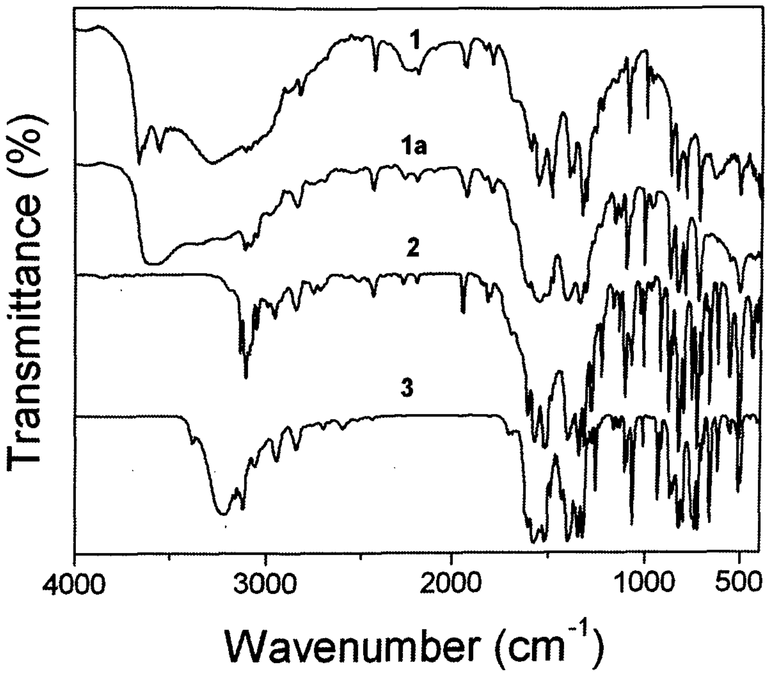

Figure 1- IR spectra of compound [Ca(H_2O)$_4$(4-nba)$_2$] **1**, [Ca(H_2O)(4-nba)$_2$] **1a**, [Ca(N-MeIm)(4-nba)$_2$] **2** and [Ca(Im)(4-nba)$_2$] **3**

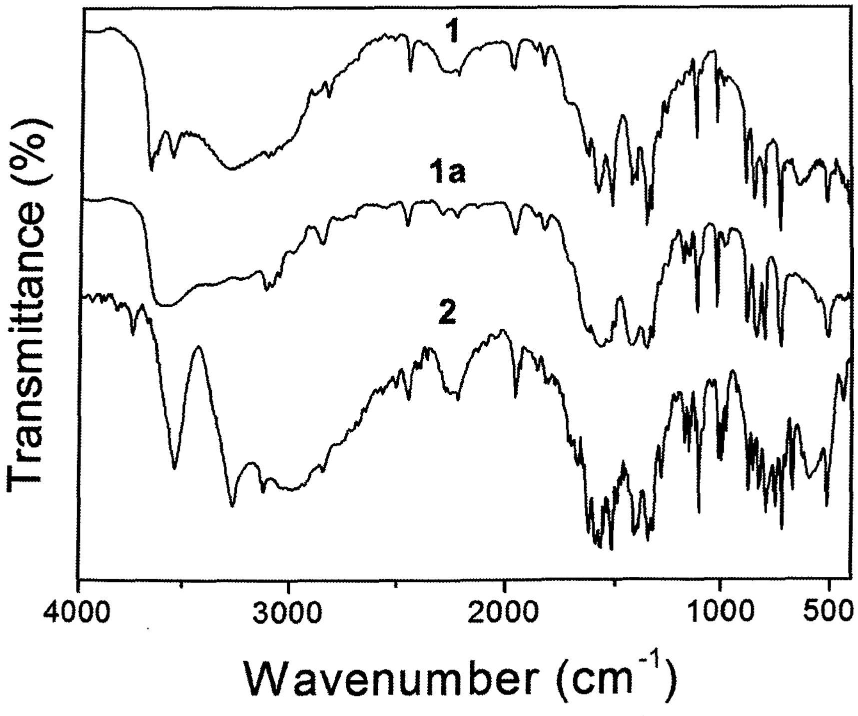

Figure 2 - Infrared spectra of compound [Ca(H_2O)$_4$(4-nba)$_2$] **1**, [Ca(H_2O)(4-nba)$_2$] **1a**, and **2**) [Ca(2-MeIm)(4-nba)$_2$] **4**

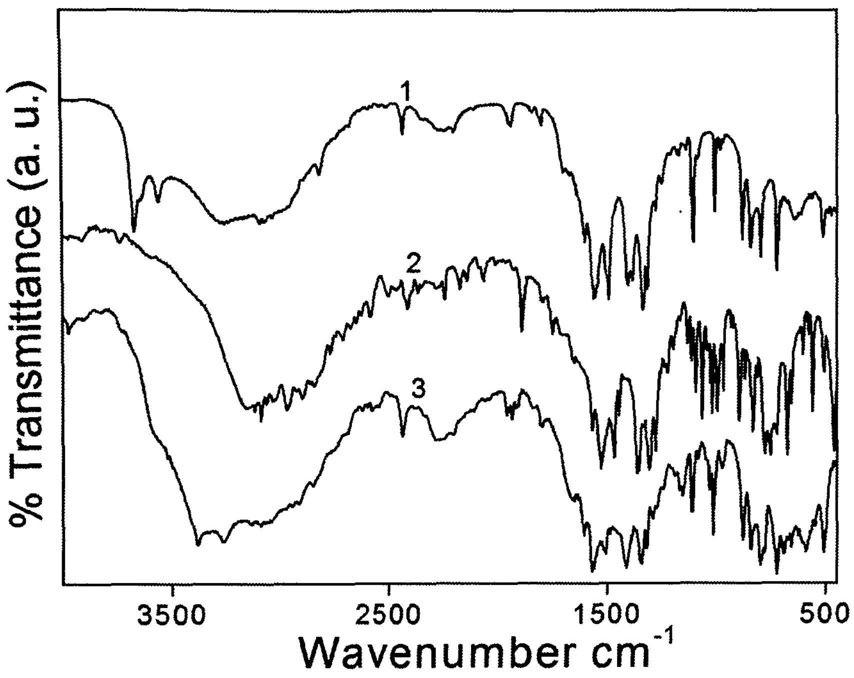

Figure 3- Infrared spectra of **1)** $[Ca(H_2O)_4(4\text{-nba})_2]$ **1**, **2)** $[Ca(pyr)_2(4\text{-nba})_2]_n$ **5**, and **3)** $[Ca(H_2O)_2(4\text{-nba})_2].2dmp]_n$ **6**

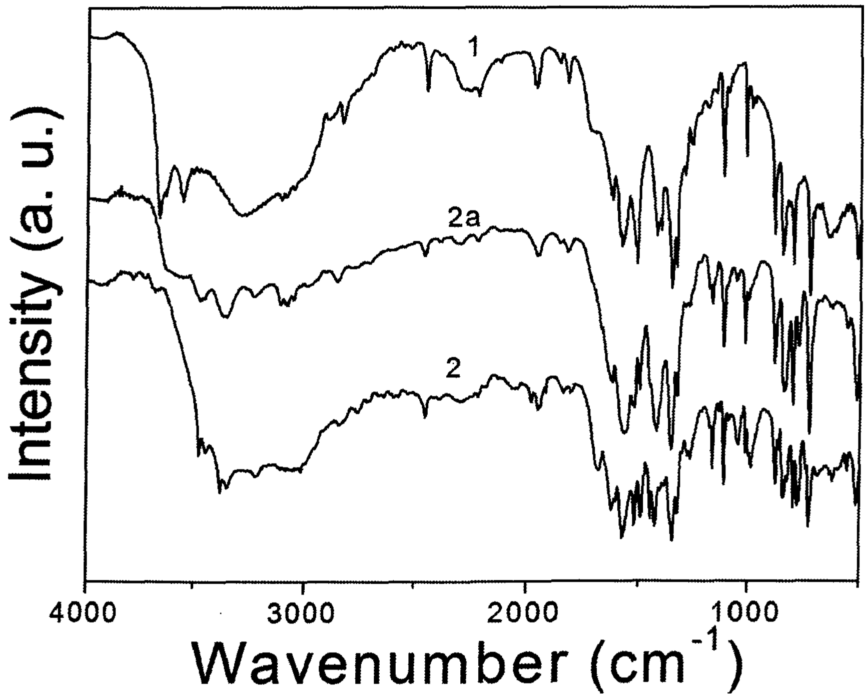

Figure 4- Infrared spectra of **1)** $[Ca(H_2O)_4(4\text{-nba})_2]$ **1**, **2a)** $[Ca(2\text{-ap})(4\text{-nba})_2]_n$ **7a**, **2)** $[Ca(H_2O)_6(4\text{-nba})].(H_2O)(4\text{-nba})(2\text{-ap})$ **7**

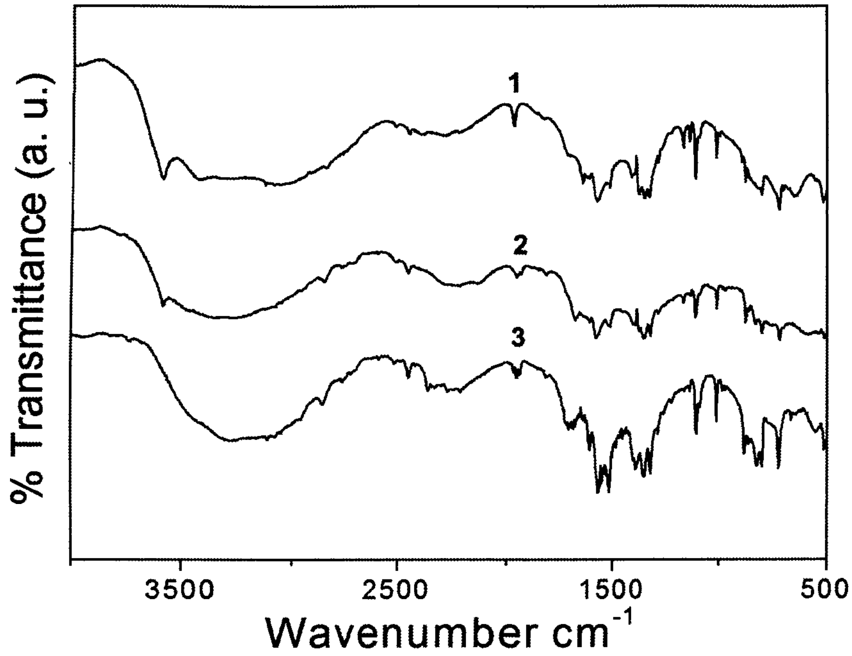

Figure 5- Comparative infrared spectra of **1**) $[(H_2O)_4Li_2(\mu\text{-}H_2O)_2](4\text{-nba})_2$ **9**, **2**) $[Na(4\text{-nba})(H_2O)_3]_n$ **9** and **3**) $[K(H_2O)_3(4\text{-nba})]$ **10**

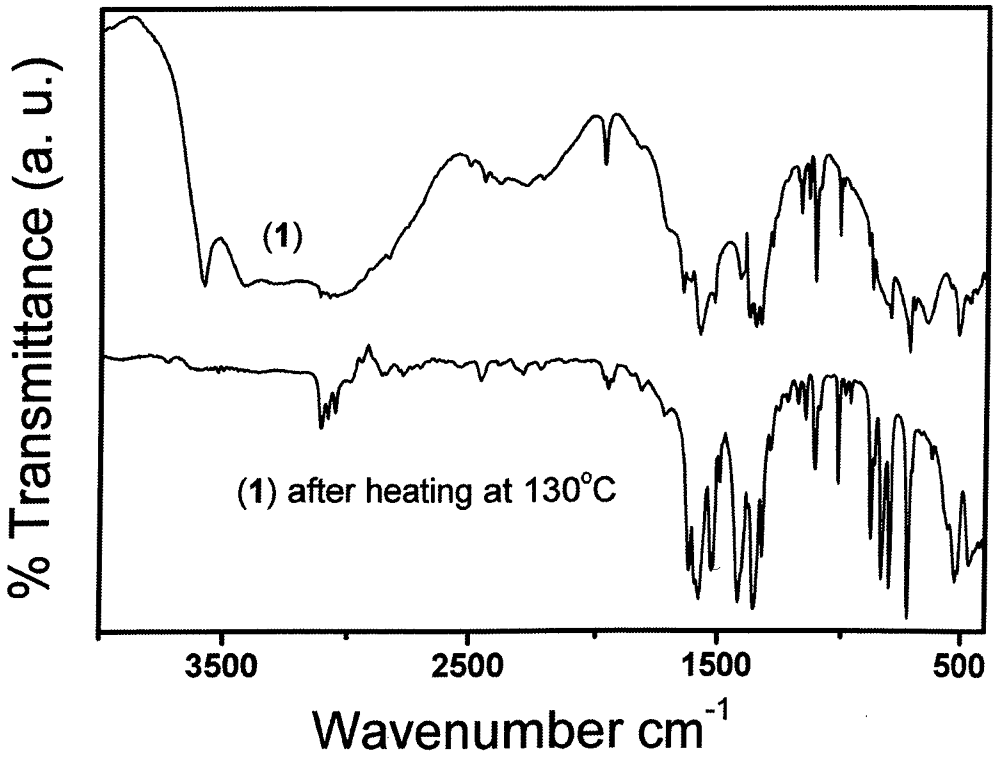

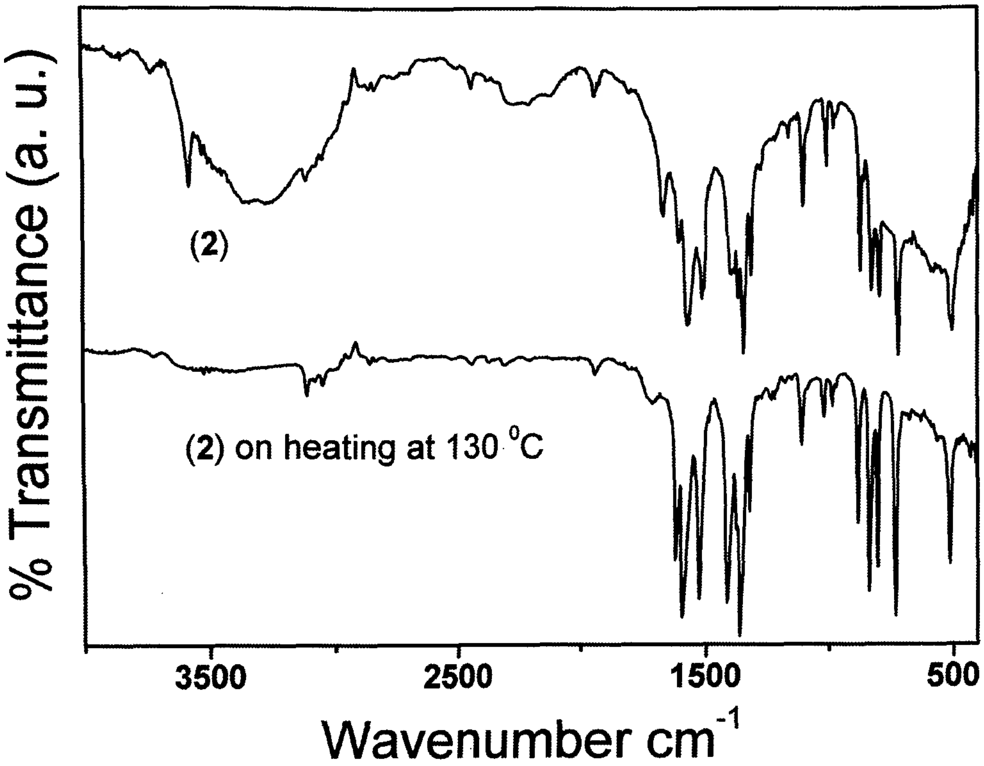

Figure 6 – comparative infrared spectra of **8** and **8a** heated at 130°C (top); Infrared spectra of **9** and **9a** heated at 130°C (bottom).

The presence of water in **11**, **11a**, **12**, **13** and **15** is evidenced by the strong and broad absorption around 3600-3500 cm^{-1} in its infrared spectrum assignable to O-H vibration. It is to be noted that the profile of the O-H signal of tetrahydrate compound **11a** is quite different as compared to that of the compound **1**. In addition the IR signals of the nitro and carboxylate functionalities, which occur between 1300 to 1650 cm^{-1} are broadened in **11a** as compared to the spectrum of **11** (Figure 7). The symmetric and asymmetric absorption due to carboxylate is observed at 1562 and 1412 cm^{-1} in **11** and **11a** while compounds **12**, **13**, **14** and **15** show asymmetric stretch at 1562 and symmetric stretch at 1414, 1406, 1398, 1400 as shown in Figure 7-8. The peaks at 3408, 3354, 3402 cm^{-1} is due to the N-H stretching of ligands like N-methylformamide in **13**, pyrazole in **14** and formamide in **15**. The presence of O-donor ligand in compounds **12**, **13** and **15** was confirmed by the presence of amide stretching signal observed at 1665, 1678 and 1689 cm^{-1} in compounds **12**, **13** and **15** respectively. This was further confirmed by presence of several sharp bands in the mid-infrared region of **12-15**, indicating the presence of the organic moieties. The asymmetric stretching and symmetric stretching frequencies of NO_2 group is mainly observed between 1524-1512 cm^{-1} and 1343-1350 cm^{-1} respectively.

The formation of the anhydrous compounds **14** is evidenced by its IR spectra, which are devoid of the signals for O-H vibrations of water and is further confirmed by the appearance of additional bands due to the incorporation of the N-donor ligand (pyr) in its mid IR spectrum. The signal at 3354 cm^{-1} can be assigned to the $\upsilon_{N\text{-}H}$ (pyr) vibration of the N-donor ligand (Figure 8).

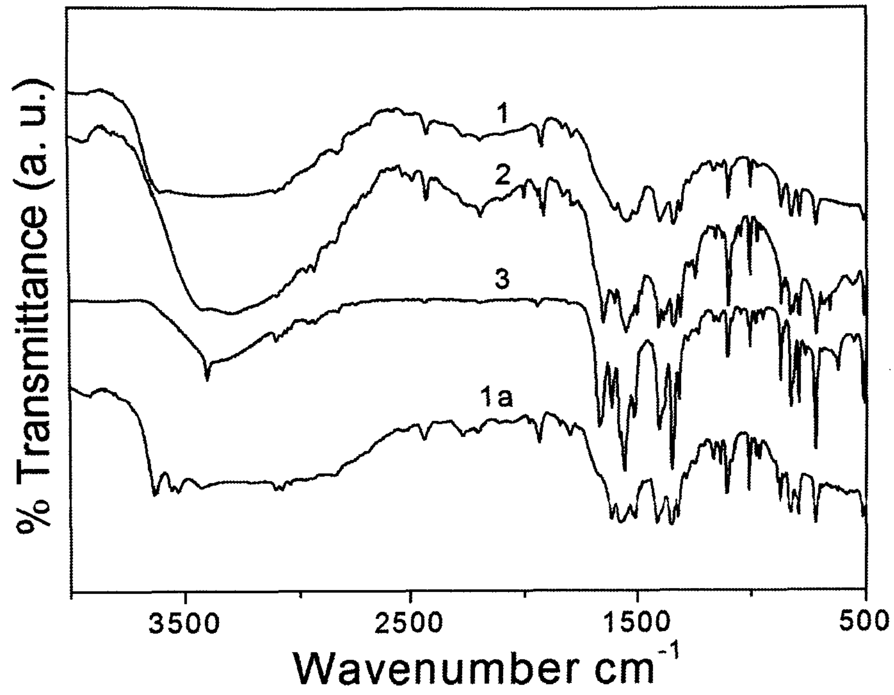

Figure 7- Infrared spectra of **1)** [Sr(4-nba)(H_2O)$_7$](4-nba).2H_2O **11**, **1a)** [Sr(4-nba)$_2$(H_2O)$_4$] **11a**, **2)** [Sr(4-nba)(DMF)(H_2O)$_3$](4-nba) **12**, **3)** [Sr(H_2O)(4-nba)$_2$(NMF)$_{1.5}$] **13**

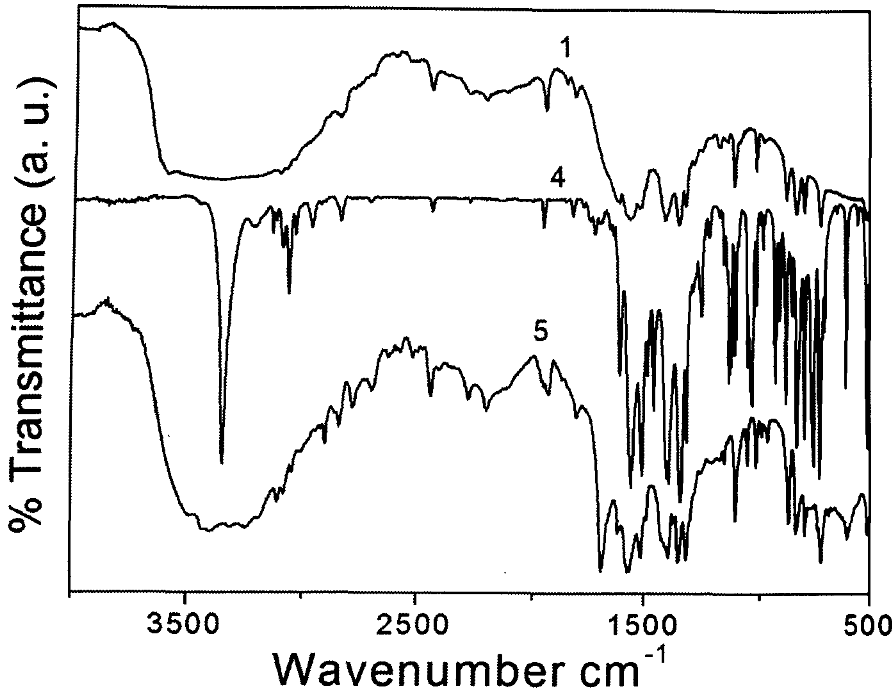

Figure 8 - Infrared spectra of **1**) $[Sr(4\text{-}nba)(H_2O)_7](4\text{-}nba).2H_2O$ **11**, **4**) $[Sr(4\text{-}nba)_2(pyr)_2]$ **14**, **5**) $[Sr(H_2O)_3(4\text{-}nba)_2(HCONH_2)]$ **15**

The IR spectrum of $[Mg(H_2O)_6](2\text{-}ca\text{-}4nba)_2$ **16** and $[Ca(H_2O)_2(2\text{-}ca\text{-}4nba)_2]_n$ **17** exhibits several signals in the mid IR region, many of which were also observed in the free acid region thus indicating the presence of the organic moiety in **16** and **17**. The presence of water in both the compounds can be readily inferred from the strong signal in its infrared spectrum at around 3600 cm^{-1}. The peaks at 3464 and 3358 cm^{-1} can be assigned for the N-H stretching vibration of the amide functionality, while the band due to the C=O of the amide is observed as a strong signal at 1680 cm^{-1}. The intense bands at 1573 and 1358 cm^{-1} can be assigned to the asymmetric and symmetric stretching vibrations of the $-NO_2$ group. The asymmetric and symmetric stretching vibrations of the carboxylate are observed as strong bands at 1605 and 1416 cm^{-1} respectively (Figure 9). The IR spectrum of **18** and **19** exhibits several signals in the mid IR region, many of which are also observed in the free acid thus indicating the presence of the organic moiety in **18** and **19**. The absence of water signal in its infrared spectrum at around 3600 cm^{-1} confirmed the anhydrous nature of **18** and **19**. The peaks at 3464 and 3358 cm^{-1} can be assigned for the N-H stretching vibration of the amide functionality, while the band due to the C=O of the amide is observed as a strong signal at 1680 cm^{-1}. The intense bands at 1573 and 1358 cm^{-1} can be assigned to the asymmetric and symmetric stretching vibrations of the $-NO_2$ group. The asymmetric and symmetric stretching vibrations of the carboxylate are observed as strong bands at 1605 and 1416 cm^{-1} respectively.

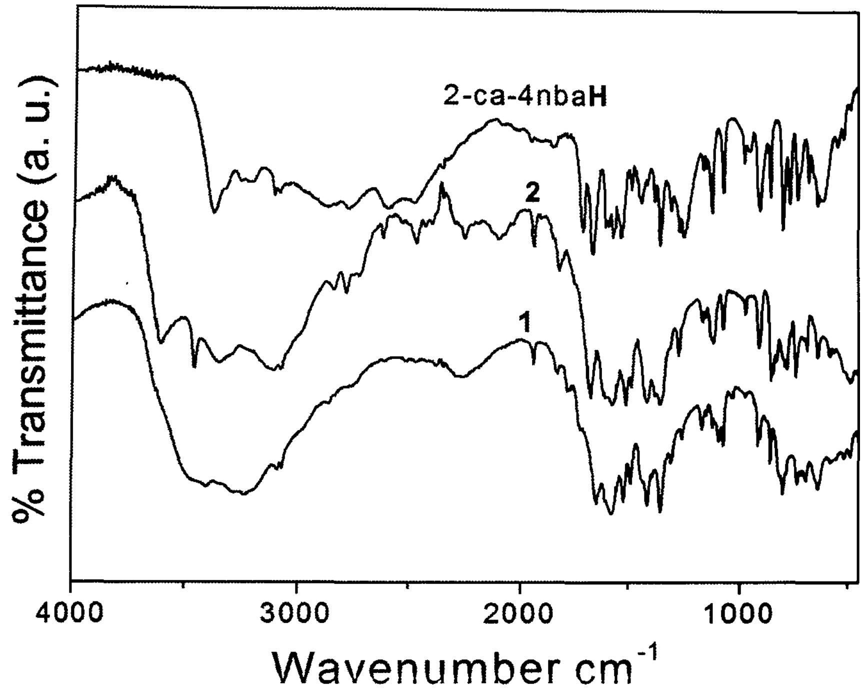

Figure 9- IR spectra of 2-ca-4nbaH and **1)** $[Mg(H_2O)_6](2\text{-ca-4nba})_2$ **16** and **2)** $[Ca(H_2O)_2(2\text{-ca-4nba})_2]_n$ **17**

The IR spectra of 2-nitrobenzoate compounds **20-23** and and the dehydrated phases **20a-23a** exhibit several sharp bands in the mid-infrared region, clearly indicating the presence of the organic moiety (Figure 10, 11). The strong signal between 3600-3500 cm^{-1} in **20-23** indicates the presence of water and can be assigned to the O-H stretching vibration. The IR spectrum of anhydrous compounds **20a-23a** is devoid of bands above 3074 cm^{-1}, which is indicative of the anhydrous nature of **20a-23a**. Below 3074 cm^{-1}, the IR spectrum of the hydrated and the dehydrated phase are very similar. Although the IR spectra of **20-23** and **20a-23a** exhibit the absorptions due to vibrations of the carboxylate and nitro groups in the expected range, no definite conclusions can be drawn on the exact nature of the binding of the 2-nba ligand based only on IR data.

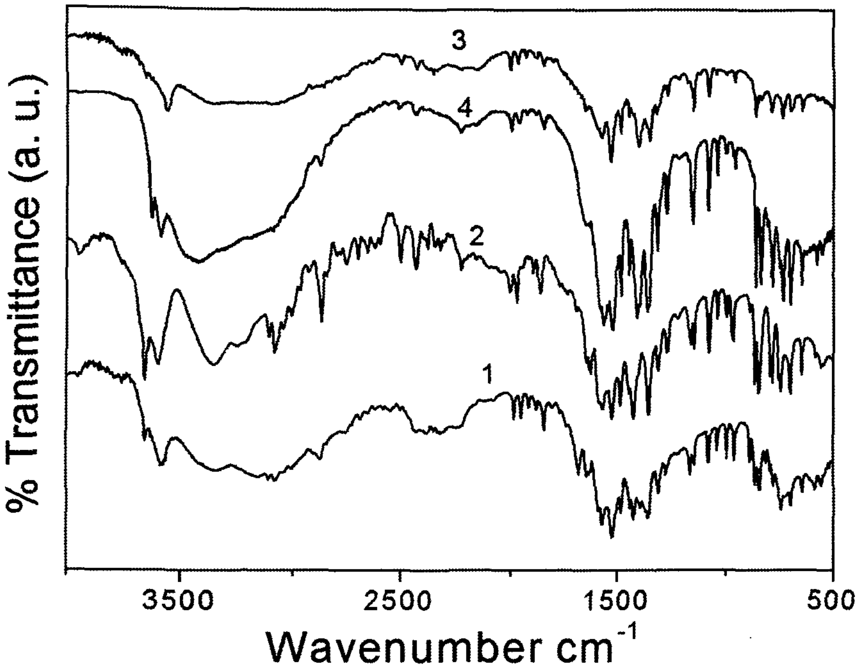

Figure 10- IR spectra of **1**) [Mg(H_2O)$_4$](2-nba)$_2$ **20, 2**) [Ca(H_2O)$_2$(2-nba)$_2$]$_n$ **21, 3**) [Ba(H_2O)$_3$(2-nba)$_2$]$_n$ **22, 4**) [Sr(H_2O)$_4$(2-nba)$_2$]$_n$ **23**.

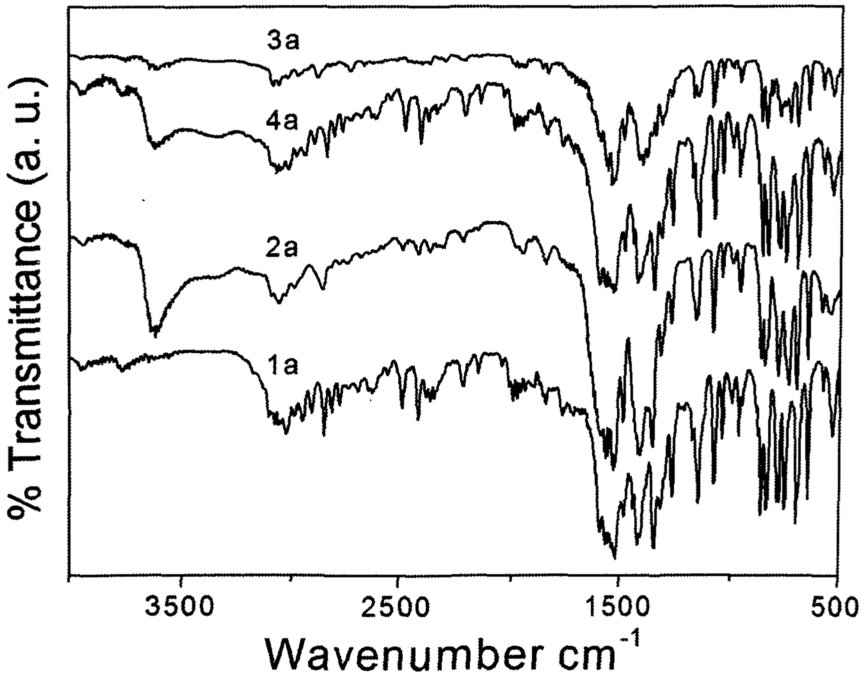

Figure 11- IR spectra of **1a**) [Mg(2-nba)$_2$] **20a, 2a**) [Ca(2-nba)$_2$]$_n$ **21a, 3a**) [Ba(2-nba)$_2$]$_n$ **22a, 4a**) [Sr(2-nba)$_2$]$_n$ **23a**

The IR spectra of **24-28** compounds exhibit several sharp bands in the mid-infrared region, many of which are also observed in the free acid clearly indicating the presence of the organic moiety (Figure 12). The anhydrous nature of **27-28** can be evidenced from its infrared spectrum which does not show any strong band above 3180 cm^{-1}, unlike the IR spectra of the hydrated compounds **24** to **26** which exhibit a strong and broad signal around 3500 cm^{-1} assignable for O-H stretching vibration. The IR spectra of all compounds exhibit characteristic signals assignable for the asymmetric and symmetric stretching absorptions of the carboxylate and nitro groups between 1600 and 1350 cm^{-1}.

The broad peak around 3600-3000 cm^{-1} in compounds **29-32** indicates the presence of water in compound **29**, **29a**, **30**, **31** and **32** respectively (Figure 13). The symmetric and asymmetric absorption due to btc is observed at 1605-1550 cm^{-1} and 1433-1378 cm^{-1} respectively. The absence of bands at 1730-1690 cm^{-1} in all the 4 compounds **29**, **29a**, **30**, **31** and **32** where the COOH is expected to appear (as observed in H_3btc) is indicative of the deprotonation of H_3btc upon reaction with metal sources. The anhydrous nature of **29a-32a** can be evidenced from its infrared spectrum which does not show any strong band above 3180 cm^{-1}, unlike the IR spectra of the hydrated compounds **29** to **32** which exhibit a strong and broad signal around 3500 cm^{-1} assignable for O-H stretching vibration (Figure 14).

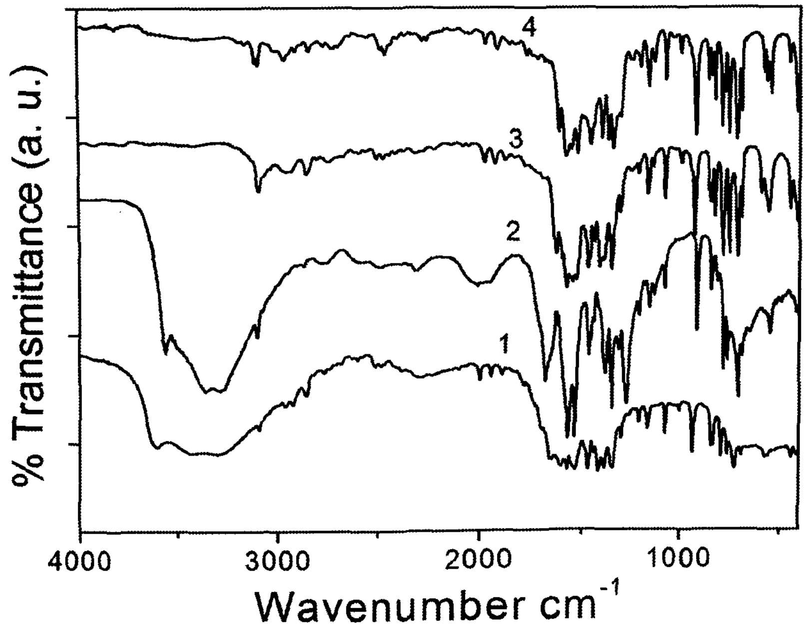

Figure 12- Infrared spectra of **1)** $[Mg(H_2O)_5(3\text{-npth})]\cdot 2H_2O$ **25**, **2)** $[[Ca(H_2O)_2(3\text{-npth})]\cdot H_2O]_n$ **26**, **3)** [Ba(3-npth)] **27**, **4)** [Sr(3-npth)] **28**

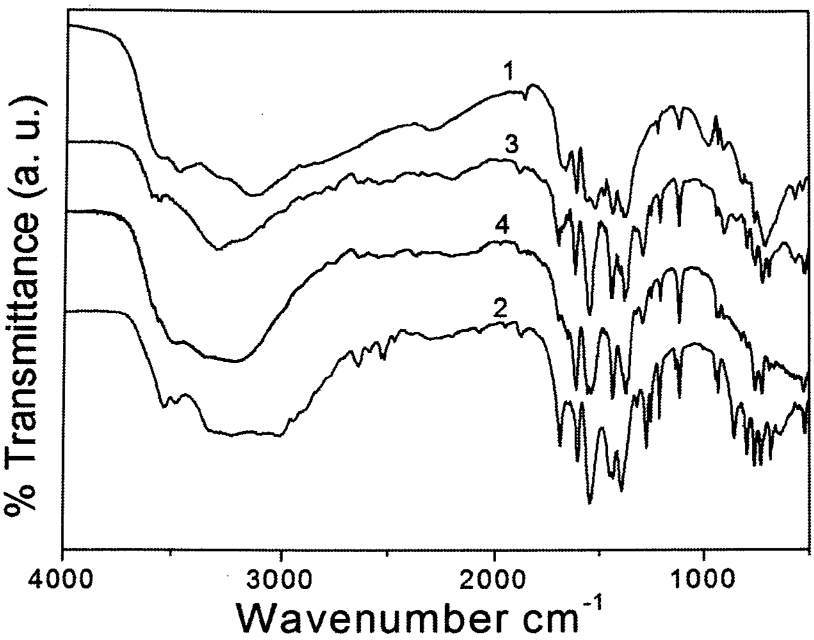

Figure 13 - Infrared spectra of **1)** [$Mg_3(btc)_2(H_2O)_{18}$] **29**, **2)** [$Ca_3(btc)_2(H_2O)_{12}$] **30**, **3)** [$Ba_3(btc)_2(H_2O)_8$].$2H_2O$ **31**, **4)** [$Sr_3(btc)_2(H_2O)_8$] **32**.

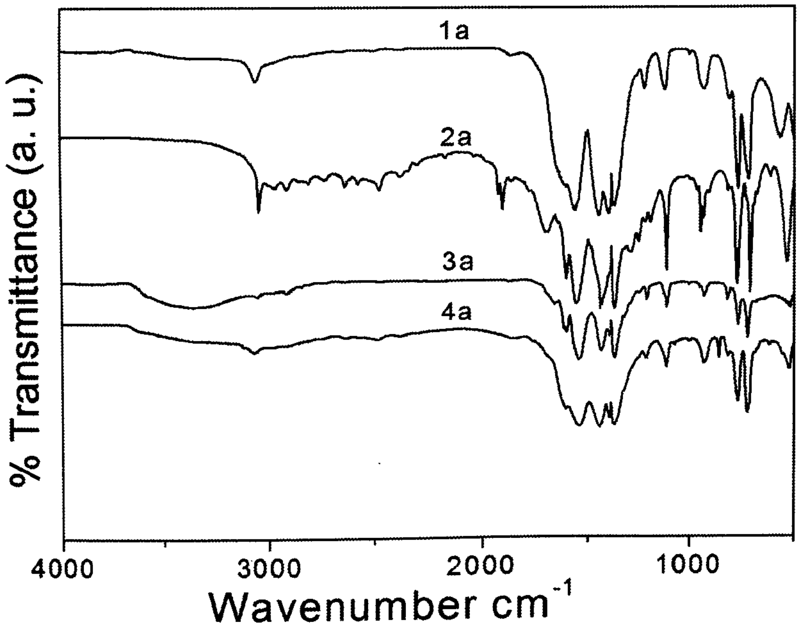

Figure 14 - Infrared spectra of dehydrated **1a)** [$Mg_3(btc)_2$] **29a**, **2a)** [$Ca_3(btc)_2$] **30a**, **3a)** [$Ba_3(btc)_2$] **31a**, **4a)** [$Sr_3(btc)_2$] **32a**

The IR spectra of compounds $[[Ca(H_2O)_2(4\text{-}OMephac)_2].H_2O]_n$ **33** $[[Ca(H_2O)_2(2\text{-}Clphac)_2].2H_2O]_n$ **34** $[Ca(H_2O)_3(phac)_2]$ **35** (Figure 15) exhibit several signals in the mid IR region indicating the presence of the organic moiety. The intense band at 3600-3610 (in **33** and **35**) and 3636 cm^{-1} (in **34**) can be assigned for the O-H stretching vibration of water. As expected, this signal is not observed in the anhydrous compounds **33a-35a**. The characteristic signals due to the symmetric and asymmetric stretching of the carboxylate are observed at 1567 and 1401 cm^{-1} (in **33**) and 1556 and 1402 cm^{-1} (in **34**) and 1545 and 1402 cm^{-1} (in **35**) respectively. The IR spectra of compounds $[Ba(H_2O)_2(2\text{-}Clphac)_2]_n$ **36** $[Mg(H_2O)_6(5\text{-}nisoph)]$ **37** and $[Ca(H_2O)_4(5\text{-}nisoph)]$ **38** and $[Mg(H_2O)_6(hip)_2]$ **39** and $[Sr(H_2O)_4(hip)_2]$ **40** exhibit several signals in the mid IR region indicating the presence of the organic moiety. The intense band at 3600-3300 cm^{-1} can be assigned for the O-H stretching vibration of water. The characteristic signals due to the asymmetric and symmetric stretching of the carboxylate are observed at 1556 and 1369 cm^{-1} (in **37**) and 1572 and 1388 cm^{-1} (in **38**) respectively (Figure 16). The intense bands at 1524 and 1350 cm^{-1} (in **37** and **38**) can be assigned to the asymmetric and symmetric stretching vibrations of the $-NO_2$ group. On the other hand, the compound **39** and **40** are devoid of such NO_2 signals and signals around 1550 cm^{-1} and 1406 cm^{-1} can be assigned to carboxylate moiety (Figure 17).

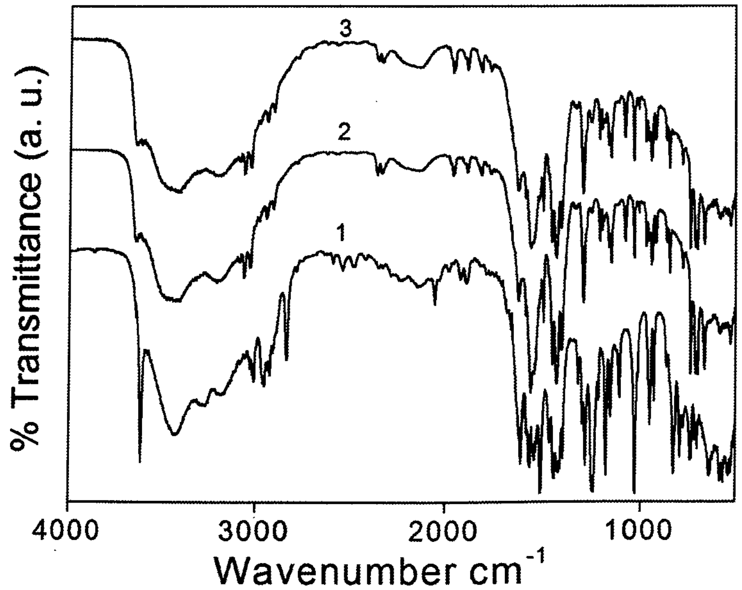

Figure 15- Infrared spectrum overlay of compound **1)** $[[Ca(H_2O)_2(4\text{-}OMephac)_2].H_2O]_n$ **33, 2)** $[[Ca(H_2O)_2(2\text{-}Clphac)_2].2H_2O]_n$ **34** and **3)** $[Ca(H_2O)_3(phac)_2]$ **35**

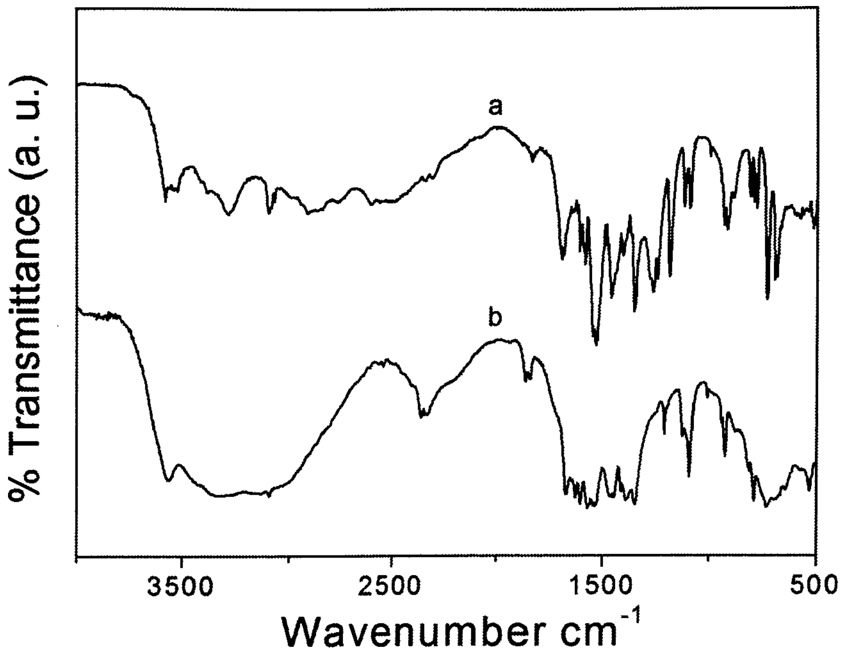

Figure 16- Infrared spectra of compounds **a)** [Mg(H_2O)$_6$(5-nisoph)] **37** and **b)** [Ca(H_2O)$_2$(5-nisoph)] **38**

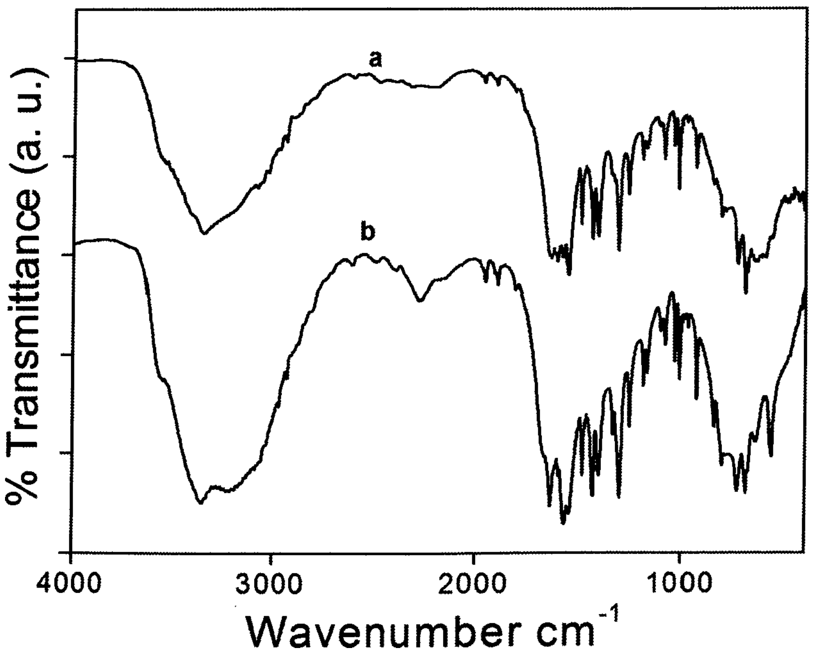

Figure 17- Infrared spectra of compounds **a)** [Mg(H_2O)$_6$(hip)$_2$] **39** and **b)** [Sr(H_2O)$_4$(hip)$_2$] **40**

3.3.2- UV-visible, diffuse reflectance and flourescence spectroscopy

All the compounds in the current study were subjected to UV-visible, solid state diffuse reflectance, fluorescence emission, and luminscence studies. The UV-Vis spectra of synthesized compounds exhibited an absorption in the region around 250-300 nm which can be assignable to the charge transfer of the aromatic carboxylic acid used as ligand. Diffuse reflectance spectrum of all the compound were identical to that of the free acid and can be assigned to the intramolecular charge transfer transition of carboxylate. The fluorescence emission spectrum of few compounds showed enhanced emission as compared to that of the free acid. These emissions are neither ligand-to-metal charge transfer (LMCT) nor metal-to-ligand charge transfer (MLCT) and can be assigned to the intraligand fluorescent emission. The luminescent property was observed in few of compounds, which can be attributed to ligand centered π or n to π* orbital transitions since similar emissions are also observed for the free ligand.

The UV-Vis spectra of compounds **1-3** exhibit an absorption in the UV region around 274 nm assignable to the charge transfer of the aromatic 4-nba ligand. In view of the insolubility of **4** in all common solvents, the diffused reflectance spectrum was recorded in the UV-Vis region. The observed signals at 251 and 330 nm in the spectrum can be attributed to the intra-ligand charge transfer bands of the 4-nba ligand based on a comparison of the reflectance spectra of compounds **4** and **1** (Figure 18). The fluorescence studies of alkaline-earth metal complexes are of considerable importance since the divalent cations Mg and Ca are the most abundant in living cells and play vital roles in many cellular processes. Two emission maxima are observed at around 450 and 490 nm for compound **4**. Interestingly both 4-nbaH and 2-MeIm exhibit emission signal around 450 nm. A scrutiny of the emission spectra reveals that the emission of the Ca(II) compound **4** is reduced as compared to that of the free ligands (Figure 19). A similar reduction in the emission intensity has been recently reported for the 1D coordination polymer $[Ca(SA)_2(phen)]_n$ (SA= salicylate; phen = 1,10-phenanthroline) [49]. The diffuse reflectance spectrum of compound **6** which absorbs strongly at ~280 nm is very similar to that of the free acid and can be assigned to the intramolecular charge transfer transition of 4-nitrobenzoate (Figure 20). The UV-Vis spectrum of a dilute aqueous solution of **6** is identical to that of the spectrum of compound **1** indicating the transformation of **6** to **1** on hydrolysis (Figure 21). Unlike the polymeric $[Ca(N\text{-}MeIm)(4\text{-}nba)_2]_n$, compound which exhibits a diminished fluorescence emission intensity, the fluorescence emission spectrum of compound **6** shows an enhanced emission as compared to that of free 4-nbaH (Figure

22). These emissions are neither ligand-to-metal charge transfer (LMCT) nor metal-to-ligand charge transfer (MLCT) and can be assigned to the intra-ligand fluorescent emission. The luminescent property of **6** can be attributed to ligand centered π or n to π^* orbital transitions since similar emissions are also observed for the free ligand. The electronic spectrum of **7** exhibits a strong absorption at 297 nm and the peak position is the same as that of a dilute aqueous solution of **1** containing 2-ap in a Ca:2-ap ratio of 1:1. The observed signal can be attributed to an internal charge transfer of the aromatic 4-nba anion. The UV-visible spectra of alkali earth metal nitrobenzoate compounds **8**, **9**, **10** in water are identical (Figure 23) and the observed λ_{max} at 299 nm can be assigned for the intra-ligand charge transfer of 4-nba. The fluorescence emission spectrum of compound **8**, **9**, **10** shows an enhanced emission as compared to that of free 4-nbaH (Figure 24). These emissions are neither ligand-to-metal charge transfer (LMCT) nor metal-to-ligand charge transfer (MLCT) and can be assigned to the intraligand fluorescent emission. Diffuse reflectance spectrum of all the compound **11-15** were identical to that of the free acid and can be assigned to the intramolecular charge transfer transition of 4-nitrobenzoate. The fluorescence emission spectrum of compounds **11-15** show enhanced emission as compared to that of the free 4-nbaH (Figure 25). These emissions are neither ligand-to- metal charge transfer (LMCT) nor metal-to-ligand charge transfer (MLCT) and can be assigned to the intra-ligand fluorescent emission. The luminescent property of compounds **12-15** can be attributed to ligand centered π or n to π^* orbital transitions since similar emissions are also observed for the free ligand. The observed chemical shifts in the NMR spectra of the free acid 2-ca-4nba**H** and the Mg(II) compound **16** are in the normal range and are nearly identical. The strong absorption at 293 nm in the UV spectra of both compounds can be attributed to an internal charge transfer of the aromatic acid. The diffused reflectance spectrum of **17** exhibits a maximum centered at around 295 nm which can be assigned for the intra ligand charge transfer transition of 2-ca-4nba. The luminescence spectrum of **17** exhibits two emission maxima at around 450 and 490 nm both of which are also observed in the free acid (Figure 26). A comparison of the emission spectra reveals that the first emission band of the Ca(II) compound is enhanced in intensity. The diffused reflectance spectrum of **18** and **19** exhibits a maximum centered at around 295 nm which can be assigned for the intra-ligand charge transfer transition of 2-ca-4nba. The UV-Visible diffuse reflectance spectrum of compound **21** which absorbs strongly at around 350 nm is very similar to that of the free acid (Figure 27) and this can be assigned to the intramolecular charge transfer transition of the aromatic 2-nitrobenzoate. In addition **21** also exhibits a signal at around 250 nm unlike the free acid and the diffused reflectance spectrum of the anhydrous compound **21a** is very similar to that of **21**. The diffuse reflectance spectrum of compounds **29-32** which absorbs strongly at ~281 nm is very similar to that of the free acid and can be assigned to the intramolecular charge transfer transition of 1,3,5-benzenetricarboxylate. In view of the insolubility of **30-32** in all common solvents, the diffuse reflectance spectrum was recorded in the UV-Vis region. The observed signals at 255 and 289 nm in the spectrum can be attributed to the intra-ligand charge transfer bands of the btc ligand based on the comparison of the reflectance spectra of compound **32** and **H_3btc** (Figure 28). Compound **30-32** exhibit diminished fluorescence emission intensity, as compared to that of free acid (Figure 29). These emissions are neither ligand-to-metal charge transfer (MLCT) nor metal to ligand charge transfer (MLCT) and can be assigned to the intraligand fluorescent emissions. The diffuse reflectance spectra of compounds **33-36** are nearly identical to that of the corresponding free acid and the signals at around 265 nm can be assigned to intra-ligand charge transfer transition of the organic acid.

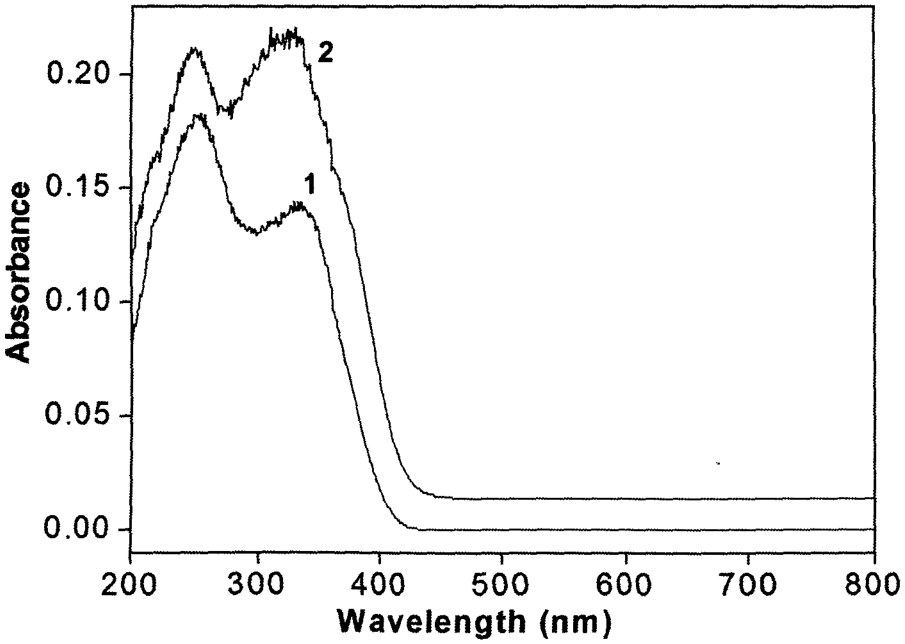

Figure 18- Diffuse reflectance spectra of compound [Ca(H_2O)$_4$(4-nba)$_2$] **1**, **2**) [Ca(H_2O)(2-MeIm)(4-nba)$_2$] **2**

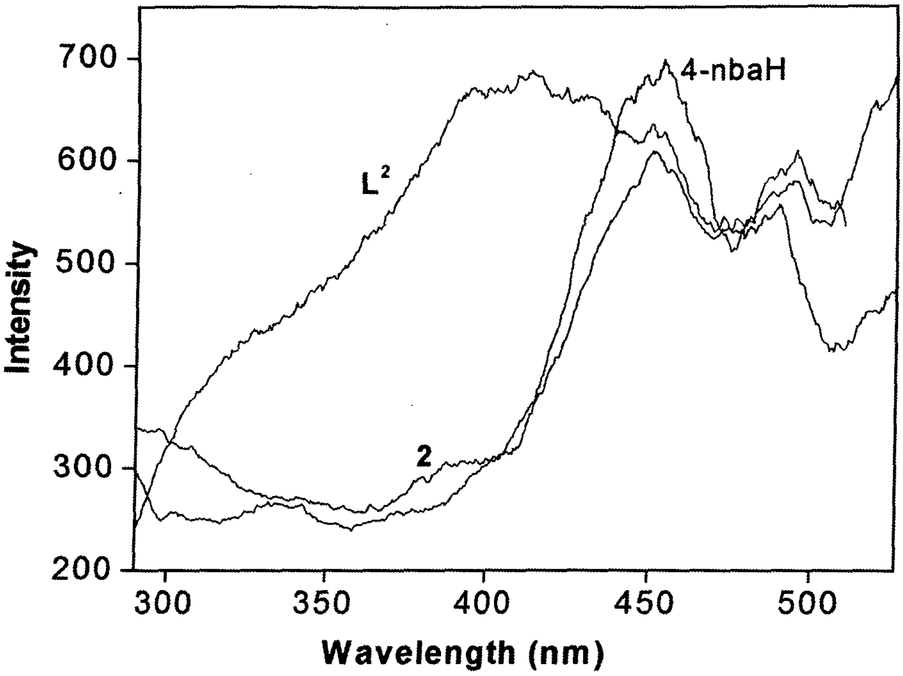

Figure 19- Luminescence spectra of free ligand L^2 = 2-MeIm; **2)** [Ca(2-MeIm)(4-nba)$_2$] **4** and free acid 4-nbaH

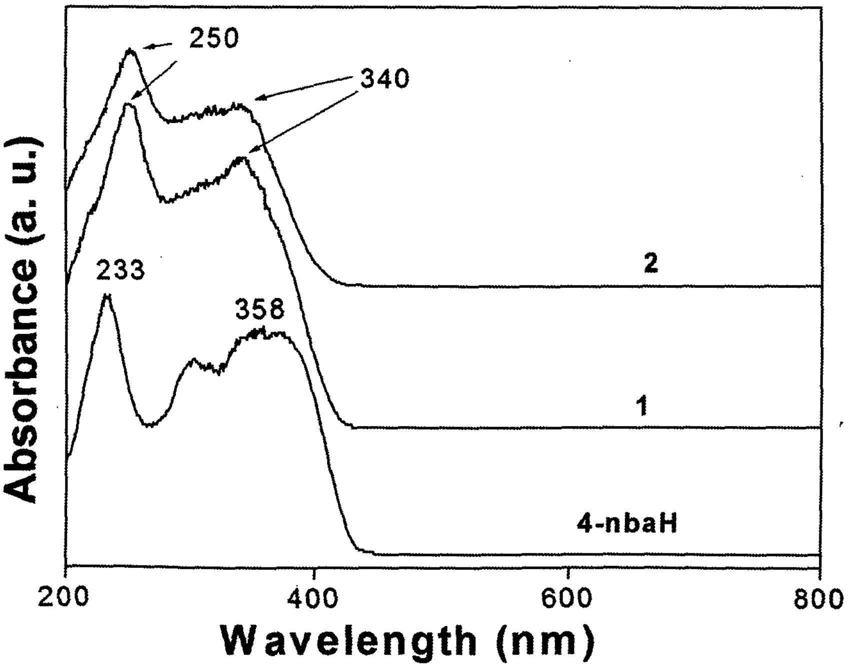

Figure 20- UV-DRS of **1)** [Ca(H$_2$O)$_4$(4-nba)$_2$] **1, 2)** [Ca(H$_2$O)$_2$(4-nba)$_2$].2dmp]$_n$ **6** and 4-nbaH

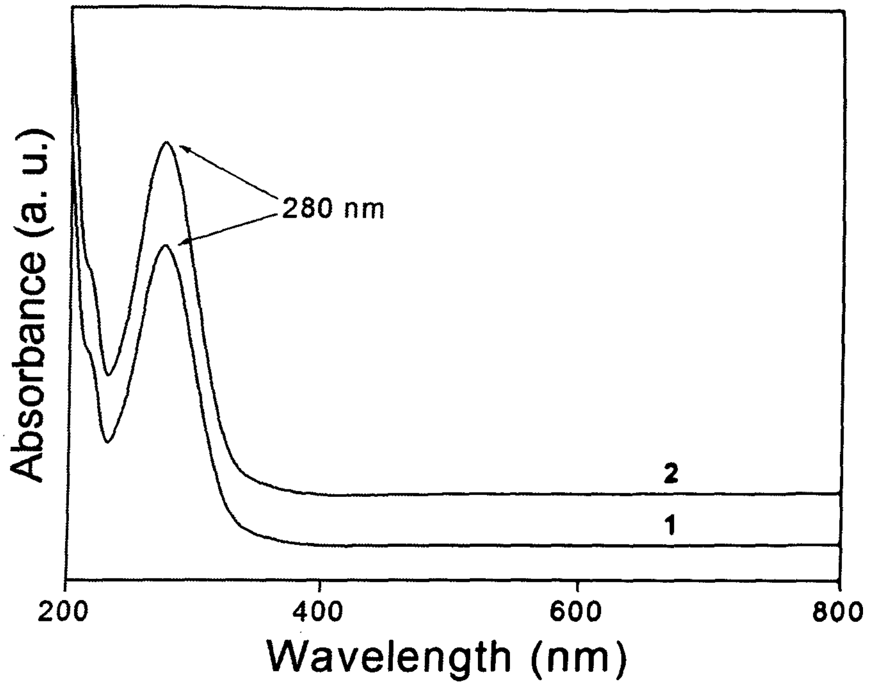

Figure 21- UV-visible spectrum of [Ca(H_2O)$_4$(4-nba)$_2$] **1** and **2**) [Ca(H_2O)$_2$(4-nba)$_2$].(dmp)$_2$]$_n$ **6**

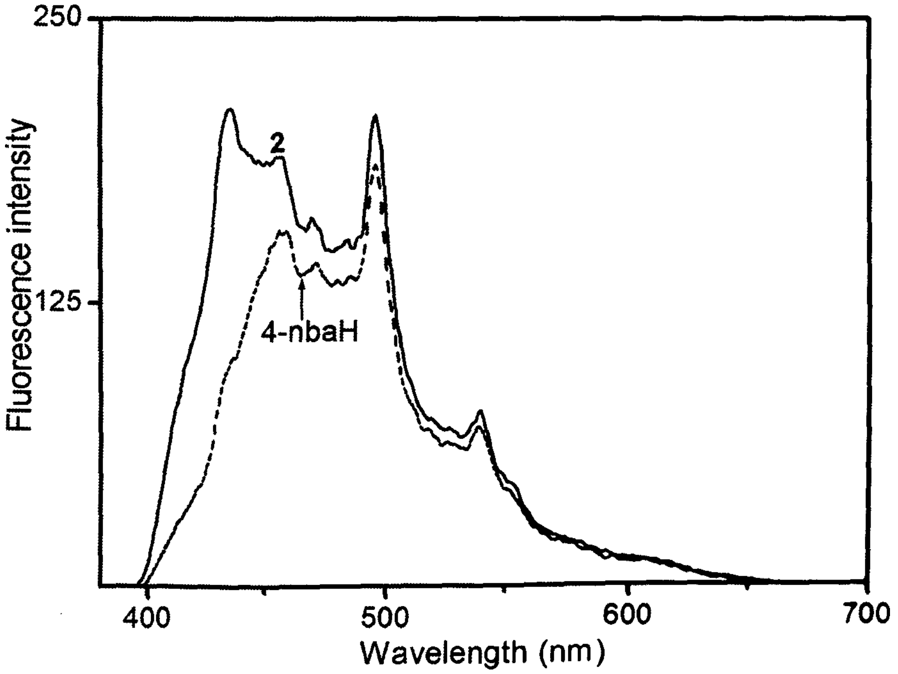

Figure 22- Flourescence spectra of 4-nbaH and **2**) [Ca(H_2O)$_2$(4-nba)$_2$]·2dmp]$_n$ **6**

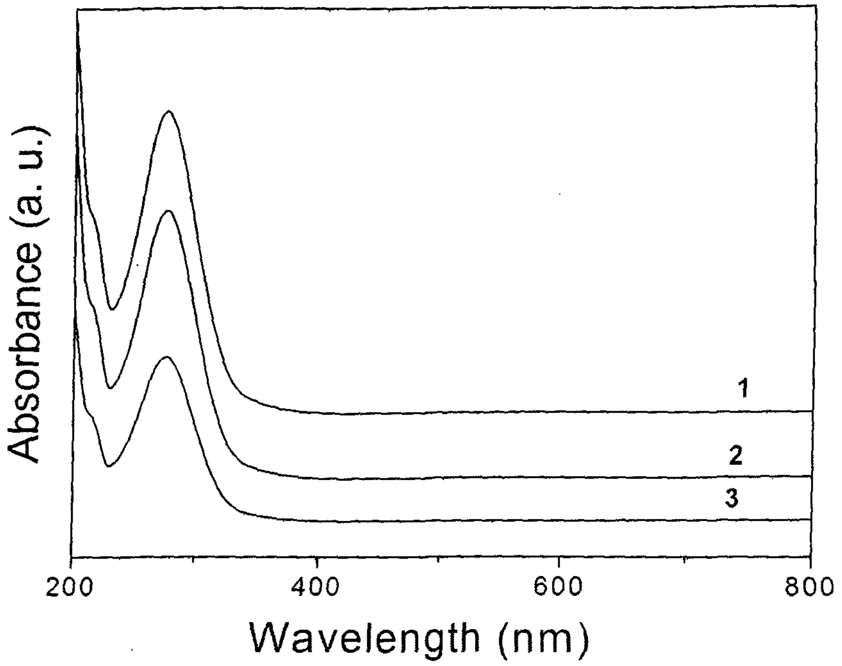

Figure 23 – UV-Visible spectra of compounds **1**) $[(H_2O)_4Li_2(\mu\text{-}H_2O)_2](4\text{-nba})_2$ **8**, **2**) $[Na(4\text{-nba})(H_2O)_3]_n$ **9** and **3**) $[K(4\text{-nba})(H_2O)_3]$ **10**

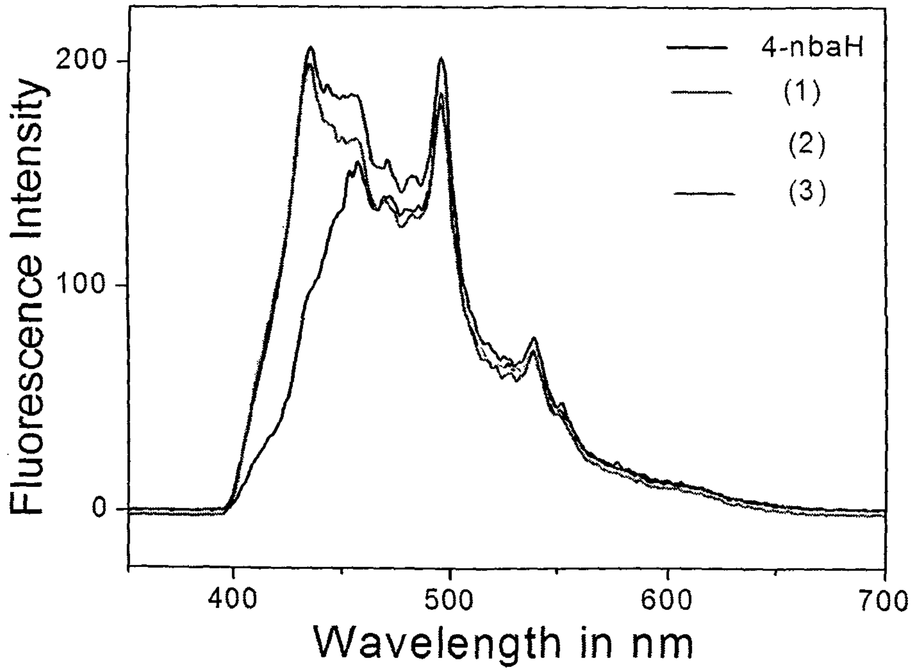

Figure 24- Flourescence spectra of 4-nbaH and **1**) $[(H_2O)_4Li_2(\mu\text{-}H_2O)_2](4\text{-nba})_2$ **8** **2**) $[Na(4\text{-nba})(H_2O)_3]_n$ **9** and **3**) $[K(H_2O)_2(4\text{-nba})]$ **10**

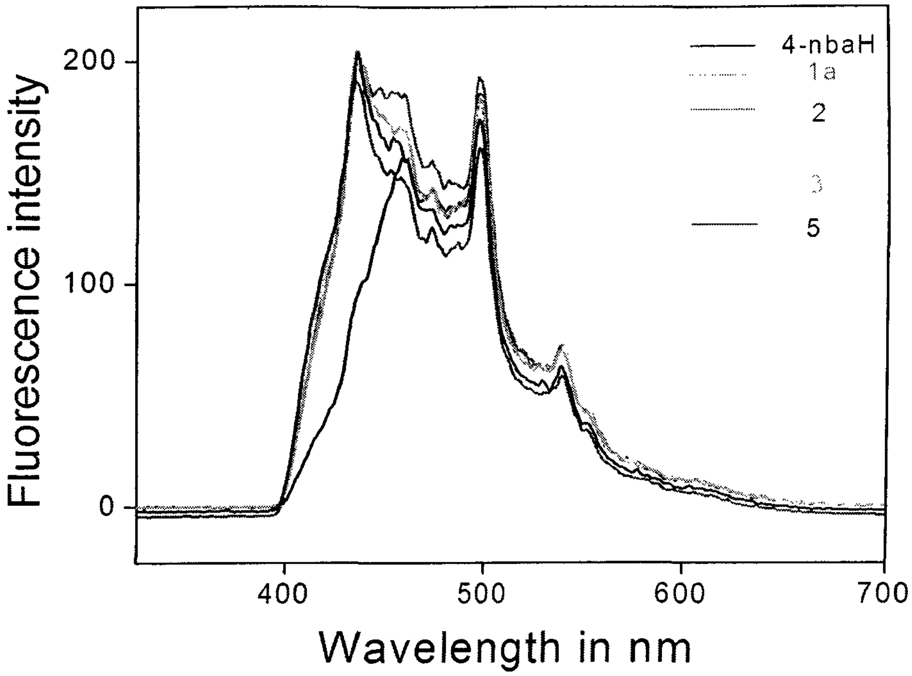

Figure 25- Fluorescence emissiion spectrum of 4-nba**H**, **1a**) [Sr(4-nba)$_2$(H$_2$O)$_4$] **11a** , **2**) [Sr(4-nba)(DMF)(H$_2$O)$_3$](4-nba) **12**, **3**) [Sr(H$_2$O)(4-nba)$_2$(NMF)$_{1.5}$] **13**, **4**) [Sr(4-nba)$_2$(pyr)$_2$] **14** and **5**) [Sr(4-nba)$_2$(HCONH$_2$)(H$_2$O)$_3$] **15** showing enhancement in emission intensity of prepared compounds as compared to that of free acid (4-nba**H**)

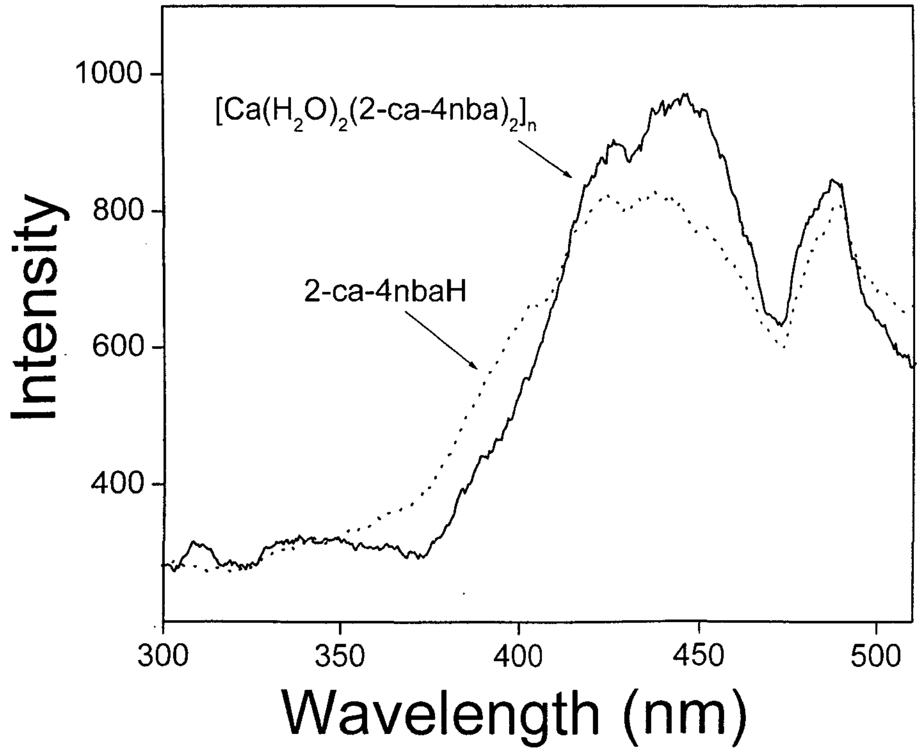

Figure 26- Luminescence spectra of [Ca(H$_2$O)$_2$(2-ca-4nba)$_2$]$_n$ **17** and 2-ca-4nbaH

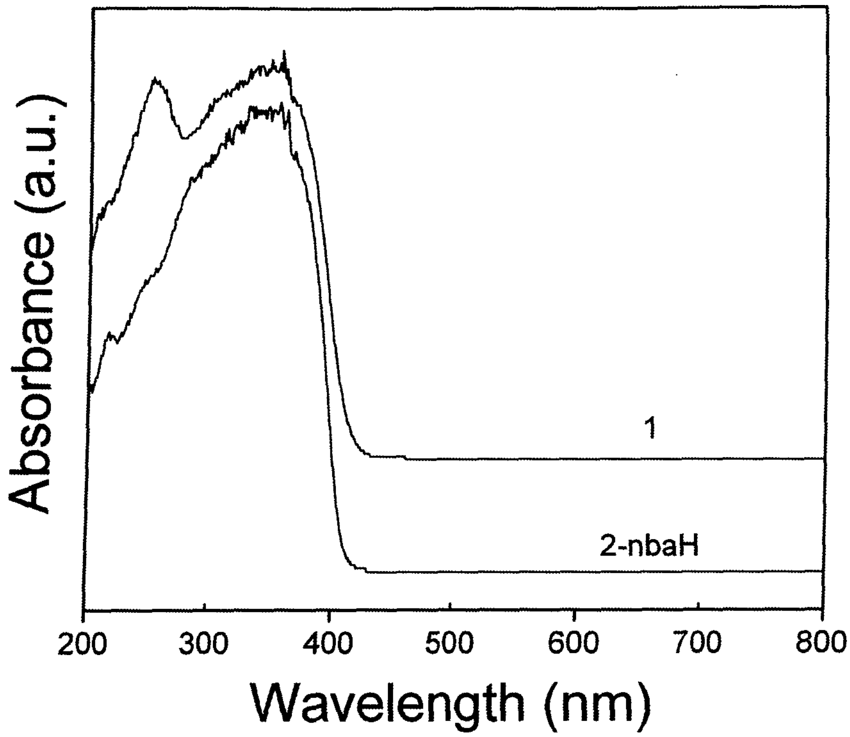

Figure 27- Diffuse Reflectance spectra of 2-nbaH and **1** $[Ca(2\text{-}nba)_2(H_2O)_2]_n$ **21**

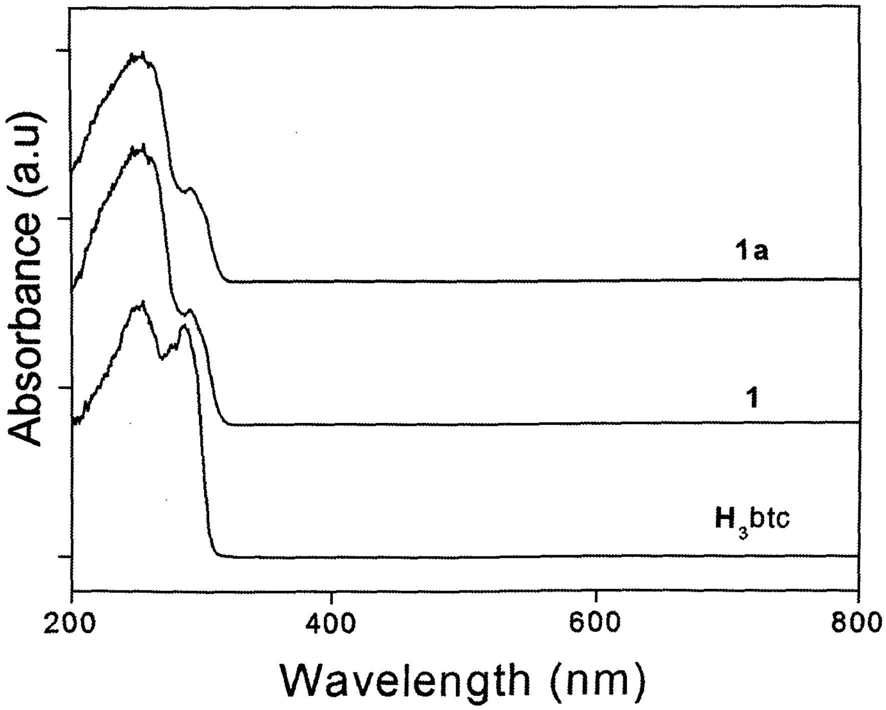

Figure 28- Diffused reflectance spectra of H_3btc, **1)** $[[Ba_3(btc)_2(H_2O)_8].2H_2O]_n$ **32** and **1a)** $[Ba_3(btc)_2]$ **32a**

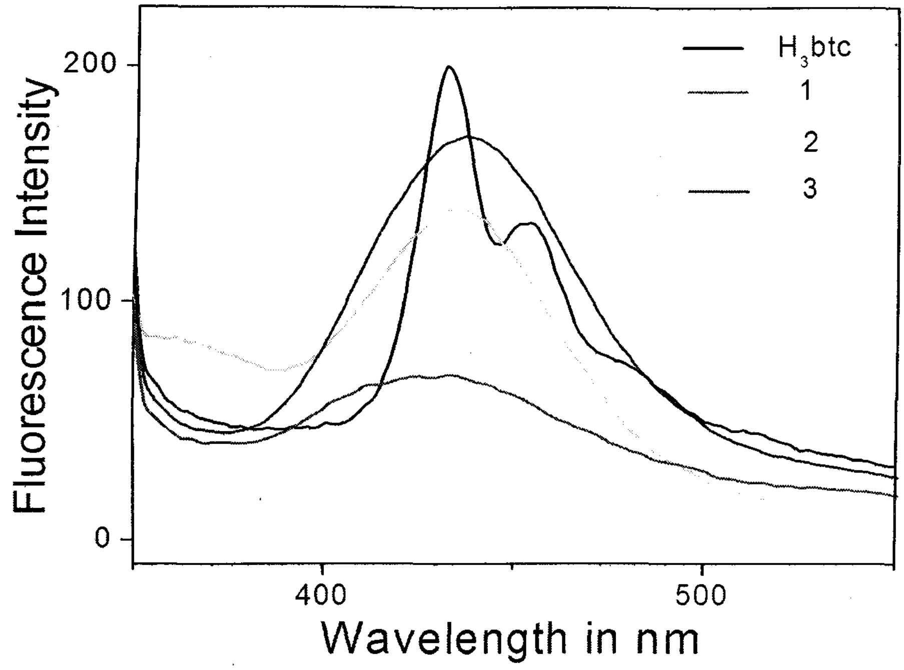

Figure 29- Fluorescence intensity spectrum of ligand H_3btc and **1**) [$Ca_3(btc)_2(H_2O)_{12}$] **30**, **3**) [$Sr_3(btc)_2(H_2O)_8$] **31**, **2**) [$Ba_3(btc)_2(H_2O)_8$].$2H_2O$ **32** showing decrease in emission intensity as compared to that of free acid (**H_3**btc)

3.3.3- NMR spectroscopy

Some of the complexes have been investigated by NMR spectroscopy. The list of compounds studied under NMR spectroscopy has been tabulated in Table 7 below. The presence of the N-donor ligands in compounds **2**, **3** and **4** can be readily confirmed by their NMR spectra which exhibit the characteristic signals of 4-nba, N-MeIm or Im, 2-MeIm. The presence of 4-nba and 2-ap in **7** can be readily evidenced from the ^{1}H NMR spectrum, which exhibits characteristic signals of both moieties (Figure 30). The ^{1}H NMR spectra of both compounds exhibit a typical AB quartet for the two sets of aromatic protons in the 4-nba anion (Figure 31) and the observed chemical shifts of **8** and **9** are nearly identical and are in agreement with the reported values [63] for [$Mg(H_2O)_6$](4-nba)$_2$·$2H_2O$. The presence of 4-nba in both compounds can be further confirmed based on the several signals in the mid IR region. The observed chemical shifts in the NMR spectra of the free acid (2-ca-4-ba**H**) and the Mg(II) compound **16** are in the normal range and are nearly identical.

Table 7 - ^{1}H NMR spectral data for few of the synthesized compounds

Compound Name	Solvent	^{1}H NMR δ (in ppm)
[Ca(N-MeIm)(4-nba)$_2$]$_n$	DMSO-d_6	3.63 (s,3H); 6.86 (s, 1H); 7.09 (s, 1H); 7.55 (s, 1H); 8.16 (m, 4H)
[Ca(Im)(4-nba)$_2$]	DMSO-d_6	7.00 (s, 1H); 7.63 (s, 1H); 8.13 (m, 4H)
[Ca(H_2O)(L^2)(4-nba)$_2$]$_n$	DMSO-d_6	2.25 (s, 3H); 6.83 (d, 2H); 7.14 (d, 2H); 8.14 (q, 2H); 11.52 (s, 1H)
[Ca(H_2O)$_6$(4-nba)](4-nba)(2-ap)·H_2O	DMSO-d_6	5.85 (s, 2H), 6.41 (m, 1H), 6.40 (m, 1H), 7.34 (m, 1H), 7.88 (d, 1H), 8.11 (d, 2H), 8.20 (d, 2H).
[(H_2O)$_4$Li$_2$(4-nba)(μ-H_2O)$_2$](4-nba)	D_2O	8.05 (d, J = 8.8 Hz, Ha), 8.31 (d, J = 9.2 Hz, Hb)
[Na(4-nba)(H_2O)$_3$]$_n$	D_2O	8.05 (d, J = 8.8 Hz, Ha), 8.31 (d, J = 8.8 Hz, Hb)
[K(4-nba)(H_2O)$_2$]	D_2O	8.05 (d, J = 8.8 Hz, Ha), 8.31 (d, J = 9.2 Hz, Hb)
2-ca-4nbaH	DMSO-d_6	7.64 (d, J = 8.4 Hz, H3), 8.20 (dd, J = 2.4 Hz, J = 8.4 Hz, H5), 8.36 (d, J = 2.4 Hz, H6), 8.94 (br s, J = 2.4, -N-H)
[Mg(H_2O)$_6$(2-ca-4nba)$_2$]	DMSO-d_6	7.65 (d, J = 8.4 Hz, H3), 8.20 (dd, J = 2.4 Hz, J = 8.4 Hz, H5), 8.4 (d, J = 2.4 Hz, H6), 9.1 (br s, J = 2.4Hz –N-H)
[Mg(H_2O)$_6$(2-ca-4nba)$_2$]	D_2O	7.65 (d, J = 8.4 Hz, H3), 8.20 (dd, J = 2.4 Hz, J = 8.4 Hz, H5), 8.4 (d, J = 2.4 Hz, H6)
[Mg(H_2O)$_5$(3-npth)]·2H_2O	DMSO-d_6	7.45 (t, 1H), 7.82 (d, 1H), 8.24 (d, 1H)
[[Ca(H_2O)$_2$(3-npth)]·H_2O]$_n$	DMSO-d_6	7.39 (t, 1H), 7.96(d, 1H), 8.03(d, 1H)

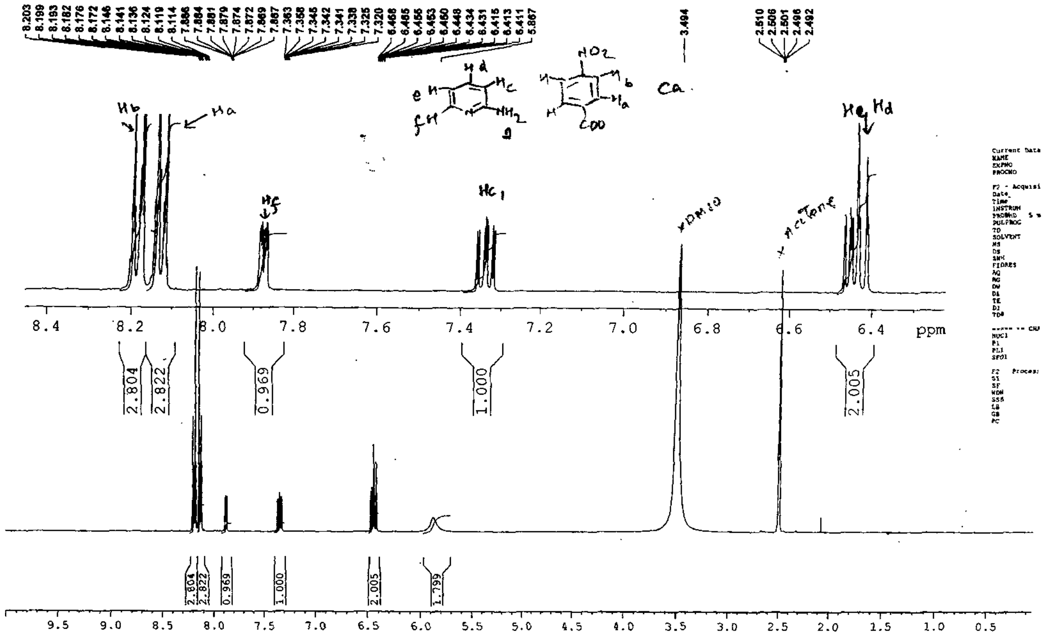

Figure 30- ^{1}H NMR (DMSO-d_6) δ (in ppm) of $[Ca(H_2O)_6(4\text{-nba})](4\text{-nba})(2\text{-ap})\cdot H_2O$ **7**: 5.85 (s, 2H), 6.41 (m, 1H), 6.40 (m, 1H), 7.34 (m, 1H), 7.88 (d, 1H), 8.11 (d, 2H), 8.20 (d, 2H).

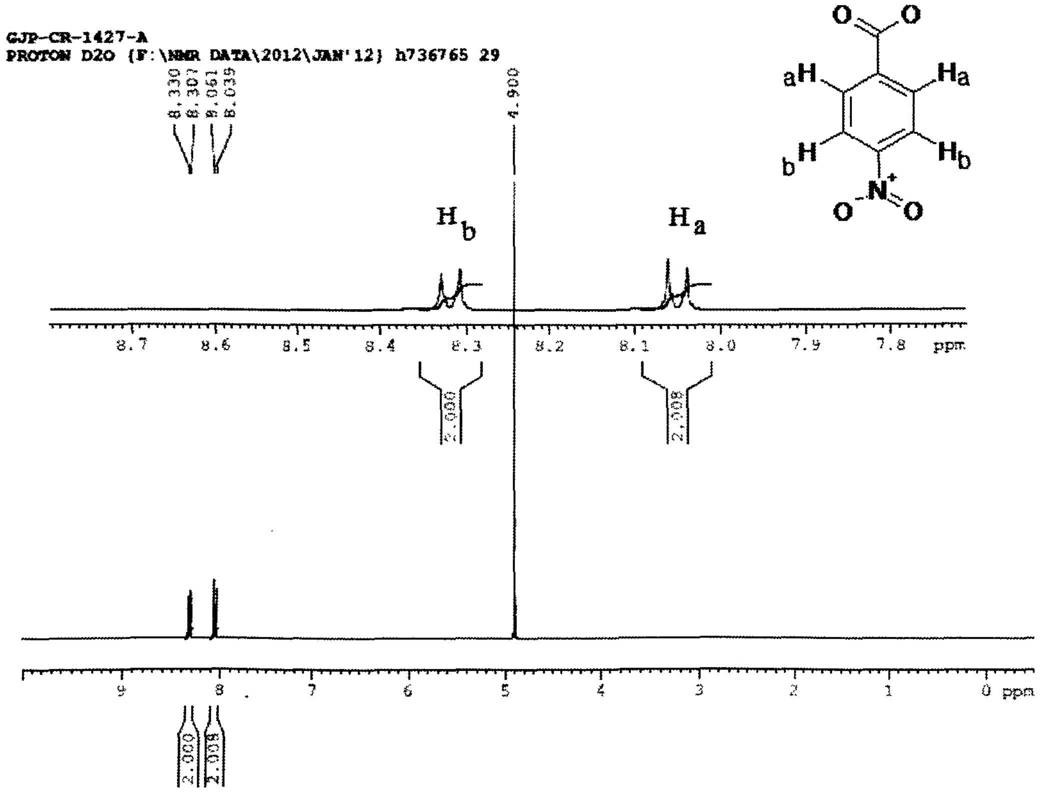

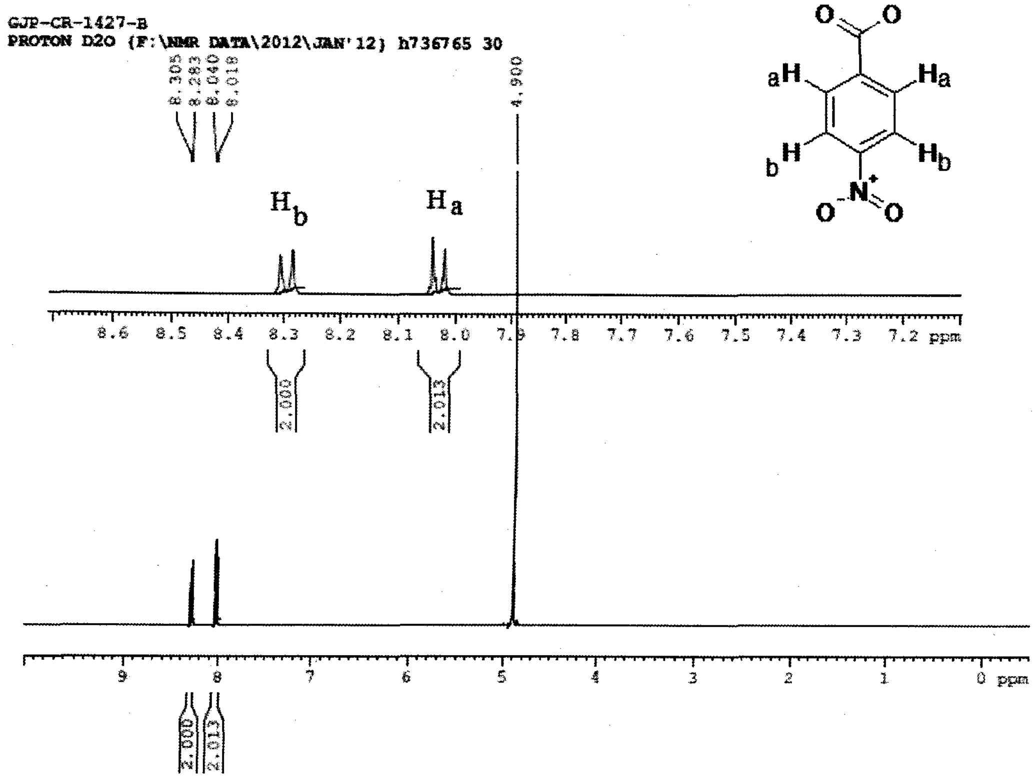

Figure 31 - ^{1}H NMR (D_2O) δ (in ppm) of $[(H_2O)_4Li_2(\mu-H_2O)_2](4\text{-nba})_2$ **8**: 8.05 (d, *J* = 8.8 Hz, Ha), 8.31 (d, *J* = 9.2 Hz, Hb) (top); ^{1}H NMR (D_2O) δ (in ppm) of $[Na(4\text{-nba})(H_2O)_3]_n$ **9**: 8.03 (d, *J* = 8.8 Hz, H_a), 8.29 (d, *J* = 8.8 Hz, H_b) (bottom)

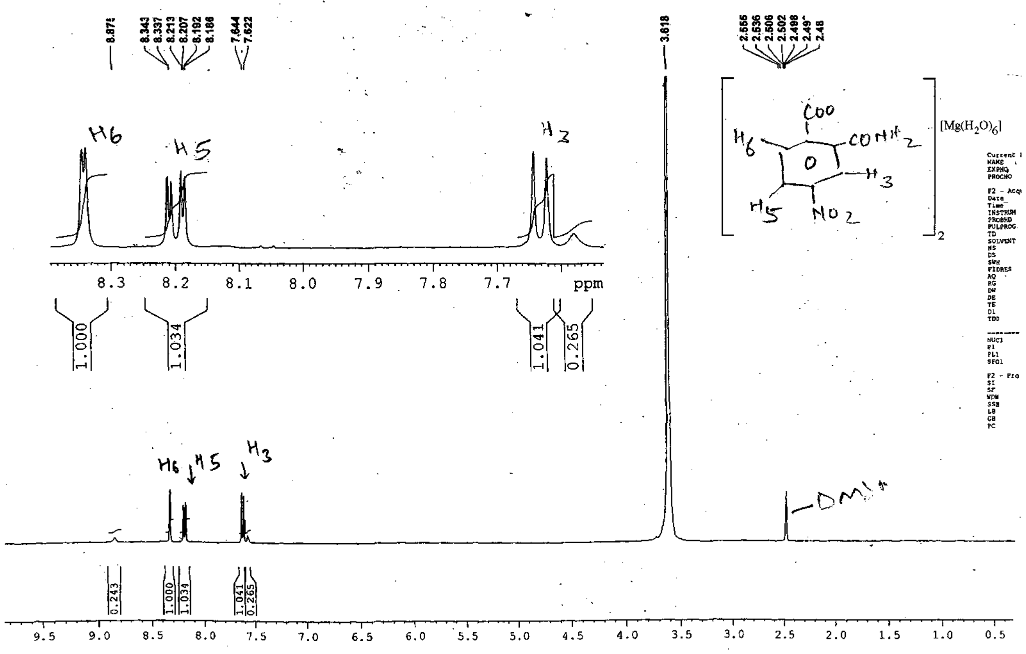

Figure 32 - ^{1}H NMR (D_2O in DMSO-d_6) δ (in ppm) of $[Mg(H_2O)_6(2\text{-ca-4nba})_2]$ (**16**): 7.65 (d, *J* = 8.4 Hz, H3), 8.20 (dd, *J* = 2.4 Hz, *J* = 8.4 Hz, H5), 8.4 (d, *J* = 2.4 Hz, H6)

3.3- X-ray powder diffraction studies

The compounds prepared in this work have been investigated by powder diffraction method. To ascertain the phase purity of the solid some of the compounds have been investigated by X-ray powder diffraction. A comparison of the powder pattern of the bulk sample of **4** with that of the theoretically calculated pattern from the single crystal data (*vide infra*) reveals the phase purity of the mixed ligand product **4** (Figure 33). The formation of a new crystalline phase of **5** and **6** (Figure 34) was evidenced based on a comparison of the X-ray powder pattern of the starting material **1** with that of the product and further confirmed by thermal and analytical data. The crystalline nature of compounds **8**, **9** and **10** (Figure 35) can be evidenced from the sharp signals in their powder diffractograms. A comparison of the powder patterns reveals that the phases are different indicating that the structure of the Li compound is different from that of the sodium compound as well as potassium compound. The X-ray powder pattern of compounds $[Sr(4\text{-nba})(H_2O)_7](4\text{-nba}).2H_2O$ **11**, $[Sr(4\text{-nba})_2(H_2O)_4]$ **11a**, $[Sr(4\text{-nba})(DMF)(H_2O)_3](4\text{-nba})$ **12**, $[Sr(H_2O)\ (4\text{-nba})_2(NMF)_{1.5}]$ **13** $[Sr(4\text{-nba})_2(pyr)_2]$ **14** and $[Sr(4\text{-nba})_2(HCONH_2)(H_2O)_3]$ **15** shows sharp signals for all the 4 compounds prepared from same starting compound **11** and are in different phases thus confirming the crystalline nature of compounds **11-15** (Figure 36). The crystalline nature of the hydrated phase of compounds **29**, **30**, **31**, **32** and dehydrated phase **29a**, **30a**, **31a**, **32a** were predicted based on the sharp intensities of the hydrated and dehydrated phases (Figure 37-38).

The X-ray powder diffractograms revealed the crystalline nature of compounds $[[Ca(H_2O)_2(4\text{-OMephac})_2].H_2O]_n$ **33** $[[Ca(H_2O)_2(2\text{-Clphac})_2].2H_2O]_n$ **34** $[Ca(H_2O)_3(phac)_2]$ **35** and the anhydrous compounds $[Ca(4\text{-OMephac})_2]$ **33a** $[Ca((2\text{-Clphac})_2]$ **34a** $[Ca(phac)_2]$ **35a** respectively (Figure 39-41). A comparison of the powder pattern of compounds **33** and **33a**, **34** and **34a,** and **35** and **35a** clearly indicate that dehydration of **33**, **34** or **35** leads to changes in structure as evidenced by the appearance of new peaks in the diffractogram of the anhydrous compound. On pyrolysis at 800°C, all the three compounds **33-35** are converted into calcium oxide as evidenced by X-ray powder pattern (Figure 42).

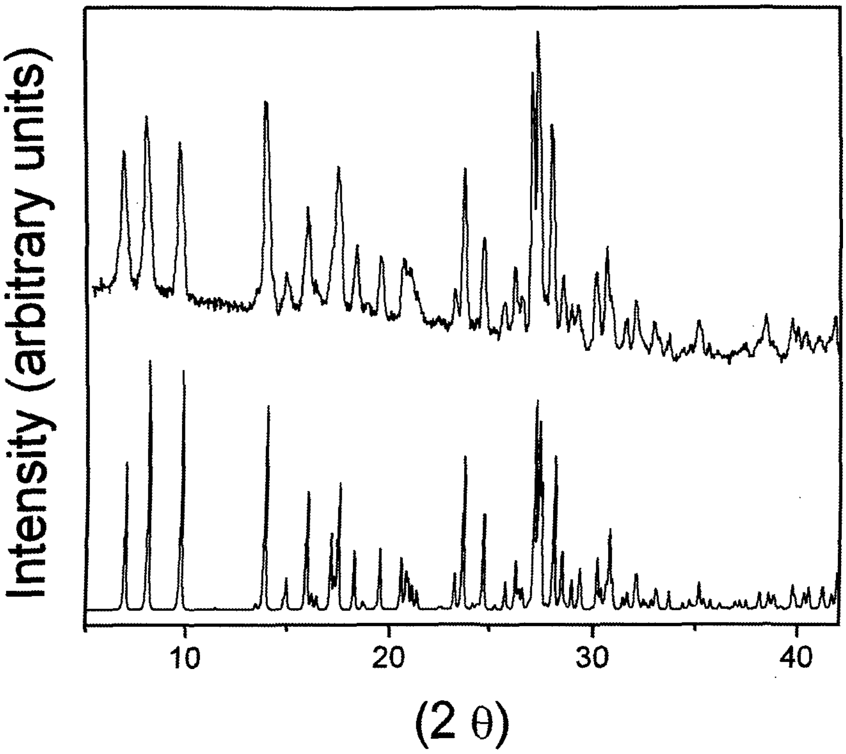

Figure 33 - X-ray powder pattern of a bulk sample of $[Ca(H_2O)(2\text{-MeIm})(4\text{-nba})_2]_n$ **4** (top); theoretical pattern calculated from single crystal data (bottom).

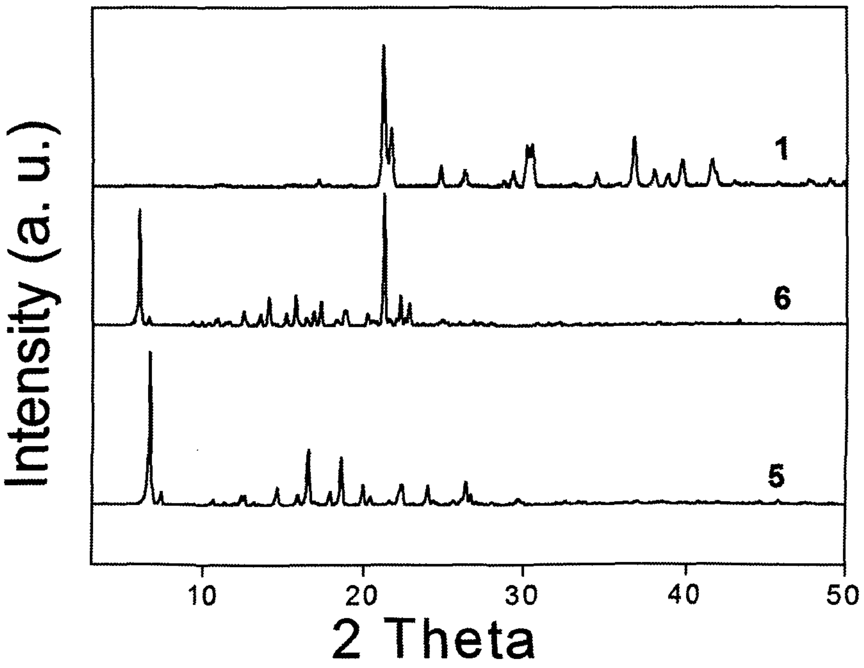

Figure 34- X-ray powder pattern of a bulk sample of $[Ca(H_2O)_4(4\text{-nba})_2]$ **1**, $[Ca(pyr)_4(4\text{-nba})_2]_n$ **5** and $[[Ca(H_2O)_2(4\text{-nba})_2].2dmp]_n$ **6**

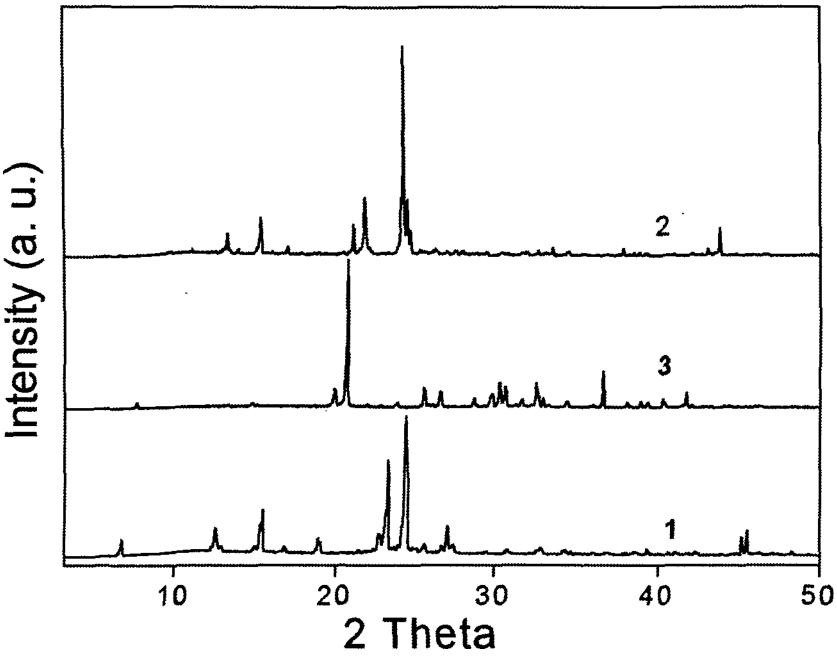

Figure 35- Comparative X-ray powder pattern of **1)** $[(H_2O)_4Li_2(\mu\text{-}H_2O)_2](4\text{-nba})_2$ **8, 2)** $[Na(4\text{-nba})(H_2O)_3]_n$ **9**, and **3)** $[K(H_2O)_3(4\text{-nba})]$ **10**

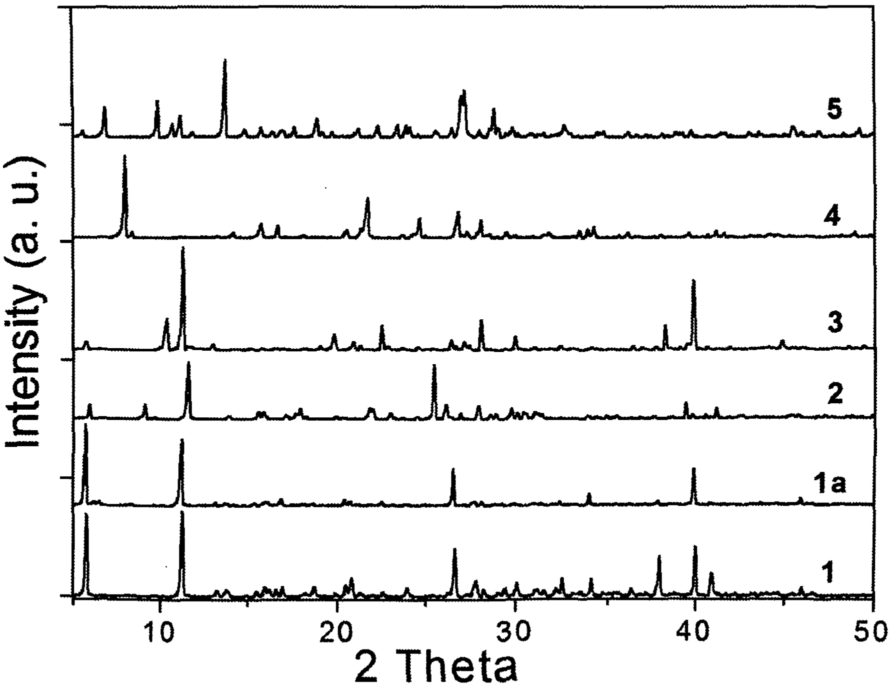

Figure 36- X-ray powder pattern of **1)** $[Sr(4\text{-nba})(H_2O)_7](4\text{-nba}).2H_2O$ **11, 1a)** $[Sr(4\text{-nba})_2(H_2O)_4]$ **11a, 2)** $[Sr(4\text{-nba})(DMF)(H_2O)_3](4\text{-nba})$ **12, 3)** $[Sr(H_2O)\ (4\text{-nba})_2(NMF)_{1.5}]$ **13, 4)** $[Sr(4\text{-nba})_2(pyr)_2]$ **14** and **5)** $[Sr(4\text{-nba})_2(HCONH_2)(H_2O)_3]$ 15

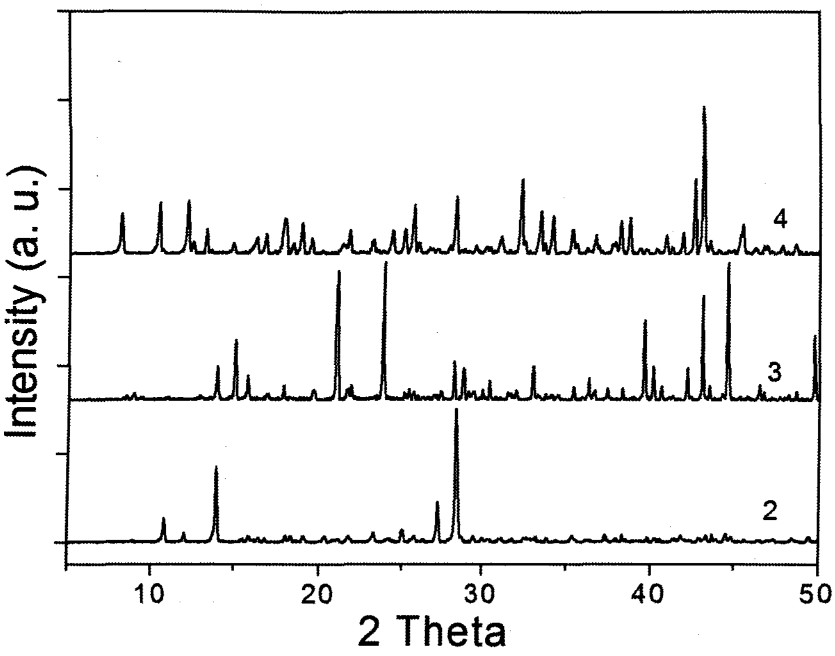

Figure 37- X-ray powder pattern of **2)** [$Ca_3(btc)_2(H_2O)_{12}$] **30**, **3)** [$Ba_3(btc)_2(H_2O)_8$].$2H_2O$ **32**, **4)** [$Sr_3(btc)_2(H_2O)_8$] **31**

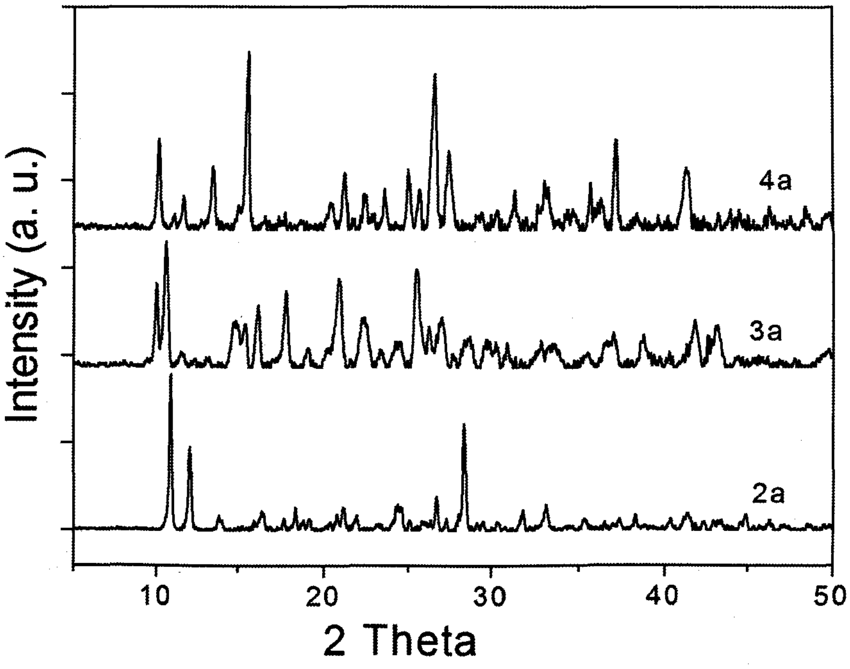

Figure 38 - X-ray powder pattern of **2a)** [$Ca_3(btc)_2$] **30a**, **3a)** [$Ba_3(btc)_2$] **32a**, and **4a)** [$Sr_3(btc)_2$] **31a**

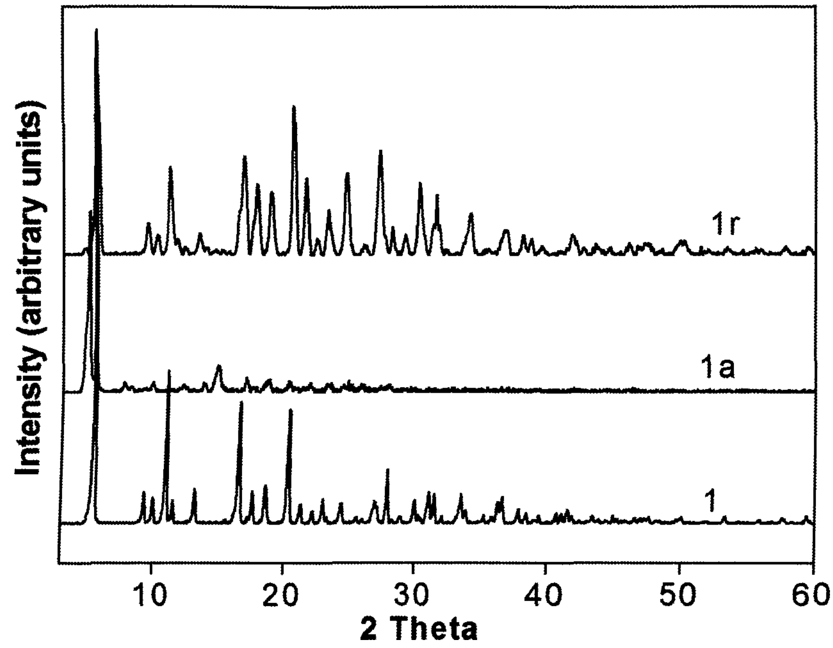

Figure 39- X-ray powder pattern of **1)** [[Ca(H_2O)$_2$(4-OMephac)$_2$].H_2O]$_n$ **33**, **1a)** [Ca(4-OMephac)$_2$] **33a** and its rehydrated compound as **1r**

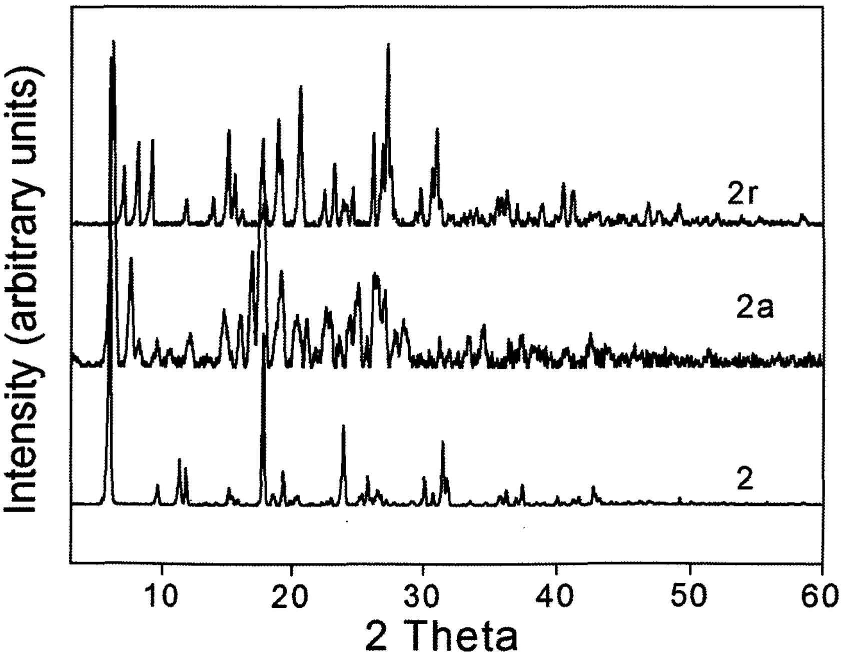

Figure 40- X-ray powder pattern of **2)** [[Ca(H_2O)$_2$(2-Clphac)$_2$].2H_2O]$_n$ **34**, **2a)** [Ca(2-Clphac)$_2$] **34a**, and its rehydrated compound **2r**

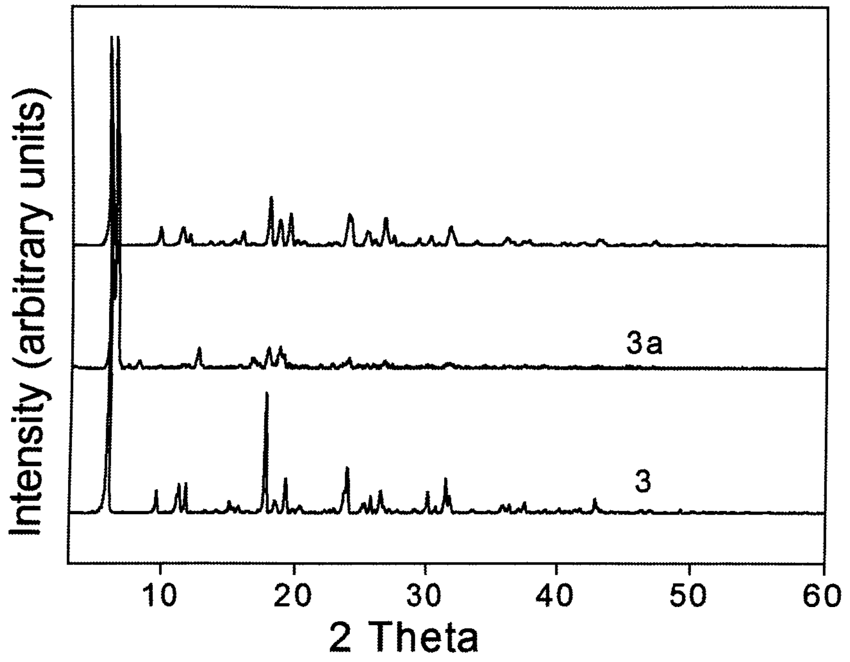

Figure 41- X-ray powder pattern of **3)** [$Ca(H_2O)_3(phac)_2$] **35**, **3a)** [$Ca(phac)_2$] **35a** and its rehydrated compound **3r** and the anhydrous compounds respectively

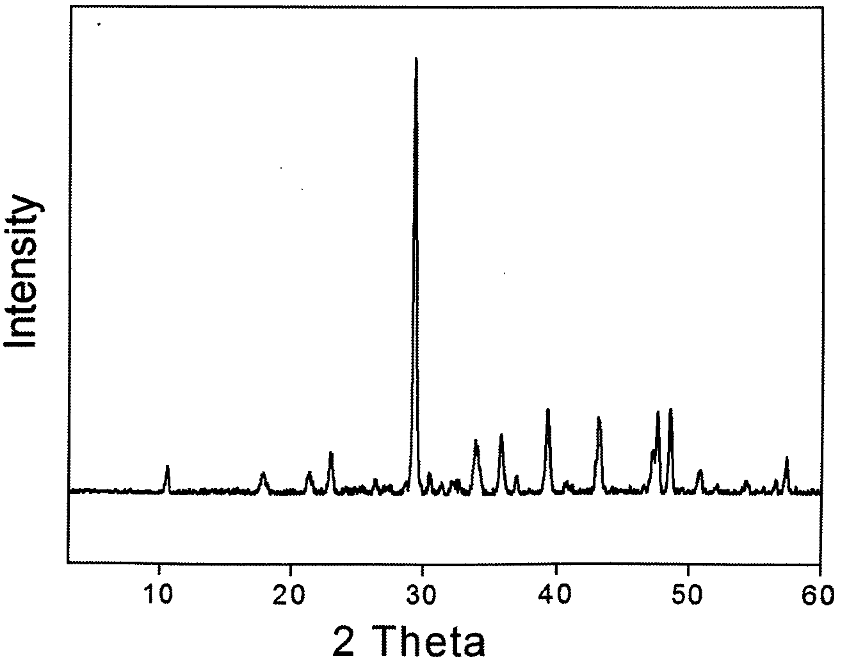

Figure 42 - X-ray powder pattern of CaO residue of [[$Ca(H_2O)_2(4\text{-}OMephac)_2$].$H_2O$]$_n$ **33** on pyrolysis.

3.4- Thermal studies

The decomposition processes of the new metal carboxylates synthesized in this work have been studied by TG-DSC/DTA and isothermal weight loss studies. The synthesized compounds show different thermal behaviours with respect to the carboxylic acid used. The TG-DTA/DSC thermograms of hydrated compounds exhibited first an endothermic event in the temperature range 100-150°C. Based on the observed weight loss and dropping profile of the TG-curve, the presence of water and its approximate percentage in the compound was predicted. The anhydrous compounds prepared from respective hydrated compounds did not show such events in the thermogram. In the case of compounds containing other neutral N-donor or O-donor ligands, this process occurred simultaneously or at higher temperatures but below 200°C. Beyond this point TG-curves showed straight line till 400°C. The carboxylate decomposition was observed as strong exothermic process above 400°C in DTA or DSC curve. The nitrobenzoate decomposition in all the 4-nitrobenzoate group containing compounds was observed around 410°C. In the absence of mass spectral data of the emitted fragments, no definite conclusion could be drawn on the exact nature of the decomposition process in majority of the compounds. The metal carboxylate compounds of Ca and Mg formed respective metal oxides as final residue when heated to 800°C while that of Sr and Ba formed respective carbonates as final residue. The formation of carbonate as final residue in case of Sr and Ba was confirmed by presence of efferevescence after acidification of the final residue.

Table 8- Thermal decomposition data of metal carboxylate complexes

Compound	TG % water loss Exp. (calc.)	DSC/DTA event at (°C)	Residue % Exp. (calc)
$[Ca(H_2O)_4(4\text{-}nba)_2]$ **1**	16.6 (16.2)	100(endo), 260(endo), 410(exo), 447(exo), 558(exo)	12.89 (12.6)
$[Ca(4\text{-}nba)_2(N\text{-}MeIm)]_n$ **2**	21.67	188(endo), 412(exo), 558(exo)	11.80
$[Ca(4\text{-}nba)_2(Im)]_n$ **3**	-	198(endo), 415(exo), 547(exo)	12.3
$[Ca(H_2O)(4\text{-}nba)_2(2\text{-}MeIm)]_n$ **4**	10.52	172(endo), 410(exo), 559(exo)	11.58 (11.87)
$[Ca(4\text{-}nba)_2(pyr)_2]_n$ **5**	25.6 (26.77)	232(endo), 421(exo), 481(exo), 575(exo)	11.08 (11.03)
$[[Ca(H_2O)_2(4\text{-}nba)_2].(dmp)_2]_n$ **6**	-	110(endo), 236(endo) 411(exo), 545(exo)	-
$[Ca(H_2O)_6(4\text{-}nba)(2\text{-}ap)](4\text{-}$	20.6 (21.28)	117(endo), 238(endo)	-

nba)(2-ap) **7**		421(exo), 534(exo)	
$[(H_2O)_4Li_2(\mu\text{-}H_2O)_2](4\text{-nba})_2$ **8**	22.0 (23.80)	100(endo), 393 (exo), 580 (exo)	-
$[Na(4\text{-nba})(H_2O)_3]_n$ **9**	19.10 (22.41)	105(endo), 404 (exo), 580 (exo)	-
$[K(4\text{-nba})(H_2O)_2]$ **10**	16.0 (13.89)	90(endo), 281(endo) 439(exo), 432(exo), 573(exo)	-
$[Sr(H_2O)_7(4\text{-nba})](4\text{-nba}).2H_2O$ **11**	28 (27.8)	115(endo), 424(exo) 534(exo)	25.29
$[[Sr(H_2O)_3(4\text{-nba})(dmf)].(4\text{-nba})]_n$ **12**	21.9	113(endo), 435(exo) 525(exo)	26
$[Sr(H_2O)(4\text{-nba})_2(nmf)_{1.5}]_n$ **13**	19	109(endo), 430(exo) 536(exo)	27.68
$[Sr(4\text{-nba})_2(pyr)_2]_n$ **14**	26.47	236(endo), 403(exo) 565(exo)	25.2
$[Sr(H_2O)_3(4\text{-nba})_2(HCONH_2)]_n$ **15**	22 (10.49)	165(endo), 415(exo) 531(exo)	26.52
$[Mg(H_2O)_6(2\text{-ca-4-nba})_2]$ **16**	19 (19.63)	94(endo), 136(endo) 245(endo), 433(exo) 545(exo)	-
$[Ca(H_2O)_2(2\text{-ca-4-nba})_2]_n$ **17**	6.0 (7.2)	152(endo), 297(endo) 440(exo), 557(exo)	-
$[Mg(H_2O)_4(2\text{-nba})_2]$ **20**	16.2 (16.80)	89(endo), 231(endo) 336(exo), 457(exo)	-
$[Ca(H_2O)_2(2\text{-nba})_2]_n$ **21**	8.5 (8.81)	144(endo), 322(exo) 354(exo), 544(exo)	14.3 (13.70)
$[Ba(H_2O)_3(2\text{-nba})_2]_n$ **22**	10.5 (10.32)	88(endo), 230(endo) 277(endo), 338(exo) 444(exo)	-
$[Sr(H_2O)_4(2\text{-nba})_2]$ **23**	13.0 (14.66)	72(endo), 116(endo), 180(exo), 266(endo), 332(exo), 358(exo), 498(exo)	-
$[Mg(H_2O)_5(3\text{-npth})].2H_2O$ **25**	33 (33.85)	125(endo), 212(endo) 412(exo), 568(exo)	-
$[[Ca(H_2O)_2(3\text{-npth})].H_2O]_n$ **26**	(17.82)	125(endo), 428(exo) 443(exo)	-
$[Mg_3(H_2O)_{18}(btc)_2]$ **29**	30.6 (30.73)	100(endo), 180(endo) 600(exo)	25.64 (17.19)
$[Ca_3(H_2O)_{12}(btc)_2]_n$ **30**	26.55 (28.79)	131(endo), 593(endo) 610(exo)	21.93 (22.41)
$[Sr_3(H_2O)_8(btc)_2]_n$ **31**	15.5 (17.54)	172(endo), 525(exo) 662(exo)	53.0 (53.93)
$[[Ba_3(H_2O)_8(btc)_2].2H_2O]_n$ **32**	(17.90)	148(endo), 525(exo) 593(exo)	58.13 (58.83)
$[Ca(H_2O)_2(4\text{-OMephac})_2].H_2O$ **33**	13 (12.72)	116(endo), 375(exo) 492(exo)	-
$[[Ca(H_2O)_2(2\text{-Clphac})_2].2H_2O]_n$ **34**	14.5 (15.95)	121(endo), 318(exo) 588(exo)	-

$[Ca(H_2O)_3(phac)_2].H_2O$ **35**	14.7 (14.82)	125(endo), 521(exo)	-
$[Ba(H_2O)_2(2\text{-}Clphac)_2]_n$ **36**	6.5	125(endo), 516(exo)	38
$[Mg(H_2O)_6(5\text{-}nisoph)]$ **37**	26.0	184(endo), 483(exo)	-
$[Ca(H_2O)_4(5\text{-}nisoph)]$ **38**	23.0 (22.4)	149(endo), 452(exo)	18.1 (17.44)
$[Mg(hip)_2(H_2O)_6]$ **39**	22 (22.0)	105(endo), 421(exo)	-
$[Sr(hip)_2(H_2O)_4]$ **40**	17(13.9)	130(endo), 539(exo)	-

Thermal behaviour of $[Ca(H_2O)_4(4\text{-}nba)_2]$ 1, $[Ca(H_2O)(4\text{-}nba)_2]$ 1a, $[Ca(N\text{-}MeIm)(4\text{-}nba)_2]_n$ 2 and $[Ca(Im)(4\text{-}nba)_2]$ 3

The temperature for the thermochemical synthesis was chosen based on the thermal characteristics of compound $[Ca(H_2O)_4(4\text{-}nba)_2]$ **1** described in Section 3.2. A comparison of the thermal behaviour of the tetrahydrate **1** and the monohydrate $[Ca(H_2O)(4\text{-}nba)_2]$ **1a** reveals that the DSC thermograms of **1a** is identical to that of compound **1** above 100 °C when the tetrahydrate **1** emits three moles of water forming the monohydrate (Figures 43 and 44). Both **1** and **1a** decompose at higher temperatures forming CaO as the final product as evidenced by the observed mass loss and also the featureless infrared spectra of the residues indicating the loss of organics. The DSC thermogram of **2** (Figure 45) exhibits an endothermic peak at 188°C, which can be attributed to the removal of N-methylimidazole and exothermic events above 400°C assignable to the decomposition of the compound resulting in the formation of CaO. The removal of N-MeIm leads to further decomposition of **2** as evidenced by a steep drop in the TG curve of **2**. A scrutiny of **2** by isothermal weight loss studies at 185°C, revealed a weight loss of 21.67 % corresponding to the loss of one mole of N-MeIm, while further heating to 800°C resulted in a total mass loss of 88% with 12% residue corresponding to the formation of CaO. However our efforts to prepare the anhydrous compound $[Ca(4\text{-}nba)_2]$ by heating **2** was not successful. The TG-DSC thermogram of compound **3** exhibits three thermal events at temperatures 198, 415 and 547°C (Figure 46). The endothermic signal at 198°C can be assigned for the loss of the neutral Im ligand. This process appears to be complex and is not well resolved as evidenced by further drop in the TG curve. The exothermic signals at 415 and 547°C can be attributed to decomposition of **3** to CaO with a residual mass of 12.3%, which is in good agreement with the calculated value. In the absence of associated mass spectral data of the emitted fragments the exact nature of the thermal decomposition cannot be commented upon for both **2** and **3**. However the formation of CaO as the final residue can be confirmed by weight loss studies of compounds **2** and **3** in a temperature controlled furnace.

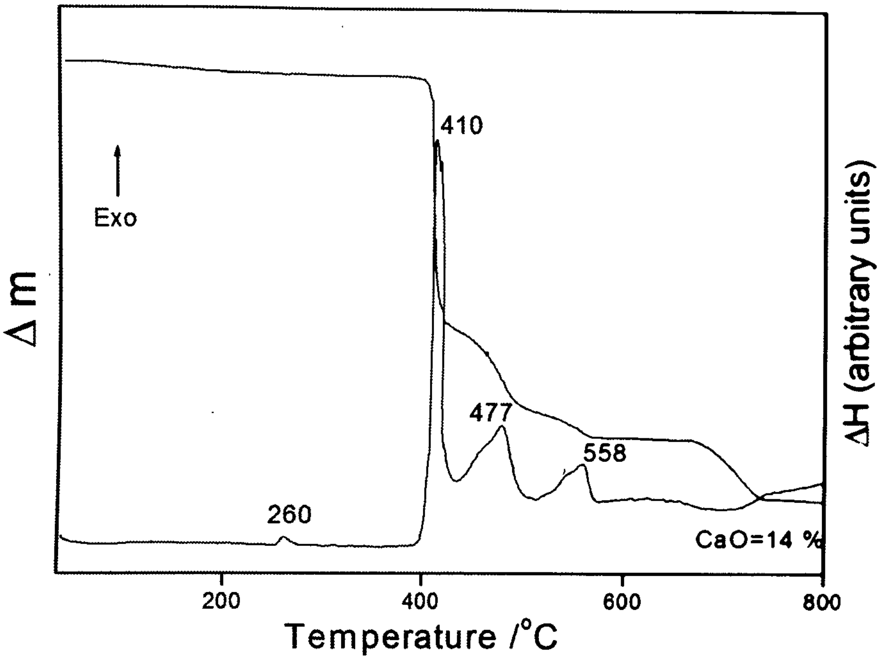

Figure 43- TG-DSC thermogram of the monohydrate $[Ca(H_2O)(4\text{-}nba)_2]$ **1a**

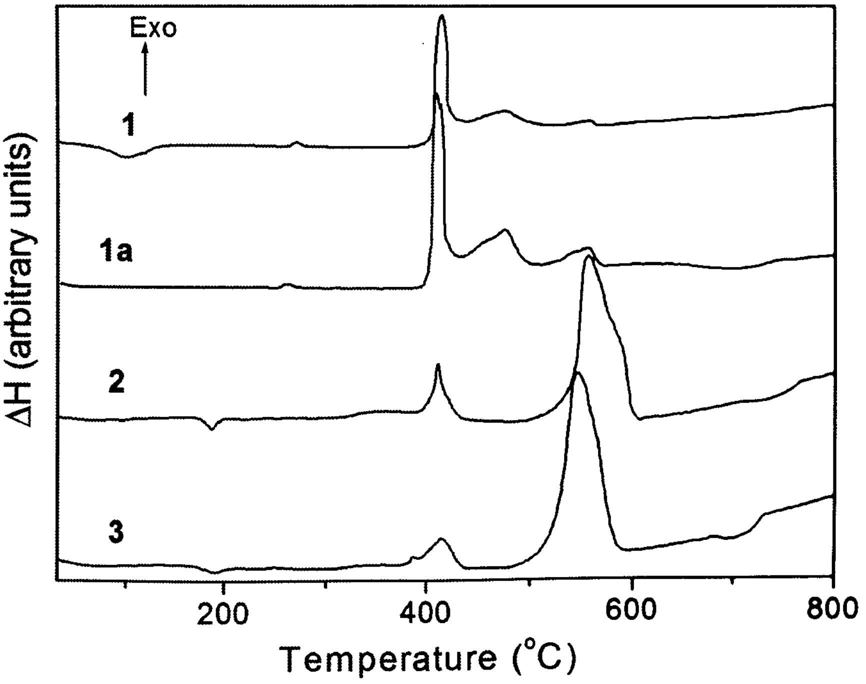

Figure 44- Comparative DSC thermograms of $[Ca(H_2O)_4(4\text{-}nba)_2]$ **1**, $[Ca(H_2O)(4\text{-}nba)_2]$ **1a**, $[Ca(N\text{-}MeIm)(4\text{-}nba)_2]_n$ **2** and $[Ca(Im)(4\text{-}nba)_2]$ **3**

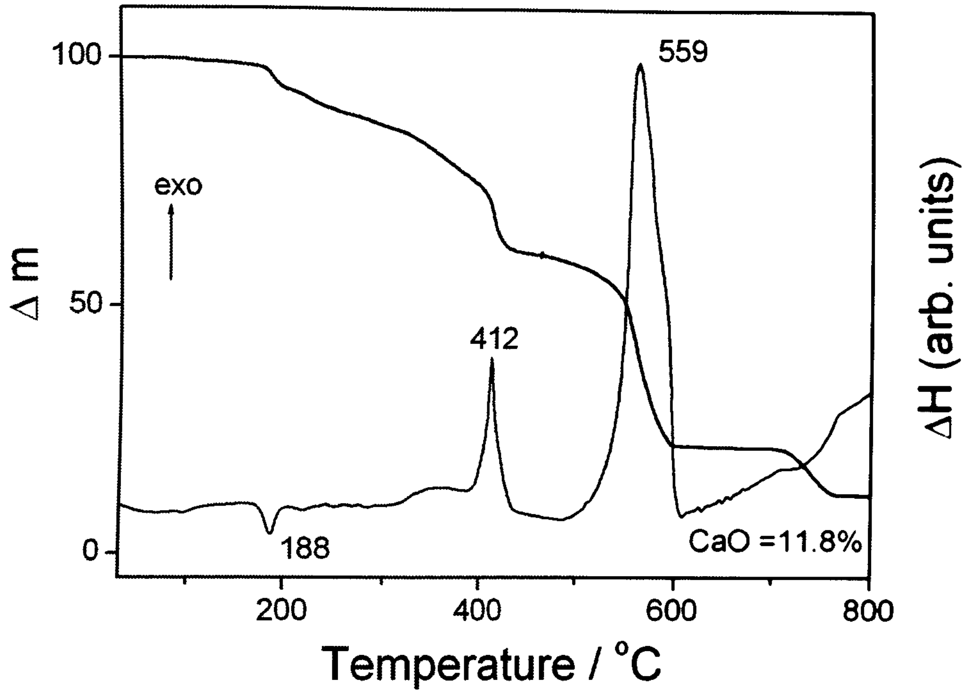

Figure 45- TG-DSC thermogram of compound [Ca(N-MeIm)(4-nba)$_2$]$_n$ **2** (Heating rate 10 K/min; Air atmosphere)

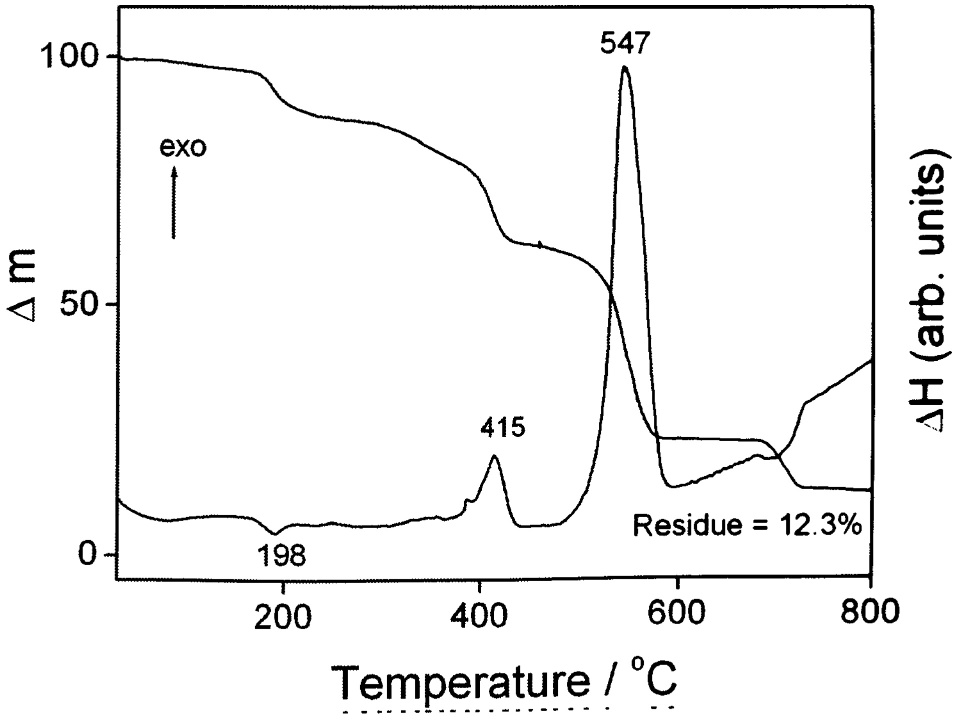

Figure 46- TG-DSC thermogram of compound [Ca(Im)(4-nba)$_2$] **3** (Heating rate 10 K/min; Air atmosphere)

$[Ca(H_2O)(2\text{-}MeIm)(4\text{-}nba)_2]_n$ 4

The TG-DSC thermogram of compound $[Ca(H_2O)(2\text{-}MeIm)(4\text{-}nba)_2]_n$ **4** is depicted in Figure 47. The DSC curve of compound **4** exhibits three thermal events. The first endothermic process at 172°C can be assigned to the loss of a neutral water ligand. The observed mass loss of 10.52% is much more than the loss expected for the loss of a mole of water. The drop in the TG curve indicates that the loss of water results in the loss of the neutral N-donor ligand. The isothermal weight loss studies at this temperature showed a mass loss of 13% which is much more than the loss expected for a mole of water and much less than loss due to either 2-MeIm or a combination of two neutral ligands in **4**. The exothermic events at 410 and 559°C correspond to the degradation of the 4-nba ligand as evidenced by the rapid drop in the TG curve. The assignment of the endothermic signal at 410°C for the decomposition of 4-nba gains more credence as a similar behaviour has been observed for the related Ca(II) compounds **1** and **1a** [24]. The TG curve above 750°C is parallel to the temperature axis and observed residue of 11.58% is in very good agreement with the expected value of 11.87% for the formation of CaO. The formation of CaO as the final residue has been confirmed based on the X-ray powder pattern of the residue as well as isothermal weight loss studies (Figure 48).

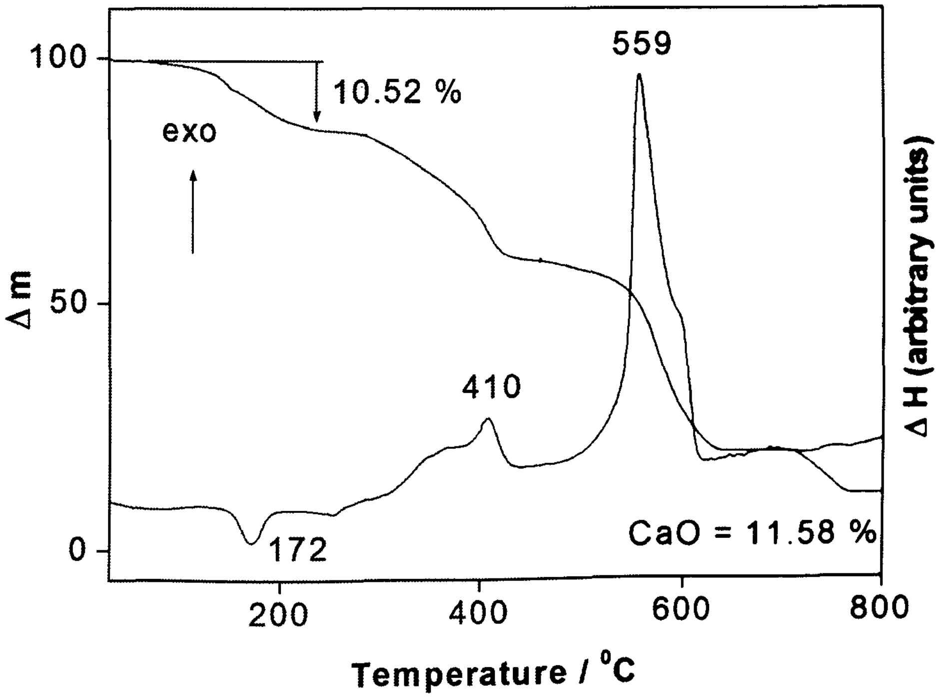

Figure 47- TG-DSC thermogram of compound $[Ca(H_2O)(2\text{-}MeIm)(4\text{-}nba)_2]_n$ **4**

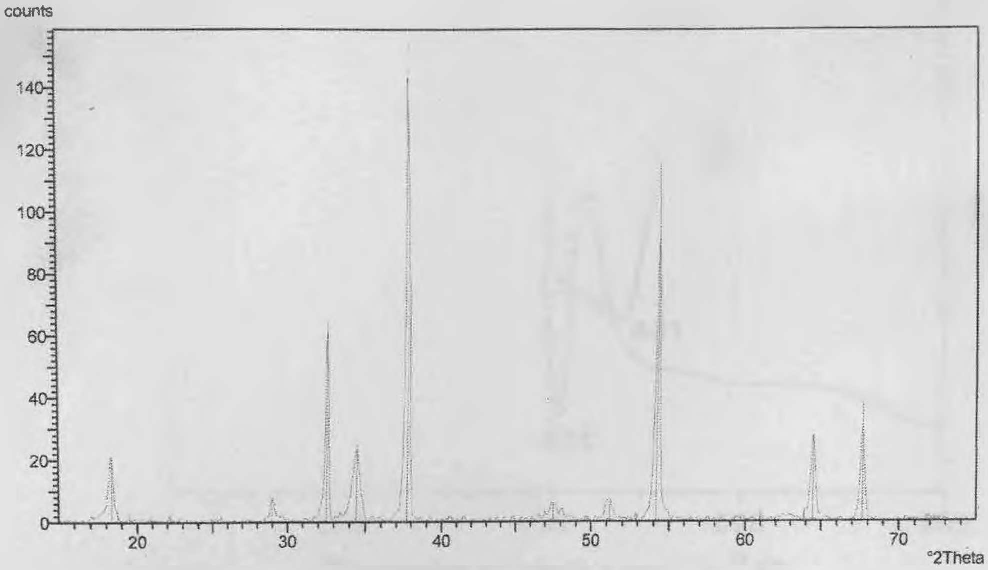

Figure 48: X-ray powder pattern of residue obtained by thermal decomposition of compound **4** at 800°C.

$[Ca(pyr)_2(4\text{-}nba)_2]_n$ 5

The TG-DTA thermogram of $[Ca(pyr)_2(4\text{-}nba)_2]_n$ **5** (Figure 49) is in accordance with the observed behavior in the isothermal weight loss studies and shows a mass loss of 25.6% (expected 26.77%) assignable for the loss of two moles of pyrazole and is accompanied by an endothermic peak in its DTA at 232°C. This is followed by two strong exothermic processes at 421, 481 and a weak exo event at 575°C. Exothermic processes have been observed at 412 and 558°C for $[Ca(L^1)(4\text{-}nba)_2]$ (L^1.= 1-methylimidazole) [24]. Based on this, the exothermic events in **5** can be assigned for the decomposition of the coordinated 4-nba leading to the formation of CaO. The complete loss of organics and the formation of oxide can be evidenced from the residual mass and the featureless infrared spectrum of the residue.

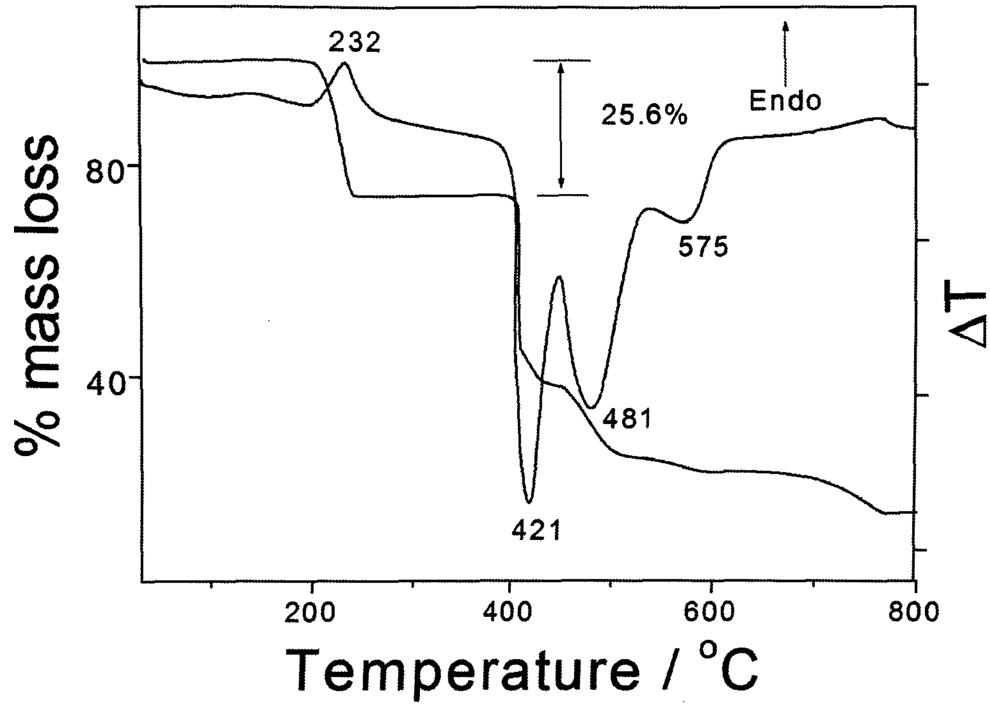

Figure 49- TG-DTA thermogram of $[Ca(pyr)_2(4\text{-}nba)_2]_n$ **5**

$[[Ca(H_2O)_2(4\text{-}nba)_2].2dmp]_n$ 6

The TG-DTA thermogram of $[[Ca(H_2O)_2(4\text{-}nba)_2].2dmp]_n$ **6** (Figure 50) exhibits two endothermic processes at 110 and 236°C which can be assigned for the loss of the neutral water ligands and lattice dmp molecules respectively. The strong exothermic signal observed at 411°C and a further exothermic event at 545°C can be attributed to the decomposition of the 4-nitrobenzoate leading to the formation of a binary oxide material. Exothermic events assignable for the decomposition of 4-nba have been reported by us for the coordination polymers $[Ca(N\text{-}MeIm)(4\text{-}nba)_2]_n$, $[Ca(H_2O)(2\text{-}MeIm)(4\text{-}nba)_2]_n$ and $[Ca(pyr)_2(4\text{-}nba)_2]_n$ at 412, 410 and 421°C respectively. The removal of organics was evidenced by the featureless infrared spectrum of the residue, while the formation of CaO as the final residue was further confirmed based on isothermal weight loss studies by heating compound **6** at 800°C in a temperature controlled furnace. The results of the isothermal weight loss studies add more credence to the thermal data.

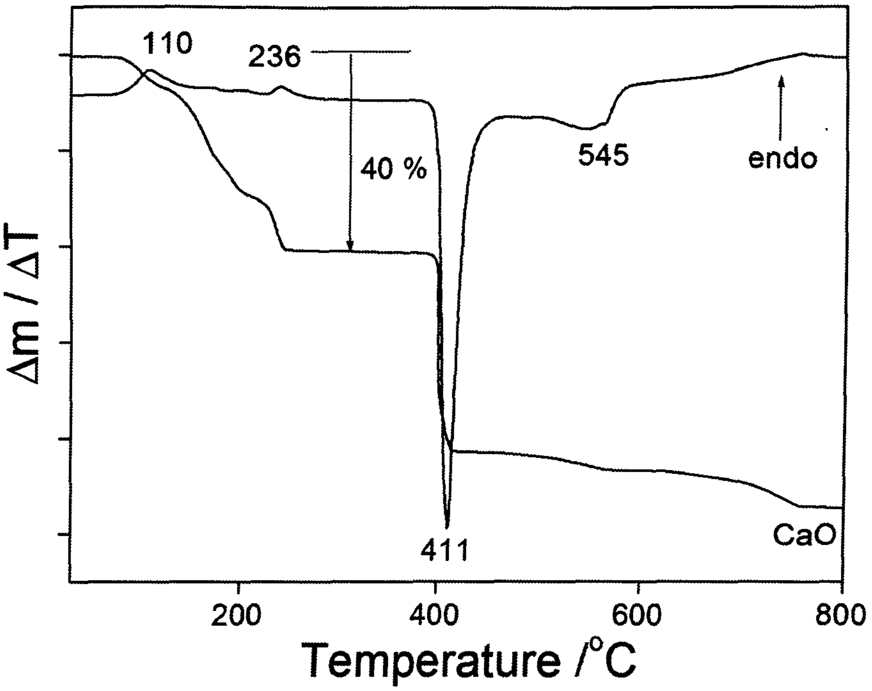

Figure 50- TG-DTA thermogram of $[[Ca(H_2O)_2(4\text{-nba})_2].2dmp]_n$ **6** in air atmosphere at heating rate of 10k/min

$[Ca(H_2O)_6(4\text{-nba})](4\text{-nba})(2\text{-ap})\cdot H_2O$ 7 and $[Ca(4\text{-nba})_2(2\text{-ap})]$ 7a

The TG-DTA thermogram of $[Ca(H_2O)_6(4\text{-nba})](4\text{-nba})(2\text{-ap})\cdot H_2O$ (7) (Figure 51) exhibits first an endothermic process at 117°C which is not observed for (**7-a**). The observed weight loss and the profile of the dropping TG curve of (7) can be attributed to the loss of the neutral water followed by 2-ap. The profile of the TG curve of (**7-a**) which is initially a straight line parallel to X-axis until about 150°C drops down, indicating the loss of 2-ap. The exothermic events at temperatures above 400°C in both compounds can be attributed to the decomposition of 4-nba [24, 26, 63, 121]. In both cases CaO is formed as the final residue. The observed mass loss of 20.6 %, on heating (7) at 120°C is in agreement with the expected value (21.28%) for the loss of seven moles of water. The formation of CaO as the final residue was further confirmed based on isothermal weight loss studies by heating compounds (7) or (**7-a**) at 800°C in a temperature controlled furnace. Thus the weight loss studies add credence to the thermal behavior of both compounds.

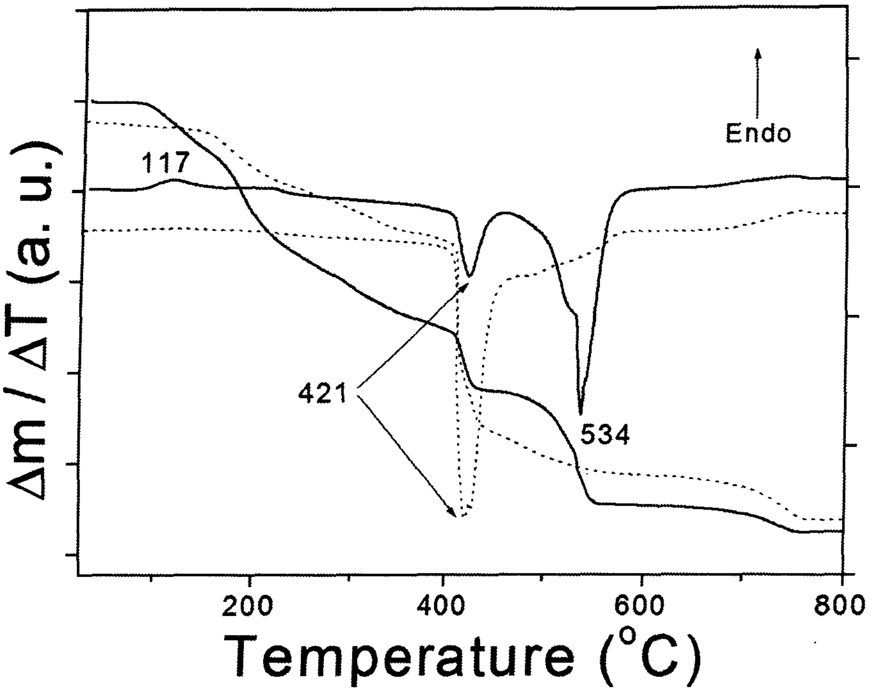

Figure 51- TG-DTA thermograms [Ca(H_2O)$_6$(4-nba)](4-nba)(2-ap)·H_2O (**7**) (solid line) and [Ca(4-nba)$_2$(2-ap)] (**7a**) (dotted line).

[K(H_2O)$_2$(4-nba)] 10

The TG-DSC thermogram of **10** (Figure 52) exhibits an endothermic event at around 90°C accompanied by a mass loss of 16% assignable for the removal of two molecules of water. The dehydration process is followed by an endothermic signal at around 281°C, which can be assigned to a phase change. Above this temperature, **10** undergo a complex decomposition process as evidenced by the strong exothermic events at 349, 432 and 573°C. In the absence of mass spectral data of the emitted fragments, no definite conclusions can be drawn on the exact nature of the decomposition processes. The observed residue is in good agreement for the formation of K_2CO_3. The results of the isothermal weight loss studies at 130°C (in temperature controlled oven) and at 800°C add more credence to the TG-DSC data.

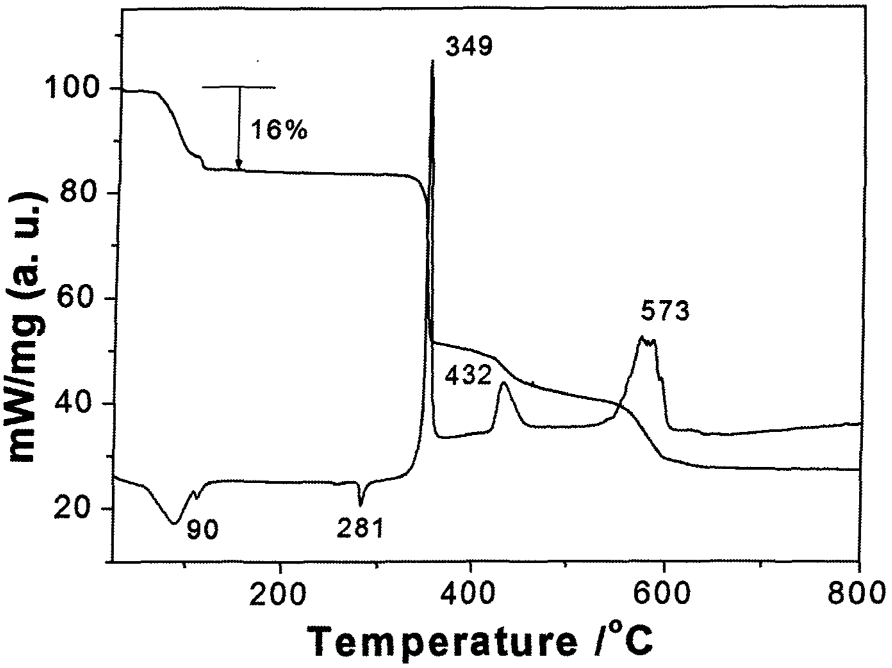

Figure 52 - TG-DSC thermogram of [$K(H_2O)_2$(4-nba)] **10** in air atmosphere at heating rate of 10k/min

Thermal behaviour of [Sr(4-nba)($H_2O)_7$](4-nba).$2H_2O$ 11, [Sr(4-nba)$_2(H_2O)_4$] 11a, [[Sr(4-nba)(DMF)($H_2O)_3$](4-nba)]$_n$ 12, [Sr(H_2O)(4-nba)$_2$(NMF)$_{1.5}$]$_n$ 13, [Sr(4-nba)$_2$(pyr)$_2$]$_n$ 14 and [Sr(4-nba)$_2$($HCONH_2$)($H_2O)_3$]$_n$ 15

On heating compounds **11**, **11a**, **12**, **13** loose water in the region 104-115°C with endothermic peaks at 115, 104, 113 and 109°C in DTA curve as shown in Table 8 above. The peak at 236 and 165°C in compound **14** and **15** are due to pyrazole decomposition in **14** and formamide in **15** respectively. The 4-nitrobenzoate decomposition in compounds **11-15** are observed as two peaks with one strong exothermic peak between 403-435°C and the other as small exothermic event above 525°C in all four compounds (Figures 53-59). The anhydrous nature of compound **14** can be seen by absence of any mass loss below 150°C in TG-DTA thermogram of compound **14**. All the compounds **11-15** when heated to 1000°C decompose giving $SrCO_3$ as final residue as shown in the Scheme **7**. Compound **11** shows an endothermic event at 115°C, followed by two exothermic events at 424°C and 534°C indicative of decomposition of 4-nitrobenzoate moiety. The tetrahydrate shows two sharp endothermic peaks at 104°C and 156°C due to the loss of water molecules. The peaks due to 4-nitrobenzoate decomposition are observed at 429°C and 556°C. Compound **12** loses its water at 113°C indicated by an endothermic peak at 113°C and two exothermic events at 435°C and 525°C representing decomposition of 4-

nitrobenzoate group. Compound **13** shows water loss at 109°C as an endothermic event followed by two exothermic peaks at 430°C and 536°C indicative of loss of 4-nitrobenzoate group (Figure 59). The decomposition product of all the process was found to be $SrCO_3$ as indicated by its DSC as well as isothermal heating to 1000°C. This was also confirmed by X-ray powder pattern of final residue $SrCO_3$ (Refer Appendix).

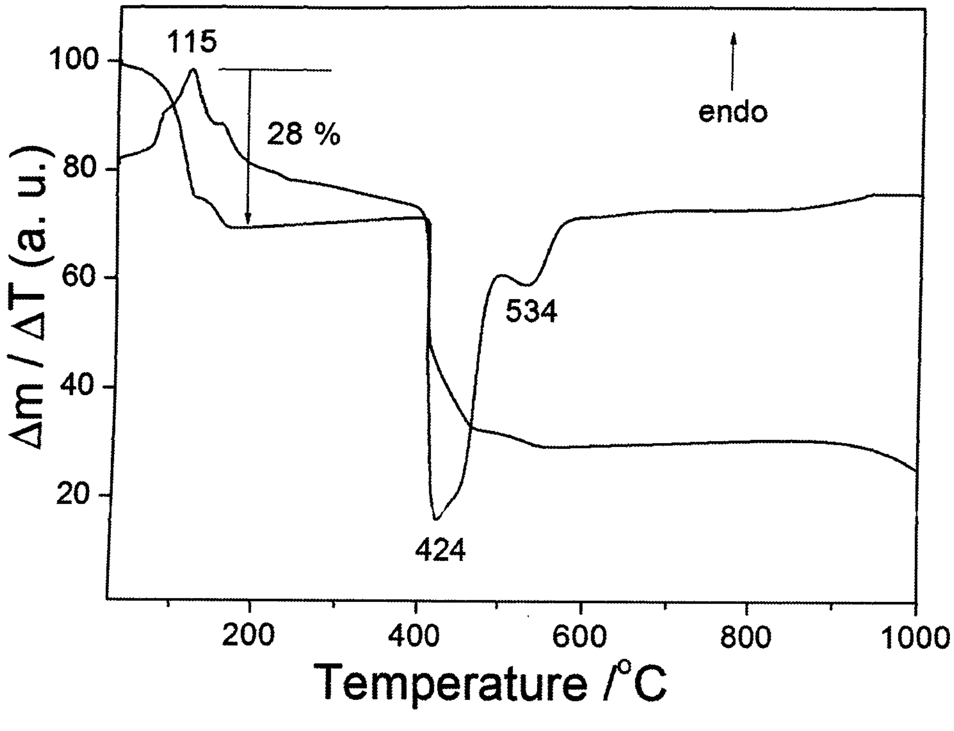

Figure 53-TG-DTA thermogram of [Sr(4-nba)$(H_2O)_7$](4-nba).$2H_2O$ **11** in air atmosphere at heating rate of 10k/min

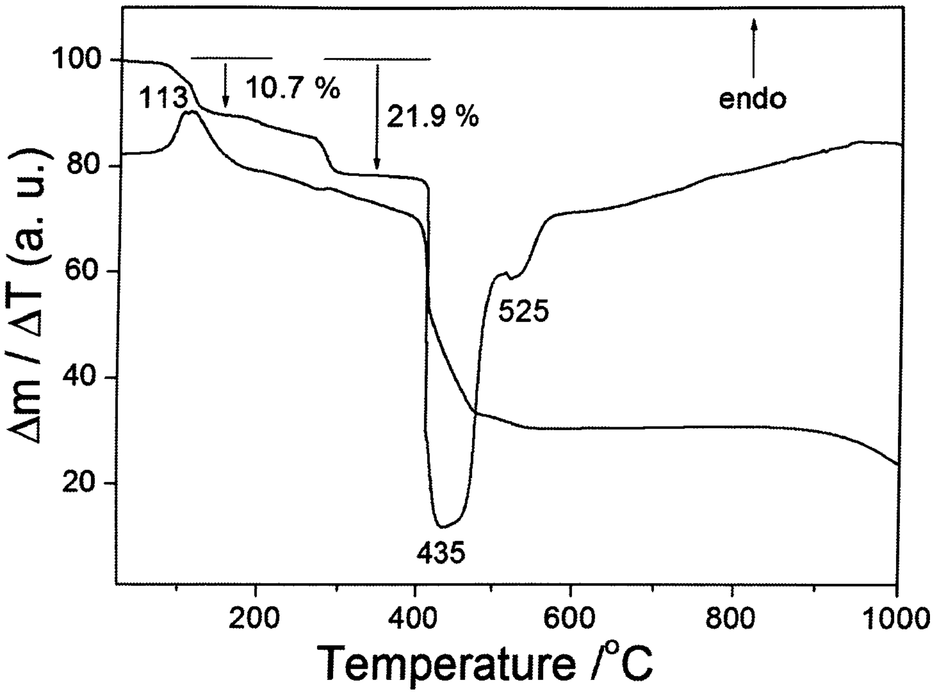

Figure 54- TG-DTA Thermogram of [Sr(4-nba)(dmf)$(H_2O)_3$](4-nba) **12** in air atmosphere at heating rate of 10k/min

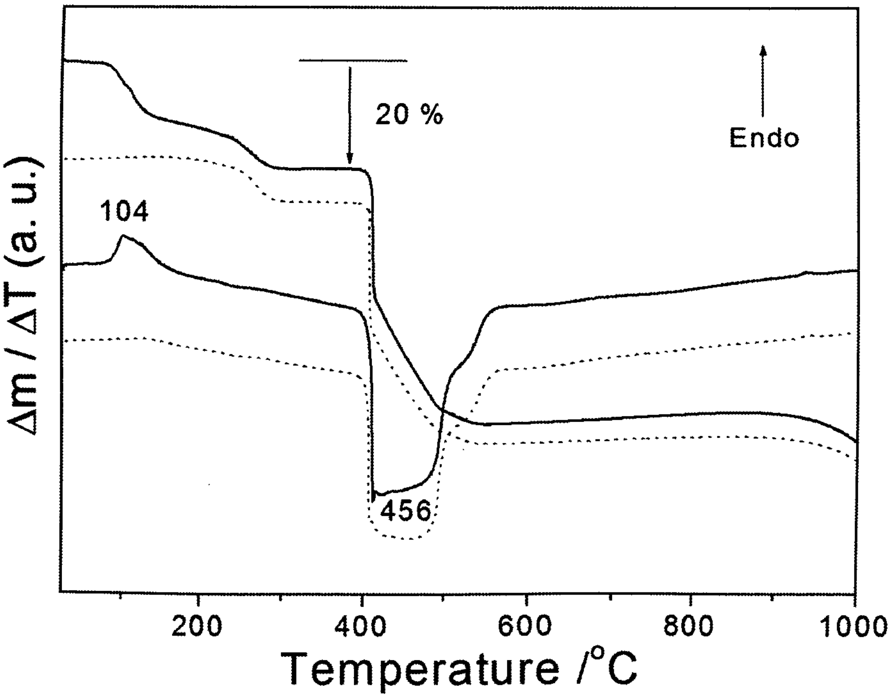

Figure 55- TG-DTA thermogram of [Sr(4-nba)(dmf)$(H_2O)_3$](4-nba) **12** and its dehydrated compound **12a** in air atmosphere at heating rate of 10k/min

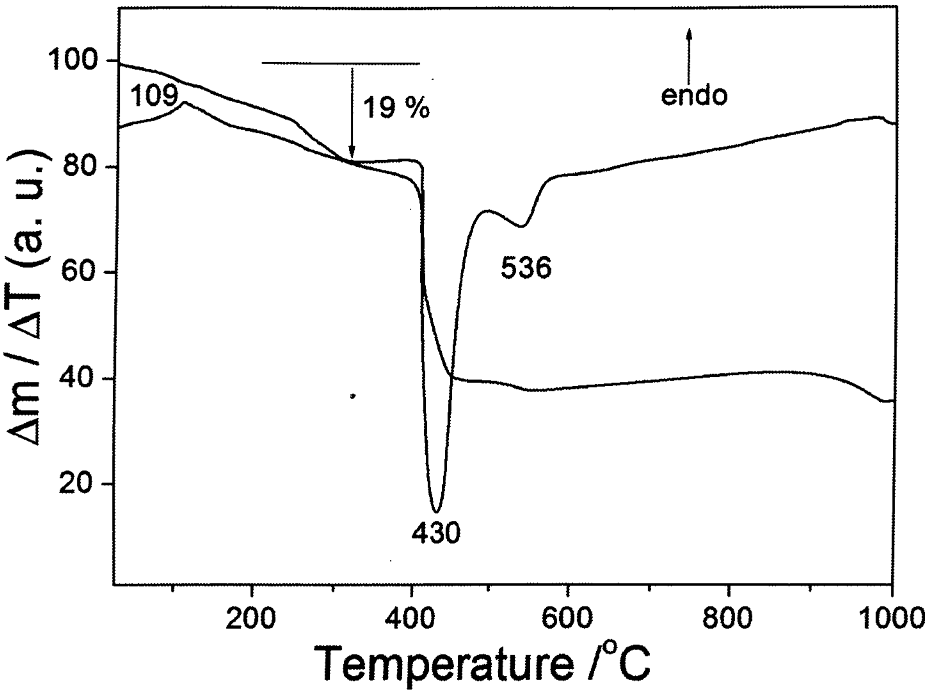

Figure 56- TG-DTA thermogram of [Sr(H_2O)(4-nba)$_2$(nmf)$_{1.5}$] **13** in air atmosphere at heating rate of 10k/min

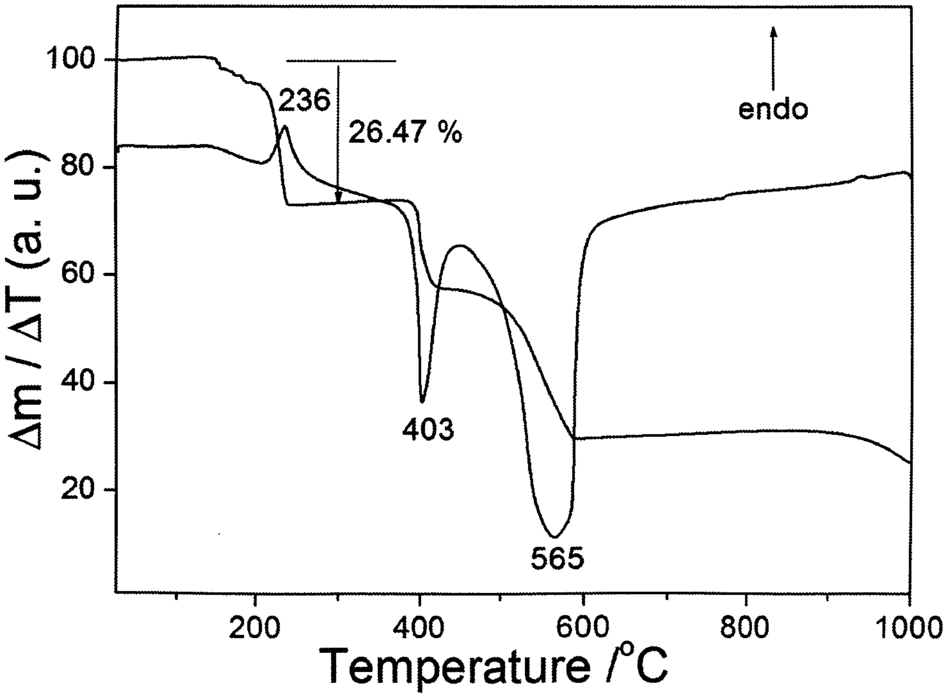

Figure 57- TG-DTA thermogram of [Sr(4-nba)$_2$(pyr)$_2$] **14** in air atmosphere at heating rate of 10K/min.

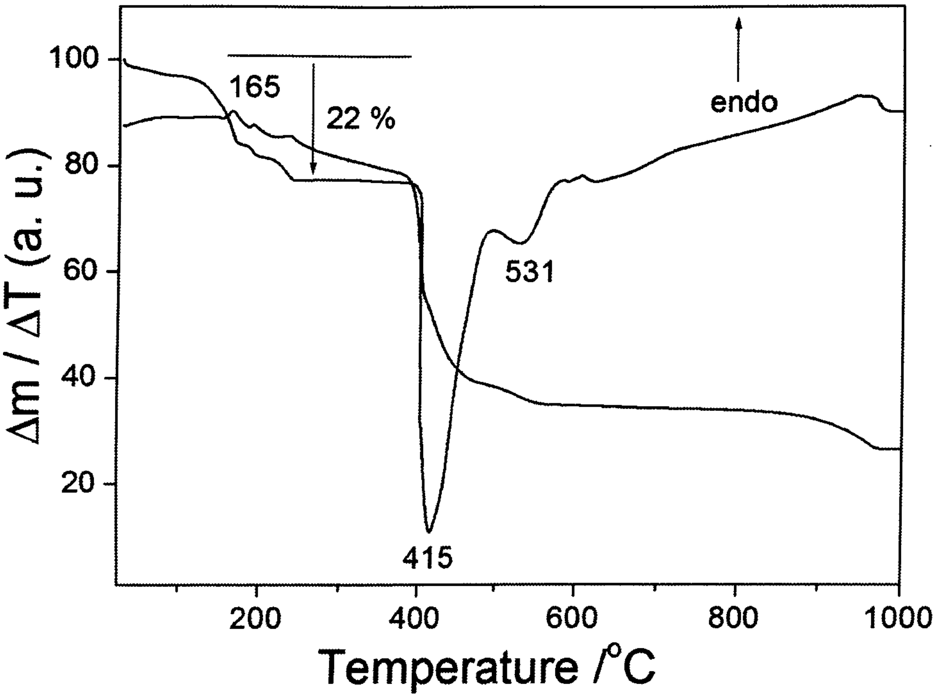

Figure 58- TG-DTA thermogram of [Sr(4-nba)$_2$(HCONH$_2$)(H$_2$O)$_3$] **15** in air atmosphere at heating rate of 10k/min

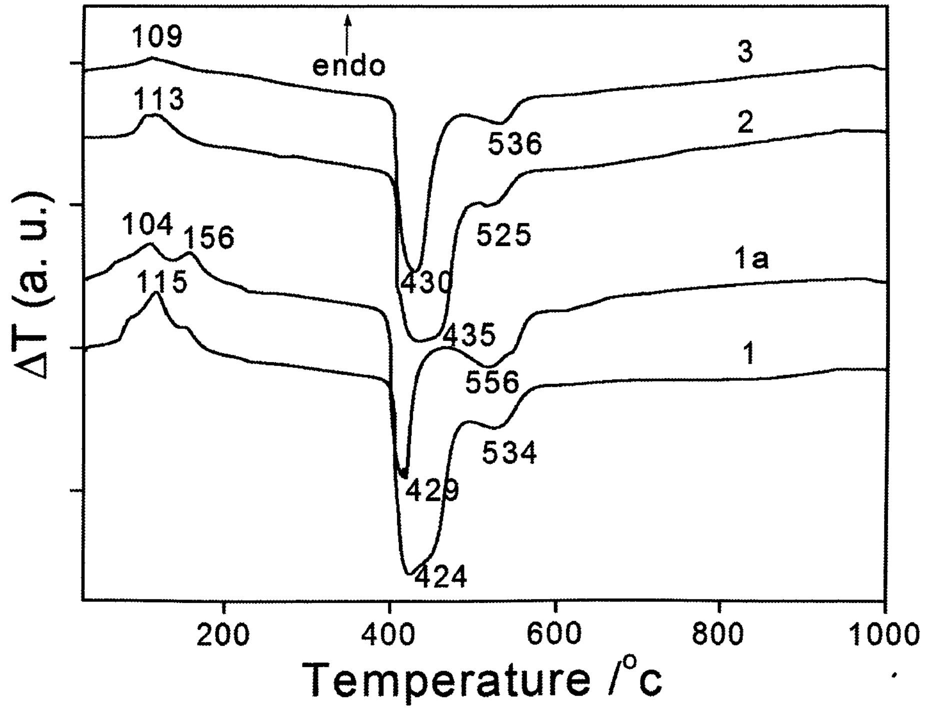

Figure 59- DTA Thermogram of [Sr(4-nba)(H$_2$O)$_7$](4-nba).2H$_2$O **11**, [Sr(4-nba)$_2$(H$_2$O)$_4$] **11a,** [Sr(4-nba)(DMF)(H$_2$O)$_3$](4-nba) **12**, [Sr(H$_2$O)(4-nba)$_2$(NMF)$_{1.5}$] **13** done in air at 10K min^{-1}.

$[Mg(H_2O)_6](2\text{-ca-4-nba})_2$ 16

The TG-DSC thermogram of $[Mg(H_2O)_6](2\text{-ca-4-nba})_2$ **16** exhibits three endothermic processes at 94, 136, and 245°C followed by two exothermic events at 433 and 545°C respectively. The mass loss of 19% for the first two processes is in good agreement for the expected (19.63%) loss of six water molecules. The third endothermic signal above 200°C is indicative of a slow decomposition of 2-ca-4nba moiety leading to further decomposition as evidenced by the two exothermic events at 433 and 545°C. Above this temperature, MgO is formed as a final decomposition product. The formation of MgO as the final residue was further confirmed based on isothermal weight loss studies by heating compound **16** at 800°C in a temperature controlled furnace (Figure 60).

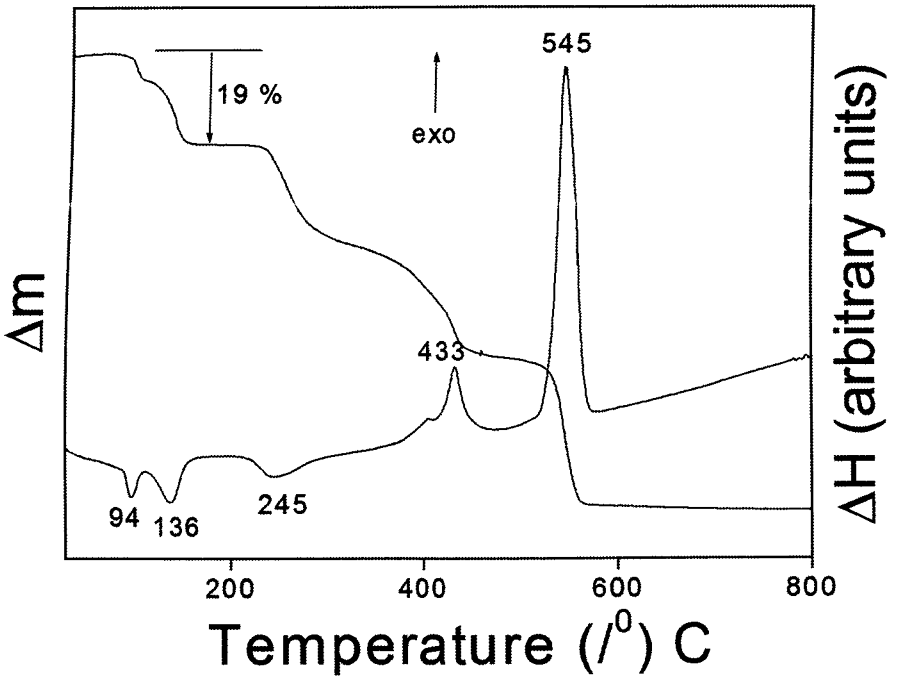

Figure 60- TG-DSC thermogram of $[Mg(H_2O)_6](2\text{-ca-4-nba})_2$ **16** (Heating rate 10K min^{-1}; air atmosphere).

$[Ca(H_2O)_2(2\text{-ca-4nba})_2]_n$ 17

The TG-DTA thermogram of $[Ca(H_2O)_2(2\text{-ca-4nba})_2]_n$ **17** (Figure 61) exhibits four thermal events. The first endothermic process at 152°C accompanied by a weight loss of 6.0% (expected 7.2%) can be assigned to the loss of two moles of coordinated water. Heating of **17** at 150°C in an oven results in the formation of an anhydrous compound. The anhydrous nature can be evidenced from its IR spectrum which is devoid of the strong O-H signal at around 3600 cm^{-1}. The second endothermic signal at 297°C as well as the exothermic events at 440 and 557°C can be assigned for the decomposition of the organic ligand leading to the formation of the oxide residue. Although the exact nature of these ligand decomposition processes cannot be commented due to the absence of associated mass spectral data of the emitted fragments, the formation of CaO as the final residue can be inferred as the residue based on mass loss. The complete loss of organics was also evidenced from the featureless IR spectrum of the residue. As expected, the thermogram of the anhydrous product (Figure 61) is nearly identical to that of **17** except for the absence of an endothermic signal at around 152°C. Similar results were obtained from the isothermal weight loss studies which add credence to the above observations.

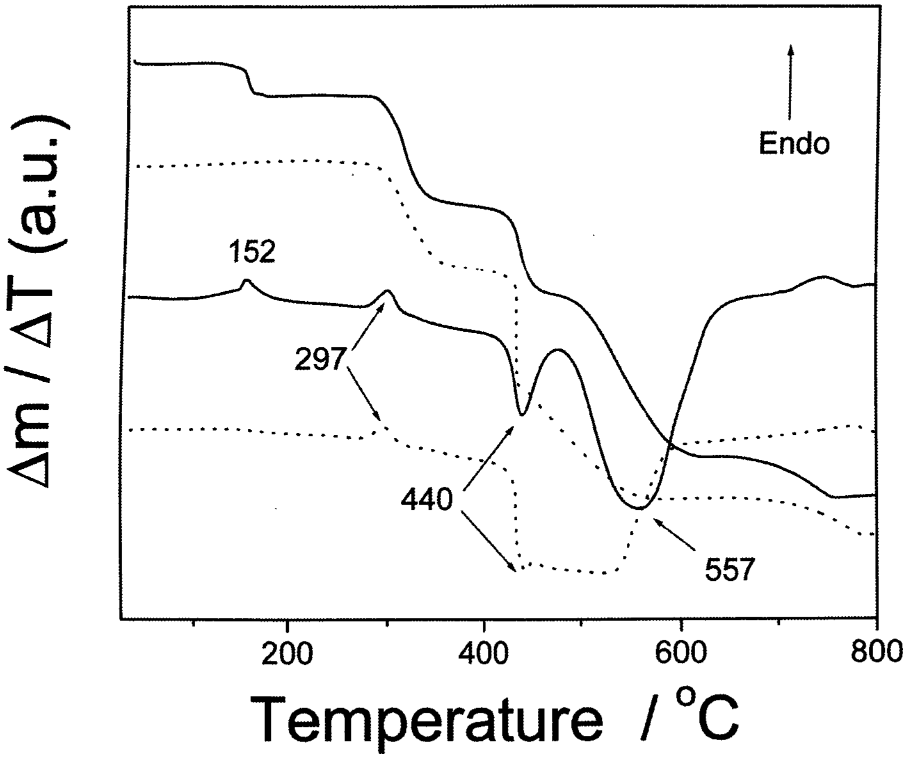

Figure 61- TG-DSC thermogram of $[Ca(H_2O)_2(2\text{-}ca\text{-}4nba)_2]_n$ **17** (solid line) and the anhydrous compound (dotted line) obtained by heating **17** at 150°C.

$[Mg(H_2O)_4(2\text{-}nba)_2]$ 20

Compound $[Mg(H_2O)_4(2\text{-}nba)_2]$ **20** gets fully dehydrated at 100°C which can be evidenced from the absence of the –OH absorption in its infrared spectrum. A comparison of TG-DSC thermal pattern of the tetrahydrate $[Mg(H_2O)_4(2\text{-}nba)_2]$ **20** and its dehydrated compound $[Mg(2\text{-}nba)_2]$ **20a** reveals that the DSC thermograms of **20a** is identical to that of compound **20** above 100°C when the tetrahydrate **20** emits four moles of water forming the anhydrous compound [Mg(2-nba)$_2$] (Figure 62). The dehydration process is followed by an endothermic signal at around 231°C, which can be assigned to a phase change. The 2-nitrobenzoate decomposition is observed as two exothermic peaks at 336 and 457°C in **20** and **20a**. Heating of **20** or **20a** at 800°C in a furnace resulted in the total removal of organics and formation of an oxide residue which does not show any features in infrared.

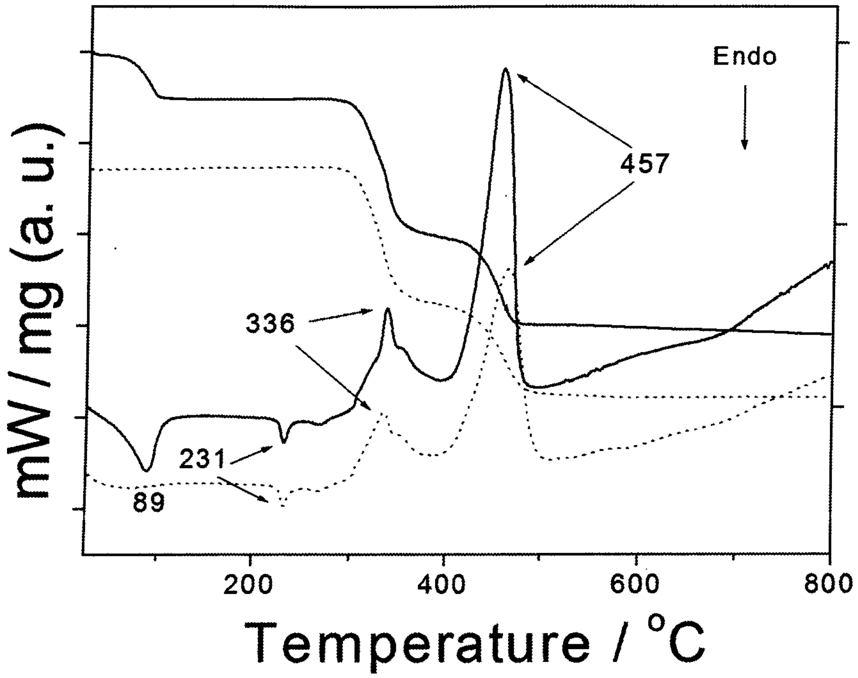

Figure 62- TG-DSC Thermogram of [Mg(H$_2$O)$_4$(2-nba)$_2$] **20** (shown as solid lines) and corresponding dehydrated product [Mg(2-nba)$_2$] **20a** (dotted lines).

[Ca(2-nba)$_2$(H$_2$O)$_2$]$_n$ 21 and [Ca(2-nba)$_2$]$_n$ 21a

The TG-DSC thermogram of [Ca(2-nba)$_2$(H$_2$O)$_2$]$_n$ **21** (Figure 63) exhibits an endothermic event at 144°C accompanied by a mass loss of 8.5%. This value is in good agreement with that expected (8.83%) for the loss of two molecules of water. Above this temperature, the thermogram exhibits only exothermic processes with signals at 322, 354 and 544°C. The first two closely related exotherms can be attributed to the decomposition of 2-nitrobenzoate. In view of the absence of mass spectral data of the emitted fragments, we do not wish to comment on the exact nature of the decomposition processes at these high temperatures. However it should be noted that the observed residual mass of 14.3% for the residue is in good agreement for the formation of CaO. The formation of the oxide phase can also be evidenced by the featureless infrared spectrum of the residue as well as the powder pattern of the residue. The residue on exposure to atmosphere shows an increase in weight corresponding to the formation of calcium carbonate. The results of the isothermal weight loss studies at 150°C and at 800°C in a furnace add more credence to the TG-DSC data. The TG-DSC thermogram of the anhydrous compound $[Ca(2\text{-}nba)_2]_n$ **21a** is devoid of the first endothermic signal observed for the dehydration of **21**. A comparison of the TG-DSC thermograms of **21** and **21a** (Figure 63) shows the identical nature of the TG-DSC curves of **21a** to that of **21** above 150°C. The observed residual mass of 13.7 % can be accounted for the formation of CaO.

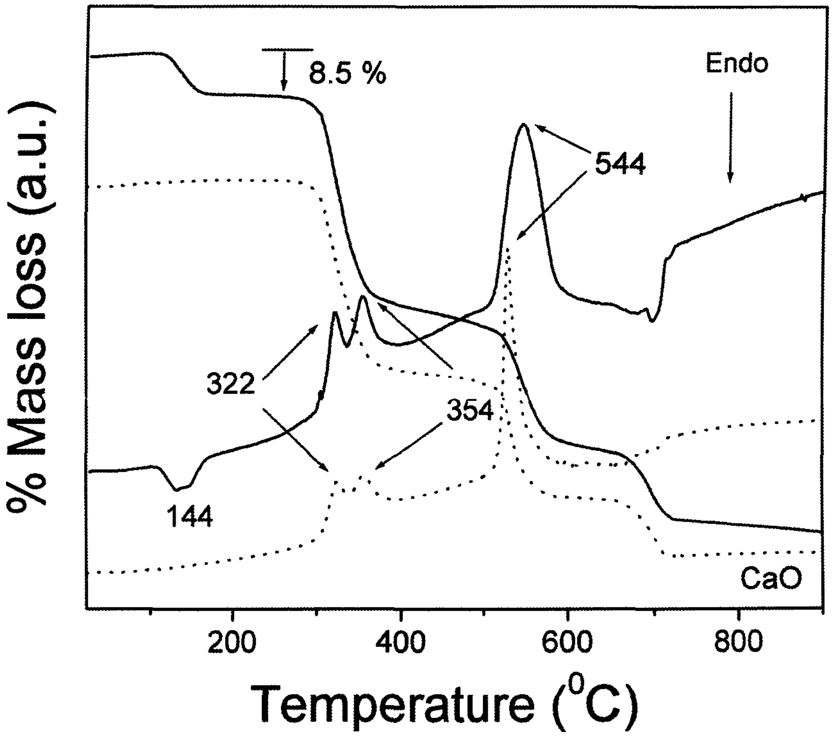

Figure 63- TG-DSC thermograms of $[Ca(2\text{-}nba)_2(H_2O)_2]_n$ **21** (solid line) and $[Ca(2\text{-}nba)_2]_n$ **21a** (dotted lines). (Heating Rate 5 K min^{-1}; Air atmosphere)

$[[Ba(H_2O)_3]_2(\mu_2\text{-}2\text{-}nba\text{-}O,O,\mu\text{-}O\text{-}NO_2)_2(\mu_2\text{-}2\text{-}nba\text{-}O,O,O')_2]_n$ 22 and dehydrated barium(II) bis(2-nitrobenzoate) 22a

The TG-DSC thermogram of **22** (Figure 64) exhibits an endothermic event at around 88°C accompanied by a mass loss of 10.5% assignable for the removal of three molecules of water. The dehydration process is followed by an endothermic signal at around 230°C, which can be assigned to a phase change. Above this temperature, **22** undergo a complex decomposition process as evidenced by the strong exothermic events at 338 and 444°C. In the absence of mass spectral data of the emitted fragments, no definite conclusions can be drawn on the exact nature of the decomposition processes. The observed residue is in good agreement for the formation of $BaCO_3$. The results of the isothermal weight loss studies at 100°C (steam bath) and at 800°C add more credence to the TG-DSC data. As expected, the TG-DSC thermogram of the anhydrous compound **22a** (Figure 64) is devoid of the first endothermic signal observed for the dehydration of **22** and the thermal decomposition pattern of **22a** is very similar to that of **22** above this temperature, resulting in the formation of $BaCO_3$ residue. Equilibriation of the anhydrous compound **22a** in an atmosphere of water vapor results in the regeneration of compound **22** as confirmed by a comparison of the IR spectrum of the rehydrated product with that of **22**.

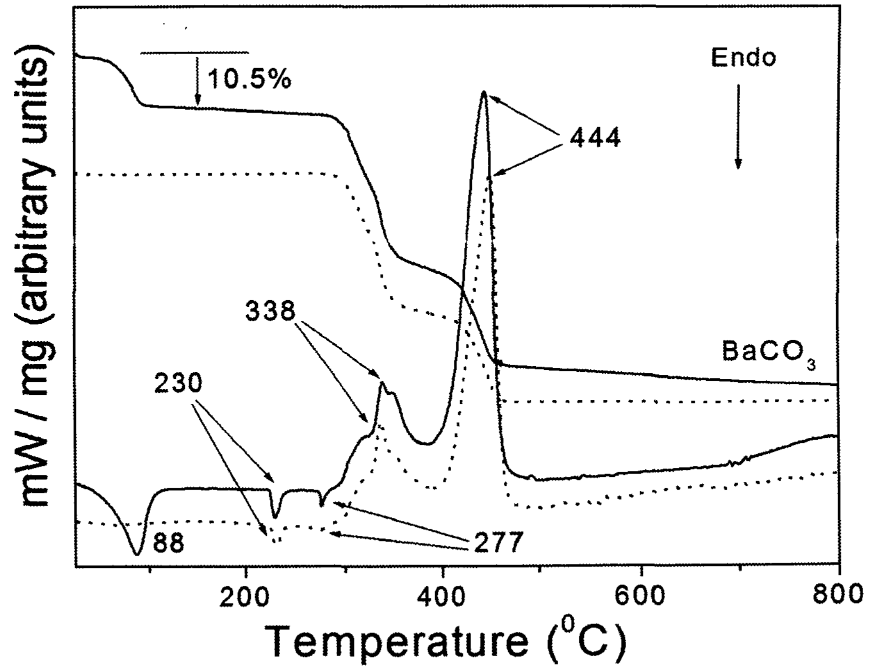

Figure 64- TG-DSC thermogram of $[[Ba(H_2O)_3]_2(\mu_2\text{-}2\text{-nba-O,O},\mu\text{-O-NO}_2)_2(\mu_2\text{-}2\text{-nba-O,O,O'})_2]_n$ **22** and dehydrated barium(II) bis(2-nitrobenzoate) **22a** (shown as dotted lines)

$[Sr(2\text{-nba})_2(H_2O)_4]_n$ 23 and **$[Sr(2\text{-nba})_2]$ 23a**

The TG-DSC thermogram of **23** (Figure 65) exhibits two endothermic events at 72°C and 116°C accompanied by a mass loss of 13.0% assignable for the removal of four molecules of water. The dehydration process is followed by an endothermic signal at around 266°C, which can be assigned to a phase change. Above this temperature, **23** undergo a complex decomposition process as evidenced by the strong exothermic events at 332 and 416°C. In the absence of mass spectral data of the emitted fragments no definite conclusions can be drawn on the exact nature of the decomposition processes. The observed residue is in good agreement for the formation of $SrCO_3$. The results of the isothermal weight loss studies at 100°C (steam bath) and at 800°C add more credence to the TG-DSC data. As expected, the TG-DSC thermogram of the anhydrous compound **23a** (Figure 65) is devoid of the first endothermic signal observed for the dehydration of **23** and the thermal decomposition pattern of **23a** is very similar to that of **23** above this temperature, resulting in the formation of $SrCO_3$ residue. Equilibriation of the anhydrous compound **23a** in an atmosphere of water vapor results in the regeneration of compound **23** as confirmed by a comparison of the IR spectrum of the rehydrated product with that of **23**.

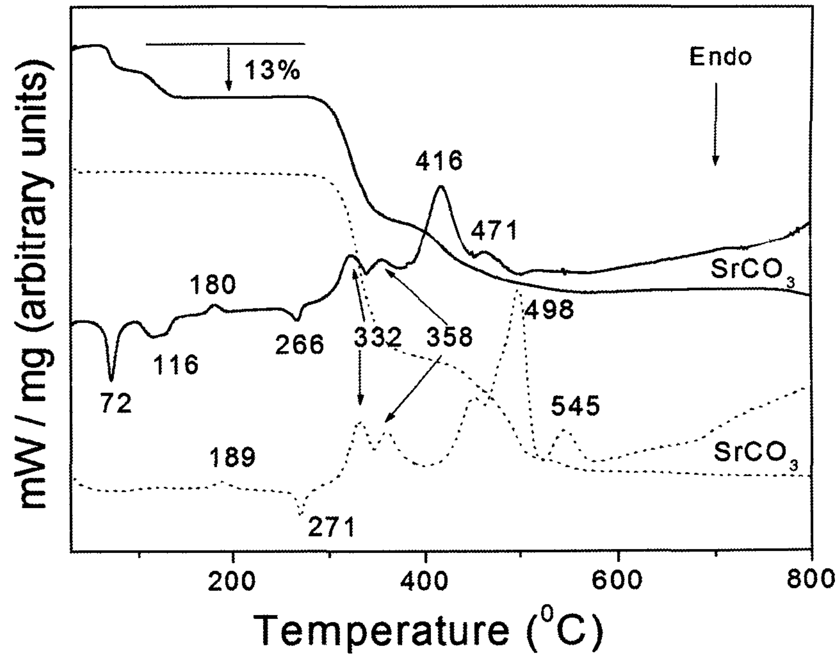

Figure 65- TG-DSC thermograms of $[Sr(2\text{-nba})_2(H_2O)_4]_n$ **23** (solid line) and $[Sr(2\text{-nba})_2]_n$ **23a** (dotted lines). (Heating Rate 5 K min^{-1}; Air atmosphere)

$[Mg(H_2O)_5(3\text{-npth})]\cdot 2H_2O$ 25 and $[[Ca(H_2O)_2(3\text{-npth})]\cdot H_2O]_n$ 26

Compound $[Mg(H_2O)_5(3\text{-npth})]\cdot 2H_2O$ **25** and $[[Ca(H_2O)_2(3\text{-npth})]\cdot H_2O]_n$ **26** gets fully dehydrated at 100°C which can be evidenced from the absence of the –OH absorption in their infrared spectra. A comparison of TG-DTA thermal pattern of the $[Mg(H_2O)_5(3\text{-npth})]\cdot 2H_2O$ **25** and its dehydrated compound [Mg(3-npth)] **25a** reveals that the DSC thermograms of **25a** is identical to that of compound **25** above 125°C when the pentahydrate **25** emits five moles of water forming the anhydrous compound [Mg(3-

npth)] **25a** (Figures 66). A similar behavior is observed in [[Ca(H_2O)$_2$(3-npth)]·H_2O]$_n$ **26** indicating a loss three moles of water around 125°C for the formation of [Ca(3-npth)] **26a**. The 3-nitrophthalate compounds of Mg(II) and Ca(II) (Figures 66 and 67) exhibit exothermic signals above 412°C in their thermograms which can be assigned for the decomposition of the carboxylate ligand. As expected, the thermal behavior of the anhydrous compounds **25a** and **26a** is identical to that of the corresponding starting hydrated compounds **25** and **26** with absence of the first endothermic signal at 125°C corresponding to the loss of water.

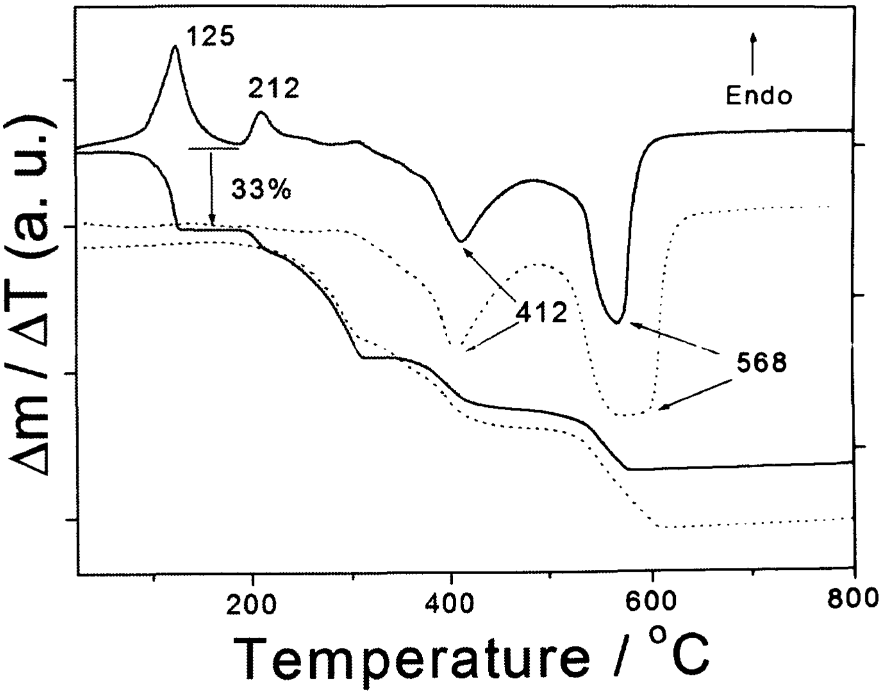

Figure 66- TG-DTA thermogram of [Mg(H_2O)$_5$(3-npth)]·$2H_2O$ **25** and the corresponding anhydrous product **25a** in dotted lines.

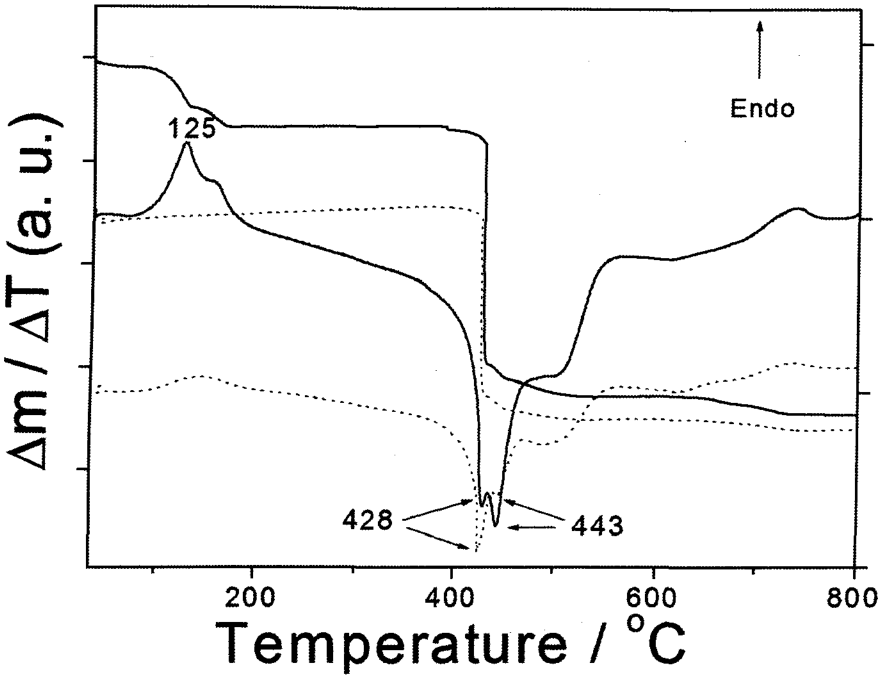

Figure 67-TG-DTA thermogram of $[[Ca(H_2O)_2(3\text{-npth})]\cdot H_2O]_n$ **26** and the corresponding anhydrous product **26a** in dotted lines.

Thermal properties of $[Mg_3(btc)_2(H_2O)_{18}]$ 29, **$[Mg_3(btc)_2(H_2O)_{12}]$ 29a, $[Mg_3(btc)_2]$, $[Ca_3(btc)_2(H_2O)_{12}]$ 30, $[Ca_3(btc)_2]$ 30a, $[Sr_3(btc)_2(H_2O)_8]$ 31, $[Sr_3(btc)_2]$ 31a, $[Ba_3(btc)_2(H_2O)_8].2H_2O$ 32,** and **$[Ba_3(btc)_2]$ 32a**

TG-DTA curve of compounds **29** show endothermic events at 100 and 180°C indicating water loss while **29a** shows peak at 178 and 210°C. Exothermic decomposition due to btc in **29a** is observed as two peaks at 599 and 674°C and its anhydrous compound is observed at 626°C (Figure 68). Compound **30** shows endothermic event at 131°C which can be attributed for water loss and exothermic decomposition due to btc ligand in **30** is observed at 593, 610°C respectively. The anhydrous phase of **30** does not show any endothermic event at 131°C however, beyond this point the TG-DSC pattern of hydrated phase of compound **30** and its dehydrated phase **30a** is same (Figure 69).

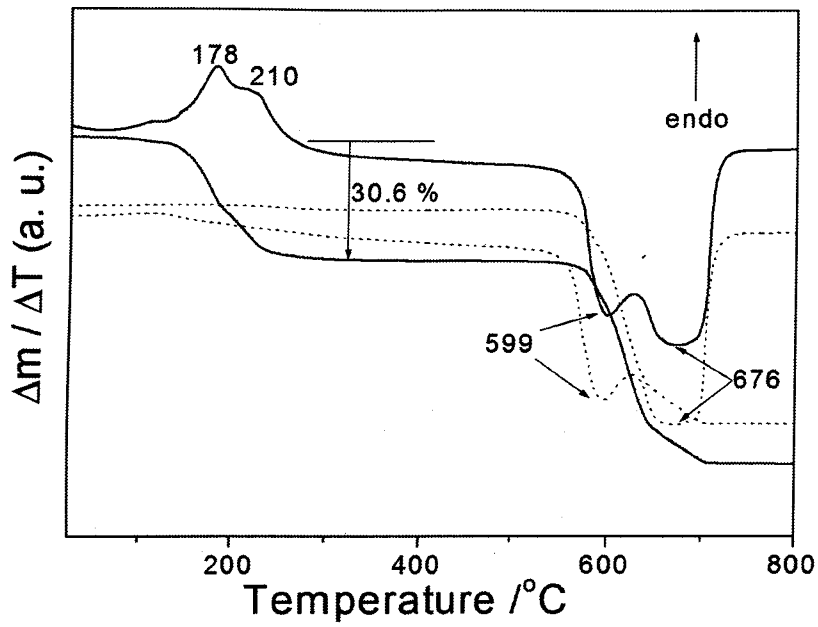

Figure 68 - TG-DTA thermogram of [$Mg_3(btc)_2(H_2O)_{12}$] **29a** and [$Mg_3(btc)_2$] shown as dotted lines in air atmosphere at heating rate of 10k/min.

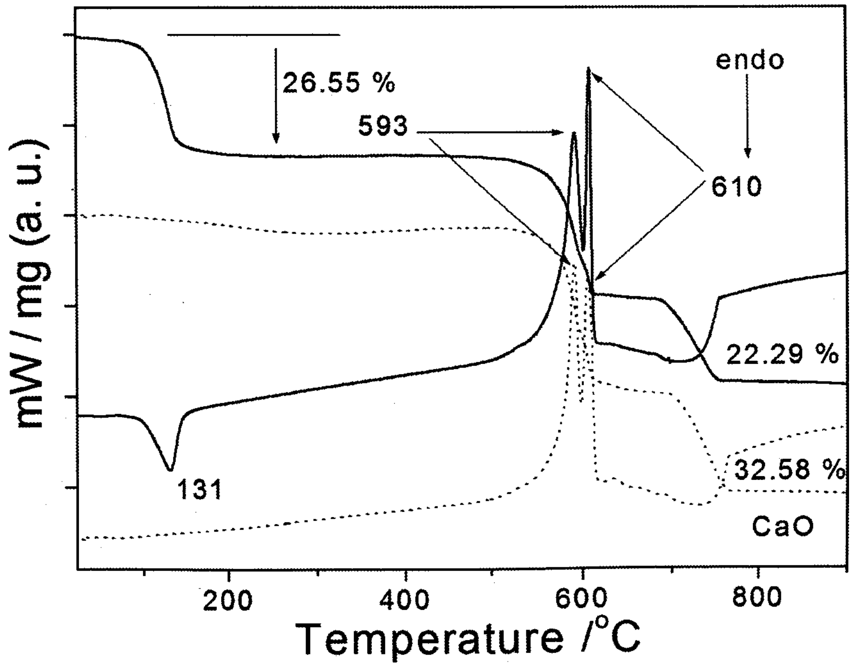

Figure 69- TG-DSC thermogram of [$Ca_3(btc)_2(H_2O)_{12}$] **30** and its dehydrated compound [$Ca_3(btc)_2$] **30a** shown as dotted lines in air atmosphere at heating rate of 10k/min

The TG-DTA profile of compound **31** shows endothermic event at 172°C indicating water loss. Beyond 172°C the TG curve of compound **31** is parallel to temperature axis until 525°C and 662°C where btc decomposition occurs as strong exothermic process. The anhydrous compound [$Sr_3(btc)_2$] **31a** does not show any endothermic events in the temperature range where hydrated compounds looses water however beyond this point both hydrated as well as dehydrated compounds show similar profile with strong exothermic decomposition at 662°C due to decomposition of btc ligand (Figure 70). The TG-DTA profile of compound **32** shows endothermic event at at 148°C indicating water loss and formation of anhydrous phase [$Ba_3(btc)_2$] **32a**. Beyond this point the TG curve of compound **32** is parallel to temperature axis until 525°C and 593°C where btc decomposition occurs as two strong exothermic processes. The anhydrous compound **32a** do not show any endothermic events in the temperature range 150-172°C where hydrated compound looses water however beyond this point both hydrated as well as dehydrated compound show similar profile with strong exothermic decomposition at 525°C and 662°C due to decomposition of btc ligand (Figure 71).

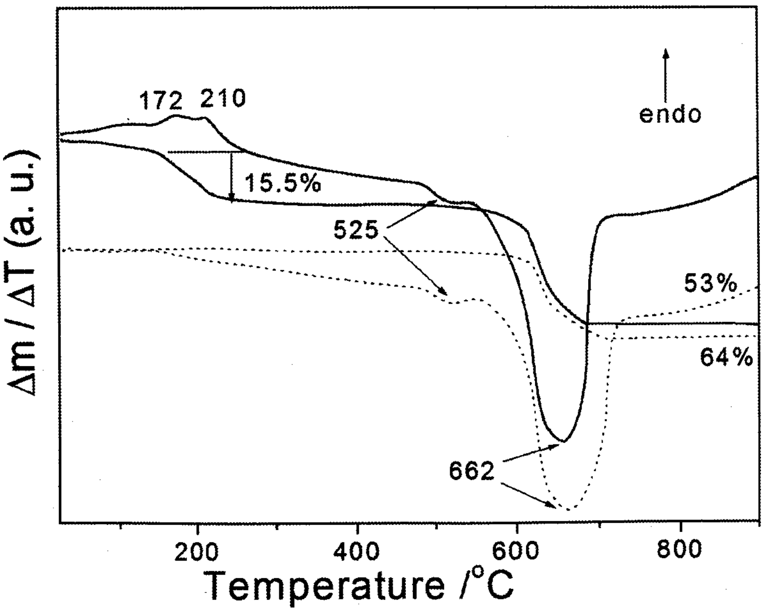

Figure 70- TG-DTA thermogram of [$Sr_3(btc)_2(H_2O)_8$] **31** and its dehydrated compound [$Sr_3(btc)_2$] **31a** shown as dotted lines in air atmosphere at heating rate of 10k/min

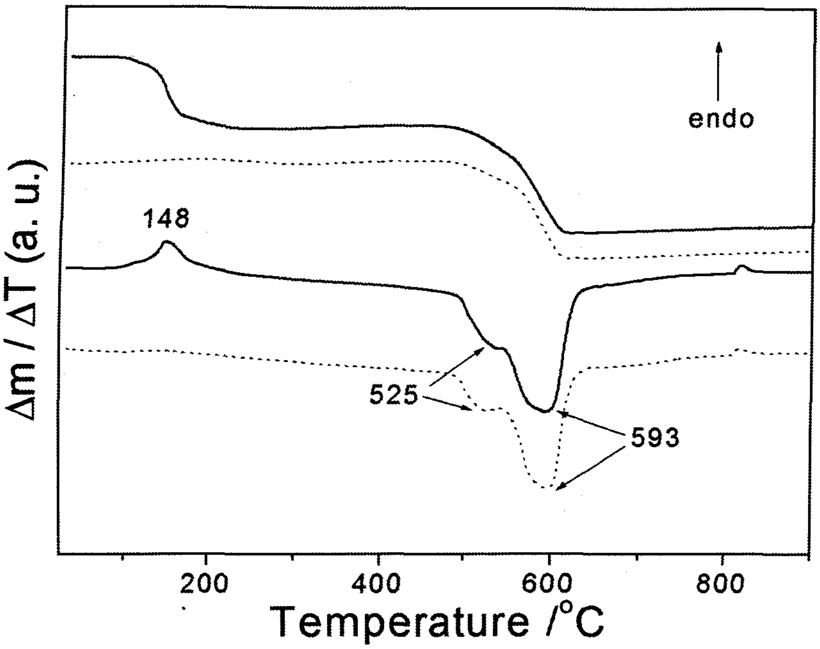

Figure 71- TG-DTA thermogram of $[Ba_3(btc)_2(H_2O)_8].2H_2O$ **32** and its dehydrated compound $[Ba_3(btc)_2]$ **32a** shown as dotted lines in air atmosphere at heating rate of 10k/min

$[Ca(H_2O)_2(L_1)_2].H_2O$ 33, $[Ca(L_1)_2]$ 33a, $[Ca(H_2O)_2(L_2)_2].2H_2O$ 34, $[Ca(L_2)_2]$ 34a

The thermal profiles of $[Ca(H_2O)_2(L_1)_2].H_2O$ **33** and $[Ca(H_2O)_2(L_2)_2].2H_2O$ **34** which exhibit an initial endothermic event at 116 and 121°C for **33** and **34** respectively assignable for loss of coordinated and lattice water molecules followed by exothermic events at higher temperatures (Figure 72) due to the decomposition of the organic linker are in accordance with the isothermal weight loss studies. As expected, the thermal behavior of the anhydrous compounds **33a** and **34a** are identical to that of the corresponding starting hydrated compounds **33** and **34** and the thermograms are devoid of the first endothermic signal corresponding to the loss of water (Figure 73).

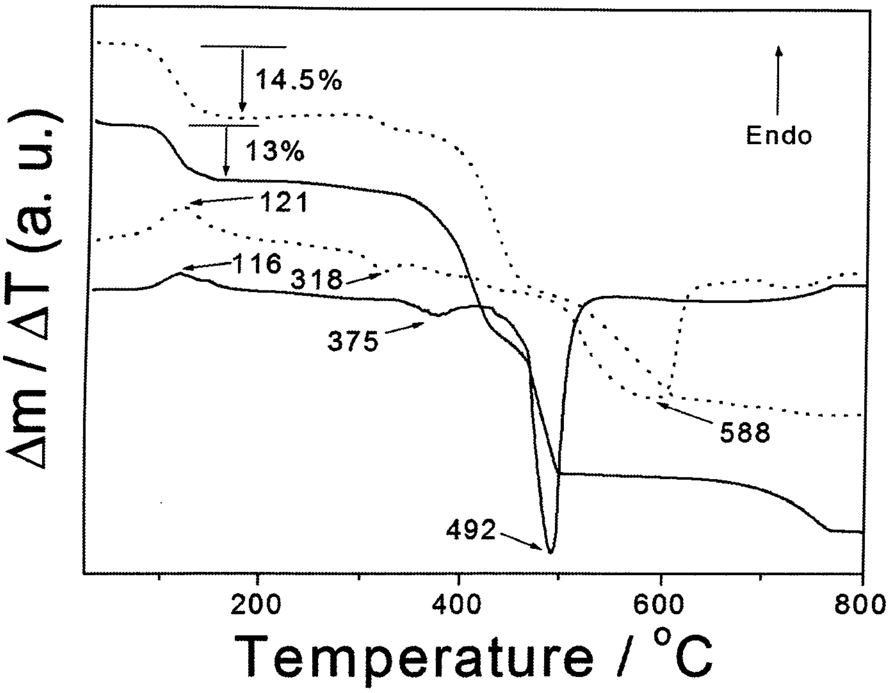

Figure 72- TG-DTA thermograms of $[Ca(H_2O)_2(L_1)_2].H_2O$ **33** (solid line) and of $[Ca(H_2O)_2(L_2)_2].2H_2O$ **34** (dotted line)

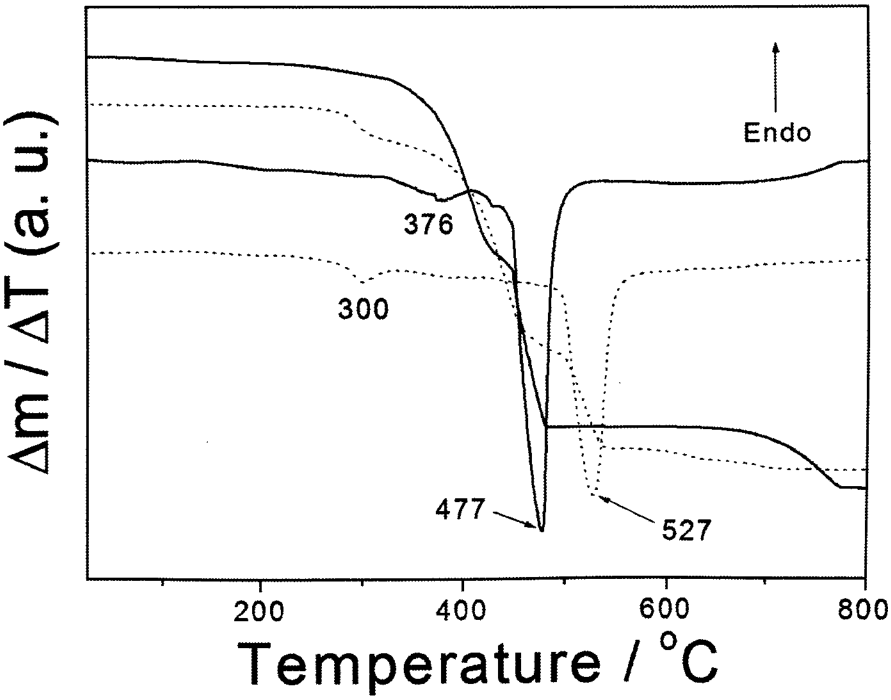

Figure 73 - TG-DTA thermograms of $[Ca(L_1)_2]$ **33a** (solid line) and of $[Ca(L_2)_2]$ **34a** (dotted line)

$[Ca(H_2O)_3(L)_2]$ 35, $[Ca(L)_2]$ 35a and $[Ba(H_2O)_3(L_2)_2].H_2O$ 36

The thermal profiles of $[Ca(H_2O)_3(L)_2]$ **35** and $[Ba(H_2O)_3(L_2)_2].H_2O$ **36** which exhibit an initial endothermic event at 125 for **35** and **36** respectively is assignable for loss of coordinated and lattice water molecules followed by exothermic events at higher temperatures above 516°C (Figure 74 and 75) due to the decomposition of the organic linker (L in **35** and L_2 in **36**) are in accordance with the isothermal weight loss studies expected for loss of three moles of water. As expected, the thermal behavior of the anhydrous compounds $[Ca(L)_2]$ **35a** and **36a** are identical to that of the corresponding starting hydrated compounds **35** and **36** and the thermograms are devoid of the first endothermic signal corresponding to the loss of water. The residue of decomposition for **35** and **35a** was analysed to be CaO while that of **36** and **36a** was found to be $BaCO_3$ as expected.

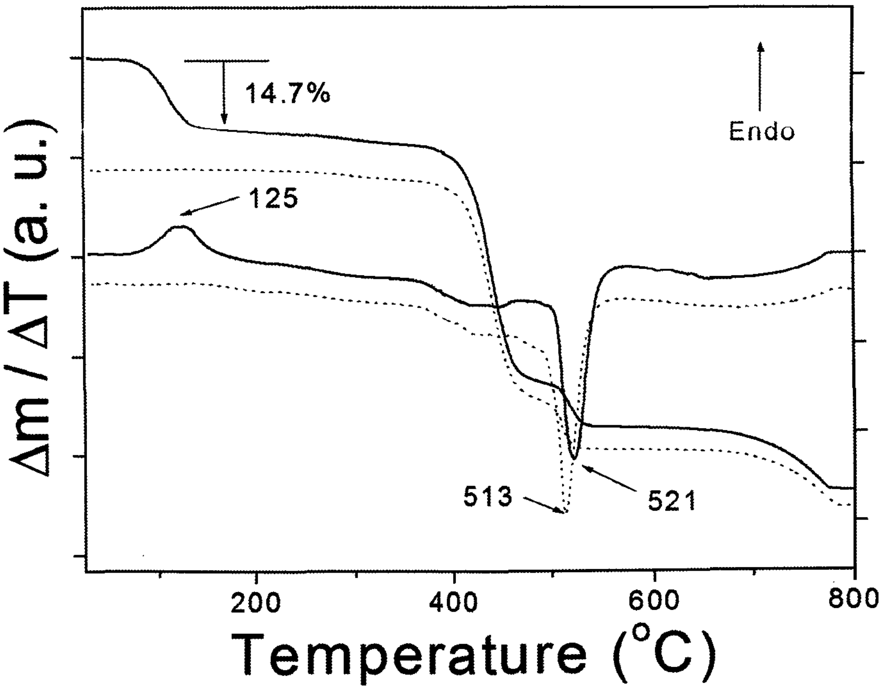

Figure 74 - TG-DTA Plot of compound $[Ca(H_2O)_3(L)_2]$ **35** and its dehydrated compound $[Ca(L)_2]$ **35a** (shown as dotted lines), done at heating rate of 10 k/min in air atmosphere

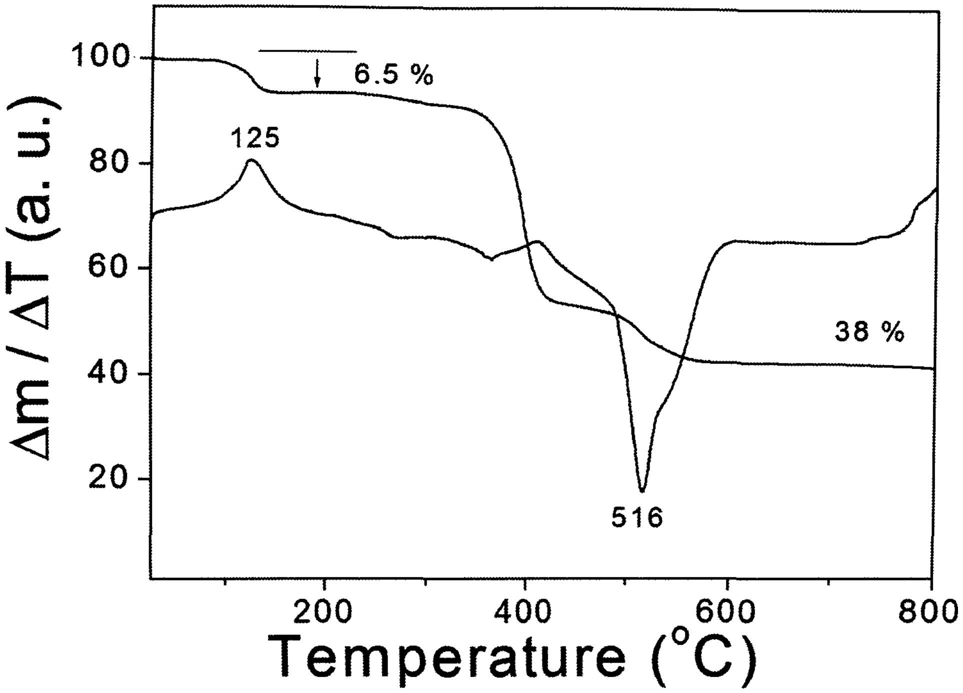

Figure 75 - TG-DTA plot of compound and $[Ba(H_2O)_3(L_2)_2].H_2O$ **36** done at heating rate of 10 k/min in air atmosphere.

$[Mg(H_2O)_6(5\text{-nisoph})]$ 37 and **$[Mg(5\text{-nisoph})]$ 37a**

Compound $[Mg(H_2O)_6(5\text{-nisoph})]$ **37** gets fully dehydrated at 184°C which can be evidenced from the absence of the –OH absorption in its infrared spectrum. A comparison of TG-DSC thermal pattern of the hexahydrate $[Mg(H_2O)_6(5\text{-nisoph})]$ **37** and its dehydrated compound $[Mg(5\text{-nisoph})]$ **37a** reveals that the DSC thermograms of **37a** is identical to that of compound **37** above 184°C when the hexahydrate **37** emits six moles of water forming the anhydrous compound $[Mg(5\text{-nisoph})]$ **37a** (Figure 76). The 5-nitroisophthalate decomposition is observed as two exothermic peaks at 483 and 566°C in **37** and **37a**. Heating of **37** or **37a** at 800°C in a furnace resulted in the total removal of organics and formation of an oxide residue which does not show any features in infrared.

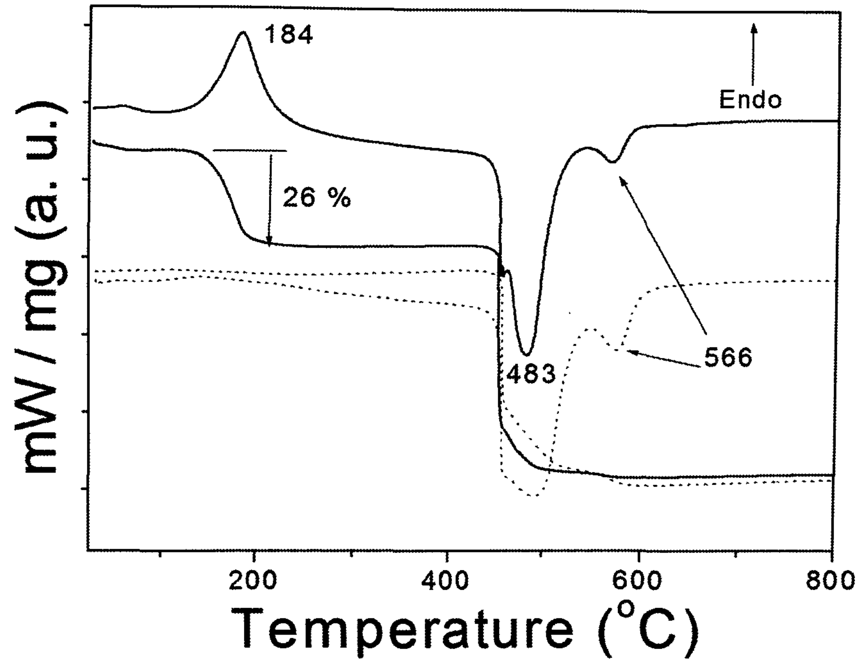

Figure 76- TG-DTA thermogram of compound [Mg$(H_2O)_6$(5-nisoph)] **37** (soild lines) and its dehydrated compound [Mg(5-nisoph)] **37a** (as dotted lines) (Heating rate 10 K/min; Air atmosphere)

[Ca$(H_2O)_4$(5-nisoph)] 38

The TG-DSC thermogram of compound [Ca$(H_2O)_2$(5-nisoph)] **38** is depicted in Figure 77. The DSC curve of compound **37** exhibits three thermal events. The first endothermic process at 149°C can be assigned to the loss of a neutral water ligand. The observed mass loss of 23% is much more than the loss expected for the loss of a four moles of water (22.4%). The exothermic events at 452 and 550°C correspond to the degradation of the 5-nitroisophthalate ligand as evidenced by the rapid drop in the TG curve. The assignment of the endothermic signal at 452°C for the decomposition of 5-nitroisophthalate gains more credence as a similar behaviour has been observed for the related Mg(II) compounds **37** and **37a** as above. The TG curve above 550°C is parallel to the temperature axis and observed residue of 18.1% is in very good agreement with the expected value of 17.44% for the formation of CaO.

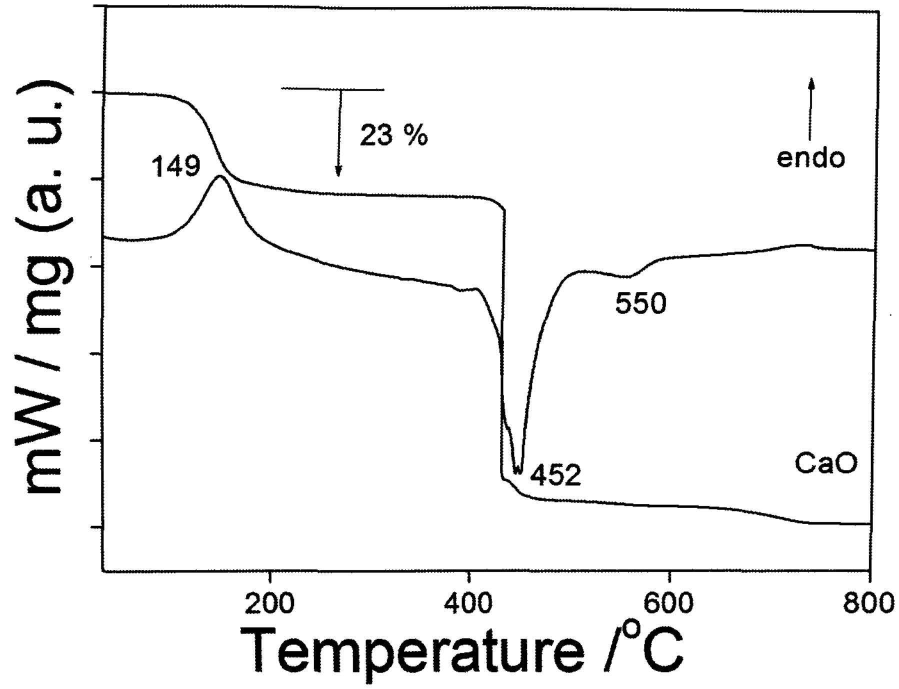

Figure 77- TG-DTA thermogram of compound [Ca$(H_2O)_2$(5-nisoph)] **38** (Heating rate 10 K/min; Air atmosphere)

[Mg$(H_2O)_6$(hip)$_2$] 39 and [Sr$(H_2O)_4$(hip)$_2$] 40

The thermal profiles of [Mg$(H_2O)_6$(hip)$_2$] **39** and [Sr$(H_2O)_4$(hip)$_2$] **40** which exhibit an initial endothermic event at 105 and 130°C for **39** and **40** respectively assignable for loss of coordinated and lattice water molecules followed by exothermic events at higher temperatures (Figure 78) due to the decomposition of the organic linker (hippurate) are in accordance with the isothermal weight loss studies. The observed mass loss of 22% (in **39**) and 17% (in **40**) at 105°C and 130°C is as expected for the loss of six moles of water in **39** (expected 22.07%) and four moles of water in **40** respectively.

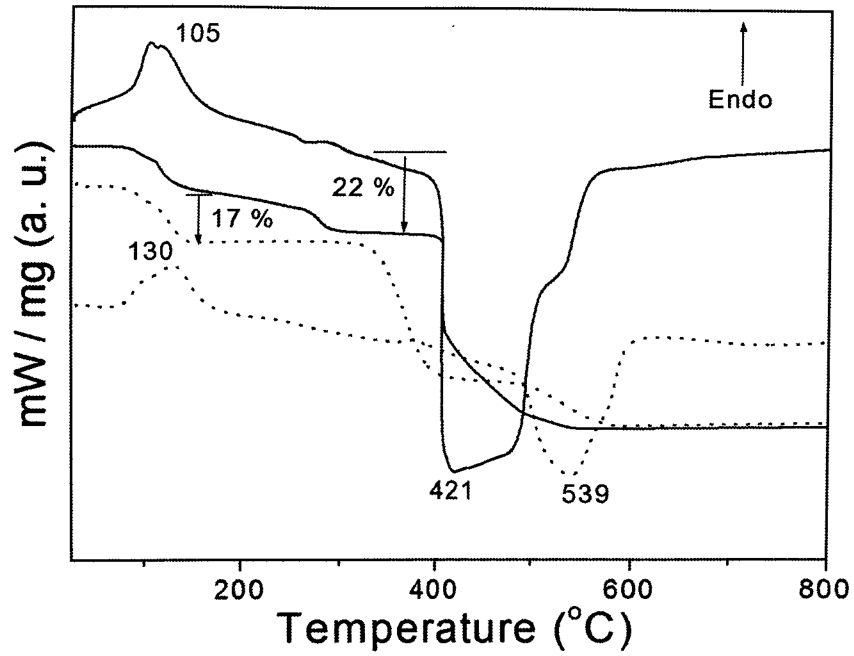

Figure 78- TG-DTA thermogram of compound [$Mg(H_2O)_6(hip)_2$] **39** (solid lines) and compound [$Sr(H_2O)_4(hip)_2$] **40** (as dotted lines) (Heating rate 10 K/min; Air atmosphere)

3.5 - Reversible hydration studies and surface area measurement

Some of the metal carboxylate polymer compounds prepared in this work subjected to reversible hydration after dehydration by equilibriating over water vapour. The results of this study are presented in Table 9. The N_2 adsorption-desorption isotherms of the anhydrous compounds **34a-35a** which show very little uptake of N_2, reveal the non porous nature of the polymers **34-36**. (Refer appendix).

Table 9- Isothermal weight loss and reversible hydration studies

Compound	Dehydrated product	Temperature °C	Isothermal mass loss	
			Exp	Theo
[Ca(H$_2$O)$_4$(4-nba)$_2$] **1**	[Ca(H$_2$O)(4-nba)$_2$] **1a**	100	12.1	12.16
[Ca(H$_2$O)$_4$(4-nba)$_2$] **1**	[Ca(4-nba)$_2$]	230	16.12	16.2
[Ca(H$_2$O)$_6$(4-nba)(2-ap)](4-nba)(2-ap) **7**	Ca(4-nba)(2-ap)](4-nba)(2-ap) **7a**	120	22.10	21.2
[(H$_2$O)$_4$Li$_2$(μ-H$_2$O)$_2$](4-nba)$_2$ **8**	[Li(4-nba)] **8a**	130	24.0	23.79
[Na(4-nba)(H$_2$O)$_3$]$_n$ **9**	[Na(4-nba)]$_n$ **9a**	130	21.98	22.22
[K(4-nba)(H$_2$O)$_2$] **10**	[K(4-nba)] **10a**	130	13.8	14.92
[Sr(H$_2$O)$_7$(4-nba)](4-nba).2H$_2$O **11**	[Sr(4-nba)$_2$] **11a**	150	28.0	27.85
[Mg(H$_2$O)$_6$(2-ca-4-nba)$_2$] **16**	[Mg(2-ca-4-nba)$_2$] **16a**	150	19.0	19.63
[Ca(H$_2$O)$_2$(2-ca-4-nba)$_2$]$_n$ **17**	[Ca(2-ca-4-nba)$_2$]$_n$ **17a**	150	6.0	7.2
[Mg(H$_2$O)$_4$(2-nba)$_2$] **20**	[Mg(2-nba)$_2$] **20a**	100	16.2	16.80
[Ca(H$_2$O)$_2$(2-nba)$_2$]$_n$ **21**	Ca(2-nba)$_2$]$_n$ **21a**	150	8.8	8.81
[Ba(H$_2$O)$_3$(2-nba)$_2$]$_n$ **22**	[Ba(2-nba)$_2$]$_n$ **22a**	120	10.5	10.32
[Sr(H$_2$O)$_4$(2-nba)$_2$] **23**	[Sr(2-nba)$_2$] **23a**	100	14.56	14.66
[Mg(H$_2$O)$_5$(3-npth)].2H$_2$O **25**	[Mg(3-npth)] **25a**	125	33.0	33.85
[[Ca(H$_2$O)$_2$(3-npth)].H$_2$O]$_n$ **26**	[Ca(3-npth)]$_n$ **26a**	125	16.2	17.82
[Mg$_3$(H$_2$O)$_{18}$(btc)$_2$] **29**	[Mg$_3$(btc)$_2$] **29a**	200	28.2	30.73
[Ca$_3$(H$_2$O)$_{12}$(btc)$_2$]$_n$ **30**	[Ca$_3$(btc)$_2$]$_n$ **30a**	200	28.65	28.79
[Sr$_3$(H$_2$O)$_8$(btc)$_2$]$_n$ **31**	[Sr$_3$(btc)$_2$]$_n$ **31a**	200	17.57	17.54
[[Ba$_3$(H$_2$O)$_8$(btc)$_2$].2H$_2$O]$_n$ **32**	[Ba$_3$(btc)$_2$]$_n$ **32a**	200	17.57	17.90
[Ca(H$_2$O)$_2$(4-OMephac)$_2$].H$_2$O **33**	[Ca(4-OMephac)$_2$]$_n$ **33a**	130	12.65	12.72
[[Ca(H$_2$O)$_2$(2-Clphac)$_2$].2H$_2$O]$_n$ **34**	[Ca(2-Clphac)$_2$]$_n$ **34a**	130	15.57	15.95
[Ca(H$_2$O)$_3$(phac)$_2$].H$_2$O **35**	[Ca(phac)$_2$]$_n$ **35a**	130	14.67	14.82

Chapter 4

Single Crystal X-ray diffractometry

The intensity data for compounds $[Ca(H_2O)(2\text{-MeIm})(4\text{-nba})_2]_n$ **4**, $[[Ca(pyr)_2(4\text{-nba})_2]_n$ **5**, $[Ca(H_2O)_2(4\text{-nba})_2].(dmp)_2]_n$ **6**, $[[Ca(H_2O)_2(3\text{-npth})]\cdot H_2O]_n$ **25**, $[Mg(H_2O)_5(3\text{-npth})]\cdot 2H_2O$ **26**, $[Mg(H_2O)_4(2\text{-nba})_2]$ **20**, $[Sr(H_2O)_3(4\text{-nba})(DMF)]\cdot 4\text{-nba}$ **12**, $[Sr(H_2O)(4\text{-nba})_2(nmf)_{1.5}]_n$ **13**, $[Sr(4\text{-nba})_2(pyr)_2]_n$ **14**, $[Sr(H_2O)_3(4\text{-nba})_2(HCONH_2)]_n$ **15** were collected on an Image Plate Diffraction System (IPDS-1) from STOE using graphite-monochromated Mo-K_α radiation. The study was done at Institut für Anorganische Chemie, Christian-Albrechts-Universität Kiel Max-Eyth Straße 2, D-24118 Kiel, Germany.

Intensity data for $[Ca(N\text{-MeIm})(4\text{-nba})_2]$ **2**, $[[Ba(H_2O)_3]_2(\mu_2\text{-2-nba-O,O'O-NO}_2)_2(\mu_2\text{-2-nba-O,O,O'})_2]_n$ **22**, $[Mg(H_2O)_6](2\text{-ca-4nba})_2$ **16**, $[Ca(2\text{-nba})_2(H_2O)_2]_n$ **21**, $[Ca_3(H_2O)_{12}(btc)_2]$ **30** and $[Ba_3(H_2O)_8(btc)_2].2H_2O$ **32** were collected on a Bruker Smart Apex CCD diffractometer using graphite-monochromated Mo-K_α radiation (λ=0.71073 Å). The single crystal X-ray diffraction study for compounds was performed at the National single crystal X-ray facility at School of Chemistry, University of Hyderabad, Hyderabad, India.

The single crystal data for $[Ca(H_2O)_2(2\text{-ca-4nba})_2]_n$ **17**, $[Ca(H_2O)_2(L_1)_2]\cdot H_2O$ (L_1= 4-methoxyphenylacetate) **33** and $[Ca(H_2O)_2(L_2)_2]\cdot 2H_2O$ **34** (L_2 = 2-chlorophenylacetate) data was recorded in Department of Chemistry, IIT-Kanpur, Kanpur India. While the single crystal of $[Ca(H_2O)_6(4\text{-nba})](4\text{-nba})(2\text{-ap})\cdot H_2O$ **7** compound was selected using a Leica polarizing microscope and was used for intensity data-collection on an X'calibur (Oxford Diffraction System) X-ray diffractometer having CCD camera, using graphite-monochromated Mo-K_α radiation. CrysAlis^{Pro} program was used for data collection. Data collection was done at X-ray Crystallography Laboratory, Department of Physics, University of Jammu, Jammu Tawi 180 006 India. The data integration and reduction were processed with SAINT [197] software. An empirical absorption correction was applied to the collected reflections with SADABS [198]. The structures were solved with direct methods using SHELXS-97 [196] and refinement were done against F^2 using SHELXL-97 [196]. All non-hydrogen atoms were refined anisotropically. Aromatic hydrogens were introduced on calculated positions and included in the refinement riding on their respective parent atoms. The hydrogen atoms of the coordinated water molecules were located in the difference map but were not stable on subsequent refinements and hence were fixed at calculated positions by using DFIX command and later refined isotropically using a riding model.

Crystal structure description of [[Ca(N-MeIm)](μ_2-η^1:η^1-4-nba)(μ_2-η^2:η^1-4-nba)]$_n$ 2

Compound **2** crystallizes in the triclinic space group P$\bar{1}$ and all atoms are situated in general positions. The structure reveals that **2** is a polymer and can be formulated as *catena*-poly[[(N-methylimidazole)calcium(II)](μ_2-η^1:η^1-4-nitrobenzoato)(μ_2-η^2:η^1-4-nitro benzoato)]. The structure of [[Ca(N-MeIm)](μ_2-η^1:η^1-4-nba)(μ_2-η^2:η^1-4-nba)]$_n$ **2** consists of a central Ca(II) ion, a terminal N-MeIm ligand and two crystallographically independent 4-nba ligands. In the crystal structure, each Ca(II) is bonded to a nitrogen atom of N-MeIm and five oxygen atoms from five symmetry related 4-nba ligands resulting in a distorted {CaO_5N} octahedron (Figure 79).

The geometric parameters of the 4-nba anions and N-MeIm are in the normal range and are comparable with literature values [63, 26, 120, 133, 175]. The Ca-O distances in **2** range from 2.2823(12) to 2.4507(11) Å (Table 1) and are in agreement with literature values [133, 175]. The Ca-N bond is longer at 2.5088(14) Å. The cis O-Ca-O and O-Ca-N angles range from 73.71(4) to 100.31(4)° while the trans O-Ca-O and O-Ca-N angles range from 163.97(4) – 175.54(4)° indicating a distorted octahedron. It is interesting to note that both 4-nitrobenzoates in each formula unit are coordinated to the central Ca(II) in different bridging modes (Figure 1). One of the two 4-nba anions in each formula unit functions as a bridging bidentate ligand (μ_2-η^1:η^1-4-nba) (Figure 2) and is linked to two symmetry related Ca(II) ions via O5 and O6 atoms resulting in the formation of an infinite chain extending along *a* axis with a Ca···Ca separation of 5.531(1) Å. The second independent ligand (μ_2-η^2:η^1-4-nba) is coordinated to three different Ca(II) ions with both the carboxylate oxygen atoms O1 and O2 linked to the same infinite chain formed earlier and one of the carboxylate oxygen atoms (O1) functioning as a monoatomic bridge between two symmetry related Ca(II) ions (Figure 3 & 4). This monoatomic bridging mode serves to link the two infinite chains with a shorter Ca···Ca separation of 3.8585(7) Å resulting in the formation of a one-dimensional ladder structure [Figure 5]. It is to be noted that Ca(II) forms a polymeric compound with 4-nba in the presence of N-MeIm unlike Mg(II) which forms a centrosymmetric dimeric complex [$Mg(H_2O)$(N-MeIm)$_2$(η^1-4-nba)(μ_2-η^1:η^1-4-nba)]$_2$ [133]. The coordination polymer **2** and the previously reported monomeric compounds [Ca(H_2O)$_4$(η^1-4-nba)(η^2-4-nba)] **1** [63] and [Ca(H_2O)$_3$(Im)(η^1-4-

nba)$_2$]·Im [175] constitute a triad of Ca(II) complexes having Ca:4-nba in a 1:2 mole ratio and showing different binding modes of the 4-nba ligand. In terms of secondary interactions **1** shows only O-H···O interactions while the monomeric imidazole compound is involved in three varieties of H-bonding interactions namely O-H···O, N-H···O and O-H···N. The absence of coordinated water as well as methylation of the nitrogen atom in N-MeIm in **2** blocks the O-H···O, N-H···O and O-H···N interactions. An analysis of the structure of **2** reveals that the anhydrous compound is involved in only C-H···O interactions (Figure 6) with the oxygen atoms of the nitro groups functioning as H-acceptors and the methyl group of imidazole as well as H atoms on the aromatic ring functioning as H-donors. The geometric parameters of these hydrogen bonds are listed in Table 2.

Table 1- Selected bond distances (Å) and bond angles (^{o}) for [Ca(N-MeIm)$_2$(4-nba)$_2$]$_n$ **2**

[Ca(N-MeIm)$_2$(4-nba)$_2$]$_n$ **2**			
Ca(1)-N(3)	2.5088(14)	Ca(1)-O(5)	2.3074(12)
Ca(1)-O(1)	2.3710(11)	Ca(1)-O(6)	2.2823(12)
Ca(1)^{i}-O(1)	2.4507(11)	Ca(1)-Ca(1)^{iii}	5.531(1)
Ca(1)-O(2)	2.3292(11)	Ca(1)-Ca(1)^{i}	3.8585(7)
O(6)-Ca(1)-O(5)	96.22(5)	O(2)-Ca(1)-O(1)^{i}	93.23(4)
O(6)-Ca(1)-O(2)	92.78(4)	O(1)-Ca(1)-O(1)^{i}	73.71(4)
O(5)-Ca(1)-O(2)	165.10(4)	O(6)-Ca(1)-N(3)	88.01(5)
O(6)-Ca(1)-O(1)	90.60(4)	O(5)-Ca(1)-N(3)	84.47(5)
O(5)-Ca(1)-O(1)	91.47(4)	O(2)-Ca(1)-N(3)	84.00(4)
O(2)-Ca(1)-O(1)	100.31(4)	O(1)-Ca(1)-N(3)	175.54(4)
O(6)-Ca(1)-O(1)^{i}	163.97(4)	O(1)^{i}-Ca(1)-N(3)	107.39(4)
O(5)-Ca(1)-O(1)^{i}	81.25(4)		

Symmetry codes i) –x+1, -y+1, -z+1 ii) x-1, y, z,

Table 2- Hydrogen- bonding geometry (Å, ^{o}) for compound [Ca(N-MeIm)$_2$(4-nba)$_2$]$_n$ **2**

D-H---A	d(D-H)	d(H---A)	D(D---A)	<DHA	Symmetry code
[Ca(N-MeIm)$_2$(4-nba)$_2$]$_n$ **2**					
C13-H13N···O8	0.93	2.67	3.456(3)	143	-x+1,-y,-z
C13-H13···O4	0.93	2.69	3.586(2)	161	-x,-y+1,-z
C6-H6···O7	0.93	2.63	3.519(2)	160	-x+1,y+1, -z
C4-H4···O3	0.93	2.62	3.495(2)	157	-x,-y+1,-z
C18-H18B···O7	0.93	2.44	3.378	167	x+1,y,z+1

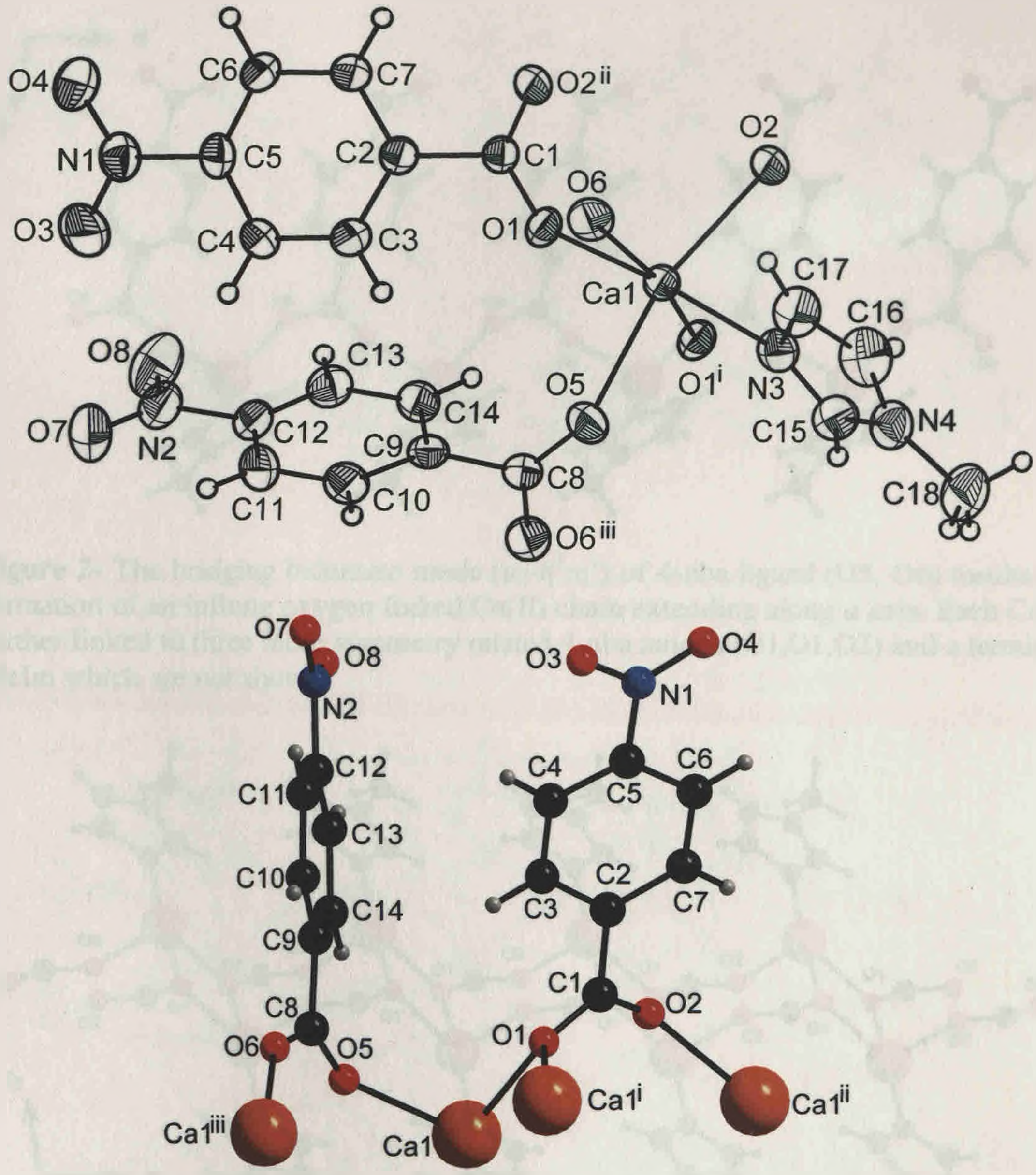

Figure 1- The coordination sphere of Ca(II) in **2** showing the atom-labeling scheme. Displacement ellipsoids are drawn at the 50% probability level except for the H atoms, which are shown as circles of arbitrary radius. (top). The μ_2-η^1:η^1 (O5, O6) and μ_3-η^2:η^1 (O1, O1, O2) binding modes of the 4-nitrobenzoate ligands in **2** (bottom). Symmetry code: i) -x+1, -y+1, -z+1 ii) -x+2, -y+1, -z+1 iii) x-1, y, z

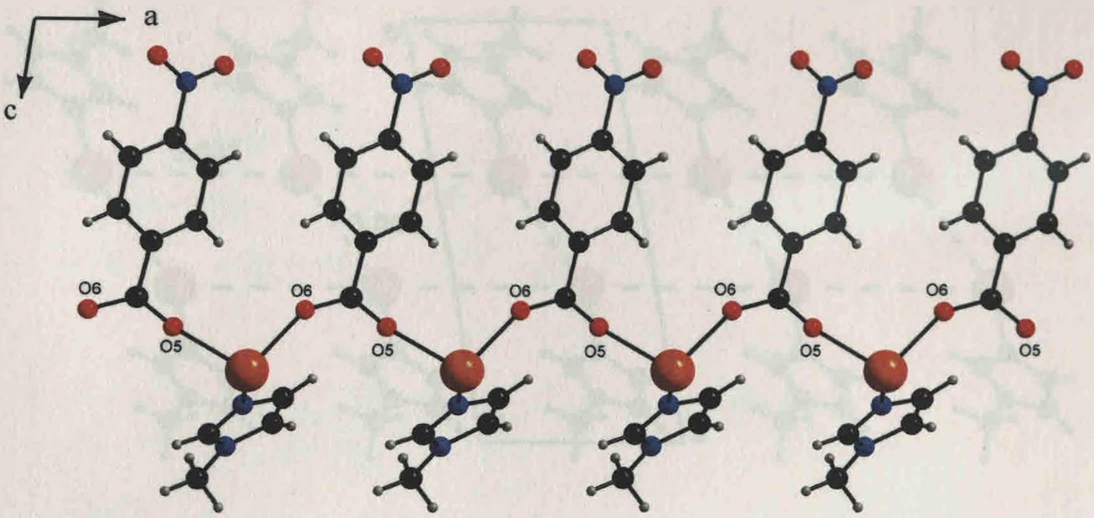

Figure 2- The bridging bidentate mode (μ_2-η^1:η^1) of 4-nba ligand (O5, O6) results in the formation of an infinite oxygen linked Ca(II) chain extending along *a* axis. Each Ca(II) is further linked to three more symmetry related 4-nba anions (O1,O1,O2) and a terminal N-MeIm which are not shown.

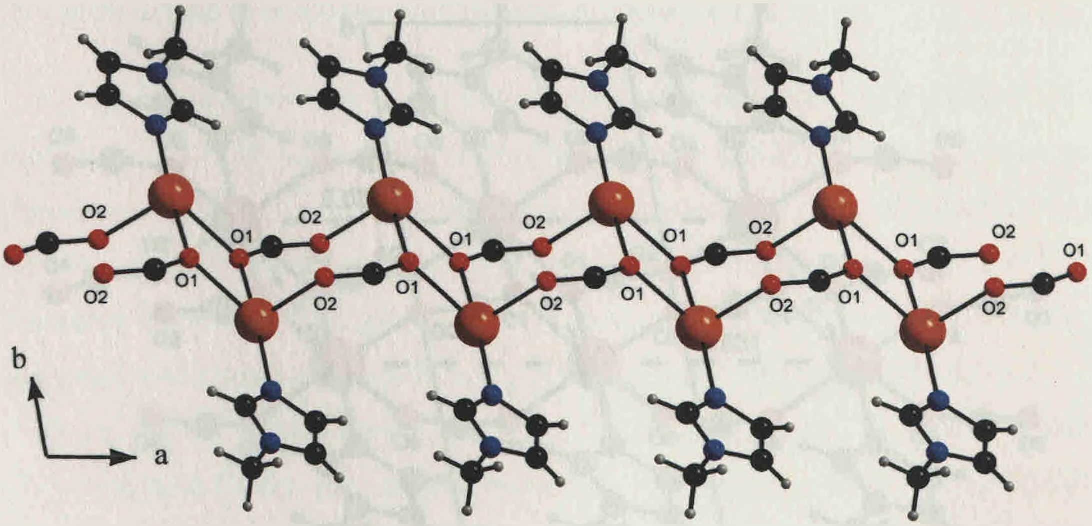

Figure 3- The bridging tridentate mode (μ_3-η^2:η^1) of the second 4-nba ligand (O1,O2) serves to link two infinite chains. For clarity only the O1 and O2 oxygen atoms involved in the chain formation are shown.

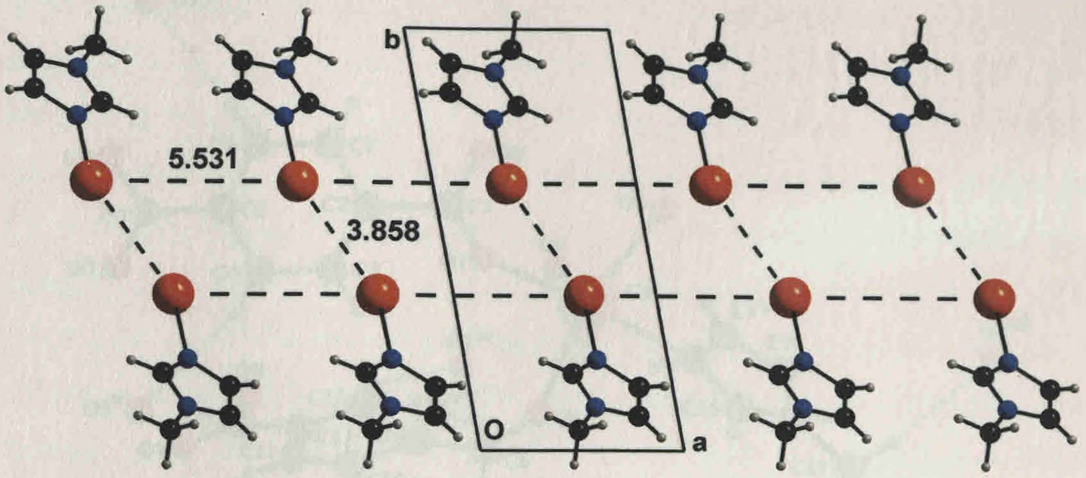

Figure 4- Two infinite chains of hexacoordinated Ca(II) complexes are linked with the aid of the monoatomic bridging O1 atom resulting in the one-dimensional ladder structure. For clarity, the linking carboxylate oxygen atoms are not shown and only the ladder points consisting of Ca(II) linked to the N atom of N-MeIm are shown.

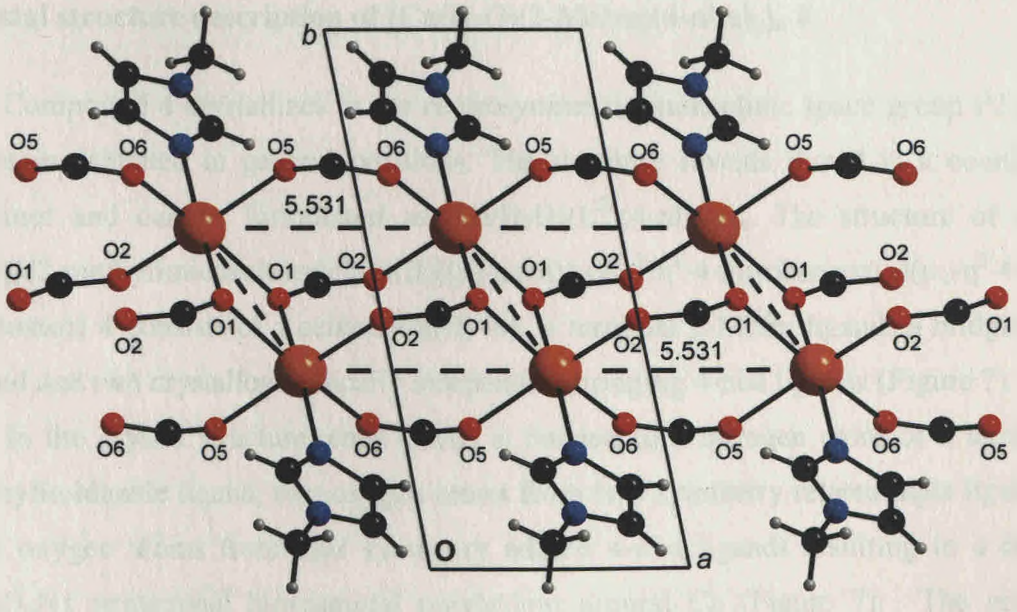

Figure 5- A view of the bridging bidentate coordination (μ_2-η^1:η^1) of 4-nba through O5 and O6 leading to a one-dimensional polymeric Ca(II) chain extending along *a* with Ca···Ca separation of 5.531(1) Å. The monoatomic bridging mode of O1 in the second 4-nba ligand results in the linking of two infinite chains. In the chains each Ca(II) is bonded to five O atoms and one N atom. For clarity only the carboxylate groups are shown

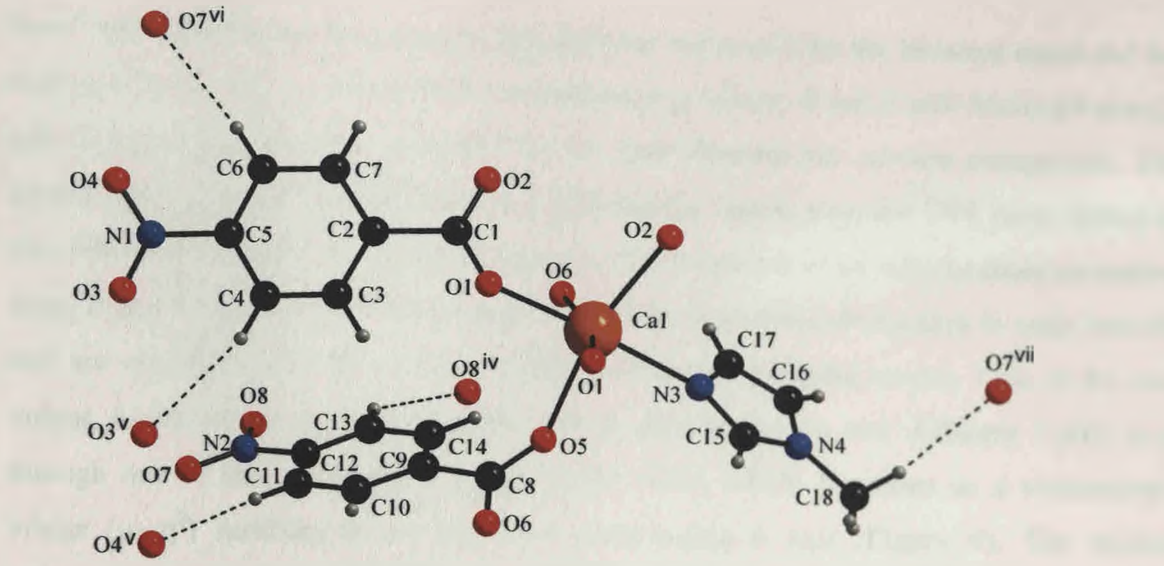

Figure 6: H-bonding situation around each six coordinated complex of **2** showing the weak C-H...O interactions. Symmetry code: iv) -x+1, -y, -z v) -x, -y+1, -z vi) -x+1, y+1, -z vii) x+1, y, z+1

Crystal structure description of $[Ca(H_2O)(2\text{-}MeIm)(4\text{-}nba)_2]_n$ 4

Compound **4** crystallizes in the centrosymmetric monoclinic space group $P2_1/n$ with all atoms situated in general positions. The structure reveals that **4** is a coordination polymer and can be formulated as $[Ca(H_2O)(L^2)(4\text{-}nba)_2]_n$. The structure of *catena*-poly[[(2-methylimidazole)calcium(II)](μ_2-aqua)(μ_2-η^1:η^1-4-nitrobenzoato)(μ_2-η^2-4-nitro benzoato)] **4** consists of a central Ca(II) ion, a terminal 2-MeIm ligand, a bridging aqua ligand and two crystallographically independent bridging 4-nba ligands (Figure 7).

In the crystal structure, each Ca(II) is bonded to a nitrogen atom of a terminal 2-methylimidazole ligand, two oxygen atoms from two symmetry related aqua ligands and four oxygen atoms from four symmetry related 4-nba ligands resulting in a distorted $\{CaO_6N\}$ pentagonal bipyramidal polyhedron around Ca (Figure 7). The geometric parameters of the 4-nba anions and 2-MeIm are in the normal range. The O-Ca-O and O-Ca-N angles range from 65.73(3) to 172.63(5)°. The Ca-O distances in **4** range from 2.3100(11)-2.5654(11) Å (Table 3) and are in agreement with literature values [24, 26, 63, 133, 175]. A Ca-N bond distance of 2.5024(13) Å is observed. The oxidation state of the central metal in compound **4** based on the bond valence sum was found to be 2.139 [199]. The bond valence sum for the precursor calcium compound $[Ca(H_2O)_4(4\text{-}nba)_2]_n$ **1**, the zero-dimensional $[Ca(H_2O)_3(Im)(4\text{-}nba)_2].Im$ and the 1-D ladder polymer $[Ca(N\text{-}MeIm)(4\text{-}nba)_2]_n$ are 2.187, 2.27 and 2.177 respectively. It is interesting to note that the bond valence sums are very close to the expected value of 2 for the bivalent metal and the estimated bond valence sums for the coordination polymers **4** and $[Ca(N\text{-}MeIm)(4\text{-}nba)_2]_n$ are slightly less than those observed for the zero-dimensional calcium compounds. The coordinated water (O41) functions as a μ_2-bridging ligand with the O41 atom linked to two symmetry related Ca(II) ions resulting in the formation of an infinite chain extending along *b* axis (Figure 8). It is interesting to note that both 4-nitrobenzoates in each formula unit are coordinated to the central Ca(II) in different bridging modes. One of the two unique 4-nba anions in each formula unit is coordinated to two different Ca(II) ions through one of the carboxylate oxygen atoms (O1), which functions as a monoatomic bridge (μ_2-η^2) resulting in an extended chain along *b* axis (Figure 9). The second independent 4-nba ligand functions as a bridging bidentate ligand (μ_2-η^1:η^1) and is linked to two symmetry related Ca(II) ions via O11 and O12 oxygen atoms. An infinite chain extending along *b* axis is formed due to this binding mode of 4-nba. Due to the bridging nature of the aqua and 4-nba ligands [(2-methylimidazole)calcium(II)] units in **2** are linked into a one-dimensional coordination polymer consisting of three chains, all of which propagate along *b*-axis (Figure 10). In the triple chain coordination polymer a Ca···Ca separation of 3.8432(3) Å is observed between neighbouring Ca(II) ions. This value is comparable with the Ca···Ca distance of 3.8585(7) Å observed in the closely related compound $[Ca(L^1)(4\text{-}nba)_2]_n$ as well as several other Ca(II) coordination polymers. A scrutiny of the structure reveals that the oxygen atoms of the carboxylate and nitro functionalities of the 4-nba ligand and the coordinated water are involved in O-H···O, N-H···O and C-H···O interactions. A total of six H-bonding interactions with H···O distances ranging from 2.002 – 2.600 Å (Table 4) are observed. These can be classified as intra- and interchain interactions. The C24-H24A···O11, O41-H41B···O2 and O41-H41B···O1 interactions occur within the triple chain 1-D polymer, while the N22-H22···O2, O41-H41A···O13 and C5-H5···O3 interactions serve to link adjacent polymeric chains (Figure 10).

Table 3- Selected bond distances (Å) and bond angles (°) for [Ca(H_2O)(4-nba)$_2$ (2-MeIm)]$_n$ **4**.

[Ca(H_2O)(4-nba)$_2$ (2-MeIm)]$_n$ **4**			
Ca(1)-O(11)	2.3100(11)	Ca(1)-O(41)	2.4978(11)
Ca(1)-O(12)^{i}	2.3119(11)	Ca(1)-N(21)	2.5024(13)
Ca(1)-O(1)^{ii}	2.4205(11)	Ca(1)-O(41)^{ii}	2.5654(11)
Ca(1)-O(1)	2.4912(11)	Ca(1)-Ca(1)^{ii}	3.8432(3)
O(11)-Ca(1)-O(12)^{i}	172.63(5)	O(12)^{i}-Ca(1)-N(21)	83.69(5)
O(11)-Ca(1)-O(12)^{ii}	87.00(4)	O(1)^{ii}-Ca(1)-N(21)	77.74(4)
O(12)-Ca(1)-O(1)^{ii}	100.11(4)	O(1)-Ca(1)-N(21)	146.38(4)
O(11)-Ca(1)-O(1)	79.52(4)	O(41)-Ca(1)-N(21)	80.64(4)
O(12)^{i}-Ca(1)-O(1)	93.94(4)	O(11)-Ca(1)-O(41)^{ii}	95.97(4)
O(1)^{ii}-Ca(1)-O(1)	135.28(3)	O(12)^{i}-Ca(1)-O(41)^{ii}	85.31(4)
O(11)-Ca(1)-O(41)	85.80(4)	O(1)^{ii}-Ca(1)-O(41)^{ii}	65.73(3)
O(12)^{i}-Ca(1)-O(41)	88.42(4)	O(1)-Ca(1)-O(41)^{ii}	73.50(4)
O(1)^{ii}-Ca(1)-O(41)	155.67(4)	O(41)-Ca(1)-O(41)^{ii}	138.19(3)
O(1)-Ca(1)-O(41)	65.76(3)	N(21)-Ca(1)-O(41)^{ii}	139.17(4)
O(11)-Ca(1)-N(21)	99.84(5)		

Symmetry codes i) x+1/2, y-1/2,- z+3/2, ii) -x+1/2, y+1/2,- z+3/2

Table 4- Hydrogen- bonding geometry (Å, °) for compound [Ca(H_2O)(4-nba)$_2$ (2-MeIm)]$_n$ **4**

D-H---A	d(D-H)	d(H---A)	D(D---A)	<DHA	Symmetry code
[Ca(H_2O)(4-nba)$_2$ (2-MeIm)]$_n$ **4**					
Intrachain interactions					
C24-H24A···O11	0.940	2.411	3.347	162	
O41-H41B···O2	0.820	2.002	2.642	170	-x+1/2, y-1/2, -z+3/2
O41-H41B···O1	0.820	2.600	3.026	114	-x+1/2, y-1/2, -z+3/2
Interchain interactions					
N22-H22···O2	0.870	2.012	2.873	170	x-1/2, -y+3/2, z-1/2
O41-H41A···O13	0.820	2.160	2.972	171	-x+1, -y+1, -z+1
C5-H5···O3	0.940	2.532	3.398	153	-x+3/2, y+1/2, -z+3/2

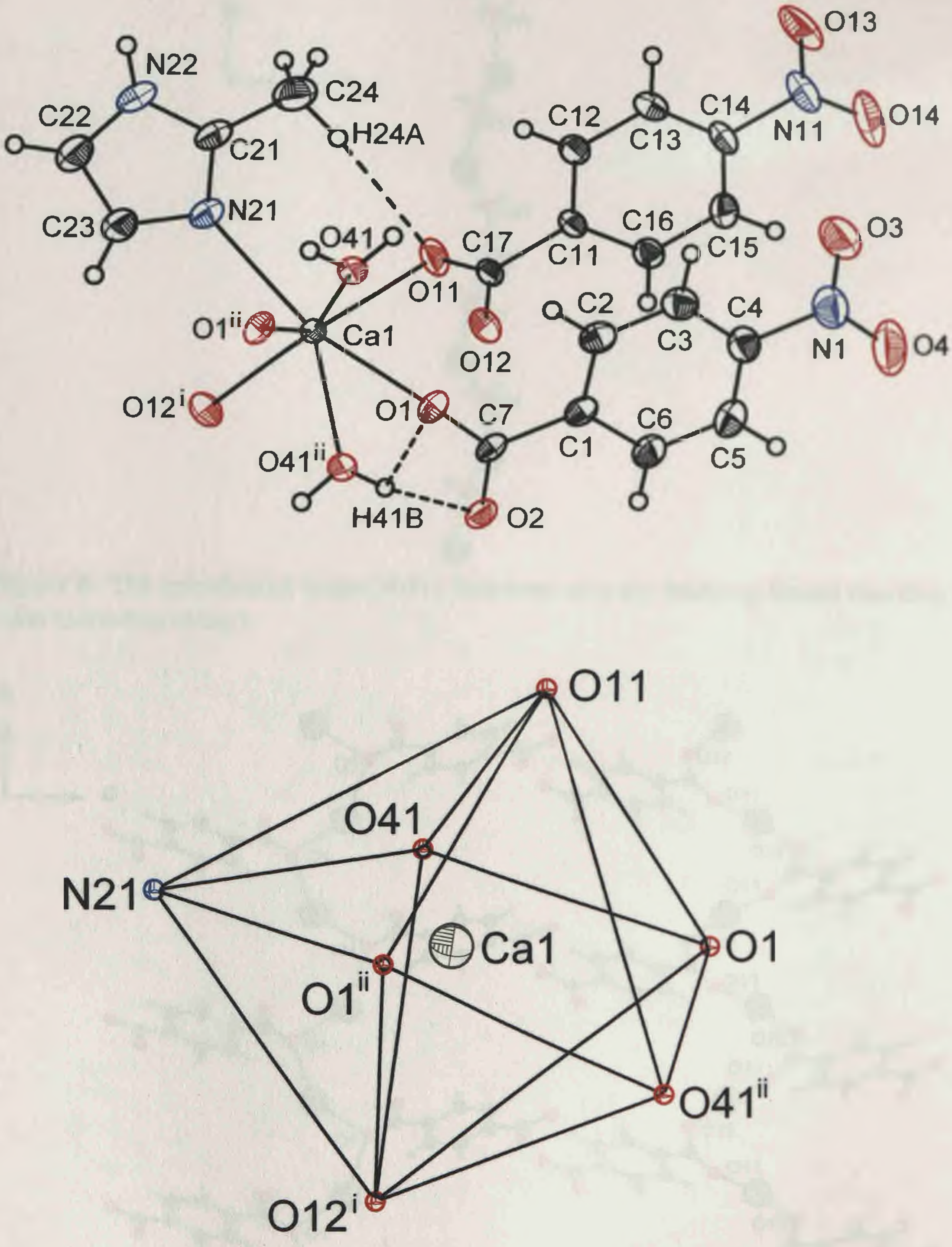

Figure 7 - A view of the coordination sphere of Ca(II) in $[Ca(H_2O)(2\text{-}MeIm)(4\text{-}nba)_2]_n$ **4**, showing the atom-labeling scheme. Displacement ellipsoids are drawn at the 50% probability level excepting for the H atoms, which are shown as circles of arbitrary radius (top). Intramolecular H-bonding is shown by the broken lines. The distorted pentagonal bipyramidal coordination polyhedron around Ca(II) in **4** (bottom). Symmetry code: i) -x+1/2, y-1/2, -z+3/2 ; ii) -x+1/2, y+1/2, -z+3/2

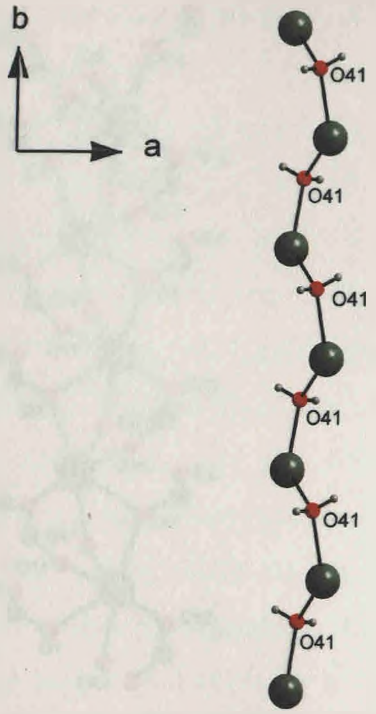

Figure 8- The coordinated water (O41) functions as a μ_2- bridging ligand resulting in a chain extending along *b*

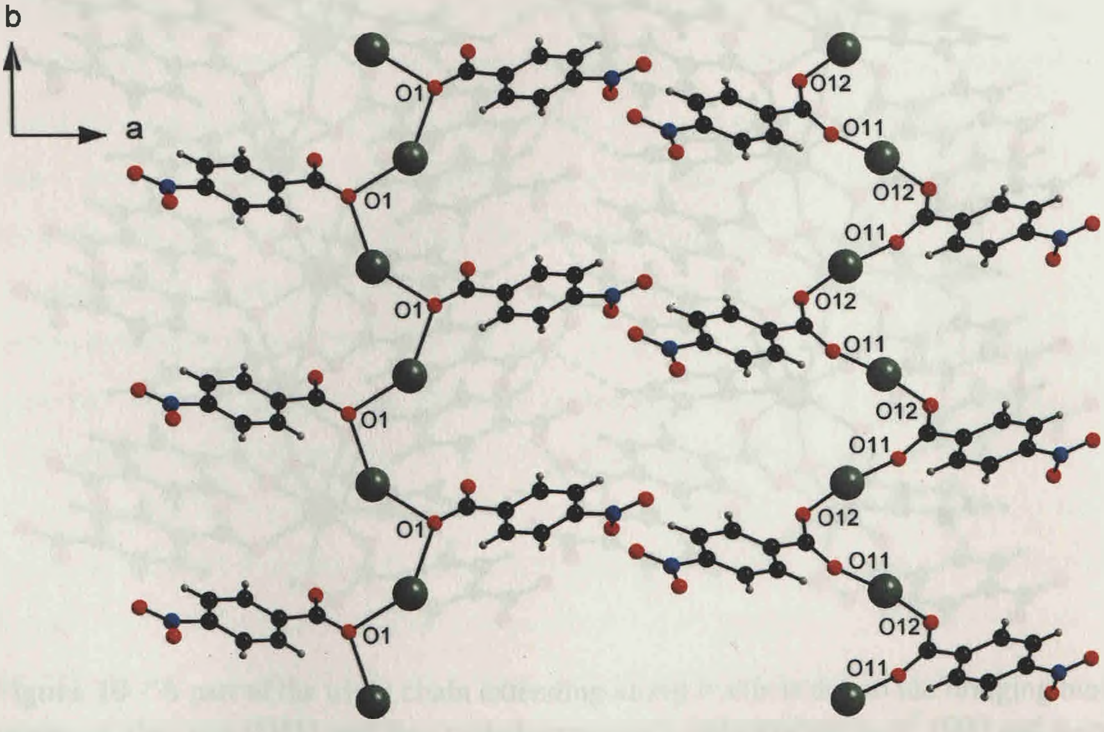

Figure 9- The μ_2-η^2 (O1) binding mode of the 4-nba ligand results in the formation of an infinite chain propagating along *b* (left). The extended chain due to the μ_2-η^1:η^1 (O11, O12) binding mode of the 4-nba ligand is shown on the right

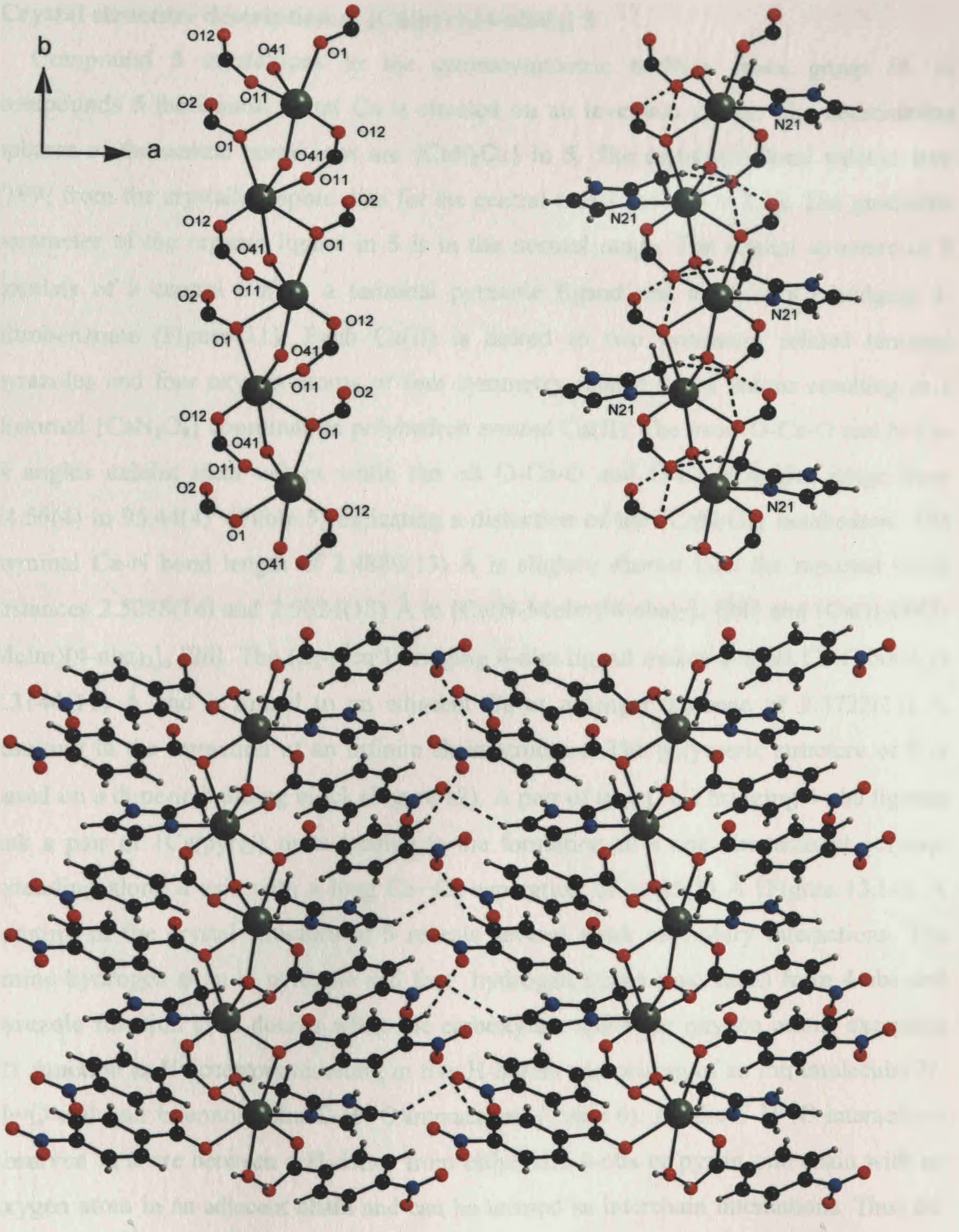

Figure 10 - A part of the triple chain extending along *b* axis is due to the bridging binding modes of the aqua (O41) and the crystallographicaly independent μ_2-η^2 (O1) and μ_2-η^1:η^1 (O11, O12) 4-nba ligands in **4**. For clarity only the -COO groups of 4-nba and the O atom of water are shown (top right). The H-atoms of the bridging water and the terminal 2-MeIm ligand (N21) are included in the triple chain to show the intrachain H-bonding interactions in broken lines (top left). A view along *c* axis is shown for the crystallographic packing of **4.** Two adjacent polymeric chains of **4** in the *ab* crystallographic plane are linked by weak C-H···O bonds shown in broken lines (bottom)

Crystal structure description of [Ca(pyr)$_2$(4-nba)$_2$] 5

Compound **5** crystallizes in the centrosymmetric triclinic space group *P1̄.* In compounds **5** the central metal Ca is situated on an inversion centre. The coordination spheres of the central metal ions are {CaN_2O_4} in **5**. The calculated bond valence sum [199] from the crystallographic data for the central metal ion in **5** is 2.23. The geometric parameter of the organic ligand in **5** is in the normal range. The crystal structure of **5** consists of a central Ca(II), a terminal pyrazole ligand and a (μ_2-η^1:η^1) bridging 4-nitrobenzoate (Figure 11). Each Ca(II) is linked to two symmetry related terminal pyrazoles and four oxygen atoms of four symmetry related 4-nba anions resulting in a distorted {CaN_2O_4} coordination polyhedron around Ca(II). The *trans* O-Ca-O and N-Ca-N angles exhibit ideal values while the *cis* O-Ca-O and O-Ca-N angles range from 84.56(4) to 95.44(4)^o (Table 5) indicating a distortion of the {CaN_2O_4} octahedron. The terminal Ca-N bond length of 2.4886(13) Å is slightly shorter than the reported Ca-N distances 2.5088(14) and 2.5024(13) Å in [Ca(N-MeIm)(4-nba)$_2$]$_n$ [24] and [Ca(H_2O)(2-MeIm)(4-nba)$_2$]$_n$ [26]. The (μ_2-η^1:η^1) bridging 4-nba ligand makes a short Ca-O bond at 2.3144(11) Å and is linked to an adjacent Ca at a longer distance of 2.3722(11) Å resulting in the formation of an infinite chain structure. The polymeric structure of **5** is based on a dimeric building block (Figure 12). A pair of (μ_2-η^1:η^1) bridging 4-nba ligands link a pair of {Ca(pyr)$_2$} units leading to the formation of a one dimensional polymer extending along *a* axis with a long Ca···Ca separation of 5.335(1) Å [Figure 13,14]. A scrutiny of the crystal structure of **5** reveals several weak secondary interactions. The amine hydrogen atom in pyrazole and four hydrogen atoms (two each) from 4-nba and pyrazole function as H-donors while the carboxylate and nitro oxygen atoms excepting O1 function as H-acceptors resulting in five H-bonds comprising of an intramolecular N-H···O and four intermolecular C-H···O interactions (Table 6). All the C-H···O interactions observed in **5** are between a H donor from either the 4-nba or pyr in one chain with an oxygen atom in an adjacent chain and can be termed as interchain interactions. Thus the intermolecular C12-H12···O4 interaction between the pyrazole H atom and the nitro oxygen atom links two adjacent one dimensional chains (Figure 15) and extends the network.

Table 5- Selected bond distances (Å) and bond angles (°) for compound [Ca(pyr)$_2$(4-nba)$_2$]$_n$ **5**

[Ca(pyr)$_2$(4-nba)$_2$]$_n$ **5**			
Ca(1)-O(1)	2.3144(11)	Ca(1)-N(11)	2.4886(13)
Ca(1)-O(2)^{ii}	2.3722(11)	Ca---Ca^{iii}	5.355(1)
O(1)-Ca(1)-O(1)^{i}	180		
O(1)-Ca(1)-O(2)^{ii}	86.06(4)	O(2)^{i}-Ca(1)-N(11)	84.56(4)
O(1)^{i}-Ca(1)-O(2)^{ii}	93.94(4)	O(2)^{iii}-Ca(1)-N(11)	95.44(4)
O(2)^{i}-Ca(1)-O(2)^{iii}	180(1)	O(1)-Ca(1)-N(11)^{i}	92.81(4)
O(1)-Ca(1)-N(11)	87.19(4)	N(11)-Ca(1)-N(11)^{i}	180.0

Symmetry codes i) –x+2, -y+1, -z+1 ii) –x+1, -y+1, -z+1, iii) x+1, y, z

Table 6- Hydrogen-bonding geometry (Å, °) for [Ca(pyr)$_2$(4-nba)$_2$]$_n$ **5**

D-H---A	d(D-H)	d(H---A)	D(D---A)	<DHA	Symmetry code
[Ca(pyr)$_2$(4-nba)$_2$]$_n$ **5**					
N11-H12N···O2	0.880	1.981	2.847	167	x,y,z
C3-H3···O3	0.950	2.538	3.327	141	-x+2,-y+2,-z+2
C5-H5···O4	0.950	2.458	3.353	157	-x,1-y,2-z
C11-H11···O2	0.950	2.656	3.546	156	-x,-y,1-z
C12-H2···O4	0.950	2.582	3.424	148	x,-1+y, -1+z

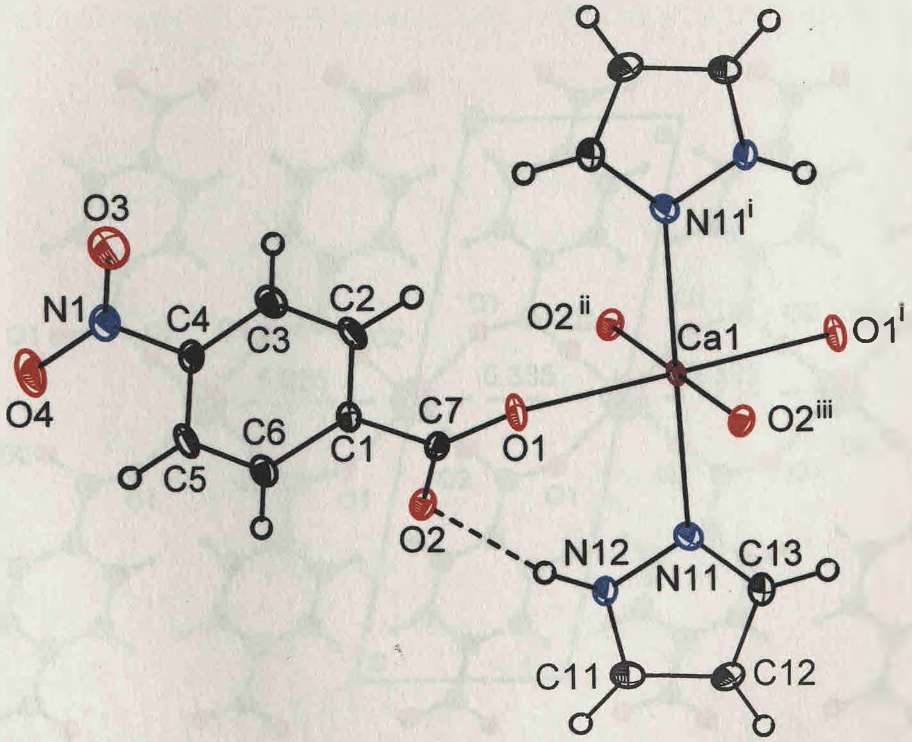

Figure 11- A view of the coordination sphere of the central metal ion in [Ca(pyr)$_2$(4-nba)$_2$]$_n$ **5** showing the atom-labeling scheme. Displacement ellipsoids are drawn at the 50% probability level excepting for the H atoms, which are shown as circles of arbitrary radius. Intramolecular H-bonding is shown as broken lines. Symmetry code: i) –x+2, -y+1, -z+1 ii) -x+1, -y+1, -z+1 iii) x+1, y, z

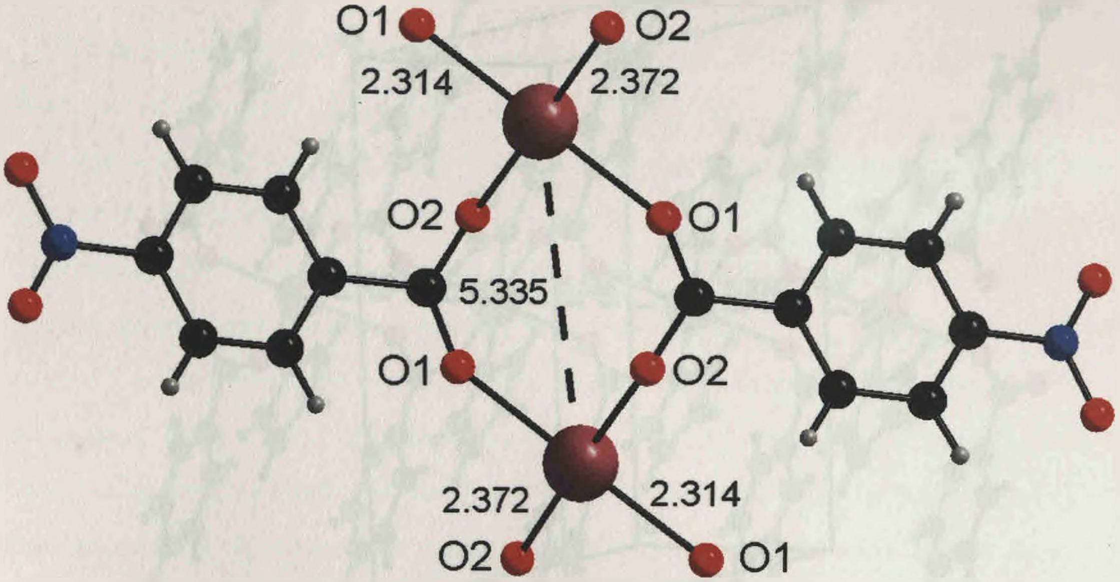

Figure 12- The dimeric building unit of the coordination polymer $[Ca(pyr)_2(4\text{-}nba)_2]_n$ **5** For clarity the terminal pyrazole ligands on Ca(II) are not shown Colour code: C, black; H, medium grey; N, blue; O, red; Ca, maroon.

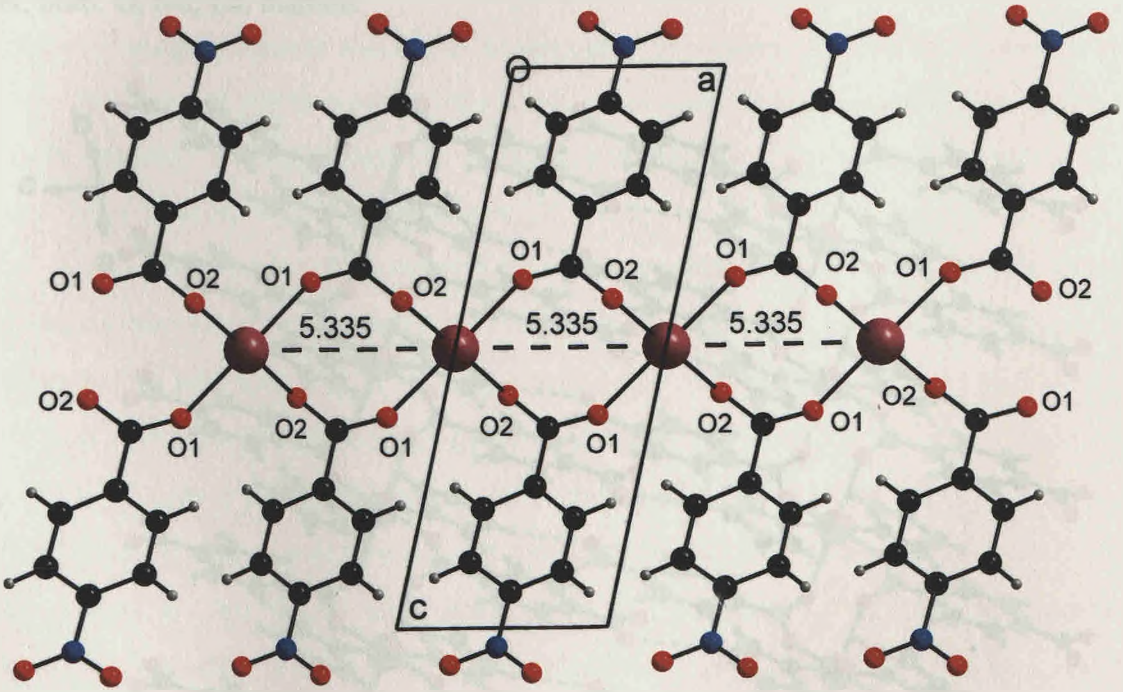

Figure 13- A portion of the 1-D polymeric chain extending along *a* axis in $[Ca(pyr)_2(4\text{-}nba)_2]_n$ **5** with a Ca···Ca separation of 5.335 Å

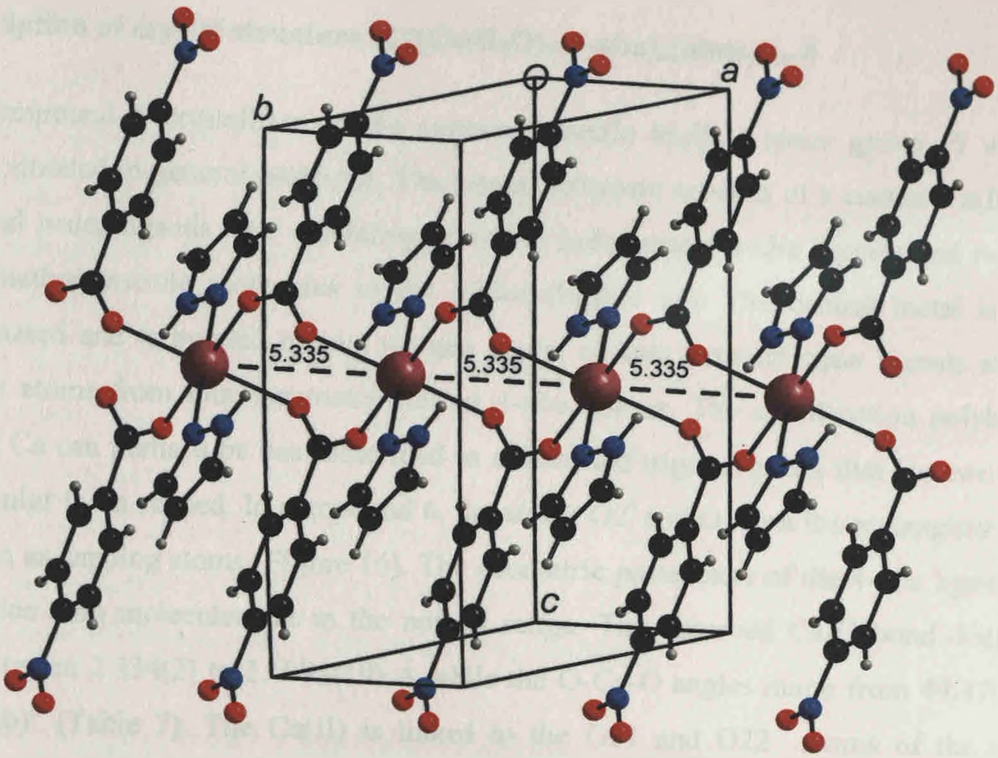

Figure 14- A portion of the 1-D polymeric chain extending along *a* axis in $[Ca(pyr)_2(4\text{-}nba)_2]_n$ **5** with a Ca···Ca separation of 5.335(1)Å. The terminal pyrazole ligands in **5** are included showing the six coordinated Ca(II) in **5**. Colour code: C, black; H, medium grey; N, blue; O, red; Ca, maroon.

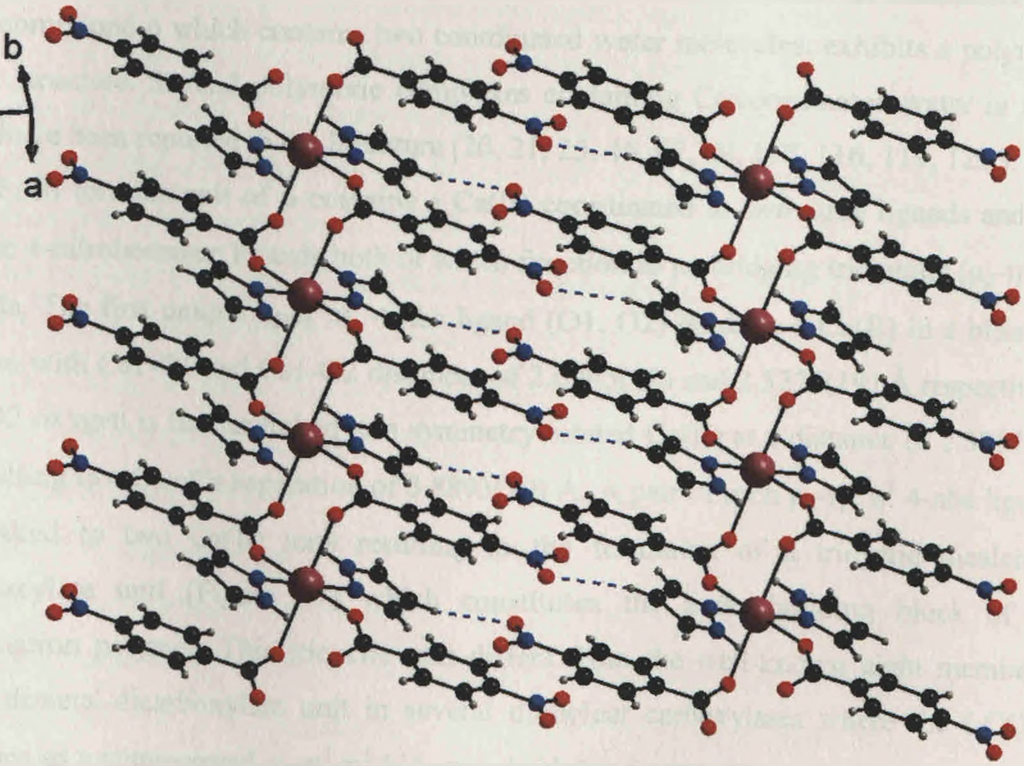

Figure 15- A view showing the interchain interactions in $[Ca(pyr)_2(4\text{-}nba)_2]_n$ **5** (top). Colour code: C, black; H, medium grey; N, blue; O, red; Ca, maroon

Description of crystal structure of $[[Ca(H_2O)_2(4\text{-}nba)_2](dmp)_2]_n$ 6

Compound **6** crystallizes in the centrosymmetric triclinic space group *P1̄* with all atoms situated in general positions. The crystal structure consists of a central Ca(II), two terminal water ligands, two crystallographically independent 4-nba ligands and two free 3,5-dimethylpyrazole molecules in the lattice (Figure 16). The central metal is eight coordinated and is bonded to two oxygen atoms of two terminal aqua ligands and six oxygen atoms from four symmetry related 4-nba anions. The coordination polyhedron around Ca can perhaps be best described as a distorted trigonal prism that has two of its rectangular faces capped. In compound **6**, the atoms $O2^i$ and O11 on the rectangluar faces function as capping atoms (Figure 16). The geometric parameters of the 4-nba ligand and the lattice dmp molecules are in the normal range. The observed Ca-O bond distances vary between 2.334(2) to 2.6995(19) Å while the O-Ca-O angles range from 49.47(5) to 155.36(6)° (Table 7). The Ca(II) is linked to the O21 and O22 atoms of the water molecules at 2.334(2) and 2.3476(19) Å respectively. Based on a study of the structural chemistry of several Ca(II)-carboxylates we have shown [25] that in Ca(II) carboxylates containing three or less number of coordinated water molecules the carboxylate ligand adopts a bridging ligation leading to the formation of a chain polymer. In accordance with this, compound **6** which contains two coordinated water molecules, exhibits a polymeric chain structure. Several polymeric complexes containing Ca:coordinated water in a 1:2 ratio have been reported in the literature [20, 21, 25, 46, 67, 89, 117, 116, 119, 122,].

Each formula unit of **6** contains a Ca(II) coordinated to two aqua ligands and two unique 4-nitrobenzoate ligands both of which function as μ_2-bridging tridentate (μ_2-η^2:η^1) ligands. The first unique μ_2-η^2:η^1 4-nba ligand (O1, O2) binds to a Ca(II) in a bidentate fashion with Ca1-O1 and Ca1-O2 distances of 2.6995(19) and 2.5277(19) Å respectively. The O2 oxygen is further linked to a symmetry related Ca(II) at a distance of 2.3857(16) Å resulting in a Ca···Ca separation of 3.8893(10) Å. A pair of such μ_2-η^2:η^1 4-nba ligands are linked to two Ca(II) ions resulting in the formation of a tricyclic dicalcium-dicarboxylate unit (Figure 17) which constitutes the basic building block of the coordination polymer. This tricyclic unit differs from the well-known eight membered cyclic dimetal-dicarboxylate unit in several dinuclear carboxylates where the $(\text{-COO})^-$ functions as a symmetrical μ_2-η^1:η^1 bidentate bridging ligand. The second independent 4-nba ligand (O11, O12) binds to two symmetry related Ca(II) ions in an identical fashion resulting in a tricylic dicalcium-dicarboxylate unit with a Ca···Ca separation of

3.9083(10) Å. The Ca-O bond lengths formed by this ligand are different. With this ligand a Ca(II) ion is linked to the O11 and O12 oxygen atoms in a bidentate manner (Ca1-O11^{ii} 2.5326(18); Ca1-O12^{ii} 2.5508(18) Å) and the O11 is further linked to a second Ca(II) ion at 2.3603(16) Å. In the crystal structure of **6** alternating pairs of the two crystallographically independent μ_2-η^2:η^1 4-nba ligands link pairs of $\{Ca(H_2O)_2\}^{2+}$ units into a 1-D polymeric chain extending along *a* axis (Figure 18,19). As a result, alternating Ca···Ca separations of 3.8893(10) and 3.9083(10) Å respectively are observed in the infinite chain. These values are comparable to the Ca···Ca separations of 3.8585(7) and 3.8432(3) Å reported for other 4-nba based coordination polymers like $[Ca(N\text{-}MeIm)(4\text{-}nba)_2]_n$ [24] and $[Ca(H_2O)(2\text{-}MeIm)(4\text{-}nba)_2]_n$ [26] respectively and shorter than the Ca···Ca separation of 5.335 Å in $[Ca(pyr)_2(4\text{-}nba)_2]_n$ [120].

Comparison of structure of 6 with $[Ca(H_2O)_2(2\text{-}nba)_2]_n$

Comparison of the structure of compound **6** with that of the earlier reported $[Ca(H_2O)_2(2\text{-}nba)_2]_n$ [25] reveals some similarities and differences. Both compounds which crystallize in the triclinic space group *P1̄* contain Ca:nitrobenzoate:water in a 1:2:2 ratio and are 1-D polymers based on tricyclic dicalcium-dicarboxylate units. The central metal in both compounds are linked to four different carboxylate ligands and the binding mode of the crystallographically unique carboxylate ligand as well as the coordination sphere of the Ca(II) are identical in both compounds. Topologically both the coordination polymers are identical. Compound **6** differs from $[Ca(H_2O)_2(2\text{-}nba)_2]_n$ in terms of the positioning of the nitro substituent in the aromatic ring and the presence of two unique 3,5-dimethylpyrazole molecules, which are located between the one dimensional polymeric chains in the lattice (Figure 20). The presence of these neutral N-ligands in the lattice results in more varieties of secondary interactions namely N-H···O and O-H···N in addition to O-H···O and C-H···O observed in $[Ca(H_2O)_2(2\text{-}nba)_2]_n$. All our efforts to incorporate dmp into the lattice of $[Ca(H_2O)_2(2\text{-}nba)_2]_n$ in view of its structural similarity with that of **6**, were not fruitful.

Secondary interactions in 6

A scrutiny of the crystal structure of **6** reveals that each eight coordinated Ca(II) complex in the polymeric chain is H-bonded to six neighboring complexes with the aid of four varieties of H-bonding interactions comprising of two O-H···O interactions, two N-H···O interactions, two O-H···N interactions and three weak C-H···O interactions. All these O···H contacts (Table 8) are shorter than the sum of their van der Waals radii. The neutral dmp molecules in the lattice function as linkers between adjacent one dimensional chains with the aid of N21-H21···O14, O22-H30···N22 and C25-H25A···O12 interactions (Figure 20) and further extend the network. Of these, the H-bonding between the nitro oxygen (O14) and the H atom (H21) attached to the N of dmp seems to be important for the formation of **6** (Figure 21).

Six different bridging binding modes of 4-nba ligand

The synthesis and structural characterization of several metal 4-nitrobenzoate compounds showing different binding modes [24-26, 120, 179-191] of the 4-nba ligand serves to demonstrate the versatile ligational behaviour of the 4-nitrobenzoate ligand. A survey of the structurally characterized metal 4-nba compounds reveals that in addition to serving as a monodentate (η^1) ligand [24-26, 120, 133, 169] or a bidentate (η^2) ligand [31, 43, 44] the anionic 4-nba exhibits six different bridging binding modes (Figure 22). An analysis of twenty two compounds (Table 9) was undertaken and in these compounds only the bridging binding modes of the 4-nba ligand are considered. It is observed in all these compounds which crystallize in the centrosymmetric triclinic or monoclinic space groups, the 4-nba ligand is involved in six different bridging binding modes, four of which (mode A to D in Figure 22) are μ_2-bridging in nature and one each of μ_3-bridging (mode E) and μ_4-bridging type (mode F) respectively. Of the four μ_2-bridging modes, there are two different symmetric μ_2-η^1:η^1 bridging modes, namely mode A (involving both the carboxylate oxygen atoms) and mode B (involving both the nitro oxygen atoms), observed so far in a single compound, namely, $[Na(H_2O)_3(4\text{-nba})]_n$ [179]. The symmetric bridging bidentate mode A appears to be the most common as this mode is observed in seventeen compounds (77%) and results in the formation of dimeric compounds in four cases [153-183] in addition to two tetramers [49, 50] and a pentamer [186] and hexamer [187]. In the remaining cases, mode A results in the formation of a chain polymer. Fourteen of the compounds are coordination polymers [24-26, 120, 133, 169, 179-180, 188-191] and the formation of the infinite O-M-O chain in these polymeric compounds is due to the presence of at least one of the six bridging binding modes of 4-nba. In addition to the symmetric bridging modes A and B, two more μ_2-bridging modes, namely μ_2-η^2:η^0 (mode C) and μ_2-η^1:η^2 (mode D), are also observed in some of the compounds. In both these binding modes one of the carboxylate oxygen atoms binds to two metal ions; it is interesting to note that compounds like $[Ca(H_2O)(2\text{-MeIm})(4\text{-nba})_2]_n$ or $[KH(4\text{-nba})_2]_n$

showing the μ_2-η^2:η^0 bridging mode are always accompanied by another binding mode like the μ_2-η^1:η^1 in the Ca coordination polymer or the μ_4-bridging mode involving both the carboxylate and nitro oxygen atoms in the K compound [180]. The μ_2-η^1:η^2 mode observed in the title compound [[Ca(H_2O)$_2$(4-nba)$_2$]·2dmp]$_n$ has earlier been reported in the isostructural *f*-block compounds [191] [M_2(4-nba)$_6$(H_2O)$_5$]$_n$ (M = Eu or Tb) and in the lead coordination polymers [54], [Pb(4-nba)(PyO)$_2$(NO_2)]$_n$ and [Pb(4-nba)$_2$(PyO)]$_n$.

Table 7- Selected bond distances (Å) and bond angles (°) for compound [Ca(H_2O)$_2$(4-nba)$_2$].(dmp)$_2$]$_n$ **6**.

[Ca(H_2O)$_2$(4-nba)$_2$].(dmp)$_2$]$_n$ **6**			
Ca(1)-O(22)	2.334(2)	Ca(1)-O(11)^{ii}	2.5326(18)
Ca(1)-O(21)	2.3476(19)	Ca(1)-O(12)^{ii}	2.5508(18)
Ca(1)-O(11)	2.3603(16)	Ca(1)-O(1)	2.6995(19)
Ca(1)-O(2)^{i}	2.3857(16)	Ca(1)-Ca(1)^{i}	3.8893(10)
Ca(1)-O(2)	2.5277(19)	Ca(1)-Ca(1)^{ii}	3.9083(10)
O(22)-Ca(1)-O(21)	100.57(7)	O(2)-Ca(1)-O(11)^{ii}	87.99(6)
O(22)-Ca(1)-O(11)	76.32(6)	O(22)-Ca(1)-O(12)^{ii}	88.53(7)
O(21)-Ca(1)-O(11)	84.32(6)	O(21)-Ca(1)-O(12)^{ii}	153.46(6)
O(22)-Ca(1)-O(2)^{i}	85.47(6)	O(11)-Ca(1)-O(12)^{ii}	122.17(6)
O(21)-Ca(1)-O(2)^{i}	76.82(6)	O(2)^{i}-Ca(1)-O(12)^{ii}	79.15(6)
O(11)-Ca(1)-O(2)^{i}	150.87(6)	O(2)-Ca(1)-O(12)^{ii}	72.94(6)
O(22)-Ca(1)-O(2)	155.36(6)	O(11)^{ii}-Ca(1)-O(12)^{ii}	51.05(5)
O(21)-Ca(1)-O(2)	90.13(7)	O(22)-Ca(1)-O(1)	153.10(6)
O(11)-Ca(1)-O(2)	127.21(6)	O(21)-Ca(1)-O(1)	83.81(6)
O(2A)-Ca(1)-O(2)	75.37(6)	O(11)-Ca(1)-O(1)	77.75(6)
O(22)-Ca(1)-O(11)^{ii}	92.87(7)	O(2)^{i}-Ca(1)-O(1)	121.20(6)
O(21)-Ca(1)-O(11)^{ii}	151.04(6)	O(2)-Ca(1)-O(1)	49.47(5)
O(11)-Ca(1)-O(11)^{ii}	74.03(6)	O(11)^{ii}-Ca(1)-O(1)	73.11(6)
O(2)^{i}-Ca(1)-O(11)^{ii}	130.19(6)	O(12)^{ii}-Ca(1)-O(1)	99.32(6)

Symmetry codes : i) –x+2, -y, -z+1, ii) –x+1, -y, -z+1

Table 8- Hydrogen- bonding geometry (Å, °) for [Ca(H_2O)$_2$(4-nba)$_2$].(dmp)$_2$]$_n$ **6**

D-H---A	d(D-H)	d(H---A)	D(D---A)	<DHA	Symmetry code
[Ca(H_2O)$_2$(4-nba)$_2$].(dmp)$_2$]$_n$ **6**					
N21-H21···O14	0.860	2.244	3.055	157	x,y, z+1
N31-H31···O1	0.860	2.058	2.889	163	
O21-H10···N32	0.820	1.960	2.770	169	
O21-H20···O12	0.820	1.994	2.798	167	x+1, y, z
O22-H30···N22	0.820	1.944	2.762	176	-x+1, -y,- z+1
O22-H40···O1	0.820	2.035	2.843	168	-x+1, -y,- z+1

Table 9 – Bridging binding modes of the 4-nba ligand

No.	Compound	Space group	Binding mode of 4-nba^b	Nuclearity	Ref.
1	$[Mg(H_2O)(N\text{-}MeIm)_2(4\text{-}nba)_2]_2$	$P\bar{1}$	A	Dimer	153
2	$[Cu_2(H_2O)_2(4\text{-}nba)_4]$	$P\bar{1}$	A	Dimer	181
3	$[Ru_2(H_2O)(CH_3CN)_2(PPh_3)_2(4\text{-}nba)_4]$	$P2_1/c$	A	Dimer	182
4	$[Rh_2(C_5H_5N)(CH_3OH)_2(4\text{-}nba)_4]\cdot CH_2Cl_2$	$P\bar{1}$	A	Dimer	183
5	$[Dy_4(H_2O)_{10}(4\text{-}nba)_{12}]\cdot 2H_2O$	$P\bar{1}$	A	Tetramer	184
6	$[Tm_4(H_2O)_{10}(4\text{-}nba)_{12}]\cdot 2H_2O$	$P\bar{1}$	A	Tetramer	185
7	$[Fe_5O(OH)(L)_4(4\text{-}nba)_4]\cdot C_7H_8$	$P\bar{1}$	A	Pentamer	186
8	$[Fe_6O_3(OH)(4\text{-}nba)_{11}(DMF)_4]$	$P\bar{1}$	A	Hexamer	187
9	$[Ag_2(DPA)(4\text{-}nba)_2]_n$	$C2/c$	A, E	Polymer	188
10	$[Pb(4\text{-}nba)(PyO)_2(NO_2)]_n$	$P2_1/n$	D	Polymer	189
11	$[Pb(4\text{-}nba)_2(PyO)]_n$	$P2_1/c$	D	Polymer	189
12	$[Pb_2(4\text{-}nba)_3(NO_3)(BPNO)]_n$	$P2_1/c$	A, D	Polymer	189
13	$[[La(4\text{-}nba)_3(DMSO)(H_2O)]\cdot DMSO]_n$	$P2_1/c$	A	Polymer	190
14	$[Eu_2(4\text{-}nba)_6(H_2O)_5]_n$	$P\bar{1}$	A, D	Polymer	191
15	$[Tb_2(4\text{-}nba)_6(H_2O)_5]_n$	$P\bar{1}$	A, D	Polymer	191
16	$[Ba(H_2O)_5(4\text{-}nba)_2]_n$	$P2_1/c$	A	Polymer	169
17	$[Ca(pyr)_2(4\text{-}nba)_2]_n$	$P\bar{1}$	A	Polymer	120
18	$[Ca(H_2O)(2\text{-}MeIm)(4\text{-}nba)_2]_n$	$P2_1/n$	A, C	Polymer	26
19	$[Ca(N\text{-}MeIm)(4\text{-}nba)_2]_n$	$P\bar{1}$	A, E	Polymer	24
20	$[Na(H_2O)_3(4\text{-}nba)]_n$	$P\bar{1}$	B	Polymer	176
21	$[KH(4\text{-}nba)_2]_n$	$P\bar{1}$	C, F	Polymer	180
22	$[[Ca(H_2O)_2(4\text{-}nba)_2]\cdot 2dmp]_n$	$P\bar{1}$	D	Polymer	121

Abbreviations used: 4-nba = 4-nitrobenzoate; N-MeIm = N-methylimidazole; L = salisylideneethylenediamine; DPA = di-2-pyridylamine; PyO = pyridine N-oxide; BPNO = 2,2'-bipyridine N-oxide; pyr pyrazole; 2-MeIm = 2-methylimidazole; dmp = 3,5-dimethylpyrazole. b) For explanation of binding mode see Fig. 22

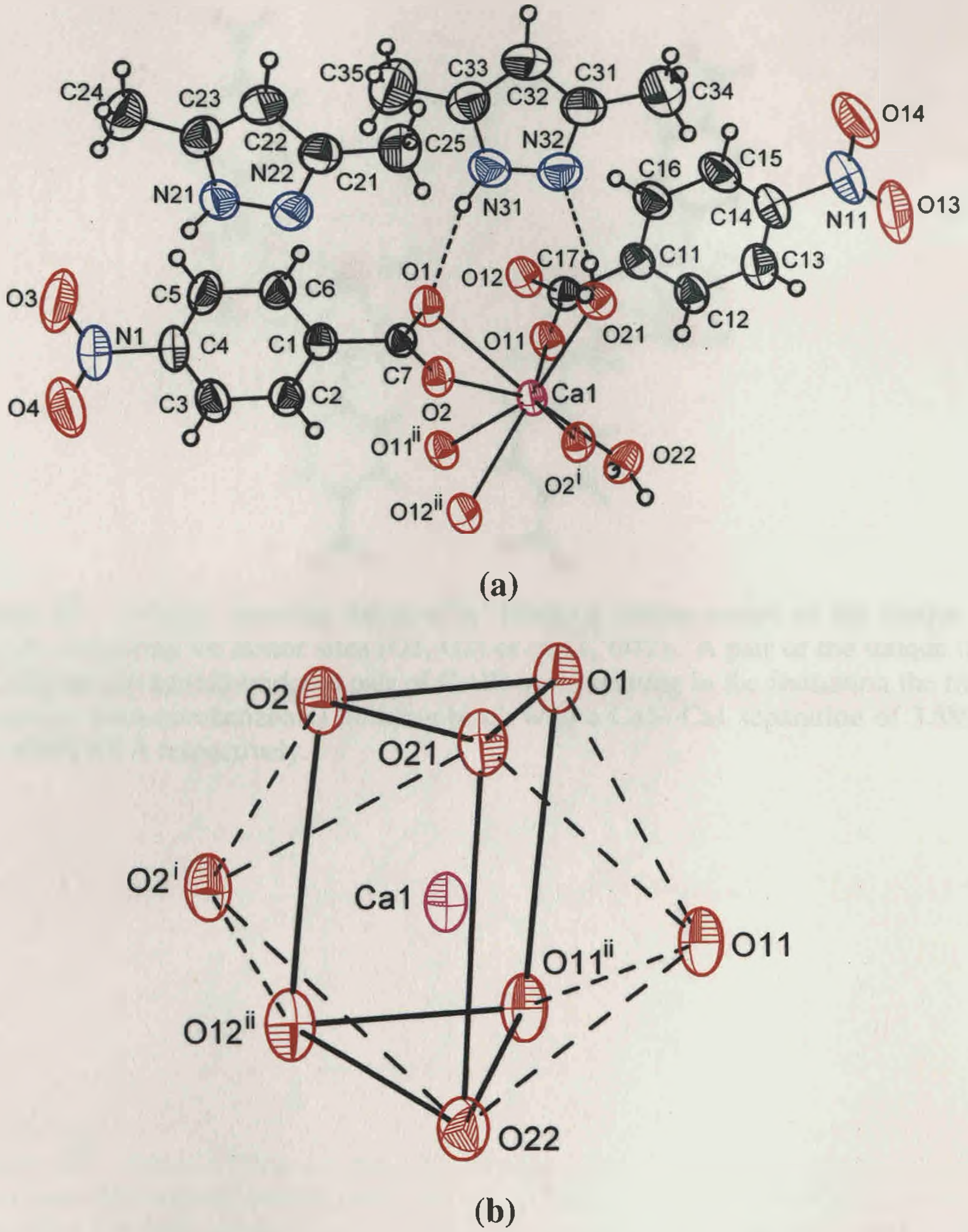

Figure 16 – (**a**) Crystal structure of $[[Ca(H_2O)_2(4\text{-}nba)_2]\cdot 2dmp]_n$ **6** showing atom-labeling scheme. Displacement ellipsoids are drawn at 50% probability level except for H atoms, which are shown as circles of arbitrary radius. Intramolecular H-bonding is shown as broken lines. (**b**) The distorted bicapped trigonal prismatic coordination environment of Ca1. The atoms O2^{i} and O11 on the rectangular faces of the trigonal prism function as capping atoms. Symmetry codes : i) *-x+2,-y,-z+1*; ii) *-x+1,-y,-z+1*

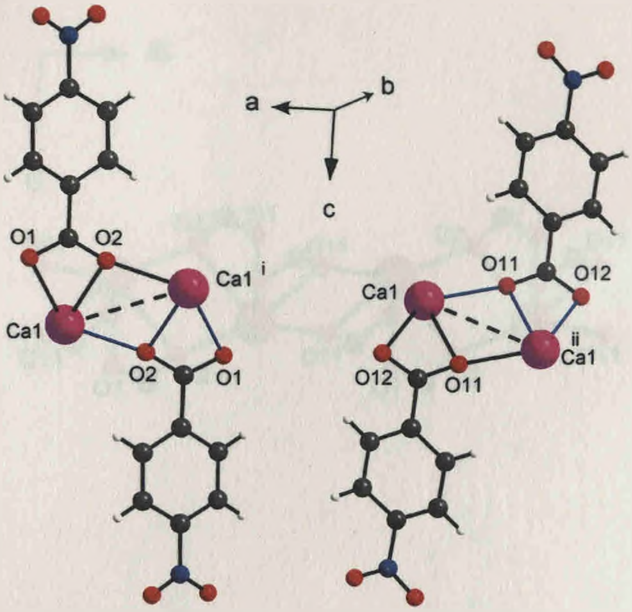

Figure 17 – A view showing the μ_2-η^2:η^1 bridging biding modes of the unique 4-nba ligands containing the donor sites (O1, O2) or (O11, O12). A pair of the unique ligands (O1,O2) or (O11,O12) bridge a pair of Ca(II) ions resulting in the formation the tricyclic dicalcium-bis(4-nitrobenzoate) building block with a Ca1···Ca1 separation of 3.8893(10) or 3.9083(10) Å respectively.

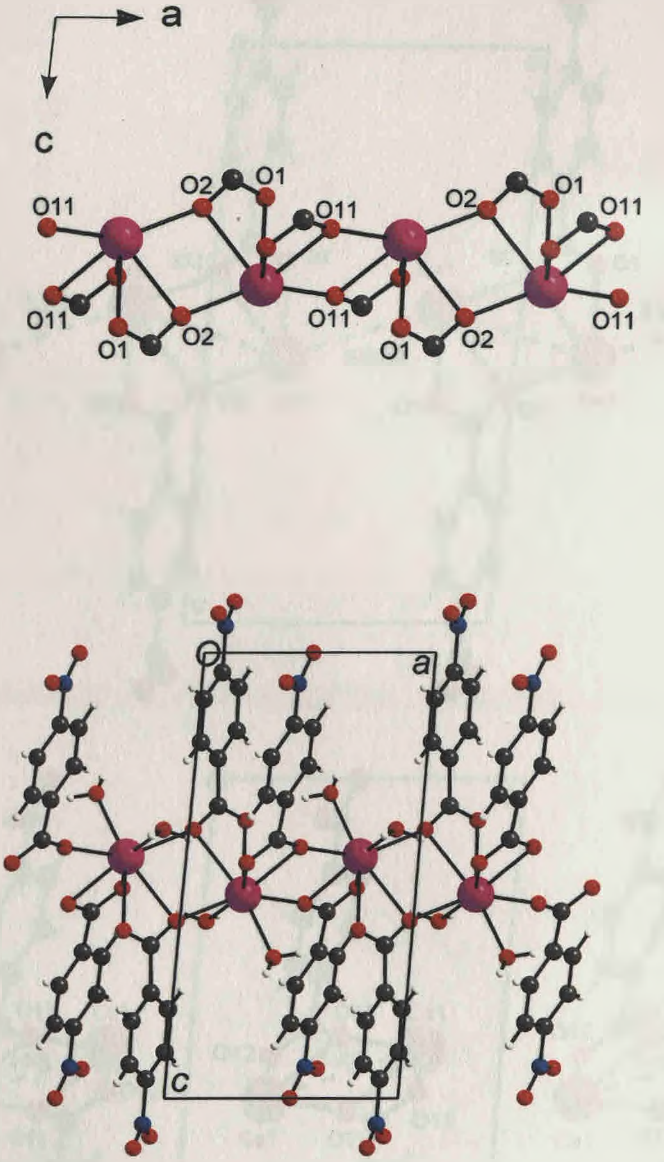

Figure 18 – (a) A portion of the 1-D polymer of **6** showing the linking of tricyclic dicalcium-bis(4-nitrobenzoate) units into an infinite chain. For clarity, coordinated H_2O molecules and aromatic ring are not shown. (b) Aromatic rings and H atoms of water are included in the polymeric chain

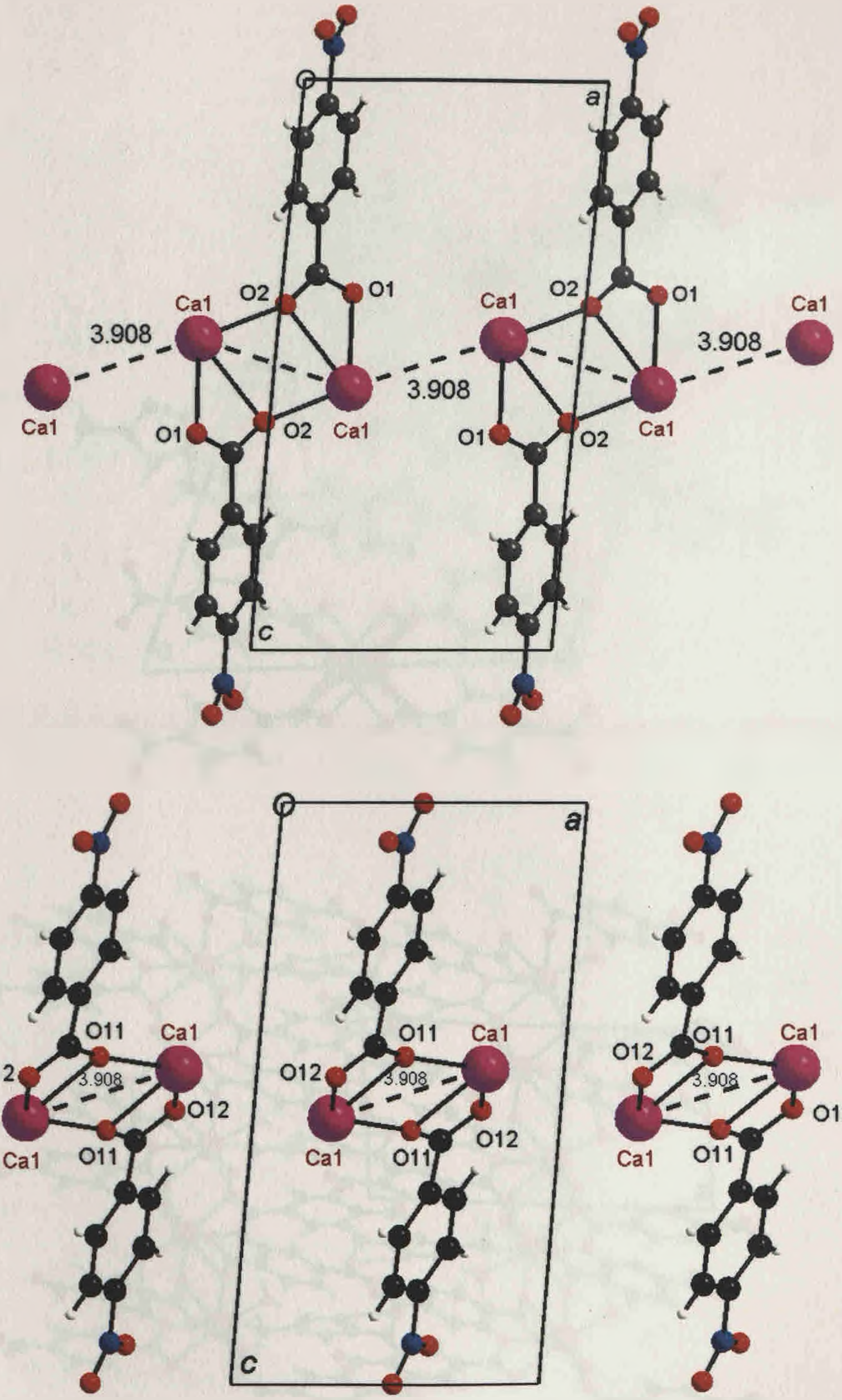

Figure 19- A view along *b* axis of the μ_2-η^2:η^1 bridging binding mode of the first unique (O1, O2) ligand. A pair of (O1, O2) ligands bridge between two Ca(II) ions resulting in a Ca···Ca separation of 3.889 Å resulting in the formation of isolated dimeric units. For clarity only the coordinated ligand is shown (top). The second independent 4-nba ligand (O11, O12) exhibits an identical bridging mode, with a Ca···Ca separation of 3.908 Å. (bottom). The identical Ca atoms in the top & bottom figures are labeled.

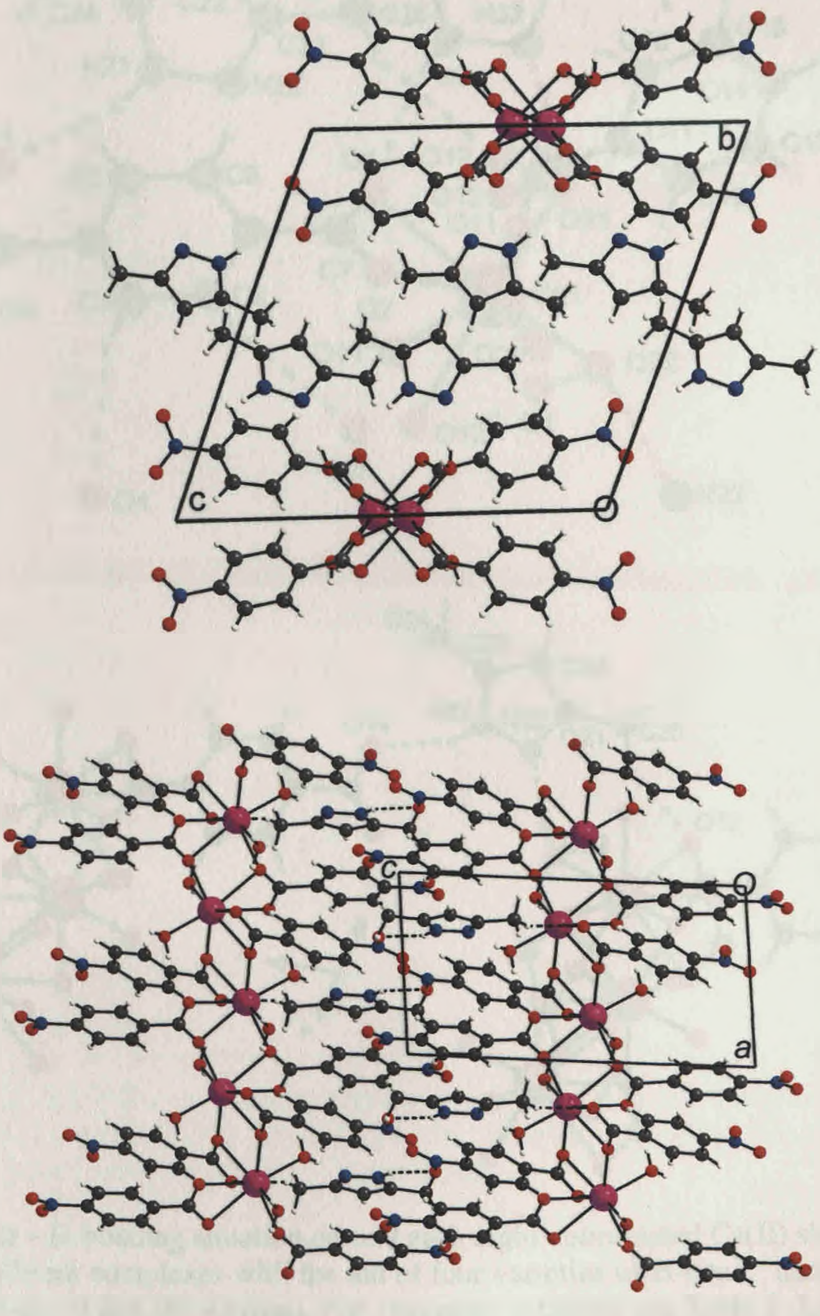

Figure 20 – (**a**) A view along *a* showing the neutral dmp molecules situated between the one dimensional parallel chains. (**b**) A view along *b* showing the lattice dmp molecules which function as linkers between adjacent polymeric chains via H-bonding interactions

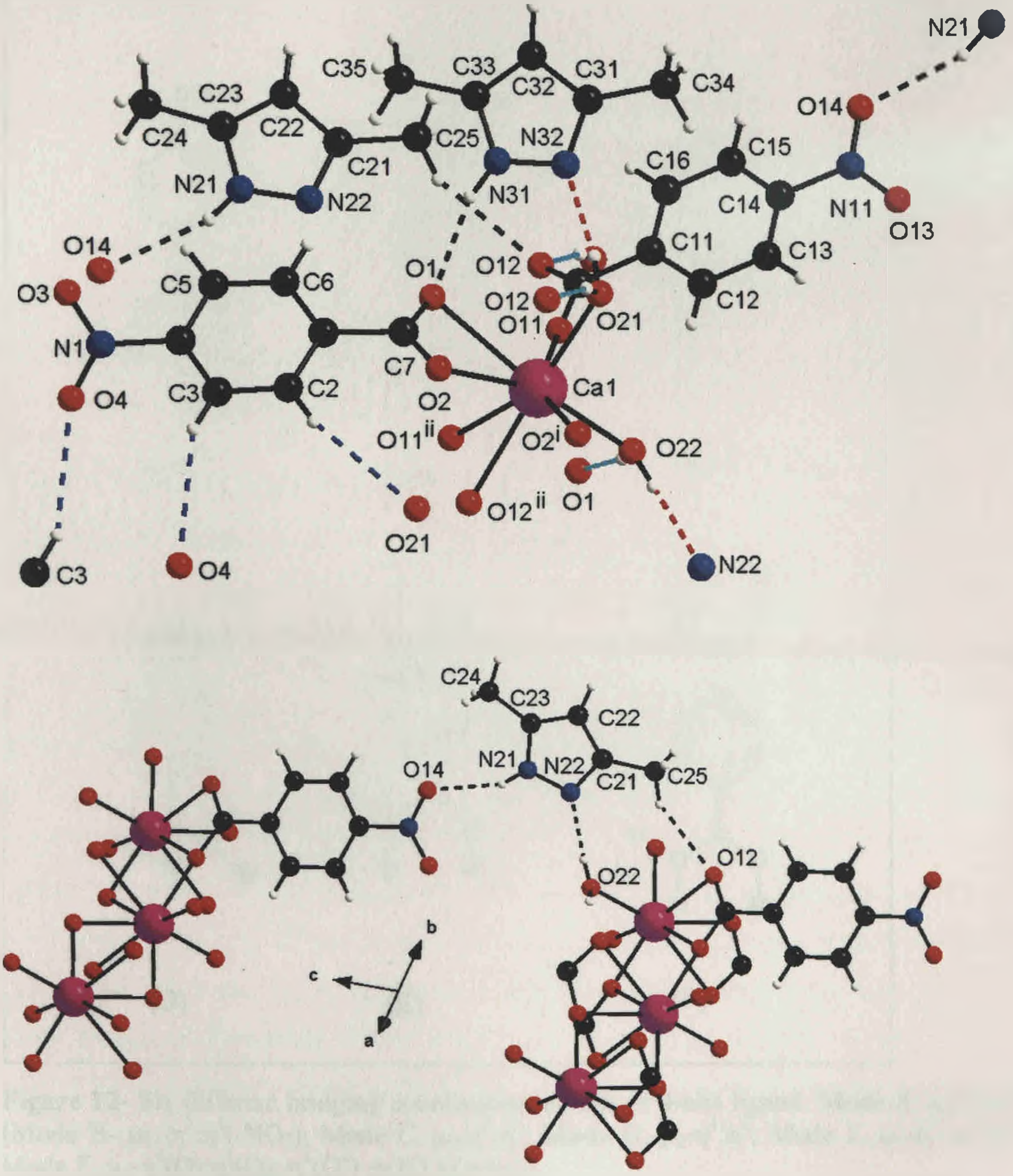

Figure 21 - H-bonding situation around each eight coordinated Ca(II) showing its linking to six different complexes with the aid of four varieties of H-bond, namely O-H···O, N-H···O, O-H···N & C-H···O (top). For symmetry relations see Table 8 Lattice dmp serves as a link between one dimensional chains via the N21-H21···O14, O22-H30···N22 and C25-H25A···O12 interactions (bottom).

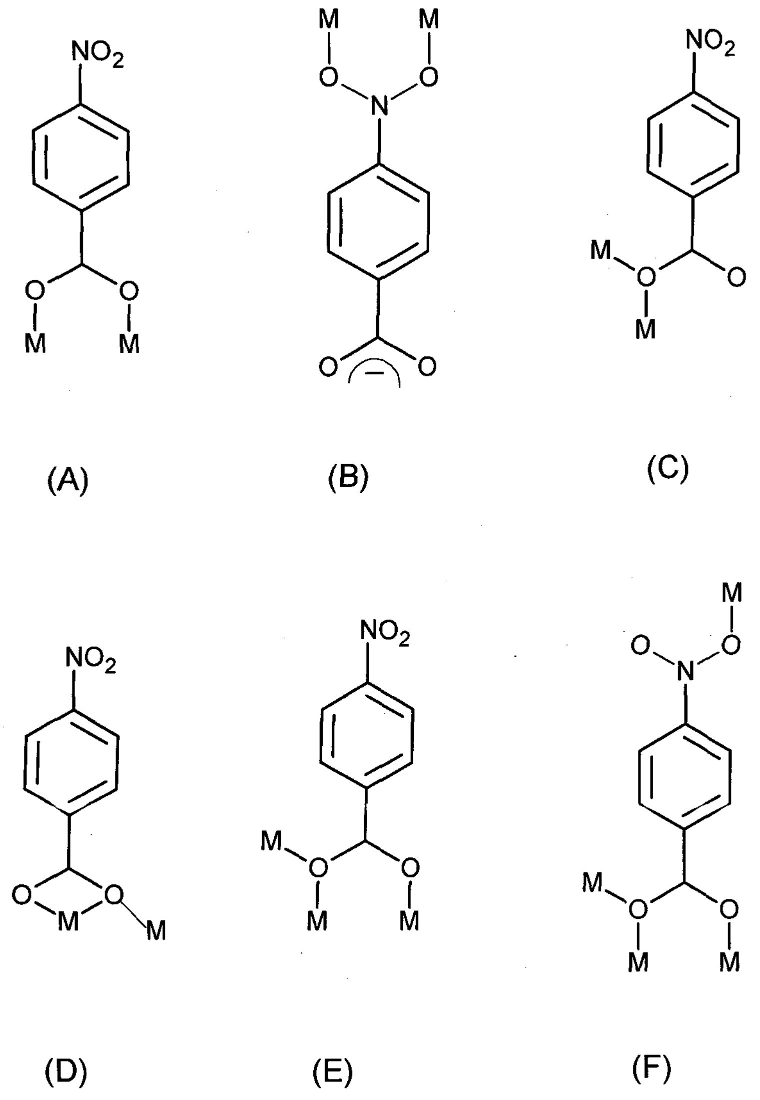

Figure 22- Six different bridging coordination modes of 4-nba ligand. Mode A, μ_2-η^1:η^1; [Mode B- μ_2:-η^1:η^1(-NO$_2$); Mode C, μ_2-η^2:η^0; Mode D, μ_2-η^1:η^2; Mode E, μ_3-η^1: η^1 :η^1; Mode F, μ_4-η^1(O):η^1(O): η^1(O') :η^1(O of nitro)].

Crystal structure description of [Ca(H_2O)$_6$(4nba)](4-nba)(2-ap)·H_2O 7

The water-rich Ca(II) compound, [Ca(H_2O)$_6$(4nba)](4-nba)(2-ap)·H_2O **7** crystallizes in the centrosymmetric triclinic space group *P1̄* with all atoms situated in general positions. The crystal structure consists of a [Ca(H_2O)$_6$(4nba)]$^+$ complex cation, a free 4-nitrobenzoate anion, a solvent 2-aminopyridne (2-ap) and a lattice water (Figure 23). In the complex cation, the central Ca(II) is seven coordinated and is bonded to six terminal water molecules and a monodentate 4-nitrobenzoate resulting in a distorted pentagonal bipyramidal {CaO_7} polyhedron (Figure 23). The water-rich Ca(II) compound differs from the known structurally characterized Ca(II)-4-nitrobenzoates [29-33] in that the central metal is coordinated to a single 4-nba ligand with the second unique 4-nba remaining uncoordinated. In all other structurally characterized 4-nitrobenzoates of Ca(II), the central metal is bonded to at least two 4-nba anions as in [Ca(H_2O)$_4$(4-nba)$_2$] [63] or to more than two 4-nba ligands as observed in the one-dimensional polymers [24, 26, 120]. The coordination of six water molecules to Ca(II) and the presence of free 4-nba in **7** clearly indicate the reorganization of the coordination sphere of Ca(II) in [Ca(H_2O)$_4$(4nba)$_2$] **1** on reaction with 2-ap. The geometric parameters of the coordinated and the free 4-nba and the 2-ap solvent are in the normal range. The Ca-O distances range from 2.360(9) to 2.531(10) Å (Table 10) and are in good agreement with reported values for several Ca(II) compounds. The O-Ca-O angles range from 47.91(3) to 159.89(4)°. A scrutiny of the crystal structure of **7** reveals that the [Ca(H_2O)$_6$(4nba)]$^+$ cation, the free 4-nba anion, lattice water and solvent 2-aminopyridine are involved in four varieties of H-bonding interactions, comprising of thirteen O-H···O, two N-H···O, one O-H···N and four C-H···O bonds (Table 11). The O···H distances ranging from 1.772 to 2.674 Å are accompanied by DHA angles ranging from 142 to 174°. All the H atoms of the coordinated and lattice water molecules, the amino group of 2-ap, H atoms attached to two of the carbon atoms (C2 and C5) of the monodentate 4-nba and H atoms bonded to C8 and C10 of 2-ap function as H-donors. All oxygen atoms of the coordinated and lattice water molecules and the N3 nitrogen atom of 2-ap, function as H-acceptors. The oxygen atom (O1) of the nitro group of coordinated 4-nba is not involved in H-bonding. The O11 and O12 atoms of the nitro group of free 4-nba are involved in weak C-H···O interactions, a feature observed in several metal 4-nitrobenzoates [24, 26, 63, 120, 169, 175]. The H-acceptor characteristics of the lattice water (O15) results in tetra coordination around O15 (Figure 24). In addition, O15 functions as H-donor, which results in the lattice water being linked to three different [Ca(H_2O)$_6$(4nba)]$^+$ cations and a free 4-nba anion. The solvent, 2-aminopyridine, serves to link three different $[Ca(H_2O)_6(4nba)]^+$ cations and a free anion with the aid of two O-H···N, two C-H···O and one N-H···O interaction (Figure 24). The secondary interactions of 2-ap with the cations and free 4-nba appears to be an important factor for the formation of the water-rich compound starting from $[Ca(H_2O)_4(4\text{-}nba)_2]$ **1** since the reaction of 4-ap with **1** does not give rise to any new compound. It is interesting to note that the H-bonding surrounding of 2-ap is identical to that of the lattice water. An analysis of the crystal structure reveals that each seven coordinated Ca(II) complex cation is H-bonded to two symmetry related lattice water molecules, two different 2-ap molecules, five different uncoordinated 4-nba anions and four symmetry related $[Ca(H_2O)_6(4nba)]^+$ ions with the aid of eleven O-H···O bonds, one N-H···O bond, one O-H···N bond and three weak C-H···O interactions (Figure 25). The free uncoordinated 4-nba anion is linked to a lattice water and five different complex cations with the aid of seven O···H contacts (Figure 25) The net result of the several H-bonding interactions in **7** is the organization of cations and anions into alternating layers with the lattice water and solvent aminopyridine serving as links between layers (Figure 26).

Table 10- Selected bond lengths and bond angles for **7**

Bond lengths (Å)			
Ca-O(4)	2.360(9)	Ca-O(7)	2.437(9)
Ca-O(8)	2.438(9)	Ca-O(6)	2.449(10)
Ca-O(9)	2.531(10)	Ca-O(10)	2.390(10)
Ca-O(5)	2.488(11)		
Bond angles (°)			
O(4)-Ca-O(7)	84.30(3)	O(4)-Ca-O(10)	98.76(4)
O(4)-Ca-O(8)	159.89(4)	O(10)-Ca-O(7)	145.92(4)
O(7)-Ca-O(8)	91.49(3)	O(10)-Ca-O(8)	95.71(4)
O(10)-Ca-O(6)	141.87(4)	O(4)-Ca-O(6)	83.71(3)
O(8)-Ca-O(6)	76.29(3)	O(7)-Ca-O(6)	72.17(4)
O(10)-Ca-O(5)	71.83(4)	O(4)-Ca-O(5)	86.86(4)
O(8)-Ca-O(5)	84.46(4)	O(7)-Ca-O(5)	142.(4)
O(4)–Ca-O(9)	122.74(3)	O(6)-Ca-O(5)	70.32(4)
O(7)-Ca-O(9)	76.31(3)	O(10)-Ca-O(9)	73.59(4)
O(6)-Ca-O(9)	136.14(3)	O(8)-Ca-O(9)	74.83(3)
O(4)-Ca-O(3)	47.91(3)	O(5)-Ca-O(9)	137.31(4)
O(7)-Ca-O(3)	74.70(3)	O(10)-Ca-O(3)	82.33(4)
O(6)-Ca-O(3)	123.11(3)	O(8)-Ca-O(3)	148.99(3)
O(9)-Ca-O(3)	74.96(3)	O(5)-Ca-O(3)	123.36 (4)

Table 11- Hydrogen-bonding geometry for $[Ca(H_2O)_6(4\text{-}nba)](4\text{-}nba)(2\text{-}ap)\cdot H_2O$ **7**

D-H···A	*D*(D-H) (Å)	*D*(H···A) (Å)	*D*(D···A) (Å)	<DHA (°)	Symmetry code
O8-H8B···O15	0.772	2.022	2.785	169	x, y, z
O6-H6A···O14	0.916	2.050	2.826	142	x, y, z
O15-H16A···O14	0.824	1.909	2.713	165	x, y, z
O8-H8A···O13	0.960	1.773	2.713	166	-x+1, -y+1, -z
O9-H9B···O13	0.878	1.958	2.821	167	-x+1, -y+1, -z
O15-H16···O7	0.802	2.014	2.809	172	-x+1, -y+1, -z
O9-H9A···O15	0.881	1.914	2.792	174	x-1, y, z
O7-H7A···O14	0.890	2.023	2.886	163	x-1, y, z
O5-H5A···O3	0.898	1.957	2.846	170	x+1, y, z
O6-H6B···O3	0.835	1.986	2.812	170	x+1, y, z
O5-H5B···O13	0.740	2.167	2.891	166	x, y-1, z
O10-H10A···O8	0.857	2.025	2.873	170	-x+1, -y, -z
O10-H10B···O9	0.805	2.202	2.961	157	-x, -y, -z
N2-H34···O4	0.821	2.399	3.174	158	x, y, z
N2-H33···O2	0.830	2.241	3.057	168	-x, -y, -z+1
O7-H7B···N3	0.911	1.772	2.671	169	x, y, z
C2-H2···O6	0.971	2.666	3.505	145	x-1, y, z
C5-H5···O11	0.997	2.526	3.204	125	x-1, y, z
C8-H8···O12	0.899	2.563	3.397	154	-x+1, -y+1,-z+1
C10-H10···O4	0.915	2.674	3.555	162	x, y+1, z

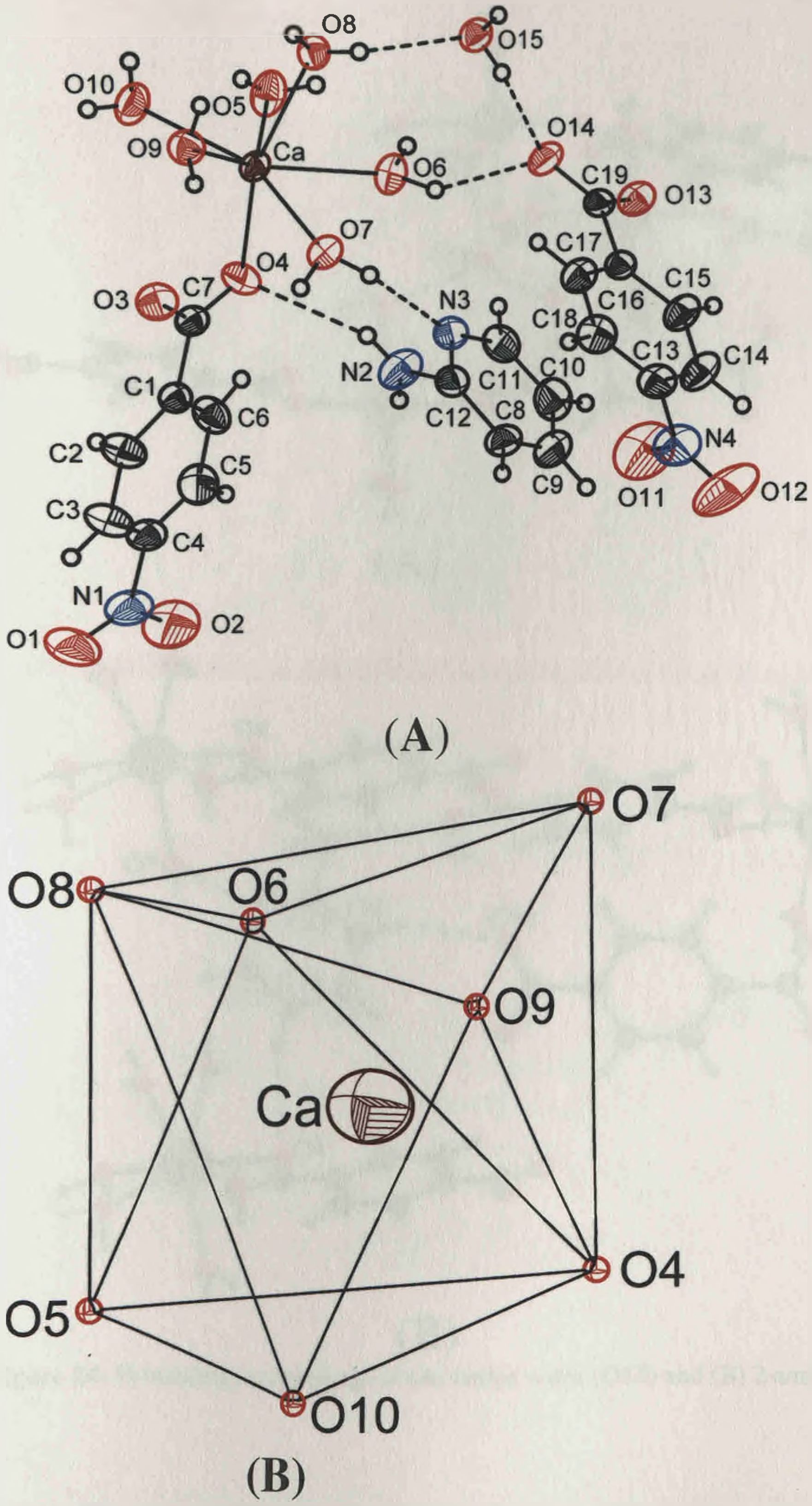

Figure 23- (A) Crystal structure of $[Ca(H_2O)_6(4\text{-nba})](4\text{-nba})(2\text{-ap})\cdot H_2O$ showing the atom-labeling scheme. Displacement ellipsoids are drawn at 50% probability level except for the H atoms, which are shown as circles of arbitrary radius. Intramolecular H-bonding is shown as broken lines. (B) The distorted pentagonal bipyramidal $\{CaO_7\}$ coordination polyhedron around Ca.

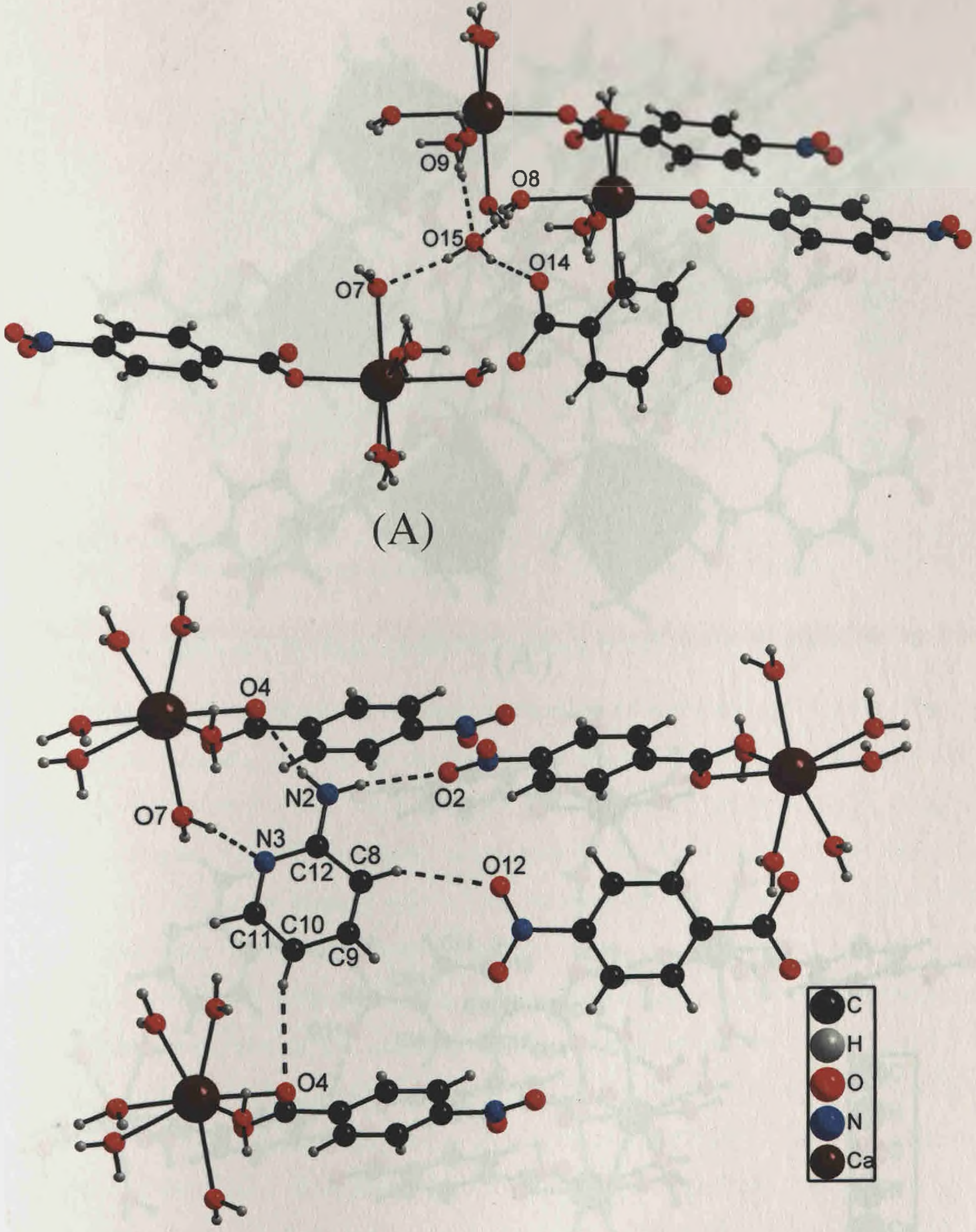

Figure 24- H-bonding surroundings of (A) lattice water (O15) and (B) 2-aminopyridine

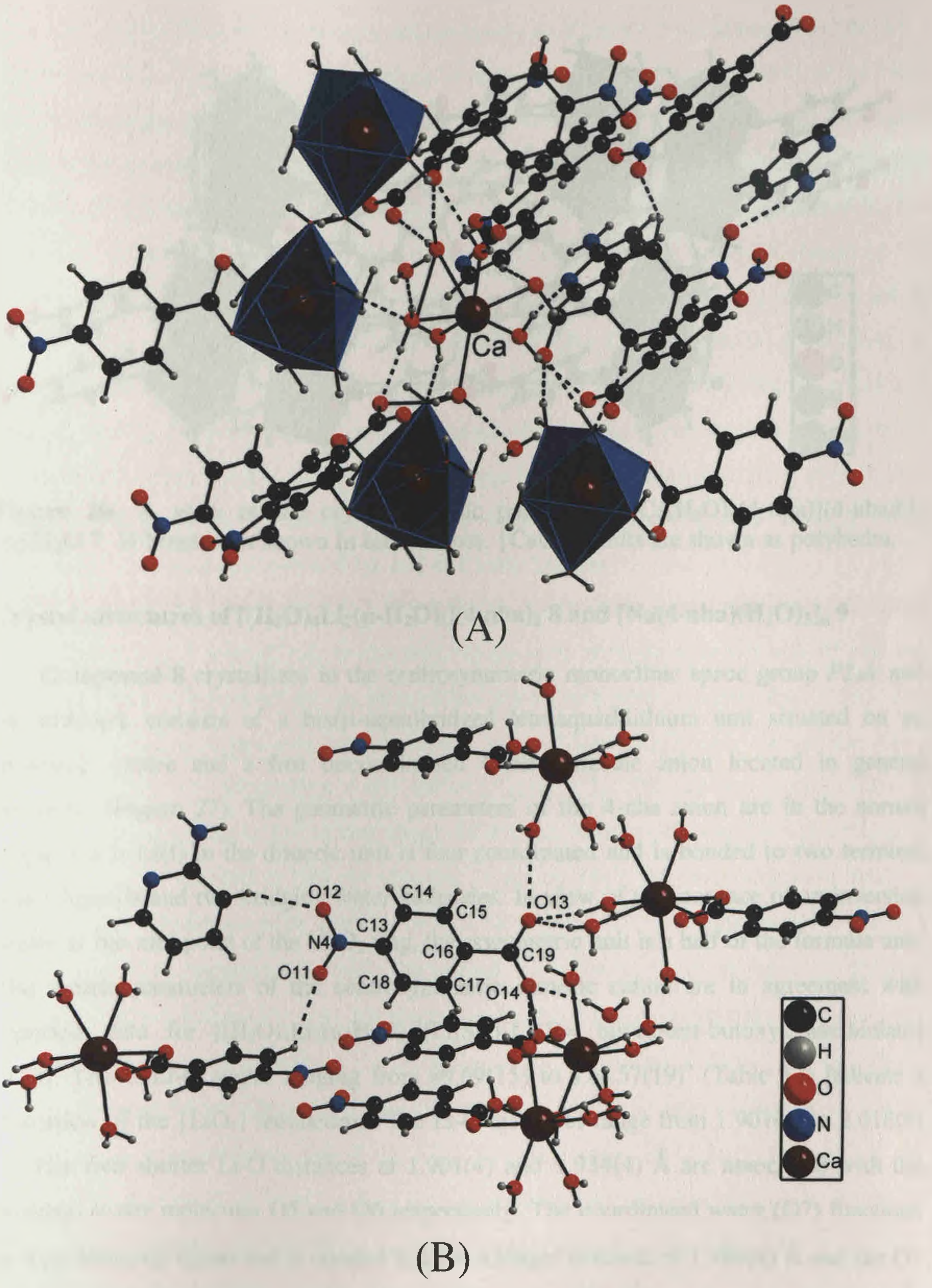

Figure 25- (A) H-bonding surroundings of the $[Ca(H_2O)_6(4nba)]^+$ cation and (B) free uncoordinated 4-nba. Each cation is H-bonded to two lattice waters, two 2-ap molecules, five free 4-nba anions and four different cations (polyhedra)

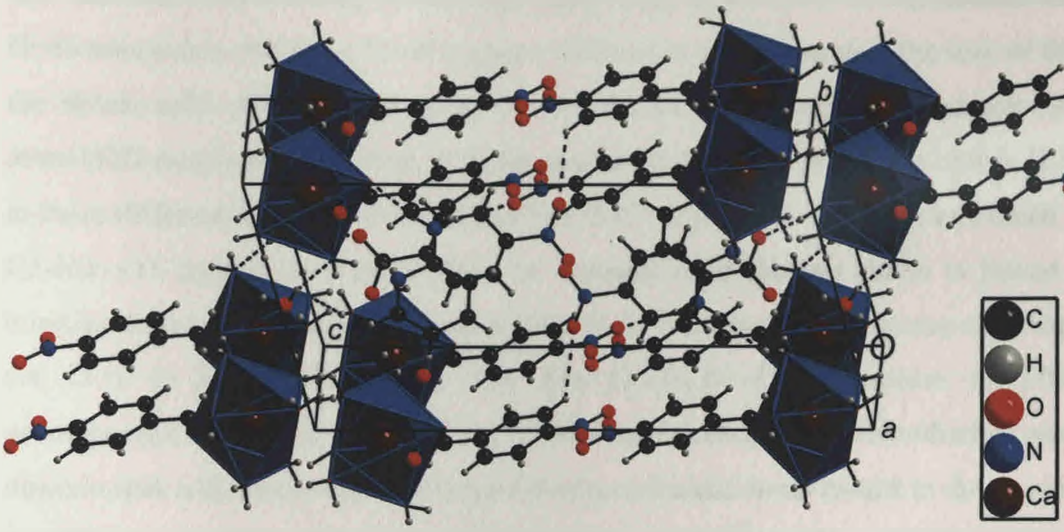

Figure 26- A view of the crystallographic packing of $[Ca(H_2O)_6(4\text{-nba})](4\text{-nba})(2\text{-ap})\cdot H_2O$ **7**. H-bonding is shown in broken lines. $\{CaO_7\}^+$ units are shown as polyhedra.

Crystal structures of $[(H_2O)_4Li_2(\mu\text{-}H_2O)_2](4\text{-nba})_2$ 8 and $[Na(4\text{-nba})(H_2O)_3]_n$ 9

Compound **8** crystallizes in the centrosymmetric monoclinic space group *P2₁/c* and its structure consists of a bis(μ-aqua)bridged tetraaquadilithium unit situated on an inversion centre and a free uncoordinated 4-nitrobenzoate anion located in general positions (Figure 27). The geometric parameters of the 4-nba anion are in the normal range. Each Li(I) in the dimeric unit is four coordinated and is bonded to two terminal water ligands and two bridging water molecules. In view of the presence of an inversion centre at the mid point of the Li_2O_2 ring, the asymmetric unit is a half of the formula unit. The metric parameters of the centrosymmetric dimeric cation are in agreement with reported data for $[(H_2O)_4Li_2(\mu\text{-}H_2O)_2][Li(SR)_2]$ [R= bis(tri-tert-butoxysilanethiolato] [178]. The O-Li-O angles ranging from 89.69(15) to 126.57(19)° (Table 12) indicate a distortion of the $\{LiO_4\}$ tetrahedron. The Li-O distances range from 1.901(4) to 2.018(4) Å. The two shorter Li-O distances at 1.901(4) and 1.934(4) Å are associated with the terminal water molecules O5 and O6 respectively. The coordinated water (O7) functions as a μ_2-bridging ligand and is bonded to Li at a longer distance of 1.989(4) Å and the O7 is further linked to symmetry related Li with a very long Li-O bond length of 2.018(4) Å. This μ_2-bridging bidentate mode of O7 results in a Li···Li separation of 2.842(7) Å in the dimeric unit which is slightly shorter than the reported value of 2.876(7) Å for $[(H_2O)_4Li_2(\mu\text{-}H_2O)_2][Li(SR)_2]$ [178].

In the crystal structure of **8** the dimeric cation and the free 4-nba anion are linked by two varieties of H-bonding interactions comprising of six O-H···O interactions and a C-H···O interaction. All these O···H contacts (Table 13) are shorter than the sum of their van der Waals radii. All the H atoms of the coordinated water molecules and one hydrogen atom (H3) attached to a carbon (C3) function as H-donors. Each 4-nba unit is H-bonded to three different dimers with the aid of five O-H···O interactions and to one anion via the C3-H3···O3 interaction (Figure 28). In contrast, each dimeric cation is linked by H-bonding to two adjacent dimers and eight symmetry related 4-nba anions with the aid of six O-H···O interaction (Figure 29). The O5-H1W···O6 interaction at 2.09(4) Å accompanied by a DHA angle of 168(3)° between the H atom of a coordinated water in a dimeric unit and the coordinated water O6 of an adjacent dimer results in the formation of an infinite supramolecular chain of $[(H_2O)_4Li_2(\mu\text{-}H_2O)_2]^{2+}$ cations extending along *b* axis (Figure 30). The chain is further H-bonded to 4-nba anions on either side resulting in the formation of alternating layers of cations and 4-nba anions.

Compound **9** crystallizes in the centrosymmetric triclinic space group $P\bar{1}$ and the observed unit cell parameters are in excellent agreement with reported data [179]. The structure consists of two crystallographically independent Na(I) ions, six unique water molecules and two independent 4-nba anions (Figure 27). The geometric parameters of the organic anions are in the normal range. Of the six water molecules, two aqua ligands (O21 and O23) attached to Na1 are terminal in nature while the remaining four function as μ_2-bridging bidentate aqua ligands. One of the two unique 4-nba anions functions as a free anion as in compound **8**, while the second 4-nba anion functions as a μ_2-bridging bidentate ligand attached to two symmetry related Na(I) ions via the oxygen atoms O3 and O4 of the nitro functionality. The μ_2-bridging binding modes of the four aqua ligands results in a two-dimensional structure (Figure 31). Although one of the 4-nba anions functions as a μ_2-bridging ligand and this binding mode alone does not lead to an extended structure. Each Na(I) in **9** is six coordinated and the observed Na-O distances and O-Na-O angles (Table 2) are in good agreement with reported data [179]. Like in **8**, two varieties of H-bonding interactions are observed (Table 13).

Recently we had shown that the charge balancing 4-nba anion is a versatile ligand and exhibits several bridging binding modes [121] in addition to binding in a monodentate or a bidentate fashion through the carboxylate oxygen atoms. A study of the 4-nba compounds of Li and Na reported in this work and earlier reported compounds [63, 133, 169, 179, 176, 177] reveals some useful trends in terms of the coordination number of the *s*-block metals. All compounds listed in (Table 14) contain coordinated water ligands and can be synthesized by an aqueous reaction of the *s*-block metal carbonate with 4-nbaH. In the alkali metal series, the lighter element Li exhibits a coordination number of four which increases to six on going to Na and a maximum value of nine is observed for the Rb and Cs compounds. In this series, the Li compound is a dimer, while all others are polymers. In the 4-nba compounds of Na, K, Rb and Cs, coordination of the central metal to the oxygen atom of the nitro functionality is observed. In contrast, for the alkaline earths Mg [133] exhibits a coordination number of six which increases to seven on going to Ca [63] and attains the maximum value of nine for Sr [177] and Ba [169]. In the alkaline earth series excepting the Ba compound which is a one-dimensional polymer all other compounds are zero-dimensional. A study of the known *s*-block metal compounds containing 4-nba and coordinated water ligands reveals that the coordination number of the central metal varies from four in Li to nine in Ba. The hydrated 4-nba compounds of K and Be are not yet known.

Table 12- Selected bond distances (Å) and bond angles (°)

$[(H_2O)_4Li_2(\mu\text{-}H_2O)_2](4\text{-nba})_2$ **8**			
Li(1)-O(5)	1.901(4)	O(5)-Li(1)-O(6)	110.1(2)
Li(1)-O(6)	1.934(4)	O(5)-Li(1)-O(7)	115.28(18)
Li(1)-O(7)	1.989(4)	O(6)-Li(1)-O(7)	126.57(19)
Li(1)-O(7)^{i}	2.018(4)	O(5)-Li(1)-O(7)^{i}	109.37(18)
Li(1)···Li(1)^{i}	2.842(7)	O(6)-Li(1)-O(7)^{I}	100.81(17)
		O(7)-Li(1)-O(7)^{i}	89.69(15)
$[Na(4\text{-nba})(H_2O)_3]_n$ **9**			
Na(1)-O(22)	2.3655(15)	O(23)-Na(1)-O(24)	96.38(5)
Na(1)-O(23)	2.3728(16)	O(21)-Na(1)-O(24)	173.77(5)
Na(1)-O(21)	2.4283(15)	O(22)^{ii}-Na(1)-O(24)	90.24(5)
Na(1)-O(22)^{ii}	2.4327(16)	O(22)-Na(1)-O(3)	166.40(6)
Na(1)-O(24)	2.4391(14)	O(23)-Na(1)-O(3)	96.30(7)
Na(1)-O(3)	2.5365(18)	O(21)-Na(1)-O(3)	79.95(6)
Na(2)-O(24)	2.4041(15)	O(22)^{ii}-Na(1)-O(3)	80.97(6)
Na(2)-O(25)^{iii}	2.4120(17)	O(24)-Na(1)-O(3)	93.82(6)
Na(2)-O(26)	2.4317(17)	O(24)-Na(2)-O(26)	149.90(6)
Na(2)-O(25)	2.4359(16)	O(25)^{iii} -Na(2)-O(26)	118.45(6)
Na(2)-O(26)^{iv}	2.4749(16)	O(24)-Na(2)-O(25)	89.62(6)
Na(2)-O(4)	2.729(2)	O(25)^{iii}-Na(2)-O(25)	77.39(5)
Na(1)···Na(1)^{ii}	3.5221(18)	O(26)-Na(2)-O(25)	101.85(5)
Na(1)···Na(2)	4.1500(13)	O(24)-Na(2)-O(26)^{iv}	91.63(5)
Na(2)···Na(2)^{iii}	3.7836(16)	O(25)^{iii}-Na(2)-O(26)^{iv}	103.52(5)
Na(2)···Na(2)^{iv}	3.8500(17)	O(26)-Na(2)-O(26)^{iv}	76.60(5)

O(22)-Na(1)-O(23)	96.87(6)	O(25)-Na(2)-O(26)^{iv}	178.43(5)
O(22)-Na(1)-O(21)	98.01(5)	O(24)-Na(2)-O(4)	73.68(6)
O(23)-Na(1)-O(21)	84.32(5)	O(25)^{iii}-Na(2)-O(4)	154.69(6)
O(22)-Na(1)-O(22)^{ii}	85.56(5)	O(26)-Na(2)-O(4)	80.33(6)
O(23)-Na(1)-O(22)^{ii}	173.01(5)	O(25)-Na(2)-O(4)	82.33(6)
O(21)-Na(1)-O(22)^{ii}	88.86(5)	O(26)^{iv}-Na(2)-O(4)	97.12(6)
O(22)-Na(1)-O(24)	88.07(5)		

Symmetry transformations used to generate equivalent atoms. Symmetry codes i) –x+1, -y-1, -z ii) -x+1, -y+1, -z+2 iii) -x+1, -y+2, -z+2 iv) –x+2, -y+2, -z+2

Table 13- Hydrogen-bonding geometry for $[(H_2O)_4Li_2(\mu\text{-}H_2O)_2](4\text{-nba})_2$ **8** and $[Na(4\text{-nba})(H_2O)_3]_n$ **9**

D-H···A	*D*(D-H) (Å)	*D*(H···A) (Å)	*D*(D···A) (Å)	<DHA (°)	Symmetry code
$[(H_2O)_4Li_2(\mu\text{-}H_2O)_2](4\text{-nba})_2$ **8**					
O5-H1W···O6	0.79(4)	2.09(4)	2.876(3)	168(3)	-x+1, -y, -z
O5-H2W···O3	0.89(4)	2.16(4)	3.028(2)	165(3)	x+1, -y+½, z-½
O6-H3W···O2	0.79(3)	2.11(3)	2.855(2)	159(3)	-x+1, y-½, -z+½
O6-H4W···O2	0.92(3)	1.81(3)	2.721(2)	171(2)	x, y, z
O7-H5W···O1	0.92(3)	1.75(3)	2.663(2)	172(2)	-x+1, -y+1, -z
O7-H6W···O2	0.82(3)	2.06(3)	2.869(3)	172(2)	-x+1, y-½, -z+½
C3-H3···O3	0.93	2.60	3.323(3)	135	-x, -y+1, -z+1
$[Na(4\text{-nba})(H_2O)_3]_n$ **9**					
O21-H1O···O1	0.820	2.031	2.785	153	-x+1, -y+1, -z+1
O21-H2O···O11	0.820	2.105	2.924	178	x+1, y, z
O22-H3O···O1	0.820	1.984	2.780	164	x, y, z+1
O22-H4O···O11	0.820	1.957	2.777	178	-x+1, -y+1, -z+2
O23-H5O···O21	0.820	2.012	2.832	178	-x+2, -y+1, -z+2
O23-H6O···O12	0.820	2.001	2.800	164	x+1, y, z
O24-H7O···O12	0.820	2.108	2.908	165	x, y, z
O24-H8O···O1	0.820	2.013	2.802	161	x, y, z+1
O25-H9O···O12	0.820	1.983	2.765	159	x, y, z
O25-H100···O2	0.820	1.888	2.707	176	-x+1, -y+2, -z+1
O26-H11O···O14	0.820	2.281	3.097	174	-x+1, -y+2, -z+1
O26-H11O···O13	0.820	2.633	3.181	126	-x+1, -y+2, -z+1
O26-H12O···O23	0.820	1.956	2.773	175	-x+2, -y+2, -z+2
C15-H15···O14	0.931	2.596	3.318	135	-x, 2-y, 1-z

Table 14 – Varying coordination number (C.N.) of s-block metals

Compound	C.N.	Nuclearity	Ref.
$[(H_2O)_4Li_2(\mu\text{-}H_2O)_2](4\text{-nba})_2$	4	Dimer	176
$[Na(H_2O)_3(4\text{-nba})]_n$	6,6	Polymer	176, 179
$[Rb(H_2O)_2(4\text{-nba})]_n$	9	Polymer	CCDC717713
$[Cs(H_2O)_2(4\text{-nba})]_n$	9	polymer	CCDC 717712
$[Mg(H_2O)_6](4\text{-nba})_2\cdot 2H_2O$	6	Monomer	133
$[Ca(H_2O)_4(4\text{-nba})_2]$	7	Monomer	63
$[Sr(H_2O)_7(4\text{-nba})](4\text{-nba})\cdot 2H_2O$	9	Monomer	177
$[Ba(H_2O)_5(4\text{-nba})_2]_n$	9	Polymer	169

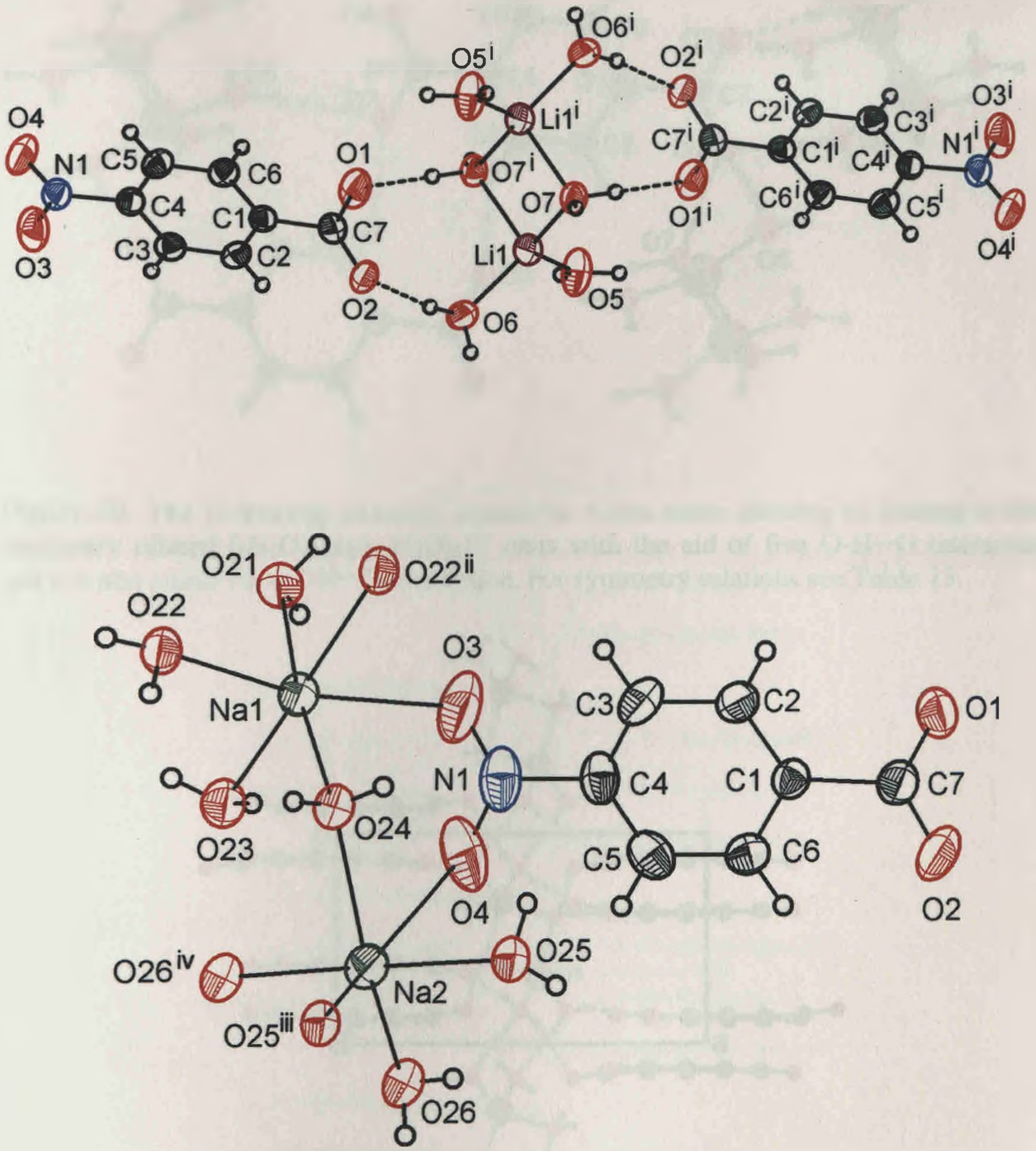

Figure 27 - Crystal structure of $[(H_2O)_4Li_2(\mu\text{-}H_2O)_2](4\text{-nba})_2$ **8** (top) and $[Na(4\text{-nba})(H_2O)_3]_n$ **9** (bottom) showing the coordination sphere of the central metal and atom-labeling scheme. Displacement ellipsoids are drawn at 50% probability level except for the H atoms, which are shown as circles of arbitrary radius. For clarity, the free uncoordinated 4-nba anion in **9** is not shown. Intramolecular H-bonding is shown as broken lines. Symmetry codes: i) –x+1, -y+1, -z. ii) -x+1, -y+1, -z+2 iii) -x+1, -y+2, -z+2 iv) -x+2, -y+2, -z+2

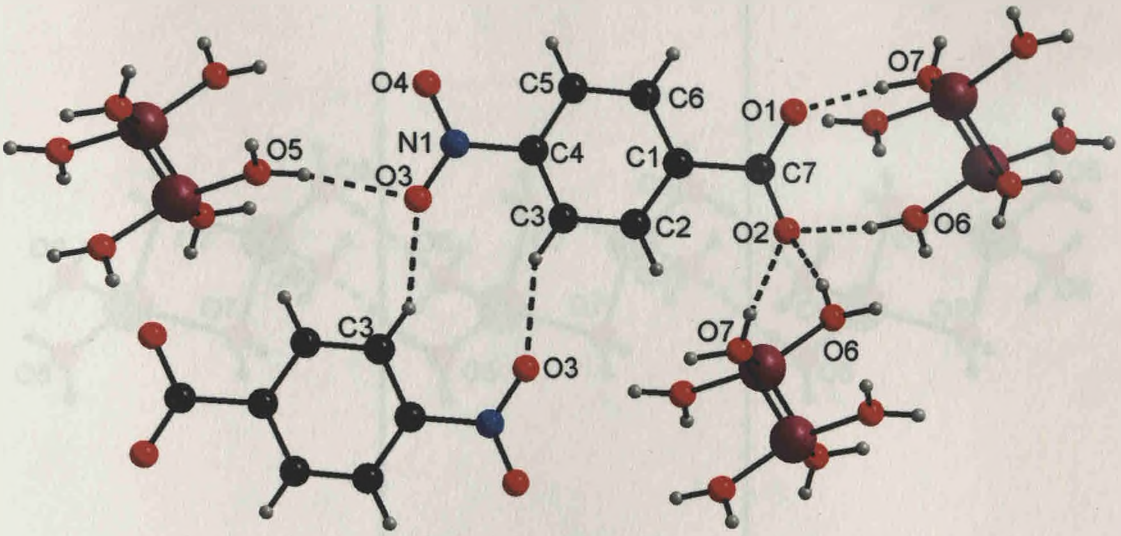

Figure 28- The H-bonding situation around the 4-nba anion showing its linking to three symmetry related $[(H_2O)_4Li_2(\mu\text{-}H_2O)_2]^{2+}$ units with the aid of five O-H···O interactions and a 4-nba anion via a C-H···O interaction. For symmetry relations see Table 13.

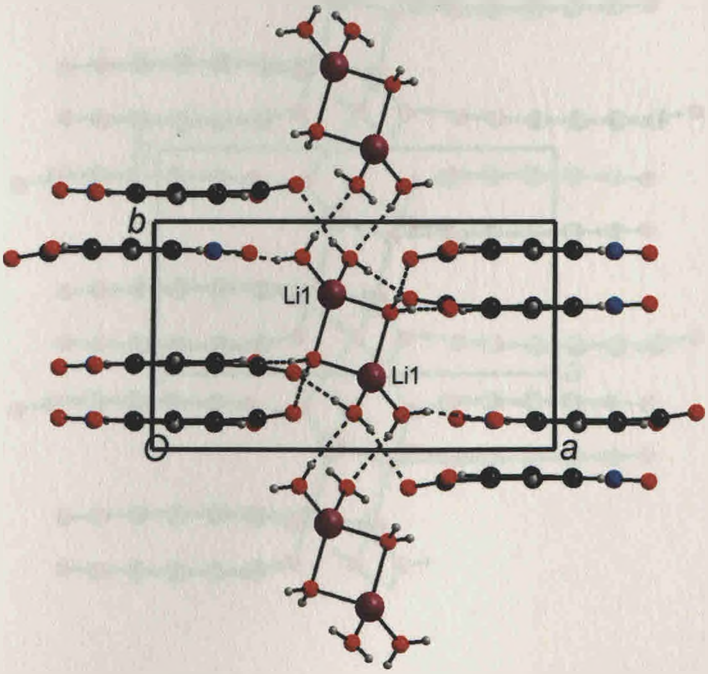

Figure 29- H-bonding situation around the dimeric cation showing its linking to eight different 4-nba anions and two symmetry elated cations.

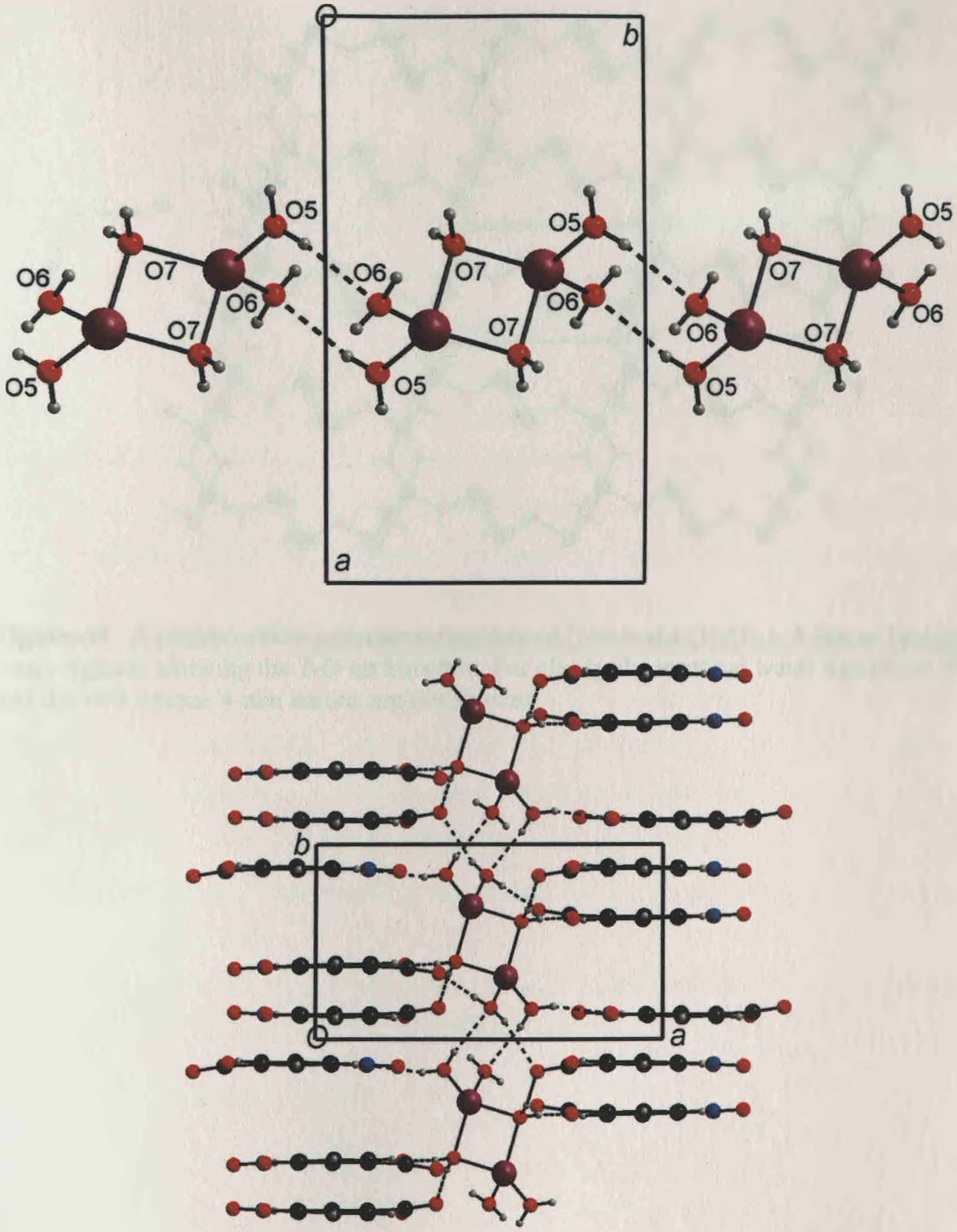

Figure 30- A portion of the supramolecular chain of $[(H_2O)_4Li_2(\mu\text{-}H_2O)_2]^{2+}$ cations in **8** extending along *b* axis (top). The cationic chain is flanked by 4-nitrobenzoate anions on either side resulting in the formation of alternating layers of catons and anions (bottom).

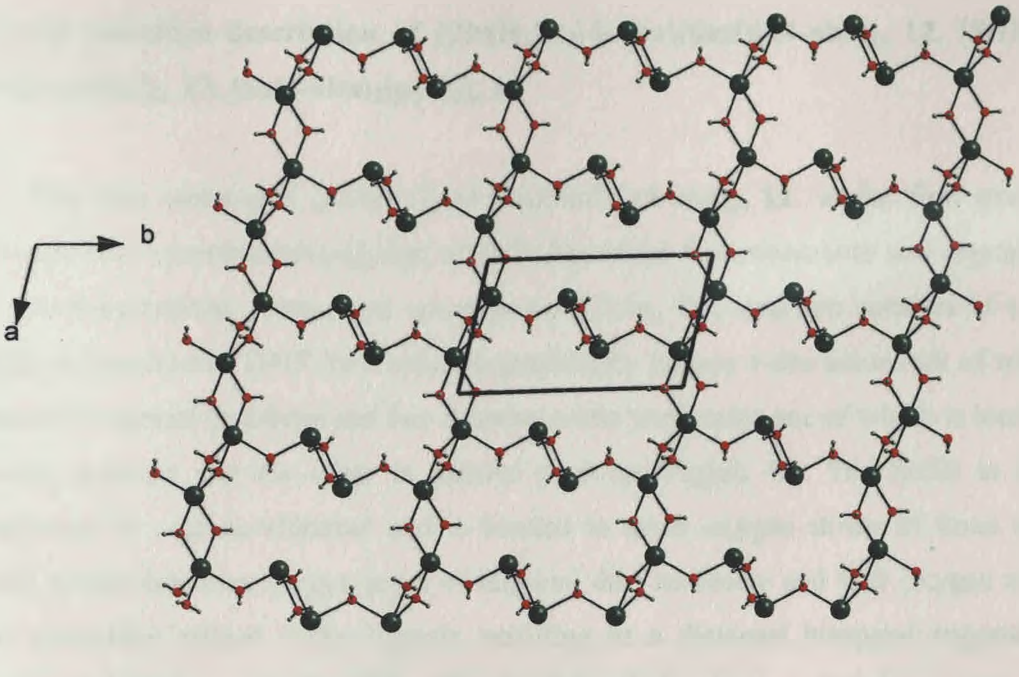

Figure 31- A portion of the polymeric structure of $[Na(4\text{-}nba)(H_2O)_3]_n$ **9** due to bridging water ligands showing the 2-D architecture. For clarity the terminal water ligands on Na and the two unique 4-nba anions are not shown.

Crystal structure description of [[Sr(H$_2$O)$_3$(4-nba)(dmf)].(4-nba)]$_n$ 12, [Sr(H$_2$O)(4-nba)$_2$(nmf)$_{1.5}$]$_n$ 13, [Sr(4-nba)$_2$(pyr)$_2$]$_n$ 14

The title compound [[Sr(H$_2$O)$_3$(4-nba)(dmf)].(4-nba)]$_n$ **12** is the first structurally characterized coordination polymer of Sr(II) based on 4-nitrobenzoate and crystallizes in the centrosymmetric monoclinic space group *P2$_1$/m*. The structure consists of a central Sr(II), a coordinated DMF, two crystallographically unique 4-nba anions all of which are situated in special positions and two terminal water molecules one of which is located in a special position and the other in general position (Figure 1a). The Sr(II) in the title compound is octa coordinated and is bonded to three oxygen atoms of three terminal water molecules, one oxygen atom of terminal dmf molecule and four oxygen atoms of two symmetry related 4-nba ligands, resulting in a distorted bicapped trigonal prism {SrO$_8$} polyhedron (Figure 32b) . The Sr-O bond distances scatter in a narrow range between 2.459(2) and 2.6869(13)(11) Å and are in good agreement with reported values [177] (Table 15). The O-Sr-O bond angles vary in a wide range between 48.54(5) and 154.15(3) (O(1)-Sr(1)-O(1) = 48.54(5) and O(21)-Sr(1)-O(1) = 154.15(3)) (Table 16). The two crystallographically independent 4-nba anions in each formula unit coordinate to the central Sr(II) in tetradentate bridging mode viz. (μ_3-η^2:η^2). This results into linking of two [Sr(H$_2$O)$_3$(dmf)]$^{2+}$ units into a one dimensional coordination polymer extending along a-axis (Figure 33).

Table 15- Selected bond distances (Å) and bond angles (°) for [Sr(H$_2$O)$_3$(4-nba)(DMF)]·4-nba **12**, [Sr(H$_2$O)(4-nba)$_2$(nmf)$_{1.5}$] **13** and [Sr(4-nba)$_2$(pyr)$_2$] **14**

[Sr(H$_2$O)$_3$(4-nba)(dmf)]·4-nba **12**

Sr(1)-O(21)	2.459(2)	Sr(1)-O(31)	2.6203(14)
Sr(1)-O(1)	2.5649(13)	Sr(1)-O(31)^{i}	2.6203(14)
Sr(1)-O(1)^{i}	2.5649(13)	Sr(1)-O(1)^{ii}	2.6869(13)
Sr(1)-O(32)	2.565(2)	Sr(1)-O(1)^{iii}	2.6869(13)
Sr(1)-Sr(1)			
O(21)-Sr(1)-O(1)	88.17(3)	O(31)-Sr(1)-O(31)^{i}	74.75(6)
O(21)-Sr(1)-O(1)^{i}	88.17(3)	O(21)-Sr(1)-O(1)^{ii}	154.15(3)
O(1)-Sr(1)-O(1)^{i}	138.28(6)	O(1)-Sr(1)-O(1)^{ii}	117.66(3)
O(21)-Sr(1)-O(32)	101.04(7)	O(1)^{i}-Sr(1)-O(1)^{ii}	72.31(4)
O(1)-Sr(1)-O(32)	70.0(3)	O(32)-Sr(1)-O(1)^{ii}	88.30(5)
O(1)^{i}-Sr(1)-O(32)	70.0(3)	O(31)-Sr(1)-O(1)^{ii}	74.26(4)
O(21)-Sr(1)-O(31)	84.09(5)	O(31)^{i}-Sr(1)-O(1)^{ii}	103.16(4)
O(1)-Sr(1)-O(31)	147.50(4)	O(21)-Sr(1)-O(1)^{iii}	154.15(3)
O(1)^{i}-Sr(1)-O(31)	73.08(4)	O(1)-Sr(1)-O(1)^{iii}	72.31(4)
O(32)-Sr(1)-O(31)	142.48(3)	O(1)^{i}-Sr(1)-O(1)^{iii}	117.66(3)

O(21)-Sr(1)-O(31)^{i}	84.09(5)	O(32)-Sr(1)-O(1)^{iii}	88.30(5)
O(1)-Sr(1)-O(31)^{i}	73.08(4)	O(31)-Sr(1)-O(1)^{iii}	103.16(4)
O(1)^{i}-Sr(1)-O(31)^{i}	147.50(4)	O(31)^{i}-Sr(1)-O(1)^{iii}	74.26(4)
O(32)-Sr(1)-O(31)^{i}	142.48(3)	O(1)^{ii}-Sr(1)-O(1)^{iii}	48.54(5)

[Sr(H_2O)(4-nba)$_2$(nmf)$_{1.5}$] **13**

Sr(1)-O(21)	2.4788(19)	Sr(1)-O(1)^{iv}	2.6565(16)
Sr(1)-O(11)	2.5072(17)	Sr(1)-O(31)	2.6720(18)
Sr(1)-O(41)	2.631(2)	Sr(1)-O(2)	2.6846(16)
Sr(1)-O(1)	2.6459(16)	Sr(1)-O(2)^{v}	2.6914(17)
Sr(1)-Sr(1)^{v}	4.1272(4)	Sr(1)-Sr(1)^{iv}	4.2864(5)
O(21)-Sr(1)-O(11)	90.93(7)	O(1)^{iv}-Sr(1)-O(31)	142.82(5)
O(21)-Sr(1)-O(41)	77.92(7)	O(21)-Sr(1)-O(2)	143.88(7)
O(11)-Sr(1)-O(41)	136.89(7)	O(11)-Sr(1)-O(2)	101.95(6)
O(21)-Sr(1)-O(1)	153.88(7)	O(41)-Sr(1)-O(2)	111.52(6)
O(11)-Sr(1)-O(1)	109.56(6)	O(1)-Sr(1)-O(2)	49.02(5)
O(41)-Sr(1)-O(1)	76.04(6)	O(1)^{iv}-Sr(1)-O(2)	115.88(5)
O(21)-Sr(1)-O(1)^{iv}	100.12(6)	O(31)-Sr(1)-O(2)	66.37(5)
O(11)-Sr(1)-O(1)^{iv}	72.79(6)	O(21)-Sr(1)-O(2)^{v}	81.30(6)
O(41)-Sr(1)-O(1)^{iv}	68.58(7)	O(11)-Sr(1)-O(2)^{v}	78.12(6)
O(1)-Sr(1)-O(1)^{iv}	72.12(5)	O(41)-Sr(1)-O(2)^{v}	138.76(7)
O(21)-Sr(1)-O(31)	83.50(6)	O(1)-Sr(1)-O(2)^{v}	117.87(5)
O(11)-Sr(1)-O(31)	144.40(6)	O(1)^{iv}-Sr(1)-O(2)^{v}	150.88(5)
O(41)-Sr(1)-O(31)	76.23(7)	O(31)-Sr(1)-O(2)^{v}	66.28(5)
O(1)-Sr(1)-O(31)	88.38(4)	O(2)-Sr(1)-O(1)^{v}	68.89(6)

[Sr(4-nba)$_2$(pyr)$_2$] **14**

Sr(1)-O(2)^{vi}	2.5220(15)	Sr(1)-N(11)^{viii}	2.6847(19)
Sr(1)-O(2)^{vii}	2.5220(15)	Sr(1)-N(11)	2.6847(19)
Sr(1)-O(1)^{viii}	2.6667(15)	Sr(1)-O(2)	2.7231(15)
Sr(1)-O(1)	2.6667(15)	Sr(1)-O(2)^{viii}	2.7231(15)
Sr(1)-Sr(1)^{vii}	4.3375(3)	Sr(1)-Sr(1)^{ix}	4.3375(3)
O(2)^{vi}-Sr(1)-O(2)^{vii}	92.61(8)	N(11)^{viii}-Sr(1)-N(11)	70.05(9)
O(2)^{vi}-Sr(1)-O(1)^{viii}	114.33(5)	O(2)^{vi}-Sr(1)-O(2)	104.01(4)
O(2)^{vii}-Sr(1)-O(1)^{viii}	86.80(5)	O(2)^{vii}-Sr(1)-O(2)	68.48(5)
O(2)^{vi}-Sr(1)-O(1)	86.80(5)	O(1)^{viii}-Sr(1)-O(2)	135.13(5)
O(2)^{vii}-Sr(1)-O(1)	114.33(5)	O(1)-Sr(1)-O(2)	48.53(5)
O(1)^{viii}-Sr(1)-O(1)	150.13(7)	N(11)^{viii}-Sr(1)-O(2)	77.32(5)
O(2)^{vi}-Sr(1)-N(11)^{viii}	168.10(6)	N(11)-Sr(1)-O(2)	111.56(5)
O(2)^{vii}-Sr(1)-N(11)^{viii}	98.80(6)	O(2)^{vi}-Sr(1)-O(2)^{viii}	68.48(5)
O(1)^{viii}-Sr(1)-N(11)^{viii}	69.99(5)	O(2)^{vii}-Sr(1)-O(2)^{viii}	104.01(4)
O(1)-Sr(1)-N(11)^{viii}	85.41(5)	O(1)^{viii}-Sr(1)-O(2)^{viii}	48.53(5)
O(2)^{vi}-Sr(1)-N(11)	98.80(6)	O(1)-Sr(1)-O(2)^{viii}	135.13(5)
O(2)^{vii}-Sr(1)-N(11)	168.10(6)	N(11)^{viii}-Sr(1)-O(2)^{viii}	111.56(5)
O(1)^{viii}-Sr(1)-N(11)	85.41(5)	N(11)-Sr(1)-O(2)^{viii}	77.32(5)
O(1)-Sr(1)-N(11)	69.99(5)	O(2)-Sr(1)-O(2)^{viii}	169.64(7)

Symmetry transformations used to generate equivalent atoms. Symmetry codes i) x, -y+1/2, z ii) -x+2, y-1/2, -z+1 iii) -x+2, -y+1, -z+1 iv) -x+1, -y+1, -z+2 v) –x+1, y, -z+3/2 vi) x, -y+1, z-1/2 vii) -x+1, -y+1, -z+1 viii) -x+1, y, -z+1/2 ix) -x+1, -y+1, -z

Table 16 - H-bonding geometry (Å, °) for $[Sr(H_2O)_3(4\text{-nba})(dmf)]\cdot 4\text{-nba}$ **12**, $[Sr(H_2O)(4\text{-nba})_2(NMF)_{1.5}]$ **13** and $[Sr(4\text{-nba})_2(Pyr)_2]$ **14**

D-H···A	d(D-H)	D(H···A)	D(D···A)	<DHA	Symmetry Code
$[Sr(H_2O)_3(4\text{-nba})(DMF)]\cdot 4\text{-nba}$ **12**					
O31-H10···O11	0.834	1.961	2.793	176	x, y-1, z
O31-H20···O12	0.938	1.793	2.721	170	-x+1, -y+1,-z+1
O32-H30···O31	0.883	1.993	2.851	164	-x+2, -y,-z+1
$[Sr(H_2O)(4\text{-nba})_2(NMF)_{1.5}]$ **13**					
N21-H1N···O14	0.860	2.520	3.273	147	-x+3/2, -y+1/2,-z+2
N31-H2N···O41	0.860	2.314	3.099	152	-x+1, y,-z+3/2
N31-H2N···O12	0.860	2.603	3.173	125	-x+1, y+1,-z+3/2
O41-H10···O12	0.800	2.035	2.816	166	x, y+1, z
O41-H20···O12	0.855	1.935	2.750	159	-x+1, -y+1, -z+2
$[Sr(4\text{-nba})_2(Pyr)_2]$ **14**					
N12-H12N···O1	0.880	2.158	2.807	130.09	x, y, z
N12-H12N···O4	0.880	2.494	3.104	127.01	-x+3/2, -y+1/2, -z+2

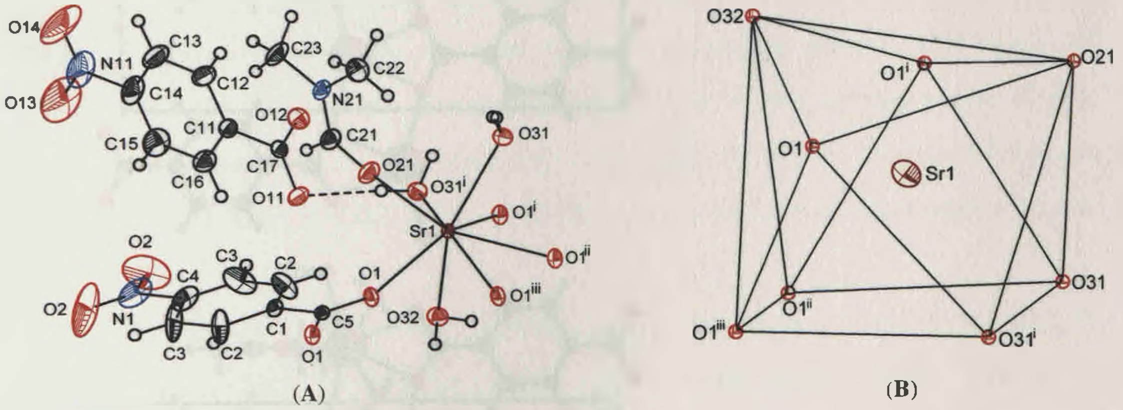

Figure 32- (A) Crystal structure of $[Sr(H_2O)_3(DMF)(4\text{-nba})](4\text{-nba})$ showing the atom labeling scheme. Displacement ellipsoids are drawn at 50% probability level except for the H atoms, which are shown as circles of arbitrary radius. Intramolecular H-bonding is shown as broken lines. (B) The distorted square antiprismatic $\{SrO_8\}$ coordination polyhedron around Sr. Symmetry code: (i) x, -y+1/2, z; (ii) –x+2, y-1/2, -z+1; (iii) –x+2, -y+1/2, -z+1

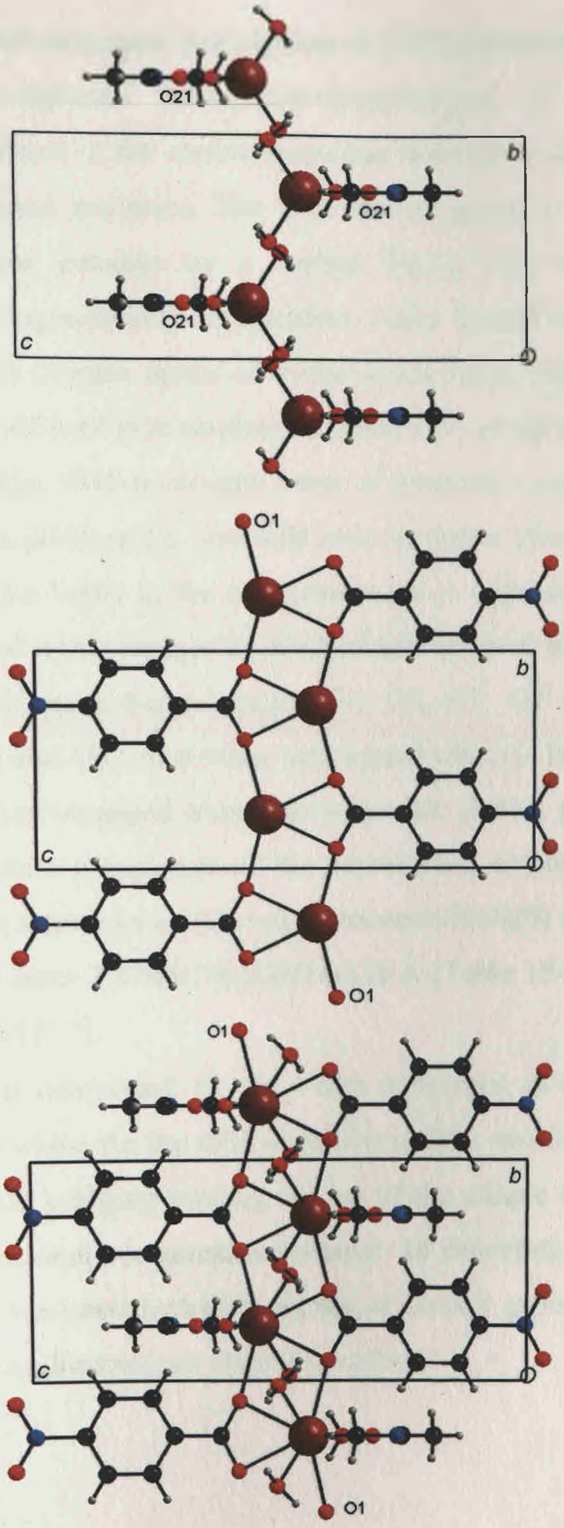

Figure 33- (top) Only terminal ligands around Sr(II) are shown. (middle) The one dimensional chain due to the bridging tetradentate ligation of 4-nba (terminal ligands are not shown). (Bottom) Both terminal and bridging ligands around Sr(II) are shown.

Crystal structure description of $[Sr(H_2O)(4\text{-}nba)_2(nmf)_{1.5}]_n$ 13

Compound $[Sr(H_2O)(4\text{-}nba)_2(nmf)_{1.5}]_n$ **13** is a one dimensional polymer and crystallizes in the centrosymmetric monoclinic space group *C2/c* with all atoms situated in general positions. The C22 methyl group is disordered due to hydrogen atoms. Its structure consists of a central Sr(II), one coordinated water molecules and two crystallographically independent 4-nba ligands and two nmf ligand (Figure 34-35). The O1, O2 oxygen atoms of 4-nba anion are μ_3-tetradentate and are bridging. O21 oxygen atoms of nmf is monodentate while O31 oxygen atom of nmf is bridging and is on two fold axis. O41 is oxygen atom of terminal water. The Oxygen atom O31 of nmf is on special position i.e. two fold axis or mirror plane and is common two Sr atoms (Figure 36). The Sr(II) in the title compound is eight coordinated and is bonded to one oxygen atom of water molecules (O41 of one terminal water molecule) and five oxygen atoms of four different 4-nba ligands (O1, O2, $O1^i$, $O2^i$ and O11) and O21 of one terminal nmf ligand and O31 of another nmf ligand which is located on two fold axis thus resulting in a distorted bicapped triangular prismatic $\{SrO_8\}$ polyhedron around Sr1 (Figure 37). The geometric parameters of the carboxylate anions are in the normal range. The O-Sr-O angles scatter in a wide range between 49.02(5) and 153.88(7)°. The Sr-O distances in **13** range from 2.4788(19)-2.6914(17) Å (Table 15-16) and are in agreement with literature values [177].

In compound **13** the 4-nba is bridged in a tetradentate μ_3-η^2:η^2 bridging binding mode while the the O31 of nmf is anf the two fold axis (Figure 38-39). The net result of the this bridging binding modes of the unique 4-nba and nmf ligand results into a one dimensional coordination polymer **13** extending along *a*-axis (Figure 40-41). Because of the disordered hydrogen atoms of methyl group of nmf molecules detailed hydrogen bonding interactions are not described.

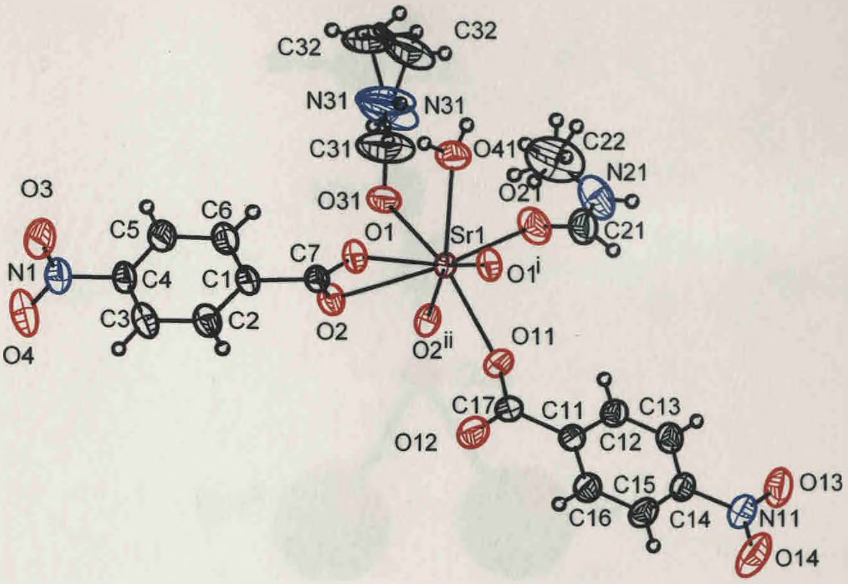

Figure 34- Crystal structure of $[Sr(H_2O)(4\text{-nba})_2(nmf)_{1.5}]_n$ **13** showing the atom labeling scheme. Displacement ellipsoids are drawn at 50% probability level except for the H atoms, which are shown as circles of arbitrary radius. Intramolecular H-bonding is not shown as hydrogen atoms on methyl group of nmf are disordered. (N31, C32 H atoms on C22 are disordered). Symmetry codes: i) -x+1, -y+1, -z+2 ii) –x+1, y, -z+3/2

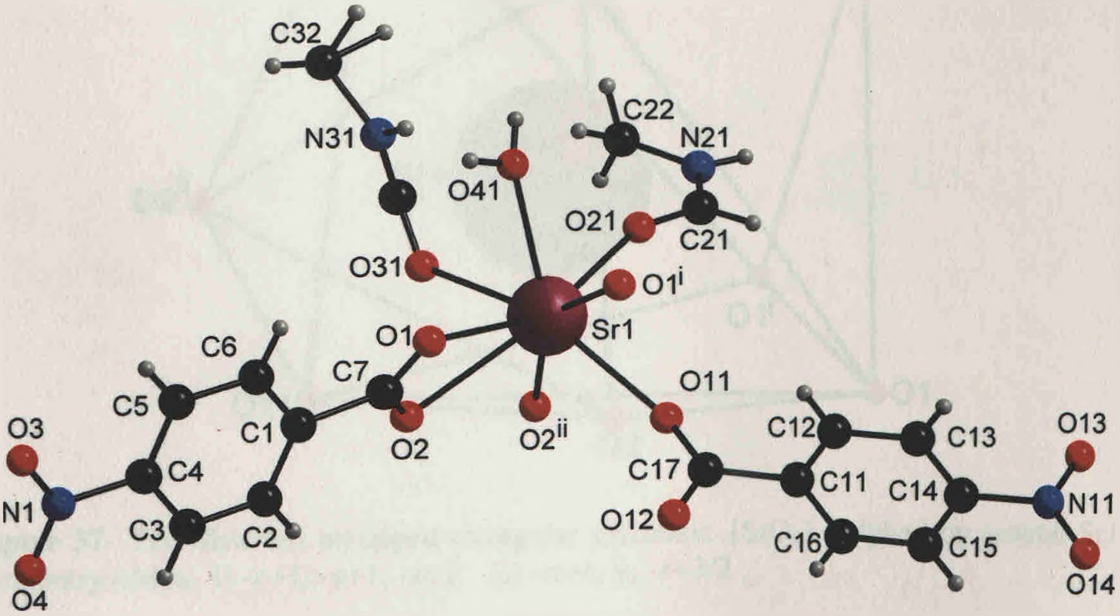

Figure 35- The coordination sphere of Sr1 in $[Sr(H_2O)(4\text{-nba})_2(nmf)_{1.5}]_n$ **13**. For clarity disordered atoms are not shown. Symmetry codes: i) -x+1, -y+1, -z+2 ii) –x+1, y, -z+3/2

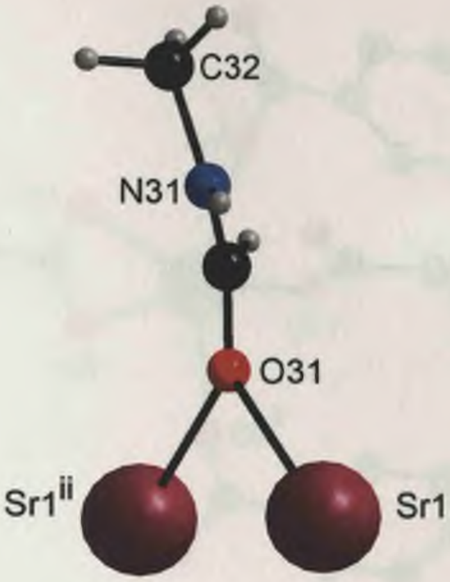

Figure 36- The O31 of the nmf is situated on a twofold axis is common two Sr atoms. Symmetry codes: ii) –x+1, y, -z+3/2

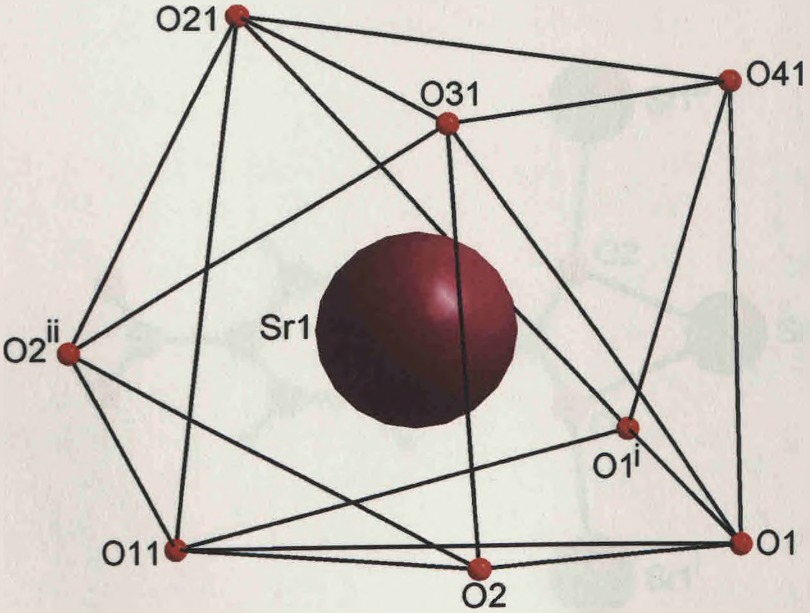

Figure 37- The distorted bicapped triangular prismatic {SrO_8} polyhedron around Sr1. Symmetry codes: i) -x+1, -y+1, -z+2 ii) –x+1, y, -z+3/2

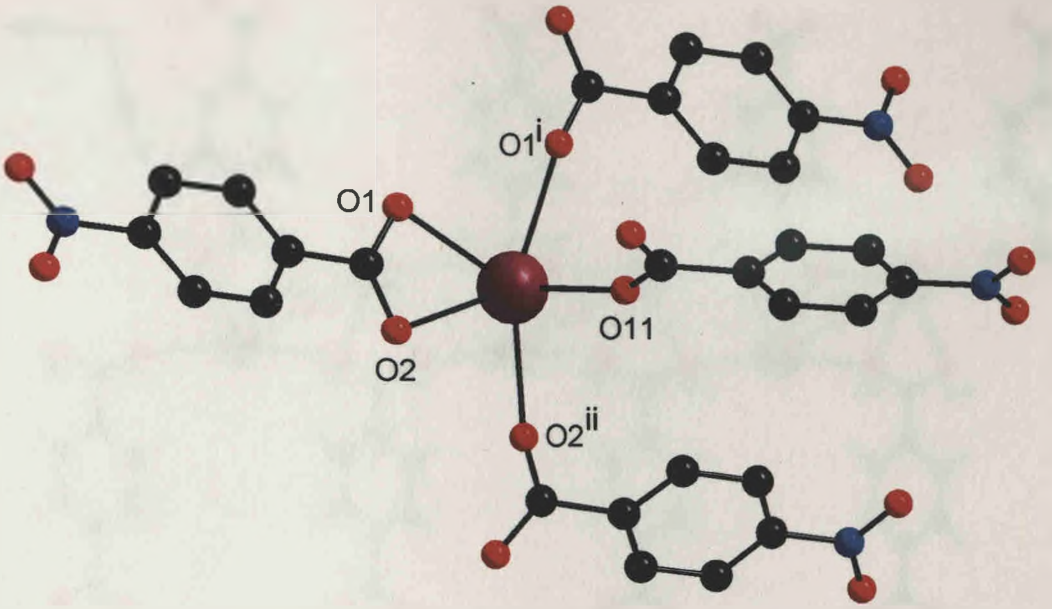

Figure 38- A view showing the four different 4-nba anions O1, O2, O1^i, O2^{ii} and O11 (monodentate 4-nba) in $[Sr(H_2O)(4\text{-nba})_2(nmf)_{1.5}]_n$ **13**. The O21, O31 and O41 coordination are not shown. Symmetry codes: i) -x+1, -y+1, -z+2 ii) –x+1, y, -z+3/2

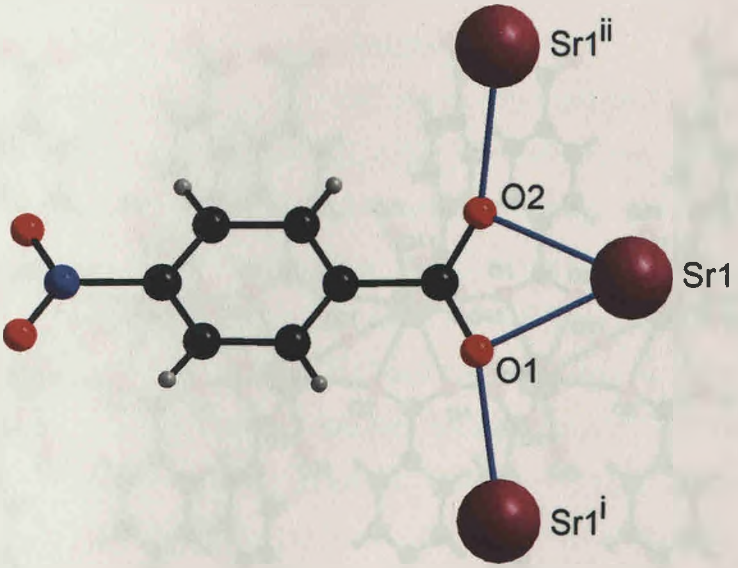

Figure 39- Binding mode of 4-nba in **13** showing one 4-nba (O1,O2) functions as a μ_3-tetradentate ligand in $[Sr(H_2O)(4\text{-nba})_2(nmf)_{1.5}]_n$ **13**. Symmetry codes: i) -x+1, -y+1, -z+2 ii) –x+1, y, -z+3/2

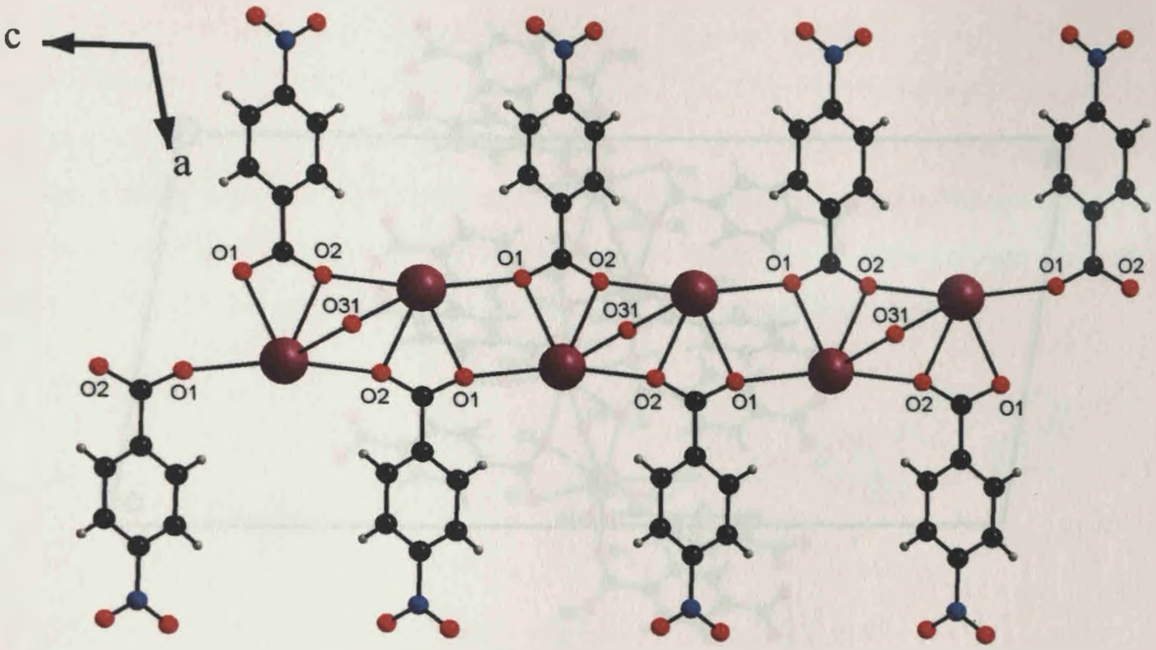

Figure 40- A portion of the $[Sr(H_2O)(4\text{-nba})_2(nmf)_{1.5}]_n$ **13** polymeric chain. For clarity, the O11 (monodentate 4-nba), O21 (terminal nmf) and O41 (terminal water) around Sr1 are not shown. Only the O31 atom of the disordered nmf is shown.

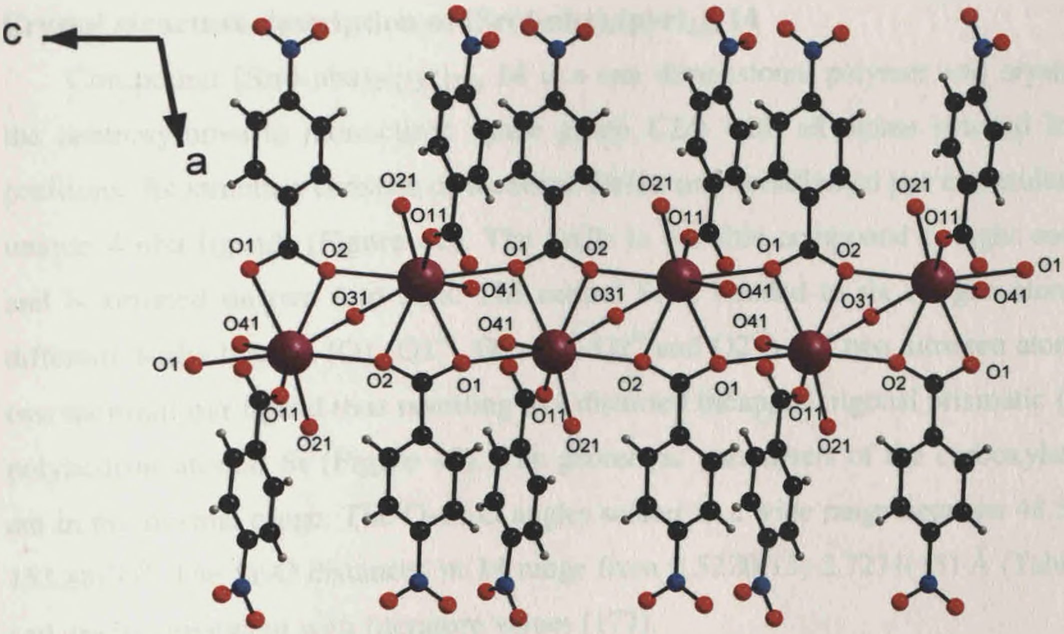

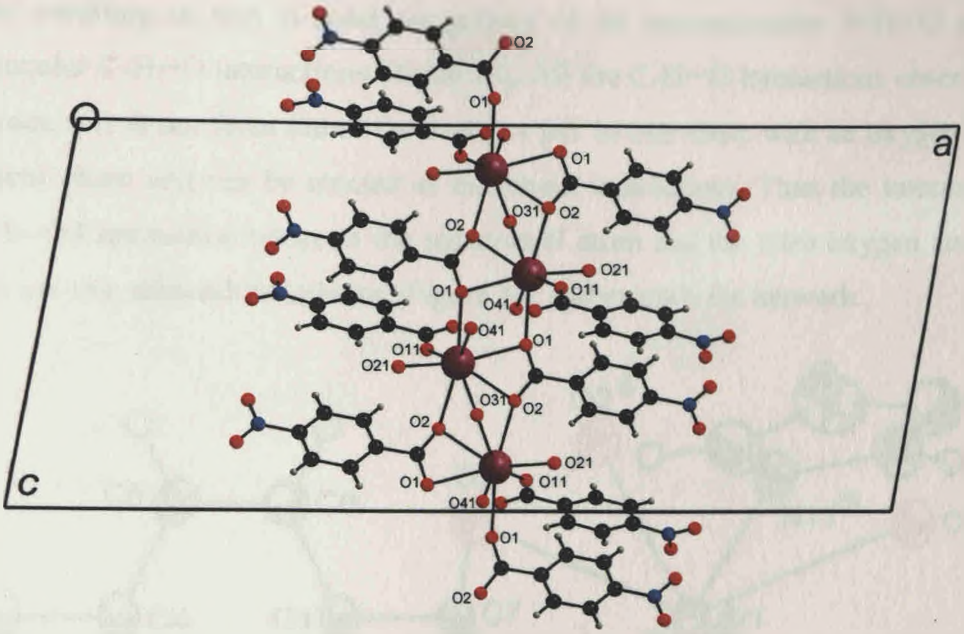

Figure 41- 1-D chain of $[Sr(H_2O)(4\text{-nba})_2(nmf)_{1.5}]_n$ **13** showing all the eight O donore around Sr1. For the first NMF only the O21 is shown. For the second NMF only the O31 is shown and for the coordinated water only the O41 is shown(top) and another view of 1-D cahin along b-axis (bottom). Symmetry codes: i) -x+1, -y+1, -z+2 ii) –x+1, y, -z+3/2

Crystal structure description of $[Sr(4\text{-nba})_2(pyr)_2]_n$ 14

Compound $[Sr(4\text{-nba})_2(pyr)_2]_n$ **14** is a one dimensional polymer and crystallizes in the centrosymmetric monoclinic space group *C2/c* with all atoms situated in general positions. Its structure consists of a central Sr(II), one coordinated pyr molecules and one unique 4-nba ligands (Figure 42). The Sr(II) in the title compound is eight coordinated and is situated on two fold axis. The central Sr is bonded to six oxygen atom of four different 4-nba ligands ($O1$, $O1^{iii}$, $O2$, $O2^{i}$, $O2^{ii}$ and $O2^{iii}$) and two nitrogen atom N11 of two terminal pyr ligand thus resulting in a distorted bicapped trigonal prismatic $\{SrO_6N_2\}$ polyhedron around Sr (Figure 43). The geometric parameters of the carboxylate anions are in the normal range. The O-Sr-O angles scatter in a wide range between 48.53(5) and 153.88(7)°. The Sr-O distances in **14** range from 2.5220(15)-2.7231(15) Å (Table 15-16) and are in agreement with literature values [177].

In the $[Sr(4\text{-nba})_2(pyr)_2]_n$ **14**, the 4-nba anions binds to two Sr atoms in μ_2-η^2:η^1) (Figure 44). The net result of the this bridging binding modes of the unique 4-nba ligands in **14** results into a one dimensional coordination polymer extending along *a*-axis (Figure 45). A scrutiny of the crystal structure of **14** reveals several weak secondary interactions. The amine hydrogen atom in pyrazole and four hydrogen atoms (two each) from 4-nba and pyrazole function as H-donors while the carboxylate oxygen atom function as H-acceptors resulting in two H-bond comprising of an intramolecular N-H···O and two intermolecular C-H···O interactions (Table 16). All the C-H···O interactions observed in **5** are between a H donor from either the 4-nba or pyr in one chain with an oxygen atom in an adjacent chain and can be termed as interchain interactions. Thus the intermolecular C11-H11···O3 interaction between the pyrazole H atom and the nitro oxygen atom links two adjacent one dimensional chains (Figure 46) and extends the network.

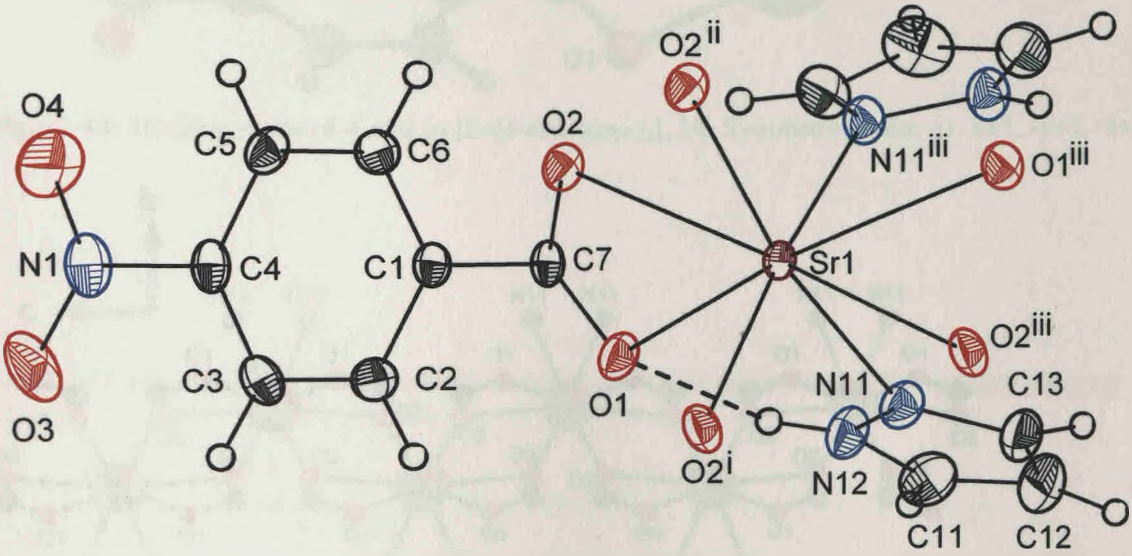

Figure 42- Crystal structure of $[Sr(4\text{-}nba)_2(pyr)_2]_n$ **14** showing the atom labeling scheme. Displacement ellipsoids are drawn at 50% probability level except for the H atoms, which are shown as circles of arbitrary radius. Intramolecular H-bonding is shown as dotted lines. Symmetry codes: i) -x+1, -y+1, -z+1 ii) -x+1, y, -z+1/2 iii) -x+1, -y+1, -z

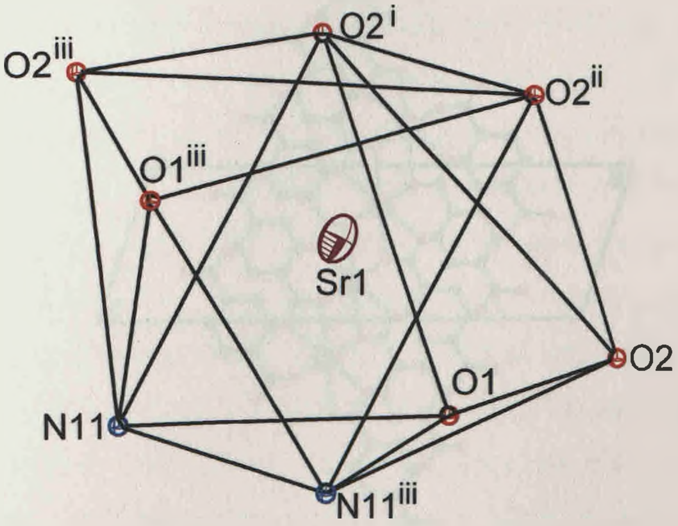

Figure 43- Distorted bicapped trigonal prismatic $\{SrO_6N_2\}$ polyhedron around Sr in 1-D polymer $[Sr(4\text{-}nba)_2(pyr)_2]_n$ **14**. Symmetry codes: i) -x+1, -y+1, -z+1 ii) -x+1, y, -z+1/2 iii) -x+1, -y+1, -z

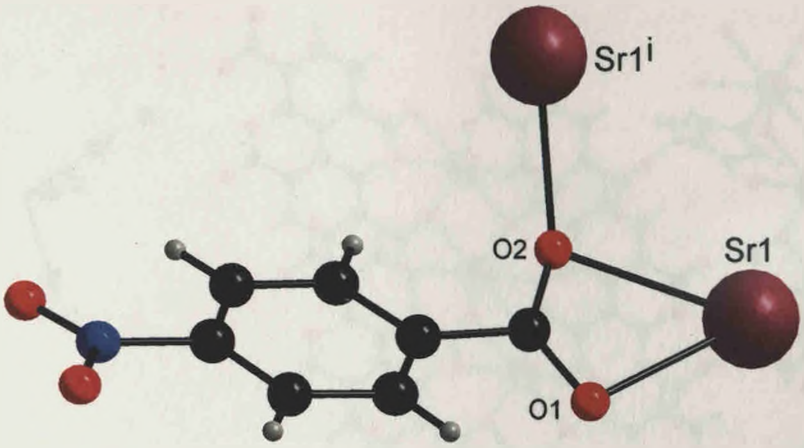

Figure 44- Binding mode of 4-nba in $[Sr(4\text{-}nba)_2(pyr)_2]_n$ **14**. Symmetry codes: i) -x+1, -y+1, -z+1

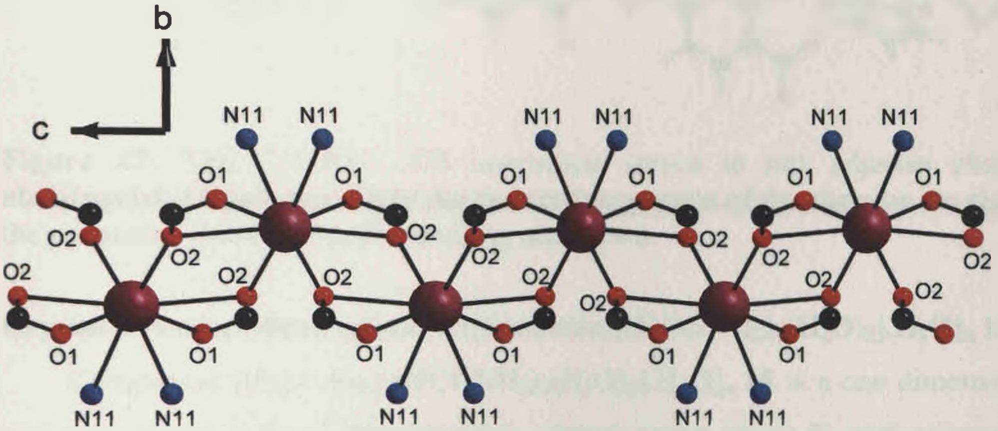

Figure 45- A portion of the $[Sr(4\text{-}nba)_2(pyr)_2]_n$ **14** polymeric chain showing only the bridging carboxylate portion of 4-nba and the terminal N atom of pyrazole.

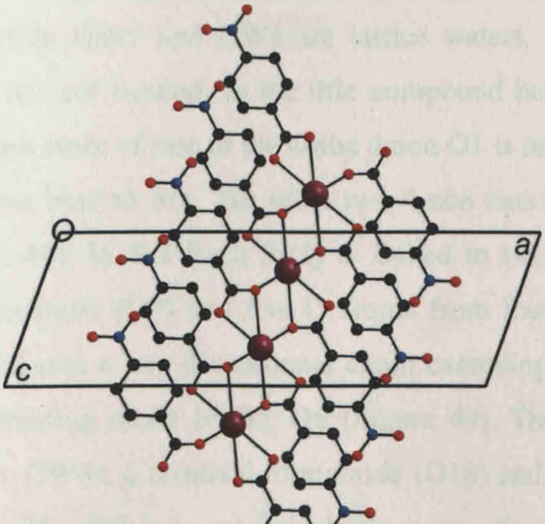

Figure 46- A portion of a chain showing only the bridging 4-nba ligands. Terminal pyrazole and the H-atoms of the aromatic ring of 4-nba are not shown for clarity.

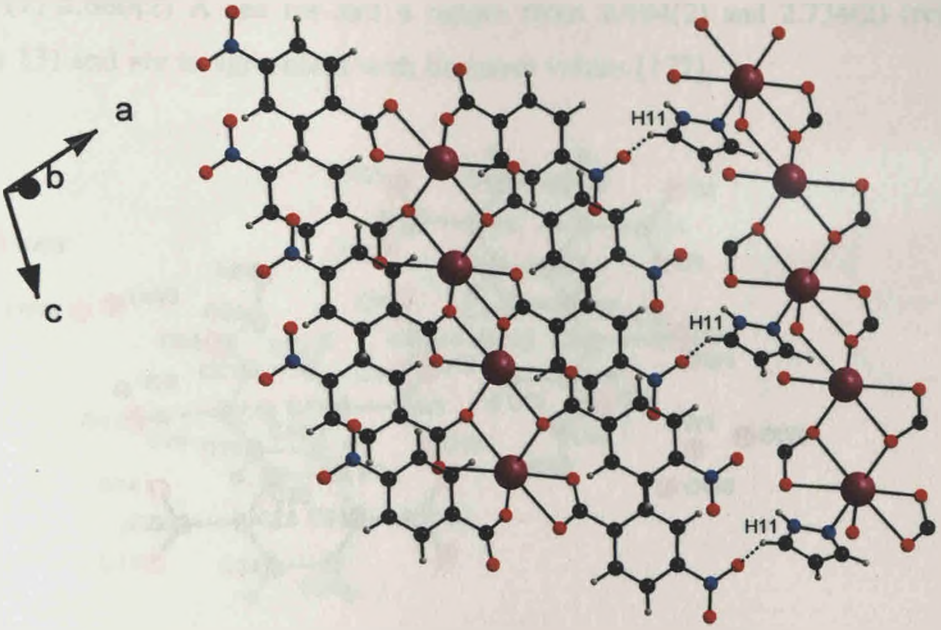

Figure 47- The C11-H11...O3 interaction serves to link adjacent chains in [Sr(4-nba)$_2$(pyr)$_2$]$_n$ **14** polymer. Only the carboxylate groups of the chain on the right and one of the pyrazoles (involved in H-bonding) are shown.

Crystal structure description of [[Sr(4-nba)$_2$(HCONH$_2$)$_2$(H$_2$O)$_2$].H$_2$O]$_n$ 15

Compound [[Sr(4-nba)$_2$(HCONH$_2$)$_2$(H$_2$O)$_2$].H$_2$O]$_n$ **15** is a one dimensional polymer and crystallizes in the centrosymmetric triclinic space group $P\bar{1}$ with all atoms situated in general positions. Its structure consists of two unique Sr(II), two coordinated formamide molecules, four unique 4-nba ligands and six water molecules (Figure 48). OW1-OW4 are terminal waters while OW5 and OW6 are lattice waters. The hydrogen atoms on water and formamide are not lacated. In the title compound both Sr1 and Sr2 are eight coordinated. The oxygen atom of one of the 4-nba anion O1 is monodentate and O5,O6 is μ_3-tetradentate and these bind to Sr1. The other two 4-nba ions behave similarly and are bonded to Sr2 (Figure 48). In Sr1 Each Sr(1) is linked to two terminal waters (OW1, OW2), a terminal formamide (O9) and five O atoms from four different 4-nba anions. The Sr1 ions are linked into a one dimensional chain extending along a axis due to the bridging tetradentate binding mode of O5, O6 (Figure 49). The Sr(2) is linked to two terminal waters (OW3, OW4), a terminal formamide (O18) and five O atoms from four different 4-nba anions. The Sr2 ions are linked into a one dimensional chain extending along a axis due to the bridging tetradentate binding mode of O10, O11 (Figure 50). The O-Sr1-O angles scatter in a wide range between 48.58(8) and 162.36(8)° while O-Sr2-O angles range from 48.68(8) and 160.87(8)°. The Sr1-O distances in **15** range from

2.483(2)-2.680(2) Å anf for Sr2 it ranges from 2.494(2) and 2.734(2) (refer appendix Table 13) and are in agreement with literature values [177].

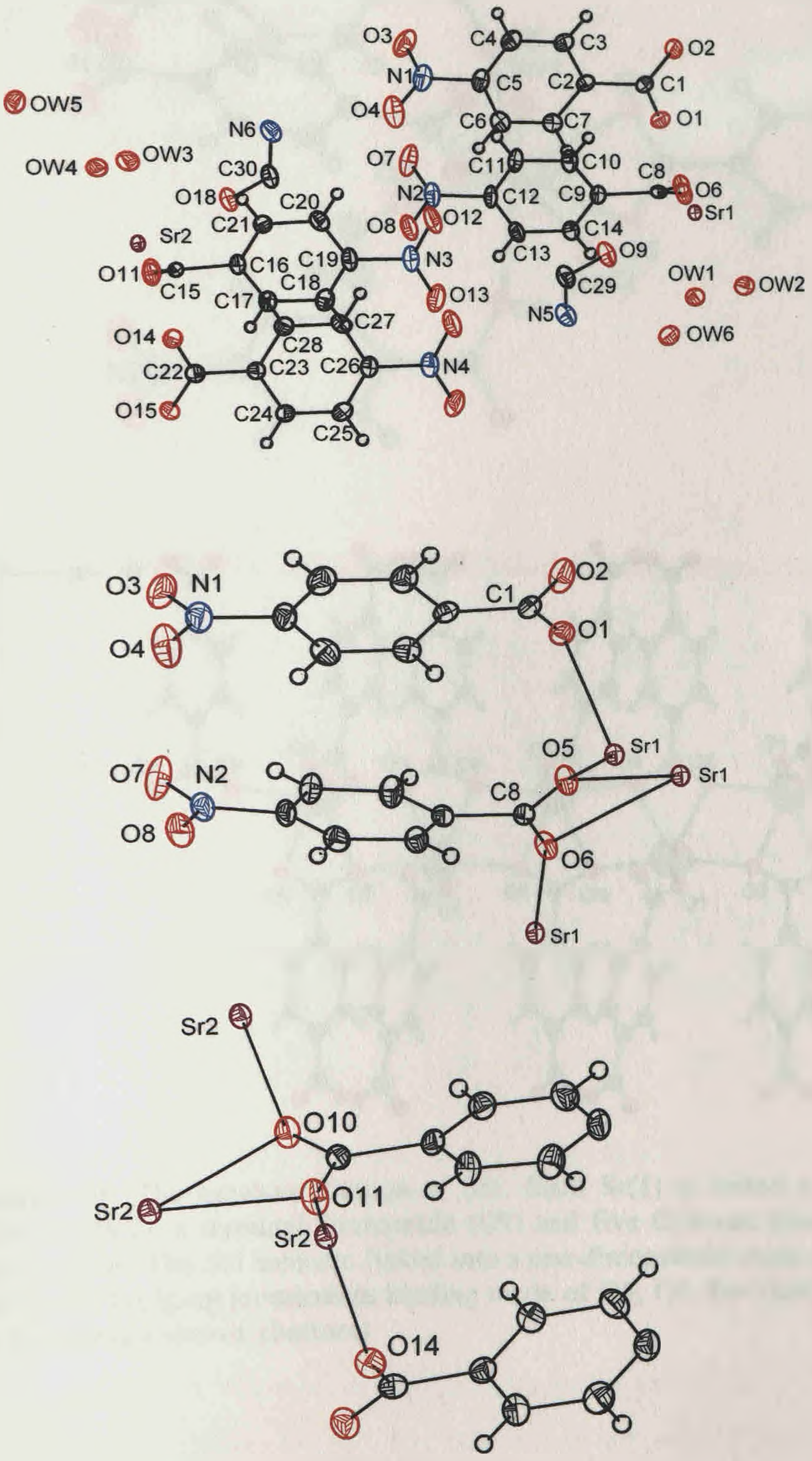

Figure 48- Structure consists of two unique Sr(II) ions, four unique 4-nba anions, two formamide molecules and six water molecules (O1W to O6W) (top); Binding mode of two of the unique 4-nba ligands are shown. O1 is monodentate and O5,O6 is μ_3-tetradentate and these bind to Sr1 (middle): The other two 4-nba ions behave similarly and are bonded to Sr2 (bottom)

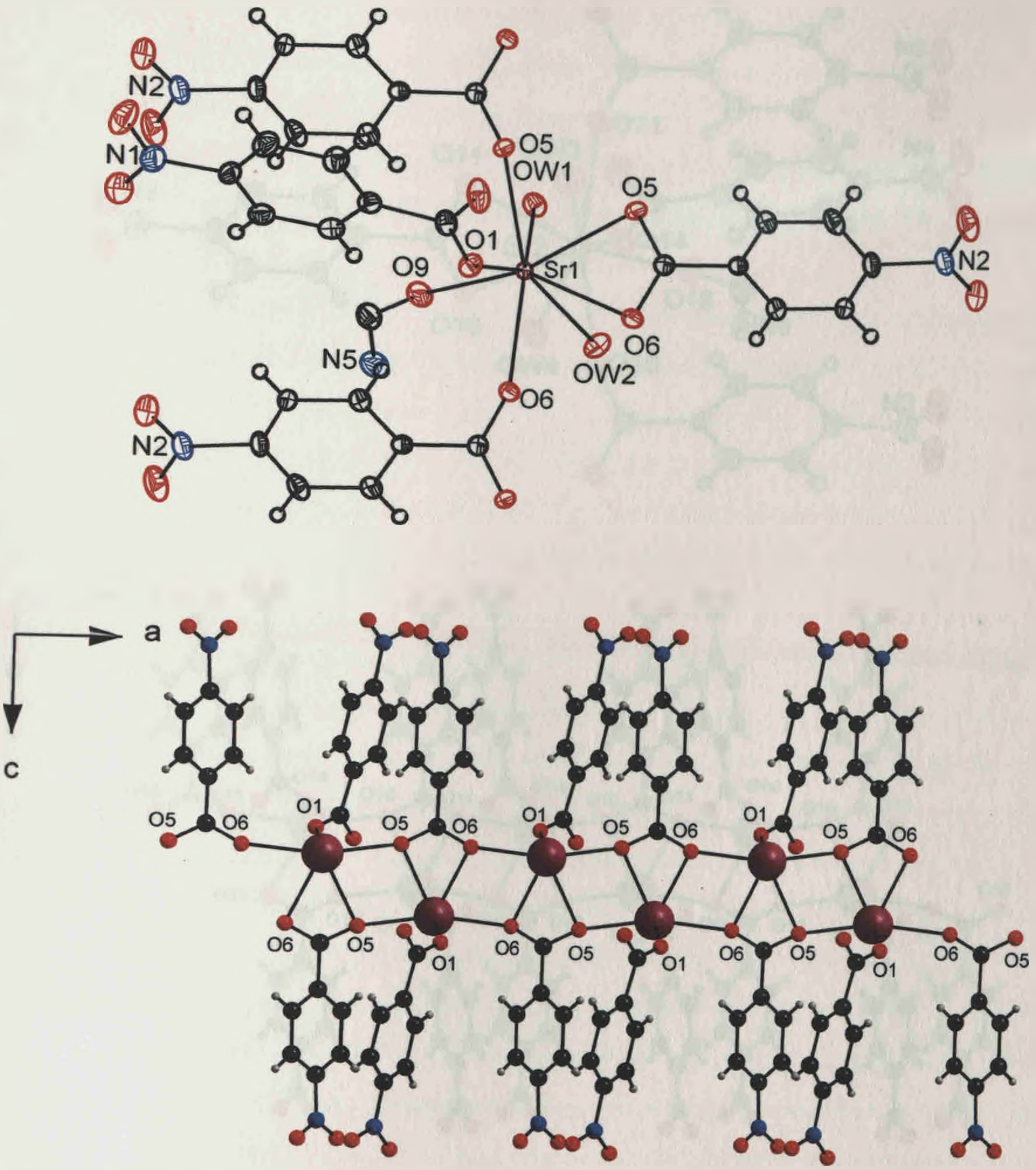

Figure 49- The octacoordination of Sr1. Each Sr(1) is linked to two terminal waters (OW1, OW2), a terminal formamide (O9) and five O atoms from four different 4-nba anions. (top) The Sr1 ions are linked into a one dimensional chain extending along a axis due to the bridging tetradentate binding mode of O5, O6. For clarity the terminal ligands on Sr1 are not shown. (bottom)

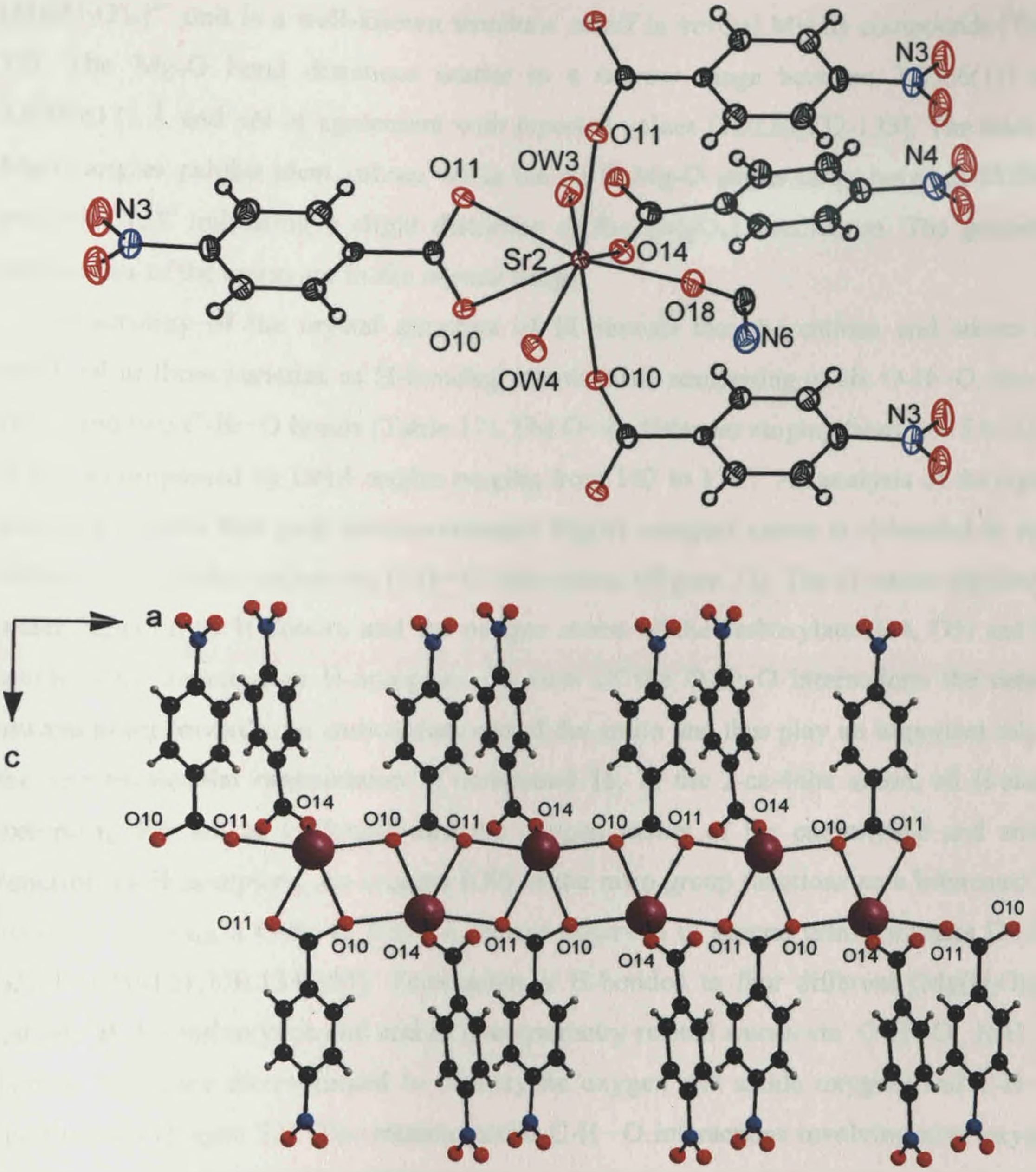

Figure 50- The octacoordination of Sr2. Each Sr(2) is linked to two terminal waters (OW3, OW4), a terminal formamide (O18) and five O atoms from four different 4-nba anions. (top) The Sr2 ions are linked into a one dimensional chain extending along a axis due to the bridging tetradentate binding mode of O10, O11. For clarity the terminal ligands on Sr2 are not shown. (bottom)

Crystal structure description of [Mg(H_2O)$_6$](2-ca-4nba)$_2$ 16

[Mg(H_2O)$_6$](2-ca-4nba)$_2$ **16** crystallizes in the centrosymmetric monoclinic space group *P2$_1$/c* and is the first structurally characterized alkaline earth salt of 2-ca-4nbaH. In **16** the Mg(II) is located on an inversion center, and the structure consists of an octahedral [Mg(H_2O)$_6$]$^{2+}$ cation and a 2-ca-4nba anion (Figure 51). The centrosymmetric

$[Mg(H_2O)_6]^{2+}$ unit is a well-known structural motif in several Mg(II) compounds (Table 17). The Mg-O bond distances scatter in a narrow range between 2.0566(11) and 2.0735(11) Å and are in agreement with reported values [120,39,132-135]. The trans O-Mg-O angles exhibit ideal values, while the cis O-Mg-O angles range between 85.03(5) and 94.97(5)° indicating a slight distortion of the $\{MgO_6\}$ octahedron. The geometric parameters of the anion are in the normal range.

A scrutiny of the crystal structure of **16** reveals that the cations and anions are involved in three varieties of H-bonding interactions, comprising of six O-H···O, two N-H···O and two C-H···O bonds (Table 17). The O···H distances ranging from 1.915 to 2.677 Å are accompanied by DHA angles ranging from 143 to 178°. An analysis of the crystal structure reveals that each hexacoordinated Mg(II) complex cation is H-bonded to eight different 2-ca-4nba anions via O-H···O interactions (Figure 52). The H atoms attached to water function as H-donors and the oxygen atoms of the carboxylate (O4, O5) and the amide (O6) function as H-acceptors. In view of the O-H···O interactions the cations always point towards the carboxylate end of the anion and thus play an important role in the supramolecular organization of compound **16**. In the 2-ca-4nba anion, all H-atoms excepting H6 act as H-donors and the oxygen atoms of the carboxylate and amide function as H-acceptors. An oxygen (O9) of the nitro group functions as a bifurcated H-acceptor forming a C-H···O bond, a feature observed in several nitrobenzoates [24-26, 63,117,119-121,130,133,169]. Each anion is H-bonded to four different $[Mg(H_2O)_6]^{2+}$ cations at the carboxylate end and to five symmetry related anions via O-H···O, N-H···O (amide hydrogen atoms linked to carboxylate oxygen and amide oxygen) and C-H···O interactions (Figure 52). The intramolecular C-H···O interactions involving nitro oxygen result in a head (nitro) to head (nitro) alignment of anions. Since the cations always point towards the carboxylate oxygen atoms due to the O-H···O interactions, a bilayer of anions sandwiched between layers of $[Mg(H_2O)_6]^{2+}$ cations is formed (Figure 53). The net result is the organization of cations and anions in the following sequence ··· $[Mg(H_2O)_6]^{2+}$ ··· $(2\text{-ca-4nba})^-$ ··· $(2\text{-ca-4nba})^-$ ··· $[Mg(H_2O)_6]^{2+}$ ··· along *a* axis.

Table 17- Selected bond distances (Å) and bond angles (°) for $[Mg(H_2O)_6](2\text{-ca-4nba})_2$ **16**

$[Mg(H_2O)_6](2\text{-ca-4nba})_2$ **16**			
Mg(1)-O(1)	2.0566(11)	Mg(1)-O(2)^{i}	2.0626(11)
Mg(1)-O(1)^{i}	2.0566(11)	Mg(1)-O(3)^{i}	2.0735(11)
Mg(1)-O(2)	2.0626(11)	Mg(1)-O(3)	2.0735(11)
O(1)-Mg(1)-O(1)^{i}	180.0(5)	O(1)^{i} -Mg(1)-O(3)^{i}	94.97(5)
O(1)-Mg(1)-O(2)	91.48(5)	O(2) -Mg(1)-O(3)^{i}	87.87(4)
O(1)^{i} -Mg(1)-O(2)	88.52(5)	O(2)^{i} -Mg(1)-O(3)^{i}	92.13(4)
O(1)-Mg(1)-O(2)^{i}	88.52(5)	O(1) -Mg(1)-O(3)	94.97(5)
O(1)^{i} -Mg(1)-O(2)^{i}	91.48(5)	O(1)^{i} -Mg(1)-O(3)	85.03(5)
O(2) -Mg(1)-O(2)^{i}	180	O(2) -Mg(1)-O(3)	92.13(4)
O(1) -Mg(1)-O(3)^{i}	85.03(5)	O(2)^{i} -Mg(1)-O(3)	87.87(4)
O(3)^{i} -Mg(1)-O(3)	180.0(3)		

Symmetry codes i)-x+2, -y, -z+1

Table 18- Hydrogen- bonding geometry (Å, °) for compound $[Mg(H_2O)_6](2\text{-ca-4nba})_2$ **16**

D-H---A	d(D-H)	d(H---A)	D(D---A)	<DHA	Symmetry code
$[Mg(H_2O)_6](2\text{-ca-4nba})_2$ **16**					
O1-H1···O5	0.820	1.950	2.770	178	-x+2, -y+1, -z+1
O1-H2···O4	0.820	1.915	2.717	166	-x+2, y-1/2,- z+3/2
O2-H1···O4	0.820	2.007	2.826	177	-x+2,-y+1,-z+1
O2-H2···O4	0.820	1.992	2.807	172	x, y, z
O3-H1···O6	0.820	1.919	2.738	177	x, y, z
O3-H2···O5	0.820	2.259	2.99	149	x, -y+1/2, z+1/2
N2-H1···O5	0.860	2.118	2.921	155	x, -y+1/2, z+1/2
N2-H2···O6	0.860	2.176	2.907	143	X,-y+1/2, z+1/2
C3-H3···O9	0.930	2.677	3.508	149	-x+1, y-1/2, -z+3/2
C5-H5···O9	0.930	2.420	3.321	163	-x+1, -y+2,- z+1

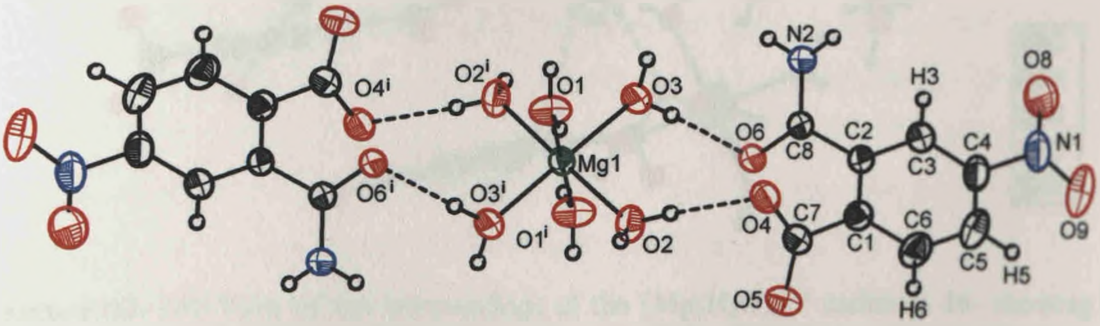

Figure 51- Crystal structure of $[Mg(H_2O)_6](2\text{-ca-4nba})_2$ **16** showing the atom-labeling scheme. Displacement ellipsoids are drawn at the 50% probability level except for the H atoms, which are shown as circles of arbitrary radius. Intramolecular H-bonding is shown as broken lines. Symmetry code: i) -x+2, -y, -z+1

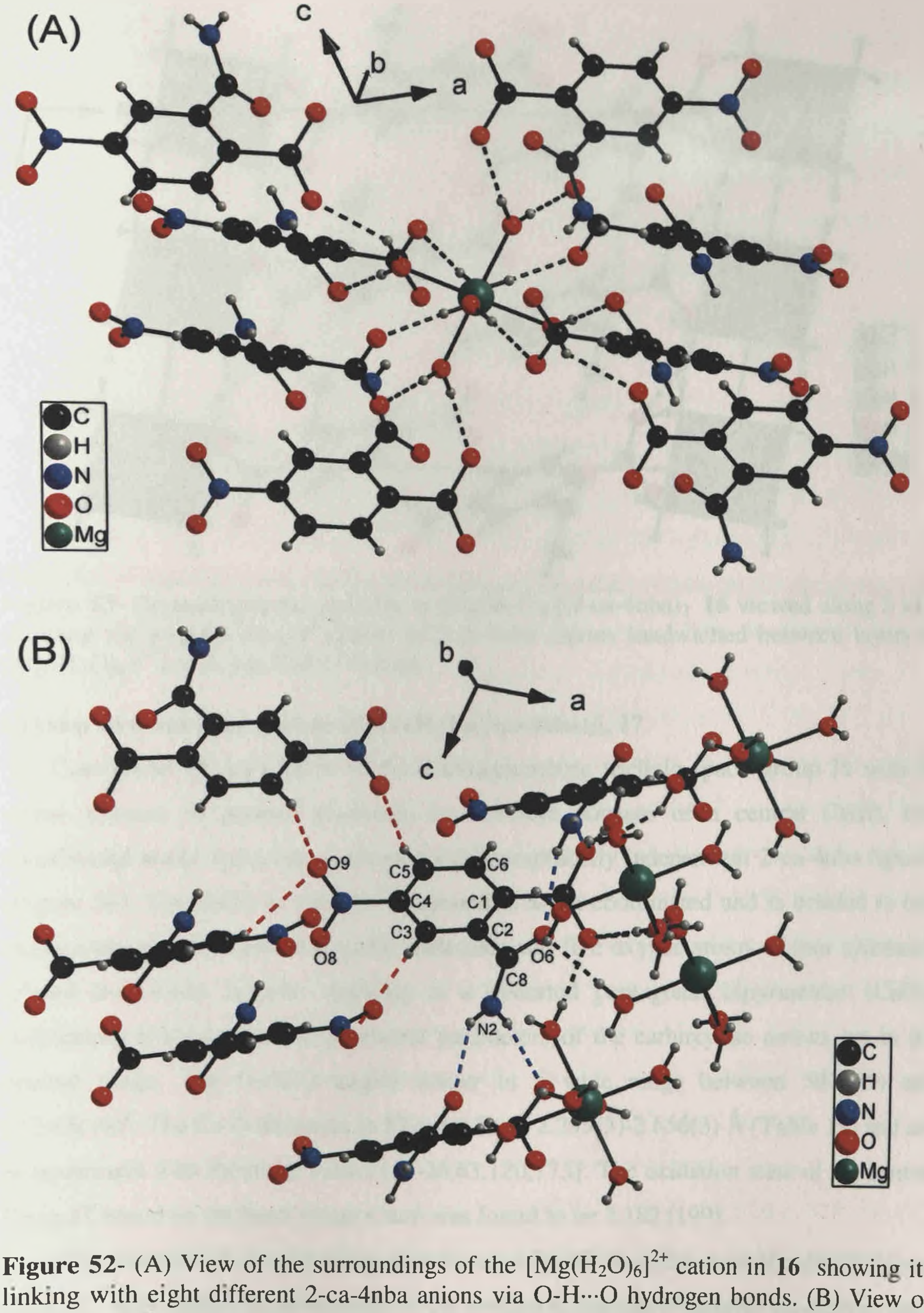

Figure 52- (A) View of the surroundings of the $[Mg(H_2O)_6]^{2+}$ cation in **16** showing its linking with eight different 2-ca-4nba anions via O-H···O hydrogen bonds. (B) View of the surroundings of the 2-ca-4nba anion in $[Mg(H_2O)_6](2\text{-ca-4nba})_2$ **16** showing its linking with four symmetry related $[Mg(H_2O)_6]^{2+}$ cations and five different 2-ca-4nba anions with the aid of three varieties of H-bonding interactions shown in broken lines.

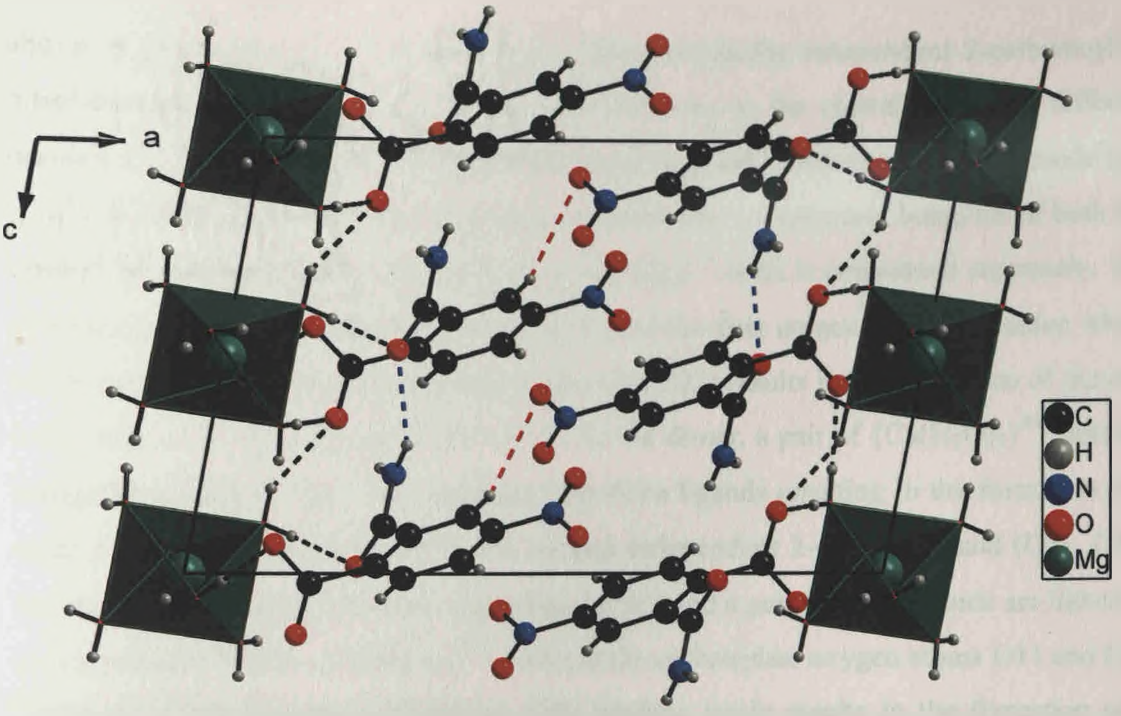

Figure 53- Crystallographic packing of $[Mg(H_2O)_6](2\text{-ca-4nba})_2$ **16** viewed along *b* axis showing the supramolecular bilayer of 2-ca-4nba anions sandwiched between layers of $[Mg(H_2O)_6]^{2+}$ (open polyhedra) cations.

Crystal structure description of $[Ca(H_2O)_2(2\text{-ca-4nba})_2]_n$ 17

Compound **17** crystallizes in the centrosymmetric triclinic space group $P\bar{1}$ with all atoms situated in general positions. Its structure consists of a central Ca(II), two coordinated water molecules and two crystallographically independent 2-ca-4nba ligands (Figure 54). The Ca(II) in the title compound is hepta coordinated and is bonded to two oxygen atoms of two terminal water molecules and five oxygen atoms of four symmetry related 2-ca-4-nba ligands, resulting in a distorted pentagonal bipyramidal $\{CaO_7\}$ polyhedron (Figure 54). The geometric parameters of the carboxylate anions are in the normal range. The O-Ca-O angles scatter in a wide range between 50.46(9) and 172.13(18)°. The Ca-O distances in **17** range from 2.299(3)-2.656(3) Å (Table 19) and are in agreement with literature values [24-26,63,120,175]. The oxidation state of the central Ca in **17** based on the bond valence sum was found to be 2.182 [199].

The structure of the polymeric compound is based on a dinuclear $\{Ca_2(H_2O)_4(2\text{-ca-}4\text{nba})_2\}^{2+}$ unit. Based on an analysis of the structural features of several Ca-carboxylates we had shown that when the number of coordinated waters in a Ca-carboxylate is 3 or less then the carboxylate ligand adopts a bridging binding mode [25]. The observation of bridging carboxylate ligation for the 2-ca-4nba ligands in **17** is in accordance with the above. It is interesting to note that the crystallographically independent 2-carbomoyl-4-nitrobenzoate anions in each formula unit coordinate to the central Ca(II) in different manner viz. a symmetrical bridging mode (μ_2-η^1:η^1) and a tridentate bridging mode (μ_3-η^2:η^1). In order to understand the crystal structure the coordination behavior of both the unique 2-ca-4nba ligands with a pair of $\{Ca(H_2O)_2\}^{2+}$ units is considered separately. The symmetrical bridging binding mode (μ_2-η^1:η^1) of the first unique 2-ca-4nba anion which binds through the carboxylate oxygen atoms (O1, O2) results in the formation of dimeric units with a Ca···Ca separation of 4.855 Å. In the dimer, a pair of $\{Ca(H_2O)_2\}^{2+}$ units are bridged by a pair of (μ_2-η^1:η^1) bridging 2-ca-4nba ligands resulting in the formation of a eight membered ring (Figure 55). The second independent 2-ca-4nba ligand (O11, O12) functions as a bridging tridentate ligand (μ_3-η^2:η^1) and a pair of such ligands are linked to two symmetry related $\{Ca(H_2O)_2\}^{2+}$ units via the carboxylate oxygen atoms O11 and O12 resulting in the formation of dimers. This binding mode results in the formation of a tricyclic dicalcium–bis(2-carbamoyl-4-nitrobenzoate) unit with a shorter Ca···Ca separation of 4.124 Å (Figure 55). A tricyclic dicalcium-bis(2-nba) (2-nba = 2-nitrobenzoate) unit has been reported by us recently in the polymer $[Ca(H_2O)_2(2\text{-nba})_2]_n$ [25]. The net result of the differing bridging binding modes of the unique 2-ca-4nba ligands in **17** is the linking of pairs of $\{Ca(H_2O)_2\}^{2+}$ units into a one dimensional coordination polymer extending along *a*-axis (Figure 56). In the infinite chain, pairs of $\{Ca(H_2O)_2\}^{2+}$ units are bridged via pairs of bridging 2-ca-4nba ligands and alternating pairs of Ca(II) ions exhibit Ca···Ca separations of 4.124 and 4.855 Å respectively. The observed values of Ca···Ca distances is comparable with the Ca···Ca distances reported by us for Ca coordination polymers based on 4-nitrobenzoate [24,26]. A scrutiny of the structure reveals that all the oxygen atoms of the amide, carboxylate and nitro functionalities of the 2-ca-4nba ligand excepting O4 and O15 function as H bond acceptors while the H atoms of coordinated water, the amide and two of the H atoms attached to carbon function as H donors resulting in three varieties of H-bonding interactions. A total of eleven H-bonding interactions with H···O distances ranging from 1.901 – 2.583 Å (Table 20) comprising of four N-H···O, five O-H···O and two C-H···O interactions are observed. In several structurally characterized nitrobenzoates, it is noted that the O atom of the nitro group functions as a H-acceptor and is involved in C-H···O interactions in addition to O-H···O bonds [24-26, 120,121]. In the title compound a similar feature is observed. The N2-H2A···O16, C5-H5···O16 and C13-H13···O6 interactions which link adjacent polymeric chains (Figure 56) are inter chain interactions and extend the H-bonding network.

Table 19- Selected bond distances (Å) and bond angles (°) for $[Ca(H_2O)_2(2\text{-}ca\text{-}4\text{-}nba)_2]_n$ **17**

$[Ca(H_2O)_2(2\text{-}ca\text{-}4\text{-}nba)_2]_n$ **17**			
Ca(1)-O(2)	2.299(3)	Ca(1)-O(12)	2.467(3)
Ca(1)-O(11)	2.337(3)	Ca(1)-O(11)^{ii}	2.656(3)
Ca(1)-O(20)	2.351(4)	Ca(1)-Ca(1)^{i}	4.855
Ca(1)-O(21)	2.380(4)	Ca(1)-Ca(1)^{ii}	4.124
Ca(1)-O(1)	2.400(3)		
O(2)-Ca(1)-O(11)	87.76(13)	O(11)-Ca(1)-O(12)	119.19(10)
O(2)-Ca(1)-O(20)	172.13(18)	O(20)-Ca(1)-O(12)	86.18(15)
O(11) –Ca(1)-O(20)	87.0(2)	O(21)-Ca(1)-O(12)	74.96(13)
O(2)-Ca(1)-O(21)	87.30(19)	O(1)-Ca(1)-O(12)	151.06(11)
O(11)-Ca(1)-O(21)	165.12(14)	O(2)-Ca(1)-O(11)^{ii}	91.83(12)
O(20)-Ca(1)-O(21)	99.2(2)	O(11)-Ca(1)-O(11)^{ii}	68.80(11)
O(2)-Ca(1)-O(1)	100.68(12)	O(20)-Ca(1)-O(11)^{ii}	80.81(15)
O(11)-Ca(1)-O(1)	87.79(11)	O(21)-Ca(1)-O(11)^{ii}	125.39(13)
O(20)-Ca(1)-O(1)	84.97(15)	O(1)-Ca(1)-O(11)^{ii}	153.05(10)
O(21)-Ca(1)-O(1)	79.36(14)	O(12)-Ca(1)-O(11)^{ii}	50.46(9)
O(2)-Ca(1)-O(12)	91.28(11)		

Symmetry codes i) -x, -y+1, -z+1 ; ii) -x+1, -y+1, -z+1

Table 20- Hydrogen- bonding geometry (Å, °) for compound $[Ca(H_2O)_2(2\text{-}ca\text{-}4\text{-}nba)_2]_n$**17**

D-H---A	d(D-H)	d(H---A)	D(D---A)	<DHA	Symmetry code
$[Ca(H_2O)_2(2\text{-}ca\text{-}4\text{-}nba)_2]_n$ **17**					
N2-H2A···O16	0.821	2.583	3.395	171	-x, -y+1, -z
N12-H12A···O5	0.970	2.465	3.412	165	-x, y+2, -z
O20-H20A···O3	0.836	2.495	3.192	142	x+1, y, z
O21-H21A···O13	0.865	2.530	3.142	128	-x, -y+1, -z+1
O21-H21A···O2	0.865	2.538	3.043	118	-x, -y+1, -z+1
N2-H2B···O12	0.926	1.965	2.884	171	-x, -y, -z+1
N12-H12B···O1	0.928	2.125	3.038	167	x, y+1, z
O20-H20B···O13	0.847	1.988	2.813	164	x, y-1, z
O21-H21B···O3	0.859	1.901	2.755	173	-x, -y, -z+1
C5-H5···O16	0.931	2.400	3.302	163	-x, 1-y, -z
C13-H13···O6	0.930	2.537	3.368	149	-x, 2-y, -z

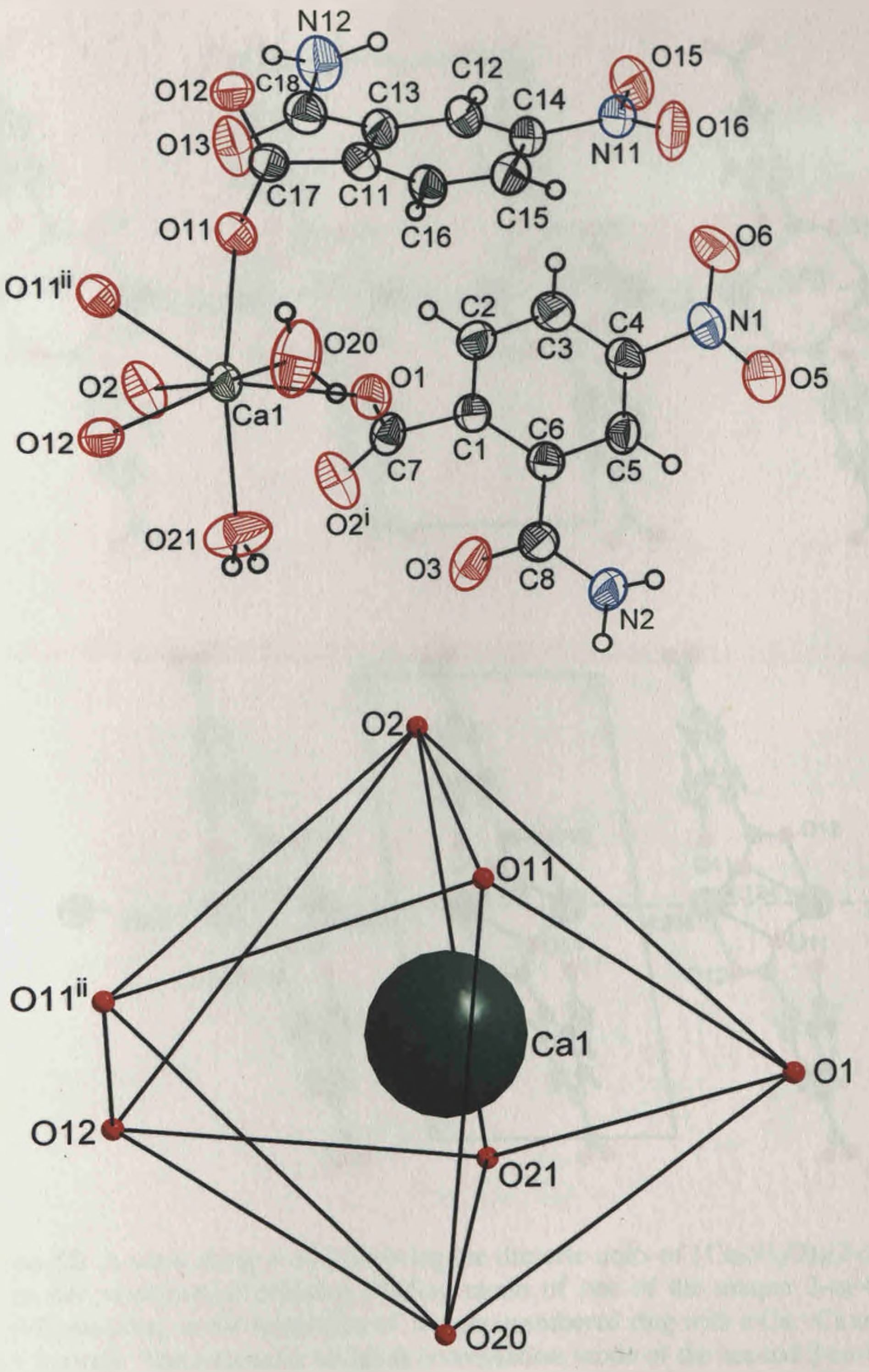

Figure 54- The coordination sphere of Ca(II) in $[Ca(H_2O)_2(2\text{-ca-4nba})_2]_n$ **17**, showing the atom-labeling scheme. Displacement ellipsoids are drawn at 50% probability level excepting for H atoms, which are shown as circles of arbitrary radius (top). The distorted pentagonal bipyram-idal coordination polyhedron around Ca(II) in **17** (bottom). Symmetry code: i) -x, -y+1, -z+1 ; ii) -x+1, y+1, -z+1. Colour code C, black ; H, grey ; N, blue ; O, red and Ca, green.

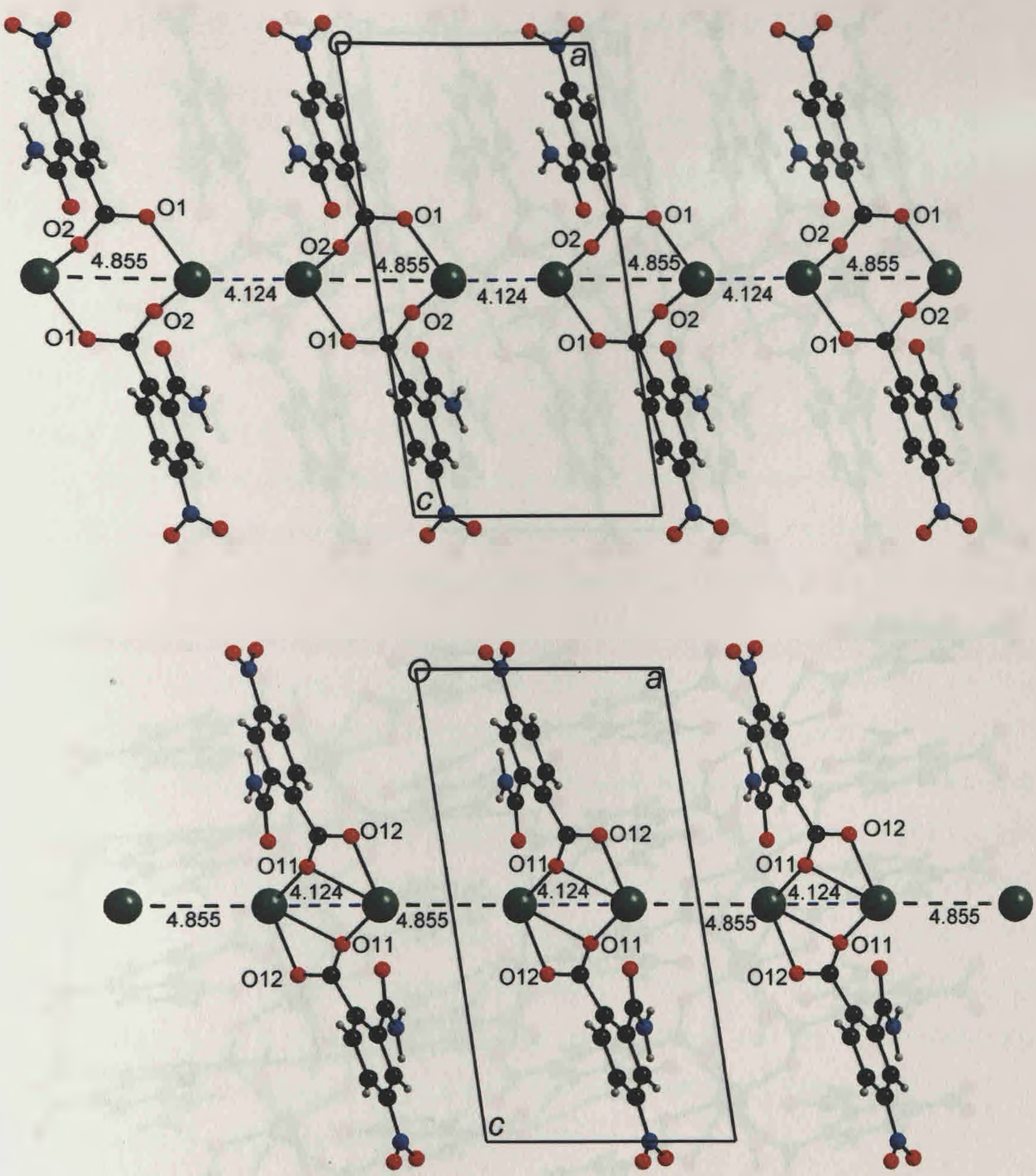

Figure 55- A view along *b* axis showing the dimeric units of $\{Ca_2(H_2O)_4(2\text{-ca-4nba})_2\}^{2+}$ due to the symmetrical bridging binding mode of one of the unique 2-ca-4nba ligand (O1,O2) resulting in the formation of a eight membered ring with a Ca···Ca separation of 4.855 Å (top). The tridentate bridging coordination mode of the second 2-ca-4nba ligand (O11, O12) results in a Ca···Ca separation of 4.124 Å (bottom). For clarity the coordinated water molecules are not shown. Colour code C, black ; H, grey ; N, blue ; O, red and Ca, green

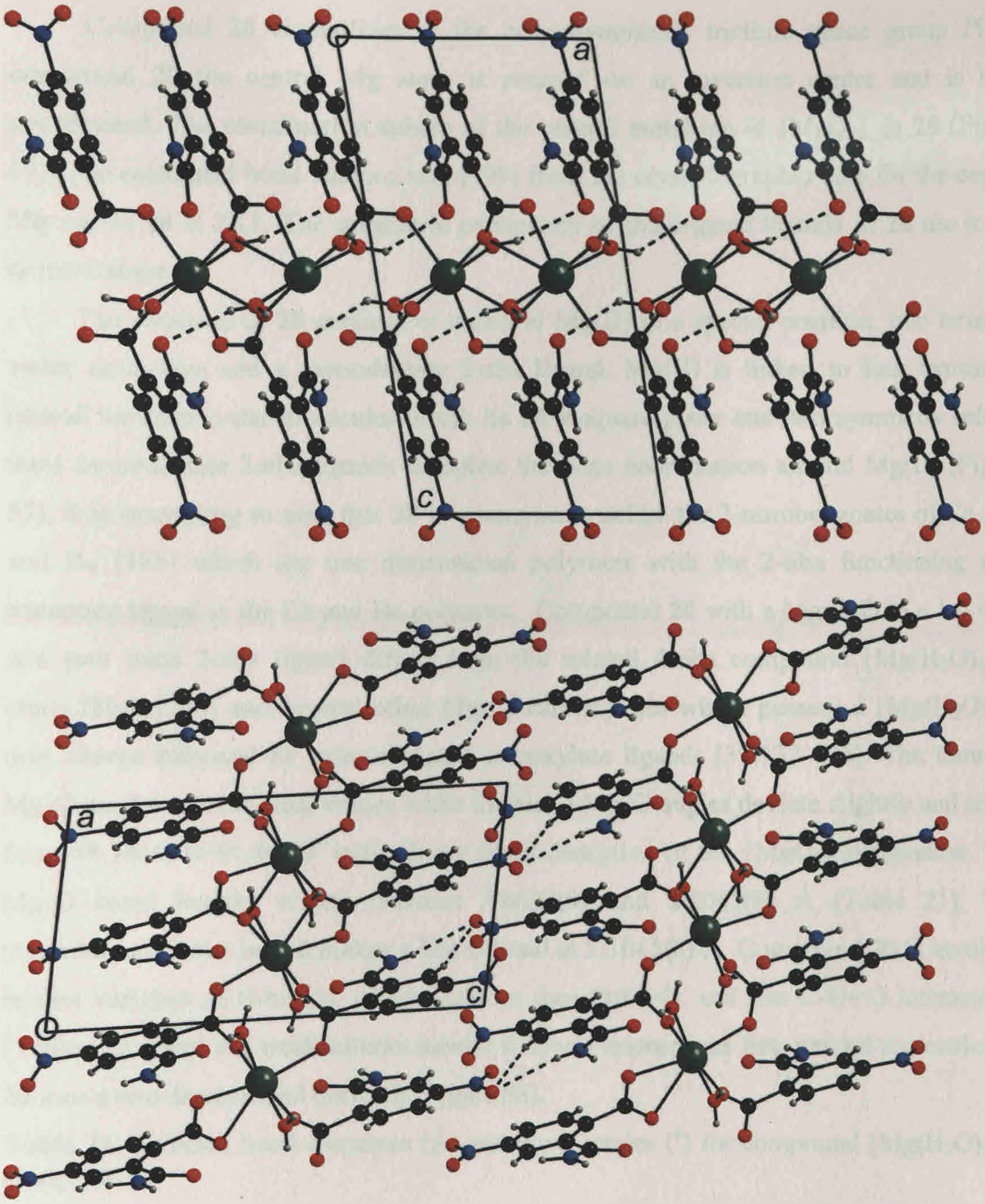

Figure 56- A view along *b* axis showing a part of the one dimensional chain extending along *a* axis due to the bridging binding modes of the unique 2-ca-4nba ligands in **17**. Intra chain H-bonding is shown by broken lines (top). Two adjacent polymeric chains of **17** in the *ac* crystallographic plane are linked by weak N-H···O and C-H···O bonds shown in broken lines (bottom). Colour code C, black ; H, grey ; N, blue ; O, red and Ca, green.

Crystal structure description of $[Mg(H_2O)_4(2\text{-nba})_2]$ 20

Compound **20** crystallizes in the centrosymmetric triclinic space group *P1̄*. In compound **20** the central Mg atom is situated on an inversion centre and is hexa coordinated. The coordination sphere of the central metal ion is $\{MgO_6\}$ in **20** (Figure 57). The calculated bond valence sum [199] from the crystallographic data for the central Mg ion in **20** is 2.11. The geometric parameters of the organic ligands in **20** are in the normal range.

The structure of **20** consists of a central Mg(II) in a special position, two terminal water molecules and a monodentate 2-nba ligand. Mg(II) is linked to four symmetry related terminal water molecules which lie on a square plane and two symmetry related trans monodentate 2-nba ligands complete the hexa coordination around Mg(II) (Figure 57). It is interesting to note that **20** is monomeric unlike the 2-nitrobenzoates of Ca [25] and Ba [165] which are one dimensional polymers with the 2-nba functioning as a tridentate ligand in the Ca and Ba polymers. Compound **20** with a Mg:H_2O in a 1:4 ratio and two trans 2-nba ligand differs from the related 4-nba compound $[Mg(H_2O)_6](4\text{-nba})_2{\cdot}2H_2O$ [133] and several other Mg(II) carboxylates which possess a $[Mg(H_2O)_6]^{2+}$ unit charge balanced by uncoordinated carboxylate ligands [39,132-136]. The trans O-Mg-O angles exhibit ideal values while the cis O-Mg-O angles deviate slightly and range from 88.16(4) to 91.84(4)° indicating a slight distortion of the $\{MgO_6\}$ octahedron. The Mg-O bond lengths scatter between 2.0638(9) and 2.1045(8) Å (Table 21). The monodentate 2-nba ligand makes a Mg-O bond at 2.1045(8) Å. Compound **20** is involved in two varieties of H-bonds, which includes four O-H···O, and two C-H···O interactions (Table 22). Both the weak intermolecular C-H···O interactions link neutral molecules of **20** into a two dimensional network (Figure 58).

Table 21- Selected bond distances (Å) and bond angles (°) for compound $[Mg(H_2O)_4(2\text{-nba})_2]$ **20**

$[Mg(H_2O)_4(2\text{-nba})_2]$			
Mg(1)-O(2)	2.1045(8)	Mg(1)-O(5)	2.0723(9)
Mg(1)-O(6)	2.0638(9)		
$O(6)^v$-Mg(1)-O(6)	180.0	$O(5)^v$-Mg(1)-O(2)	91.84(4)
$O(6)^v$-Mg(1)-O(5)	91.00(4)	O(5)-Mg(1)-O(2)	88.16(4)
O(6)-Mg(1)-O(5)	89.0(4)	O(2)-Mg(1)-$O(2)^v$	180.0(3)
$O(5)^v$-Mg(1)-O(5)	180.0(5)	$O(6)^v$-Mg(1)-O(2)	91.79(4)
O(6)-Mg(1)-O(2)	88.21(4)		

Symmetry code v) -x+1,-y+1,-z,

Table 22- Hydrogen bonding geometry (Å,°) for compound $[Mg(H_2O)_4(2\text{-nba})_2]$ **20**

D-H---A	d(D-H)	d(H---A)	D(D---A)	<DHA	Symmetry code
$[Mg(H_2O)_4(2\text{-nba})_2]$					
O5-H1O5···O4	0.840	2.126	2.944	164	-x+1, -y+1, -z
O5-H2O5···O2	0.840	1.888	2.720	171	-x, -y+1, -z
O6-H1O6···O1	0.840	1.999	2.817	164	x, y+1, z
O6-H2O6···O1	0.840	1.898	2.736	175	-x, -y+1, -z
C3-H3----O4	0.950	2.567	3.44	153	2-x,1-y,-1-z
C6-H6----O5	0.950	2.600	3.302	131	1-x,-y,-z

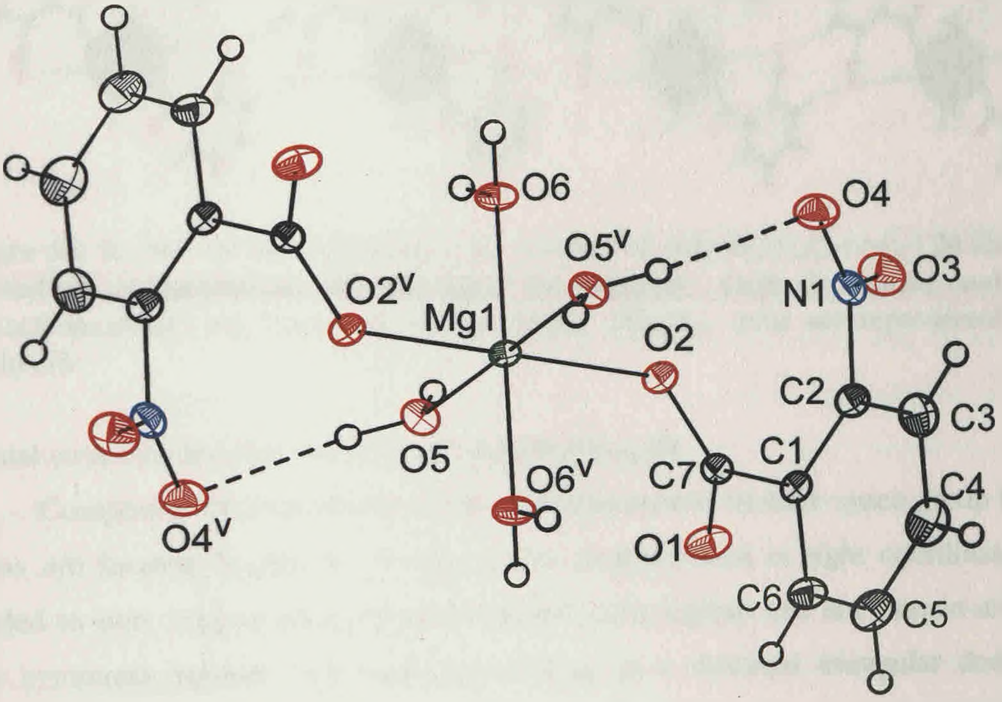

Figure 57- $[Mg(H_2O)_4(2\text{-nba})_2]$ showing the atom-labeling scheme. Displacement ellipsoids are drawn at the 50% probability level excepting for the H atoms, which are shown as circles of arbitrary radius. Intramolecular H-bonding is shown as broken lines. Symmetry code, v) -x+1,-y+1,-z

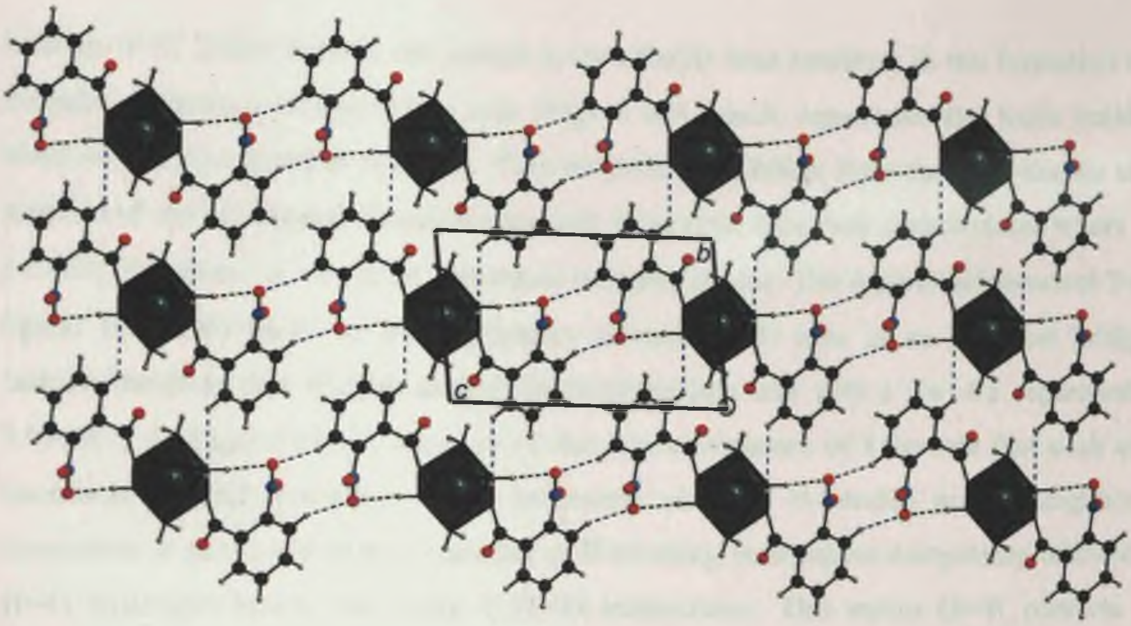

Figure 58: A view of the crystallographic packing of $[Mg(H_2O)_4(2\text{-nba})_2]$ **20** showing the H-bonding characteristics of the nitro functionality. O-H···O (black) and C-H···O interactions.(blue) are shown as broken lines. $\{MgO_6\}$ units are represented as open octahedra.

Crystal structure description of $[Ca(2\text{-nba})_2(H_2O)_2]_n$ **21**

Compound **21** crystallizes in the centrosymmetric triclinic space group P1̄ and all atoms are located in general positions. The central metal is eight coordinated and is bonded to two oxygen atoms of two terminal aqua ligands and six oxygen atoms from four symmetry related 2-nba anions resulting in a distorted triangular dodecahedral $\{CaO_8\}$ coordination polyhedron (Figure 59). The geometric parameters of the 2-nba ligand are in the normal range and are in agreement with reported values [165]. The observed Ca-O bond distances vary between 2.3442(13) to 2.6539(15) Å (Table 23) while the O-Ca-O angles range from 77.32(6) to 150.25(5)°. These values are comparable with those reported for other Ca(II)-carboxylates [24,26,117,119,120]. The Ca(II) is linked to the O9 and O10 atoms of the water molecules at 2.3918(18) and 2.4121(17) Å respectively. The structure of compound **21** is a one-dimensional (1-D) polymer and hence it is formulated as $[Ca(2\text{-nba})_2(H_2O)_2]_n$. Each formula unit of **21** contains a Ca(II) coordinated to two aqua ligands and two unique 2-nitrobenzoate ligands both of which function as bridging ligands. The first unique μ_2-η^2:η^1 2-nba ligand (O1, O2) binds to a Ca(II) in a bidentate fashion with Ca1-O1 and Ca1-O2 distances of 2.4548(15) and 2.6313(15) Å respectively. The O2 oxygen is further linked to a symmetry related Ca(II) at a distance of 2.3498(14) Å resulting in a Ca···Ca separation of 3.9865(8) Å. A pair of such μ_2-η^2:η^1 2-nba ligands are linked to two Ca(II) ions resulting in the formation of a tricyclic dicalcium-dicarboxylate unit (Figure 60) which constitutes the basic building block of the coordination polymer. This tricyclic unit differs from the well-known eight membered cyclic dimetal-dicarboxylate unit in several dinuclear carboxylates where the $(\text{-COO})^-$ functions as a μ_2-η^1:η^1 bidentate bridging ligand. The second independent 2-nba ligand (O5, O6) binds to two symmetry related Ca(II) ions in an identical bridging fashion resulting in a tricylic dicalcium-dicarboxylate unit with a Ca···Ca separation of 3.9967(9) Å (Figure 61). A scrutiny of the crystal structure of **1** reveals that each eight coordinated Ca(II) complex in the polymeric chain is H-bonded to six neighboring complexes with the aid of two varieties of H-bonding interactions comprising of three O-H···O hydrogen bonds and three C-H···O interactions. This entire O···H contacts are shorter than the sum of their van der Waals radii and their geometric parameters are listed in Table 24. The O9-H9···O1^{i} and O10-H10B···O5^{ii} (Table 24) interactions between the coordinated water molecules and the carboxylate oxygen atoms O1 and O5 occur within the 1-D polymeric chain (Figure 62) and thus are intrachain interactions. The oxygen atoms of the nitro group function as H-acceptors and this behavior has been observed in several nitrobenzoates [24-26, 120,121,130,133,169,177]. The nitro oxygen atoms O4 and O7 in one polymeric chain are hydrogen bonded to the H11 and H10A atoms in an adjacent chian via C11-H11···O4^{v} and O10-H10A···O7^{iii} and these can be termed as interchain interactions. Likewise the H-bonding between O9 (water) and O1 (carboxylate) with the H atoms of the aromatic ring serve to link parallel chains resulting in a two-dimensional H-bonded network (Figure 63). It is to be noted that the Ca-O bond lengths formed by this ligand are different. With this ligand a Ca(II) ion is linked to the O5 and O6 oxygen atoms in a bidentate manner (Ca1-O5 2.4213(14); Ca1-O6 2.3442(13) Å) and the O6 is further linked to a second Ca(II) ion at 2.6539(15) Å. In the crystal structure of **21** alternating pairs of the two crystallographically independent μ_2-η^2:η^1 2-nba ligands link pairs of $\{Ca(H_2O)_2\}^{2+}$ units into a 1-D polymeric chain extending along *a* axis (Figure 62). In the infinite chain, alternating pairs of Ca(II) ions are bridged by a pair of bridging 2-nba ligands resulting in alternating Ca···Ca separations of 3.9865(8) and 3.9967(9) Å respectively across the chain (Figure 62). These values are in very good agreement with Ca···Ca separations of 3.8585(7) and 3.8432(3) Å reported for the coordination polymers $[Ca(L^1)(4\text{-nba})_2]_n$ (L^1=N-methylimidazole) [24] and $[Ca(L^2)(H_2O)(4\text{-nba})_2]_n$ (L^2 is 2-methylimidazole) respectively [26]. A comparison of the structure of the recently reported polymeric barium compound [165] of 2-nba namely $[Ba(H_2O)_3(2\text{-nba})_2]_n$ with that of the title Ca compound **21** reveals certain similarities and several differences. Both compounds contain alkaline-earth:2-nba in a 1:2 ratio and are 1-D polymers based on dinuclear units. The alkali-earth metals in both compounds are linked to four different carboxylate ligands. However the compounds are differently hydrated and Ba adopts nine coordination. Of the two crystallographically independent 2-nba ligands in the Ba compound, one ligand binds in a μ_2-η^2:η^1 manner as observed in the Ca compound, while the other 2-nba ligand functions as a monoatomic bridge between two adjacent Ba ions in the chain with one of the nitro oxygen atoms bonded to one Ba resulting in a denticity of three for this second 2-nba ligand. This binding mode of the carboxylate moiety in $[Ba(H_2O)_3(2\text{-nba})_2]_n$ can be designated as μ_2-η^1:η^1. In the 1-D polymeric chain alternating pairs of bivalent metals are bridged by a pair of 2-nba ligands.

In order to understand the role of the nitro group in the structural chemistry of Ca-nitrobenzoates, a comparison of the structural features of the title Ca compound **21** with the related monomeric Ca compound [63] of 4-nba namely $[Ca(H_2O)_4(\eta^1\text{-4-nba})\text{-}(\eta^2\text{-4-nba})]$ is made. In the 4-nba compound containing the nitro group para to the carboxylate functionality, the heptacoordinated Ca(II) is linked to two crystallographically independent 4-nba ligands which coordinate in monodentate (η^1) and bidentate (η^2) manner respectively. In our original report [63] on the structural aspects of $[Ca(H_2O)_4(\eta^1\text{-4-nba})(\eta^2\text{-4-nba})]$ only the O-H···O interactions were described but the weak C-H···O interactions were not mentioned. A reinvestigation of the structure data reveals that one nitro oxygen atom on each unique 4-nba is involved in a C-H···O interaction at distances of 2.61 and 2.45 Å accompanied by CHO angles of 158 and 166° respectively. Hence the $-NO_2$ group in the 4-nba and 2-nba compounds of Ca, which are differently disposed with respect to the carboxylate in the benzene ring are very similar in terms of their secondary interactions. However there is a noticeable difference between **21** and $[Ca(H_2O)_4(\eta^1\text{-4-nba})(\eta^2\text{-4-nba})]$ in terms of the number of coordinated waters, which can account for the observed structural variation in these two compounds.

Table 2- Selected bond distances (Å) and bond angles (°) for compound $[Ca(H_2O)_2(2\text{-}nba)_2]_n$ **21**

$[Ca(H_2O)_2(2\text{-}nba)_2]_n$			
Ca(1)-O(6)	2.3442(13)	Ca(1)-O(5)	2.4213(14)
Ca(1)-O(2)^{ii}	2.3498(14)	Ca(1)-O(1)	2.4548(15)
Ca(1)-O(9)	2.3918(18)	Ca(1)-O(2)	2.6313(15)
Ca(1)-O(10)	2.4121(17)	Ca(1)-O(6)^{i}	2.6539(15)
Ca(1)-Ca(1)^{ii}	3.9865(8)	Ca(1)-Ca(1)^{i}	3.9967(9)
O(6)-Ca(1)-O(2)^{ii}	148.82(5)	O(5)-Ca(1)-O(1)	88.01(5)
O(6)-Ca(1)-O(9)	77.32(6)	O(6)-Ca(1)-O(2)	128.87(5)
O(2)^{ii} -Ca(1)-O(9)	82.91(6)	O(2)^{ii}-Ca(1)-O(2)	73.82(5)
O(6)-Ca(1)-O(10)	84.37(5)	O(9)-Ca(1)-O(2)	153.76(6)
O(2)^{ii} -Ca(1)-O(10)	77.70(6)	O(10)-Ca(1)-O(2)	82.04(5)
O(9)-Ca(1)-O(10)	104.97(7)	O(5)-Ca(1)-O(2)	75.15(5)
O(6)-Ca(1)-O(5)	124.91(5)	O(1)-Ca(1)-O(2)	50.88(4)
O(2)^{ii} -Ca(1)-O(5)	77.78(5)	O(6)-Ca(1)-O(6)^{i}	73.97(5)
O(9)-Ca(1)-O(5)	88.40(6)	O(2)^{ii}-Ca(1)-O(6)^{i}	124.74(5)
O(10)-Ca(1)-O(5)	150.25(5)	O(9)-Ca(1)-O(6)^{i}	77.23(6)
O(6)-Ca(1)-O(1)	80.89(5)	O(10)-Ca(1)-O(6)^{i}	157.29(5)
O(2)^{ii}-Ca(1)-O(1)	124.69(5)	O(5)-Ca(1)-O(6)^{i}	50.95(4)
O(9)-Ca(1)-O(1)	150.53(5)	O(1)-Ca(1)-O(6)^{i}	77.85(5)
O(10)-Ca(1)-O(1)	92.27(6)	O(2)-Ca(1)-O(6)^{i}	106.15(5)

Symmetry codes i) –x+1, -y+2, -z ; ii) -x+2, -y+2, -z

Table 3- Hydrogen bonding geometry (Å,°) for compound $[Ca(H_2O)_2(2\text{-}nba)_2]_n$ **21**

D-H---A	d(D-H)	d(H---A)	D(D---A)	<DHA	Symmetry code
$[Ca(H_2O)_2(2\text{-}nba)_2]_n$					
Intrachain interactions					
O9-H9···O1	0.817	1.965	2.769	168	-x+1, -y+2, -z
O10-H10B···O5	0.832	1.953	2.754	161	-x+2, -y+2, -z
Interchain interactions					
O10-H10A···O7	0.823	2.257	2.999	150	x, y+1, z
C3-H3···O9	0.930	2.623	3.548	173	x, y, 1+z
C11-H11···O4	0.929	2.523	3.404	158	1-x, 1-y, 1-z
C10-H10···O1	0.929	2.539	3.464	174	x, -1+y, z

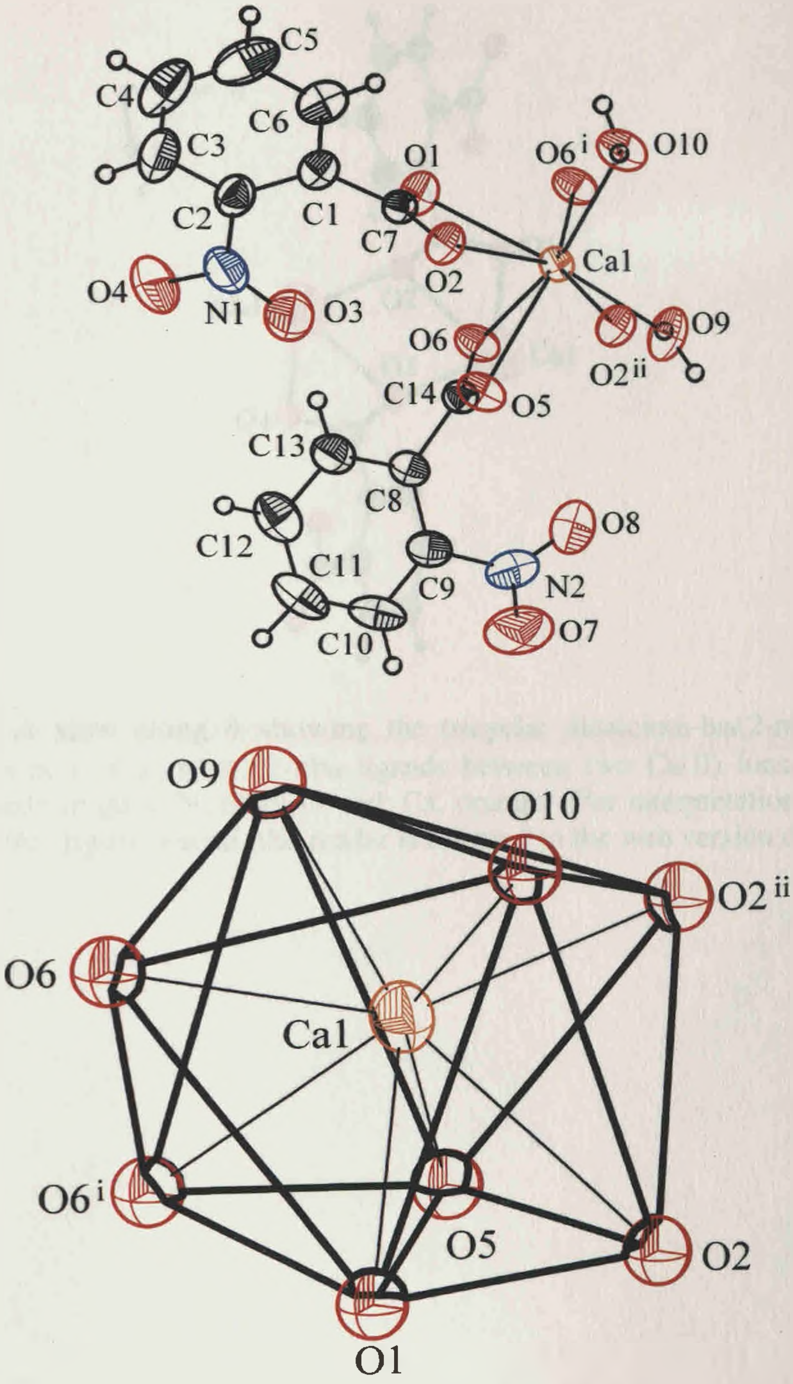

Figure 59-A view of the coordination sphere of Ca(II) in $[Ca(2\text{-}nba)_2(H_2O)_2]_n$ **21**, showing the atom-labelling scheme. Displacement ellipsoids are drawn at the 50% probability level excepting for the H atoms, which are shown as circles of arbitrary radius (top). The coordination polyhedron around Ca(II) in **21** (bottom). Symmetry code: i) -x+1, -y+2, -z; ii) -x+2, -y+2, -z. Colour code: C, black; N, blue; O, red; Ca, orange. (For interpretation of the references to colour in this figure legend, the reader is referred to the web version of this article)

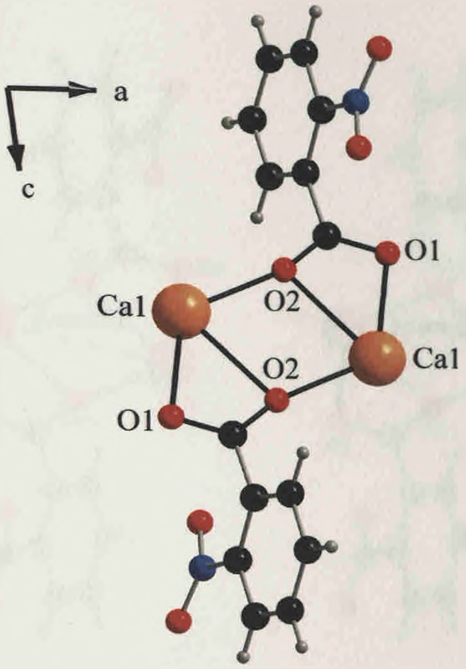

Figure 60- A view along *b* showing the tricyclic dicalcium-bis(2-nitrobenzoate) unit formed by a pair of μ_2-η^2:η^1 2-nba ligands between two Ca(II) ions. Colour code: C, black; H, medium grey; N, blue; O, red; Ca, orange. (For interpretation of the references to colour in this figure legend, the reader is referred to the web version of this article)

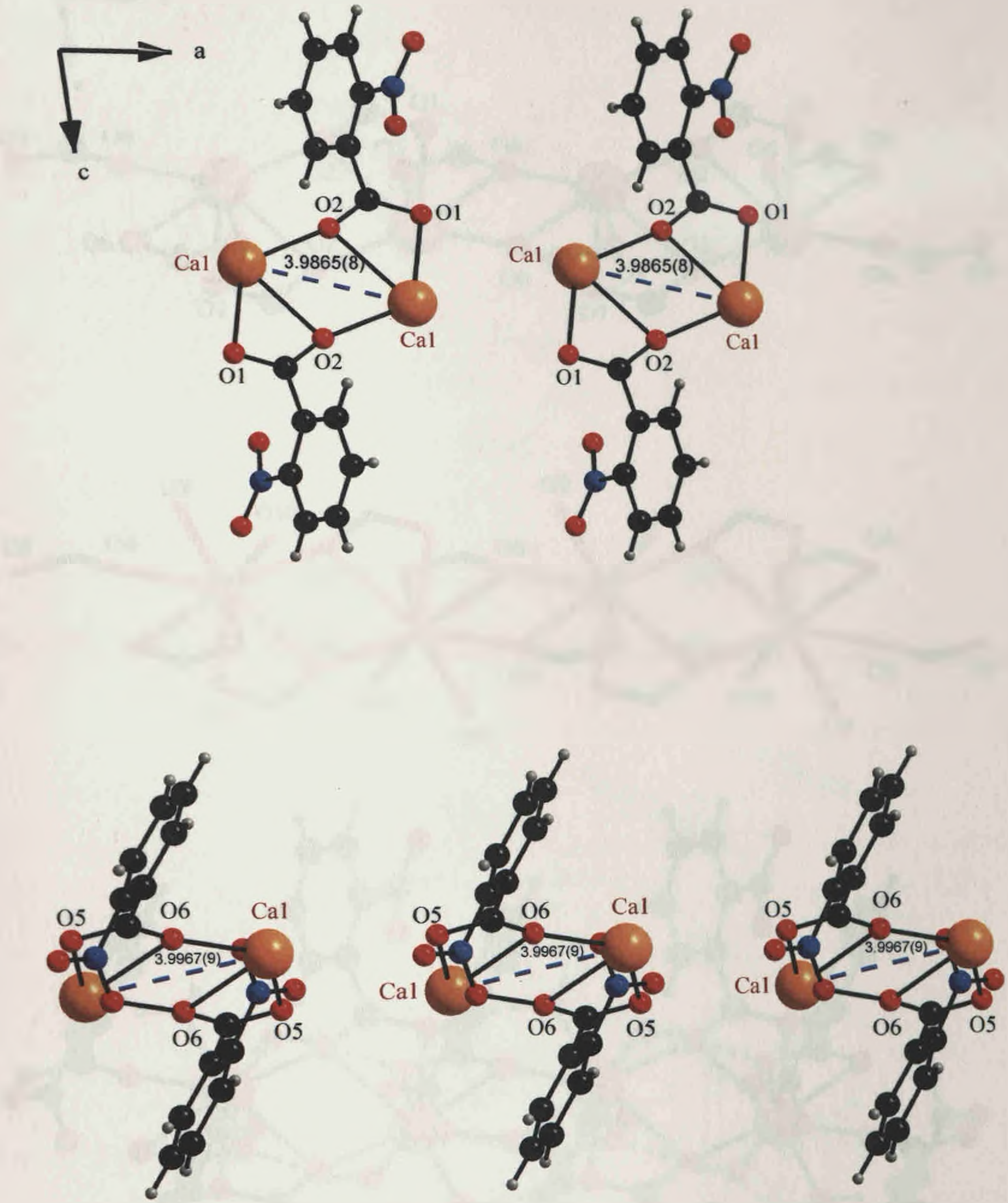

Figure 61- A view along *b* axis of the μ_2-η^2:η^1 bridging binding mode of the first unique (O1, O2) ligand. A pair of (O1, O2) ligands bridge between two Ca(II) ions resulting in a Ca···Ca separation of 3.9865(8) Å. For clarity only the coordinated ligand is shown (top). The second independent 2-nba ligand (O5, O6) exhibits an identical bridging mode, with a Ca···Ca separation of 3.9967(9) Å. (bottom). The identical Ca atoms in the top & bottom figures are labeled.

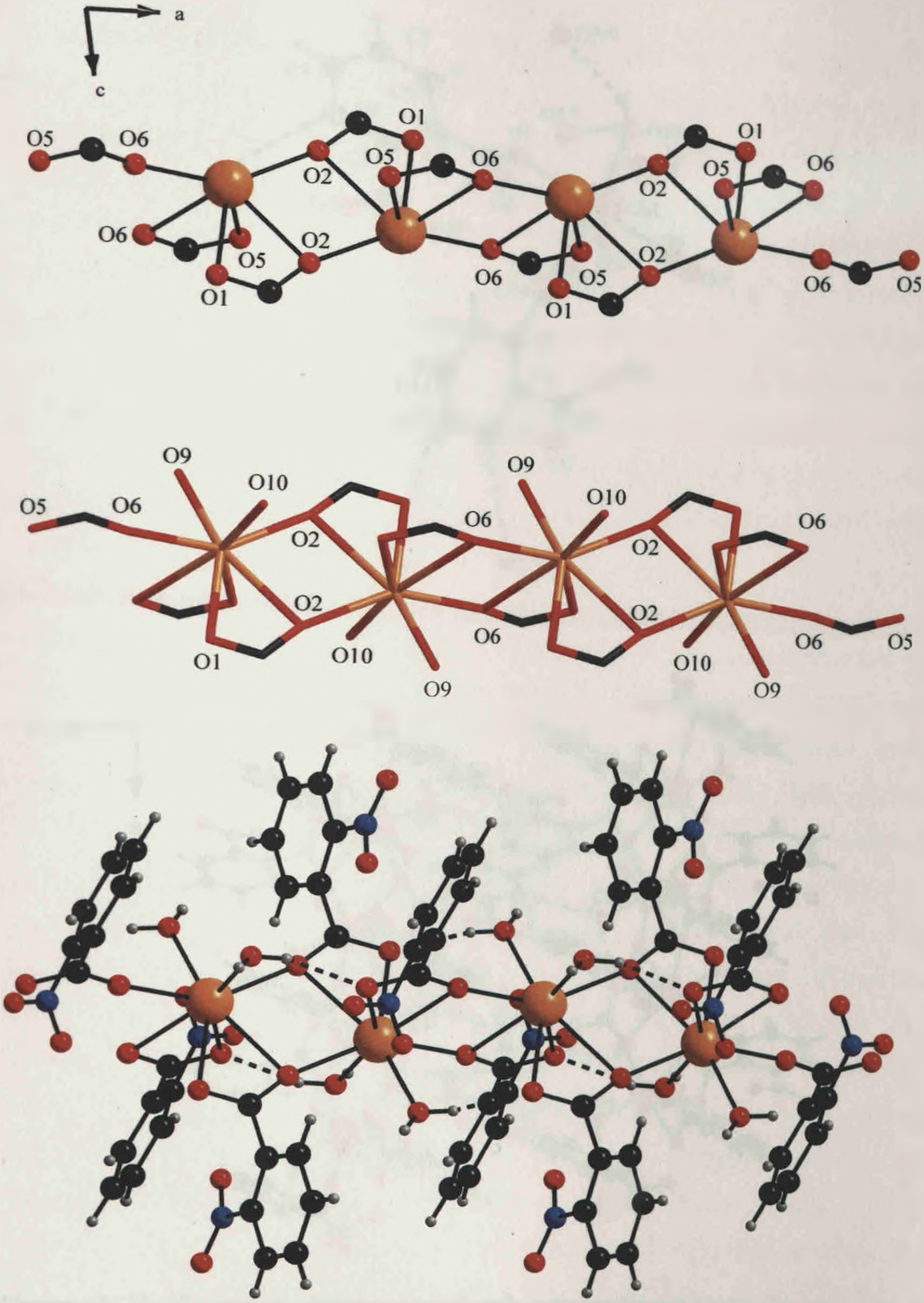

Figure 62- A portion of the 1-D polymeric chain in **21** showing the linking of tricyclic dicalcium-bis(2-nitrobenzoate) units into an infinite chain extending along *a* axis. For clarity the coordinated water molecules and aromatic ring are not shown (top). A wireframe model of the polymeric chain wherein the oxygen atoms O9 and O10 of water are included (middle). The aromatic rings and the H atoms of water are included in the polymeric chain to show the intrachain O-H···O bonds in broken lines. Colour code: C, black; H, medium grey; N, blue; O, red; Ca, orange. (For interpretation of the references to colour in this figure legend, the reader is referred to the web version of this article)

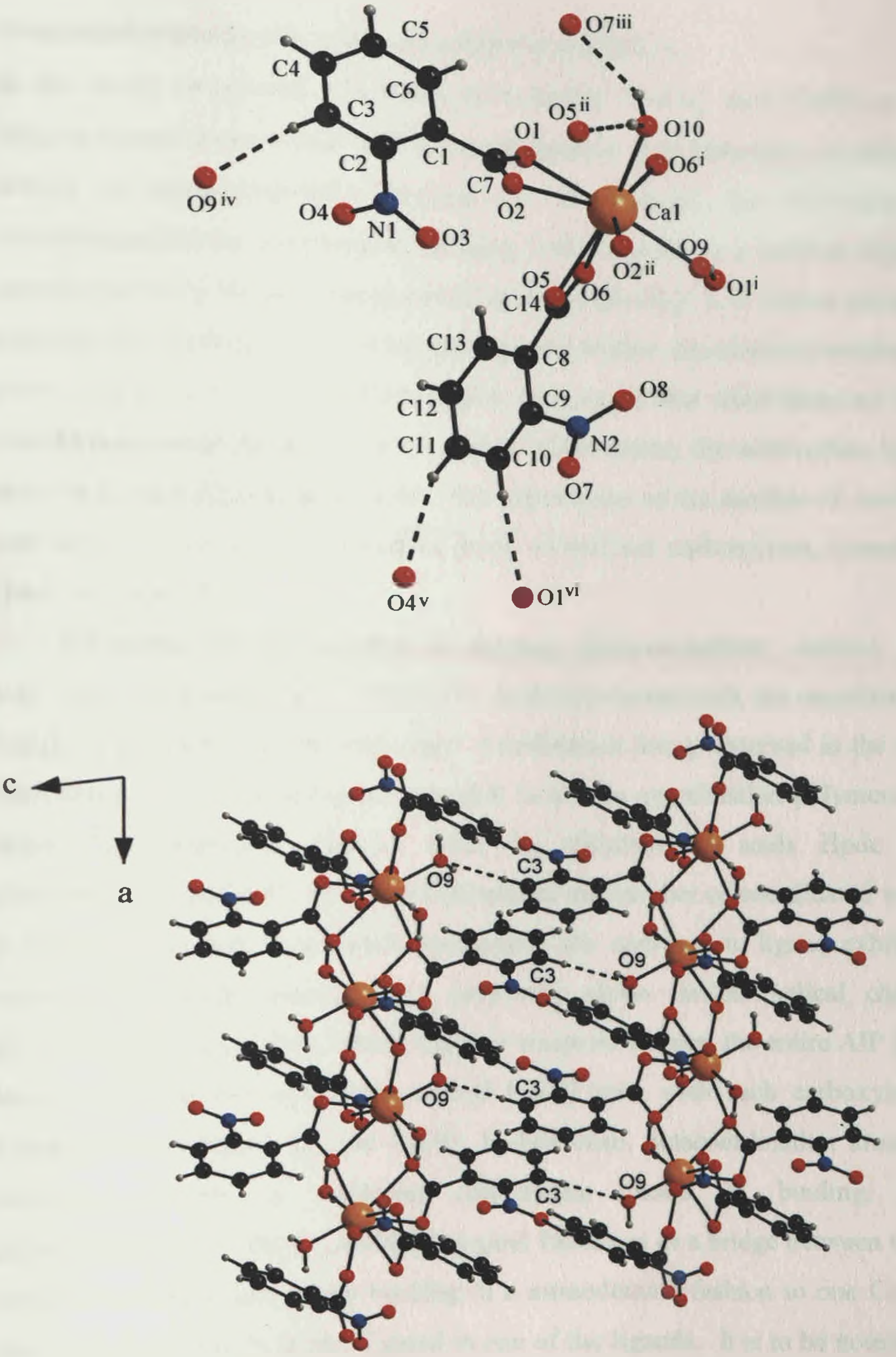

Figure 63: The H-bonding situation around each octacoordinated Ca(II) showing its kinking to six different complexes with the aid of three O-H···O and three C-H···O interactions (**top**). Symmetry code: i) -x+1, -y+2, -z ; ii) -x+2, -y+2, -z iii) x, y+1, z; iv) x, y, 1+z; v) 1-x, 1-y, 1-z; vi) x, -1+y, z .The interchain C3-H3···O9 interaction serves to link two parallel chains as shown in the crystallographic ac plane (**bottom**).

Comparative study of Ca(II) coordination polymers

In the 4-nba compound $[Ca(H_2O)_4(\eta^1\text{-4-nba})(\eta^2\text{-4-nba})]$ each Ca(II) is linked to four oxygen atoms from water and the monodentate and bidentate coordination of 4-nba results in heptacoordination around Ca. In contrast, the tridenticity of the two crystallographically independent bridging 2-nba ligands in **1** leads to eight coordination around Ca in the diaqua compound $[Ca(2\text{-nba})_2(H_2O)_2]_n$ **1**, a feature observed in several calcium carboxylates [25]. The attainment of a higher coordination number appears to be a key feature in Ca structural chemistry. It is noted that when there are less number of coordinated water molecules in a calcium- carboxylate, the carboxylate ligand prefers to adopt a bridging mode of ligation. The importance of the number of coordinated waters can be evidenced by a comparative study of calcium carboxylates, several of which are listed in Table 25.

Polymeric Ca-carboxylates of varying dimensionalities, derived from different carboxylic acids are listed in Table 25. In all the compounds, the coordination number of Ca(II) varies from 6 to 10 with eight coordination being observed in the majority of the compounds. It is interesting to note that in all the coordination polymers excepting the three Ca compounds derived from the dicarboxylic acids Hpdc (3,5-pyrazole-dicarboxylate) and AIP (5-aminoisophthalate) the number of coordinated water molecules is three or less and in all such compounds the carboxylate ligand exhibits a bridging coordination mode leading to a polymeric chain. In the helical chain compound $[[Ca(H_2O)_4(AIP)_2](H_2O)]_n$ which has four water molecules, the entire AIP ligand acts as a bridge between two symmetry related Ca(II) ions with each carboxylate showing a bidentate coordination to one Ca(II). In this case, octacoordination around Ca can be achieved without a bridging carboxylate mode of binding. Likewise in $[[Ca(H_2O)_4(Hpdc)].2H_2O]_n$ the Hpdc ligand functions as a bridge between two Ca(II) ions with each carboxylate group binding in a monodentate fashion to one Ca. Additionally one of the pyrazole N is also ligated in one of the ligands. It is to be noted that both AIP and Hpdc are ditopic ligands as they contain two carboxylate groups anchored on to a ring and the ditopicity is responsible for the polymeric structure, without making use of a bridging carboxylate mode in these compounds. It is interesting to note that in the 1-D polymer $[[Ca(H_2O)_4(Hpdc)].H_2O]_n$ synthesized at a more acidic pH, a bridging carboxylate ligation is observed even though the Ca is coordinated to four water molecules. In this case the pyrazole N ligation is not observed. From Table 25 it is very clear that when the number of coordinated water molecules is three or less than three, a bridging carboxylate binding mode is always observed. In Ca(II) compounds derived from mono carboxylic acids, for example [Ca(H_2O)$_4$(η^1-4-nba)(η^2-4-nba)] [63] seven coordination around Ca can be achieved due to the mono and chelating binding modes of the crystallographically independent 4-nba ligands and this compound exhibits a zero-dimensional structure. When the number of water ligands in this compound is reduced by heating, the 4-nba adopts a bridging binding mode leading to a polymeric structure as has been shown by us in recent reports [24,26]. Another noteworthy feature is the tendency for a majority of the compounds to crystallize in centrosymmetric space groups.

Table 25- List of calcium compounds in increasing water content

Compound	C.N.	Bridging (RCOO)$^-$ present	S.G.	D	Ref.
[Ca(pyr)$_2$(4-nba)$_2$]$_n$	6	Yes	P$\bar{1}$	1-D	120
[Ca(H_2dhtp)]	8	Yes	C2/c	3-D	110
[Ca($C_5H_3N_2O_2$)$_2$]$_n$	8	Yes	I4$_1$/amd	1-D	113
[Ca(l-tartarate)]$_n$	8	Yes	C222(1)	3-D	118
[Ca(m-tartarate)]$_n$	8	Yes	C2/c	3-D	118
[Ca(DMF)$_2$(TTF)]$_n$	7	Yes	P$\bar{1}$	1-D	123
[Ca(DMF)(ABDC)]$_n$	8	Yes	Pnma	1-D	125
[Ca(H_2dhtp)(DMF)]	7	Yes	P$\bar{1}$	dimer	125
[Ca(H_2dhtp)(DMF)$_2$]	6	Yes	C2/c	Discrete	125
[Ca$_2$(OH)$_2$(ndc)]$_n$	7	Yes	P2$_1$/c	3-D	53
[Ca(NH_2.NH.CO_2)$_2$]$_n$	7	Yes	P2$_1$/c	3-D	37
[Ca($C_3H_3O_4$)$_2$]$_n$	8	Yes	P2$_1$/c	3-D	56
[Ca(N-MeIm)(4-nba)$_2$]$_n$	6	Yes	P$\bar{1}$	1-D	24
[Ca(μ-DMF)(μ-DADC)]$_n$	8	Yes	Pnma	3-D	73
[Ca(Sa)$_2$(Phen)]$_n$	6	Yes	Pnab	1-D	49
[Ca($C_5H_3O_3$)$_2$]$_n$	8	Yes	P2/c	3-D	64
[Ca($C_{10}H_9O_4$)$_2$]$_n$	7	Yes	P2$_1$/n	1-D	93
[Ca(μ-DMF)(μ-NDC)]$_n$	8	Yes	Pnma	3-D	73
[Ca(μ-DEF)(μ-TPDC)]$_n$	8	Yes	Pnma	3-D	73
[Ca$_{1.5}$(DEF)(μ-BDC)$_{1.5}$]$_n$	6,7	Yes	I2/a	1-D	73
[α-Ca(HCOO)$_2$]$_n$	8	Yes	Pcab	2-D	80
[Ca$_3$($C_{57}H_{102}N_9O_{18}$)$_6$]$_n$.3CH_3CN	6	Yes	P2$_1$/n	2-D	94
[Ca($C_8H_4O_4$)]$_n$.H_2O	7	Yes	P2$_1$/c	1-D	83
[[Ca(NH_2-$NHCO_2$)$_2$].H_2O]$_n$	8	Yes	P$\bar{1}$	1-D	37
[[Ca($C_5H_3N(CO_2)_2$](H$_2$O)$_{1.5}$]$_n$	7	Yes	P21/n	1-D	126

$[[Ca(C_5H_3N(CO_2)_2](H_2O)_2]_n$	7	Yes	$C2/c$	1-D	126
$[[Ca_3(H_2O)_2(DMF)_2(BTC)_2].3H_2O]_n$	7,8	Yes	$C2$	1-D	125
$(C_3H_7N_6)_4[Ca(C_7H_3NO_4)_3].6H_2O$	9	No	$C2/c$	0-D	115
$[Ca(H_2O)(DMF)(BDC)]_n$	8	Yes	Pnma	1-D	125
$[Ca(H_2O)(dnSa)]_n$	7	Yes	$P2_1/c$	1-D	38
$[Ca(H_2O)(C_{10}H_8O_6)]_n$	8	Yes	$P2_1/c$	3-D	59
$[Ca(H_2O)(Hpdc)]_n$	7	No	$P2_1/c$	3-D	48
$[[Ca(H_2O)(ptaH)].6H_2O]_n$	6	Yes	$P\bar{1}$	3-D	75
$[Ca(H_2O)(val)_2]_n$	8	Yes	$C2/c$	1-D	22
$[Ca_2(H_2O)(A_3Br).4H_2O]_n$	6	Yes	Pnma	3-D	60
$[Ca(H_2O)(gly)_2]_n$	8	Yes	$P\bar{1}$	1-D	22
$[Ca(H_2O)((O_2C)_2C_6H_3CO_2H)]_n$	8	Yes	$P\bar{1}$	2-D	23
$[Ca(H_2O)(tda)]_n$	8	Yes	$P\bar{1}$	2-D	58
$[[Ca_2(H_2O)_2(TTF)_2(EtOH)].MeOH]_n$	7	Yes	$P\bar{1}$	2-D	123
$[Ca(H_2O)(C_3H_2O_4)]_n.H_2O$	8	Yes	$C2$	3-D	87
$[Ca(H_2O)(Oac)_2]_n$	7,8	Yes	$P\bar{1}$	2-D	102
$[Ca(H_2O)(bpdc)]_n$	7	Yes	$P2_1$	3-D	53
$[Ca(H_2O)(DMF)(benz)_2]_n$	8	Yes	$P2_1/n$	1-D	40
$[Ca(H_2O)(C_4H_5O_2)_2]_n$	7	Yes	$P2_1/n$	2-D	90
$[Ca(H_2O)(4\text{-}nba)_2(2\text{-}MeIm)]_n$	7	Yes	$P2_1/n$	1-D	26
$[Ca(H_2O)_{1.5}(DPA)]_2$	8	Yes	$C2/c$	Dimer	105
$[Ca(H_2O)_2(C_3H_2O_4)]_n$	7	Yes	$P2_1/c$	2-D	79
$[Ca(H_2O)_2HN(CH_2COO)_3]_n$	7	Yes	$P2_1/c$	3-D	85
$[Ca(H_2O)_2(2\text{-}ca\text{-}4nba)_2]_n$	7	Yes	$P\bar{1}$	1-D	117
$[[Ca(H_2O)_2(3\text{-}npth)].H_2O]_n$		Yes		1-D	
$[Ca(H_2O)_2(H_2dhtp)_2]$	7	Yes	$P\bar{1}$	dimer	125
$[Ca(H_2O)_2(C_3H_2O_4)]_n.2H_2O$	8	Yes	$P2_1/c$	3-D	96
$[Ca(H_2O)_2(todd)]$	8	Yes	$P2_1/c$	Dimer	101
$[Ca(H_2O)_2(C_8H_5O_3)_2]_n$	8	Yes	$C2/c$	1-D	45
$[Ca(H_2O)_2(C_4H_4O_5)_2]_n$	8	Yes	$C2/c$	1-D	68
$[Ca(H_2O)_2(C_7H_3O_2F_2)_2]_n$	8	Yes	$C2/c$	1-D	106
$[Ca(H_2O)_2(DTBB)(C_2H_5OH)_{0.5}]_n$	8	Yes	$C2/c$	2-D	129
$[Ca_2(H_2O)_2(Oac)_3(NO_3)]_n$	8	Yes	Pnma	1-D	41
$[Ca(H_2O)_2(4\text{-}aba)_2]_n$	8	Yes	$P2_12_12_1$	1-D	39
$[Ca(H_2O)_2(L\text{-}Asp)]_n$	8	Yes	$P2_12_12_1$	1-D	109
$[Ca(H_2O)_2(3\text{-}aba)_2]_n$	8	Yes	Pbcn	1-D	42
$[Ca(H_2O)_2(4\text{-}Cnbenz)_2]_n$	8	Yes	$P2/n$	1-D	20
$[Ca(H_2O)_2(2\text{-}OPA)_2]_n$	8	Yes	$Pna2_1$	1-D	46
$[Ca_2(H_2O)_2(C_{14}H_4O_8)]_n$	7	Yes	P-1	3-D	57
$[Ca(H_2O)_2(HBTC)]_n$	8	Yes	$P1$	2-D	70

$[Ca(H_2O)_2(C_7H_2O_6)_2].N_2H_6$	8	No	$P2/c$	0-D	65
$[Ca_{1.5}(H_2O)_2(ptc)]_n$	7	Yes	$P\bar{1}$	3-D	76
$[Ca(H_2O)_2(CMA)_2]$	8	Yes	$P\bar{1}$	1-D	108
$[Ca(H_2O)_2(2\text{-}nba)_2]_n$	8	Yes	$P\bar{1}$	1-D	25
$[Ca(H_2O)_2(C_4H_2O_4)]_n$	8	Yes	$Pna2_1$	1-D	89
$[Ca(H_2O)_2(L_1)_2]$	6	No	$C222_1$	O-D	67
$[Ca(H_2O)_2(H_2dhtp)]$	8	Yes	$P2_1/n$	3-D	110
$[Ca(H_2O)_2(C_6H_3ClNO_2)_2]_n$	8	Yes	$P\bar{1}$	1-D	112
$[Ca(H_2O)_2(C_8H_9N_2O_4)_2]_n$	8	Yes	$C2/c$	1-D	114
$[Ca(H_2O)_2(C_8H_9NO_6)].H_2O$	8	Yes	$P2_1/c$	1-D	116
$[[Ca(H_2O)_2(L\text{-}OMe)_2].H_2O]_n$	8	Yes	$P2_1$	1-D	119
$[[Ca(H_2O)_2(L\text{-}Cl)_2].2H_2O]_n$	8	Yes	$P2_1$	1-D	119
$[Ca(H_2O)_2(4\text{-}nba)_2].(dmp)_2]_n$	7	Yes	$P\bar{1}$	1-D	121
$[Ca(H_2O)_2(hip)_2].H_2O]_n$	8	Yes	$P2_{1/c}$	1-D	122
$[[Ca(H_2O)_2(C_8H_5Cl_2O_3)_2].H_2O]_n$	8	Yes	$P2_1/c$	1-D	91
$[Ca(H_2O)_2(C_4H_4O_4)].H_2O]_n$	8	Yes	$P\bar{1}$	1-D	55
$[Ca(H_2O)_2(C_5H_7NO_4)]_n.H_2O$	8	Yes	$P3_121$	1-D	81
$[[Ca(H_2O)_2(PY\text{-}Thr)_2].2H_2O]_n$	8	Yes	$C2$	1-D	50
$[Ca(H_2O)_2(C_5H_8NO_4)_2]_n.2H_2O$	6	No	$P4_32_12$	1-D	82
$[Ca_3(H_2O)_2(C_4H_4O_4)_3]_n.2H_2O$	7	Yes	$C2/c$	2-D	92
$[Ca(H_2O)_2(C_9H_8NO_4)_2].2.5H_2O]_n$	6	No	$C2/c$	1-D	51
$[[Ca(H_2O)_2(Nic)_2].3H_2O]_n$	7	Yes	$C2/c$	1-D	44
$[Ca(H_2O)_2(C_{84}H_{126}O_{16})\ (L_2)_2].L_2(H_2O)_4$	7	No	$P\bar{1}$	2-D	72
$[[Ca(H_2O)_2(1,3\text{-}bdc)]_{2.5}.4\ H_2O]_n$	8	Yes	$C2/c$	1-D	21
$[[Ca_5(H_2O)_9(1,3\text{-}bdc)_5].8H_2O]_n$	8	Yes	$C2/c$	1-D	35
$[Ca_2(H_2O)_5(C_{30}H_{32}O_{24}N_{12})].3H_2O]_n$	8	Yes	$P1$	3-D	62
$[[Ca(H_2O)_3(4\text{-}fba)](4\text{-}fba)]_n$	8	Yes	$P2_1/c$	1-D	32
$[Ca(H_2O)_3(benz)_2]_n$	8	Yes	$P2_1/c$	1-D	33
$[Ca(H_2O)_3(C_6H_6O_7)]_n$	8	Yes	$P2_1/c$	1-D	103
$[Ca(H_2O)_3(C_8H_4O_4)]_n$	8	Yes	$P2_1/c$	1-D	104
$[Ca(H_2O)_3(DPA)]_2$	8	Yes	$P2_1/c$	Dimer	105
$[Ca(H_2O)_3(CaEDTA)].4H_2O]_n$	7,8	Yes	$P\bar{1}$	2-D	98
$[Ca(H_2O)_3(C_9H_{11}N_6O_5)_2]_n$	10	Yes	$C2/c$	1-D	52
$[[Ca(H_2O)]_2(L)(\mu\text{-}H_2O)]_n$	8	Yes	$P\bar{1}$	1-D	36
$[Ca(H_2O)_3(leu)_2]_n$	8	Yes	$P\bar{1}$	1-D	22
$[Ca(H_2O)_3(5\text{-}OH\text{-}BDC)]_n.H_2O$	8	Yes	$P2_1/c$	2-D	61
$[Ca(H_2O)_3(2\text{-}aba)_2]_n$	7	Yes	$Pbcn$	1-D	47
$[Ca(H_2O)_3(bpdc)]_n$	8	Yes	$Ima2$	1-D	53
$[Ca(H_2O)_3(edoda)]_2$	8	Yes	$P\bar{1}$	Dimer	84
$[[Ca(H_2O)_3(C_2H_5NO_2)_2].I_2]_n$	7	Yes	$Pca2_1$	1-D	111

$[CaCl_2(Hgly)(H_2O)_3]_n$	8	Yes	$P2_{1/c}$	1-D	124
$[Ca(TBbA)(H_2O)_3].H_2O$	7	yes	$P2_1/n$	2-D	128
$[[Ca(H_2O)_4][Ca(L^1)(H_2O)_2]_2.7H_2O]_n$	7	Yes	$P\bar{1}$	1-D	43
$[Ca(H_2O)_4(1,4\text{-bdc})]_n$	8	Yes	$P2_1/c$	1-D	34
$[Ca(H_2O)_4(\eta^1\text{-4-nba})(\eta^2\text{-4-nba})]$	7	No	$P2_1/c$	0-D	63
$[Ca_3(H_2O)_4(Sa)_6(4\text{-bpy})_2]_n$	7,6,7	Yes	$P\bar{1}$	1-D	49
$[Ca(H_2O)_4(Tartarate)]_n$	8	No	$P2_12_12_1$	1-D	77
$[Ca(dl\text{-tartarate})(H_2O)_4]_n$	8	No	$P\bar{1}$	0-D	118
$[Ca(H_2O)_4Br(C_{12}H_{21}O_{12})]$	8	No	$P2_12_12_1$	0-D	95
$[Ca(H_2O)_4(L\text{-Asp})]_n$	7	No	C2	1-D	109
$[Ca(H_2O)_4(C_8H_6N_2O_6)]_n$	8	Yes	P2/c	1-D	66
$[Ca(H_2O)_4(C_4H_4O_6)]_n$	8	No	$P\bar{1}$	1-D	78
$[[Ca(H_2O)_4(Hpdc)].2H_2O]_n$	7	Yes	$P2_1/n$	1-D	48
$[Ca_2(H_2O)_7(C_{12}H_2O_{12}).2H_2O]_n$	7	Yes	$P2_12_12_1$	2-D	86
$[Ca_3(H_2O)_8(BTA)_2]_n.3H_2O$	7,8	Yes	$P\bar{1}$	2-D	71
$[Ca_3(H_2O)_{12}(BTC)_2]_n$	8,7	Yes	C2/c	2-D	69
$[Ca(H_2O)_4(H_2L^1)][(H_2L^1)].4H_2O$	7	No	Cc	0-D	43
$[[Ca(H_2O)_4(AIP)_2](H_2O)]_n$	8	No	R-3	1-D	19
$[[Ca(H_2O)_4(Hpdc)].H_2O]_n$	8	Yes	$P2_1/c$	1-D	48
$[Ca(H_2O)_5(C_9H_7O_4)_2]_n$	8	No	$P\bar{1}$	1-D	88
$[Ca(H_2O)_5(O(CH_2CO_2)_2)_2].H_2O$	8	No	$P2_1/a$	0-D	99
$[Ca(H_2O)_6(PY\text{-Valinato})_2]_n$	8	No	$P2_1$	2-D	50
$[Ca_2(H_2O)_6(C_5H_3O_2N_2)_2]$	8	Yes	$P2_1/n$	Dimer	54
$[Ca(H_2O)_6(C_{16}H_{12}O_4)]_n.H_2O$	8	No	$P\bar{1}$	1-D	107
$[Ca(H_2O)_4(Hbtc)]_n$	7	yes	P21/c	2-D	127
$[Ca(H_2O)_6(4\text{-nba})(2\text{-ap})](4\text{-nba})(2\text{-ap})$	7	No	$P\bar{1}$	0-D	130
$[(H_2O)_6Ca(\mu\text{-3,5-Hpdc})Ca(H_2O)_3(3,5\text{-Hpdc})_2](3,5\text{-Hpdc}).2H_2O$	7	No	$P\bar{1}$	0-D	171

Abbreviations used: C.N. = coordination number; S. G. = Space group; D = dimensionality; pyr = pyrazole; H_2dhtp = 2,5 dihydroxyterephalic acid, $C_5H_3N_2O_2$ = Pyrimidine-2-carboxylate, TTF = tetrathiafulvenebicarboxylate; DMF = N,N- Dimethyl formamide; ABDC = 2-aminobenzene-1,4-dicarboxylate; ndc = 2,6 Naphathalenedicarboxylate; $NH_2.NH.(CO_2)_2$ = Hydrazine carboxylate; $C_3H_3O_4$ = Malonate; N-MeIm = 1-Methyl imidazole; 4-nba = 4- nitrobenzoate; DADC = 5,10-dihydroanthracene-2,7-dicarboxylate;; Sa = Salicylato; Phen = 1, 10-phenanthroline; $C_5H_3O_3$ = 2-Furancarboxylate; $C_{10}H_9O_4$ = Benzylmalonate; NDC = Naphthalene 2, 6-dicarboxylate; DEF = N-N diethylformamide; TPDC = 4,5,9,10-Tetrahydropyrene-2,7-dicarboxylate; BDC- Benzene-1,4-dicarboxylate; HCOO = Formate; $C_{57}H_{102}N_9O_{18}$ = t-butyl-Glycyl–N-isobutylglycine-N-isobutylglycine; $C_8H_4O_4$ = Terephthalate; $C_3H_7N_6$ = 2,4,6-triamino-1,3,5-triazine, $C_7H_3NO_4$ = pyridine-2,6-dicarboxylate, $C_6H_3ClNO_2$ = 2-chloronicotinate,

$C_8H_9N_2O_4$ = 4-carboxy-2-propyl-1H-imidazole-5-carboxylate dnSa = 3,5 dinitrosalicylato; $C_{10}H_8O_6$ = benzene 1,4 dioxylacetate; Hpdc = 3,5 Pyrazoledicarboxylate; ptaH = tris-{2-(4-carboxyphenoxy)ethyl}amine; val = rac-valinate; A_3Br = 1, 3-biscarboxyethylimidazolium bromide; gly = glycinate; $(O_2C)_2C_6H_3CO_2H$ = 1,2,4-benzenetricarboxylate or trimellitate; tda = $S(CH_2COO)_2$; Oac = Acetate; bpdc = 4,4'- biphenyldicarboxylate; benz = benzoate; $C_4H_5O_2$ = 3-butenoate; 2-MeIm = 2-methylimidazole; DPA = dipicolinate; $N(CH_2COO)_3$ = Nitrilotriacetate; 2-ca-4nba = 2-carbamoyl-4-nitrobenzoate; $C_3H_2O_4$ = malate; todd = 3,6,9- trioxaundecanedioate; $C_8H_5O_3$ = 2-Formylbenzoate; $C_4H_4O_5$ = Malate; $C_7H_3O_2F_2$ = 2,6 difluorobenzoate; DTBB = 2,2'-dithiobis(benzoate); NO_3 = nitrate; 4-aba = 4-amino benzoate; L- Asp = L -aspartate; 3-aba = 3-amino benzoate; 4-CNbenz = 4-Cyanobenzoate; 2-OPA = 2-oxo-1, 2-dihydropyridine-1-acetate; $C_{14}H_4O_8$ = 1,4,5,8 naphthalenetetracarboxylate; BTC = 1,3,5 benzenetricarboxylate; $C_7H_2O_6$ =Chelidonic acid; ptc = pyridine-2,4,6-tricarboxylate; CMA = 9,10-Dihydro-9-oxo-10-acridineacetate; 2-nba = 2-nitrobenzoate; $C_4H_2O_4$ = Fumarate; L_1 = $C_{34}H_{46}N_4O_8$ = 2,6-bis(2,2 dimethylpropionylamino)benzoate; $C_8H_9NO_6$ = 3-nitrophthalate, L-Ome = P-methoxy phenyl acetate; L-Cl = 2-Chloro-phenyl acetate; dmp = 3,5 dimethylpyrazole; hip = Hippurate; $C_8H_5Cl_2O_3$ = (2,4-dichlorophenoxy)acetate; $C_4H_4O_4$ = Methylmalonate; $C_5H_7NO_4$ = L-Glutamate; PY = N-(6-amino-3,4-dihydro-3-methyl-5-nitroso-4-oxopyrimidin-2-yl); Thr = Threonate; $C_5H_8NO_4$ = L-Glutamate; $C_4H_4O_4$ = methylmalate; $C_9H_8NO_4$ = 2-(pyridinium-1-yl) butanedioate; Nic = 3-carboxypyridine; L_2 = DMSO; $C_{84}H_{126}O_{16}$ = 5,11,17,23-tetracarboxy-4,6,10,12,16,18,22,24-octa-O-methyl-2,8,14,20-tetra(n-undecyl)resorc[4] arene; 1,3-bdc = 1,3-benzenedicarboxylate; $C_{30}H_{32}O_{24}N_{12}$ = 1,3,5 –Triazine-2,4,6-triamine hexaacetate; 4-fba = 4-fluorobenzoate; benz = benzoate; $C_6H_6O_7$ = citrate; $C_8H_4O_4$ = Pthalate; EDTA = Ethylenediaminetetraacetate; $C_9H_{11}N_6O_5$ = Bis[N-(6-amino-3,4-dihydro-3-methyl-5-nitroso-4-oxopyrimidine-2-yl) glycylglycinate; L = 4-(2-nitrophenyl)-3,6-dioxaoctane dioate; leu = rac-leucinate; 5-OH-BDC = 5 hydroxy isophthalate; 2-aba = 2-amino benzoate; $C_2H_5NO_2$ = Glycine, Hgly = H-glycinate, edoda = ethylenedioxydiacetate; L^1 = 2,2',2''-Nitrilotribenzoate; 1,4-bdc = 1,4 benzenedicarboxylate; 4-nba = 4-nitro benzoate; 4-bpy = 4-4' bipyridine; $C_4H_4O_6$ = Tartrate; $C_{12}H_{21}O_{12}$ = Lactobionic acid; $C_8H_6N_2O_6$ = 3,6-Dioxo-2,5-diazabicyclo[2.2.2.]octane-1,4-dicarboxylate; $C_{12}H_2O_{12}$ = Benzenehexacarboxylic acid; BTA = 1,3,5-benzenetriacetate; AIP = 5-Aminoisopthalate; $C_9H_7O_4$ = Homophthalate; $O(CH_2CO_2)_2$ = Oxydiacetate; $C_5H_3O_2N_2$ = Pyridazine-3-carboxylate; $C_{16}H_{12}O_4$ = meso 2,3 diphenyl succinate; $C_5H_3N(CO_2)_2$ = 2,6-pyridinedicarboxylate (PDC); TBbA = Terephthaloyl-bis-β-alanine, 2-ap = 2-aminopyridine, 3,5-Hpdc = pyridine-3,5-dicarboxylate

Crystal structure description of $[[Ba(H_2O)_3]_2(\mu_2\text{-2-nba-O,O'O-NO}_2)_2(\mu_2\text{-2-nba-O,O,O'})_2]_n$ 22

The coordination polymer $[[Ba(H_2O)_3]_2(\mu_2\text{-2-nba-O,O'O-NO}_2)_2(\mu_2\text{-2-nba-O,O,O'})_2]_n$ **22** crystallizes in the centrosymmetric triclinic space group $P\bar{1}$ and all atoms are located in general positions. The observed Ba-O bond distances vary between 2.703(2) to 2.906(2) Å (Table 26). These values are comparable with those reported for other Ba(II)-carboxylates [169]. In the crystal structure, the Ba(II) is nine coordinated and is bonded to three O atoms from the three aqua ligands and six oxygen atoms from four symmetry related 2-nba anions (Figure 64). The central metal is linked to the O atoms (O9-O11) of three water molecules and the Ba-O(H_2O) distances range from 2.744(2) to 2.807(4) Å.

The polymeric structure is based on a dimer and each formula unit of **22** contains three coordinated water ligands and two unique 2-nitrobenzoate ligands both of which function as tridentate ligands in different fashion. The first unique 2-nba ligand (O1, O2, O3) functions as a monodentate bridging ligand, linking two symmetry related Ba(II) ions via O1 with Ba1-O1 bond distances of 2.816(2) and 2.833(2) Å respectively. It is interesting to note that the O3 oxygen of the nitro functionality makes a Ba1-O3 bond at 2.900(2) Å. This unique tridentate 2-nba ligand is designated as (μ_2-2-nba-O,O,O-NO_2). It is to be noted that the proximity of the nitro group to the carboxylate has resulted in this bond. A similar behavior was earlier reported for the 2D-coordination polymer of Ba(II) derived from 2-aminobenzoic acid with a Ba-N bond at 3.047(4) Å [47]. To the best of our knowledge compound **22** constitutes the first example of a structurally characterized 2-nitrobenzoate showing a coordinated nitro group. The second independent 2-nba ligand (O5, O6) also functions as a tridentate ligand with each Ba(II) linked to O5 and O6 in a bidentate manner (Ba1-O5 2.703(2); Ba1-O6 2.777(2) Å) and the O5 further linked to a symmetry related Ba(II) ion at 2.906(2) Å resulting in a monoatomic bridging mode. However the nitro oxygen atoms are not at bonding distance to Ba(II) for this ligand. This second tridentate 2-nba ligand is designated as (μ_2-2-nba-O,O,O'). The structure of **22** can be explained as being composed of a pair of $\{Ba(H_2O)_3\}$ units linked via two μ_2-carboxylate bridges by a pair of (μ_2-2-nba-O,O,O-NO_2) ligands leading to a (Ba_2O_2) four membered ring (Figure 65) with a Ba···Ba distance of 4.5726(14) Å resulting in the formation of dimeric units of composition $[Ba(H_2O)_3(\mu_2\text{-2-nba-O,O,O-NO}_2)_2]_2$ along *b* axis. The linking of a pair of $\{Ba(H_2O)_3\}$ units by a pair of tridentate (μ_2-2-nba-O,O,O') ligands results in the formation of dimeric units of composition $[Ba(H_2O)_3(\mu_2\text{-2-nba-O,O'O'})_2]_2$ along *b* axis (Figure 65). It is interesting to note that this binding mode of 2-

nba results in a Ba···Ba separation of 4.5406(15) Å, which is slightly shorter than the Ba···Ba separation observed earlier for the tridentate 2-nba ligand binding through the nitro oxygen. The extended structure is arrived at by the linking of two $[Ba(H_2O)_3(\mu_2\text{-}2\text{-}nba\text{-}O,O,O\text{-}NO_2)_2]$ units by a pair of (μ_2-2-nba-O,O,O′) ligands. Thus the two different tridentate 2-nba ligands link the $\{Ba(H_2O)_3\}$ units into a one dimensional polymeric chain along *b* axis. In the infinite chain, each nine coordinated Ba(II) is bonded to three water molecules and further linked to six oxygen atoms of four different 2-nba anions with alternating pairs of Ba(II) ions in the chain bridged by a pair of (μ_2-2-nba-O,O′,O-NO_2) and (μ_2-2-nba-O,O,O′) ligands resulting in alternating Ba···Ba distances of 4.5406(15) and 4.5726(14) Å across the chain (Figure 66). An analysis of the crystal structure of **22** reveals that each nine coordinated Ba(II) complex in the polymeric chain is H-bonded to neighbouring complexes in the polymeric chain with the aid of two varieties of H-bonding interactions. All the hydrogen atoms attached to the coordinated waters excepting H10B and one hydrogen atom on a benzene ring function as H-donors. Two oxygen atoms from the coordinated water molecules O9 and O10, the free carboxylate oxygen O2 and the coordinated oxygen O6 and the nitro oxygen O8 function as H-acceptors. Thus each Ba(II) complex in **22** is linked to five other complexes with the aid of five O-H···O bonds and a C-H···O interaction (Table 27). The C-H···O interaction between the nitro oxygen O8 and an aromatic H serves to link parallel chains resulting in a two dimensional H-bonded network (Figure 67). The short ring interactions and distances between the ring centroids (Cg-Cg) in **22** were analysed by using the program PLATON [204]. The Cg-Cg distance between the two 2-nba ligands is 4.089 Å and the perpendicular distance from the center of the first ring to the second (interplanar distance) is 3.644 Å accompanied by a dihedral angle of 5.58°. These values indicate that the rings do not overlap and the magnitude of the values is suggestive of no stacking interactions.

The availability of structural information of many Ba(II) coordination polymers of varying dimensionalities derived from several carboxylic acids permits a comparative study of Ba(II) coordination polymers. In these compounds the Ba···Ba distance across the polymeric chain varies from 4.069(2) in the three dimensional (3-D) coordination polymer derived from 2,2′-dithiobis(benzoic acid) to 7.467 Å in the 1-D Ba(II) polymer derived from the N-substituted amino acid containing the N-(6-amino-3,4-dihydro-3-methyl-5-nitroso-4-oxopyrimidin-2-yl) group (Table 28). In all these compounds, the carboxylate anions function as bridging ligands. The coordination number of Ba(II) varies from 8 to 10 with nine coordination observed in several compounds. In four of the polymers the Ba···Ba separations are shorter than the sum of the van der Waals radii (4.28 Å) indicating weak metal-metal interactions, while in other compounds the observed metal-metal contacts are longer. Interestingly the observed Ba···Ba distances of 4.5406(15) and 4.5726(14) Å in **22** are much shorter than the Ba···Ba separation of 6.750(1) Å in the related 1-D polymer $[Ba(H_2O)_5(4\text{-nba})_2]_n$ derived from 4-nitrobenzoic acid where the nitro group is disposed trans to the carboxylate. It is to be noted that the polymeric complex $[Ba(H_2O)_5(4\text{-nba})_2]_n$ contains two unique 4-nba ligands one of which functions as a bidentate ligand with the other functioning as a bridging bidentate ligand [169]. In the Ba(II) polymer of 4-nba the oxygen atoms of the nitro group are not involved in coordination unlike in compound **22.** It is interesting to note that both the oxygen atoms of the nitro functionalities in both the unique 4-nba ligands in $[Ba(H_2O)_5(4\text{-nba})_2]_n$ are involved in C-H···O interactions unlike in compound **22** where one oxygen atom (O8) of the tridentate (μ_2-2-nba-O,O,O') ligand is involved in C-H···O bonding. In the Ba(II) coordination polymer derived from 2-aminobenzoic acid the Ba(II) exhibits a Ba-N bond but the coordination polymer is three dimensional. Hence it appears that the Ba···Ba distances in Ba-carboxylate coordination polymers are probably determined by a combination of several factors, which include the electronic and steric requirements of the central metal, the denticity, flexibility, bridging behaviour and H-bonding characteristics of the carboxylate ligand.

Table 26- Selected bond distances (Å) and bond angles (°) for compound $[Ba(H_2O)_3(2\text{-nba})_2]_n$ **22**

$[Ba(H_2O)_3(2\text{-nba})_2]_n$			
Ba(1)-O(5)	2.703(2)	Ba(1)-O(1)	2.816(2)
Ba(1)-O(11)	2.744(2)	$Ba(1)-O(1)^{ii}$	2.833(2)
Ba(1)-O(10)	2.767(3)	Ba(1)-O(3)	2.900(2)
$Ba(1)-O(6)^{i}$	2.777(2)	$Ba(1)-O(5)^{i}$	2.906(2)
Ba(1)-O(9)	2.807(4)	$Ba(1)-Ba(1)^{i}$	4.5406(15)
$Ba(1)-Ba(1)^{ii}$	4.5726(14)		

Symmetry codes (i) -x+1, -y+1, -z+1 ; ii) -x+1, -y+2, -z+1

Table 27- Hydrogen bonding geometry (Å,°) for compound $[Ba(H_2O)_3(2\text{-nba})_2]_n$

D-H---A	d(D-H)	d(H---A)	D(D---A)	<DHA	Symmetry code
$[Ba(H_2O)_3(2\text{-nba})_2]_n$					
O11-H11A···O9	0.836	1.949	2.780	173	-x+1, -y+1, -z+1
O9-H9A···O10	0.797	2.275	2.775	121	-x+1, -y+2, -z+1
O10-H10A···O6	0.857	1.899	2.752	174	x-1, y+1, z
O11-H11B···O2	0.847	1.870	2.714	175	x-1, y, z
O9-H9B···O2	0.817	2.429	3.224	165	
C12-H12···O8	0.930	2.689(3)	3.612	172	x+1, y, z

Table 28- Ba···Ba distances across the chain in some Ba(II) coordination polymers containing bridging carboxylates

Compound	C.N.	Ba···Ba distance (Å)*	Dimensionality (D) of polymer	Reference
$[\{Ba_2(DTBB)_2(H_2O)_2\}0.5H_2O]_n^{\#}$	9, 8, 8	4.069(2)	3-D	136
$[Ba(C_6H_4(COO)_2)]_n$	8	4.123	3-D	153
$[Ba(Hbpdc)_2(H_2O)_2]_n$	9	4.1386(17)	1-D	151
$[Ba_9(CH_3COO)_{14}(ClO_4)_4]_n^{\#}$	8,9,9	4.27	3D	152
$[Ba(2\text{-aba})_2(H_2O)_2]_n$	9	4.32	2-D	47
$[Ba(C_7H_5O_2S)_2(H_2O)_4]_n$	9	4.335	1-D	150
$[Ba(C_8H_5O_3)_2(H_2O)_2]_n$	8	4.4336(3)	1-D	154
$[[Ba(PY\text{-met})_2(H_2O)_4].3H_2O]_n$	10	4.4451(2)	3-D	50
$[[Ba(H_2O)_3(2\text{-nba})_2]_2]_n$ **1**	9	4.5406(15) 4.5726(14)	1-D	165
$[Ba(C_5H_4O_4)_2(H_2O)_4]_n$	9	4.595(4)	2-D	155
$[Ba(1,3\text{-BDOA})(H_2O)_2]_n$	10	4.755(3)	3-D	156
$[Ba(C_{10}H_{12}N_5O_6)_2(H_2O)_6]_n$	9	6.575(0)	1-D	157
$[Ba(H_2PMA)(H_2O)_5]_n$	9	6.65	2-D	135
$[Ba(H_2O)_5(4\text{-nba})_2]_n$	9	6.750(1)	1-D	169
$[[Ba(H_2IDC)_2(H_2O)_4].2H_2O]_n$	10	6.765(3)	2-D	156
$[[Ba(PY\text{-glycinato})_2(H_2O)_5].H_2O]_n$	9	6.916(1)	1-D	50
$[[Ba(PY\text{-serinato})_2(H_2O)_4].3H_2O]_n$	10	7.139(0)	1-D	50
$[[Ba(PY\text{-glycilglycinato})_2(H_2O)_2]_n$	8	7.467	2-D	50
$[Ba(\mu\text{-dmf})(\mu\text{-ndc})]_n$	8	4.039	2-D	73
$[Ba(H_2O)_4(H_2pdc)_2].2H_2O$	10	8.856(4)	1-D	48
$[Ba(H_2O)(Hpdc)_2]$	9,10	4.0771(15)	3-D	48
$[Ba(Sa)_2(Phen)_2]_n$	8		1-D	49
$[[Ba(Sa)_2(H_2O)_3](4\text{-bpy})_{1.5}(H_2O)]_n$	7		1-D	49
$[Ba_3(H_2O)_8(bta)_2]_n.3H_2O$	8	4.2835(3) 4.3317(4)	2-D	71
$[Ba_3(H_2O)_8(BTC)_2].2\ H_2O]_n$	8,10		3-D	This work
$[[Ba(C_7H_2N_2O_7)(H_2O)_2]\ .H_2O]_n$	10	4.767(5)	1-D	162

Abbreviations used: C.N. = coordination number; #three unique Ba(II) ions; DTBB = 2,2′-dithiobis(benzoate); $(C_6H_4(COO)_2)]$ = terephthalate; Hbpdc = 2′carboxybiphenyl-2-carboxylate; 2-aba = 2-aminobenzoate; $(C_7H_5O_2S)$ = thiosalicylate; $(C_8H_5O_3)$ = 2-formylbenzoate; PY = N-(6-amino-3,4-dihydro-3-methyl-5-nitroso-4-oxopyrimidin-2-yl); met = monoanion of methionine; $C_5H_4O_4$ = mesaconate anion; (1,3-BDOA) = m-phenylenedioxyacetate; ($C_{10}H_{12}N_5O_6$) = N-4-amino-1,6-dihydro-1-methyl-5-nitroso-6-oxopyrimidin-2-yl-(S)-glutamato; (H_4PMA) = pyromellitic acid; 4-nba = 4-nitrobenzoate; H_2IDC = 1H-imidazole-4,5-dicarboxylato monoanion; 2,6-ndc = 2,6 naphthalenedicarboxylate; dmf = dimethylformamide; pdc = pyridine-3,5-dicarboxylate; Sa = salicylate; Phen = 1, 10-phenanthroline; 4-bpy = 4,4′-bipyridine; bta = 1,3,5-benzenetriacetate; *For 2-D and 3-D polymers only the shortest Ba···Ba contact is given.

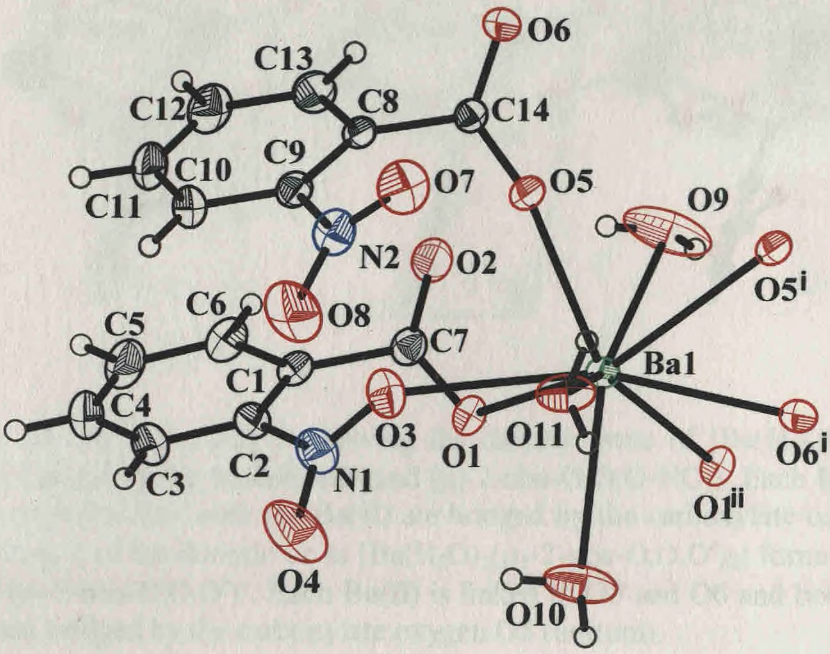

Figure 64- The coordination sphere of Ba(II) in $[[Ba(H_2O)_3]_2(\mu_2\text{-}2\text{-nba-O,O,}\mu O\text{-}NO_2)_2(\mu_2\text{-}2\text{-nba-O,O,O}')_2]_n$ **1** showing the atom-labeling scheme. Displacement ellipsoids are drawn at the 50% probability level except for the H atoms, which are shown as circles of arbitrary radius. Symmetry code: i) -x+1, -y+1, -z+1 ; ii) -x+1, -y+2, -z+1

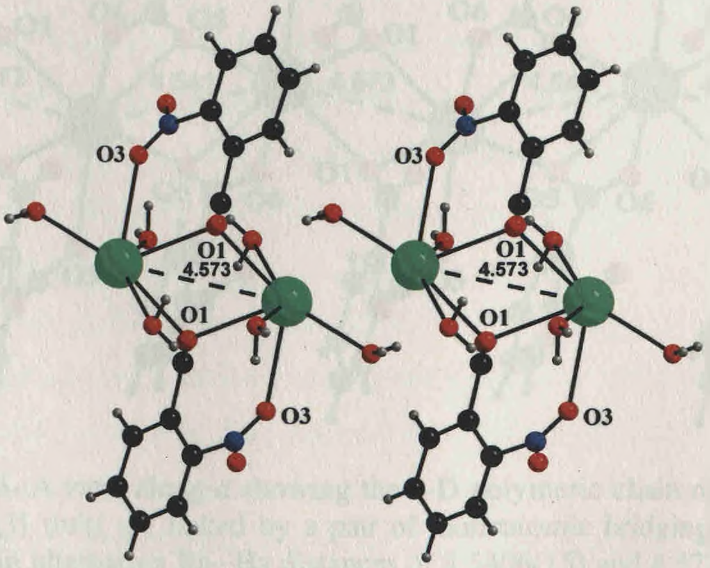

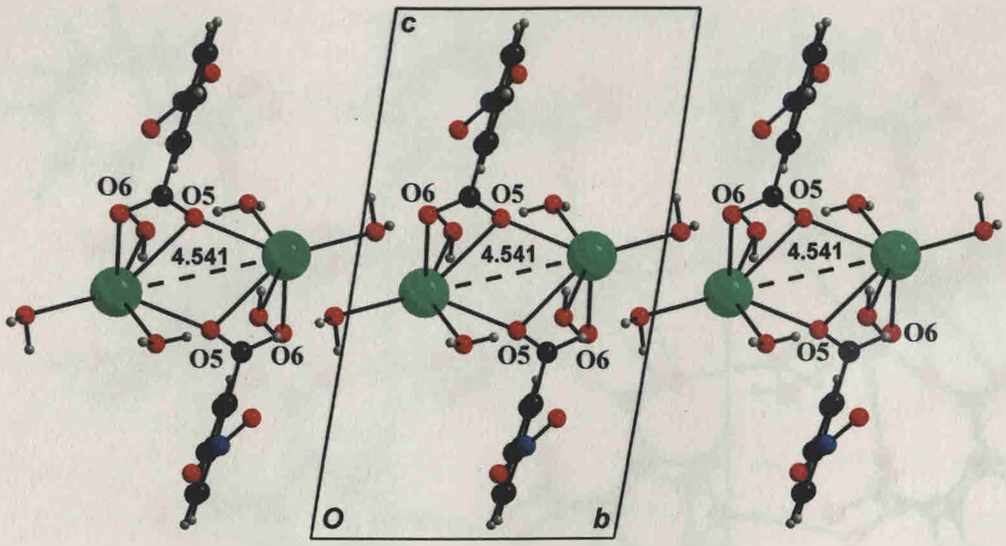

Figure 65- A view along *a* showing the dimeric units of $[Ba(H_2O)_3(\mu_2\text{-2-nba-O,O,O-}NO_2)_2]$ formed by the tridentate ligand (μ_2-2-nba-O,O,O-NO_2). Each Ba(II) is linked to a nitro oxygen O3 and both the Ba(II) are bridged by the carboxylate oxygen O1 (top). A view along *a* of the dimeric units $[Ba(H_2O)_3(\mu_2\text{-2-nba-O,O,O}')_2]$ formed by the tridentate ligand (μ_2-2-nba-O,O,O′) . Each Ba(II) is linked to O5 and O6 and both the Ba(II) in the dimer are bridged by the carboxylate oxygen O5 (bottom).

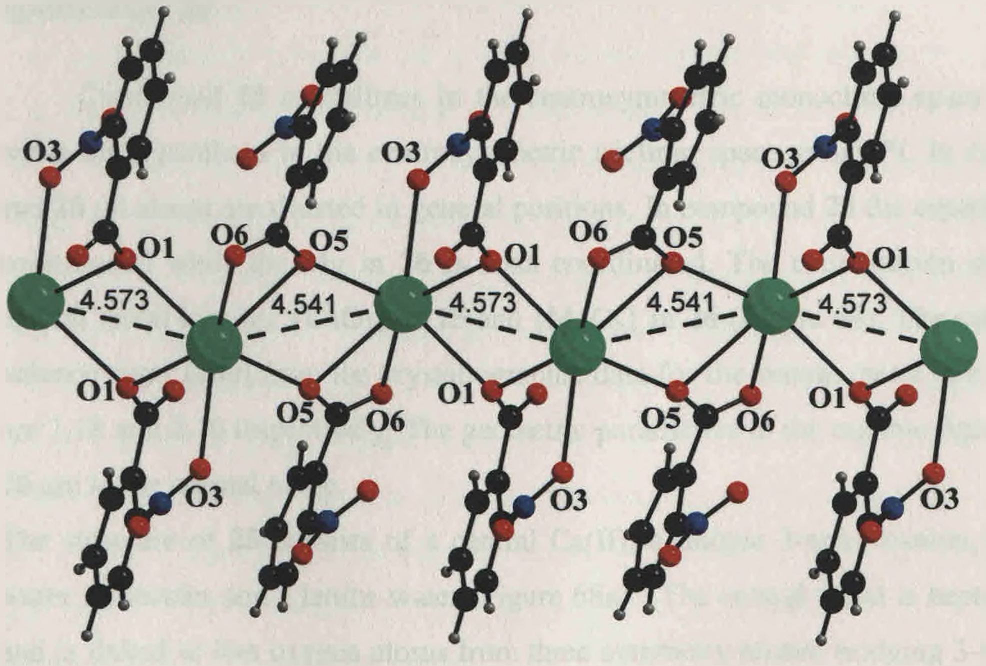

Figure 66- A view along *a* showing the 1-D polymeric chain of **22.** Alternating pairs of $\{Ba(H_2O_3)\}$ units are linked by a pair of monoatomic bridging tridentate 2-nba ligands resulting in alternating Ba···Ba distances of 4.5406(15) and 4.5726(14) Å. For clarity, the coordinated water molecules on Ba(II) are not shown.

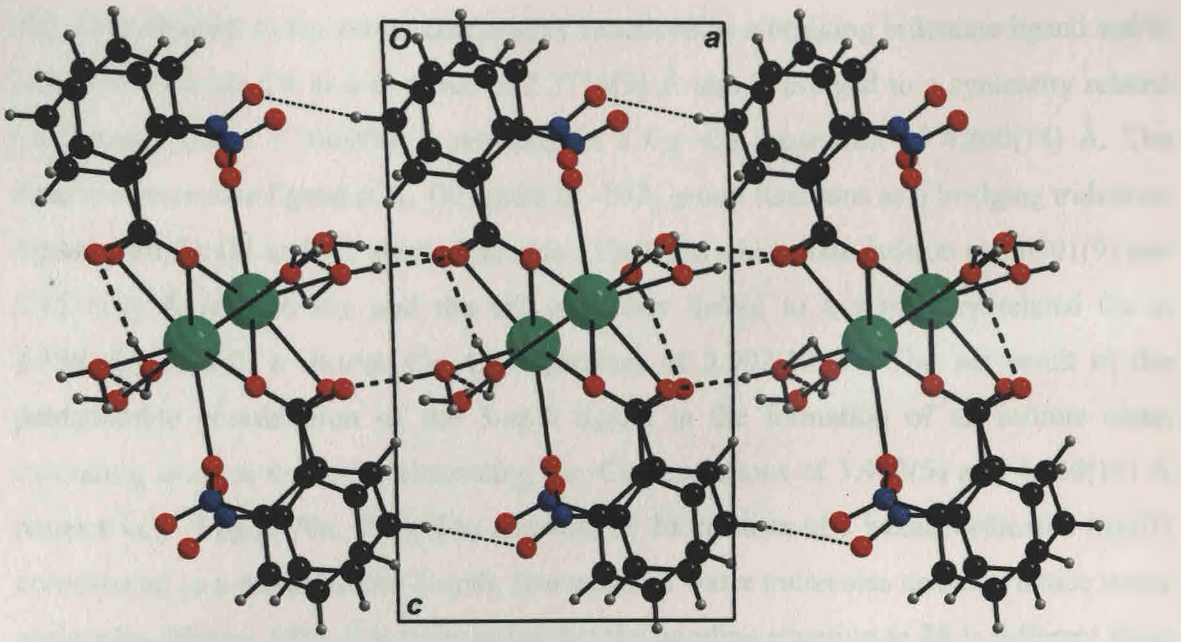

Figure 67: Packing diagram of $[[Ba(H_2O)_3]_2(\mu_2\text{-2-nba-O,O}, \mu\text{-O-NO}_2)_2(\mu_2\text{-2-nba-O,O,O}')_2]_n$ **22** viewed along *b* axis showing the O-H···O (dashed lines) and C-H···O (dotted lines) interactions.

Crystal structure description of $[[Ca(H_2O)_2(\text{3-npth})].H_2O]_n$ 25 and $[Mg(H_2O)_5(\text{3-npth})].2H_2O$ 26

Compound **25** crystallizes in the centrosymmetric monoclinic space group $P2_1/c$ while **26** crystallizes in the centrosymmetric triclinic space group $P\bar{1}$. In compounds **25** and **26** all atoms are situated in general positions. In compound **25** the central Ca is seven coordinated while the Mg in **26** is hexa coordinated. The coordination spheres of the central metal ions are $\{CaO_7\}$ in **25** and $\{MgO_6\}$ in **26** (Figure 68). The calculated bond valence sums [199] from the crystallographic data for the central metal ions in **25** and **26** are 2.18 and 2.10 respectively. The geometric parameters of the organic ligands in **25** and **26** are in the normal range.

The structure of **25** consists of a central Ca(II), a unique 3-npth dianion, two terminal water molecules and a lattice water (Figure 68a). The central metal is hepta coordinated and is linked to five oxygen atoms from three symmetry related bridging 3-nitrophthalate anions, two terminal water molecules resulting in a distorted pentagonal bipyramidal $\{CaO_7\}$ polyhedron (Figure 69). The Ca-O bond distances vary between 2.3310(9) to 2.6301(9) Å, while the O-Ca-O angles range from 51.43(3) to 157.73(3)° (Table 29). The 3-npth functions as a bridging pentadentate ligand (Figure 69). The carboxylate group

(O3, O4) adjacent to the nitro functionality functions as a bridging bidentate ligand and is linked to a Ca via O4 at a distance of 2.3718(9) Å and is bridged to a symmetry related Ca through O3 at 2.3669(9) Å resulting in a Ca···Ca separation of 4.860(18) Å. The distant carboxylate ligand (O1, O2) meta to $-NO_2$ group functions as a bridging tridentate ligand with the O1 and O2 atoms linked to a Ca(II) in a bidentate fashion at 2.6301(9) and 2.4516(9) Å respectively and the O2 is further linked to a symmetry related Ca at 2.3504(9) Å with a shorter Ca···Ca separation of 3.902(12) Å. The net result of the pentadentate coordination of the 3-npth ligand is the formation of an infinite chain extending along *a* axis with alternating Ca···Ca separations of 3.902(5) and 4.860(18) Å respectively (Figure 70a, 70b). The structure of **26** consists of a hexacoordinated Mg(II) coordinated to a monodentate 3-npth, five terminal water molecules and two lattice water molecules (Figure 68b). It is to be noted that the bonding situation in **26** is different from that normally observed for several known Mg(II) compounds consisting of an octahedral $[Mg(H_2O)_6]^{2+}$ unit [39, 44, 131-136]. The trans O-Mg-O angles deviate from ideal values and range from 169.73(4) to 176.70(5)° while the cis O-Mg-O angles range between 84.20(4) and 100.47(5)° (Table 29) indicating a distortion of the $\{MgO_6\}$ octahedron. The Mg-O bond lengths scatter in a very narrow range between 2.0351(11) to 2.1255(8) Å. The npth dianion functions as a monodentate ligand and makes a Mg-O bond at 2.0351(11) Å. The supramolecular structure of **26** is similar to that of **25** in that only O-H···O interactions (Table 30) between the hydrogen atoms of coordinated and lattice water molecules and all the oxygen atoms excepting O2, O11 and O15 are observed. The O17-H13O···O16 bond between the lattice waters O16 and O17 results in the formation of a water dimer, which is H-bonded to six different $[Mg(H_2O)_5(3\text{-npth})]$ units (Figure 71). The water dimers are linked into an infinite H-bonded chain along *a* axis (Figure 72) by the O1 atom of 3-npth ligand with the aid of O17-H14O···O1 and O16-H12O···O1 interactions. The nitro group in compound **25** is not involved in any C-H···O interactions, and exhibits only O-H···O interactions (Table 30) involving the H atoms of coordinated and lattice water molecules (H-donors) and the oxygen atoms of nitro and carboxylate groups and the lattice water (Figures 73 and 74).

Table 29. Selected bond distances (Å) and bond angles (°) for [[Ca(H$_2$O)$_2$(3-npth)]·H$_2$O]$_n$ **25** and [Mg(H$_2$O)$_5$(3-npth)]·2H$_2$O **26**

[Mg(H$_2$O)$_5$(3-npth)]·2H$_2$O **26**			
Mg(1)-O(2)	2.0351(11)	Mg(1)-O(12)	2.0861(10)
Mg(1)-O(15)	2.0491(10)	Mg(1)-O(14)	2.1132
Mg(1)-O(11)	2.0804(11)	Mg(1)-O(13)	2.1255(8)
O(2)-Mg(1)-O(15)	91.13(5)	O(11)-Mg(1)-O(14)	169.73(4)
O(2)-Mg(1)-O(11)	100.47(5)	O(12)-Mg(1)-O(14)	90.33(4)
O(15)-Mg(1)-O(11)	92.50(4)	O(2)-Mg(1)-O(13)	172.94(4)
O(2)-Mg(1)-O(12)	89.49(4)	O(15)-Mg(1)-O(13)	88.67(4)
O(15) -Mg(1)-O(12)	176.70(5)	O(11) -Mg(1)-O(13)	86.58(4)
O(11)-Mg(1)-O(12)	84.20(4)	O(12)-Mg(1)-O(13)	91.11(4)
O(2)-Mg(1)-O(14)	88.13(4)	O(14)-Mg(1)-O(13)	84.84(3)
O(15) -Mg(1)-O(14)	92.93(4)		
[[Ca(H$_2$O)$_2$(3-npth)]·H$_2$O]$_n$ **25**			
Ca(1)-O(7)	2.3310(9)	Ca(1)-O(4)	2.3718(9)
Ca(1)-O(2)	2.3504(9)	Ca(1)-O(2)^{ii}	2.4516(9)
Ca(1)-O(8)	2.3590(9)	Ca(1)-O(1)^{ii}	2.6301(9)
Ca(1)-O(3)^{i}	2.3669(9)	Ca^{ii} (1)-O(2)	2.4516(9)
Ca^{ii}(1)-O(1)	2.6301(9)	Ca(1)-Ca(1)^{ii}	3.9016(5)
Ca^{i}(1)-O(3)	2.3669(9)		
O(7)-Ca(1)-O(2)	153.61(3)	O(7)-Ca(1)-O(2)^{ii}	131.29(3)
O(7)-Ca(1)-O(8)	83.13(3)	O(2)-Ca(1)-O(2)^{ii}	71.34(3)
O(2) –Ca(1)-O(8)	86.59(3)	O(8)-Ca(1)-O(2)	84.48(3)
O(7)-Ca(1)-O(3)^{i}	93.58(3)	O(3)^{i}-Ca(1)-O(2)^{ii}	81.00(3)
O(2)-Ca(1)-O(3)^{i}	104.81(3)	O(4)-Ca(1)-O(2)^{ii}	146.14(3)
O(8)-Ca(1)-O(3)^{i}	157.44(3)	O(7)-Ca(1)-O(1)^{ii}	80.63(3)
O(7)-Ca(1)-O(4)	82.31(3)	O(2)-Ca(1)-O(1)^{ii}	122.67(3)
O(2)-Ca(1)-O(4)	77.56(3)	O(8)-Ca(1)-O(1)^{ii}	85.07(3)
O(8)-Ca(1)-O(4)	107.01(3)	O(3)^{i}-Ca(1)-O(1)^{ii}	72.38(3)
O(3)^{i}-Ca(1)-O(4)	94.58(3)	O(4)-Ca(1)-O(1)^{ii}	157.73(3)
O(2)^{ii}-Ca(1)-O(1)^{ii}	51.43(3)		

Symmetry codes i) –x+1, -y+1, -z+1 ii) 2-x, -y+1, -z+1

Table 30- Hydrogen- bonding geometry (Å, °) for compound [[Ca(H$_2$O)$_2$(3-npth)]·H$_2$O]$_n$ **25** and [Mg(H$_2$O)$_5$(3-npth)]·2H$_2$O **26**

D-H---A	d(D-H)	d(H---A)	D(D---A)	<DHA	Symmetry code
[Mg(H$_2$O)$_5$(3-npth)]·2H$_2$O **26**					
O7-H107···O	0.840	1.947	2.761	163	x, y, z-1
O7-H207···O9	0.840	1.920	2.753	171	
O8-H108···O4	0.840	2.057	2.890	171	x-1, y, z
O8-H108···O5	0.840	2.603	3.019	112	x-1, y, z
O8-H208···O9	0.840	2.230	2.899	137	x-1, y, z
O8-H208···O6	0.840	2.360	3.061	141	x-1, -y+1/2, z-1/2
O9-H109···O3	0.840	2.143	2.964	166	x, y, z-1
O9-H209···O1	0.840	2.183	3.009	168	-x+1, -y+1, -z+1
[[Ca(H$_2$O)$_2$(3-npth)]·H$_2$O]$_n$ **25**					
O11-H1O···O13	0.840	2.080	2.916	173	-x+2, -y+2, -z+2

O11-H2O···O12	0.840	1.947	2.771	167	-x+1, -y+2, -z+1
O12-H3O···O1	0.840	1.817	2.654	175	-x+1, -y+2, -z+1
O12-H4O···O4	0.840	1.879	2.714	172	-x+1, -y+1, -z+1
O13-H5O···O14	0.840	2.141	2.947	161	-x+2, -y+1, -z+1
O13-H6O···O17	0.840	1.852	2.677	167	
O14-H7O···O3	0.840	1.847	2.684	175	-x+1, -y+1, -z+1
O14-H8O···O4	0.840	1.876	2.713	174	
O15-H9O···O3	0.840	1.846	2.681	172	x+1, y, z
O15-H10O···O17	0.840	1.915	2.747	171	-x+2, -y+2, -z+1
O17-H13O···O16	0.840	1.943	2.754	162	
O17-H13O···O6	0.840	2.626	3.059	114	x+1, y+1, z-1
O17-H14O···O1	0.840	2.263	2.945	138	-x+1, -y+2, -z+1
O17-H14O···O5	0.840	2.518	2.953	113	-x+1, -y+1, -z+1
O16-H11O···O4	0.837	1.986	2.819	173	-x+2, -y+1, -z+1
O16-H12O···O1	0.863	2.122	2.930	156	-x+2, -y+2, -z+1

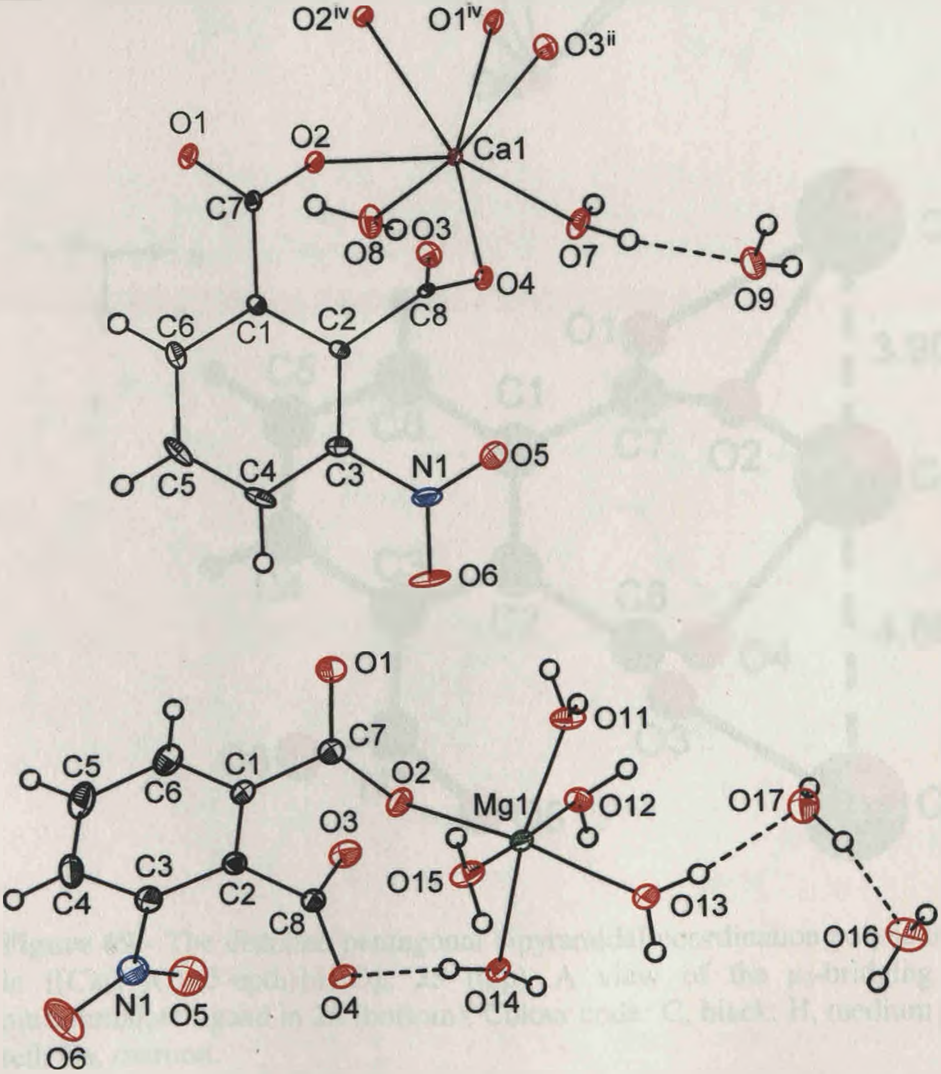

Figure 68- A view of the coordination sphere of the central metal ion in $[[Ca(H_2O)_2(3\text{-}npth)]\cdot H_2O]_n$ **25** (a), $[Mg(H_2O)_5(3\text{-}npth)]\cdot 2H_2O$ **26** (b) showing the atom-labeling scheme. Displacement ellipsoids are drawn at the 50% probability level excepting for the H atoms, which are shown as circles of arbitrary radius. Intramolecular H-bonding is shown as broken lines. Symmetry code: ii) -x+1, -y+1, -z+1 iv) -x, -y+1, -z+1

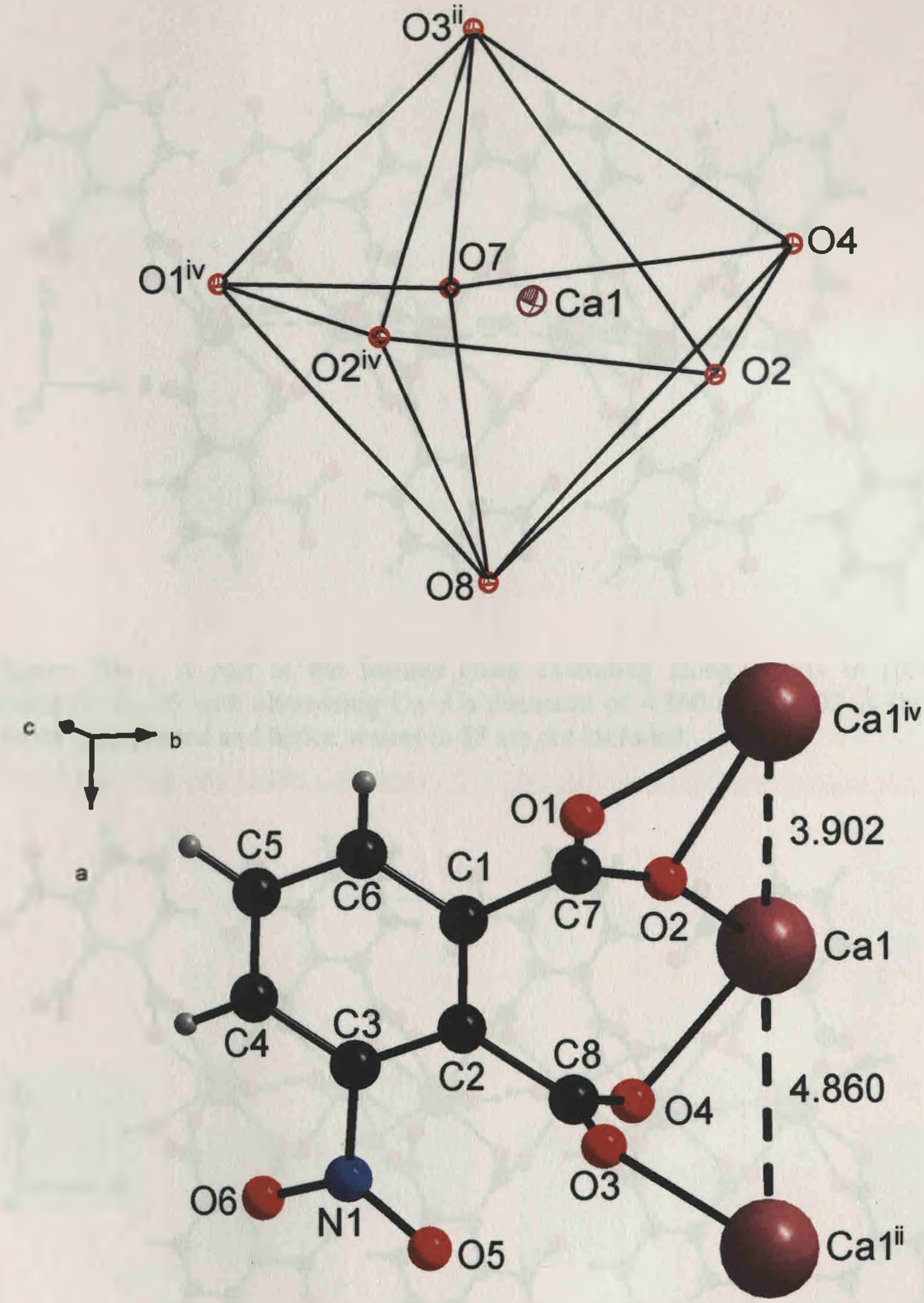

Figure 69 - The distorted pentagonal bipyramidal coordination polyhedron around Ca(II) in $[[Ca(H_2O)_2(3\text{-npth})]\cdot H_2O]_n$ **25** (top). A view of the μ_3-bridging pentadentate 3-nitrophthalate ligand in **25** (bottom). Colour code: C, black; H, medium grey; N, blue; O, red; Ca, maroon.

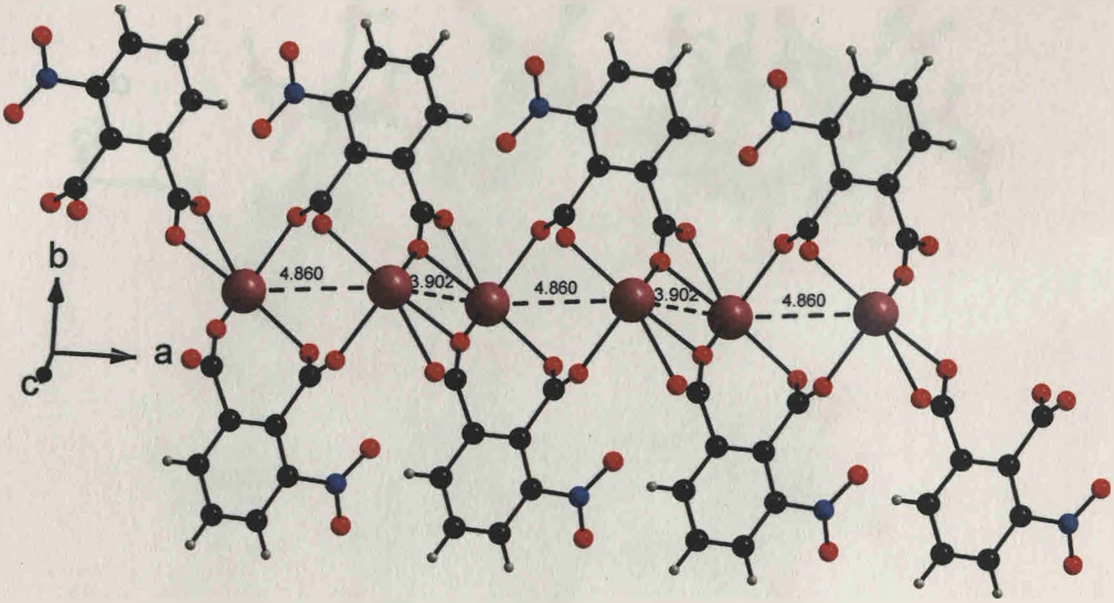

Figure 70a - A part of the infinite chain extending along *a* axis in [[Ca(H_2O)$_2$(3-npth)]·H_2O]$_n$ **25** with alternating Ca···Ca distances of 4.860 and. 3.902 Å (bottom). For clarity coordinated and lattice waters in **25** are not included.

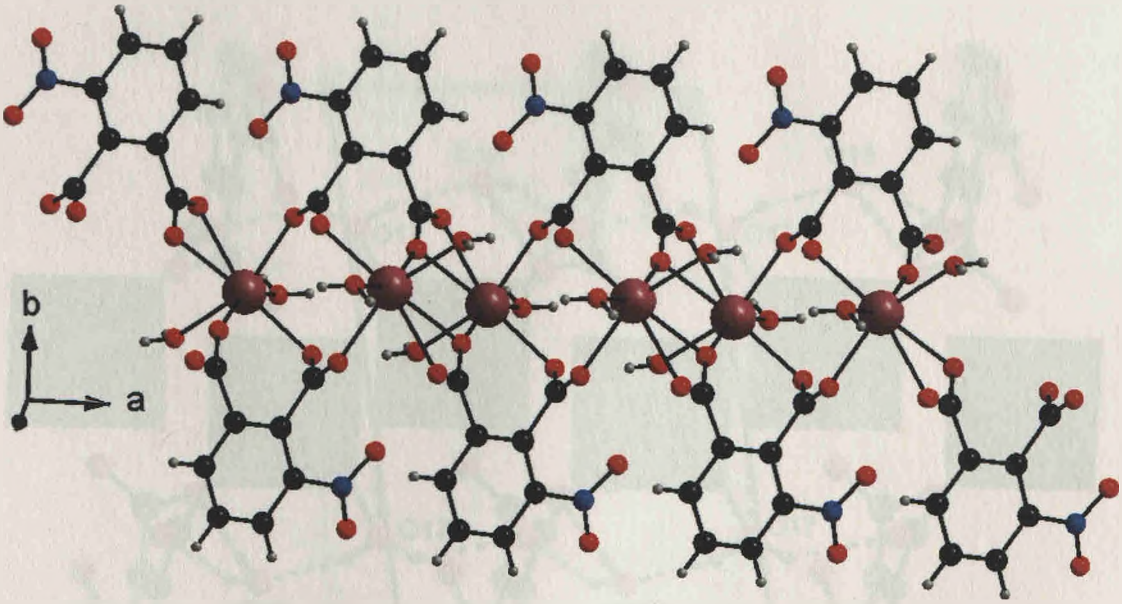

Figure 70b- A portion of the 1-D polymeric chain extending along *a* axis in [[Ca(H_2O)$_2$(3-npth)]·H_2O]$_n$ **25** with alternating Ca···Ca separations of 4.860 and. 3.902 Å. Colour code: C, black; H, medium grey; N, blue; O, red; Ca, maroon.

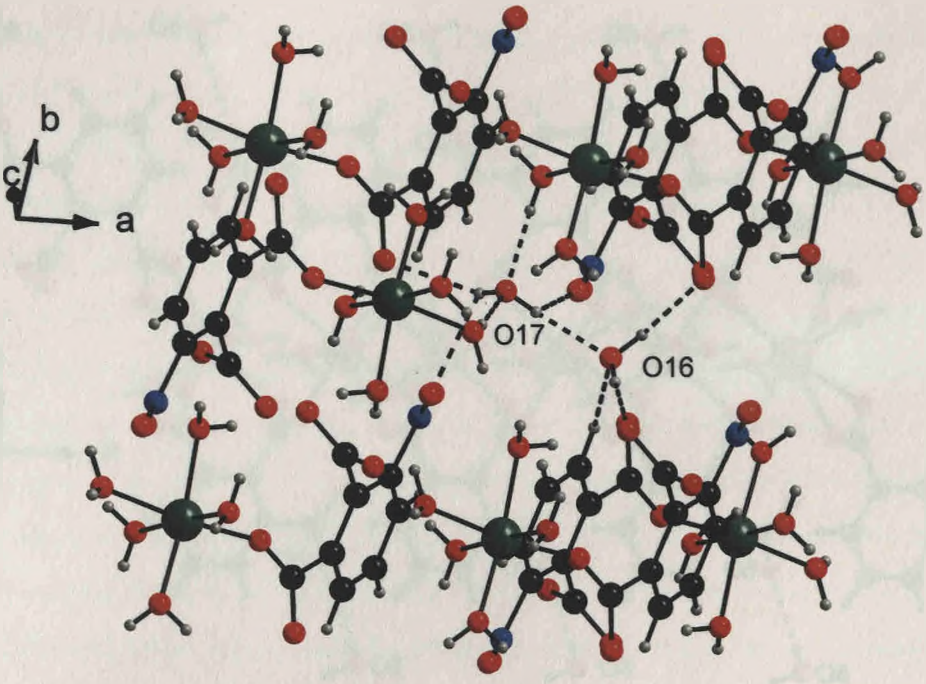

Figure 71- H-bonding situation around the water dimer in $[Mg(H_2O)_5(3\text{-npth})]\cdot 2H_2O$ **26** showing the linking of water dimer to seven different Mg(II) complexes with the aid of O-H···O interactions. Colour code: C, black; H, medium grey; N, blue; O, red; Mg, green.

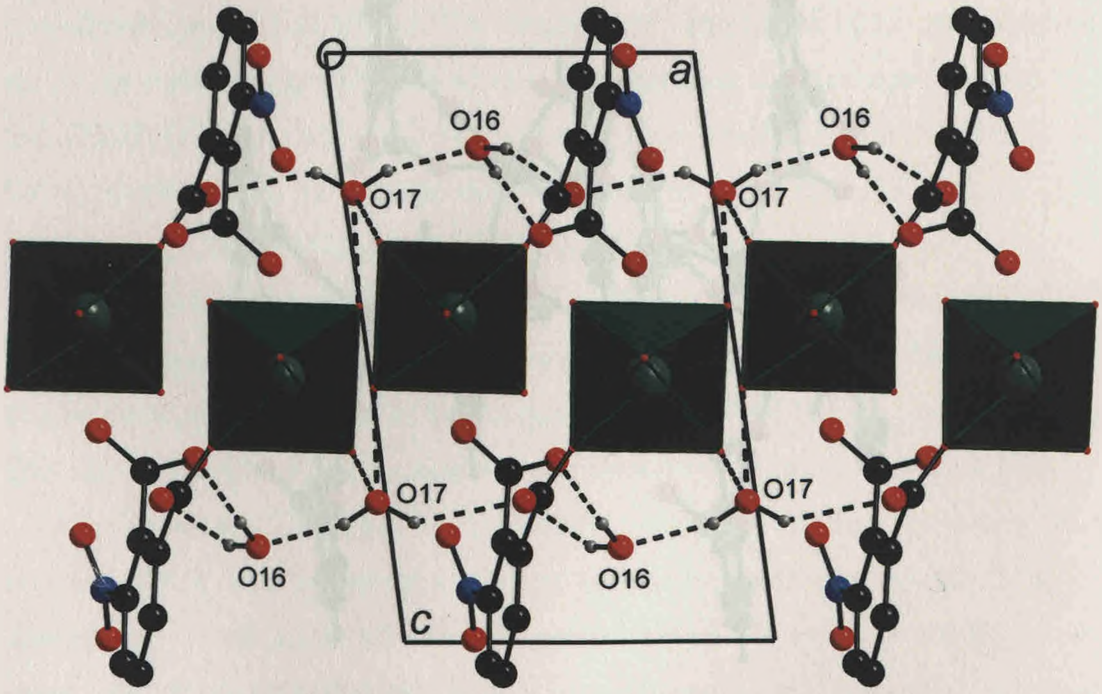

Figure 72- The O1 atom of $[Mg(H_2O)_5(3\text{-npth})]\cdot 2H_2O$ **26** links adjacent water dimers into a H-bonded chain along *a* axis. $\{MgO_6\}$ units are represented as open octahedra.

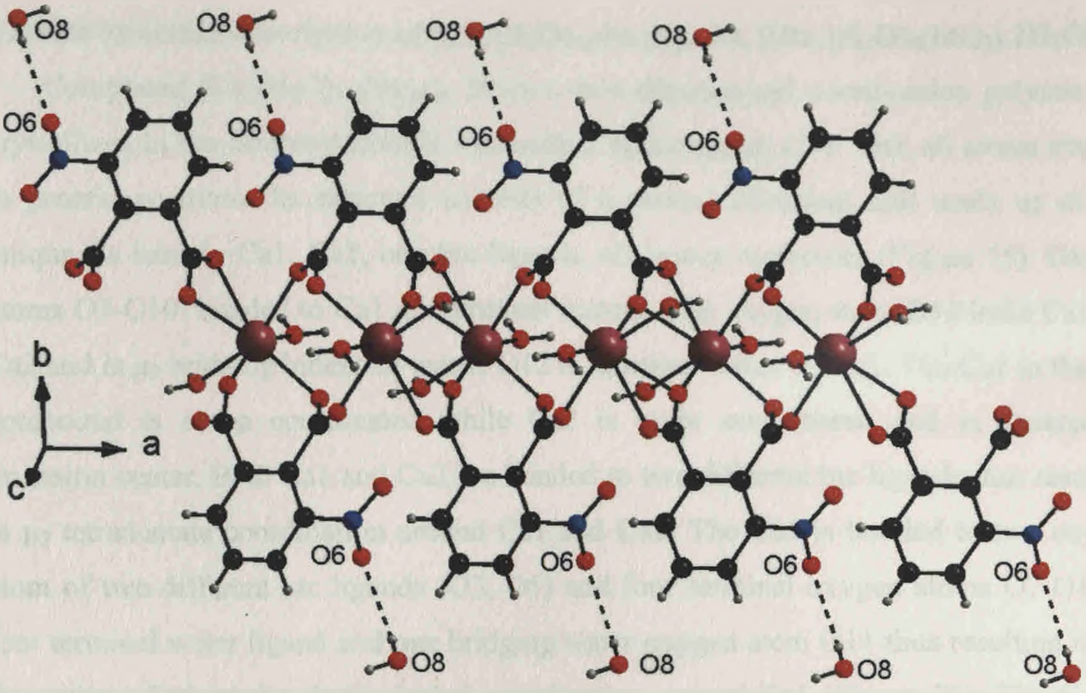

Figure 73- A view showing the interchain interactions in $[[Ca(H_2O)_2(3\text{-npth})]\cdot H_2O]_n$ **25.** Colour code: C, black; H, medium grey; N, blue; O, red; Ca, maroon.

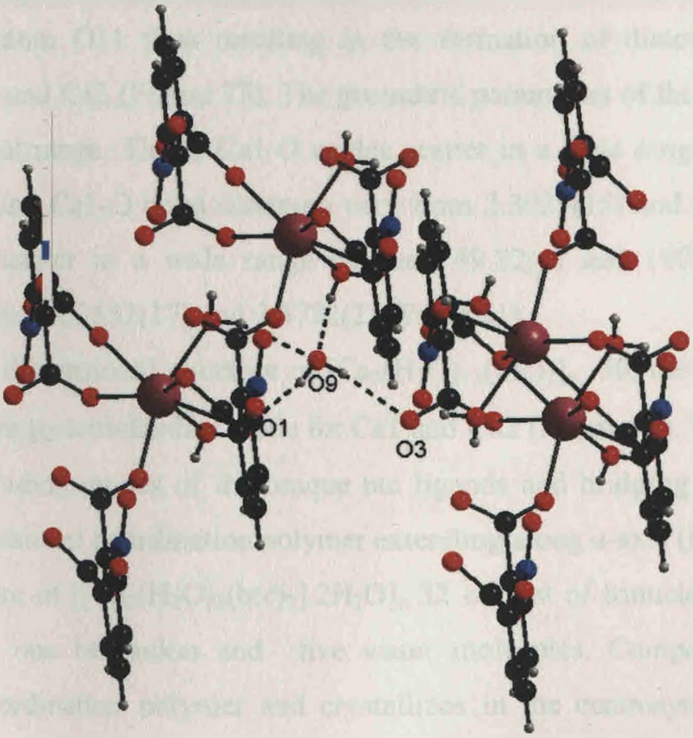

Figure 74- H-bonding situation around the lattice water in $[[Ca(H_2O)_2(3\text{-npth})]\cdot H_2O]_n$ **26** showing its linking to four different hepta coordinated Ca(II) complexes via O-H···O interactions. Colour code: C, black; H, medium grey; N, blue; O, red; Ca, maroon.

Crystal structure description of $[Ca_3(H_2O)_{12}(btc)_2]_n$ 30, $[[Ba_3(H_2O)_8(btc)_2].2H_2O]_n$32

Compound $[Ca_3(H_2O)_{12}(btc)_2]_n$ **30** is a two dimensional coordination polymer and crystallizes in the centrosymmetric monoclinic space group *C2/c* with all atoms situated in general positions. Its structure consists of a central trinuclear unit made up of two unique Ca namely Ca1, Ca2, one btc ligands, six water molecules (Figure 75). Oxygen atoms O7-O10 bonded to Ca1 are terminal waters. The oxygen atom O11 links Ca1 and Ca2 and is μ_2 bridging bidentate water, O12 is terminal water on Ca2. The Ca1 in the title compound is seven coordinated while Ca2 is eight coordinated and is situated on inversion center. Both Ca1 and Ca2 are bonded to two different btc ligands thus resulting in μ_3 tetradentate coordination around Ca1 and Ca2. The Ca1 is bonded to two oxygen atom of two different btc ligands (O3, O5) and four terminal oxygen atoms O7-O10 of four terminal water ligand and one bridging water oxygen atom O11 thus resulting in the formation of triangular dodecahedral coordination around Ca1 (Figure 76). The Ca2 is bonded to two oxygen atom of two different btc ligands in chelating mode (O1, O2) and two symmetry related oxygen atoms O12 of two terminal water ligand and two bridging water oxygen atom O11 thus resulting in the formation of distorted trigonal prism coordination around Ca2 (Figure 77). The geometric parameters of the carboxylate anions are in the normal range. The O-Ca1-O angles scatter in a wide range between 49.82(4) and 172.28(4)° and Ca1-O bond distances vary from 2.3025(15) and 2.7182(18). The O-Ca2-O angles scatter in a wide range between 49.82(4) and 180° and Ca2-O bond distances vary from 2.3552(17) and 2.5772(2) (Table 31)

In the two dimensional structure of $[Ca_3(H_2O)_{12}(btc)_2]_n$ **30**, the btc anions binds to three Ca atoms in μ_3-tetradendate mode for Ca1 and Ca2 (Figure 78). The net result of the this bridging binding modes of the unique btc ligands and bridging water in **30** results into a two dimensional coordination polymer extending along *a*-axis (Figure 78).

The structure of $[[Ba_3(H_2O)_8(btc)_2].2H_2O]_n$ **32** consist of trinuclear unit made up of two Ba atoms, one btc anion and five water molecules. Compound **32** is a three dimensional coordination polymer and crystallizes in the centrosymmetric monoclinic space group *P2₁/c* with all atoms situated in general positions (Figure 79). The unique btc ligand shows μ_6-η^2:η^2: η^2 bridging binding modes in this compound (Figure 80). In the crystal structure Ba1 is eight coordinated while Ba2 is ten coordinated and is located on an inversion center. Oxygen atoms O7, O8 bonded to Ba1 are terminal water molecules while O9 and O10 are bridging waters. The four oxygen atoms O1,O2,O3 and O6 binding to Ba1 are the oxygen atoms coming from 4 different btc ligand and are symmetry related. This results in the eight coordinated [BaO_8] unit around Ba1 this gives rise to distorted square antiprism coordination polyhedron around Ba1 (Figure 81). The Ba2 is surrounded by four btc ligands two of which are binding in the chelating mode via O3 and O4, while the other two bind in a monodentate via O5 oxygen atom of btc anion and the four water molecules bind to Ba2 via O9 and O10 in the bridging mode and are symmetry related and are linked to Ba1 (Figure 82). The geometric parameters of the carboxylate anions are in the normal range. The O-Ba1-O angles scatter in a wide range between 63.92(6) and 147.29(7)° and Ba1-O bond distances vary from 2.6548(18) and 2.874(2). The O-Ba2-O angles scatter in a wide range between 45.16(5) and 180(12)° and Ba2-O bond distances vary from 2.7545(18) and 3.013(2) (Table 31)

The water molecule present in the crystal lattice of **32** results in H-bonding of coordinated btc ligand resulting in weak C-H...O interaction between H4 hydrogen atom of btc and O11 of lattice water (Figure 83). In the crystal structure of $[[Ba_3(H_2O)_8(btc)_2].2H_2O]_n$ **32**, the btc anions binds to six Ba atoms in μ_6-hexadendate mode while the water forms a bridge between Ba1 and Ba2. The net result of the this bridging binding modes of the unique btc ligands and bridging water results into a three dimensional coordination polymer of **32** extending along *a*-axis (Figure 84). The crystal water present in **32** the is trapped in the pores of 3-D network (Figure 84).

Table 31- Selected bond lengths and bond angle (Å,°) for compound $[Ca_3(H_2O)_{12}(btc)_2]_n$ **31** and $[[Ba_3(H_2O)_8(btc)_2].2H_2O]_n$ **32**.

$[Ca_3(H_2O)_{12}(btc)_2]$ **31**			
Ca(1)-O(3)	2.3025(15)	Ca(2)-O(12)#1	2.3552(17)
Ca(1)-O(7)	2.3412(18)	Ca(2)-O(12)	2.3552(17)
Ca(1)-O(5)	2.3694(15)	Ca(2)-O(11)	2.4961(14)
Ca(1)-O(8)	2.3940(16)	Ca(2)-O(11)#1	2.4961(14)
Ca(1)-O(9)	2.4080(16)	Ca(2)-O(2)#1	2.5199(16)
Ca(1)-O(10)	2.4431(16)	Ca(2)-O(2)	2.5199(16)
Ca(1)-O(11)	2.7182(18)	Ca(2)-O(1)	2.577(2)
		Ca(2)-O(1)#1	2.577(2)
O(3)-Ca(1)-O(7)	145.44(5)	O(12)#1-Ca(2)-O(11)#1	97.95(6)
O(3)-Ca(1)-O(5)	87.64(5)	O(11)-Ca(2)-O(11)#1	180.0(4)
O(7)-Ca(1)-O(5)	75.99(4)	O(12)#1-Ca(2)-O(2)#1	78.61(6)
O(3)-Ca(1)-O(8)	78.57(6)	O(12)-Ca(2)-O(2)#1	101.39(6)
O(7)-Ca(1)-O(8)	121.54(5)	O(11)-Ca(2)-O(2)#1	70.14(5)
O(5)-Ca(1)-O(8)	162.28(5)	O(11)#1-Ca(2)-O(2)#1	109.86(5)
O(3)-Ca(1)-O(9)	77.73(5)	O(12)#1-Ca(2)-O(2)	101.39(6)
O(7)-Ca(1)-O(9)	77.15(5)	O(12)-Ca(2)-O(2)	78.61(6)

O(5)-Ca(1)-O(9)	104.17(6)	O(11)-Ca(2)-O(2)	109.86(5)
O(8)-Ca(1)-O(9)	83.87(6)	O(11)#1-Ca(2)-O(2)	70.14(5)
O(3)-Ca(1)-O(10)	95.20(6)	O(2)#1-Ca(2)-O(2)	180.0
O(7)-Ca(1)-O(10)	110.57(6)	O(12)#1-Ca(2)-O(1)	81.17(5)
O(5)-Ca(1)-O(10)	78.36(6)	O(12)-Ca(2)-O(1)	98.83(5)
O(8)-Ca(1)-O(10)	91.75(6)	O(11)-Ca(2)-O(1)	68.29(5)
O(9)-Ca(1)-O(10)	172.28(4)	O(11)#1-Ca(2)-O(1)	111.71(5)
O(3)-Ca(1)-O(11)	145.87(4)	O(2)#1-Ca(2)-O(1)	130.18(4)
O(7)-Ca(1)-O(11)	67.02(4)	O(2)-Ca(2)-O(1)	49.82(4)
O(5)-Ca(1)-O(11)	118.78(5)	O(12)#1-Ca(2)-O(1)#1	98.83(5)
O(8)-Ca(1)-O(11)	70.69(5)	O(12)-Ca(2)-O(1))#1	81.17(5)
O(9)-Ca(1)-O(11)	112.43(4)	O(11)-Ca(2)-O(1))#1	111.71(5)
O(10)-Ca(1)-O(11)	71.78(4)	O(11)#1-Ca(2)-O(1)#1	68.29(5)
O(12)#1-Ca(2)-O(12)	180.0(4)	O(2)#1-Ca(2)-O(1)#1	49.82(4)
O(12)#1-Ca(2)-O(11)	97.95(6)	O(2)-Ca(2)-O(1)#1	130.18(4)
O(12)-Ca(2)-O(11)	82.05(6)	O(1)-Ca(2)-O(1)#1	180.0
O(12)#1-Ca(2)-O(11)#1	82.05(6)		

$[Ba_3(H_2O)_8(btc)_2].2H_2O$ **32**

Ba(1)-O(2)	2.6548(18)	Ba(2)-O(4)^{i}	2.7545(18)
Ba(1)-O(1)	2.7320(18)	Ba(2)-O(5)	2.8127(19)
Ba(1)-O(6)	2.7662(19)	Ba(2)-O(5)^{i}	2.8127(19)
Ba(1)-O(3)	2.7829(19)	Ba(2)-O(9)^{i}	2.966(2)
Ba(1)-O(10)	2.823(2)	Ba(2)-O(9)	2.966(2)
Ba(1)-O(9)	2.850(2)	Ba(2)-O(3)	2.979(2)
Ba(1)-O(7)	2.851(2)	Ba(2)-O(3)^{i}	2.979(2)
Ba(1)-O(8)	2.874(2)	Ba(2)-O(10)^{i}	3.013(2)
Ba(2)-O(4)	2.7545(18)	Ba(2)-O(10)	3.013(2)
O(2)-Ba(1)-O(1)	78.62(6)	O(5)^{i}-Ba(2)-O(9)^{i}	118.11(6)
O(2)-Ba(1)-O(6)	148.70(6)	O(4)-Ba(2)-O(9)	107.10(6)
O(1)-Ba(1)-O(6)	75.63(5)	O(4)^{i}-Ba(2)-O(9)	72.90(6)
O(2)-Ba(1)-O(3)	125.10(6)	O(5)-Ba(2)-O(9)	118.11(6)
O(1)-Ba(1)-O(3)	155.84(6)	O(5)^{i}-Ba(2)-O(9)	61.89(6)
O(6)-Ba(1)-O(3)	80.44(6)	O(9)^{i}-Ba(2)-O(9)	180.0(12)
O(2)-Ba(1)-O(10)	134.65(7)	O(4)-Ba(2)-O(3)	45.16(5)
O(1)-Ba(1)-O(10)	103.98(6)	O(4)^{i}-Ba(2)-O(3)	134.84(5)
O(6)-Ba(1)-O(10)	69.78(6)	O(5)-Ba(2)-O(3)	110.45(6)
O(3)-Ba(1)-O(10)	63.92(6)	O(5)^{i}-Ba(2)-O(3)	69.55(6)
O(2)-Ba(1)-O(9)	75.48(6)	O(9)^{i}-Ba(2)-O(3)	117.37(6)
O(1)-Ba(1)-O(9)	131.17(6)	O(9)-Ba(2)-O(3)	62.63(6)
O(6)-Ba(1)-O(9)	135.54(6)	O(4)-Ba(2)-O(3)^{i}	134.84(5)
O(3)-Ba(1)-O(9)	66.53(6)	O(4)^{i}-Ba(2)-O(3)^{i}	45.16(5)
O(10)-Ba(1)-O(9)	69.30(7)	O(5)-Ba(2)-O(3)^{i}	69.55(6)
O(2)-Ba(1)-O(7)	81.43(7)	O(5)^{i}-Ba(2)-O(3)^{i}	110.45(6)
O(1)-Ba(1)-O(7)	93.95(7)	O(9)^{i}-Ba(2)-O(3)^{i}	62.63(6)
O(6)-Ba(1)-O(7)	82.88(7)	O(9)-Ba(2)-O(3)^{i}	117.37(6)
O(3)-Ba(1)-O(7)	86.21(7)	O(3)-Ba(2)-O(3)^{i}	180.0(7)
O(10)-Ba(1)-O(7)	141.85(8)	O(4)-Ba(2)-O(10)^{i}	95.93(7)
O(9)-Ba(1)-O(7)	121.65(7)	O(4)^{i}-Ba(2)-O(10)^{i}	84.07(7)
O(2)-Ba(1)-O(8)	69.45(6)	O(5)-Ba(2)-O(10)^{i}	118.39(6)
O(1)-Ba(1)-O(8)	66.56(6)	O(5)^{i} -Ba(2)-O(10)^{i}	61.61(6)

O(6)-Ba(1)-O(8)	114.74(5)	O(9)^{i}-Ba(2)-O(10)^{i}	65.28(6)
O(3)-Ba(1)-O(8)	122.50(6)	O(9)-Ba(2)-O(10)^{i}	114.72(6)
O(10)-Ba(1)-O(8)	70.53(7)	O(3)-Ba(2)-O(10)^{i}	120.63(6)
O(9)-Ba(1)-O(8)	65.80(6)	O(3)^{i}-Ba(2)-O(10)^{i}	59.37(6)
O(7)-Ba(1)-O(8)	147.29(7)	O(4)-Ba(2)-O(10)	84.07(7)
O(4)-Ba(2)-O(4)^{i}	180.00(8)	O(4)^{i}-Ba(2)-O(10)	95.93(7)
O(4)-Ba(2)-O(5)	96.86(6)	O(5)-Ba(2)-O(10)	61.61(6)
O(4)^{i}-Ba(2)-O(5)	83.14(6)	O(5)^{i}-Ba(2)-O(10)	118.39(6)
O(4)-Ba(2)-O(5)^{i}	83.14(6)	O(9)^{i}-Ba(2)-O(10)	114.72(6)
O(4)^{i}-Ba(2)-O(5)^{i}	96.86(6)	O(9)-Ba(2)-O(10)	65.28(6)
O(5)-Ba(2)-O(5)^{i}	180.0(5)	O(3)-Ba(2)-O(10)	59.37(6)
O(4)-Ba(2)-O(9)^{i}	72.90(6)	O(3)^{i}-Ba(2)-O(10)	120.63(6)
O(4)^{i}-Ba(2)-O(9)^{i}	107.10(6)	O(10)^{i}-Ba(2)-O(10)	180.0(7)
O(5)-Ba(2)-O(9)^{i}	61.89(6)		

Symmetry transformations used to generate equivalent atoms: #1 –x+1/2,-y+3/2,-z, i) -x+2, -y, -z.

Table 32- Hydrogen-bonding geometry (Å, °) for compound $[Ca_3(H_2O)_{12}(btc)_2]_n$ **30** and $[[Ba_3(H_2O)_8(btc)_2].2H_2O]_n$ **32**

D-H···A	d(D-H)	d(H···A)	D(D···A)	<DHA	Symmetry code
$[Ca_3(H_2O)_{12}(btc)_2]$ **30**					
O7-H7A···O9	0.799	1.989	2.788	177	-x+1/2, -y+1/2, -z
O7-H7B···O2	0.780	1.852	2.623	170	-x+1/2, -y+3/2, -z
O8-H8A···O1	0.859	1.754	2.606	171	
O8-H8B···O10	0.804	2.023	2.826	177	-x, -y+1, -z
O9-H9A···O6	0.785	1.984	2.762	171	-x+1/2, -y+1/2, -z
O9-H9B···O4	0.808	1.926	2.719	166	-x, y, -z-1/2
O10-H10A···O8	0.827	2.395	3.140	150	x, -y+1, z+1/2
O10-H10B···O4	0.807	1.843	2.650	178	-x, -y+1, -z
O11-H11A···O6	0.839	1.983	2.818	173	-x+1/2, y+1/2, -z+1/2
O11-H11B···O4	0.825	1.987	2.784	162	-x, -y+1, -z
O12-H12A···O5	0.813	2.029	2.834	170	-x+1/2, y+1/2, -z+1/2
O12-H12B···O6	0.815	1.972	2.783	174	x-1, -y+1/2, z+1/2
$[Ba_3(H_2O)_8(btc)_2].2H_2O$ **32**					
O7-H7A···O6	0.816	2.001	2.815	175	-x+1, -y, -z+1
O8-H8A···O1	0.870	1.928	2.792	172	x, -y+1/2, z-1/2
O8-H8A···O2	0.870	2.613	3.154	121	
O9-H9A···O8	0.754	2.106	2.825	160	x, -y+1/2, z-1/2
O10-H10A···O11	0.771	2.063	2.824	169	-x+1, -y+1, -z+1
O11-H11A···O4	0.838	1.907	2.745	178	x-1, y+1, z
O7-H7B···O2	0.808	2.190	2.966	161	-x+1, -y, -z
O8-H8B···O11	0.822	1.958	2.775	173	-x+1, y-1/2, -z+1/2
O9-H9B···O6	0.741	2.130	2.856	167	x, y, z-1
O9-H9B···O5	0.741	2.479	2.974	126	-x+2, -y, -z
O10-H10B···O5	0.739	2.245	2.981	174	-x+2, -y, -z+1
O11-H11B···O4	0.783	2.019	2.787	167	x-1, -y+1/2, z+1/2

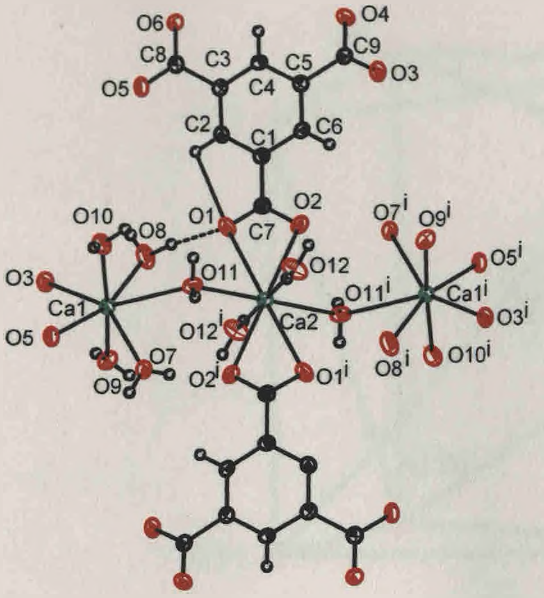

Figure 75- Crystal structure of $[Ca_3(btc)_2(H_2O)_{10}]_n$ **30** showing atom-labeling scheme. Displacement ellipsoids are drawn at 50% probability level except for the H atoms, which are shown as circles of arbitrary radius (top). Symmetry codes: i) –x+1/2,-y+3/2,-z

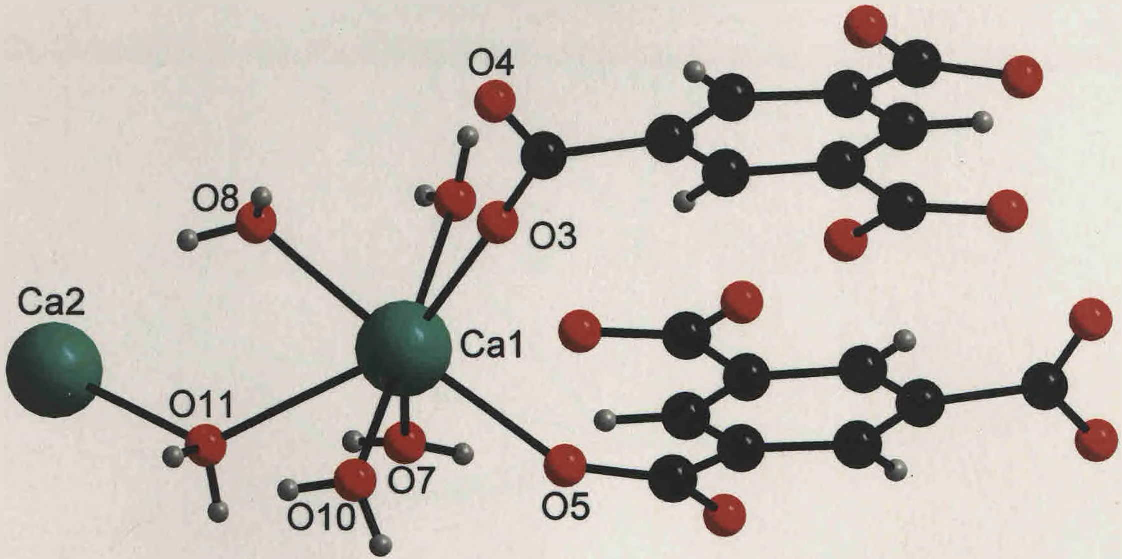

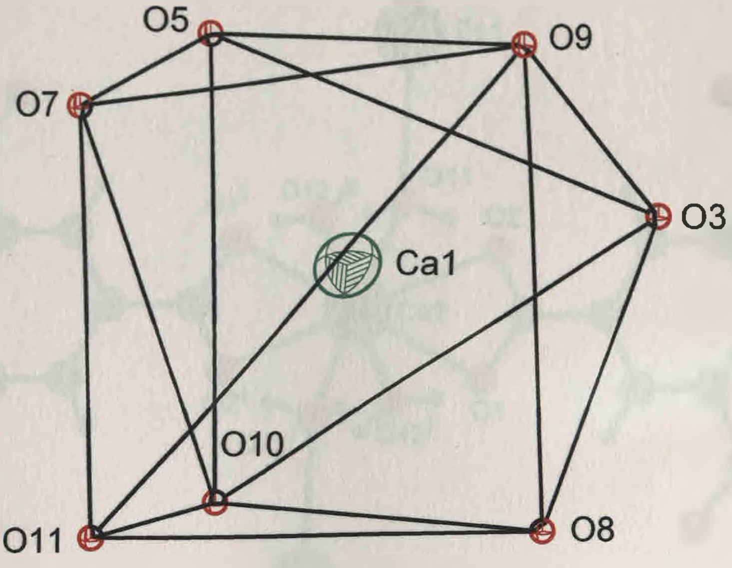

Figure 76- The coordination sphere of Ca1 in $[Ca_3(H_2O)_{12}(btc)_2]_n$ **30** showing O11 of water as linker betweem Ca1 and Ca2 (top). The distorted triangular dodecahedron coordination polyhedron around Ca1 in $[Ca_3(H_2O)_{12}(btc)_2]_n$ **30** (bottom).

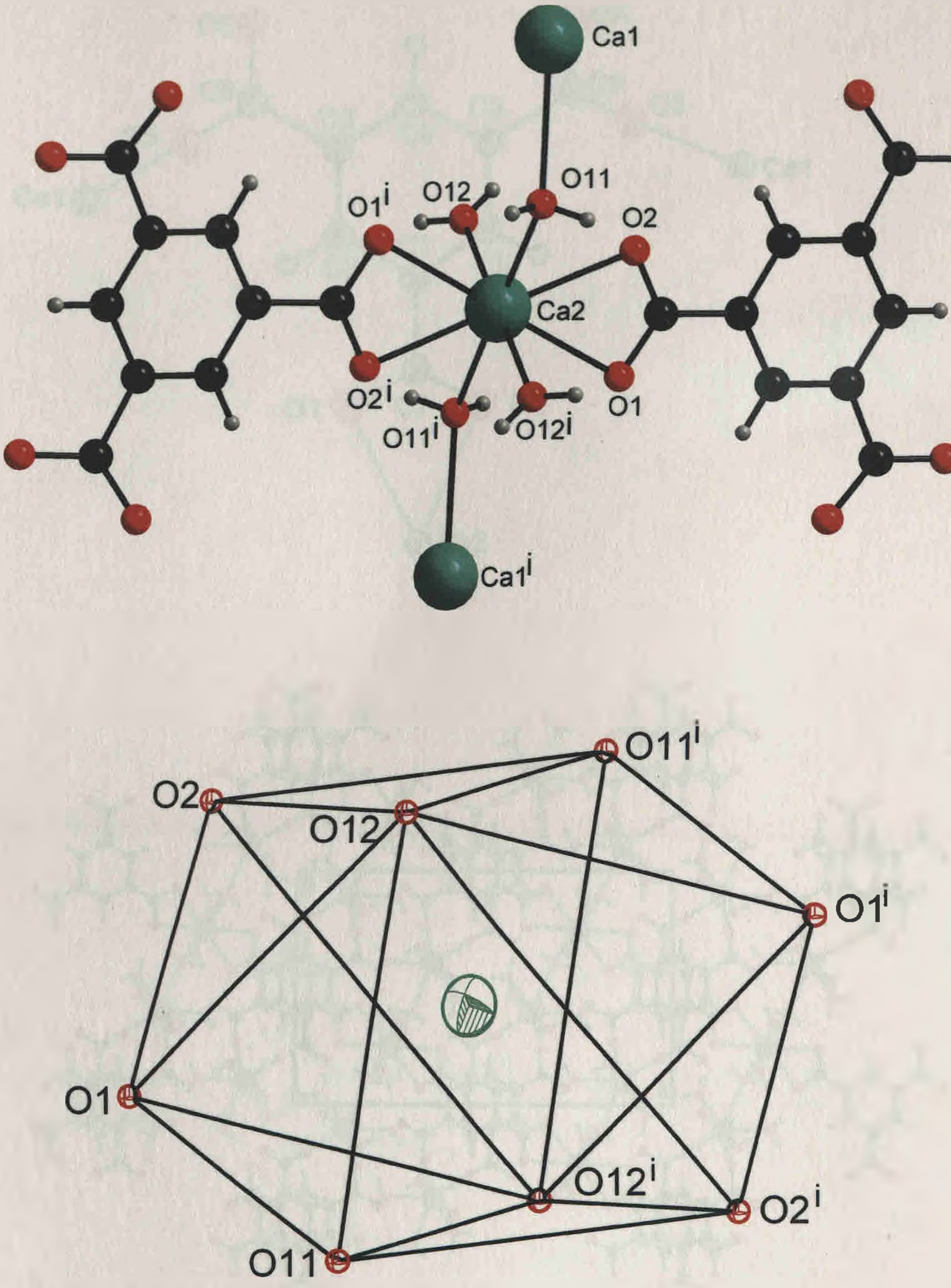

Figure 77- The coordination sphere of Ca2 in $[Ca_3(H_2O)_{12}(btc)_2]_n$ **30** showing O11 of water as linker betweem Ca1 and Ca1^{i} (top), The distorted triangular dodecahedron coordination polyhedron around Ca2 in $[Ca_3(H_2O)_{12}(btc)_2]_n$ **30** (bottom). Symmetry codes: i) –x+1/2,-y+3/2,-z;

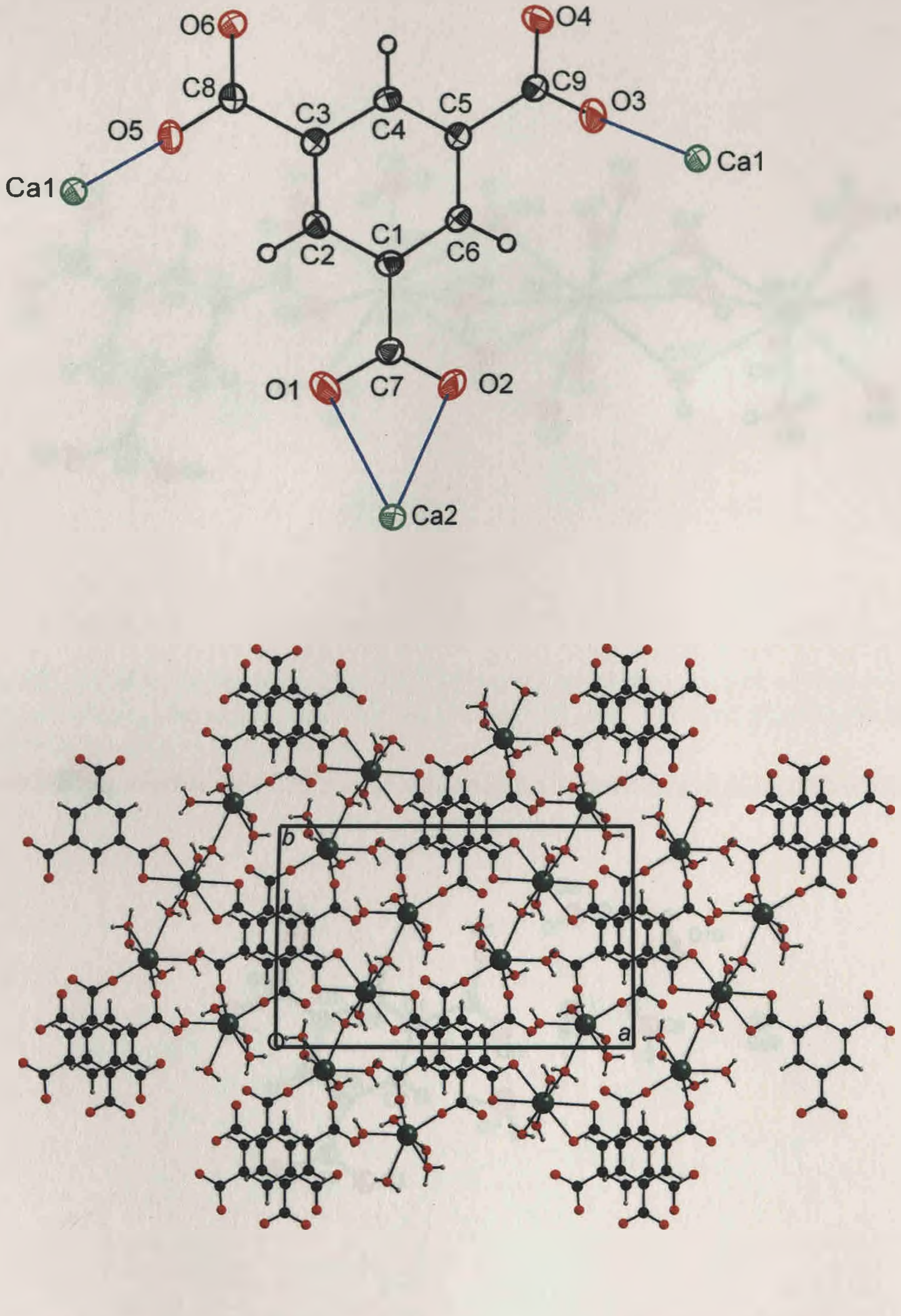

Figure 78- A view of the μ_3-bridging teradentate btc ligand in **30**. Colour code: C, black; H, medium grey; O, red; Ca, green(top). A portion of a 2-D network expanding along a and b axis.

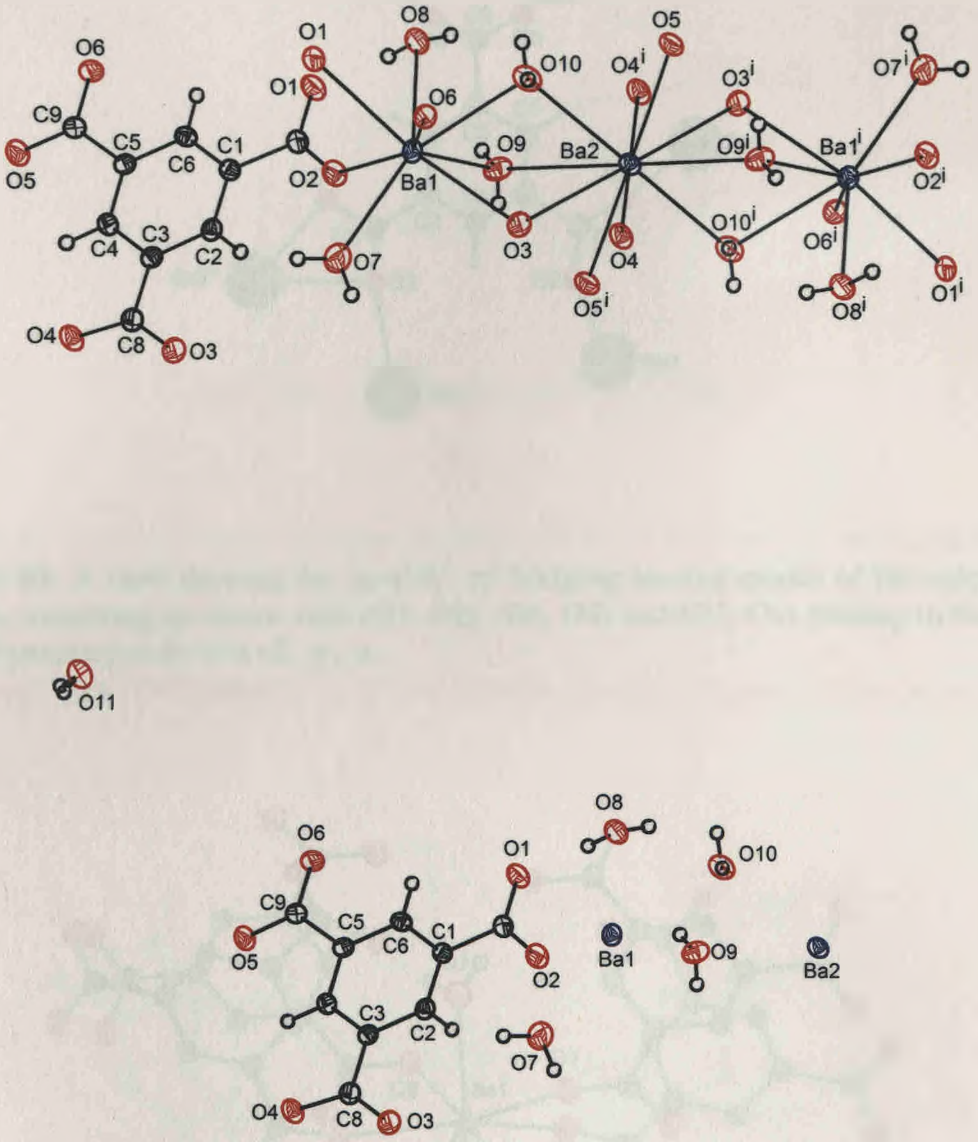

Figure 79- Crystal structure of $[[Ba_3(btc)_2(H_2O)_8].2H_2O]_n$ **32** showing the trinuclear unit and atom-labeling scheme. Displacement ellipsoids are drawn at 50% probability level except for the H atoms, which are shown as circles of arbitrary radius. Symmetry codes; i) -x+2, -y, -z.

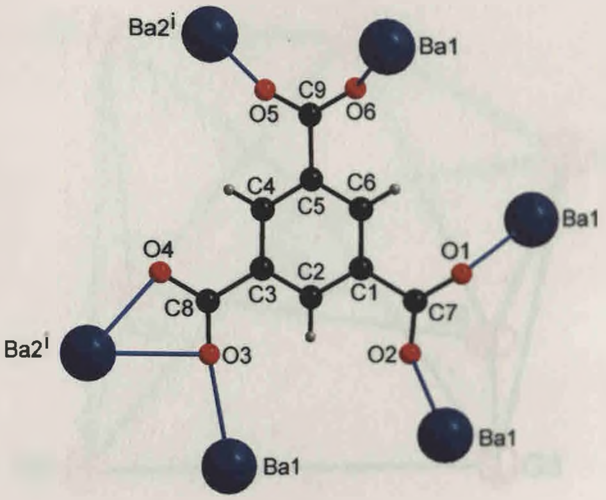

Figure 80- A view showing the μ_6-η^2:η^2: η^2 bridging binding modes of the unique btc ligands containing the donor sites (O1, O2), (O3, O4) and (O5, O6) binding to Ba1 and Ba2^{i}. Symmetry code: i) -x+2, -y, -z.

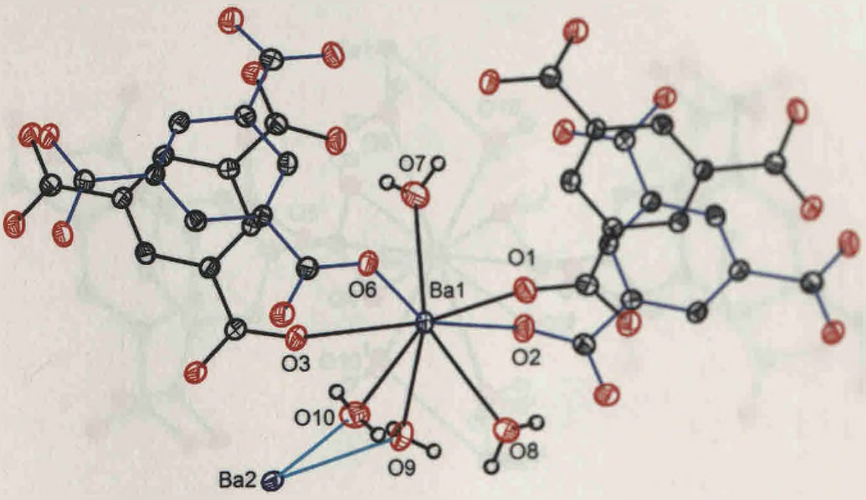

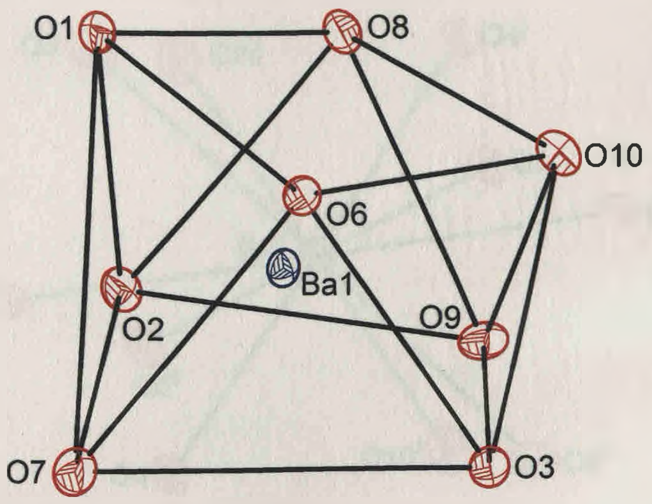

Figure 81- Distorted square antiprism coordination polyhedron around eight coordinated Ba1(II) in **32** showing four btc ligands, two terminal water ligands and two bridging water molecules(top). Ba1 coordination polyhedron around eight coordinated Ba1(II) in $[[Ba_3(H_2O)_8(btc)_2].2H_2O]_n$ **32** (bottom). Symmetry codes : i) -x+2, -y, -z

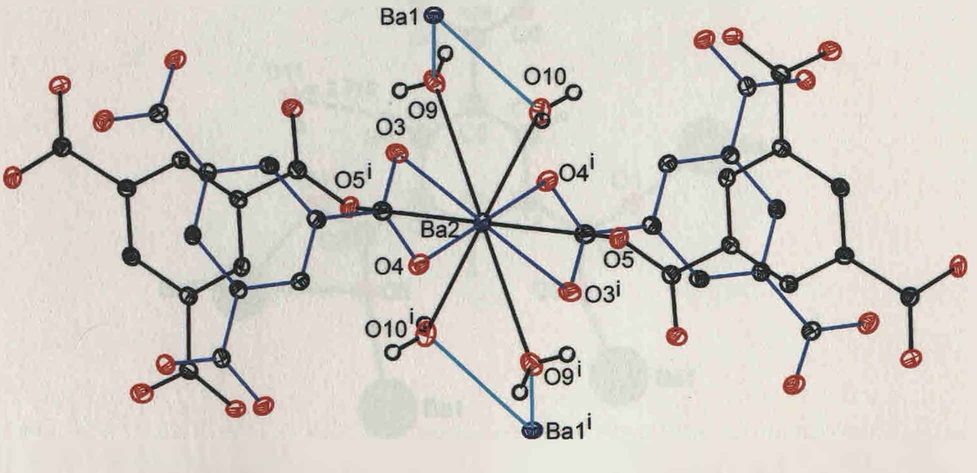

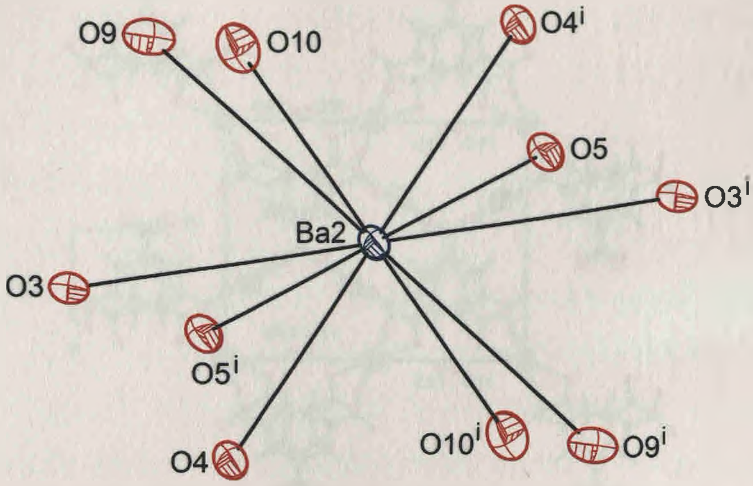

Figure 82- Coordination environment around Ba2 showing four unique btc ligands (top). Coordination environment around Ba2 showing four unique btc ligands coordinated to central Ba2 located on an inversion center (bottom).

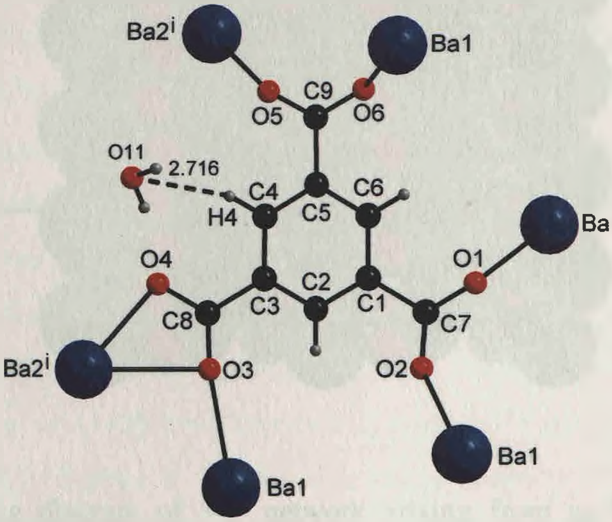

Figure 83- A view showing the μ_6-η^2:η^2: η^2 bridging binding modes of the unique btc ligands containing the donor sites (O1, O2), (O3, O4) and (O5, O6), binding to Ba1 and Ba2^i and H-bonding of coordinated btc ligand showing the weak C-H...O interaction between H4 hydrogen atom of btc and O11 of lattice water. Symmetry code: i) -x+2, -y, -z.

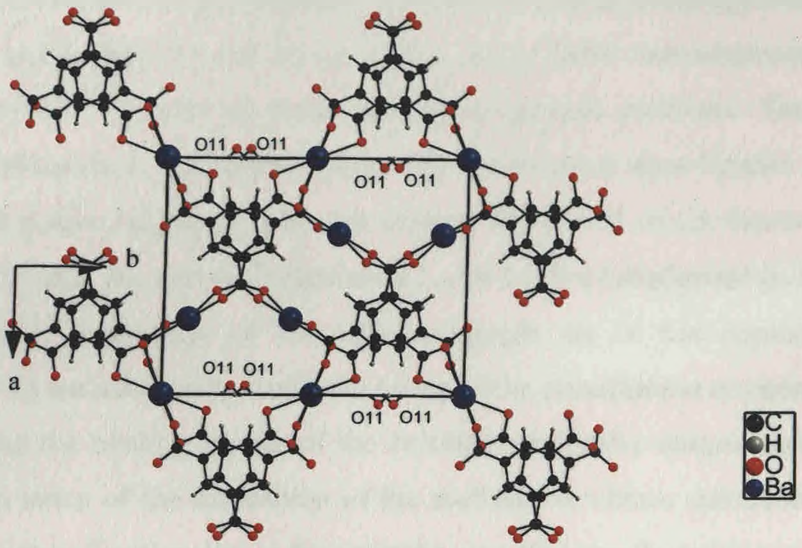

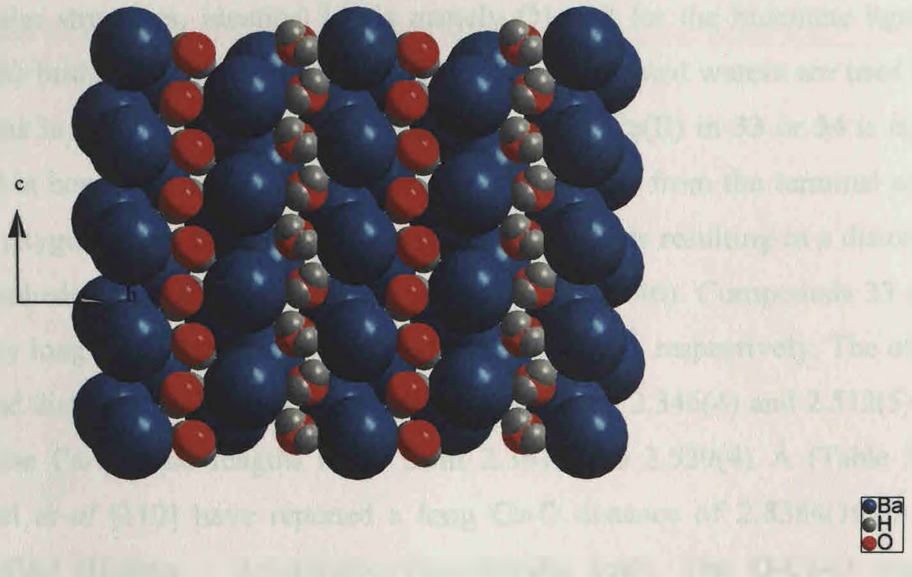

Figure 84- Packing diagram of 3-D network arising from μ_6 bridging of btc ligand showing water trapped between the pores (top) and The porous water trapped between the pores in **32**.

Crystal structure description of $[Ca(H_2O)_2(L_1)_2]\cdot H_2O$ 33, $[Ca(H_2O)_2(L_2)_2]\cdot 2H_2O$ 34

The polymeric compounds **33** and **34** crystallize in the chiral non-centrosymmetric monoclinic space group *P2₁* with all atoms situated in general positions. The crystal structure of **33** or **34** consists of a central Ca(II) ion, two terminal aqua ligands and two crystallographically unique (L_1) or (L_2) ligands (Figure 85) one of which functions as a chelating bidentate ligand. The second independent L_1 (or L_2) is a tetradentate μ_3-bridging ligand. The geometric parameters of the organic ligands are in the normal range. Compounds **33** and **34** are structurally similar in terms of the coordination environment of the central metal and the binding modes of the crystallographically unique carboxylate ligands but differ in terms of the disposition of the methoxy or chloro substituents with respect to the carboxylate functionality in the aromatic ring (Scheme 2) and the number of lattice waters. In **33** which contains a single lattice water, the $-OCH_3$ group is *trans* to the carboxylate while the –Cl group is *ortho* to the –COO functionality in **34** which has two lattice waters.

In view of similar structures, identical labels namely O1, O2 for the bidentate ligand, O11, O12 for the bridging ligand and O21, O22 for the coordinated waters are used for the oxygen atoms in **33** and **34**. In the crystal structure, each Ca(II) in **33** or **34** is eight coordinated and is bonded to two oxygen atoms (O21 and O22) from the terminal aqua ligands and six oxygen atoms from four different L_1 or L_2 ligands resulting in a distorted triangular dodecahedral $\{CaO_8\}$ polyhedron around Ca (Figure 86). Compounds **33** and **34** exhibit a very long Ca-O distance of 2.753(4) and 2.704(3) Å respectively. The other seven Ca-O bond distances in **33** vary in a small range between 2.346(4) and 2.512(5) Å, while in **34** these Ca-O bond lengths range from 2.361(3) to 2.529(4) Å (Table 33). Recently Dietzel *et al* [110] have reported a long Ca-O distance of 2.8384(16) Å in $[Ca(H_2dhtp)(H_2O)_2]$ (H_4dhtp = 2,5-dihydroxyterephthalic acid). The O-Ca-O angles (49.13(10) to 154.04(13)° in **33**; 49.62(8) to 154.79(13)° in **34**) scatter in a very wide range.

The first independent L_1 (or L_2) is coordinated to the central metal through O1 and O2 and the observed Ca-O distances of 2.501(5) and 2.512(5) Å in **33** (2.495(5) and 2.529(4) Å in **34**) indicate the symmetrical bidentate behavior of this ligand. The second unique L_1 (or L_2) ligand which binds through O11 and O12 is tetradentate, the $\mu_3-\eta^2:\eta^2$ binding mode of which results in a one dimensional coordination polymer. Both O11 and O12 are bonded to two Ca(II) each, of which one Ca(II) is common to both. The polymeric structure of **33** or **34** is based on a dimer and can be visualized as follows. A pair of μ_3-bridging L_1 (or L_2) ligands link a pair of $\{Ca(H_2O)_2(L_1)\}$ (or $\{Ca(H_2O)_2(L_2)\}$) units resulting in the formation of a tricyclic dicalcium-dicarboxylate block with a Ca···Ca separation of 3.9467(11) in **33** or 3.9533(11) Å in **34** (Figure 86). This tricyclic unit can be considered as the basic building block of the one dimensional polymer. A similar tricyclic unit has been recently reported in the one dimensional polymers $[Ca(H_2O)_2(2\text{-}nba)_2]_n$ (2-nba = 2-nitrobenzoate) [25] and $[Ca(H_2O)_2(2\text{-}ca\text{-}4nba)_2]_n$ (2-ca-4nba = 2-carbamoyl-4-nitrobenzoate) [117]. It is interesting to note that in these compounds the organic linker coordinates in a $\mu_2\text{–}\eta^2\text{:}\eta^1$ fashion leading to the formation of the tricyclic unit. The net result of the differing coordination modes of the L_1 (or L_2) ligands in **33** and **34** is the formation of a one dimesional polymeric chain extending along *b* axis with two terminal water molecules (O21, O22), a chelating bidentate (O1, O2) L_1 (or L_2) accounting for four of the eight binding sites of each Ca(II) in the chain (Figure 87). The remaining four oxygen atoms for Ca(II) are provided by three symmetry related μ_3-bridging L_1 (or L_2) ligands. A scrutiny of the structure reveals that the H atoms of the coordinated and lattice water molecules function as H-donors and are involved in several O-H···O interactions (Table 34) and the O atoms of the chelating L_1 (or L_2) ligands and the lattice water molecules function as H-donors.

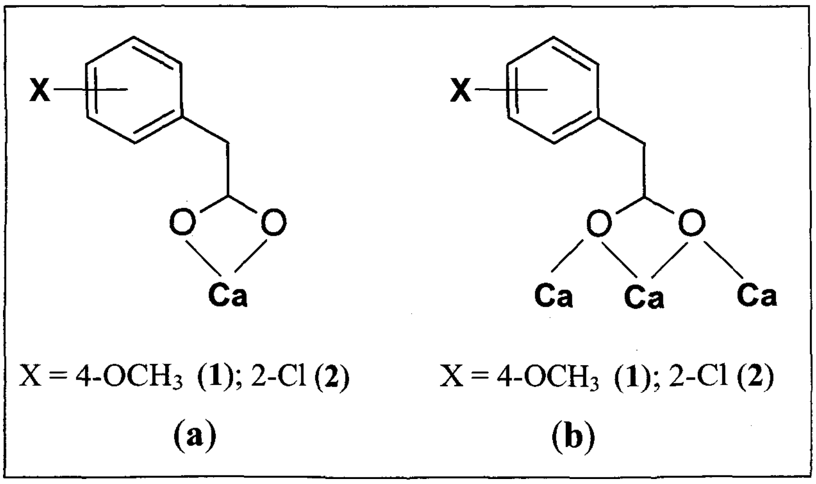

Scheme 2- Bidentate (**a**) and μ_3-bridging (**b**) binding modes of the unique ligands In **1** and **2**

Table 33- Selected bond distances (Å) and bond angles (°) for compounds **33** and **34**

$[Ca(H_2O)_2(L_1)_2]\cdot H_2O$ **33**		$[Ca(H_2O)_2(L_2)_2]\cdot 2H_2O$ **34**	
Ca(1)-O(12)^{i}	2.346(4)	Ca(1)-O(12)	2.361(3)
Ca(1)-O(11)	2.358(4)	Ca(1)-O(11)^{i}	2.368(3)
Ca(1)-O(22)	2.410(2)	Ca(1)-O(22)	2.387(3)
Ca(1)-O(21)	2.417(2)	Ca(1)-O(21)	2.415(3)
Ca(1)-O(12)^{ii}	2.454(4)	Ca(1)-O(12)^{iv}	2.460(3)
Ca(1)-O(2)	2.501(5)	Ca(1)-O(2)	2.495(4)
Ca(1)-O(1)	2.512(5)	Ca(1)-O(1)	2.529(4)
Ca(1)-O(11)^{ii}	2.753(4)	Ca(1)-O(11)^{iv}	2.704(3)
Ca(1)-Ca(1)^{iii}	3.9461(11)	Ca(1)-Ca(1)^{iv}	3.9533(11)
O(12)^{i}-Ca(1)-O(11)	145.32(13)	O(12)-Ca(1)-O(11)^{i}	145.61(10)
O(12)^{i}-Ca(1)-O(22)	75.55(14)	O(12)-Ca(1)-O(22)	88.38(14)
O(11)-Ca(1)-O(22)	75.54(13)	O(11)^{i}-Ca(1)-O(22)	83.62(13)
O(12)^{i}-Ca(1)-O(21)	89.11(13)	O(12)-Ca(1)-O(21)	74.80(13)
O(11)-Ca(1)-O(21)	82.77(13)	O(11)^{i}-Ca(1)-O(21)	76.13(13)
O(22)-Ca(1)-O(21)	109.34(9)	O(22)-Ca(1)-O(21)	108.27(10)
O(12)^{i}-Ca(1)-O(12)^{ii}	118.51(11)	O(12)-Ca(1)-O(12)^{iv}	119.22(9)
O(11)-Ca(1)-O(12)^{ii}	77.04(13)	O(11)^{i}-Ca(1)-O(12)^{iv}	76.05(10)
O(22)-Ca(1)-O(12)^{ii}	84.45(12)	O(22)-Ca(1)-O(12)^{iv}	151.94(13)
O(21)-Ca(1)-O(12)^{ii}	151.88(12)	O(21)-Ca(1)-O(12)^{iv}	85.60(11)
O(12)^{i}-Ca(1)-O(2)	78.29(16)	O(12)-Ca(1)-O(2)	79.13(12)
O(11)-Ca(1)-O(2)	132.73(15)	O(11)^{i}-Ca(1)-O(2)	132.23(12)
O(22)-Ca(1)-O(2)	151.65(13)	O(22)-Ca(1)-O(2)	82.20(11)
O(21)-Ca(1)-O(2)	80.80(11)	O(21)-Ca(1)-O(2)	151.43(13)
O(12)^{ii}-Ca(1)-O(2)	98.73(14)	O(12)^{iv}-Ca(1)-O(2)	97.24(12)
O(12)^{i}-Ca(1)-O(1)	129.60(16)	O(12)-Ca(1)-O(1)	130.21(12)
O(11)-Ca(1)-O(1)	82.33(15)	O(11)^{i}-Ca(1)-O(1)	80.94(12)
O(22)-Ca(1)-O(1)	154.04(13)	O(22)-Ca(1)-O(1)	79.10(12)
O(21)-Ca(1)-O(1)	80.67(12)	O(21)-Ca(1)-O(1)	154.79(13)
O(12)^{ii}-Ca(1)-O(1)	77.43(15)	O(12)^{iv}-Ca(1)-O(1)	78.76(12)
O(2)-Ca(1)-O(1)	51.42(11)	O(2)-Ca(1)-O(1)	51.64(8)
O(12)^{i}-Ca(1)-O(11)^{ii}	71.51(13)	O(12)-Ca(1)-O(11)^{iv}	71.58(10)
O(11)-Ca(1)-O(11)^{ii}	124.49(11)	O(11)^{i}-Ca(1)-O(11)^{iv}	123.83(9)
O(22)-Ca(1)-O(11)^{ii}	85.60(11)	O(22)-Ca(1)-O(11)^{iv}	152.08(13)
O(21)-Ca(1)-O(11)^{ii}	152.12(11)	O(21)-Ca(1)-O(11)^{iv}	85.54(11)
O(12)^{ii}-Ca(1)-O(11)^{ii}	49.13(10)	O(12)^{iv}-Ca(1)-O(11)^{iv}	49.62(8)
O(2)-Ca(1)-O(11)^{ii}	75.85(13)	O(2)-Ca(1)-O(11)^{iv}	75.22(11)
O(1)-Ca(1)-O(11)^{ii}	96.13(14)	O(1)-Ca(1)-O(11)^{iv}	98.84(12)

Symmetry codes i) x, y-1, z ii) -x+1, y-1/2, -z+1 iii) -x+1, y+1/2, -z+1, iv) -x+2, y-1/2, -z+1 v) –x+2, y+1/2, -z+1

Table 34- H-bonding geometry (Å, °) for $[Ca(H_2O)_2(L_1)_2]\cdot H_2O$ **33** and $[Ca(H_2O)_2(L_2)_2]\cdot 2H_2O$ **34**

D-H···A	d(D-H)	D(H···A)	D(D···A)	<DHA	Symmetry Code
$[Ca(H_2O)_2(L_1)_2]\cdot H_2O$ **33**					
O21-H20···O23	0.820	1.938	2.752	172	x, y, z
O22-H30···O1	0.820	2.143	2.837	142	-x+1, y-1/2,-z+1
O22-H40···O2	0.820	2.120	2.822	144	-x+1, y+1/2,-z+1
O23-H50···O2	0.820	2.120	2.896	158	-x+2, y+1/2,-z+1
O23-H60···O1	0.820	2.160	2.890	148	-x+2, y-1/2,-z+1
$[Ca(H_2O)_2(L_2)_2]\cdot 2H_2O$ **34**					
O21-H10···O2	0.820	2.033	2.824	162	-x+2, y-1/2,-z+1
O21-H20···O1	0.820	2.097	2.894	164	-x+2, y+1/2,-z+1
O22-H40···O24	0.820	1.949	2.692	150	-x+1, y-1/2,-z+1
O23-H50···O2	0.820	2.098	2.897	165	x, y, z
O23-H60···O1	0.820	2.068	2.853	160	x, y+1, z
O24-H7O···O23	0.820	2.097	2.905	168	-x+1, y+1/2,-z+1
O24-H80···O23	0.820	2.276	2.824	125	x, y, z

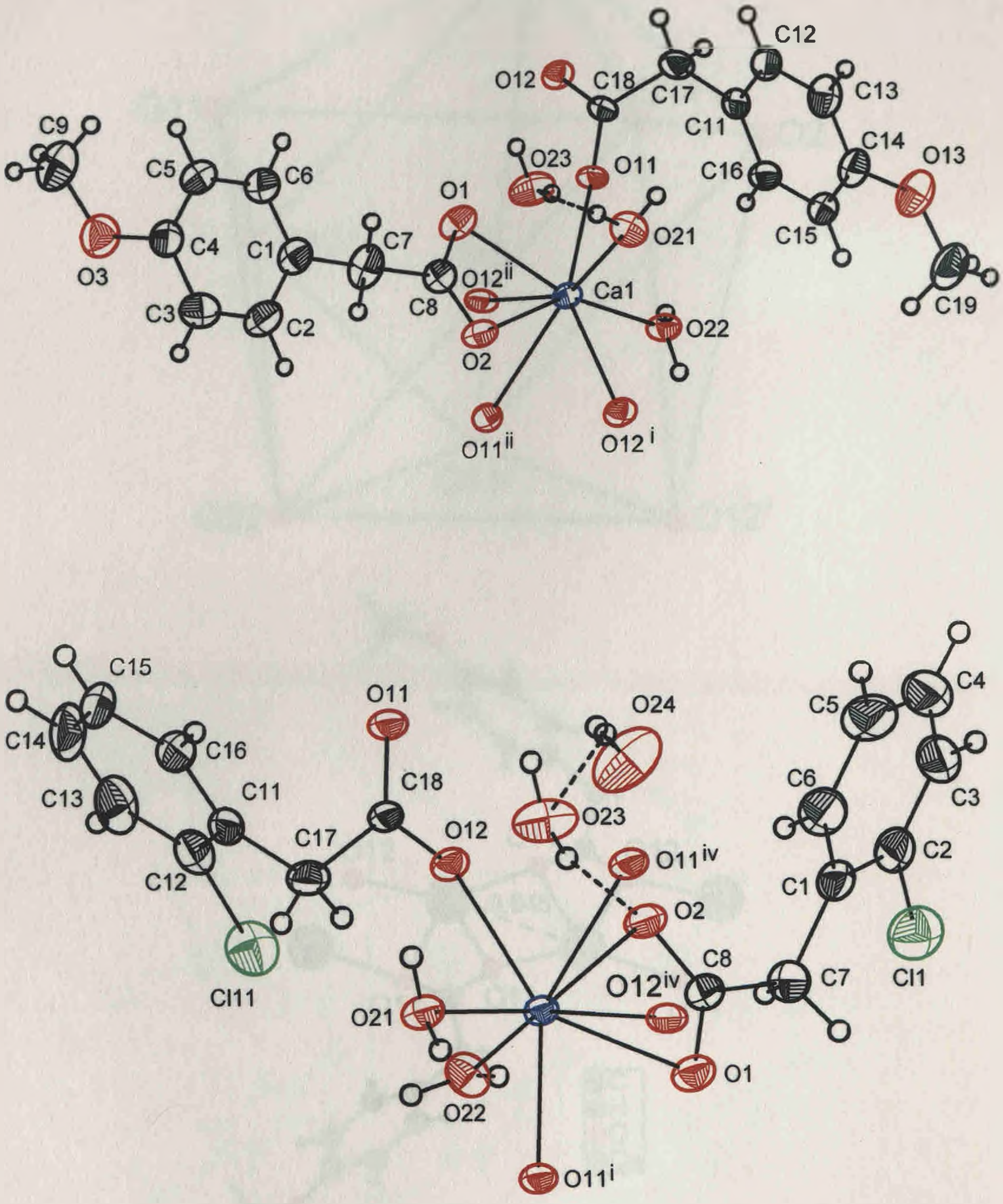

Figure 85 - A view of the coordination sphere of Ca(II) in $[Ca(H_2O)_2(L_1)_2]\cdot H_2O$ **33** (**a**) and $[Ca(H_2O)_2(L_2)_2]\cdot 2H_2O$ **34** (**b**), showing the atom-labeling scheme. Displacement ellipsoids are drawn at the 50% probability level excepting for the H atoms, which are shown as circles of arbitrary radius. Intramolecular H-bonding is shown as broken lines. Symmetry codes i) x, y-1, z ii) -x+1, y-1/2, -z+1 iv) -x+2, y-1/2, -z+1

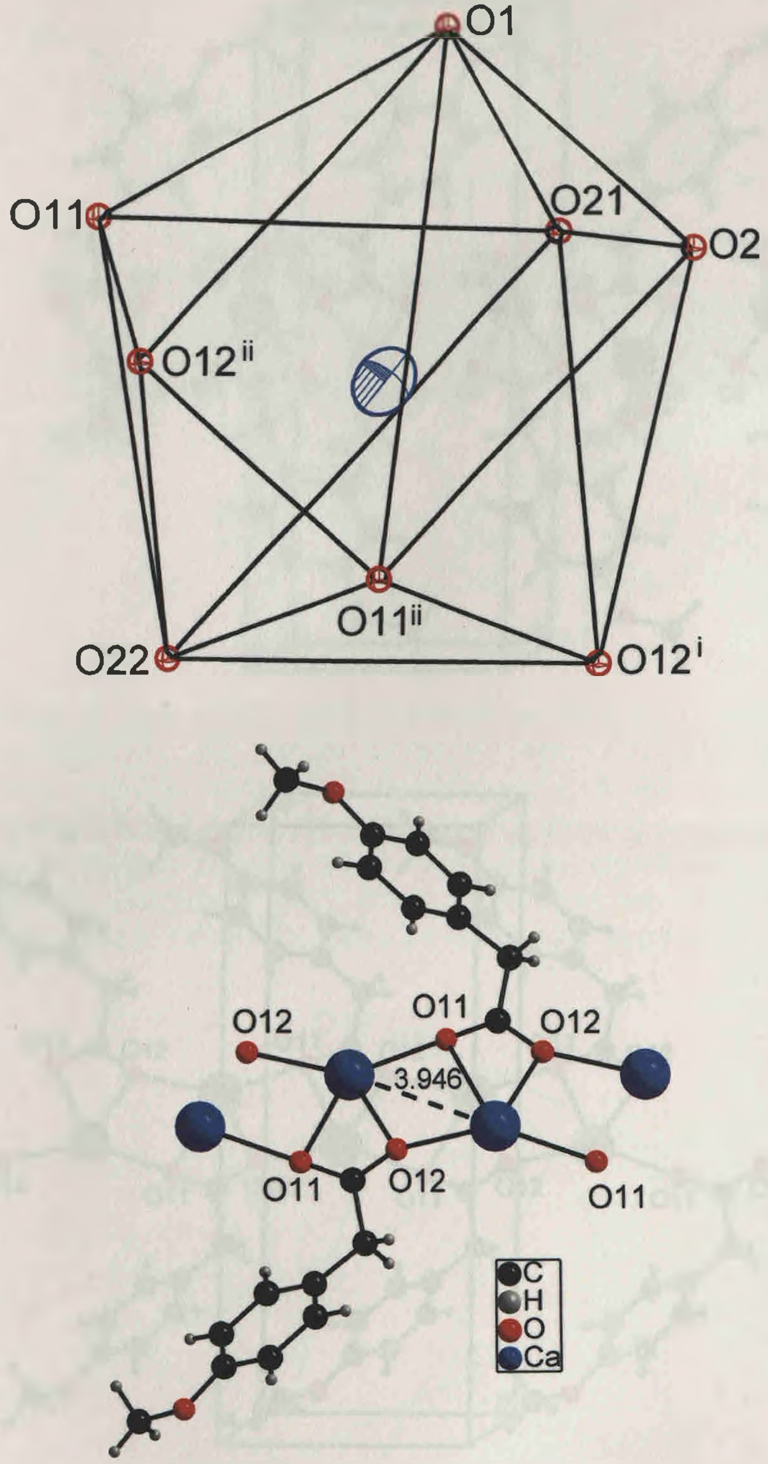

Figure 87 - (**A**) The distorted triangular dodecahedral coordination polyhedron around Ca(II) in **33**. (**B**) A pair of μ_3–η^2:η^2 ligands form a tricyclic dicalcium-dicarboxylate unit. Symmetry codes i) x, y-1, z ii) -x+1, y-1/2, -z+1.

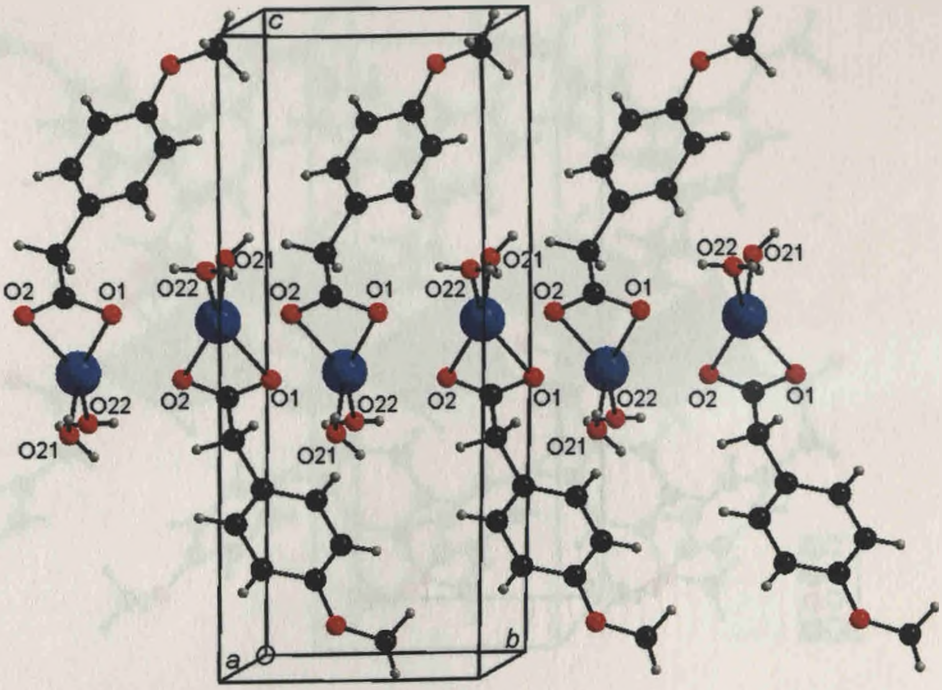
c
O22
O21
O2
O1
O22
O21
O2
O1
O22
O21
O2
O1
O22
O21
O2
O1
O22
O21
O2
O1
O22
O21
O2
O1
O22
O21
O2
O1
a
b

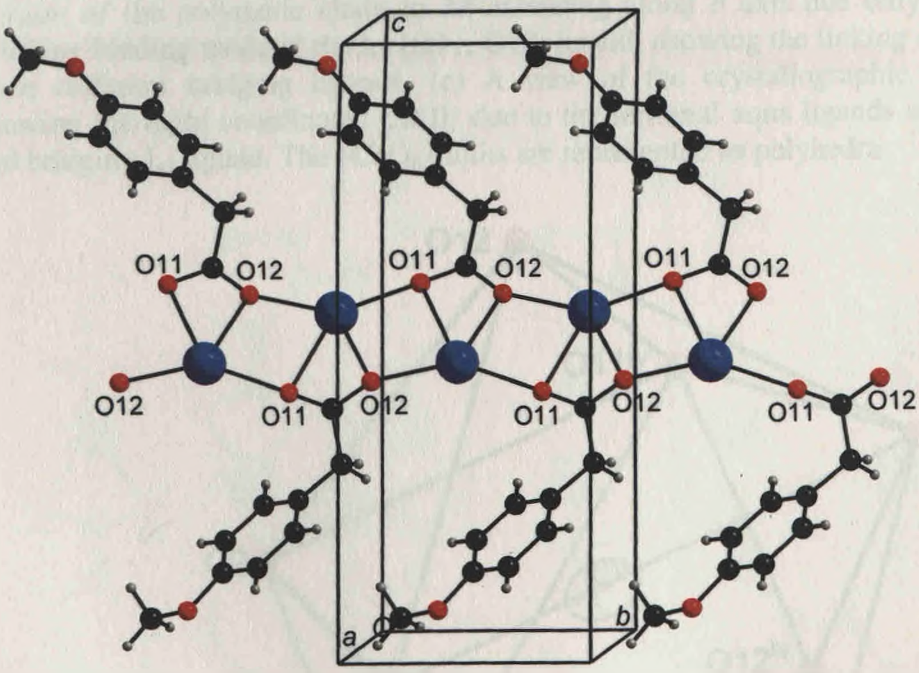
c
O11
O12
O11
O12
O11
O12
O12
O11
O12
O11
O12
O11
O12
a
b

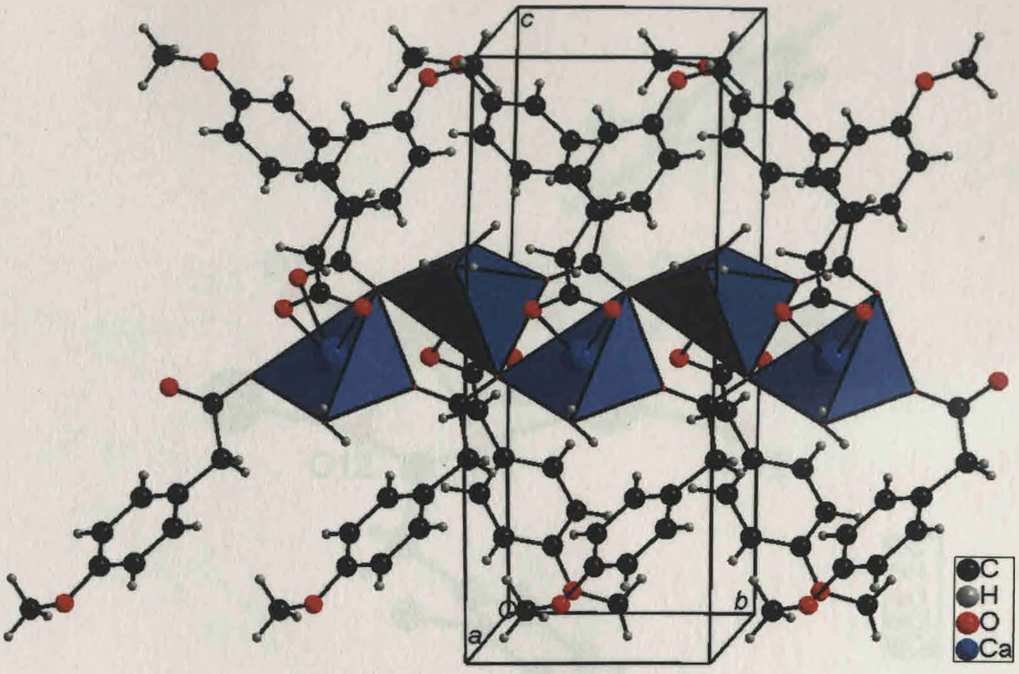

Figure 88- **(a)** A view of the crystal structure of **33** along *a* axis showing only the bidentate L_1 ligand (O1, O2), and the coordinated waters (O21, O22) around Ca(II) (**b**) A portion of the polymeric chain in **33** extending along *b* axis due only to the μ_3-η^2:η^2 bridging binding mode of the L_1 (O11, O12) ligand, showing the linking of each Ca(II) to three different bridging ligands. (**c**) A view of the crystallographic packing of **33**, showing the eight coordinated Ca(II) due to the terminal aqua ligands and the chelating and bridging L_1 ligand. The $\{CaO_8\}$ units are represented as polyhedra.

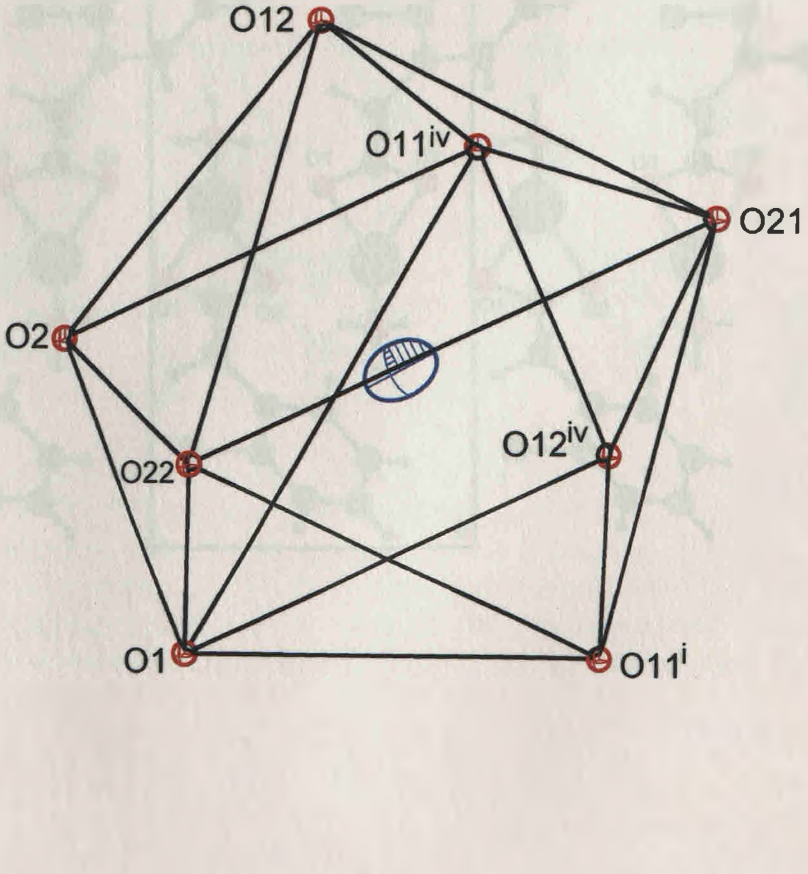

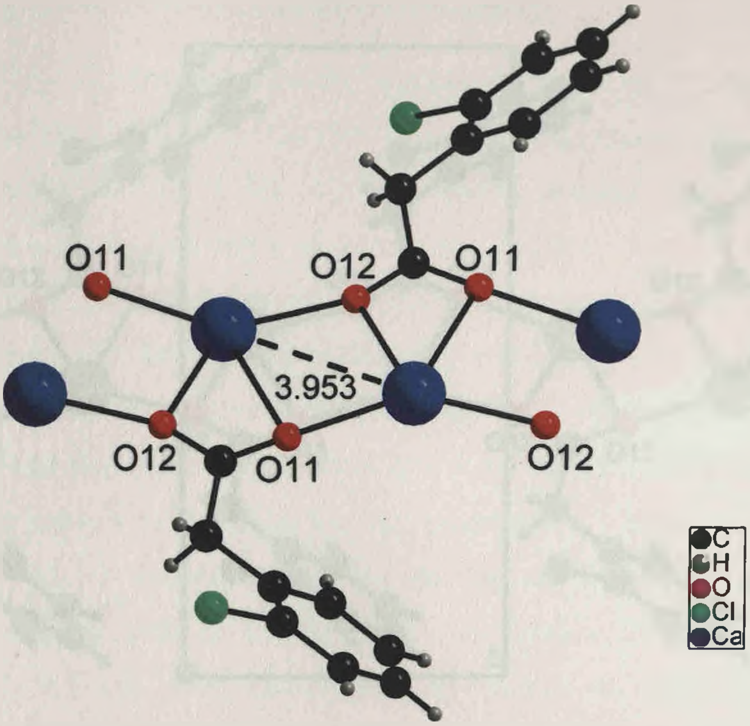

Figure 88- (**A**) The distorted triangular dodecahedral coordination polyhedron around Ca(II) in **34**. (**B**) A pair of μ_3–η^2:η^2 L_2 ligands form a tricyclic dicalcium-dicarboxylate unit. Symmetry codes i) x, y-1, z iv) -x+2, y-1/2, -z+1.

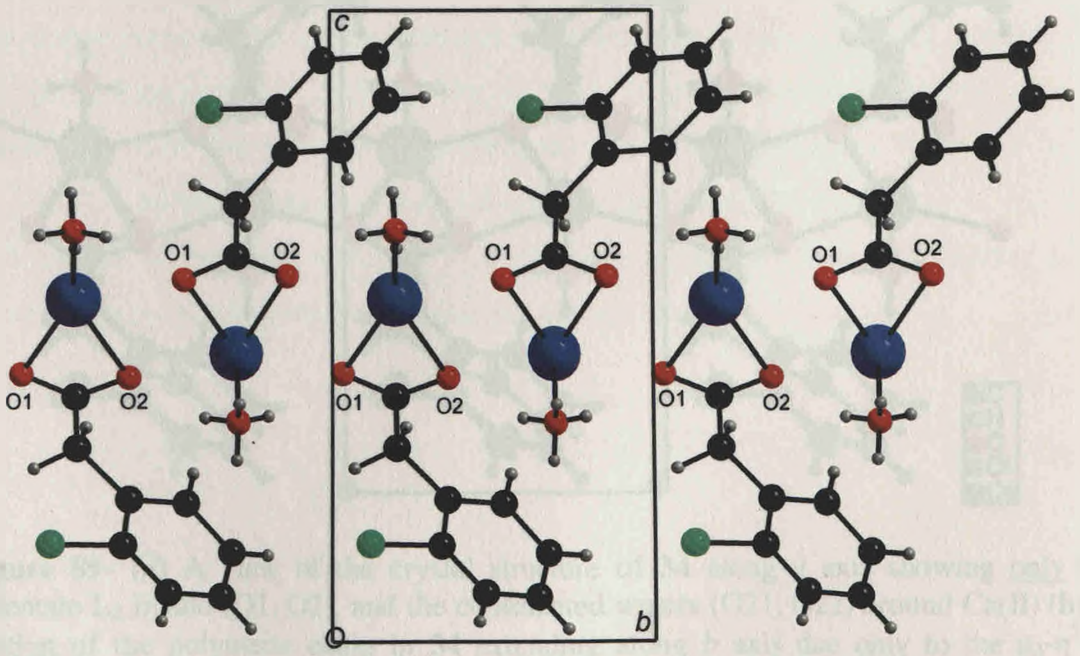

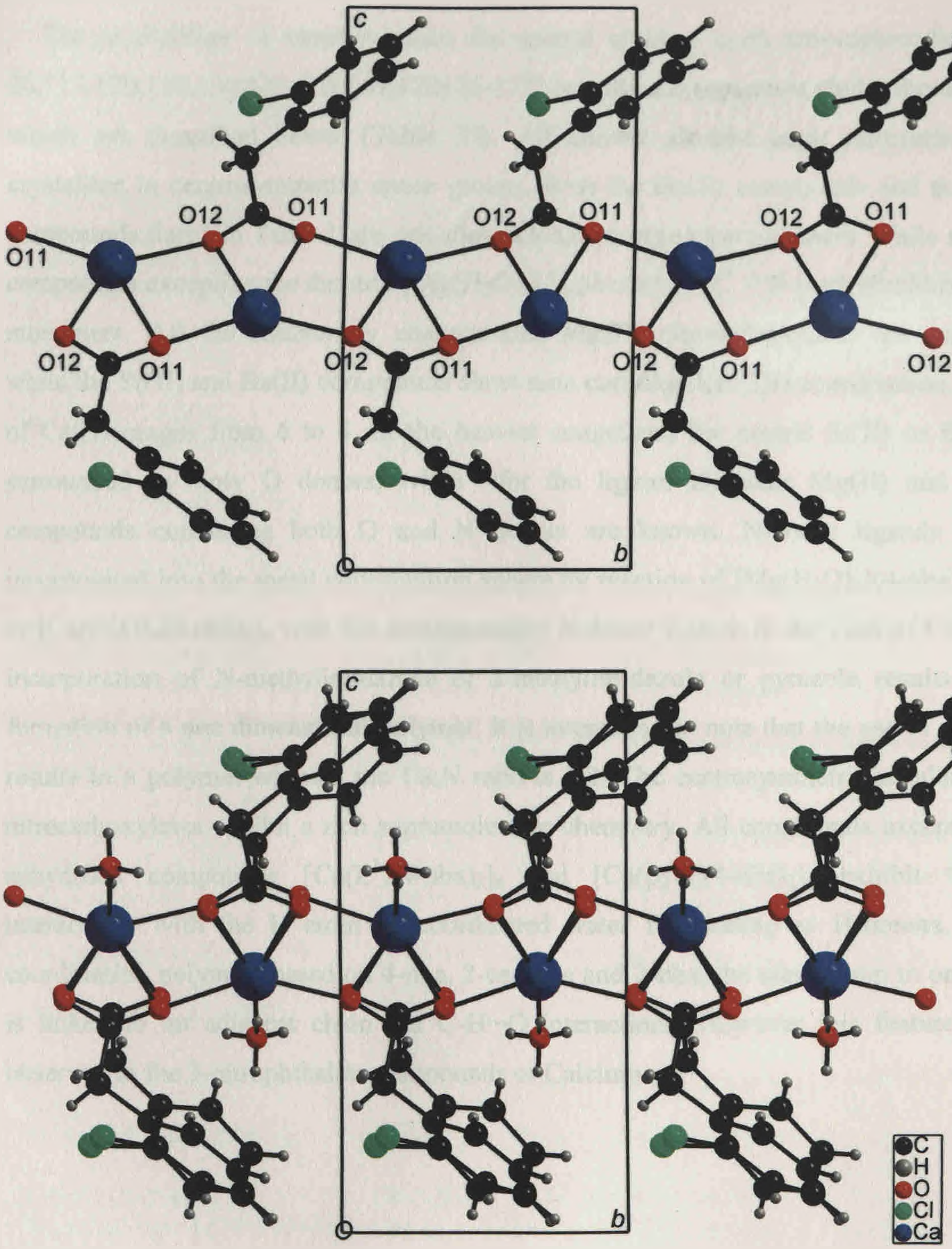

Figure 89- **(a)** A view of the crystal structure of **34** along *a* axis showing <u>only</u> the bidentate L_2 ligand (O1, O2), and the coordinated waters (O21, O22) around Ca(II) **(b)** A portion of the polymeric chain in **34** extending along *b* axis due <u>only</u> to the μ_3-η^2:η^2 bridging binding mode of the L_2 (O11, O12) ligand, showing the linking of each Ca(II) to three different bridging ligands. **(c)** A view of the crystallographic packing of **34**, showing the eight coordinated Ca(II) due to the terminal aqua ligands and the chelating and bridging L_2 ligand.

Comparative study of alkaline earth nitrocarboxylates

The availability of structural data for several alkaline earth nitrocarboxylates [24-26,117,120,121,130,133,165,169,170176-177] permits a comparative study, the details of which are described below (Table 35). All known alkaline earth nitrocarboxylates crystallize in centrosymmetric space groups. Both the Ba(II) compounds and six Ca(II) compounds listed in Table 1 are one dimensional coordination polymers, while all other compounds excepting the dimeric $[Mg(H_2O)(L^1)_2(4\text{-nba})_2]_2$ (L^1 = N-methylimidazole) are monomers. All the structurally characterized Mg(II) nitrocarboxylates are octahedral while the Sr(II) and Ba(II) compounds show nine coordination. The coordination number of Ca(II) ranges from 6 to 8. In the heavier congeners, the central Sr(II) or Ba(II) is surrounded by only O donors, while for the lighter elements Mg(II) and Ca(II), compounds containing both O and N donors are known. N-donor ligands can be incorporated into the metal coordination sphere by reaction of $[Mg(H_2O)_6](4\text{-nba})_2{\cdot}2H_2O$ or $[Ca(H_2O)_4(4\text{-nba})_2]_n$ with the corresponding N-donor ligand. In the case of Ca(II) the incorporation of N-methylimidazole or 2-methylimidazole or pyrazole results in the formation of a one dimensional polymer. It is interesting to note that the use of pyrazole results in a polymer wherein the Ca:N ratio is 1:2. The centrosymmetric alkaline earth nitrocarboxylates exhibit a rich supramolecular chemistry. All compounds excepting the anhydrous compounds $[Ca(L^1)(4\text{-nba})_2]_n$ and $[Ca(pyr)_2(4\text{-nba})_2]_n$ exhibit O-H···O interactions with the H atom of coordinated water functioning as H-donors. In the coordination polymers based on 4-nba, 2-ca-4nba and 2-nba, the nitro group in one chain is linked to an adjacent chain via C-H···O interactions. However this feature is not observed in the 3-nitrophthalate compounds of Calcium.

Table 35- showing comparative structural features of synthesized *s*-block metal carboxylates

Compound *	C.S.	Space Group	M : H$_2$O	Nuclearity	H-bonding
[Mg(H$_2$O)$_6$](4-nba)$_2$·2H$_2$O	{MgO$_6$}	$P\bar{1}$	1:6	monomer	O-H···O
[Mg(H$_2$O)$_6$](2-ca-4nba)$_2$	{MgO$_6$}	$P2_1/c$	1:6	monomer	O-H···O, N-H···O, C-H···O
[Mg(H$_2$O)$_5$(3-npth)]·2H$_2$O	{MgO$_6$}	$P\bar{1}$	1:5	monomer	O-H···O
[Mg(H$_2$O)$_4$(2-nba)$_2$]	{MgO$_6$}	$P\bar{1}$	1:4	monomer	O-H···O, C-H···O
[Ca(H$_2$O)$_4$(4-nba)$_2$]$_n$	{CaO$_7$}	$P2_1/c$	1:7	monomer	O-H···O, C-H···O
[[Sr(H$_2$O)$_7$(4-nba)](4nba)·2H$_2$O]	{SrO$_9$}	$P2_1/c$	1:5	monomer	O-H···O, C-H···O
[Ba(H$_2$O)$_5$(4-nba)$_2$]$_n$	{BaO$_9$}	$P2_1/c$	1:3	polymer	O-H···O, C-H···O
[Ba(H$_2$O)$_3$(2-nba)$_2$]$_n$	{BaO$_9$}	$P\bar{1}$	1:2	polymer	O-H···O, C-H···O
[Ca(H$_2$O)$_2$(2-nba)$_2$]$_n$	{CaO$_8$}	$P\bar{1}$	1:2	polymer	O-H···O, C-H···O
[Ca(H$_2$O)$_2$(2-ca-4nba)$_2$]$_n$	{CaO$_7$}	$P\bar{1}$	1:2	polymer	O-H···O, N-H···O, C-H···O
[[Ca(H$_2$O)$_2$(3-npth)]·H$_2$O]$_n$	{CaO$_7$}	$P2_1/c$	1:2	polymer	O-H···O
[Mg(H$_2$O)$_2$(Im)$_2$(4-nba)$_2$]	{MgO$_4$N$_2$}	$P\bar{1}$	1:2	monomer	O-H···O, N-H···O
[Mg(H$_2$O)(N-MeIm)$_2$(4-nba)$_2$]$_2$	{MgO$_4$N$_2$}	$P\bar{1}$	1:1	Dimer	O-H···O
[Ca(H$_2$O)$_3$(Im)(4-nba)$_2$]·Im	{CaO$_5$N}	$P2_1/c$	1:3	monomer	O-H···O, N-H···O, O-H···N
[Ca(N-MeIm)(4-nba)$_2$]$_n$	{CaO$_5$N}	$P\bar{1}$	1:0	polymer	C-H···O
[Ca(H$_2$O)(2-MeIm)(4-nba)$_2$]$_n$	{CaO$_6$N}	$P2_1/n$	1:1	polymer	O-H···O, N-H···O, C-H···O
[Ca(pyr)$_2$(4-nba)$_2$]$_n$	{CaO$_4$N$_2$}	$P\bar{1}$	1:0	polymer	N-H···O, C-H···O
[[Ca(H$_2$O)$_2$(4-nba)$_2$](dmp)$_2$]$_n$	{CaO$_8$}	$P\bar{1}$	1:2	polymer	O-H···O, N-H···O O-H···N, C-H···O
[[Ca(H$_2$O)$_2$(L$_1$)$_2$]·H$_2$O]$_n$	{CaO$_8$}	$P2_1$	1:2	polymer	O-H···O, C-H···O
[[Ca(H$_2$O)$_2$(L$_2$)$_2$]·2H$_2$O]$_n$	{CaO$_8$}	$P2_1$	1:2	polymer	O-H···O, C-H···O
[Ca(H$_2$O)$_6$(4-nba)](4-nba)(2-ap)·H$_2$O	{CaO$_7$}	$P\bar{1}$	1:6	monomer	O-H···N, C-H···O, N-H···O
[Ca$_3$(btc)$_2$(H$_2$O)$_{12}$]$_n$	{CaO$_7$} {CaO$_8$}	C2/C	1:4	polymer	C-H···O
[[Ba$_3$(btc)$_2$(H$_2$O)$_8$].2H$_2$O]$_n$	{BaO$_8$} {BaO$_{10}$}	$P2_{1/c}$	1:2.75	polymer	C-H···O
[[Sr(4-nba)(dmf) (H$_2$O)$_3$](4-nba)]$_n$	{SrO$_8$}	$P2_{1/m}$	1:3	polymer	O-H···N, C-H···O, N-H···O
[Sr(H$_2$O)(4-nba)$_2$(nmf)$_{1.5}$]$_n$	{SrO8}	$C2/c$	1:1	polymer	C-H···O, O-H···O, N-H···O
[Sr(pyr)$_2$(4-nba)$_2$]$_n$	{SrO$_6$N$_2$}	$C2/c$	1:0	polymer	C-H···O, N-H···O
[Sr(H$_2$O)$_2$(4-nba)$_2$(HCONH$_2$)] .H$_2$O]$_n$	{SrO$_8$}	$P\bar{1}$	1:3	polymer	O-H···N, C-H···O, N-H···O
[(H$_2$O)$_4$Li$_2$(μ-H$_2$O)$_2$](4-nba)$_2$	{LiO$_4$}	$P2_1/c$	1.3	dimer	O-H···O, C-H···O
[Na(4-nba)(H$_2$O)$_3$]$_n$	{NaO$_6$}	$P\bar{1}$	1:3	Polymer	O-H···O, C-H···O

Abbreviations- C.S. = coordination sphere of central metal; 4-nba = 4-nitrobenzoate; 2-ca-4nba = 2-carbamoyl-4-nitrobenzoate; 3-npth = 3-nitrophthalate; 2-nba = 2-nitrobenzoate; Im = imidazole; N-MeIm = N-methylimidazole; 2-MeIm = 2-methylimidazole; pyr = pyrazole; dmp = dimethylpyrazole; L$_1$= P-methoxy phenylacetate; L$_2$= 2-chlorophenylacetate; 2-ap = 2-aminopyridine; btc = 1,3,5-benzenetricarboxylate; DMF = dimethylformamide; NMF = N-methylformamide

* All the compounds given herein are from the present work.

Conclusions

The important findings of the present work are as follows -

- A simple method has been developed for the synthesis of $[Ca(H_2O)_4(4\text{-}nba)_2]$. Thermochemical route has been developed for the synthesis of calcium 4-nitrobenzoates containing N-donor ligands like Im, N-MeIm, pyr and 2-ap.
- It is shown that zero dimensional mononuclear tetraaqua Ca(II) 4-nitrobenzoate compound can be transformed into the Ca(II) coordination polymers by heating in the presence of N-donor ligands like N-MeIm, 2-MeIm, pyr and dmp.
- The reaction of mononuclear tetraaqua Ca(II)-4-nitrobenzoate with 2-ap results in the formation of water rich compound in aqueous condition and an anhydrous compound under solid state condition.
- New alkaline earth metal carboxylate compounds of 2-nitrobenzoic acid have been synthesized and characterized.
- Chemistry of 3-nitrophthalic acid and 4-nitrophthalamic acid has been investigated for their reactivity with alkaline earth metal salts.
- Two new metal carboxylates compounds of Mg and Ca have been synthesized under ambient condition using 2-ca-4nbaH and the role of the 2-carbamoyl (amide) sustituent in 2-ca-4nbaH forming differently hydrated products has been shown by comparison of the reaction of $CaCO_3$ or $MgCO_3$ with 2-ca-4nbaH and 4-nbaH under identical conditions.
- Reactivity and structural features of alkaline earth metal carboxylates of 1,3,5-benzene tricarboxylic has been investigated.
- The chemistry of strontium-4-nitrobenzoate has been studied for its reactivity with the O-donor ligands like dmf, nmf, formamide as well as neutral N-donor ligands.
- Two new non-centrosymmetric calcium compounds using flexible phenylacetate based ligands have been structurally characterized.
- This work demonstrates that new coordination polymers can be prepared under ambient condition.

REFERENCES

[1] S. R. Batten, S.M. Neville, D. R. Turner, Coordination Polymers: Design, Analysis and Application, RSC Publishing, Cambridge UK (2009).

[2] C. Janiak, J. K. Vieth, New J. Chem., **34** (2010) 2366

[3] A. U. Czaja, N. Trukhan, U. Müller Chem. Soc. Rev., **38** (2009) 1284

[4] M. D. Allendorf, C. A. Bauer, R. K. Bhakta, R. J. T. Houk, Chem. Soc. Rev., **38** (2009) 1330

[5] D. Britt, D. Tranchemontagne, O. M. Yaghi, Proc. Natl. Acad. Sci., **105** (2008) 11623

[6] D. Laurencin, C. Gervais, A. Wong, C. Coelho, F. Mauri, D. Massiot, M. E. Smith, C. Bonhomme, J. Am. Chem. Soc., **131** (2009) 13430

[7] L. J. Murray, M. Dincă, J. R. Long, Chem. Soc. Rev., **38** (2009) 1294

[8] J. R. Li, R. J. Kuppler, H-C. Zhou, Chem. Soc. Rev., **38** (2009) 1477

[9] S. S. Iremonger, P. D. Southon, C. J. Kepert, J. Chem. Soc. Dalton Trans., (2008) 6103

[10] C. Janiak, J. Chem. Soc. Dalton Trans., (2003) 2781

[11] R. Robson, J. Chem. Soc. Dalton Trans., (2008) 5113

[12] S. R. Batten, N. R. Champness, X-M. Chen, J. Garcia-Martinez, S. Kitagawa, L. Öhrström, M. O'Keeffe, M. P. Suh, J. Reedijk, Cryst. Eng. Comm., **14** (2012) 3001

[13] Coordination polymers: In Wikipedia, The Free Encyclopedia. http://en.wikipedia.org/wiki/Coordination_polymers

[14] J. W. Steed, J. L. Atwood, Supramolecular Chemistry, 2nd ed. Wiley Chichester, UK, (2009) 538

[15] K. Biradha, A. Ramanan, J. J. Vittal, Cryst. Growth Des., **9** (2009) 2969

[16] A. Y. Robin, K.M. Fromm, Coord. Chem. Rev. **250** (2006) 2127

[17] K. M. Fromm, E. D. Gueneau, A. Y. Robin, W. Maudez, J. Saue, R. Bergougnant Z. Anorg. Allg. Chem., **631** (2005) 1725

[18] S. Chen, S. Hoffmann, Y. Prots, J-T. Zhao, R. Kniep Z. Anorg. Allg. Chem., **636**, (2010) 1710

[19] R. Murugavel, P. Kumar, M.G. Walawalkar, R. Mathialagan, Inorg. Chem., **46** (2007), 6828

[20] R-X.Yuan, R-G. Xiong, Z-F. Chen, X-Z. You, S-M. Peng, G-H. Lee, Inorg. Chem. Commun., **4** (2001), 430

[21] L-C. Yu, Z-F. Chen, H. Liang, C-S. Zhou, Y. Li, J. Mol. Struct., **750** (2005) 35

[22] S. Fox, I. Büsching, W. Barklage, H. Strasdeit, Inorg. Chem., **46** (2007), 818

[23] C. Volkringer, T. Loiseau, G. Férey, J. H. Warren, D. S Wragg, R. E Morris, Solid State Sci., **9** (2007) 455

[24] B. R. Srinivasan, S.Y. Shetgaonkar, J. V. Sawant, P. Raghavaiah, Polyhedron, **27** (2008) 3299

[25] B. R. Srinivasan, S.Y. Shetgaonkar, P. Raghavaiah, Polyhedron, **28** (2009) 2879

[26] B. R. Srinivasan, S.Y. Shetgaonkar, C. Nather, W. Bensch, Polyhedron, **28** (2009) 534

[27] P. J. Calderone, D. Banerjee, Q. Nizami, R. L. La Duca, J. B. Parise, Polyhedron, **37** (2012) 42

[28] D. Banerjee, J. B. Parise, Cryst. Growth Des., **11** (2011) 4704

[29] J. D. Lee, Concise Inorganic Chemistry; Chapman and Hall: New York, (1991)

[30] R. C. Mehrotra and M. Bohra, Metal carboxylates (Academic press, London), 1983; R.C. Mehrotra, A. Singh, Prog. Inorg. Chem., **46** (1997) 239

[31] F. A. Cotton, G. Wilkinson, C. A. Murillo, M. Bochmann, Advanced Inorganic Chemistry, 6th Edition, John Wiley & Sons, Inc, Chichester (1999) 487

[32] A. Karipides, C. Mc Kinney, K. Peiffer, Acta Crystallogr., **C44** (1988) 46

[33] I. Senkovska, U. Thewalt Acta Crystallogr., **C61** (2005) m488

[34] R. H. Groeneman, J. L. Atwood, Cryst. Eng., **2** (1999) 241

[35] S.H. Dale, M.R.J Elsegood, Acta Crystallogr., **C59** (2003) m540

[36] A. Bacchi, M. Carcelli, C. Pelizzi, G. Pelizzi, P. Pelagatti, D Rogolino, M. Tegoni, C. Viappiani, Inorg. Chem., **42** (2003) 5871

[37] A. Brainbanti, A. M.M. Lanfredi , M. A. Pellinghelli, A. Tiripicchio, Chem. Commun., (1970) 377

[38] W-D. Song, X-X. Guo, C-H. Zhang, Acta Crystallogr., **E63** (2007) m399

[39] R. Murugavel, V.V. Karambelkar, G. Anantharaman, Indian J. Chem. **39A** (2000) 843

[40] S. Yano, M. Numata, M. Kato, S. Motoo, T. Nishimura, Acta Crystallogr., **E57** (2001) m488

[41] B. G. Cooksey, L. T. Gibson, A. R. Kennedy, D. Littlejohn, L. Stewart, N. H. Tennent, Acta Crystallogr., **C55** (1999) 324

[42] R. Murugavel, S. Banerjee Inorg. Chem. Commun., **6** (2003) 810

[43] S. Wörl, I. O. Fritsky, D. Hellwinkel, H. Pritzkow, R. Krämer, Eur. J. Inorg. Chem., (2005) 759

[44] B. L. Cole, E. M. Holt., Inorg. Chim. Acta, **108** (1985) 159

[45] M. Odabaşoğlu, O. Büyükgüngör, Acta Crystallogr., **E63** (2007) m712

[46] J-G. Zhao, S. Gao, Z-Y. Zhang, L-H. Huo, H. Zhao, Acta Crystallogr., **E62** (2006) m278

[47] R. Murugavel, V. V. Karambelkar, G. Anantharaman, M. G. Walawalkar Inorg. Chem., **39** (2000) 1381

[48] L. Pan , T. Frydel, M B. Sander, X. Huang, J. Li. Inorg. Chem., **40** (2001) 1271

[49] R. Murugavel, R. Korah, Inorg. Chem., **46** (2007) 11048

[50] M. L. G. Salido, P. A. Mascaros, R. L. Garzon, M. D. G. Valero, J. N. Low, J. F. Gallagher, C. Glidewell, Acta Crystallogr., **B60** (2004) 46

[51] D. K. Tian, S. L. Li, J. F. Hou, Acta Crystallogr., **E62** (2006) m130

[52] J. N. Low, P. Arranz, J. Cobo, M. A. Fontecha, M.L Godino, R. Lopez, D. Cannon, A. Quesada, C. Glidewell, Acta Crystallogr., **C57** (2001) 680

[53] C. Volkringer, J. Marrot, G. Ferey, T. Loiseau, Cryst. Growth Des., **8** (2008) 685

[54] W. Starosta, J. Leciejewicz, Acta Crystallogr., **E63** (2007) m1662

[55] A. Karipides, A. T. Reed, Acta Crystallogr., **B36** (1980) 1377

[56] K. Aliouane, N. Rahahlia, A. Guehria-Laidoudi, S. Dahaoui, C. Lecomte, Acta Crystallogr., **E63** (2007) m1834

[57] R. K. B. Nielsen, K. O. Kongshaug, H. Fjellvåg, Solid State Sci., **8** (2006) 1237

[58] A. Grirrane, A. Pastor, E. Álvarez, R. Moyano, A. Galindo, Inorg. Chem. Comm., **10** (2007) 1125

[59] Y. Yang, G. Jiang, Y-Z. Li, J. Bai, Y. Pan, X-Z. You, Inorg. Chimi. Acta., **359** (2006) 3257

[60] Z. Fei, T. J. Geldbach, R. Scopelliti, P. J. Dyson, Inorg. Chem., **45** (2006) 6331

[61] Q. Shuai, S. Chen, S. Gao, Inorg. Chim. Acta., **360** (2007) 1381

[62] S. N. G. Acharya, R. S. Gopalan, G. U. Kulkarni, K. Venkatesan, S. Bhattacharya Chem. Comm., (2000) 1351

[63] B. R. Srinivasan, J. V. Sawant, P. Raghavaiah, J. Chem. Sci., **119** (2007) 11

[64] B. Paluchowska, J. K. Maurin, Leciejewicz, Acta Crystallogr., **C52** (1996) 347

[65] V. Yasodha, S. Govindarajan, J. N. Low, C. Glidewell, Acta Crystallogr., **C63** (2007) m207

[66] D. A. Lenev, K. A. Lyssenko, R. G. Kostyanovsky, Eur. J. Inorg. Chem., (2003) 2979

[67] J. D. Crane, D. J. Moreton, E. Rogerson, Eur. J. Inorg. Chem., (2004) 4237

[68] T. Jini, K. V. Saban, G. Varghese, S. Naveen, M. A. Shridhar, J.S. Prasad, J. Alloys Comp., **433** (2007) 211

[69] Y-Y. Yang, Z-Q. Huang, L. Szeto, W-T.Wong, Appl. Organometal. Chem., **18** (2004) 97

[70] M. J. Platers, R. A. Howie, A. J. Roberts, Chem. Commun., (1997) 893

[71] H. Zhu, Z. Zhang, W. Sun, T. Okamura, N. Ueyama, Crys. Growth Des., **5** (2005) 177

[72] D. Volkmer, M. Fricke, C. Agena, J. Mattay, Cryst. Eng. Comm., **4** (2002) 288

[73] C. A. Williams, A. J. Blake, C. Wilson, P. Hubberstey, M. Schroder, Cryst. Growth Des., **8** (2008) 911

[74] N. Ueyama, J. Takeda, Y. Yamada, A. Onoda, T-a Okamura, Inorg. Chem., **38** (1999) 475

[75] S. Neogi, J. A. R. Navarro, P. K. Bharadwaj, Cryst. Growth Des., **8** (2008) 1554

[76] M. C. Das, S. K. Ghosh, E. C. Sanudo, P. K. Bharadwaj, Dalton Trans., (2009) 1644

[77] A. L. Bail, D. Bazin, M. Daudon, A. Brochot, V. Robbez-Masson, V. Maisonneuve, Acta Crystallogr., **B65** (2009) 350

[78] G. K. Ambady, Acta Crystallogr., **B24** (1968) 1548

[79] J. Albertsson, Å. Oskarsson, C. Svensson, Acta Crystallogr. **B34** (1978) 2737

[80] N. Burger, H. Fuess, Acta Crystallogr., **B33** (1977) 1968

[81] H. Einspahr, C. E. Bugg, Acta Crystallogr., **B30** (1974) 1037

[82] H. Einspahr, C. E. Bugg, Acta Crystallogr., **B35** (1979) 316

[83] W. Schukmann, H. Fuess, J. W. Bats, Acta Crystallogr., **B34** (1978) 3754

[84] F. Ancillotti, G. Boschi, G. Perego, A. Zazzetta, J. Chem. Soc. Dalton Trans., (1977) 901

[85] S. H. Whitlow, Acta Crystallogr., **B28** (1972) 1914

[86] V. A. Uchtman, R. J. Jandacek, Inorg. Chem., **19** (1980) 350

[87] A. Karipides, J. Ault, A. T. Reed, Inorg. Chem., **16** (1977) 3299

[88] M. P. Gupta, N. Prasad, Acta Crystallogr., **B32** (1976) 3257

[89] M. P. Gupta, S. M. Prasad, R. G. Sahu, B. N. Sahu, Acta Crystallogr., **B28** (1972) 135

[90] M. J. Vela, B. B. Snider, B. M. Foxman, Chem. Mater., **10** (1998) 3167

[91] W-D. Song, X-H. Huang, J-B. Yan, D-Y Ma, Acta Crystallogr., **E64** (2008) m654

[92] M. E. Curry, D. S. Eggleston, D. J. Hodgson, J. Am. Chem. Soc., **107** (1985) 8234

[93] Y. Yokomori, D. J. Hodgson, Inorg. Chem., **27** (1988) 2008

[94] E. A. Jefferson, P. Gantzel, E. Benedetti, M. Goodman, J. Am. Chem. Soc., **119** (1997) 3187

[95] W. J. Cook, C. E. Bugg, Acta Crystallogr., **B29** (1973) 215

[96] D. J. Hodgson, R. O. Asplund, Inorg. Chem., **29** (1990) 3612

[97] A. T. H. Lenstra, W. V. Havere, Acta Crystallogr., **B36** (1980) 156

[98] B. L. Barnett, V. A. Uchtman, Inorg. Chem., **18** (1979) 2674

[99] V. A. Uchtman, R. P. Oertel, J. Am. Chem. Soc., **95** (1973) 1802

[100] C. K. Schauer, O. P. Anderson, J. Am. Chem. Soc., **109** (1987) 3646

[101] A. M. Bahl, S. Krishnaswamy, N. G. Massand, D. J. Burkey T. P. Hanusa, Inorg. Chem., **36** (1997) 5413

[102] P. V. D. Sluis, A. Schouten, A. L. Spek, Acta Crystallogr, **C43** (1987) 1922

[103] B. Sheldrick, Acta Crystallogr., **B30** (1974) 2056

[104] T. Matsuzaki, Acta Crystallogr., **B28** (1972) 1977

[105] G. Strahs, R. E. Dickerson, Acta Crystallogr., **B24** (1968) 571

[106] A. Karipides, C. White, K. Peiffer, Acta Crystallogr., **C48** (1992) 1015

[107] G. Morin, M. Shang, B. D. Smith, Acta Crystallogr., **C56** (2000) 544

[108] D. Miernik, T. Lis, Acta Crystallogr., **C52** (1996) 1171

[109] H. Schmidbaur, I. Bach, D. L. Wilkinson, G. Muller Chem. Ber., **122** (1989) 1439

[110] P. C. Dietzel, R. Blom, H. Fjellvåg, Z. Anorg. Allg. Chem., **635** (2009) 1953

[111] S. Natarajan, G. Shanmugan, S. A. Martin Britto Dhas, S. Athimoolam, Acta Crystallogr., **E63** (2007) m2897

[112] L. Quan, H. Yin, L. Cui, M. Yang, Acta Crystallogr., **E65** (2009) m167

[113] B-Y Zhang, J-J. Nie, D-J Xu, Acta Crystallogr. **E65** (2009) m878

[114] W-D. Song, J-B. Yan, S-J. Li, D-L. Miao, X-F. Li, Acta Crystallogr., **E66** (2010) m53

[115] H. Aghabozorg, S. Daneshvar, A. Nimati, Acta Crystallogr., **E64** (2008) m1063

[116] M. Guo, Acta Crystallogr., **C65** (2009) m395

[117] B. R. Srinivasan, S.Y. Shetgaonkar, J. Coord. Chem., **63** (2010) 3403

[118] L. N. Appelhans, M. Kosa, A. V. Radha, P. Simoncic, A. Navrotsky, M. Parrinello, A. K. Cheetham, J. Am. Chem. Soc. **131** (2009) 15375

[119] B.R. Srinivasan, S. Y. Shetgaonkar, N. N. Ghosh, J. Coord. Chem., **64** (2011) 1113

[120] B. R. Srinivasan, S. Y. Shetgaonkar, C. Nather, Z. Anorg. Allg. Chem., **637** (2011) 130

[121] B. R. Srinivasan, S.Y. Shetgaonkar, C. Nather, Indian J. Chem., **51A** (2012) 435

[122] K. R. Jisha, S. Suma, M. R. Sudarsanakumar, Polyhedron, **29** (2010) 3164

[123] J-P. Wang, Z-J. Lu, Q-Y. Zhu, Y-P. Zhang, Y-R. Qin, G-Q. Bian, J. Dai, Cryst. Growth Des., **10** (2010) 2090

[124] K. Yusenko, S. Fox, P. Guni, H. Strasdeit, Z. Anorg. Allg. Chem., **634** (2008) 2347

[125] P-C. Liang, H-K. Liu, C-T. Yeh, C-H. Lin, V. Zima, Cryst. Growth Des., **11** (2011) 699

[126] M. K. Kim, K-L. Bae, K. M. Ok, Cryst. Growth Des., **11** (2011) 930

[127] B. M. Borah, S. K. Dey, G. Das, Cryst. Growth Des., **11** (2011) 2773

[128] C. N. Morrison, A. K. Powell, G. E. Kostakis, Cryst. Growth Des., **11** (2011) 3653

[129] R. Murugavel, K. Baheti, G. Anantharaman, Inorg. Chem. **40** (2001), 6870

[130] B. R. Srinivasan, S. Y. Shetgaonkar, S. Kohli, Rajnikant, Indian J. Chem., **49A** (2010) 1468

[131] H-K. Liu, T-H. Tsao, Y-T. Zhang, C-H. Lin. Cryst. Eng. Comm., **11** (2009) 1462

[132] G. Morgant, J. Angelo, D. Desmaele, E. Dichi, M. Sghaier, B. Fraisse, P.Retailleau, V. Brumas, M. M. L. Fiallo, A. Tomas, Polyhedron., **27** (2008) 2097

[133] B. R. Srinivasan, J. V. Sawant, C. Näther, W. Bensch, J. Chem. Sci., **119** (2007) 243

[134] F. Wiesbrock, A. Schier, H. Schmidbaur, Z. Naturforsch., **B57** (2002) 251

[135] S. H. Dale, M. R. J. Elsegood, S. Kainth, Acta Crystallogr., **59C** (2003) m505

[136] M. Kariuki, W. Jones, Acta Crystallogr., **C45** (1989) 1297

[137] B-H. Ye, T. Mak, I. D. Williams, X-Y. Li, J. Chem. Soc. Dalton Trans., (1998) 1935

[138] H. Schmidbaur, I. Bach, D. L. Wilkinson, G. Müller, Chem. Ber., **122** (1989) 1445

[139] S. R. Drake, K. D. Sanderson, M. B. Hursthouse, K. M. AbdulMalik, Inorg. Chem., **32** (1993) 1041

[140] F. Huang, W. D. Song, Acta Crystallogr., **E64** (2008) m552

[141] X-Y. Liu, L-H. Liu, Acta Crystallogr., **E66** (2010) m305

[142] Y. L. Li, X. Guo, J. X. Wang, Y. C. Wang, Acta Crystallogr., **E65** (2009) m772

[143] X-M. Hao, C-S. Gu, W-D. Song, J-W. Liu, Acta Crystallogr., **E64** (2008) m1052

[144] I. Senkovska, S. Kaskel, Eur. J. Inorg. Chem., (2006) 4564

[145] I. Senkovska, J. Fritsch, S. Kaskel, Eur. J. Inorg. Chem., (2007) 5475

[146] M. Dinca, J. R. Long, J. Am. Chem. Soc., **127** (2005) 9376

[147] Z. Guo, G. Li, L. Zhou, S. Shenqqun, Y. Lei, S. Dang, H. Zhang, Inorg. Chem. **48**

(2009) 8069

[148] M. Indrani, R. Ramasubramanian, F. R. Fronczek, D. Braga, N. Y. Vasanthacharya, S. Kumaresan, J. Chem. Sci., **121** (2009) 413

[149] D. Banerjee, J. Finkelstein, A. Smirov, P. M. Forster, L. A. Borkowski, S. J. Teat, J. B. Parise, Cryst. Growth. Des., **11** (2011) 2572

[150] B. H. Lee, C. H. Kim, S. G. Lee, Acta Crystallogr., **C59** (2003) m196

[151] A. Briceno, J. M. Delgado, G. D. Delgado, Acta Crystallogr., **E58** (2002) m602

[152] G. Dong, Z. Bing-guang, P. Ke-liang, D. Chun-ying, M. Qing-jin, J. Chem. Soc. Dalton Trans., (2002) 3783

[153] F. S. M. Lo, Y. S. S. Chui, D. I. Williams, Acta Crystallogr., **C54** *(1998) 1846*

[154] M. Odabasoglu, O. Büyükgüngör, Acta Crystallogr., **E62** (2006) m402

[155] S. Djehni, F. Balegroune, A. Guehria-Laidoudi, S. Dahaoui, C. Lecomte, Acta Crystallogr., **C63** (2007) m91

[156] S. Gao, W. J. Liu, H. L. Huo, H. Zhao, Acta Crystallogr., **C61** (2005) m348

[157] R. L. Garzon, L. M. D. Leon, N. J. Low, C. Glidewell, Acta Crystallogr., **C61** (2005) m224

[158] X. Zhang, S. Gao, H. L. Huo, H. Zhao, Acta Crystallogr., **E61** (2005) m2488

[159] S. Chen, Q. Shuai, S. Gao, Z. Anorg. Allg. Chem., **634**, (2008) 1591

[160] H. Lin, Y-H. He., Acta Crystallogr., **E63** (2007) m3204

[161] H. Aghabozorg, A. Nemati, Z. Derikvand, M. Ghadermazi, S. Daneshvar, Acta Crystallogr., **E64** (2008) m375

[162] W-D. Song, R-Z. Fan, C-S. Gu, X-M. Hao, Acta Crystallogr., **E64** (2008) m551

[163] J-W. Liu, S-W Ng, Acta Crystallogr., **E63** (2007) m808

[164] D. J. Hodgson, R. O. Asplund, Inorg. Chem., **30** (1991) 3577

[165] B. R. Srinivasan, S.Y. Shetgaonkar, P Raghavaiah, J. Chem. Sci., **120** (2008) 249

[166] M. Dan, A. K. Cheetam, C.N. R. Rao, Inorg. Chem., **45** (2006) 8227

[167] Z. Fei, T.J. Geldbach, D. Zhao, R. Scopelliti, P.J. Dyson, Inorg. Chem., **44** (2005) 5200

[168] D. T. Tran, D. Chu, A. G. Oliver, S. R. J. Oliver, Inorg. Chem. Comm., **12** (2009) 351

[169] B. R. Srinivasan, J. V. Sawant, S. C. Sawant, P Raghavaiah, J. Chem. Sci., **119** (2007) 593

[170] B. R. Srinivasan, S. Y. Shetgaonkar, P. Raghavaiah, Indian J. Chem., **48A** (2009) 1662

[171] W. Starosta, H. Ptasiewicz-bak, J. Leciejewicz, J. Coord. Chem., **56** (2003) 33

[172] M. J. Plater, A. J. Roberts, J. Marr, E. E. Lachowski, R. A. Howie, J. Chem. Soc. Dalton Trans., (1998) 797

[173] R. P. Davies, R. J. Less, P. D. Lickiss, A. J. P. White, Dalton Trans., (2007) 2528

[174] C. Volkringer, T. Loiseau, J. Marrot, G. Férey, Cryst Eng Comm., **11** (2009) 58

[175] B. R. Srinivasan, J. V. Sawant, P. Raghavaiah, Indian J. Chem., **45A** (2006) 2392

[176] B. R. Srinivasan, S. Y. Shetgaonkar, K. T. Dhavskar, J. K. Sundar, S. Natarajan, Indian. J. Chem., **51A** (2012) 564

[177] B. R. Srinivasan, P. Raghavaiah, J. V. Sawant, Acta Crystallogr., **E63** (2007) m2251

[178] M. Kloskowska, J. Chojnacki, W. Wojnowski, B. Becker, Acta Crystallogr., **C62** (2006) m541

[179] I. Turowska-Tyrk, T. M. Krygowski, M. Gdaniec, G. Hafelinger, G. Ritter., J. Mol. Struc., **172** (1988) 401

[180] H. N. Shrivastava, J. C. Speakman, J. Chem. Soc., (1961) 1151

[181] B. T. Usubaliev, E. M. Movsumov, I. R. Amiraslanov, K. S. Mamedov, Dokl Akad Nauk Az SSR., **36** (1980) 40

[182] B. K. Das, A. R. Chakravorty, Inorg Chem, **30** (1991) 4978

[183] M. Ebihara, K. Yamada, T. Kawamura, Acta Crystallogr, **C62** (2006) m451

[184] M. S. Khiyalov, I. R. Amiraslanov, K. S. Mamedov, E. M. Movsumov, Proc. Nat. Acad. Sci. Azebaidzhan., **37** (1981) 42

[185] M. Jian-Fang, J. Zhong-Sheng, N. Jia-Zuan, Chinese J. Struct. Chem., **10** (1991) 56

[186] C. Boskovic, A. Sieber, G. Chaboussant, H. U. Guedel, J. Ensling, W. Wernsdorfer, A. Neels, G. Labat, H. Stoeckli-Evans, S. Janssen, Inorg Chem., **43** (2004) 5053

[187] G. Trettenhahn, M. Nagl, N. Neuwirth, V. B. Arion, W. Jary, P. Pochlauer, W. Schmid, Angew Chem. Int. Ed., **45** (2006) 2794

[188] M. Odoko, T. Ise, N. Okabe, Acta Crystallogr., **C63** (2007) m22

[189] R. Sarma, J. B. Baruah, Inorg Chim Acta., **362** (2009) 1681

[190] H. Bußkamp, G. B. Deacon, M. Hilder, P. C. Junk, U. H. Kynast, W. W. Lee, D. R. Turner, Cryst Eng Comm., **9** (2007) 394

[191] A. D. Dias, S. Viswanathan, Dalton Trans, (2006) 4093

[192] H. Einspahr, C. E. Bugg, Acta Crystallogr, B37 (1981) 1044

[193] H. Schmidbaur, P. Mikulcik, G. Müller, Chem. Ber. 123 (1990) 1599

[194] K. Nakamoto, Infrared spectra of Inorganic and coordination compounds, Wiley

New York., (1986)

[195] R. M. Silverstein, F. X. Webster, Spectrometric identification of organic Compounds., Wiley India sixth edition., (2006)

[196] G. M. Sheldrick, Acta Crystallgr., **A64** (2008) 112

[197] Bruker SMART V5.630 and SAINT-PLUS V6.45, Bruker-Nonius Analytical X-ray System Inc.: Madison, Wisconsin, USA, (2003)

[198] SADABS (1997) Empirical absorption correction program, Bruker AXS Inc., Madison, Wisconsin, USA

[199] Bond valence sums were determined using the software VaList. A.S. Wills, VaList, Program available from www.ccp14.ac.uk

[200] B. R. Srinivasan, S. C. Sawant, Thermochim. Acta., **402** (2003) 45

[201] S. Prabhakar, V.W. Bhagwat, V. Vijaywargiya, N. S. Poonia, Curr. Sci., **53**, (1984) 1287

[202] E. Regulska, M. Samsonowicz, R. Swislocka, W. Lewandowski, J. Phys. Org. Chem., **20**, (2007) 93

[203] J. G. Z. Young, W. Onyebuagu, J. Org. Chem., **55** (1990) 2155

[204] A. L. Spek, J. Appl. Cryst., **36** (2003) 7

[205] A. I. Vogel, Longman, A Textbook of Quantitative Inorganic Analysis, London, 4th edn., (1978) 472

APPENDIX - I

Table 1- Crystal data and structure refinement for $[Ca(N\text{-}MeIm)_2(4\text{-}nba)_2]_n$ **2** and $[Ca(H_2O)(4\text{-}nba)_2\,(L^2)]_n$ **4** (L^2 = 2MeIm).

	$[Ca(N\text{-}MeIm)_2(4\text{-}nba)_2]_n$ **2**	$[Ca(H_2O)(4\text{-}nba)_2(L^2)]_n$ **4**
Empirical formula	$C_{18}H_{14}CaN_4O_8$	$C_{18}H_{16}CaN_4O_9$
Formula weight(g mol^{-1})	454.41	472.43
Temperature (K)	293(2)	220(2)
Crystal system	Triclinic	Monoclinic
Wavelength (Å)	0.71073	0.71073
Space group	P-1	$P2_1/n$
Unit cell dimensions		
A (Å)	5.5313(5)	15.5486(13)
B (Å)	12.7904(12)	7.0358(4)
C (Å)	14.9226(15)	18.4282(15)
A (°)	113.08(1)	90
B (°)	95.72(1)	98.789(10)
Γ (°)	97.64(1)	90
Volume (Å^3)	950.11(16)	1992.3(3)
Z	2	4
Density (calculated) (mg/m^3)	1.588	1.575
Absorption coefficient (mm^{-1})	0.388	0.377
F (000)	468	976
Crystal size (mm^3)	0.38x0.28x0.2	0.4x0.3x0.2
Theta range for data collection (°)	1.5 to 26.00	2.65 to 28.09
Index ranges	$-6\le h\le 6$, $-15\le k\le 15$, $-18\le l\le 18$	$-20\le h\le 20$, $-8\le k\le 9$, $-24\le l\le 24$
Reflections collected	9475	18549
Independent reflections (R_{int})	3696(0.0205)	4768(0.0334)
Completeness to theta = 26.00° (%)	99.3	98
Refinement method	Full-matrix least-square on F^2	
Data / restraints / parameters	3696 / 0 / 285	4768/0/291
Goodness-of-fit on F^2	1.057	1.055
Final R indices [I>2sigma(I)]	R1 = 0.0348 wR2 = 0.0900	R1 = 0.0399 wR2 = 0.1069
R indices (all data)	R1 = 0.0392 wR2 = 0.0929	R1 = 0.0484 wR2 = 0.1123
Extinction coefficient		0.027(3)
Largest diff. peak and hole (e. Å^{-3})	0.338 and -0.235	0.337 and -0.386

Table -2 Crystal data and structure refinement for [Ca(pyr)$_2$(4-nba)$_2$]$_n$ **5** and [Ca(H$_2$O)$_2$(4-nba)$_2$].(dmp)$_2$]$_n$ **6**.

	[Ca(pyr)$_2$(4-nba)$_2$]$_n$ **5**	[Ca(H$_2$O)$_2$(4-nba)$_2$].(dmp)$_2$]$_n$ **6**
Empirical formula	$C_{20}H_{16}CaN_6O_8$	$C_{24}H_{28}CaN_6O_{10}$
Formula weight(g mol^{-1})	508.47	600.60
Temperature (K)	170(2)	293(2)
Crystal system	Triclinic	Triclinic
Wavelength (Å)	0.71073	0.71073
Space group	P-1	P-1
Unit cell dimensions		
A (Å)	5.3346(5)	7.4030(4)
B (Å)	7.8475(8)	14.4078(7)
C (Å)	13.7756(14)	14.8293(6)
A (°)	96.582(12)	110.419(3)
Β (°)	99.934(12)	91.214(4)
Γ (°)	107.703(12)	99.765(4)
Volume (Å^3)	532.50(9)	1455.31(12)
Z	1	2
Density (calculated) (mg/m^3)	1.586	1.371
Absorption coefficient (mm^{-1})	0.358	0.278
F (000)	262	628
Crystal size (mm^3)	0.3x0.2x0.2	0.4x0.2x0.03
Theta range for data collection (°)	2.77 to 27.00	1.54 to 26.00
Index ranges	$-6 \leq h \leq 6$, $-10 \leq k \leq 10$, $-17 \leq l \leq 17$	$-9 \leq h \leq 9$, $-17 \leq k \leq 17$, $-18 \leq l \leq 18$
Reflections collected	4537	17792
Independent reflections (R_{int})	2261(0.0327)	5713(0.0624)
Completeness to theta = 27.00° (%)	97.4	99.8
Refinement method	Full-matrix least-square on F^2	
Data / restraints / parameters	2261 / 0 / 161	5713/0/374
Goodness-of-fit on F^2	1.045	1.156
Final R indices [I>2sigma(I)]	R1 = 0.0356 wR2 = 0.0916	R1 = 0.0577 wR2 = 0.1103
R indices (all data)	R1 = 0.0439 wR2 = 0.0957	R1 = 0.0813 wR2 = 0.1178
Extinction coefficient	0.070(12)	
Largest diff. peak and hole (e. Å^{-3})	0.380 and -0.433	0.254 and -0.187

Table 3- Crystal data and structure refinement for $[Ca(H_2O)_6(4\text{-nba})(2\text{-ap})](4\text{-nba})(2\text{-ap})$ **7**

Empirical formula	$C_{19}H_{28}CaN_4O_{15}$
Formula weight(g mol^{-1})	592.52
Temperature (K)	293 (2)
Wavelength (Å)	0.71073
Crystal system / Space group	Triclinic / $P\bar{1}$
Unit cell dimensions	
a (Å)	6.8667(4)
b (Å)	10.1174(4)
c (Å)	19.4741(8)
α (°)	75.700(4)
β (°)	87.453(4)
γ (°)	84.675(4)
Volume (Å^3) / Z	1305.03(11) / 2
Density (calculated) (mg / m^3)	1.508
Absorption coefficient (mm^{-1})	0.321
F (000)	620
Crystal size (mm^3)	0.15 × 0.2 × 0.30
Θ range for data collection (°)	3.15 to 32.35
Completeness to theta (32.35°)	90.0 %
Index ranges	$-10\leq h\leq 10$, $-15\leq k\leq 5$, $-28\leq l\leq 28$
Reflections collected	19968
Independent reflections	8439 [R(int) = 0.0201]
Refinement method	Full-matrix least-square on F^2
Data / restraints / parameters	8439 / 0 / 465
Goodness-of-fit on F^2	0.936
Final R indices [I>2sigma(I)]	R1 = 0.0373 wR2 = 0.0961
R indices (all data)	R1 = 0.0556 wR2 = 0.1008
Extinction coefficient	0.0060(19)
Largest diff. peak and hole (e. Å^{-3})	0.325 and -0.276

Table 4 - Crystal data and structure refinement for $[(H_2O)_4Li_2(\mu\text{-}H_2O)_2](4\text{-nba})_2$ **8** and $[Na(4\text{-nba})(H_2O)_3]_n$ **9**

Empirical formula	$C_{14}H_{20}Li_2N_2O_{14}$	$C_7H_{10}NaNO_7$
Formula weight (g mol^{-1})	454.20	243.15
Temperature (K)	293(2)	298(2)
Wavelength (Å)	0.71073	0.71073
Crystal system	Monoclinic	Triclinic
Space group	$P2_1/c$	$P\bar{1}$
Unit cell dimensions	a = 12.324(4) Å α = 90°	a = 7.2109(14) Å α = 96.42(3)°
	b = 6.719(5) Å β = 104.29(3)°	b = 12.033(2) Å β = 91.65(3)°
	c = 12.402(3) Å γ = 90°	c = 12.382(3) Å γ = 104.43(3)°
Volume [Å^3]	995.2(8)	1032.2(4)
Z	2	4
Density (calculated) mg/m^3	1.516	1.565
Absorption coefficient (mm^{-1})	0.135	0.174
F(000)	472	504
Crystal size (mm^3)	0.25 × 0.19 × 0.17	0.12 × 0.10 × 0.08
Theta range for data collection (°)	3.39 to 24.96	1.76 to 25.98
Completeness to theta	99.9 %	98.8%
Index ranges	$0 \le h \le 14$, $-1 \le k \le 7$, $-14 \le l \le 14$	$-8 \le h \le 8$, $-14 \le k \le 14$, $-15 \le l \le 15$
Reflections collected	2170	10532
Independent reflections	1741 [R(int) = 0.0364]	3990 [R(int) = 0.0228]
Refinement method	Full-matrix least-squares on F^2	Full-matrix least-squares on F^2
Data / restraints / parameters	1741 / 0 / 164	3990 / 0 / 290
Goodness-of-fit on F^2	1.194	0.948
Final R indices [I>2sigma(I)]	R1 = 0.0377, wR2 = 0.1112	R1 = 0.0390, wR2 = 0.1044
R indices (all data)	R1 = 0.0437, wR2 = 0.1154	R1 = 0.0458, wR2 = 0.1105
Extinction coefficient	0.203(9)	0.022(2)
Largest diff. peak and hole (e.Å^{-3})	0.219 and -0.173	0.411 and -0.256
Bond valence sum[a] of central metal	1.059, 1.058	1.117, 0.999

[a] Bond valence sums were determined from the crystallographic data using the software Valist [199]

Table 5 – Selected refinement data for $[Sr(H_2O)_3(4\text{-nba})(DMF)]\cdot 4\text{-nba}$ **12** and $[Sr(H_2O)(4\text{-nba})_2(NMF)_{1.5}]$ **13** and $[Sr(4\text{-nba})_2(Pyr)_2]$ **14**

Empirical formula	$[Sr(H_2O)_3(4\text{-nba})(DMF)]\cdot 4\text{-nba}$	$[Sr(H_2O)(4\text{-nba})_2(NMF)_{1.5}]$	$[Sr(4\text{-nba})_2(Pyr)_2]$
Formula weight(g mol^{-1})	546.99	1052.93	556.01
Temperature (K)	200(2)	293(2)	170(2)
Wavelength (Å)	0.71073	0.71073	0.71073
Crystal system	monoclinic	monoclinic	monoclinic
space group	$P2_{1/m}$	$C2/c$	$C2/c$
a (Å)	10.1712(5)	32.1274(9)	22.5885(14)
b (Å)	7.0022(4)	8.9601(3)	13.1532(7)
c (Å)	15.9352(8)	14.5598(4)	7.7101(4)
β (°)	102.149(6)	100.147(2)	109.608(7)
Volume ($Å^3$)	1109.50(10)	4125.7(2)	2157.9(2)
D_{calc} (mg/m^3), Z	1.637, 2	1.695, 4	1.711, 4
Absorption coefficient (mm^{-1})	2.498	2.679	2.561
F(000)	556	2128	1120
Crystal size(mm^3)	0.14 x 0.11 x 0.08	0.07 x 0.10 x 0.14	0.11 x 0.08 x 0.06
θ range for data collection (°)	2.61 to 26.99	2.36 to 27.95	3.06 to 27.00
Index ranges	$-12\leq h\leq 12$, $-8\leq k\leq 8$, $-20\leq l\leq 20$	$-42\leq h\leq 35$, $-11\leq k\leq 11$, $-17\leq l\leq 19$	$-28\leq h\leq 28$, $-16\leq k\leq 16$, $-8\leq l\leq 9$
Reflections collected	9011	21317	9715
Independent reflections (R_{int})	2609 (0.036)	4924 (0.0371)	2272 (0.0343)
Completeness to theta	99.5 %	99.3 %	96.5 %
Refinement method	Full-matrix least-squares on F^2		
Data / restraints / Parameters	2609 / 0 / 185	4924 / 0 / 307	2272 / 0 / 160
Goodness-of-fit on F^2	1.038	1.179	1.051
Final R indices[$I>2\sigma$ (I)]	R1 = 0.0283, wR2 = 0.0691	R1 = 0.0385, wR2 = 0.0609	R1 = 0.0275, wR2 = 0.0655
R indices (all data)	R1 = 0.0322, wR2 = 0.0709	R1 = 0.0492, wR2 = 0.0633	R1 = 0.0322, wR2 = 0.0674
Extinction coefficient	0.016(2)		0.0029(5)
Largest difference peak and hole (e.$Å^{-3}$)	0.368 and -0.402	0.374 and -0.510	0.294 and -0.395

Table 6 - Crystal data and structure refinement for $[Mg(H_2O)_6](2\text{-ca-4nba})_2$ **16** and $[Ca(H_2O)_2(2\text{-ca-4-nba})_2]_n$ **17**.

	$[Mg(H_2O)_6](2\text{-ca-4nba})_2$ **1**	$[Ca(H_2O)_2(2\text{-ca-4-nba})_2]_n$ **2**
Empirical formula	$C_{16}H_{22}MgN_4O_{16}$	$C_{16}H_{14}CaN_4O_{12}$
Formula weight(g mol^{-1})	550.69	494.39
Temperature (K)	298(2)	220(2)
Crystal system	Monoclinic	Triclinic
Wavelength (Å)	0.71073	0.71073
Space group	$P2_1/c$	P-1
Unit cell dimensions		
a (Å)	15.729(3)	7.8884(16)
b (Å)	7.5571(16)	8.2028(16)
c (Å)	9.982(2)	15.5763(16)
α (°)	90	75.15(3)
β (°)	100.658(3)	80.71(3)
γ (°)	90	87.58(3)
Volume (Å^3)	1166.1(4)	961.5(3)
Z	2	2
Density (calculated) (mg/m^3)	1.568	1.708
Absorption coefficient (mm^{-1})	0.165	0.406
F (000)	572	508
Crystal size (mm^3)	0.42x0.32x0.12	
Theta range for data collection (°)	1.32 to 26.02	2.57 to 28.35
Index ranges	$-19\leq h\leq 19$, $-9\leq k\leq 9$, $-12\leq l\leq 12$	$-9\leq h\leq 10$, $-10\leq k\leq 8$, $-18\leq l\leq 20$
Reflections collected	11523	6349
Independent reflections (R_{int})	2289(0.0238)	4556(0.0208)
Completeness to theta = 28.35.00° (%)	99.5	95
Refinement method	Full-matrix least-square on F^2	
Data / restraints / parameters	2289 / 0 / 169	4556/0/330
Goodness-of-fit on F^2	1.062	1.127
Final R indices [I>2sigma(I)]	R1 = 0.0360 wR2 = 0.0972	R1 = 0.0615 wR2 = 0.1617
R indices (all data)	R1 = 0.0397 wR2 = 0.0999	R1 = 0.0919 wR2 = 0.2385
Extinction coefficient	0.018(2)	0.027(3)
Largest diff. peak and hole (e. Å^{-3})	0.212 and -0.202	0.863and -0.694

Table 7 - Crystal data and structure refinement for $[Mg(H_2O)_4(2\text{-nba})_2]$ **20**, $[Ca(H_2O)_2(2\text{-nba})_2]_n$ **21**, $[Ba(H_2O)_3(2\text{-nba})_2]_n$ **23**

	$[Mg(H_2O)_4(2\text{-nba})_2]$	$[Ca(H_2O)_2(2\text{-nba})_2]_n$	$[Ba(H_2O)_3(2\text{-nba})_2]_n$
Empirical formula	$C_{14}H_{16}MgN_2O_{12}$	$C_{14}H_{12}CaN_2O_{10}$	$C_{14}H_{14}BaN_2O_{11}$
Formula weight(g mol^{-1})	428.60	408.34	523.61
Temperature (K)	170(2)	293(2)	293(2)
Crystal system	Triclinic	Triclinic	Triclinic
Wavelength (Å)	0.71073	0.71073	0.71073
Space group	P-1	P-1	P-1
Unit cell dimensions			
A (Å)	5.2587(5)	7.7477(10)	8.360(3)
B (Å)	7.6309(7)	10.1953(13)	8.475(3)
C (Å)	11.7095(10)	11.2808(15)	14.077(6)
A (°)	81.745(11)	80.851(2)	79.78(6)
B (°)	78.443(10)	82.233(2)	85.52(5)
Γ (°)	73.797(11)	89.333(2)	70.49(5)
Volume ($Å^3$)	440.15(7)	871.6(2)	925(6)
Z	1	2	2
Density (calculated) (mg/m^3)	1.617	1.556	1.880
Absorption coefficient (mm^{-1})	0.174	0.418	2.209
F (000)	222	420	512
Crystal size (mm^3)	0.3x0.2x0.2	0.38x0.32x0.2	0.42x0.34x0.2
Theta range for data collection (°)	2.79 to 27.94	1.85 to 25.93	2.58 to 25.85
Index ranges	$-6\leq h\leq 6$, $-10\leq k\leq 10$, $-15\leq l\leq 15$	$-9\leq h\leq 9$, $-11\leq k\leq 12$, $-13\leq l\leq 13$	$-10\leq h\leq 10$, $-10\leq k\leq 10$, $-17\leq l\leq 17$
Reflections collected	4989	6780	8554
Independent reflections (Rint)	2007 (0.0423)	3753 (0.0204)	3526 (0.0187)
Completeness to theta = 25.93° (%)	95.2	98.4	98.6
Refinement method	Full-matrix least-square on F^2		
Data / restraints / parameters	2007 / 0 / 134	3353 / 4 / 260	3526 / 9 / 271
Goodness-of-fit on F^2	1.019	1.077	1.113
Final R indices [I>2sigma(I)]	R1 = 0.0346 wR2 = 0.0931	R1 = 0.0395 wR2 = 0.0863	R1 = 0.0227 wR2 = 0.0589
R indices (all data)	R1 = 0.0427 wR2 = 0.0966	R1 = 0.0461 wR2 = 0.0896	R1 = 0.0230 wR2 = 0.0592
Extinction coefficient	0.092(16)	0.0040(2)	0.0040(2)
Largest diff. peak and hole (e. $Å^{-3}$)	0.273 and -0.339	0.215 and -0.202	0.707 and -0.885

Table 8 – Selected refinement data for $[[Ca(H_2O)_2(3\text{-npth})]\cdot H_2O]_n$ **25** and $[Mg(H_2O)_5(3\text{-npth})]\cdot 2H_2O$ **26**

	$[Mg(H_2O)_5(3\text{-npth})]\cdot 2H_2O$ **25**	$[[Ca(H_2O)_2(3\text{-npth})]\cdot H_2O]_n$ **26**
Empirical formula	$C_8H_{17}MgNO_{13}$	$C_8H_9CaNO_9$
Formula weight(g mol^{-1})	359.54	303.24
Temperature (K)	170(2)	170(2)
Crystal system	Triclinic	monoclinic
Wavelength (Å)	0.71073	0.71073
Space group	P-1	$P2_1/c$
Unit cell dimensions		
A (Å)	7.3921(5)	6.1289(4)
B (Å)	8.6642(6)	20.9606(11)
C (Å)	12.0943(9)	8.9218(6)
A (°)	76.948(9)	90
β (°)	81.120(8)	96.006(8)
γ (°)	82.391(8)	90
Volume ($Å^3$)	741.7(9)	1139.85(12)
Z	2	4
Density (calculated) (mg/m^3)	1.610	1.767
Absorption coefficient (mm^{-1})	0.191	0.596
F (000)	376	624
Crystal size (mm^3)	0.15x0.1x0.1	0.2x0.1x0.1
Theta range for data collection (°)	2.43 to 28.06	2.49 to 28.03
Index ranges	-9<=h<=9, -11<=k<=11, -15<=l<=15	-8<=h<=8, -27<=k<=27, -11<=l<=11
Reflections collected	7767	13362
Independent reflections (Rint)	3419 (0.0370)	2645 (0.0387)
Completeness to theta = 25.93° (%)	95.1	96.3
Refinement method	Full-matrix least-square on F^2	
Data / restraints / parameters	3419 / 0 / 212	2645 / 0 / 173
Goodness-of-fit on F^2	1.043	1.043
Final R indices [I>2sigma(I)]	R1 = 0.0364 wR2 = 0.0967	R1 = 0.0252 wR2 = 0.0653
R indices (all data)	R1 = 0.0457 wR2 = 0.1014	R1 = 0.0292 wR2 = 0.0668
Extinction coefficient	0.062(7)	0.016(2)
Largest diff. peak and hole (e. $Å^{-3}$)	0.335 and -0.315	0.357and -0.314

Table 9- Crystal data and structure refinement for $[Ca_3(H_2O)_{12}(btc)_2]$ **30** and $[Ba_3(H_2O)_8(btc)_2].2H_2O$ **32**.

	$[Ca_3(H_2O)_{12}(btc)_2]$ **30**	$[Ba_3(H_2O)_8(btc)_2].2H_2O$ **32**
Empirical formula	$C_{18}H_{30}Ca_3O_{24}$	$C_{18}H_{26}Ba_3O_{22}$
Formula weight (g mol^{-1})	750.66	1006.41
Temperature (K)	298(2)	298(2)
Wavelength (Å)	0.71073	0.71073
Crystal system	monoclinic	monoclinic
space group	C2/C	$P2_{1/c}$
Unit cell dimensions		
a (Å)	19.288(11)	12.589(3)
b (Å)	11.445(7)	16.004(3)
c (Å)	12.975(8)	6.8171(14)
β (°)	106.317(9)	91.153(3)
Volume ($Å^3$)	2749(3)	1373(5)
Z	4	2
D_{calc} (mg/m^3)	1.814	2.434
Absorption coefficient (mm^{-1})	0.709	4.353
F(000)	1560	956
Crystal size (mm^3)	0.38x0.24x0.22	0.42x0.19x0.16
Theta range for data collection (°)	2.09 to 26	1.62 to 25.97
Index ranges	$-23\leq h\leq 18$, $-13\leq k\leq 14$, $-15\leq l\leq 15$	$-15\leq h\leq 15$, $-19\leq k\leq 19$, $-8\leq l\leq 8$
Reflections collected	6880	13080
Independent reflections (Rint)	2666 (0.0200)	2678 (0.0273)
Completeness to theta = 28.49°	98.4 %	99.3 %
Refinement method	Full-matrix least-squares on F^2	
Data / restraints / parameters	2666 / 2 / 213	2678 / 0 / 237
Goodness-of-fit on F^2	1.056	1.153
Final R indices [I>2sigma(I)]	R1 = 0.0275, *w*R2 = 0.0714	R1 = 0.0184, wR2 = 0.0461
R indices (all data)	R1 = 0.0299, *w*R2 = 0.0729	R1 = 0.0188, wR2 = 0.0463
Largest diff. peak and hole ($eÅ^{-3}$)	0.264 and -0.355	0.599 and -0.674

Table10- Selected refinement data for $[Ca(H_2O)_2(L_1)_2]\cdot H_2O$ **33** and $[Ca(H_2O)_2(L_2)_2]\cdot 2H_2O$ **34**

Empirical formula	$[Ca(H_2O)_2(L_1)_2]\cdot H_2O$ **33**	$[Ca(H_2O)_2(L_2)_2]\cdot 2H_2O$ **34**
Formula weight(g mol^{-1})	424.45	451.30
Temperature (K)	293(2)	293(2)
Wavelength (Å)	0.71069	0.71069
Crystal system	monoclinic	monoclinic
space group	$P2_1$	$P2_1$
a (Å)	9.568(2)	11.669(3)
b (Å)	6.6381(16)	6.6737(18)
c (Å)	16.165(4)	13.508(4)
β (°)	99.196(4)	105.295(5)
Volume (Å^3)	1013.5(4)	1014.7(5)
Z	2	2
D_{calc} (mg/m^3)	1.391	1.477
Absorption coefficient (mm^{-1})	0.356	0.612
F(000)	448	468
θ range for data collection (°)	2.16 to 28.33	2.69 to 28.49
Index ranges	$-8\leq h\leq 12$, $-8\leq k\leq 8$, $-21\leq l\leq 21$	$-15\leq h\leq 13$, $-8\leq k\leq 8$, $-17\leq l\leq 15$
Reflections collected	6663	6740
Independent reflections (R_{int})	4544 (0.0447)	4597 (0.0312)
Completeness to theta	98.3 %	97.4 %
Refinement method	Full-matrix least-squares on F^2	
Data / restraints / Parameters	4544 / 1 / 248	4597 / 1 / 244
Goodness-of-fit on F^2	1.103	1.117
Final R indices[$I>2\sigma(I)$]	R1 = 0.0711, wR2 = 0.1840	R1 = 0.0501, wR2 = 0.1140
R indices (all data)	R1 = 0.0989, wR2 = 0.2385	R1 = 0.0763, wR2 = 0.1516
Flack X parameter	0.00(14)	-0.03(6)
Largest difference peak and hole (e.Å^{-3})	0.799 and -0.647	0.389 and -0.490

Table 11. Crystal data and structure refinement for Sr-Formamide.

Empirical formula	C15 H17 N3 O12 Sr
Formula weight	518.94
Temperature	293(2) K
Wavelength	0.71069 A
Crystal system, space group	triclinic, P-1
Unit cell dimensions	a = 7.122(5) A alpha = 98.016(5) deg. b = 8.941(5) A beta = 90.433(5) deg. c = 31.889(5) A gamma = 93.135(5) deg.
Volume	2007.5(18) A^3
Z, Calculated density	4, 1.717 Mg/m^3
Absorption coefficient	2.756 mm^-1
F(000)	1048
Crystal size	x, x, x, mm
Theta range for data collection	3.16 to 27.88 deg.
Limiting indices	-9<=h<=8, -11<=k<=11, -41<=l<=35
Reflections collected / unique	36360 / 9367 [R(int) = 0.0554]
Completeness to theta = 27.88	97.7 %
Absorption correction	None
Refinement method	Full-matrix least-squares on F^2
Data / restraints / parameters	9367 / 0 / 559
Goodness-of-fit on F^2	1.027
Final R indices [I>2sigma(I)]	R1 = 0.0406, wR2 = 0.0899
R indices (all data)	R1 = 0.0799, wR2 = 0.1030
Largest diff. peak and hole	0.741 and -0.430 e.A^-3

Table 12 - Selected bond lengths [A] and angles [deg] for Sr-Formamide.

Sr(1)-O(9)#1	2.483(2)
Sr(1)-O(1)	2.532(3)
Sr(1)-O(5)	2.547(3)
Sr(1)-O(6)#1	2.556(3)
Sr(1)-OW1	2.642(3)
Sr(1)-OW2	2.656(3)
Sr(1)-O(6)#2	2.680(2)
Sr(1)-O(5)#2	2.698(2)
Sr(1)-Sr(1)#3	4.330(2)
Sr(1)-Sr(1)#2	4.331(2)
Sr(2)-O(18)	2.494(2)
Sr(2)-O(14)#4	2.544(3)
Sr(2)-OW3	2.558(3)
Sr(2)-O(10)	2.577(3)
Sr(2)-O(11)#4	2.589(3)
Sr(2)-O(10)#5	2.635(2)
Sr(2)-OW4	2.700(3)
Sr(2)-O(11)#5	2.734(2)
Sr(2)-Sr(2)#5	4.260(2)
Sr(2)-Sr(2)#6	4.427(2)

O(9)#1-Sr(1)-O(1)	95.69(8)
O(9)#1-Sr(1)-O(5)	98.19(8)
O(1)-Sr(1)-O(5)	74.43(8)
O(9)#1-Sr(1)-O(6)#1	80.71(8)
O(1)-Sr(1)-O(6)#1	75.38(8)
O(5)-Sr(1)-O(6)#1	149.53(8)
O(9)#1-Sr(1)-OW1	74.56(8)
O(1)-Sr(1)-OW1	142.32(8)
O(5)-Sr(1)-OW1	71.23(9)
O(6)#1-Sr(1)-OW1	135.76(8)
O(9)#1-Sr(1)-OW2	92.47(8)
O(1)-Sr(1)-OW2	144.36(8)
O(5)-Sr(1)-OW2	138.42(8)
O(6)#1-Sr(1)-OW2	71.81(8)
OW1-Sr(1)-OW2	73.23(9)
O(9)#1-Sr(1)-O(6)#2	147.72(8)
O(1)-Sr(1)-O(6)#2	85.89(8)
O(5)-Sr(1)-O(6)#2	113.15(7)
O(6)#1-Sr(1)-O(6)#2	68.47(8)
OW1-Sr(1)-O(6)#2	121.74(7)
OW2-Sr(1)-O(6)#2	69.49(8)
O(9)#1-Sr(1)-O(5)#2	162.36(8)
O(1)-Sr(1)-O(5)#2	92.09(8)
O(5)-Sr(1)-O(5)#2	68.70(8)
O(6)#1-Sr(1)-O(5)#2	116.65(7)
OW1-Sr(1)-O(5)#2	89.64(8)
OW2-Sr(1)-O(5)#2	90.37(8)
O(6)#2-Sr(1)-O(5)#2	48.58(8)
O(18)-Sr(2)-O(14)#4	98.63(8)

O(18)-Sr(2)-OW3	78.43(9)
O(14)#4-Sr(2)-OW3	142.70(9)
O(18)-Sr(2)-O(10)	83.07(8)
O(14)#4-Sr(2)-O(10)	71.76(8)
OW3-Sr(2)-O(10)	142.76(9)
O(18)-Sr(2)-O(11)#4	99.66(8)
O(14)#4-Sr(2)-O(11)#4	72.05(8)
OW3-Sr(2)-O(11)#4	71.88(9)
O(10)-Sr(2)-O(11)#4	143.70(9)
O(18)-Sr(2)-O(10)#5	146.06(8)
O(14)#4-Sr(2)-O(10)#5	92.86(8)
OW3-Sr(2)-O(10)#5	110.36(8)
O(10)-Sr(2)-O(10)#5	70.37(8)
O(11)#4-Sr(2)-O(10)#5	114.27(7)
O(18)-Sr(2)-OW4	83.59(8)
O(14)#4-Sr(2)-OW4	142.08(8)
OW3-Sr(2)-OW4	75.05(9)
O(10)-Sr(2)-OW4	70.96(9)
O(11)#4-Sr(2)-OW4	145.29(8)
O(10)#5-Sr(2)-OW4	68.24(8)
O(18)-Sr(2)-O(11)#5	160.87(8)
O(14)#4-Sr(2)-O(11)#5	90.91(8)
OW3-Sr(2)-O(11)#5	83.92(8)
O(10)-Sr(2)-O(11)#5	115.79(7)
O(11)#4-Sr(2)-O(11)#5	67.48(8)
O(10)#5-Sr(2)-O(11)#5	48.68(8)
OW4-Sr(2)-O(11)#5	99.03(8)

Symmetry transformations used to generate equivalent atoms:
#1 x+1,y,z #2 -x,-y,-z #3 -x+1,-y,-z
#4 x-1,y,z #5 -x,-y,-z+1 #6 -x-1,-y,-z+1

APPENDIX - II

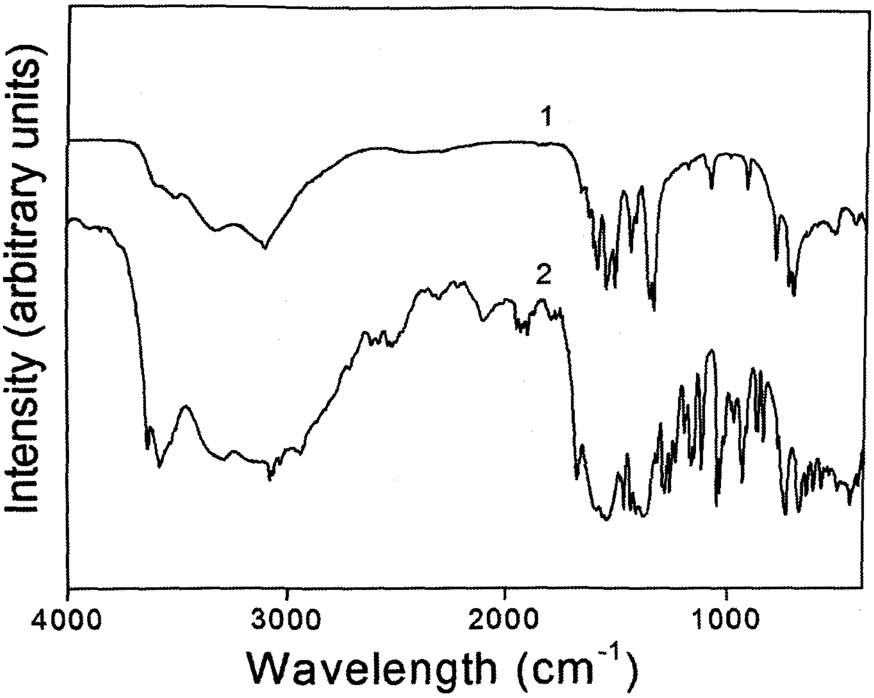

Figure 1- Infrared spectra of compounds 1) [$Cs_2(H_2O)_5$(3-npth)] **24** and 2) [$Ba(H_2O)_2$(2-Clphac)$_2$]$_n$ **36**

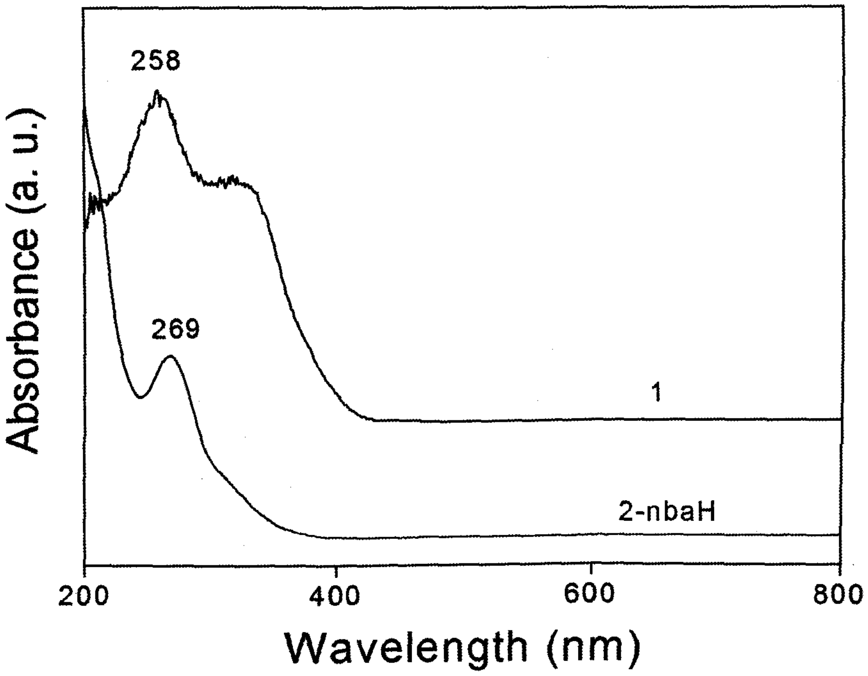

Figure 2- Diffuse Reflectance spectra of 2-nbaH and **1** [$Sr(H_2O)_4$(2-nba)$_2$]

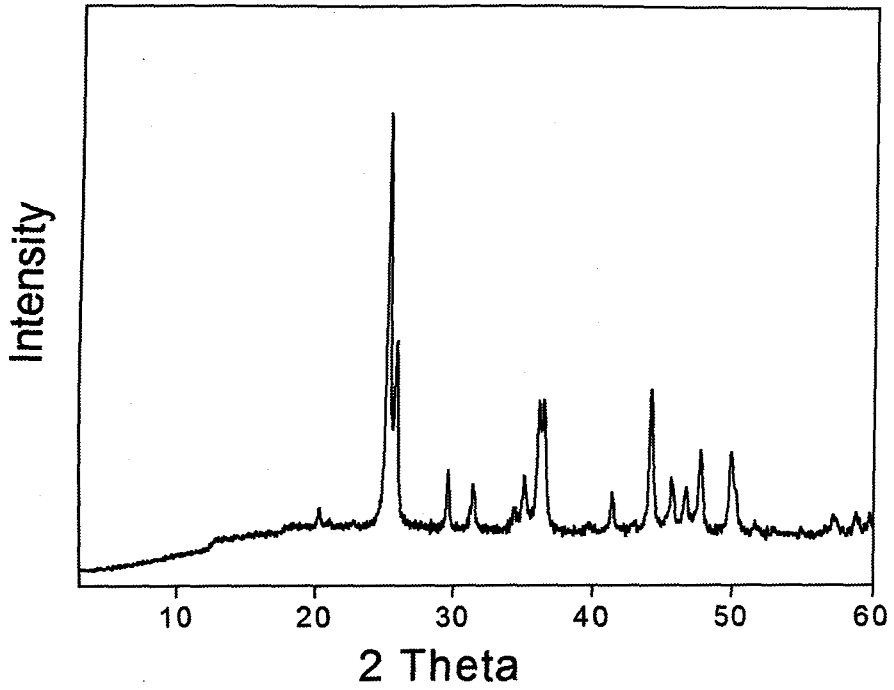

Figure 3- X-ray powder pattern of $SrCO_3$ residue of $[Sr(4\text{-nba})(DMF)(H_2O)_3](4\text{-nba})$ **12** on pyrolysis to 1000°C.

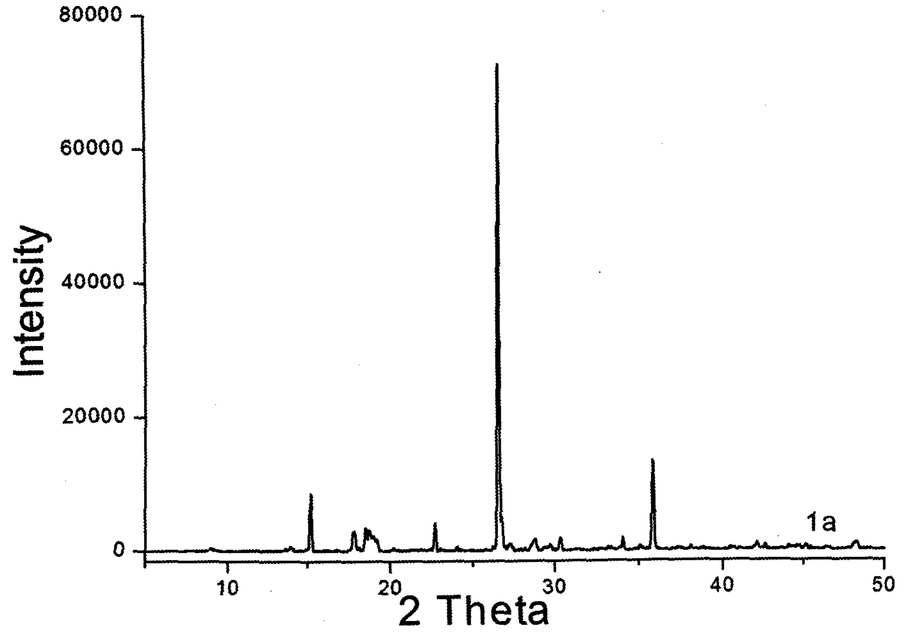

Figure 4 - X-ray powder pattern of $[Mg_3(btc)_2(H_2O)_{12}]$ **1a**

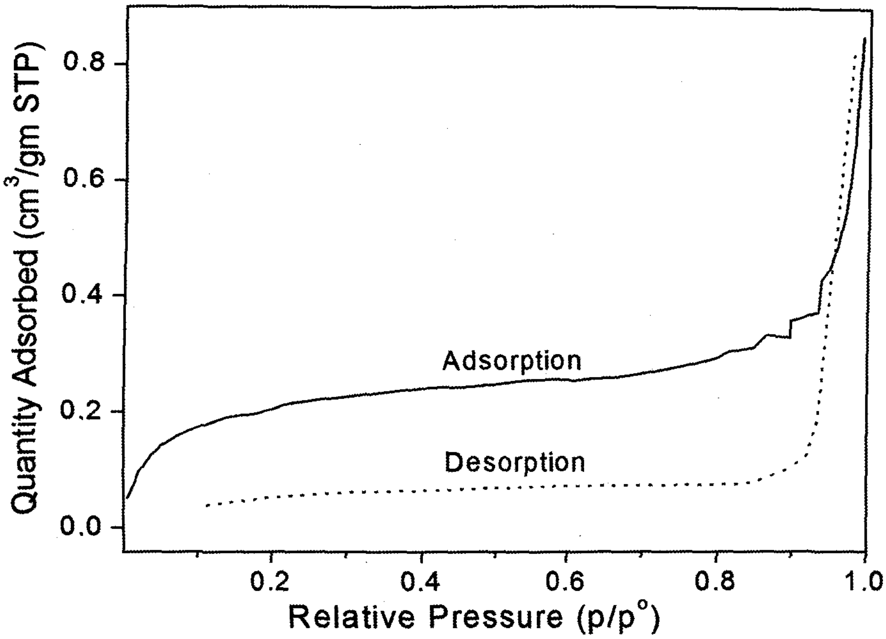

Figure 5 - Surface area of compound [Ca(4-OMephac)$_2$] **33a**

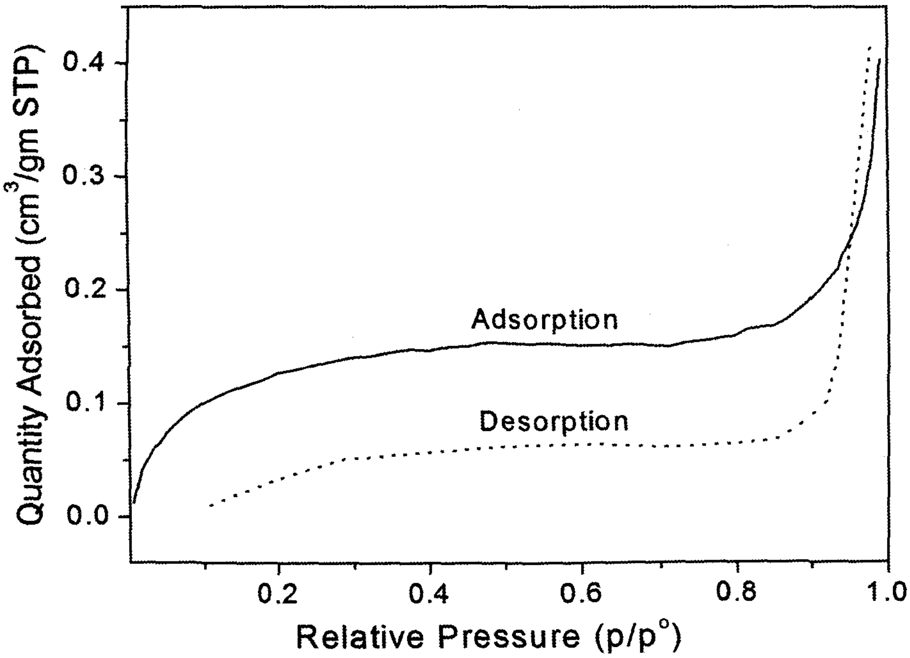

Figure 6 - Surface area of compound [Ca(2-Clphac)$_2$] **34a**

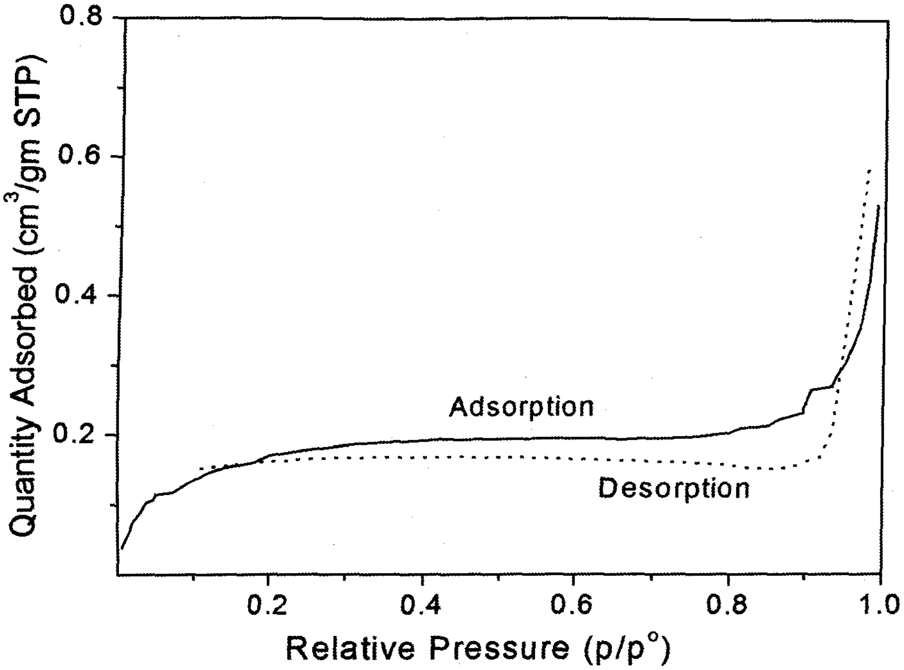

Figure 7 - Surface area of compound [Ca(phac)$_2$] **35a**

List of publications of Santosh Shetgaonkar in peer reviewed journals

1. A new calcium (II) coordination polymer based on a μ_2-bridging tridentate 4-nitrobenzoate B.R. Srinivasan, S.Y. Shetgaonkar, M. Saxena, C. Näther, *Indian. J. Chem.* **51A** 435-443 (2012)

2. Soft synthesis of a metal-organic framewok basd on a tribarium building block, B. R. Srinivasan, S. Y. Shetgaonkar, P. Raghavaiah, *Indian J. Chem.* **51A** 1064-1072(2012)

3. Synthesis and structural characterization of bis(μ_2-aqua)tetrakis(aqua)dilithium(I) bis(4-nitrobenzoate) B.R. Srinivasan, S.Y. Shetgaonkar, K. T. Dhavskar, J. K. Sundar, S. Natarajan, *Indian. J. Chem.* **51A** 564-570 (2012)

4. Synthesis and characterization of calcium(II) coordination polymers based on phenylacetic acid, B.R. Srinivasan, S.Y. Shetgaonkar, N.N. Ghosh, *J. Coord Chem.* **64** 1113-1124 (2011)

5. Preparation, crystal structures and thermal studies of alkaline earth nitrocarboxylates, B.R. Srinivasan, S.Y. Shetgaonkar, C. Näther, *Z. Anorg. Allg. Chem.* **637** 130-136 (2011)

6. Synthesis, characterization and properties of a water-rich calcium(II) 4-nitrobenzoate, B.R. Srinivasan, S.Y. Shetgaonkar, S. Kohli, Rajnikant, *Indian. J. Chem.* **49A** 1468-1477 (2010)

7. A calcium(II) coordination polymer showing two different bridging 2-carbamoyl-4-nitrobenzoate coordination modes, B.R. Srinivasan, S.Y. Shetgaonkar, *J. Coord Chem.* **63** 3403-3412 (2010)

8. First alkaline earth 2-carbamoyl-4-nitrobenzoate: Synthesis and supramolecular structure, B.R. Srinivasan, S.Y. Shetgaonkar, P. Raghavaiah, *Indian J. Chem.* **48A** 1662-1666 (2009)

9. A calcium(II) coordination polymer based on a tricyclic dicalcium-bis(2-nitrobenzoate) building block, B.R. Srinivasan, S.Y. Shetgaonkar, P. Raghavaiah, *Polyhedron* **28** 2879-2886 (2009)

10. Solid state synthesis and characterization of a triple chain calcium(II) coordination polymer showing two different bridging 4-nitrobenzoate coordination modes, B.R. Srinivasan, S.Y. Shetgaonkar, C. Näther, W. Bensch, *Polyhedron* **28** 534-540 (2009)

11. Synthesis, X-ray structure and properties of a calcium(II) coordination polymer showing μ_2-η^1:η^1 and μ_3-η^2:η^1 coordination modes of 4-nitrobenzoate, B.R. Srinivasan, S.Y. Shetgaonkar, J.V. Sawant P. Raghavaiah, *Polyhedron* **27** 3299-3305 (2008)

12. A one dimensional barium(II) coordination polymer with a coordinated nitro group of 2-nitrobenzoate, B.R. Srinivasan, S.Y. Shetgaonkar, P. Raghavaiah, *J. Chem. Sci* **120** 249-257 (2008)

List of presentations in Conference / Symposia

1. Structural chemistry of calcium carboxylates, B. R. Srinivasan, S. Y. Shetgaonkar, Poster presented at TIFR (Tata Institute of fundamental research, Mumbai) in 3rd Nov 2009

2. Preparation and properties of alkaline earth coordination polymers, B. R. Srinivasan, S. Y. Shetgaonkar, 3rd Sep 2010, oral 4 pg 18, Presentation at RSC west India section Ph.D. students symposium, Department of Chemistry, Goa University.

Indian Journal of Chemistry
Vol. 51A, March 2012, pp. 435-443

A new calcium(II) coordination polymer based on a μ_2-bridging tridentate 4-nitrobenzoate

Bikshandarkoil R Srinivasan[a, *], Santosh Y Shetgaonkar[a], Manav Saxena[b] & Christian Näther[c]

[a]Department of Chemistry, Goa University, Goa 403 206, India
Email: srini@unigoa.ac.in

[b]Department of Chemistry, Indian Institute of Technology, Kanpur, 208 016 India

[c]Institut für Anorganische Chemie, Christian-Albrechts-Universität Kiel, Max-Eyth Strasse 2, D-24118 Kiel, Germany

Received 17 September 2011; revised and accepted 16 January 2012

Reaction of a heptacoordinated Ca(II) compound $[Ca(H_2O)_4(4\text{-nba})_2]$ (4-nba = 4-nitrobenzoate) with 3,5-dimethyl-pyrazole (dmp) leads to the formation of an eight coordinated Ca(II) compound, $[[Ca(H_2O)_2(4\text{-nba})_2]\cdot 2dmp]_n$, containing two coordinated water molecules, two unique 4-nba ligands and two free dmp molecules in the lattice. The μ_2-bridging tridentate binding mode of the unique 4-nba ligands results in the formation of a one-dimensional (1-D) coordination polymer. The title compound exhibits enhanced fluorescence emission. An analysis of the six different bridging binding modes of the 4-nba ligand in twenty two different structurally characterized 4-nitrobenzoate compounds is described.

Keywords: Coordination chemistry, Calcium, 4-Nitrobenzoates, 3,5-Dimethylpyrazole, Coordination polymers, Metal organic frameworks

Coordination polymers (CPs) also known as metal organic frameworks (MOFs) have attracted much attention because of their topology and applications in catalysis, adsorption (gas storage), separation and luminescence[1-3]. Compared to the extensive chemistry of CPs based on transition metals, the coordination chemistry of *s*-block metals with organic linkers has remained a relatively less explored area. The reluctance in using alkali metal or alkaline earth cations as building blocks for open framework materials can be attributed to their unpredictable coordination numbers and geometries as no ligand field stabilization effects govern their bonding. Although the closed shell *s*-block metal cations lack useful properties like magnetism or variable oxidation states, alkali and alkaline-earth metals are preferred to transition or lanthanide metal ions because many of the *s*-block cations have the advantage of being non-toxic, cheap and soluble in aqueous media. Several recent reports reveal the growing interest in the coordination chemistry of *s*-block elements[4-17] and the chemistry of *s*-block metal compounds has been recently reviewed[18,19].

Depending on the electronic and steric requirements of the central metal, the flexibility, binding modes and hydrogen bonding characteristics of the organic ligand, coordination polymers of differing dimensionalities can be constructed. For the oxophilic *s*-block metals, carboxylic acids are useful linkers for the construction of coordination polymers as the metals can be linked into an extended chain with the aid of bridging binding modes of the carboxylate ligand. In view of their known affinity for oxygen donors, especially water, *s*-block metal carboxylates are normally synthesized in aqueous medium by reactions between alkaline earth metal sources and aromatic carboxylic acids under ambient conditions[13-17,20-30]. Reaction of metal source with carboxylic acids under hydrothermal conditions is another method employed by many groups for compound synthesis[5-12].

As part of an ongoing research program we are investigating the chemistry of alkaline earth nitrocarboxylates[30]. The seven coordinated Ca(II) compound $[Ca(H_2O)_4(4\text{-nba})_2]$[31] (**1**) reported by us in a very early work differs from several other Ca-carboxylates in that the 4-nba ligand does not exhibit bridging coordination. We have shown in earlier work[32,35] that on reaction with N-donor ligands the zero-dimensional compound, $[Ca(H_2O)_4(4\text{-nba})_2]$, can be transformed into mixed ligand Ca(II) compounds containing less or no water as evidenced by the characterization of $[Ca(Im)(H_2O)_3(4\text{-nba})_2]\cdot Im$[32], $[Ca(N\text{-MeIm})(4\text{-nba})_2]_n$, $[Ca(H_2O)(2\text{-MeIm})(4\text{-nba})_2]_n$

and $[Ca(pyr)_2(4\text{-nba})_2]_n$ (Im = imidazole[33]; N-MeIm = N-methylimidazole[33]; 2-MeIm = 2-methylimidazole[34]; pyr = pyrazole[30]). Recently we reported that compound (**1**) on reaction with 2-aminopyridine in an aqueous medium is transformed into a water-rich Ca(II) compound[35]. In this work, we have investigated the reaction of $[Ca(H_2O)_4(4\text{-nba})_2]$ with 3,5-dimethylpyrazole (dmp) and the results of this research are described herein.

Materials and Methods

All the chemicals used in this study were of reagent grade and were used as received. The starting materials and reaction products are air stable and hence were prepared under normal laboratory conditions. The compound $[Ca(H_2O)_4(4\text{-nba})_2]$ (**1**) was prepared by a published procedure[31,35]. 3,5-Dimethylpyrazole (dmp) was prepared by condensation of acetylacetone with hydrazine[36]. Infrared (IR) spectra of the solid samples diluted with KBr were recorded on a Shimadzu (IR Prestige-21) FT-IR spectrometer in the range 4000-400 cm^{-1}. UV-visible spectra were recorded on a Shimadzu UV-2450 double beam spectrophotometer. X-ray powder pattern were recorded on a Rigaku Miniflex II diffractometer using Cu-K_α radiation. Photoluminescence of solid samples was studied using a Perkin Elmer LS55 fluoroscence spectrometer. TG-DTA studies were performed in flowing air, in Al_2O_3 crucibles on a STA-409PC simultaneous thermal analyzer from Netzsch. A heating rate of 10 K min^{-1} was employed for all measurements. Isothermal weight loss studies were performed in a temperature controlled electric furnace.

Preparation of $[[Ca(H_2O)_2(4\text{-nba})_2]\cdot 2dmp]_n$ (2)

A mixture of $[Ca(H_2O)_4(4\text{-nba})_2]$ (**1**) (0.445 g, 1 mmol) and 3,5-dimethylpyrazole (0.392 g, 4 mmol) was taken in water (~5 mL) and the reaction mixture was heated on a steam bath to obtain a clear solution. The clear reaction mixture was left aside for crystallization. The pale yellow crystalline blocks suitable for structure determination which separated after ~3 h were isolated by filtration, washed with a little ice cold water followed by ether and air dried. $[[Ca(H_2O)_2(4\text{-nba})_2]\cdot 2dmp]_n$ (**2**) (Yield 0.46 g, 77%). Anal. (%): Found (calcd) for $CaC_{24}H_{28}N_6O_{10}$ (600.60): C 46.92 (48.00), H 4.54 (4.70), N 13.75 (13.99), CaO 9.2 (9.34). 4-nbaH 54.84 (55.65). IR (KBr cm^{-1}): 3600 (br, υ_{OH}), 3387, 3269 (υ_{NH}), 3148, 3105, 1614, 1568 υ_{as}(-COO), 1514 υ_{as}(-NO_2), 1416 υ_s(-COO), 1342 υ_s(-NO_2), 1317, 1288, 1151, 1105, 1015, 974, 878, 843, 797, 726, 694, 660, 592, 511. DTA data (in °C): 110 (endo), 236 (endo), 411 (exo), 545 (exo).

X-ray crystal structure determination

Intensity data for (**2**) were collected on an Image Plate Diffraction System (IPDS-II) from STOE. All non-hydrogen atoms were refined using anisotropic displacement parameters. The C-H hydrogen atoms were positioned with idealized geometry and refined using a riding model. The hydrogen atoms attached to the O21 and O22 of water and N21 and N31 of lattice dmp were located in the difference map and were refined isotropically using a riding model. Crystal data of (**2**) $C_{24}H_{28}CaN_6O_{10}$, $M = 600.60$ g mol^{-1}, triclinic, space group = $P\bar{1}$, $\lambda = 0.71073$ Å, $a = 7.4030(4)$ Å, $b = 14.4078(7)$ Å, $c = 14.8293(6)$ Å, $\alpha = 110.419(3)°$, $\beta = 91.214(4)°$, $\gamma = 99.765(4)°$, $V = 1455.31(12)$ Å^3, $Z = 2$, $D_{calc} = 1.371$ mg m^{-3}, $\mu = 0.278$ mm^{-1}, F(000) = 628, index range = $-9 \leq h \leq 9$, $-17 \leq k \leq 17$, $-18 \leq l \leq 18$; completeness to theta = 26.00° (99.8 %). A total of 17792 reflections ($1.54 < \theta < 26.0°$) were collected, of which 5713 were unique ($R_{int} = 0.0624$) and used for the structure solution. Structure was solved using SHELXS-97[37] and refined using SHELXL-97[37] to $R1$ ($wR2$) = 0.0577 (0.1103) for 4473 reflections with ($I > 2\sigma(I)$) using 374 parameters. The final Fourier difference synthesis showed minimum and maximum peaks of -0.187 and +0.254 eÅ^{-3}.

Results and Discussion

Synthetic aspects, spectral and thermal studies

The nature of products of the reaction of $CaCO_3$ with the isomeric 2- or 4-nitrobenzoic acids depends on the positioning of the nitro group with respect to the carboxylate functionality in the aromatic ring as can be evidenced by the formation of a one-dimensional polymer $[Ca(H_2O)_2(2\text{-nba})_2]_n$ for the *ortho* isomer[17], while a zero-dimensional compound $[Ca(H_2O)_4(4\text{-nba})_2]$ (**1**) is the only isolable product for the *para* isomer[31,35]. In earlier works we have demonstrated that N-donor ligands like N-methylimidazole[33] (N-MeIm), 2-methylimidazole[34] (2-MeIm), pyrazole[30] (pyr) and imidazole[32] (Im) can be incorporated into the coordination sphere of Ca(II) by an aqueous reaction of the zero-dimensional compound $[Ca(H_2O)_4(4\text{-nba})_2]$ (**1**) with an excess of N-donor ligand. Use of excess ligand is essential to suppress the hydrolysis of mixed ligand compounds into the starting tetraaqua compound (**1**) (Supplementary Data Fig. S1). In the present study we have investigated the reaction of (**1**) with an excess of 3,5-dimethylpyrazole, which results in the formation of a new Ca(II) coordination polymer (**2**) as shown in Eq. 1. In contrast, reaction of $[Ca(H_2O)_2(2\text{-nba})_2]_n$ with dmp under similar conditions does not result in the formation of any new product.

$[Ca(H_2O)_4(4\text{-nba})_2]$ (**1**) + dmp (excess) → (**2**) ...(1)

The formation of a new crystalline product was evidenced based on a comparison of the powder diffractograms of the starting material and (**2**) (Supplementary Data Fig. S2). Thermal and analytical data provide additional evidence for the proposed formula. Pyrolysis of (**2**) leads to the formation of binary oxide, while reaction with dilute HCl results in decomposition leading to the quantitative formation of insoluble 4-nbaH, which can be filtered and weighed as described earlier[38]. The composition of (**2**) was arrived at based on elemental analysis, 4-nbaH content obtained by acidification and CaO formed on pyrolysis and weight loss studies. Analytical data of (**2**) indicates the presence of Ca:4-nba:dmp:water in a 1:2:2:2 ratio. The two moles each of water and dmp in (**2**) can be accounted for by two coordinated water molecules and two lattice dmp molecules based on the single crystal data (*vide infra*).

The diffuse reflectance spectrum of compound (**2**) (Supplementary Data Fig. S3) with a strong signal at ~280 nm is very similar to that of the free acid and can be assigned to the intramolecular charge transfer transition of 4-nitrobenzoate. The UV-vis spectrum of a dilute aqueous solution of (**2**) is identical to that of the spectrum of compound (**1**) (Supplementary Data Fig. S4) indicating the transformation of (**2**) to (**1**) on hydrolysis. Unlike the polymeric $[Ca(N\text{-MeIm})(4\text{-nba})_2]_n$ compound which exhibits a diminished fluorescence emission intensity, the fluorescence emission spectrum of compound (**2**) shows an enhanced emission as compared to that of free 4-nbaH (Fig. 1). These emissions are neither ligand-to-metal charge transfer (LMCT) nor metal-to-ligand charge transfer (MLCT) and can be assigned to the intraligand fluorescent emission. The luminescent property of (**2**) can be attributed to ligand centered π or n to π^* orbital transitions since similar emissions are also observed for the free ligand. The IR spectrum of (**2**) exhibits several sharp bands in the mid-infrared region, indicating the presence of the organic moieties. A comparison of the IR spectra of (**2**) and that of $[Ca(H_2O)_4(4\text{-nba})_2]$ (**1**) (Supplementary Data Fig. S5) reveals changes in profile of the spectra in the 3000-3500 cm^{-1} region and the 1600-1300 cm^{-1} region due to the differently hydrated nature of (**1**) and (**2**). Although the IR spectrum of (**2**) exhibits absorptions due to the vibrations of the carboxylate and nitro groups, no definite conclusions can be drawn on the exact nature of the binding of the 4-nba ligand based only on IR data. The symmetric (υ_s) and asymmetric (υ_{as}) stretching vibrations of the carboxylate group are observed at 1568 and 1416 cm^{-1}, while those of the nitro group are observed at around 1514 and 1342 cm^{-1}.

The TG-DTA thermogram of (**2**) (Supplementary Data Fig. S6) exhibits two endothermic processes at 110 and 236 °C which can be assigned to the loss of the neutral water ligands and lattice dmp molecules respectively. The strong exothermic signal observed at 411 °C and a further exothermic event at 545 °C can be attributed to the decomposition of the 4-nitrobenzoate leading to the formation of a binary oxide material. Exothermic events assignable for the decomposition of 4-nba have been reported by us for the coordination polymers $[Ca(N\text{-MeIm})(4\text{-nba})_2]_n$, $[Ca(H_2O)(2\text{-MeIm})(4\text{-nba})_2]_n$ and $[Ca(pyr)_2(4\text{-nba})_2]_n$ at 412, 410 and 421 °C respectively. The removal of organics was evidenced by the featureless infrared spectrum of the residue, while the formation of CaO as the final residue was further confirmed based on isothermal weight loss studies by heating

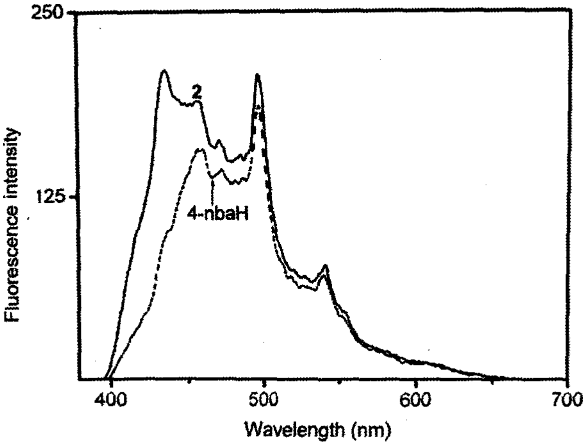

Fig. 1 — Fluorescence spectra of 4-nbaH and the complex, $[[Ca(H_2O)_2(4\text{-nba})_2]\cdot 2dmp]_n$ (**2**).

compound (2) at 800 °C in a temperature controlled furnace. The results of the isothermal weight loss studies add more credence to the thermal data.

Crystal structure of $[[Ca(H_2O)_2(4\text{-nba})_2]\cdot 2dmp]_n$ (2)

Compound (2) crystallizes in the centrosymmetric triclinic space group $P\bar{1}$ with all atoms situated in general positions. The crystal structure consists of a central Ca(II), two terminal water ligands, two crystallographically independent 4-nba ligands and two free 3,5-dimethylpyrazole molecules in the lattice (Fig. 2). The central metal is eight coordinated and is bonded to two oxygen atoms of two terminal aqua ligands and six oxygen atoms from four symmetry related 4-nba anions. The coordination polyhedron around Ca can perhaps be best described as a distorted trigonal prism that has two of its rectangular faces capped. In compound (2), the atoms $O2^i$ and O11 on the rectangular faces function as capping atoms (Fig. 2). The geometric parameters of the 4-nba ligand and the lattice dmp molecules are in the normal range. The observed Ca-O bond distances vary between 2.334(2) to 2.6995(19) Å (Table 1) while the O-Ca-O angles range from 49.47(5) to 155.36(6)°. The Ca(II) is linked to the O21 and O22 atoms of the water molecules at 2.334(2) and 2.3476(19) Å respectively. Based on a study of the structural chemistry of several Ca(II)-carboxylates, we have shown that in Ca(II) carboxylates containing three or fewer coordinated water molecules the carboxylate ligand adopts a bridging ligation leading to the formation of a chain polymer[17]. In accordance with this, compound (2) which contains two coordinated water molecules exhibits a polymeric chain structure. Several polymeric complexes containing Ca:coordinated water in a 1:2 ratio have been reported in the literature[17,39-42].

Each formula unit of (2) contains a Ca(II) coordinated to two aqua ligands and two unique 4-nitrobenzoate ligands both of which function as μ_2-bridging tridentate (μ_2-η^2:η^1) ligands. The first unique μ_2-η^2:η^1 4-nba ligand (O1, O2) binds to Ca(II) in a bidentate fashion with Ca1-O1 and Ca1-O2 distances of 2.6995(19) and 2.5277(19) Å respectively. The O2 oxygen is further linked to a symmetry related Ca(II) at a distance of 2.3857(16) Å, resulting in a Ca···Ca separation of 3.8893(10) Å. A pair of such μ_2-η^2:η^1 4-nba ligands are linked to two Ca(II) ions resulting in the formation of a tricyclic dicalcium-dicarboxylate unit (Fig. 3) which constitutes the basic building block of the coordination polymer. This tricyclic unit differs from the well-known eight membered cyclic dimetal-dicarboxylate unit in several dinuclear carboxylates where the $(\text{-COO})^-$ functions as a symmetrical μ_2-η^1:η^1 bidentate bridging ligand. The second independent 4-nba ligand (O11, O12) binds to two symmetry related Ca(II) ions in an identical fashion resulting in a tricylic dicalcium-dicarboxylate unit with a Ca···Ca separation of 3.9083(10) Å (Supplementary Data Fig. S7). The Ca-O bond lengths formed by this ligand are different. With this ligand a Ca(II) ion is linked to the O11 and O12 oxygen atoms in a bidentate manner (Ca1-$O11^{ii}$ 2.5326(18); Ca1-$O12^{ii}$ 2.5508(18) Å) and the O11 is further linked to a second Ca(II) ion at 2.3603(16) Å. In the crystal structure of (2) alternating pairs of the two crystallographically

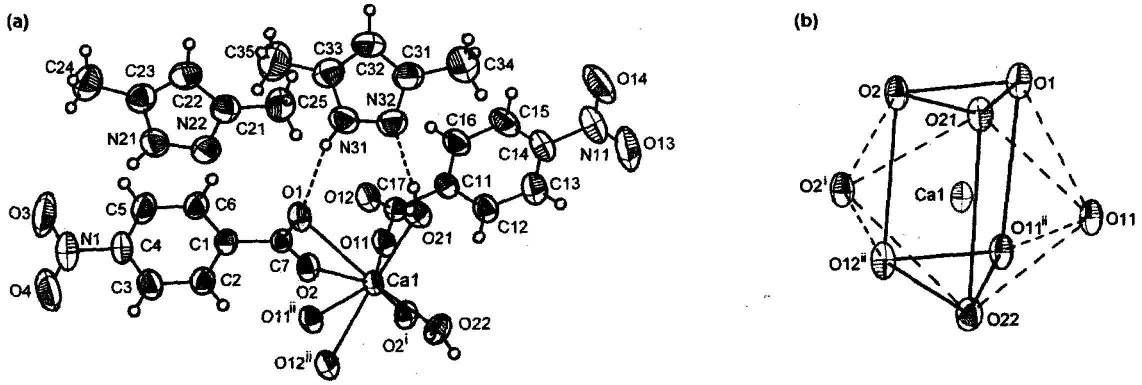

Fig. 2 — (a) Crystal structure of $[[Ca(H_2O)_2(4\text{-nba})_2]\cdot 2dmp]_n$ (2) showing atom-labeling scheme. Displacement ellipsoids are drawn at 50% probability level except for H atoms, which are shown as circles of arbitrary radius. Intramolecular H-bonding is shown as broken lines. (b) The distorted bicapped trigonal prismatic coordination environment of Ca1. The atoms $O2^i$ and O11 on the rectangular faces of the trigonal prism function as capping atoms. [Symmetry codes: (i) $-x+2,-y,-z+1$; (ii) $-x+1,-y,-z+1$].

Table 1 — Selected bond lengths (Å) and angles (°) for $[[Ca(H_2O)_2(4\text{-nba})_2]\cdot 2dmp]_n$ (**2**)

Bond lengths (Å)			
Ca1-O(22)	2.334(2)	Ca1-O(2)	2.5277(19)
Ca1-O(21)	2.3476(19)	Ca1-O(11)^{ii}	2.5326(18)
Ca1-O(11)	2.3603(16)	Ca1-O(12)^{ii}	2.5508(18)
Ca1-O(2)^{i}	2.3857(16)	Ca1-O(1)	2.6995(19)
Ca1···Ca1^{i}	3.8893(10)	Ca1···Ca1^{ii}	3.9083(10)
Bond angles (°)			
O(22)-Ca1-O(21)	100.57(7)	O(2)-Ca1-O(11)^{ii}	87.99(6)
O(22)-Ca1-O(11)	76.32(6)	O(22)-Ca1-O(12)^{ii}	88.53(7)
O(21)-Ca1-O(11)	84.32(6)	O(21)-Ca1-O(12)^{ii}	153.46(6)
O(22)-Ca1-O(2)^{i}	85.47(6)	O(11)-Ca1-O(12)^{ii}	122.17(6)
O(21)-Ca1-O(2)^{i}	76.82(6)	O(2)^{i}-Ca1-O(2)^{ii}	79.15(6)
O(11)-Ca1-O(2)^{i}	150.87(6)	O(2)-Ca1-O(12)^{ii}	72.94(6)
O(22)-Ca1-O(2)	155.36(6)	O(11)^{ii}-Ca1-O(12)^{ii}	51.05(5)
O(21)-Ca1-O(2)	90.13(7)	O(22)-Ca1-O(1)	153.10(6)
O(11)-Ca1-O(2)	127.21(6)	O(21)-Ca1-O(1)	83.81(6)
O(2)^{i}-Ca1-O(2)	75.37(6)	O(11)-Ca1-O(1)	77.75(6)
O(22)-Ca1-O(11)^{ii}	92.87(7)	O(2)^{i}-Ca1-O(1)	121.20(6)
O(21)-Ca1-O(11)^{ii}	151.04(6)	O(2)-Ca1-O(1)	49.47(5)
O(11)-Ca1-O(11)^{ii}	74.03(6)	O(11)^{ii}-Ca1-O(1)	73.11(6)
O(2)^{i}-Ca1-O(11)^{ii}	130.19(6)	O(12)^{ii}-Ca1-O(1)	99.32(6)

Symmetry transformations used to generate equivalent atoms: (i) $-x+2, -y, -z+1$; (ii) $-x+1, -y, -z+1$.

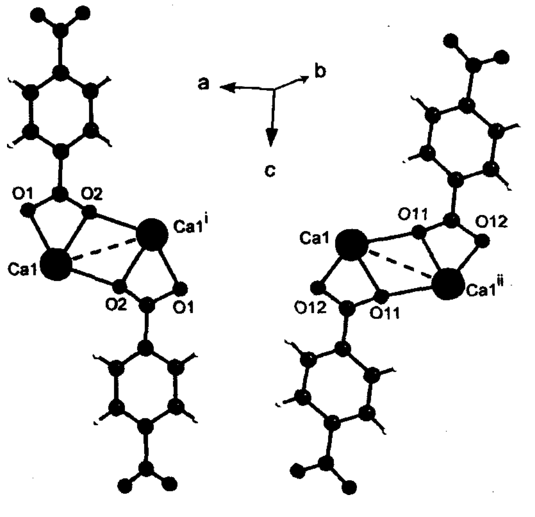

Fig. 3 — A view showing the μ_2-η^2:η^1 bridging binding modes of the unique 4-nba ligands containing the donor sites (O1, O2) or (O11, O12). A pair of the unique ligands (O1, O2) or (O11, O12) bridge a pair of Ca(II) ions resulting in the formation the tricyclic dicalcium-bis(4-nitrobenzoate) building block with a Ca1···Ca1 separation of 3.8893(10) or 3.9083(10) Å respectively.

independent μ_2-η^2:η^1 4-nba ligands link pairs of $\{Ca(H_2O)_2\}^{2+}$ units into a 1-D polymeric chain extending along *a* axis (Fig. 4). As a result, alternating Ca···Ca separations of 3.8893(10) and 3.9083(10) Å respectively are observed in the infinite chain. These values are comparable to the Ca···Ca separations of 3.8585(7) and 3.8432(3) Å reported for other 4-nba based coordination polymers like $[Ca(N\text{-MeIm})(4\text{-nba})_2]_n$[33] and $[Ca(H_2O)(2\text{-MeIm})(4\text{-nba})_2]_n$[34] respectively and shorter than the Ca···Ca separation of 5.335 Å in $[Ca(pyr)_2(4\text{-nba})_2]_n$[30].

Comparison of structure of (2) with $[Ca(H_2O)_2(2\text{-nba})_2]_n$

Comparison of the structure of compound (**2**) with that of the earlier reported $[Ca(H_2O)_2(2\text{-nba})_2]_n$[17] reveals both similarities and differences. Both compounds which crystallize in the triclinic space group *P*$\bar{1}$ contain Ca:nitrobenzoate:water in a 1:2:2 ratio and are 1-D polymers based on tricyclic dicalcium-dicarboxylate units. The central metal in both compounds are linked to four different carboxylate ligands and the binding mode of the crystallographically unique carboxylate ligand as well as the coordination sphere of the Ca(II) are identical in both compounds. Topologically both the coordination polymers are identical. Compound (**2**) differs from $[Ca(H_2O)_2(2\text{-nba})_2]_n$ in terms of the positioning of the nitro substituent in the aromatic ring and the presence of two unique 3,5-dimethylpyrazole molecules, which are located between the one dimensional polymeric chains in

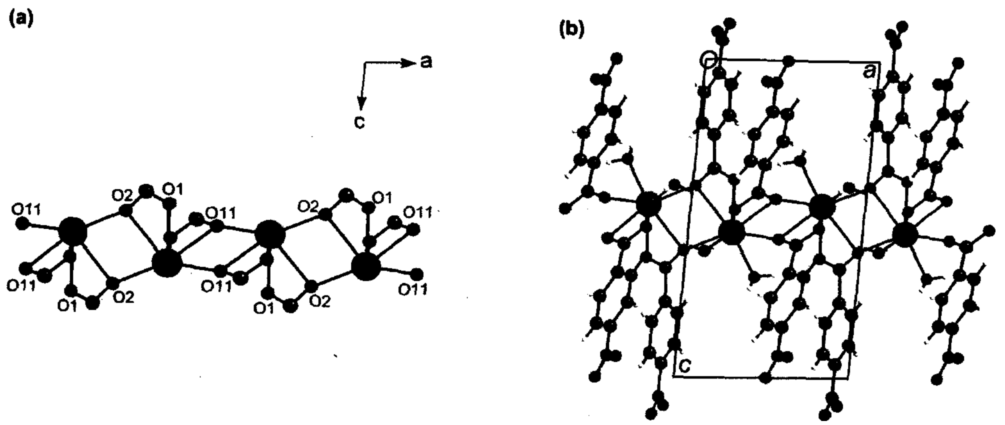

Fig. 4 – (a) A portion of the 1-D polymer of (**2**) viewed along *b* axis, showing the linking of tricyclic dicalcium-bis(4-nitrobenzoate) units into an infinite chain. For clarity, coordinated H_2O molecules and aromatic ring are not shown. (b) Aromatic rings and coordinated water molecules are included in the polymeric chain.

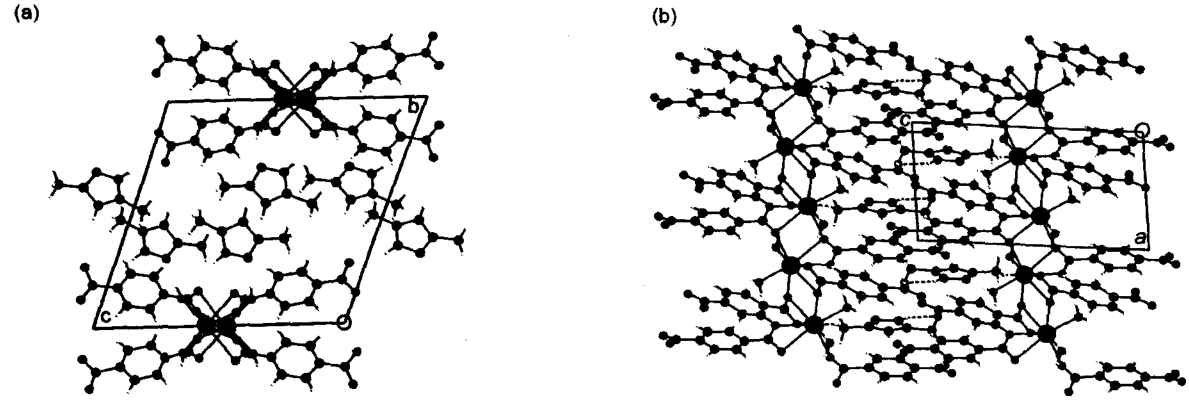

Fig. 5 — (a) A view along *a* showing the neutral dmp molecules situated between the one dimensional parallel chains. (b) A view along *b* showing the lattice dmp molecules which function as linkers between adjacent polymeric chains via H-bonding interactions shown in broken lines.

the lattice (Fig. 5). The presence of these neutral N-ligands in the lattice results in more varieties of secondary interactions, namely N-H···O and O-H···N, in addition to O-H···O and C-H···O observed in $[Ca(H_2O)_2(2\text{-nba})_2]_n$. Our efforts to incorporate dmp into the lattice of $[Ca(H_2O)_2(2\text{-nba})_2]_n$ in view of its structural similarity with that of (**2**) have not been fruitful so far.

Secondary interactions in (2)

An analysis of the crystal structure of (**2**) reveals that each eight coordinated Ca(II) complex in the polymeric chain is H-bonded to six neighboring complexes with the aid of four varieties of H-bonding interactions comprising of two O-H···O interactions, two N-H···O interactions, two O-H···N interactions and three weak C-H···O interactions (Supplementary Data Fig. S8). All these O···H contacts (Table 2) are shorter than the sum of their van der Waals radii. The neutral dmp molecules in the lattice function as linkers between adjacent one-dimensional chains with the aid of N21-H21···O14, O22-H30···N22 and C25-H25A···O12 interactions (Fig. 5) and further extend the network. Of these, the H-bonding between the nitro oxygen (O14) and the H atom (H21) attached to the N of dmp seems to be important for the formation of (**2**).

Six different bridging binding modes of 4-nba ligand

The synthesis and structural characterization of several metal 4-nitrobenzoate compounds showing different binding modes[31-35, 43-58] of the 4-nba ligand serves to demonstrate the versatile ligational behaviour of the 4-nitrobenzoate ligand. A survey of

Table 2 — Hydrogen-bonding geometry for $[[Ca(H_2O)_2(4\text{-}nba)_2]\cdot 2dmp]_n$ (**2**)

D-H···A	*D* (D-H) (Å)	*D* (H···A) (Å)	*D* (D···A) (Å)	<DHA (°)	Symmetry code
N21-H21···O14	0.860	2.244	3.055	157	*x*, *y*, *z*+1
N31-H31···O1	0.860	2.058	2.889	162	*x*, *y*, *z*
O21-H10···N32	0.820	1.960	2.770	169	*x*, *y*, *z*
O21-H20···O12	0.820	1.994	2.798	166	*x*+1, *y*, *z*
O22-H30···N22	0.820	1.944	2.762	176	-*x*+1, -*y*, -*z*+1
O22-H40···O1	0.820	2.035	2.843	168	-*x*+1, -*y*, -*z*+1
C2-H2···O21	0.930	2.664	3.565	163	2-*x*, -*y*, 1-*z*
C3-H3···O4	0.930	2.630	3.460	149	2-*x*, -*y*, 2-*z*
C25-H25A···O12	0.959	2.576	3.452	152	*x*, *y*, *z*

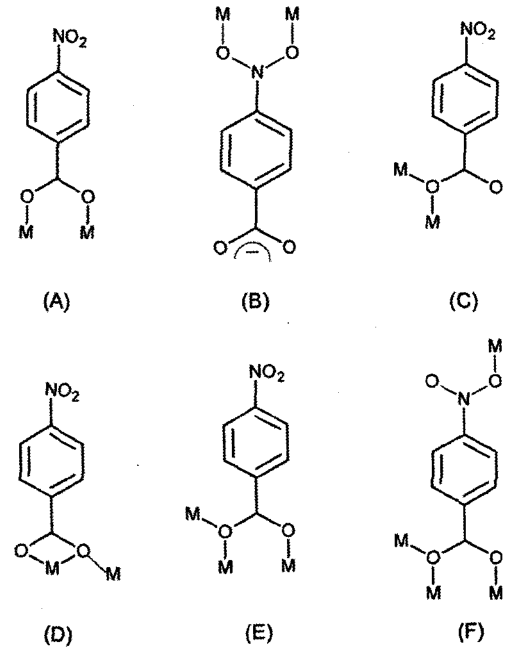

Fig. 6 — Six different bridging coordination modes of 4-nba ligand. [Mode A, μ_2-η^1:η^1; Mode B, μ_2:-η^1:η^1(-NO_2); Mode C, μ_2-η^2:η^0; Mode D, μ_2-η^1:η^2; Mode E, μ_3-η^1: η^1:η^1; Mode F, μ_4-η^1(O):η^1(O): η^1(O') :η^1(O of nitro)].

the structurally characterized metal 4-nba compounds reveals that in addition to serving as a monodentate (η^1) ligand[31,35,44,45] or a bidentate (η^2) ligand[31,43,44], the anionic 4-nba exhibits six different bridging binding modes (Fig. 6). An analysis of twenty two compounds (Supplementary Data Table S1) was undertaken and in these compounds only the bridging binding modes of the 4-nba ligand are considered. It is observed in all these compounds which crystallize in the centrosymmetric triclinic or monoclinic space groups, the 4-nba ligand is involved in six different bridging binding modes, four of which (mode A to D in Fig. 6) are μ_2-bridging in nature and one each of μ_3-bridging (mode E) and μ_4-bridging type (mode F) respectively. Of the four μ_2-bridging modes, there are two different symmetric μ_2-η^1:η^1 bridging modes, namely mode A (involving both the carboxylate oxygen atoms) and mode B (involving both the nitro oxygen atoms), observed so far in a single compound, namely, $[Na(H_2O)_3(4\text{-}nba)]_n$[57]. The symmetric bridging bidentate mode A appears to be the most common as this mode is observed in seventeen compounds (77 %) and results in the formation of dimeric compounds in four cases[45-48] in addition to two tetramers[49,50] and a pentamer[51] and hexamer[52]. In the remaining cases, mode A results in the formation of a chain polymer. Fourteen of the compounds are coordination polymers[30,33-35,44,53-58] and the formation of the infinite O-M-O chain in these polymeric compounds is due to the presence of at least one of the six bridging binding modes of 4-nba. In addition to the symmetric bridging modes A and B, two more μ_2-bridging modes, namely μ_2-η^2:η^0 (mode C) and μ_2-η^1:η^2 (mode D), are also observed in some of the compounds. In both these binding modes one of the carboxylate oxygen atoms binds to two metal ions; it is interesting to note that compounds like $[KH(4\text{-}nba)_2]_n$ or $[Ca(H_2O)\,(2\text{-}meIm)(4\text{-}nba)_2]_n$ showing the μ_2-η^2:η^0 bridging mode are always accompanied by another binding mode like the μ_2-η^1:η^1 in the Ca coordination polymer or the μ_4-bridging mode involving both the carboxylate and nitro oxygen atoms in the K compound[58]. The μ_2-η^1:η^2 mode observed in the title compound $[[Ca(H_2O)_2(4\text{-}nba)_2]\cdot 2dmp]_n$ has earlier been reported in the isostructural *f*-block compounds[56] $[M_2(4\text{-}nba)_6(H_2O)_5]_n$ (M = Eu or Tb) and in the lead coordination polymers[54], $[Pb(4\text{-}nba)(PyO)_2(NO_2)]_n$ and $[Pb(4\text{-}nba)_2(PyO)]_n$.

Conclusions

In this work, we have described the synthesis and characterization of a new calcium(II) coordination polymer $[[Ca(H_2O)_2(4\text{-nba})_2]\cdot 2dmp]_n$ based on a μ_2-bridging tridentate 4-nba ligand. An analysis of the six bridging binding modes of 4-nba ligand reveals that the symmetrical μ_2-η^1:η^1 bridging binding mode is very common and observed in a majority of 4-nba compounds. The two binding modes involving the oxygen atom of the nitro group is observed only in the alkali metal 4-nitrobenzoates, where the alkali metal Na[57] or K[58] is linked to the oxygen of the nitro functionality. The compounds $[Ca(pyr)_2(4\text{-nba})_2]_n$[30] $[Ca(N\text{-MeIm})(4\text{-nba})_2]_n$[33] and $[Ca(H_2O)(2\text{-MeIm})(4\text{-nba})_2]_n$[34] which contain terminal N-donor ligands and a solvent dmp in the lattice in the title compound (**2**) constitute examples of coordination polymers which show the four different bridging modes of the 4-nba ligand involving only the carboxylate oxygen atoms.

Supplementary Data

Crystallographic data (excluding structure factors) for the structure of $[[Ca(H_2O)_2(4\text{-nba})_2]\cdot 2dmp]_n$ reported herein have been deposited with the Cambridge Crystallographic Data Centre as supplementary publication no. CCDC 799281. Copies of the data can be obtained, free of charge, on application to CCDC, 12 Union Road, Cambridge CB2 1 EZ, UK (fax: +44-(0)1223-336033 or Email: deposit@ccdc.cam.ac.uk). The other supplementary data associated with this article, viz., Table S1 and Figs S1–S8, are available in electronic form at http://www.niscair.res.in/jinfo/ijca/IJCA 51A(03) 435-443_Suppl Data.pdf.

Acknowledgement

BRS thanks Prof W Bensch, University of Kiel, Kiel, Germany, for helpful discussions. Financial support under Nanomission program (SR/NM/NS-86, 2009) of Department of Science and Technology, New Delhi, India, and the Special Assistance Programme [F.540/25/DRS/2007/(SAP-I)] of University Grants Commission, New Delhi, India, is gratefully acknowledged.

References

1 Janiak C & Vieth J K, *New J Chem*, 34 (2010) 2366.

2 Batten S R, Neville S M & Turner D R, *Coordination Polymers: Design, Analysis and Application* (RSC Publishing, Cambridge, UK) 2009.

3 Biradha K, Ramanan A & Vittal J J, *Cryst Growth Des*, 9 (2009) 2969.

4 Turner D R, Hatton J S & Batten S R, *Z Anorg Allg Chem*, 635 (2009) 439.

5 Chen S, Hoffmann S, Prots Y, Zhao J T & Kniep R, *Z Anorg Allg Chem*, 636 (2010) 1710.

6 Dietzel P C, Blom R & Fjellvag H, *Z Anorg Allg Chem*, 635 (2009) 1953.

7 Guo Z, Li G, Zhou L, Su S, Lei Y, Dang S & Zhang H, *Inorg Chem*, 48 (2009) 8069.

8 Appelhans L N, Kosa M, Radha A V, Simoncic P, Navrotsky A, Parrinello M & Cheetham A K, *J Am Chem Soc*, 131 (2009) 15375.

9 Tran D T, Chu D, Oliver A J & Oliver S R J, *Inorg Chem Commun*, 12 (2009) 351.

10 Williams C A, Blake A J, Wilson C, Hubberstey P & Schroder M, *Cryst Growth Des*, 8 (2008) 911.

11 Das M C, Ghosh S K, Sanudo E C & Bharadwaj P K, *Dalton Trans*, (2009) 1644.

12 Rossin A, Ienco A, Costantino F, Montini T, Credico B D, Caporali M, Gonsalvi L, Fornasiero P & Peruzzini M, *Cryst Growth Des*, 8 (2008) 3302.

13 Bolligarla R, Tripuramullu B K, Sreenivasulu V & Das S K, *Indian J Chem*, 50A (2011) 1410.

14 Korah R, Kalita L & Murugavel R, *Indian J Chem*, 50A (2011) 763.

15 Borah B M, Dey S K & Das G, *Cryst Growth Des*, 11 (2011) 2773.

16 Fox S, Büsching I, Barklage W & Strasdeit H, *Inorg Chem*, 46 (2007) 818.

17 Srinivasan B R, Shetgaonkar S Y & Raghavaiah P, *Polyhedron*, 28 (2009) 2879.

18 Banerjee D & Parise J B, *Cryst Growth Des*, 11 (2011) 4704.

19 Fromm K M, *Coord Chem Rev*, 252 (2008) 856.

20 Zhu H F, Zhang Z H, Sun W Y, Okamura T & Ueyama N, *Cryst Growth Des*, 5 (2005) 177.

21 Dan M, Cheetham A K & Rao C N R, *Inorg Chem*, 45 (2006) 8227.

22 Yusenko K, Fox S, Guni P & Strasdeit H, *Z Anorg Allg Chem*, 634 (2008) 2347.

23 Morin G, Shang M & Smith B D, *Acta Crystallogr*, 56C (2000) 544.

24 Bacchi A, Carcelli M, Pelizzi C, Pelizzi G, Pelagatti P, Rogolino D, Tegoni M & Viappiani C, *Inorg Chem*, 42 (2003) 5871.

25 Yang Y, Huang Z, Szeto L & Wong W, *Appl Organomet Chem*, 18 (2004) 97.

26 Murugavel R & Korah R, *Inorg Chem*, 46 (2007) 11048.

27 Song W D, Guo X X & Zhang C H, *Acta Crystallogr*, 63E (2007) m399.

28 Morrison C N, Powell A K & Kostakis G E, *Cryst Growth Des*, 11 (2011) 3653.

29 Dale S H & Elsegood M R J, *Acta Crystallogr*, 59C (2003) m540.

30 Srinivasan B R, Shetgaonkar S Y & Näther C, *Z Anorg Allg Chem*, 637 (2011) 130 and references therein.

31 Srinivasan B R, Sawant J V & Raghavaiah P, *Indian J Chem*, 45A (2006) 2392.

32 Srinivasan B R, Sawant J V & Raghavaiah P, *J Chem Sci*, 119 (2007) 11.

33 Srinivasan B R, Shetgaonkar S Y, Sawant J V & Raghavaiah P, *Polyhedron*, 27 (2008) 3299.

34 Srinivasan B R, Shetgaonkar S Y, Näther C & Bensch W, *Polyhedron*, 28 (2009) 534.

35 Srinivasan B R, Shetgaonkar S Y, Kohli S & Rajnikant, *Indian J Chem*, 49A (2010) 1468.
36 Furniss B S, Hannaford A J, Rogers V, Smith P W J & Tatchell A R, 1978 *Vogel's Textbook of Practical Organic Chemistry*, ELBS 4th Edition 881.
37 Sheldrick G M, *Acta Crystallogr*, 64A (2008) 112.
38 Srinivasan B R & Sawant S C, *Thermochim Acta*, 402 (2003) 45.
39 Karipides A, Ault J & Reed A T, *Inorg Chem*, 16 (1977) 3299.
40 Karipides A & Miller C J, *J Am Chem Soc*, 106 (1984) 1494.
41 Kim M K, Bae K L & Ok K M, *Cryst Growth Des*, 11 (2011) 930.
42 Liang P C, Liu K-K, Yeh C-T, Lin C-H & Zima V, *Cryst Growth Des*, 11 (2011) 699.
43 Srinivasan B R, Raghavaiah P & Sawant J V, *Acta Crystallogr*, 63E (2007) m2251.
44 Srinivasan B R, Sawant J V, Sawant S C & Raghavaiah P, *J Chem Sci*, 119 (2007) 593.
45 Srinivasan B R, Sawant J V, Näther C & Bensch W, *J Chem Sci*, 119 (2007) 243.
46 Usubaliev B T, Movsumov E M, Amiraslanov I R & Mamedov Kh S, *Dokl Akad Nauk Az SSR*, 36 (1980) 40.
47 Das B K & Chakravorty A R, *Inorg Chem*, 30 (1991) 4978.
48 Ebihara M, Yamada K & Kawamura T, *Acta Crystallogr*, 62C (2006) m451.
49 Khiyalov M S, Amiraslanov I R, Mamedov Kh S & Movsumov E M, *Proc Nat Acad Sci Azebaidzhan*, 37 (1981) 42, (CCDC Refcode BAKPIM).
50 Jian-Fang M, Zhong-Sheng J & Jia-Zuan N, *Chinese J Struct Chem*, 10 (1991) 56, CCDC Refcode SIXVEA.
51 Boskovic C, Sieber A, Chaboussant G, Guedel H U, Ensling J, Wernsdorfer W, Neels A, Labat G, Stoeckli-Evans H & Janssen S, *Inorg Chem*, 43 (2004) 5053.
52 Trettenhahn G, Nagl M, Neuwirth N, Arion V B, Jary W, Pochlauer P & Schmid W, *Angew Chem Int Ed*, 45 (2006) 2794.
53 Odoko M, Ise T & Okabe N, *Acta Crystallogr*, 63C (2007) m22.
54 Sarma R & Baruah J B, *Inorg Chim Acta*, 362 (2009) 1681.
55 Bußkamp H, Deacon G B, Hilder M, Junk P C, Kynast U H, Lee W W & Turner D R, *Cryst Eng Comm*, 9 (2007) 394.
56 Dias A D & Viswanathan S, *Dalton Trans*, (2006) 4093.
57 Turowska-Tyrk I, Krygowski T M, Gdaniec M, Hafelinger G & Ritter G, *J Mol Struc*, 172 (1988) 401.
58 Shrivastava H N & Speakman J C, *J Chem Soc*, (1961) 1151.

Indian Journal of Chemistry
Vol. 51A, August 2012, pp. 1064-1072

Soft synthesis of a metal-organic framework based on a tribarium building block

Bikshandarkoil R Srinivasan[a, *], Santosh Y Shetgaonkar[a] & Pallepogu Raghavaiah[b]
[a]Department of Chemistry, Goa University, Goa 403 206 India
Email: srini@unigoa.ac.in
[b]National Single Crystal X-ray Diffractometer Facility, School of Chemistry,
University of Hyderabad, Hyderabad 500 046 India

Received 16 May 2012; revised and accepted 18 July 2012

Reaction of MCO_3 (M = Ba or Ca) with benzene-1,3,5-tricarboxylic acid (H_3btc) in aqueous medium at room temperature affords in good yields the metal-organic framework material $[Ba_3(btc)_2(H_2O)_8]\cdot 2H_2O$ (**1**) or the layer compound $[Ca_3(btc)_2(H_2O)_{12}]$ (**2**). The structure of (**1**) is a three-dimensional polymer based on a tribarium building unit. In the trinuclear building block, the central Ba(II) situated on an inversion centre exhibits ten coordination, while the symmetry equivalent terminal Ba(II) ions are eight coordinated. The μ_6-heptadentate bridging binding mode of the unique btc ligand in (**1**) results in a 3-D structure with two water molecules situated in the pores. Compound (**2**) exhibits a two-dimensional structure, unlike the compositionally similar *d*-block compounds $[M_3(btc)_2(H_2O)_{12}]$ (M = Co, Ni, Zn) which are one-dimensional. A comparative study of several compounds containing the $\{M_3(btc)_2\}$ unit is described.

Keywords: Coordination chemistry, Metal-organic framework, Coordination polymers, Barium, Calcium, Trinuclear compounds, Benzene-1,3,5-tricarboxylic acid

The chemistry of metal-organic frameworks (MOFs), also known as coordination polymers (CPs) is currently a frontier area of research. Interest in this field can be evidenced by the publication of special issues of journals on MOF chemistry and several recent review articles[1,2]. In this rapidly developing area of inorganic materials research, different terminologies like metal-organic frameworks, coordination polymers, hybrid inorganic and organic solids, porous coordination polymers, etc., are employed to designate solids with extended structures[2g-2j]. Taking note of this, the inorganic chemistry division of IUPAC has initiated a project to formulate terminology and nomenclature guidelines for CPs and MOFs[3]. In the present work, the term 'framework' is used to designate a barium carboxylate compound which exhibits a three-dimensional (3-D) structure, in accordance with the proposal of Biradha *et al.*[2j]

Most syntheses of extended solids are performed under hydro/solvothermal conditions by combining metal sources with di-, tri-, or tetratopic organic linkers especially carboxylic acids[2d]. Using this principle several metal-organic framework materials have been synthesized and structurally characterized, the most prominent of these being the MOF-5, HKUST-1, MIL-53 (MIL = Materials Institute Lavoisier), MIL-101, etc.[4] In the past two decades *d*-block metals have been extensively employed for the construction of framework materials, while the use of *s*-block metals is comparatively less. Currently, there is a steady growth of papers reporting *s*-block materials and recent developments in this area have been reviewed[2e]. Since the early days of MOF research[2g], the tritopic benzene-1,3,5-tricarboxylic acid (H_3btc) also known as trimesic acid has been the subject of several investigations and has been shown to exhibit several bridging binding modes[5]. Using these connectivities, several extended solids based on btc of varying dimensionalities have been structurally characterized[5-9]. Interestingly a majority of the reported syntheses of alkaline-earth benzene-1,3,5-tricarboxylates have so far been performed under hydrothermal conditions[8]. In this report, we show that a Ba-carboxylate (**1**) and a Ca-carboxylate (**2**), which exhibit 3-D and 2-D connectivities respectively, can be readily assembled under mild reaction (non-hydrothermal) conditions, using H_3btc as an organic linker.

Materials and Methods

All the chemicals used in this study were of reagent grade and were used as received. The starting materials and reaction products are air stable and hence were prepared under normal laboratory conditions. Infrared (IR) spectra of the solid samples diluted with KBr were recorded on a Shimadzu (IR Prestige-21) FT-IR spectrometer in the range 4000-400 cm^{-1}. UV-visible spectra were recorded on a Shimadzu UV-2450 double beam spectrophotometer. Photoluminescence of solid samples were recorded using a Perkin Elmer LS55 fluorescence spectrometer. TG-DTA studies were performed in flowing air in Al_2O_3 crucibles on a STA-409PC simultaneous thermal analyzer from Netzsch, at a heating rate of 10 K min^{-1} for all measurements. Isothermal weight loss studies were performed in a temperature controlled electric furnace. X-ray powder pattern were recorded on a Rigaku Miniflex II powder diffractometer using Cu-Kα radiation with a Ni filter.

Preparation of $[Ba_3(btc)_2(H_2O)_8].2H_2O$ (1) and $[Ca_3(btc)_2(H_2O)_{12}]$ (2)

H_3btc (0.42 g, 2 mmol) was dissolved in water (50 mL). To this barium carbonate (0.59 g, 3 mmol) was added slowly under stirring at room temperature. Brisk effervescence was observed during addition of $BaCO_3$ to H_3btc solution followed by the immediate separation of compound (**1**) as fine crystals. After 1 h, the fine crystals were filtered, washed well with cold water, followed by alcohol and ether and dried. From the mother liquor colorless crystals of (**1**) suitable for single crystal work were obtained. (Yield = 0.78 g). The use of $CaCO_3$ instead of $BaCO_3$ in the above synthesis afforded colorless crystals of $[Ca_3(btc)_2(H_2O)_{12}]$ (**2**) in 80 % yield.

Anal. (%): Calc. for $Ba_3C_{18}H_{26}O_{22}$ (1006.37) (**1**): $BaCO_3$, 58.83; C, 21.48; H, 2.60; Found: $BaCO_3$, 58.12; C, 21.45; H, 2.64. IR data: 3600-3000 (υ_{O-H}), 1697(s), 1614(s), 1549 (s, υ_{as}-COO), 1433 (s, υ_s-COO), 1378 (s), 1284 (s), 1197 (s), 1110 (s), 899 (s), 792 (s), 754 (s), 723 (s), 692 (s), 667 (s), 520 (s) cm^{-1}. DTA data (in °C): 148 (endo), 525 (exo), 593 (exo). UV-vis (diffused reflectance): 281 nm.

Anal. (%): Calc. for $Ca_3C_{18}H_{30}O_{24}$ (750.65) (**2**): Ca, 16.02; CaO, 22.41; C, 28.80; H, 4.03; Found: Ca, 15.80; CaO, 21.93; C, 30.87; H, 5.22 %; IR data: 3600-3000 (br, υ_{O-H}), 1692 (s), 1607(s), 1549 (s, υ_{as}-COO), 1445 (s), 1433 (s, υ_s-COO), 1390 (s), 1271(s), 1250 (s), 1207 (s), 1111 (s), 930 (s), 856 (s), 795 (s), 762 (s), 729 (s), 687 (s), 529 (s) cm^{-1}. DSC data (in °C): 131 (endo), 593 (exo), 610 (exo). UV-vis (diffused reflectance): 281 nm.

Dehydration of $[Ba_3(btc)_2(H_2O)_8].2H_2O$ (1) and $[Ca_3(btc)_2(H_2O)_{12}]$ (2)

A weighed amount of compound (**1**) or (**2**) was heated for 1 h at 150 °C in a temperature controlled oven. This resulted in the formation of the anhydrous compounds $[Ba_3(btc)_2]$ (**1a**) or $[Ca_3(btc)_2]$ (**2a**) respectively. The observed mass loss on heating was in good agreement with the expected loss of all water molecules in the starting materials. Equilibration of the anhydrous compounds over water vapour in a dessiccator did not result in any rehydration to form the respective starting compounds.

Anal. (%): Calc. for $Ba_3C_{18}H_6O_{12}$ (826.21) (**1a**): $BaCO_3$, 71.65; Found: $BaCO_3$, 70.21; IR data: 1603 (s), 1543 (s, υ_{as}-COO), 1433 (s, υ_s-COO), 1368 (s), 1207 (s), 1107 (s), 932 (m), 818 (m), 768 (s), 721 (s), 518 (s) cm^{-1}. DTA data (in °C): 525 (exo), 593(exo). UV-vis (diffused reflectance): 281 nm.

Anal. (%): Calc. for $Ca_3C_{18}H_6O_{12}$ (534.47) (**2a**): CaO, 37.03; Found: CaO, 37.15. IR (KBr) data: 3057 (m), 2983-2486 (br), 1705 (m), 1607 (s), 1555 (s, υ_{as}-COO), 1433 (s, υ_s-COO), 1368 (s), 1109 (s), 984 (s), 772 (s), 710 (s), 532 (s), 460 (m) cm^{-1}. DSC data (in °C): 593(exo), 610(exo).

X-ray crystal structure determination

Intensity data for (**1**) and (**2**) were collected on a Bruker Smart Apex CCD diffractometer using graphite-monochromated Mo-Kα radiation. The structures were solved with direct methods using SHELXS-97[10] and refinement was carried out against F^2 using SHELXL-97[10]. All non-hydrogen atoms were refined using anisotropic displacement parameters. C-H hydrogen atoms of the btc ligand were positioned with idealized geometry and refined using a riding model. H atoms attached to the O atoms of water were located in the difference map and were refined isotropically using a riding model. The technical details of data acquisition and some selected refinement results are summarized in Table 1.

Results and Discussion

Synthetic aspects of alkaline-earth btc compounds

Since the first report of a 1:1 Ca-Hbtc compound in 1997 by the Plater group[8a], a total of sixteen alkaline-earth btc compounds have been characterized[8]. The synthesis of all these compounds excepting two Ca compounds[9a,9b] has been performed under hydrothermal conditions (Supplementary Data Table S1). An important requirement of the

Table 1—Crystal data and structure refinement for $[Ba_3(btc)_2(H_2O)_8]\cdot 2H_2O$ (**1**) and $[Ca_3(btc)_2(H_2O)_{12}]$ (**2**)

	(**1**)	(**2**)
Emp. formula	$C_{18}H_{26}Ba_3O_{22}$	$C_{18}H_{30}Ca_3O_{24}$
Formula wt (g mol^{-1})	1006.41	750.66
Temp. (K)	298(2)	298(2)
Wavelength (Å)	0.71073	0.71073
Crystal system	Monoclinic	Monoclinic
Space group	$P2_1/c$	$C2/c$
Unit cell dimensions		
a (Å)	12.589(3)	19.288(11)
b (Å)	16.004(3)	11.445(7)
c (Å)	6.8171(14)	12.975(8)
β (°)	91.153(3)	106.317(9)
Vol. ($Å^3$)	1373(5)	2749(3)
Z	2	4
D_{calc} (mg/m^3)	2.434	1.814
Abs coeff. (mm^{-1})	4.353	0.709
F(000)	956	1560
Crystal size (mm^3)	$0.42 \times 0.19 \times 0.16$	$0.38 \times 0.24 \times 0.22$
θ range for data collect. (°)	1.62 to 25.97	2.09 to 26
Index ranges	$-15 \le h \le 15$, $-19 \le k \le 19$, $-8 \le l \le 8$	$-23 \le h \le 18$, $-13 \le k \le 14$, $-15 \le l \le 15$
Reflections collected	13080	6880
(Rint)	2678 (0.0273)	2666 (0.0200)
Completeness to θ = 28.49°	99.3 %	98.4 %
Refinement method	Full-matrix least-squares on F^2	
Data/ restraints /parameters	2678 / 0 / 237	2666 / 2 / 213
Goodness-of-fit on F^2	1.153	1.056
Final R indices [I >2σ (I)]	R1 = 0.0184, wR2 = 0.0461	R1 = 0.0275, wR2 = 0.0714
R indices (all data)	R1 = 0.0188, wR2 = 0.0463	R1 = 0.0299, wR2 = 0.0729
Largest diff. peak and hole ($eÅ^{-3}$)	0.599 & –0.674	0.264 & –0.355
Bond valence sum of central metal[a]	2.072 & 1.946	2.13 & 2.01

Bond valence sums were calculated from crystallographioc data using VaList. A.S. Wills, VaList, program available from www.ccp14.ac.uk

hydrothermal reactions is maintenance of a high reaction temperature for prolonged periods which in some cases is as high as 8 or 10 days as reported for the Be-btc frameworks[8f]. In the present work, synthesis has been performed under non-hydrothermal conditions and the water soluble nature of H_3btc permits a convenient assembly of compounds (**1**) and (**2**) at room temperature. Thus, the reaction of MCO_3 (M = Ba or Ca) with H_3btc in a 3:2 mole ratio in an aqueous medium results in the formation of (**1**) or (**2**) in good yields, which can be represented as follows:

$$3MCO_3 + 2H_3btc \rightarrow [M_3(btc)_2(H_2O)_x] \text{ (M=Ba or Ca)}$$
$$x = 10 \text{ for } (\mathbf{1});\ x = 12 \text{ for } (\mathbf{2})$$

Both compounds can also be prepared by reacting aqueous MCl_2 solutions with *in situ* generated trisodium salt of btc in a 3:2 mole ratio. The high formation tendency of (**1**) or (**2**) can also be evidenced by the fact that both compounds can be prepared by a carboxylate exchange reaction, i.e., by the direct reaction of the alkaline-earth acetate with the aromatic acid. The synthesis of a 1:1 compound[8b] $[Ba(Hbtc)(H_2O)_2]\cdot 0.5H_2O$ and the 3:2 compounds[8i,8j] $[Ba_3(btc)_2(H_2O)_4]\cdot 0.5H_2O$ and $[Ba_3(btc)_2(H_2O)_4]$ containing less coordinated water than (**1**) have been performed under hydrothermal conditions. It is interesting to note that the hemihydrate compound $[Ba_3(btc)_2(H_2O)_4]\cdot 0.5H_2O$ was prepared at a reaction temperature of 170 °C, while the solvothermal reaction of a mixture of Zn and Ba nitrates in aqueous DMF at 110 °C has been reported to yield $[Ba_3(btc)_2(H_2O)_4]$ without any incorporation of either the DMF or Zn in the product. In contrast, the use of a mixture of zinc nitrate and $Ca(OH)_2$ in aqueous DMF has been shown to result in the formation of the heterometallic compound $[CaZn_2(btc)_2(H_2O)_2](DMF)_2$ in a solvothermal reaction[8k]. Under hydrothermal conditions the use of Ba- or Ca-acetate as metal source yielded the 1:1 compounds $[M(Hbtc)(H_2O)_2]$ containing the $(Hbtc)^{-2}$ dianion as the linker[8a,b]. It has also been reported that a solvothermal reaction of $Ca(NO_3)_2$ with H_3btc in aqueous DMF in the presence of HCOOH results in the formation of $[Ca_3(btc)_2(H_2O)_2(dmf)_2]\cdot 3H_2O$ in low yield[8d]. The above instances show the differing and unpredictable nature of the products in solvothermal reactions. This can also be evidenced by the fact that the DMF solvent used in the synthesis of the anionic Be frameworks undergoes decomposition providing the dimethylammonium counter cation[8f] while the F^- ion used in the synthesis in the form of HF is not incorporated in the final product given the fact that Be has great affinity for F ligands. Prior to our work, a brief structure report of compound (**2**) prepared by a slow diffusion of NEt_3 (Et = ethyl) into a reaction mixture of $[Ca(acetate)_2]$ and H_3btc in isopropanol-water has appeared[9a]. More recently the synthesis of a 1:1 compound of Ca namely $[Ca(Hbtc)(H_2O)_4]$ has been reported by the reaction of $CaCl_2$ with H_3btc and Na_2CO_3 in aqueous methanolic medium under refluxing conditions[9b].

Spectral and thermal investigations

The characteristic infrared spectra of (**1**) and (**2**) (Supplementary Data Fig. S1), showing no signals in the 1730-1690 cm^{-1} region, serve to demonstrate the formation of a metal:btc compound containing a fully deprotonated btc trianion and the absence of any free –COOH group in the product. The composition of (**1**) and (**2**) was arrived at based on elemental analysis, and thermal and spectral studies. Both compounds which contain metal:btc in a 3:2 ratio are differently hydrated and the metal:water ratio are 3:10 and 3:12 for (**1**) and (**2**) respectively. Compounds (**1**) and (**2**) can be fully dehydrated to the corresponding anhydrous phases, $[Ba_3(btc)_2]$ (**1a**) and $[Ca_3(btc)_2]$ (**2a**) respectively by heating at 150 °C. The anhydrous crystalline materials thus formed cannot be rehydrated to the starting materials. The intense O-H vibration observed in (**1**) or (**2**) are not observed in the spectra of (**1a**) and (**2a**), thus confirming the formation of the anhydrous phases (Supplementary Data Fig. S1). The crystalline nature of (**1a**) and (**2a**) can be evidenced by the sharp lines in their X-ray powder pattern (Supplementary Data Fig. S2). A comparison of the powder pattern of (**1a**) with that of (**1**), reveals the differing nature of the starting and the anhydrous material. The thermograms of (**1**) or (**2**) exhibit a first endothermic event (148 °C for (**1**); 131 °C for (**2**)) followed by exothermic events above 500 °C. The endothermic event can be assigned for the dehydration process and has been verified by isothermal weight loss studies by heating (**1**) or (**2**) at 150 °C. The thermal profile of the anhydrous phases is identical to that of the starting hydrated compounds excepting for the absence of the first endothermic event in (**1**) and (**2**), which accounts for the loss of water molecules (Supplementary Data Fig. S3). The optical spectra of the hydrated and the anhydrous phases are very similar to that of the free ligand indicating that the absorptions are ligand centred (Supplementary Data Fig. S4). Both compounds exhibit diminished fluorescence (Supplementary Data Fig. S4) and the luminescence property can be attributed to ligand centered π or $n \rightarrow \pi^*$ orbital transitions since similar emissions are also observed for the free ligand.

Structural features

The barium-organic framework compound $[Ba_3(btc)_2(H_2O)_8]\cdot 2H_2O$ (**1**) crystallizes in the centrosymmetric monoclinic space group $P2_1/c$ and its structure consists of two crystallographically unique Ba(II) ions, an independent trianionic btc ligand and five water molecules (Supplementary Data Fig. S5). The structure of compound (**1**) is polymeric based on a tribarium building block consisting of a central Ba2 linked to two symmetry equivalent Ba1 ions on either side. In the trinuclear unit, Ba2 is situated on an inversion centre and exhibits a coordination number of ten while Ba1 is eight coordinated (Fig. 1). The five water molecules in the crystal structure can be classified into two sets namely four coordinated water molecules (O7 to O10) and an uncoordinated water molecule (O11). The water molecules O7 and O8 are monodentate ligands bonded to Ba1 in a terminal fashion, while O9 and O10 function as μ_2-bridging bidentate ligands linking Ba1 with Ba2 (Supplementary Data Fig. S6). The unique btc trianion functions as a μ_6-heptadentate bridging ligand and is bonded to six different Ba(II) ions, four of which are Ba1 and two are Ba2 (Fig. 2). Each Ba1 is linked to four different btc units via the oxygen atoms O1, O2, O3 and O6 and to four water molecules O7, O8, O9 and O10, resulting in a distorted square antiprismatic $\{BaO_8\}$ polyhedron (Fig. 3). Like Ba1, the Ba2 situated on a special position is also linked to four different btc ligands via six oxygen atoms O3, O4, O5, $O3^i$, $O4^i$ and $O5^i$ and to four different water molecules O9, O10, $O9^i$ and $O10^i$ leading to ten coordination (Supplementary Data Fig. S6). The $\{BaO_{10}\}$ polyhedron around Ba2 has a distorted bicapped square antiprismatic geometry. The μ_6-heptadentate bridging binding mode of the unique btc ligand in (**1**) results in a three-dimensional structure with the free water molecules (O11) situated in the pores (Fig. 4). The geometric parameters of the organic ligand in (**1**) are in the

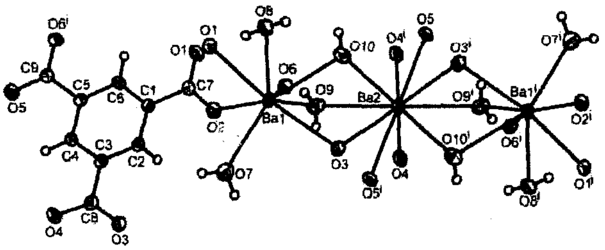

Fig. 1—The basic trinuclear building unit in $[Ba_3(btc)_2(H_2O)_8]\cdot 2H_2O$ (**1**) showing the coordination sphere of the unique Ba(II) ions (Ba1 and Ba2) and the crystallographic labeling scheme. Displacement ellipsoids are drawn at the 50 % probability level except for H atoms, which are shown as circles of arbitrary radius. Symmetry code: (i) $-x+2$, $-y$, $-z+1$.

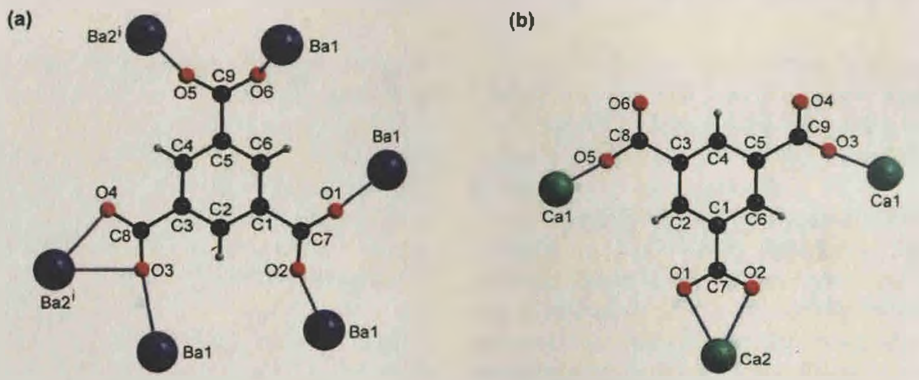

Fig. 2—(a) The μ_6-heptadentate bridging binding mode of the trianionic btc ligand in (1) showing its linking to six Ba(II) ions (Ba-O bonds are shown in blue). Symmetry code: (i) -x+2, -y, -z+1. (b) The μ_3-tetradentate bridging binding mode of the trianionic btc ligand in (2) showing its linking to three Ca(II) ions (Ca1-O5, Ca1-O3, Ca2-O1 and Ca2-O2 bonds are shown in blue).

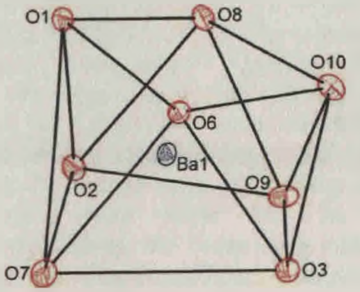

Fig. 3—The distorted square antiprismatic $\{BaO_8\}$ polyhedron around Ba1 in (1).

normal range and the O-Ba-O angles scatter in a wide range (Supplementary Data Table S2). The observed Ba-O distances (2.6548(18) to 2.874 Å for Ba1-O; 2.7545(18) to 3.013 Å for Ba2-O) are in good agreement with reported data[8i,8j] for $[Ba_3(btc)_2(H_2O)_4]\cdot 0.5H_2O$ and $[Ba_3(btc)_2(H_2O)_4]$. Compound (1) differs considerably from these compounds which contain less number of coordinated water. The compounds $[Ba_3(btc)_2(H_2O)_4]\cdot 0.5H_2O$ and $[Ba_3(btc)_2(H_2O)_4]$ which crystallize in the non-centrosymmetric $Pna2_1$ space group contain three unique Ba ions and two independent btc trianions. The unique btc ligands in these water deficient Ba-btc compounds exhibit a higher denticity (nona or decadentate) and function as μ_7-bridging ligands (Supplementary Data Fig. S7).

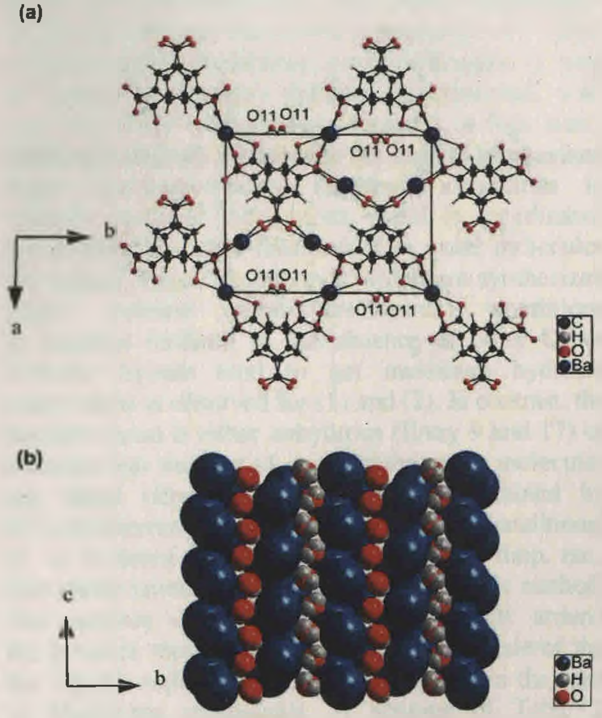

Fig. 4—(a) A view of the unit cell packing of $[Ba_3(btc)_2(H_2O)_8]\cdot 2H_2O$ (1) showing the free water molecules (O11) trapped in the pore of the 3-D framework. For clarity, the bridging and terminal waters around Ba1 and Ba2 are not shown. (b) A space filling model of the framework showing only the Ba ions and the trapped water (O11). For clarity, the bridging btc ligands and coordinated waters around Ba are not shown.

Compound (2) crystallizes in the centrosymmetric monoclinic space group *C2/c* and the observed unit cell parameters are in agreement with the earlier reported data[9a]. Like in (1) the basic building block of compound (2) is a trinuclear unit with the central calcium (Ca2) situated on an inversion centre. Unlike in (1), both the unique Ca(II) ions Ca1 and Ca2 in (2) are linked to two different btc ligands (Supplementary Data Fig. S8). In (2), two of the three –COO groups in the organic linker bind in a monodentate fashion while the third is linked in a bidentate manner resulting in a μ_3-tetradentate btc ligand (Fig. 2). It is to be noted that none of the three carboxylic group of the unique btc ligand in (**2**) exhibit a bridging binding mode unlike in (**1**). A similar feature is observed in the 1:1 compound[8d] [Ca(Hbtc)(H_2O)$_4$] where each unique Ca is bonded to four terminal water molecules and each of the three –COO groups in the unique btc ligand functions as a monodentate ligand. In contrast, in the water deficient compound[8d] [Ca_3(btc)$_2$(H_2O)$_2$(DMF)$_2$]·3H_2O, each of the carboxylate groups in the two independent btc ligands exhibit bridging binding modes (Supplementary Data Fig. S9). This indicates that the number of coordinated water molecules around the alkaline earth metal influences the binding mode of the carboxylate ligand.

The geometric parameters of the organic btc ligand are in the normal range and the Ca-O bond distances and O-Ca-O bond angles (Supplementary Data Table S3) are in agreement with reported data[9a]. The H atoms of the coordinated water molecules in both compounds and the uncoordinated water (O11) in (**1**) are involved in several weak H-bonding interactions (Supplementary Data Table S4). In terms of secondary interactions, the framework compound (**1**) differs from the two-dimensional compound (**2**) in that the H4 atom attached to C4 is involved in a weak C-H···O interaction with the lattice water O11.

Coordination behavior of btc ligand towards *s*- and *d*-block metals

The extended solids (**1**) and (**2**) described in this work are members of a group of compounds which contain bivalent metal:btc in a 3:2 ratio. A comparison of several compositionally similar [M_3(btc)$_2$(H_2O)$_x$] (M = bivalent metal) compounds reveals the differing coordination behavior of the btc ligand towards *d*- and *s*-block metals. In all these extended solids of differing dimensionalities (Table 2) interesting structural features like (i) varying levels of hydration of the *s*- or *d*-block metal, (ii) different coordination number of the central metal, (iii) varying denticity of the bridging btc ligand, (iv) tendency to crystallize in non-centrosymmetric space groups (Entry 3-5 and 10-16 in Table 2), and, (v) different dimensionality of the extended solid can be observed. The isotypic *d*-block compounds [M_3(btc)$_2$(H_2O)$_{12}$] (M = Co, Ni and Zn) are compositionally identical to the Ca compound [Ca_3(btc)$_2$(H_2O)$_{12}$] (**2**) and their structure consists of two unique bivalent metal ions and two independent btc ligands, one of which exhibits a μ_3-tetradentate bridging mode as in (**2**). The second unique btc ligand is a μ_2-bridging bidentate ligand and each metal in the trinuclear unit is bonded to four terminal water molecules thus accounting for the twelve water molecules in the formula unit. Hexacoordination around the *d*-block metal is achieved by bonding to btc ligands (Fig. 5), resulting in the formation of a 1-D corrugated chain structure unlike in [Ca_3(btc)$_2$(H_2O)$_{12}$] (**2**) which exhibits a 2-D layer structure. The μ_2-bridging binding mode of one of the water molecules extends the structure of (**2**) in the second dimension and the presence of bridging water molecule enhances the coordination number of the unique Ca ions in (**2**) to 7 and 8 respectively unlike the hexacoordination for the *d* block metals. The twelve water molecules provide a total of fourteen Ca-O(water) bonds, two more than that observed for the *d*-block compounds. In the Ba-organic framework compound (**1**) which contains eight coordinated water molecules, a total of twelve Ba-O(water) linkages are observed, with each Ba in the trinuclear unit bonded to four water molecules. In both compounds (**1**) and (**2**) synthesized under non-hydrothermal (ambient) conditions in aqueous medium, the *s*-block metal is coordinated to four/four (Ba) and five/four (Ca) water molecules per unique metal. Compounds which are synthesized under ambient (non-hydrothermal) conditions in aqueous medium in the absence of other O- or N-donor ligands tend to get maximum hydrated (water-rich) as observed for (**1**) and (**2**). In contrast, the bivalent metal is either anhydrous (Entry 9 and 17) or contains less number of coordinated water molecules per metal (Entry 6-17) in products obtained by (i) hydrothermal synthesis and/ or (ii) use of additional N- or O-donor ligands like py, eg, DMF, dmp, etc., (for abbreviations see Table 2) in the synthetic method. The number of coordinated water ligands around the bivalent metal influences the binding mode of the btc ligand, and has been earlier explained in the case of Ba/Ca-btc compounds. A scrutiny of Table 2 reveals that a reduction in the number of coordinated water molecules (water deficient) leads to an enhanced denticity of the btc ligand. In all the *s*-block compounds, which are synthesized under hydrothermal conditions (Entry 10–14), the btc ligand exhibits both higher denticity and bridging. In the compounds [Ba_3(btc)$_2$] (**1a**) or [Ca_3(btc)$_2$] (**2a**) which are devoid of coordinated water molecules, the btc ligands in the formula unit attain an enhanced denticity in order to fulfill the high coordination demands of the alkaline-earth metal, resulting in a reorganization of the structure, which is different from that of the starting water-rich materials

Table 2—Different binding modes of btc ligand in $[M_3(btc)_2(H_2O)_x]$ (M = bivalent metal)

No.	Compound	C. No.	Space group	Binding mode of the independent btc ligands	D	Ref.
1	$[Ba_3(btc)_2(H_2O)_8]\cdot 2H_2O$ **(1)**	8,10 [a]	$P2_1/c$	μ_6-heptadentate	3-D	This work#
2	$[Ca_3(btc)_2(H_2O)_{12}]$ **(2)**	7, 8 [a]	$C2/c$	μ_3-tetradentate	2-D	This work#
3	$[Co_3(btc)_2(H_2O)_{12}]$*	6, 6 [a]	$C2$	μ_3-tetradentate; μ_2-bidentate	1-D	5b
4	$[Ni_3(btc)_2(H_2O)_{12}]$*	6, 6 [a]	$C2$	μ_3-tetradentate; μ_2-bidentate	1-D	5b, 7b
5	$[Zn_3(btc)_2(H_2O)_{12}]$*	6, 6 [a]	$C2$	μ_3-tetradentate; μ_2-bidentate	1-D	5b, 5d#
6	$[Cu_3(btc)_2(H_2O)_3]$* (HKUST-1)	5	$Fm\text{-}3m$	μ_6-hexadentate	3-D	4b
7	$[Cd_3(btc)_2(pipH)(H_2O)_3(OH)]\cdot H_2O$*	6, 6, 6 [b]	$Pbca$	μ_4-tetradentate; μ_5-octadentate	2-D	5e
8	$[Cd_2Co(btc)_2(H_2O)_4]\cdot 2H_2O$*	6, 6, 6 [b]	$C2/c$	μ_5-pentadentate	3-D	5e
9	$[Mn_3(btc)_2]$*	6, 6 [a]	$R\text{-}3$	μ_6-nonadentate	3-D	5f
10	$[Ca_3(btc)_2(H_2O)_2(DMF)_2]\cdot 3H_2O$*	7, 7, 8 [b]	$C2$	μ_6-octadentate; μ_7-nonadentate	3-D	8d
11	$[CaZn_2(btc)_2(H_2O)_2]\cdot(DMF)_2$*	6 (Ca); 4 (Zn)	$C222_1$	μ_6-hexadentate	3-D	8k
12	$[Sr_3(btc)_2(H_2O)_4]\cdot H_2O$*	7, 9, 9 [b]	$Pna2_1$	μ_7-octadentate; μ_7-decadentate	3-D	8c
13	$[Ba_3(btc)_2(H_2O)_4]\cdot 0.5H_2O$ *	7, 9, 9 [b]	$Pna2_1$	μ_7-decadentate; μ_7-decadentate	3-D	8i
14	$[Ba_3(btc)_2(H_2O)_4]$*	7, 8, 9 [b]	$Pna2_1$	μ_7-nonadentate; μ_7-decadentate	3-D	8j
15	$[Ni_3(btc)_2(py)_6(eg)_6]\cdot 3(eg)4H_2O$	6	$P4_332$	μ_3-tridentate	3-D	5g#
16	$[Zn_3(btc)_2(DMF)_3(H_2O)]\cdot(DMF)(H_2O)$	5, 5, 6 [b]	$P\,4_12_12$	μ_6-hexadentate; μ_5-hexadentate	3-D	5h#
17	$[Zn_3(btc)_2(dmp)_6]\cdot 2.5H_2O$	4,4 [a]	$Pbcn$	μ_2-bidentate	1-D	5d#

Abbreviations: C.N. = coordination number; D = dimensionality; a - two crystallographically unique bivalent metals; b - three crystallographically unique bivalent metals; pip = piperazine; DMF = dimethylformamide; py = pyridine; eg = ethylene glycol; dmp = 3,5-dimethylpyrazole; *Compound synthesis performed under hydrothermal conditions; # non-hydrothermal synthesis

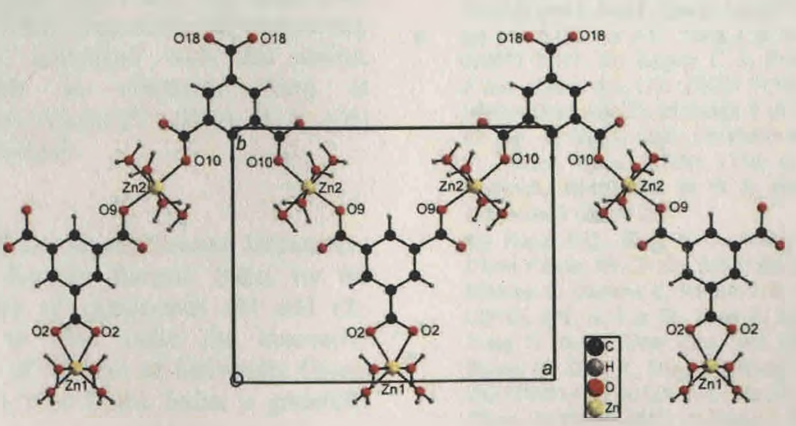

Fig. 5—The corrugated 1-D chain structure of $[M_3(btc)_2(H_2O)_{12}]$ compounds (M = Co, Ni and Zn) due to the μ_3-tetradentate and μ_2-bidentate binding modes of the unique btc ligands. The central metal is hexacoordinated with each metal linked to four terminal H_2O ligands. [Figure drawn for M= Zn using the reported cif data in Ref. 5d].

(**1**) or (**2**). The importance of the coordinated water ligands in (**1**) and (**2**) can thus be evidenced by the fact that on heating at ~150°C both compounds can be fully dehydrated but the anhydrous phases cannot be rehydrated to the original phase indicating the collapse of the original structure.

Conclusions

In summary, we have described the structural characterization of a new barium-organic framework material synthesized under mild reaction conditions. A comparative study of several compounds containing the $\{M_3(btc)_2\}$ unit reveals the versatile ligational behavior of the btc ligand towards *d*- and *s*-block metal ions and that the number of coordinated water molecules around the bivalent metal influences the binding mode of the btc ligands. The Ca-compound $[Ca_3(btc)_2(H_2O)_{12}]$ (**2**) exhibits a two-dimensional structure unlike other compositionally similar *d*-block compounds $[M_3(btc)_2(H_2O)_{12}]$ (M = Co, Ni, Zn), which are one-dimensional.

Supplementary Data

Crystallographic data (excluding structure factors) for the structures of $[Ba_3(btc)_2(H_2O)_8]\cdot 2H_2O$ (**1**) and $[Ca_3(btc)_2(H_2O)_{12}]$ (**2**) reported herein have been deposited with the Cambridge Crystallographic Data Centre as supplementary publication no. CCDC 754975 and CCDC 882229. Copies of the data can be obtained, free of charge, on application to CCDC, 12 Union Road, Cambridge CB2 1 EZ, UK. (Fax: +44-(0)1223-336033 or Email: deposit@ccdc.cam.ac.uk). Supplementary data associated with this article, viz., are available in electronic form at http://www.niscair.res.in/jinfo/IJCA/IJCA 51A (08) 1064-1072_Suppl Data.pdf.

Acknowledgement

The authors thank Dr. Manav Saxena, Department of Chemistry, IIT Kanpur, Kanpur, India, for the luminescence spectra of compounds (**1**) and (**2**). Financial support to BRS under the Innovative Research Activities of XI plan of University Grants Commission (UGC), New Delhi, India, is gratefully acknowledged.

References

1 *Special issue on MOF, Chem Soc Rev,* 38 (2009) 1203; *Themed issue Coordination polymers: Structure and Function, New J Chem,* 34 (2010) 2339; Biradha K, *New J Chem,* 34 (2010) 2353; *Metal-organic Frameworks Special issue, Chem Rev,* 112 (2012); Zhou H-C, Long J R & Yaghi O M, *Chem Rev,* 112 (2012) 673.

2 (a) Batten S R, Neville S M & Turner D R, *Coordination Polymers: Design, Analysis and Application,* (RSC Publishing, Cambridge UK) 2009; (b) Janiak C & Vieth J K, *New J Chem,* 34 (2010) 2366; (c) Natarajan S, Mahata P & Sarma D, *J Chem Sci,* 124 (2012) 339; (d) Stock N & Biswas S, *Chem Rev,* 112 (2012) 933; (e) Banerjee D & Parise J B, *Cryst Growth Des,* 11 (2011) 4704; (f) Fromm K M, *Coord Chem Rev,* 252 (2008) 856; (g) Yaghi O M & Li H, *J Am Chem Soc,* 117 (1995) 10401; (h) Janiak C, *Dalton Trans,* (2003) 2781; (i) Robson R, *Dalton Trans,* (2008) 5113; (j) Biradha K, Ramanan A & Vittal J J, *Cryst Growth Des,* 9 (2009) 2969.

3 (a) *Coordination Polymers and Metal Organic Frameworks: Terminology and Nomenclature Guidelines,* http://www.iupac.org/web/ins/2009-012-2-200; (b) Ohrstrom L, *Chem Int,* 32 (2010) 23; (c) Batten S R, Champness N R, Chen X-M, Garcia-Martinez J, Kitagawa S, Ohrstrom L, O'Keeffe M, Suh M P & Reedijk J, *Cryst Eng Comm,* 14 (2012) 3001.

4 (a) Li H, Eddaoudi M, O'Keeffe M & Yaghi O M, *Nature* 402 (1999) 276; (b) Chui S S Y, Lo S M F, Charmant J P H, Orpen A G & Williams I D, *Science,* 283 (1999) 1148; (c) Serre C, Millange F, Thouvenot C, Nogues M, Marsolier G, Louer D & Ferey G, *J Am Chem Soc,* 124 (2002) 13519; (d) Ferey G, Mellot-Drazineks C, Serre C, Millange F, Dutour J, Surble S & Margiolaki I, *Science,* 309 (2005) 2040.

5 (a) Yaghi O M, Li G & Li H, Nature 378 (1995) 703; (b) Yaghi O M, Li H & Groy T L, *J Am Chem Soc,* 118 (1996) 9096; (c) Yaghi O M, Davis C E, Li G & Li H, *J Am Chem Soc,* 119 (1997) 2861; (d) Krishnamurthy D & Murugavel R, *Indian J Chem* 42A (2003) 2267; (e) Chen J-X, Liu S-X & Gao E-Q, *Polyhedron* 23 (2004) 1877; (f) Gutschke S O H, Molinier M, Powell A K, Winpenny R E P, Wood P T, *Chem Comm,* (1996) 823; (g) Kepert C J, Rosseinsky M, *Chem Comm,* (1998) 31; (h) Fang Q, Zhu G, Xue M, Sun J, Sun F, Qiu S, Inorg Chem, 45 (2006) 3582.

6 (a) Liu Y-Y, Ma J-F, Yang J & Su Z-M, *Inorg Chem* 46 (2007) 3027; (b) Kepert C J, Prior T J, Rosseinsky M, *J Am Chem Soc,*122 (2000) 5158; (c) Ferey G, Serre C, Mellot-Drazineks C, Millange F & Surble S *Angew Chem Int Ed* , 43 (2004) 6296; (d) Habib H A, Sanchiz J & Janiak C, *Dalton Trans,* (2008) 1734; (e) Foreman M R St J, Gelbrich, Hursthouse M B & Plater M J, *Inorg Chem Commun,* 3 (2000) 234.

7 (a) Jiang Z-Q, Jiang G-Y, Wang F, Zhao Z, Zhang J, *Chem Comm,* 48 (2012), 3653; (b) Sarma R, Chowdhury P, Bikkina C, Gumma S, Baruah J B, *J Chem Crystallogr,* 40 (2010), 892; (c) Liu M, Yang Z, Sun W, Li X, Li J, Ma J, Yang G, *Inorg Chim Acta,* 362 (2009) 2884; (d) Zhu S, Zhang H, Zhao Y, Shao M, Wang Z, Li M, *J Mol Struct,* 892 (2008) 420; (e) Liu Y-Y; Ma J-F, Yang J, Su Z-M, *Inorg Chem,* 46 (2007) 3027; (f) Meng J, Wang X, Wang E, Li Y, Qin C, Xu X, *Inorg Chim Acta,* 361 (2008) 2447; (g) Liang S-W, Li M-X, Shao M, Liu H-J, *Inorg Chem Commun,* 10 (2007) 1347; (h) Zhou, Y- F, Lou B-Y, Yuan D-Q, Xu Y-Q, Jiang, F-L, Hong M-C, *Inorg Chim Acta,* 358 (2005) 3057; (i) Liu Y-Y, Ma J-C, Xie Y-P, Ma J-F, *J Coord Chem,* 61 (2008) 3450.

8 (a) Plater M J, Howie R A & Roberts A J, *Chem Commun,* (1997) 893; (b) Plater M J, Roberts A J, Marr J, Lachowski E E & Howie R A, *J Chem Soc Dalton Trans,* (1998) 797; (c) Tran D T, Chu D, Oliver A G & Oliver S R J, *Inorg Chem Comm,* 12 (2009) 351; (d) Liang P-C, Liu H-K, Yeh C-T, Lin C-H & Zima V, *Cryst Growth Des,* 11 (2011) 699; (e) Davies R P, Less R J, Lickiss P D & White A J P, *Dalton Trans,* (2007) 2528; (f) Kang M, Luo D, Luo X, Chen Z, Lin Z, *Cryst Eng Comm,* 14 (2012) 95; (g) Lee D W, Jo V, Ok K M, *Cryst Growth Des,* 11 (2011) 2698; (h) Ma S, Fillinger J A, Ambrogio M W, Zuo J-L, Zhou H-C, *Inorg Chem Commun,* 10 (2007) 220; (i) Ma K-R, Zhu Y-L, Yin Q-F, Hu H-Y, Ma F, *J Chem Res,* 34 (2010) 705; (j) Zhang X, Huang Y-Y, Zhang M-J, Zhang J & Yao Y G, *Crystal Growth Des,* 12 (2012) 3231; (k) Zou R, Zhong R, Han S, Xu H, Burrell A K, Henson N, Cape J L, Hickmott D D, Timofeeva T V, Larson T E, Zhao Y, *J Am Chem Soc,* 132 (2010) 17996; (l) Song L-F, Jiang C-H, Zhang J, Sun L-X, Xu F, Tian Y-Q, You W-S, Cao Z, Zhang L, Yang D-W, *J Therm Anal Calorim,* 101 (2010) 365.

9 (a) Yang Y-Y, Huang Z-Q, Szeto L & Wong W-T, *Appl Organometal Chem* 18 (2004) 97; (b) Borah B M, Dey S K & Das G, *Cryst Growth Des,* 11 (2011) 2773.

10 Sheldrick G M, *Acta Crystallogr A*, 64 (2008) 112.

Indian Journal of Chemistry
Vol. 51A, April 2012, pp. 564-570

Synthesis and structural characterization of bis(μ_2-aqua)tetrakis(aqua)dilithium(I) bis(4-nitrobenzoate)

Bikshandarkoil R Srinivasan[a, *], Santosh Y Shetgaonkar[a], Kiran T Dhavskar[a],
Jeyaperumal Kalyana Sundar[b] & Subramanian Natarajan[b]

[a]Department of Chemistry, Goa University, Goa 403 206, India
Email: srini@unigoa.ac.in

[b]School of Physics, Madurai Kamaraj University,
Madurai 625 021, Tamil Nadu, India

Received 19 May 2011; revised and accepted 15 March 2012

Reaction of alkali metal carbonates M_2CO_3 (M = Li or Na) with 4-nitrobenzoic acid (4-nbaH) results in the formation of $[(H_2O)_4Li_2(\mu\text{-}H_2O)_2](4\text{-nba})_2$ (4-nba = 4-nitrobenzoate) (**1**) and $[Na(4\text{-nba})(H_2O)_3]$ (**2**). Compounds (**1**) and (**2**) have been characterized by analytical, spectral and thermal data. The structure of (**1**) consists of bis(μ_2-aqua)tetrakis(aqua)dilithium(I) dication situated on an inversion centre and a free 4-nba anion. In compound (**2**), one of the two independent 4-nba functions as a μ_2-bridging bidentate ligand, bridging the two unique Na(I) ions via the oxygen atoms of the nitro functionality. Hydrogen bonding of coordinated water ligands in a dinuclear lithium cation with coordinated water molecules in an adjacent unit leads to the formation of a supramolecular chain of $[(H_2O)_4Li_2(\mu\text{-}H_2O)_2]^{2+}$ cations. The cationic chain is further H-bonded to 4-nba anions resulting in alternating layers of $[(H_2O)_4Li_2(\mu\text{-}H_2O)_2]^{2+}$ cations and 4-nba anions. Compounds (**1**) and (**2**) exhibit enhanced fluorescence emission. A study of the known *s*-block metal compounds containing 4-nba and coordinated water ligands reveals that the coordination number of the central metal varies from four in Li to nine in Ba.

Keywords: Coordination chemistry, Lithium, Sodium, Nitrobenzoates, Supramolecular chains

Recent years have witnessed a steady growth of publications describing the chemistry of *s*-block elements[1-22]. Non-toxic and water soluble nature, variable structural chemistry, affinity for O-donor ligands and relevance in biology are some factors responsible for the current interest in the chemistry of alkali and alkaline earths. The closed shell *s*-block metal cations lack properties like magnetism or variable oxidation states. Unlike the transition metals, no ligand field stabilization effects govern the bonding of *s*-block metal cations and hence the coordination numbers and geometries of alkali and alkaline earth metal cannot be accurately predicted. For example, the alkaline earth metal Ca adopts a range of coordination numbers from six to nine with eight coordination being the most preferred in several Ca(II) compounds[23]. An important property of *s*-block metals is their affinity for O-donor ligands, especially water. When synthesis is performed in aqueous media, the products invariably contain coordinated and lattice water molecules. In the case of Mg(II), coordination of six aqua ligands is a typical feature and several Mg(II) compounds possessing an octahedral $[Mg(H_2O)_6]^{2+}$ unit have been characterized[24-31]. Lighter elements like Li(I) in the alkali metal series or Be(II) in the alkaline earth series are known to prefer four coordination while cations like Na(I) and especially Mg(II) prefer a coordination number of six. As part of our research program we have developed an extensive structural chemistry of alkaline earth 4-nitrobenzoates[32]. In contrast, very few reports have appeared in the literature on the chemistry of alkali metal 4-nitrobenzoates[33-35]. Hence, we have extended our work to include the 4-nitrobenzoates of alkali metals. Herein, we describe the synthesis, spectral and structural characterization of the 4-nitrobenzoates of lithium and sodium.

Materials and Methods

All the chemicals used in this study were of reagent grade and were used as received. The starting materials and reaction products are air stable and hence were prepared under normal laboratory conditions. Infrared (IR) spectra were recorded on a Shimadzu (IR Prestige-21) FT-IR spectrometer in the range 4000-400 cm^{-1}. The samples for the IR spectra were diluted with KBr in the solid state and the signals referenced to polystyrene bands. UV-visible spectra of aqueous solutions were recorded on a Shimadzu UV-2450 double beam spectrophotometer using matched quartz cells. Photoluminescence of solid samples was studied using a Perkin Elmer LS55 fluorescence spectrometer. ^{1}H NMR spectra were recorded on a 400 MHz Bruker Ultrashield spectrometer. X-ray powder pattern were recorded on a Rigaku Miniflex II powder diffractometer using Cu-K_α radiation with a Ni filter. Thermal studies were performed in flowing air, in Al_2O_3 crucibles on a STA-409PC simultaneous thermal analyzer from Netzsch. A heating rate of 10 K min^{-1} was employed for all measurements. The insoluble 4-nbaH obtained on acid treatment of (**1**) and (**2**) was weighed as described earlier[36].

A mixture of 4-nitrobenzoic acid (3.340 g, 20 mmol) and lithium carbonate (0.739 g, 10 mmol) in water (50 mL) was heated on a water bath till all the 4-nitrobenzoic acid dissolved completely to give a clear solution. The hot reaction mixture was filtered and left aside for crystallization. Pale yellow crystalline blocks of (**1**) that separated out were filtered, washed with ether and dried in air. Yield: 3.1 g (68 %). Use of sodium carbonate (1.06 g, 10 mmol) instead of lithium carbonate in the above reaction resulted in the formation of 3.6 g of (**2**) in 70% yield.

Anal. (%): Calcd for $Li_2C_{14}H_{20}N_2O_{14}$ (**1**): 4-nbaH, 73.59; C, 37.02, H, 4.44; N, 6.17. Found: 4-nbaH, 73.03; C, 36.52; H, 3.82; N, 6.03. IR data (cm^{-1}): 3582, 3400-2800 (br), 1641, 1566 υ_{as}(-COO), 1512 υ_{as}(-NO_2), 1408 υ_s(-COO), 1369, 1344 υ_s(-NO_2), 1323, 1161, 1105, 1011, 802, 723, 648, 517. UV–vis (in H_2O): 299 nm. ^{1}H NMR (D_2O) δ (in ppm): 8.05 (d, J = 8.8 Hz, H_a), 8.31 (d, J = 9.2 Hz, H_b). Thermal data (in °C): 105 (endo) and 389 (exo).

Anal. (%): Calcd for $NaC_7H_{10}NO_7$ (**2**): 4-nbaH, 68.73; C, 34.58; H, 4.15; N, 5.76. Found: 4-nbaH, 68.39; C, 34.32; H, 4.11; N, 5.87. IR data (cm^{-1}): 3578, 3500-2800 (br) 1678, 1572 υ_{as}(-COO), 1514 υ_{as}(-NO_2), 1393 υ_s(-COO), 1350 υ_s(-NO_2), 1319, 1107, 1011, 833, 804, 723, 511. UV–vis (in H_2O): 299 nm. ^{1}H NMR (D_2O) δ (in ppm): 8.03 (d, J = 8.8 Hz, H_a), 8.29 (d, J = 8.8 Hz, H_b). Thermal data (in °C): 105 (endo) and 368 (exo).

Intensity data were collected on a Nonius MACH3/ CAD-4 single crystal diffractometer for (**1**) and on a Bruker Smart Apex Diffractometer for (**2**) using graphite-monochromated Mo-K_α radiation. Structures were solved with direct methods using SHELXS-97[37] and refinement was done against F^2 using SHELXL-97[37]. All non-hydrogen atoms were refined using anisotropic displacement parameters. The C-H hydrogen atoms of 4-nba anion were positioned with idealized geometry and were refined using a riding model. H atoms attached to water oxygen were located in difference map, and were refined with fixed isotropic displacement parameters. The calculated bond valence sum from the crystallographic data for the central metal in both compounds is close to 1. Selected refinement results are listed in Table 1.

Results and Discussion

An aqueous solution containing a mixture of 4-nbaH and alkali metal carbonate M_2CO_3 (M = Li or Na) in 2:1 mole ratio was heated till the 4-nbaH dissolved. Filtration of the reaction mixture followed by slow evaporation afforded in good yields the alkali metal 4-nitrobenzoates $[(H_2O)_4Li_2(\mu\text{-}H_2O)_2](4\text{-nba})_2$ (**1**) or $[Na(4\text{-nba})(H_2O)_3]$ (**2**) respectively. The unit cell parameters of a trihydrate of Li(I) charge balanced by 4-nba, with no details on compound synthesis, have been reported by Prabhakar *et al.*[35] More recently, the synthesis of anhydrous [M(4-nba)] (M = Li or Na) by an aqueous reaction of MOH with 4-nbaH followed by removal of solvent under reduced pressure, has been reported by Regulska *et al.*[38] For synthesis of compound (**2**), $NaHCO_3$ can also be used instead of Na_2CO_3. Compounds (**1**) and (**2**), which were isolated from a neutral reaction mixture, are freely soluble in water but unstable in acidic medium. On reaction with dilute HCl, (**1**) and (**2**) decompose forming quantitatively 4-nbaH, the insoluble nature of which provides a convenient method for the gravimetric analysis of (**1**) and (**2**). The composition of (**1**) and (**2**) was arrived at based on elemental analysis, and the 4-nbaH content obtained by acidification. Analytical data of (**1**) and (**2**) reveals the presence of three moles of water per mole of alkali metal. Despite this similarity, both compounds adopt different structures (*vide infra*). The presence of water in both compounds was also confirmed based on their characteristic infrared spectra in the O-H region and weight loss studies on heating at 130 °C. Presence of three moles of water in (**1**) and (**2**) is evidenced by mass loss of 24.0 and 22.0 % respectively.

The UV-visible spectra of both compounds in water are identical (Supplementary Data Fig. S1) and the observed λ_{max} at 299 nm can be assigned to the

Table 1—Selected refinement data for $[(H_2O)_4Li_2(\mu\text{-}H_2O)_2](4\text{-nba})_2$ (**1**) and $[Na(4\text{-nba})(H_2O)_3]_n$ (**2**)

Empirical formula	$C_{14}H_{20}Li_2N_2O_{14}$	$C_7H_{10}NaNO_7$
Formula weight (g mol^{-1})	454.20	243.15
Temp. (K)	293(2)	298(2)
Wavelength (Å)	0.71073	0.71073
Crystal system	Monoclinic	Triclinic
Space group	$P2_1/c$	$P\bar{1}$
Unit cell dimensions	a = 12.324(4) Å; α = 90°	a = 7.2109(14) Å; α = 96.42(3)°
	b = 6.719(5) Å; β = 104.29(3)°	b = 12.033(2) Å; β = 91.65(3)°
	c = 12.402(3) Å; γ = 90°	c = 12.382(3) Å; γ = 104.43(3)°
Volume (Å^3)	995.2(8)	1032.2(4)
Z	2	4
Density (calc.) (mg/m^3)	1.516	1.565
Abs. coeff. (mm^{-1})	0.135	0.174
F(000)	472	504
Crystal size (mm^3)	0.25 × 0.19 × 0.17	0.12 × 0.10 × 0.08
Theta range for data collection (°)	3.39 to 24.96	1.76 to 25.98
Completeness to theta	99.9 %	98.8%
Index ranges	$0 \leq h \leq 14, -1 \leq k \leq 7, -14 \leq l \leq 14$	$-8 \leq h\, 8, -14 \leq k \leq 14, -15 \leq l \leq 15$
Reflections collected	2170	10532
Independent reflections	1741 [R(int) = 0.0364]	3990 [R(int) = 0.0228]
Refinement method	Full-matrix least-squares on F^2	Full-matrix least-squares on F^2
Data/restraints/parameters	1741/ 0 / 164	3990/ 0 / 290
Goodness-of-fit on F^2	1.194	0.948
Final R indices [I >2sigma(I)]	$R1$ = 0.0377, w$R2$ = 0.1112	$R1$ = 0.0390, w$R2$ = 0.1044
R indices (all data)	$R1$ = 0.0437, w$R2$ = 0.1154	$R1$ = 0.0458, w$R2$ = 0.1105
Extinction coefficient	0.203(9)	0.022(2)
Largest diff. peak and hole (e.Å^{-3})	0.219 and -0.173	0.411 and -0.256
Bond valence sum of central metal[a]	1.059, 1.058	1.117, 0.999

[a] Bond valence sums were determined from the crystallographic data using Valist. A.S. Wills, VaList, Program available from www.ccp14.ac.uk.

intra ligand charge transfer of 4-nba. The fluorescence emission spectra of compounds (**1**) and (**2**) exhibit an enhanced emission as compared to that of free 4-nitrobenzoic acid (Supplementary Data Fig. S2). A similar enhancement of fluorescence has been recently reported by us in a Ca(II) coordination polymer based on 4-nitrobenzoate[39] and as in the case of the Ca compound, the emissions can be assigned to the intraligand fluorescent emission. The luminescent property of (**1**) and (**2**) can be assigned for ligand centered orbital transitions since similar emissions are also observed for the free ligand. The ^{1}H NMR spectra of both compounds exhibit a typical AB quartet for the two sets of aromatic protons in the 4-nba anion (Supplementary Data Fig. S3) and the observed chemical shifts of (**1**) and (**2**) are nearly identical and in agreement with the reported values[36] for $[Mg(H_2O)_6](4\text{-nba})_2\cdot 2H_2O$. The presence of 4-nba in both compounds can be further confirmed based on the several signals in the mid IR region. It is interesting to note that the infrared spectra of both compounds are nearly similar excepting for a change in the profile of the spectra in the 3500-3000 cm^{-1} region (Supplementary Data Fig. S4). The broad signal in this region assignable for the $\upsilon_{O\text{-}H}$ vibration disappears in the spectra of samples obtained on heating (**1**) and (**2**) at 130 °C. The values of the symmetric (υ_s) and asymmetric (υ_{as}) stretching vibrations of the carboxylate and the nitro groups are in the expected range (for assignment see Experimental section). Both compounds exhibit characteristic signals assignable to the vibrations of the carboxylate and nitro groups. The crystalline nature of both compounds (Supplementary Data Fig. S5) can be evidenced from the sharp signals in their powder diffractograms. A comparison of the powder patterns reveals that the phases are different indicating that the structure of the Li compound is different from that of the sodium compound.

Thermal studies reveal that both compounds exhibit an initial endothermic event centered at 105 °C followed by a strong exothermic signal at 368 and 389 °C for (**1**) and (**2**) respectively. The endothermic signal can be assigned for the removal of three moles of water in both compounds while the exothermic event can be attributed to the decomposition of 4-nba. It is to be noted that the decomposition of 4-nba occurs at lower temperatures in the alkali metal compounds unlike in alkaline earth 4-nba compounds which exhibit exothermic decomposition above 400 °C. The results of the isothermal weight loss studies at 130 °C and the characteristic IR spectra of the anhydrous compounds (Supplementary Data Fig. S6) obtained on heating add credence to the thermal data.

Compound (**1**) crystallizes in the centrosymmetric monoclinic space group *P2₁/c* and its structure consists of a bis(μ-aqua)bridged tetraaquadilithium unit situated on an inversion centre and a free uncoordinated 4-nitrobenzoate anion located in general positions (Fig. 1). Each Li(I) in the dimeric unit is four coordinated and is bonded to two terminal water ligands and two bridging water molecules. In view of the presence of an inversion centre at the mid point of the Li_2O_2 ring, the asymmetric unit is a half of the formula unit. The metric parameters of the centrosymmetric dimeric cation are in agreement with reported data for $[(H_2O)_4Li_2(\mu\text{-}H_2O)_2][Li(SR)_2]$ [R= bis(tri-tert-butoxysilanethiolato]^{40}. The O-Li-O angles ranging from 89.69(15) to 126.57(19)° (Table 2)

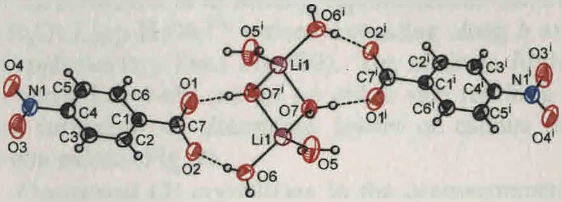

Fig. 1—Crystal structure of $[(H_2O)_4Li_2(\mu\text{-}H_2O)_2](4\text{-nba})_2$ (**1**) showing the coordination sphere of Li(I) and atom-labeling scheme. Displacement ellipsoids are drawn at 50 % probability level except for the H atoms, which are shown as circles of arbitrary radius. Intramolecular H-bonding is shown as broken lines. [Symmetry code: (i) –*x*+1, -*y*+1, -*z*].

Table 2—Selected bond distances (Å) and bond angles (°) of (**1**) and (**2**)

$[(H_2O)_4Li_2(\mu\text{-}H_2O)_2](4\text{-nba})_2$ (**1**)

Li(1)-O(5)	1.901(4)	O(5)-Li(1)-O(6)	110.1(2)
Li(1)-O(6)	1.934(4)	O(5)-Li(1)-O(7)	115.28(18)
Li(1)-O(7)	1.989(4)	O(6)-Li(1)-O(7)	126.57(19)
Li(1)-O(7)^{i}	2.018(4)	O(5)-Li(1)-O(7)^{i}	109.37(18)
Li(1)···Li(1)^{i}	2.842(7)	O(6)-Li(1)-O(7)^{i}	100.81(17)
		O(7)-Li(1)-O(7)^{i}	89.69(15)

$[Na(4\text{-nba})(H_2O)_3]_n$ (**2**)

Na(1)-O(22)	2.3655(15)	O(23)-Na(1)-O(24)	96.38(5)
Na(1)-O(23)	2.3728(16)	O(21)-Na(1)-O(24)	173.77(5)
Na(1)-O(21)	2.4283(15)	O(22)^{ii}-Na(1)-O(24)	90.24(5)
Na(1)-O(22)^{ii}	2.4327(16)	O(22)-Na(1)-O(3)	166.40(6)
Na(1)-O(24)	2.4391(14)	O(23)-Na(1)-O(3)	96.30(7)
Na(1)-O(3)	2.5365(18)	O(21)-Na(1)-O(3)	79.95(6)
Na(2)-O(24)	2.4041(15)	O(22)^{ii}-Na(1)-O(3)	80.97(6)
Na(2)-O(25)^{iii}	2.4120(17)	O(24)-Na(1)-O(3)	93.82(6)
Na(2)-O(26)	2.4317(17)	O(24)-Na(2)-O(26)	149.90(6)
Na(2)-O(25)	2.4359(16)	O(25)^{iii} -Na(2)-O(26)	118.45(6)
Na(2)-O(26)^{iv}	2.4749(16)	O(24)-Na(2)-O(25)	89.62(6)
Na(2)-O(4)	2.729(2)	O(25)^{iii}-Na(2)-O(25)	77.39(5)
Na(1)···Na(1)^{ii}	3.5221(18)	O(26)-Na(2)-O(25)	101.85(5)
Na(1)···Na(2)	4.1500(13)	O(24)-Na(2)-O(26)^{iv}	91.63(5)
Na(2)···Na(2)^{iii}	3.7836(16)	O(25)^{iii}-Na(2)-O(26)^{iv}	103.52(5)
Na(2)···Na(2)^{iv}	3.8500(17)	O(26)-Na(2)-O(26)^{iv}	76.60(5)
O(22)-Na(1)-O(23)	96.87(6)	O(25)-Na(2)-O(26)^{iv}	178.43(5)
O(22)-Na(1)-O(21)	98.01(5)	O(24)-Na(2)-O(4)	73.68(6)
O(23)-Na(1)-O(21)	84.32(5)	O(25)^{iii}-Na(2)-O(4)	154.69(6)
O(22)-Na(1)-O(22)^{ii}	85.56(5)	O(26)-Na(2)-O(4)	80.33(6)
O(23)-Na(1)-O(22)^{ii}	173.01(5)	O(25)-Na(2)-O(4)	82.33(6)
O(21)-Na(1)-O(22)^{ii}	88.86(5)	O(26)^{iv}-Na(2)-O(4)	97.12(6)
O(22)-Na(1)-O(24)	88.07(5)		

Symmetry transformations used to generate equivalent atoms.
Symmetry codes; (i) –*x*+1, -*y*-1, -*z* (ii) -*x*+1, -*y*+1, -*z*+2 (iii) -*x*+1, -*y*+2, -*z*+2 (iv) –*x*+2, -*y*+2, -*z*+2

indicate a distortion of the $\{LiO_4\}$ tetrahedron. The Li-O distances range from 1.901(4) to 2.018(4) Å. The two shorter Li-O distances at 1.901(4) and 1.934(4) Å are associated with the terminal water molecules O5 and O6 respectively. The coordinated water (O7) functions as a μ_2-bridging ligand and is bonded to Li at a longer distance of 1.989(4) Å and the O7 is further linked to a symmetry related Li with a very long Li-O bond length of 2.018(4) Å. This μ_2-bridging bidentate mode of O7 results in a Li···Li separation of 2.842(7) Å in the dimeric unit which is slightly shorter than the reported value of 2.876(7) Å for $[(H_2O)_4Li_2(\mu\text{-}H_2O)_2][Li(SR)_2]$[40].

In the crystal structure of (**1**) the dimeric cation and the free 4-nba anion are linked by two varieties of H-bonding interactions comprising of six O-H···O bonds and a C-H···O interaction. All these O···H contacts (Table 3) are shorter than the sum of their van der Waals radii. All the H atoms of the coordinated water molecules and one hydrogen atom (H3) attached to a carbon (C3) function as H-donors. Each 4-nba unit is H-bonded to three different dimers with the aid of five O-H···O interactions and to one anion via the C3-H3···O3 interaction (Supplementary Data Fig. S7). In contrast, each dimeric cation is linked by H-bonding to two adjacent dimers and eight symmetry related 4-nba anions with the aid of six O-H···O interaction (Supplementary Data Fig. S8). The O5-H1W···O6 interaction at 2.09(4) Å accompanied by a DHA angle of 168(3)° between the H atom of a coordinated water in a dimeric unit and the coordinated water O6 of an adjacent dimer results in the formation of an infinite supramolecular chain of $[(H_2O)_4Li_2(\mu\text{-}H_2O)_2]^{2+}$ cations extending along *b* axis (Supplementary Data Fig. S9). The chain is further H-bonded to 4-nba anions on either side resulting in the formation of alternating layers of cations and 4-nba anions (Fig. 2).

Compound (**2**) crystallizes in the centrosymmetric triclinic space group $P\bar{1}$ and the observed unit cell parameters are in excellent agreement with reported data[34]. The structure consists of two crystallographically independent Na(I) ions, six unique water molecules and two independent 4-nba anions (Supplementary Data Fig. S10). Of the six water molecules, two aqua ligands (O21 and O23) attached to Na1 are terminal in nature while the remaining four function as μ_2-bridging bidentate aqua ligands (Fig. 3). One of the two unique 4-nba anions functions as a free anion as in compound (**1**), while the second 4-nba anion functions as a μ_2-bridging bidentate ligand attached to the unique Na(I) ions Na1

Table 3—Hydrogen-bonding geometry for $[(H_2O)_4Li_2(\mu\text{-}H_2O)_2](4\text{-nba})_2$ (**1**) and $[Na(4\text{-nba})(H_2O)_3]_n$ (**2**)

D-H···A	*D*(D-H) (Å)	*D*(H···A) (Å)	*D*(D···A) (Å)	<DHA (°)	Symmetry code
$[(H_2O)_4Li_2(\mu\text{-}H_2O)_2](4\text{-nba})_2$ (**1**)					
O5-H1W···O6	0.79(4)	2.09(4)	2.876(3)	168(3)	-*x*+1, -*y*, -*z*
O5-H2W···O3	0.89(4)	2.16(4)	3.028(2)	165(3)	*x*+1, -*y*+½, *z*-½
O6-H3W···O2	0.79(3)	2.11(3)	2.855(2)	159(3)	-*x*+1, *y*-½, -*z*+½
O6-H4W···O2	0.92(3)	1.81(3)	2.721(2)	171(2)	*x*, *y*, *z*
O7-H5W···O1	0.92(3)	1.75(3)	2.663(2)	172(2)	-*x*+1, -*y*+1, -*z*
O7-H6W···O2	0.82(3)	2.06(3)	2.869(3)	172(2)	-*x*+1, *y*-½, -*z*+½
C3-H3···O3	0.93	2.60	3.323(3)	135	-*x*, -*y*+1, -*z*+1
$[Na(4\text{-nba})(H_2O)_3]_n$ (**2**)					
O21-H1O···O1	0.820	2.031	2.785	153	-*x*+1, -*y*+1, -*z*+1
O21-H2O···O11	0.820	2.105	2.924	178	*x*+1, *y*, *z*
O22-H3O···O1	0.820	1.984	2.780	164	*x*, *y*, *z*+1
O22-H4O···O11	0.820	1.957	2.777	178	-*x*+1, -*y*+1, -*z*+2
O23-H5O···O21	0.820	2.012	2.832	178	-*x*+2, -*y*+1, -*z*+2
O23-H6O···O12	0.820	2.001	2.800	164	*x*+1, *y*, *z*
O24-H7O···O12	0.820	2.108	2.908	165	*x*, *y*, *z*
O24-H8O···O1	0.820	2.013	2.802	161	*x*, *y*, *z*+1
O25-H9O···O12	0.820	1.983	2.765	159	*x*, *y*, *z*
O25-H10O···O2	0.820	1.888	2.707	176	-*x*+1, -*y*+2, -*z*+1
O26-H11O···O14	0.820	2.281	3.097	174	-*x*+1, -*y*+2, -*z*+1
O26-H11O···O13	0.820	2.633	3.181	126	-*x*+1, -*y*+2, -*z*+1
O26-H12O···O23	0.820	1.956	2.773	175	-*x*+2, -*y*+2, -*z*+2
C15-H15···O14	0.931	2.596	3.318	135	-*x*, 2-*y*, 1-*z*

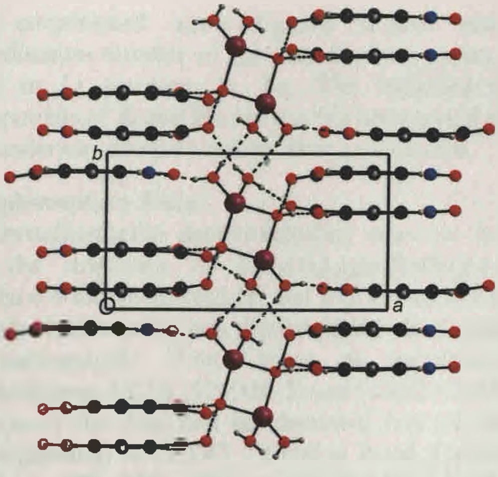

Fig. 2—A portion of the supramolecular chain of $[(H_2O)_4Li_2(\mu\text{-}H_2O)_2]^{2+}$ cations in (**1**) extending along *b* axis and flanked by 4-nitrobenzoate anions on either side.

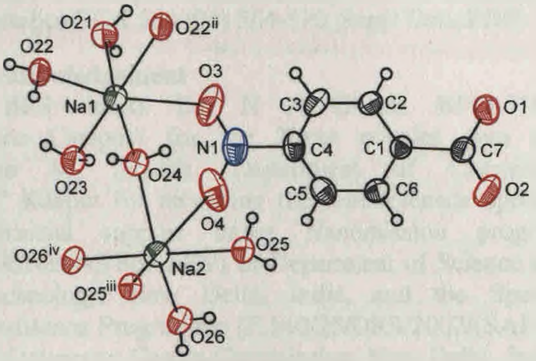

Fig. 3—Crystal structure of $[Na(4\text{-}nba)(H_2O)_3]_n$ (**2**) showing the coordination sphere of the unique Na(I) ions and atom-labeling scheme. Displacement ellipsoids are drawn at 50 % probability level except for the H atoms, which are shown as circles of arbitrary radius. For clarity, the free uncoordinated 4-nba anion in (**2**) is not shown. [Symmetry codes: (ii) -*x*+1, -*y*+1; -*z*+2; (iii) -*x*+1, -*y*+2, -*z*+2; (iv) -*x*+2, -*y*+2, -*z*+2].

and Na2 via the oxygen atoms O3 and O4 of the nitro functionality. The μ_2-bridging binding modes of the four aqua ligands results in a two-dimensional structure (Fig. 4). Although one of the 4-nba anions functions as a μ_2-bridging ligand, this binding mode alone does not lead to an extended structure (Supplementary Data Fig. S11). Each Na(I) in (**2**) is six coordinated and the observed Na-O distances and O-Na-O angles (Table 2) are in agreement with reported data[34]. Like in (**1**), two varieties of H-bonding interactions are observed (Table 3).

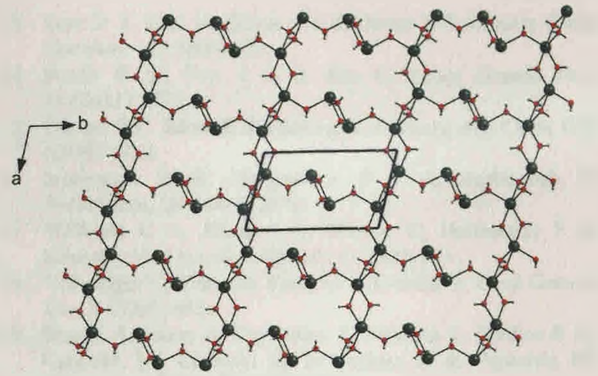

Fig. 4—A portion of the polymeric structure of $[Na(4\text{-}nba)\ (H_2O)_3]_n$ (**2**) due to bridging water ligands showing the 2-D architecture. For clarity the terminal water ligands on Na and the two unique 4-nba anions are not shown.

Table 4—Varying coordination number (C.N) of *s*-block metals

Compound	C.N.	Nuclearity	Ref.
$[(H_2O)_4Li_2(\mu\text{-}H_2O)_2](4\text{-}nba)_2$	4	Dimer	This work
$[Na(H_2O)_3(4\text{-}nba)]_n$	6, 6	Polymer	34 & this work
$[Rb(H_2O)_2(4\text{-}nba)]_n$	9	Polymer	CCDC 717713
$[Cs(H_2O)_2(4\text{-}nba)]_n$	9	Polymer	CCDC 717712
$[Mg(H_2O)_6](4\text{-}nba)_2\cdot 2H_2O$	6	Monomer	30
$[Ca(H_2O)_4(4\text{-}nba)_2]$	7	Monomer	41
$[Sr(H_2O)_7(4\text{-}nba)](4\text{-}nba)\cdot 2H_2O$	9	Monomer	42
$[Ba(H_2O)_5(4\text{-}nba)_2]_n$	9	Polymer	43

Recently we had shown that the charge balancing 4-nba anion is a versatile ligand and exhibits several bridging binding modes[39], in addition to binding in a monodentate or a bidentate fashion through the carboxylate oxygen atoms. A study of the 4-nba compounds of Li and Na reported in this work and earlier reported compounds[30,34,41-43] reveals some useful trends in terms of the coordination number of the *s*-block metals. All compounds listed in Table 4 contain coordinated water ligands and can be synthesized by an aqueous reaction of the *s*-block metal carbonate with 4-nbaH. In the alkali metal series, the lighter element Li exhibits a coordination number of four which increases to six on going to Na and a maximum value of nine is observed for the Rb and Cs compounds. In this series, the Li compound is a dimer, while all others are polymers. In the 4-nba compounds of Na, K, Rb and Cs, coordination of the central metal to the oxygen atom of the nitro functionality is observed. In contrast, for the alkaline earths, Mg exhibits a coordination number of six[30] which increases to seven on going to Ca[41] and attains the maximum value of nine for Sr[42] and Ba[43]. In the alkaline earth series excepting the Ba compound which is a one-dimensional polymer, all other compounds are zero-dimensional. A study of the known *s*-block metal compounds containing 4-nba and coordinated water ligands reveals that the coordination number of the central metal varies from four in Li to nine in Ba. The hydrated 4-nba compounds of K and Be are not yet known and efforts are underway to characterize these compounds.

Supplementary Data

Crystallographic data (excluding structure factors) for the structures of $[(H_2O)_4Li_2(\mu\text{-}H_2O)_2](4\text{-nba})_2$ (4-nba = 4-nitrobenzoate) (**1**) and $[Na(4\text{-nba})(H_2O)_3]$ (**2**) reported herein have been deposited with the Cambridge Crystallographic Data Centre as supplementary publication no. CCDC 822969 (**1**) and CCDC 822970 (**2**). Copies of the data can be obtained, free of charge, on application to CCDC, 12 Union Road, Cambridge CB2 1 EZ, UK. (Fax: +44-(0)1223-336033 or Email: deposit@ccdc. cam.ac.uk). Other supplementary data associated with this article, viz., (Figs S1-S11) are available in electronic form at http://www.niscair.res.in/jinfo/ijca/IJCA 51A(04) 564-570_Suppl Data.PDF.

Acknowledgement

BRS thanks Dr. N N Ghosh, BITS-Pilani (Goa Campus) for the X-ray powder data and Shri M. Saxena, Department of Chemistry, IIT Kanpur for recording the luminescence spectra. Financial support under Nanomission program (SR/NM/NS-86, 2009) of Department of Science and Technology, New Delhi, India, and the Special Assistance Programme [F.540/25/DRS/2007/(SAP-I)] of University Grants Commission, New Delhi, India, is gratefully acknowledged.

References

1 Banerjee D & Parise J B, *Cryst Growth Des*, 11 (2011) 4704 and references therein.
2 Fromm K M, *Coord Chem Rev*, 252 (2008) 856
3 Kim M K, Bae K L & Ok K M, *Cryst Growth Des*, 11 (2011) 930.
4 Liang P C, Liu K K, Yeh C T, Lin C H & Zima V, *Cryst Growth Des*, 11 (2011) 699.
5 Saalfrank R W, Scheurer A, Puchta R, Hampel F, Maid H & Heinemann F W, *Angew Chem Int Ed. Engl*, 46 (2007) 265.
6 Masci B, Pasquale S & Thuery P, *Cryst Growth Des*, 10 (2010) 2004.
7 Smith G, Wermutha U D, Young D J & White J M, *Polyhedron*, 26 (2007) 3645.
8 Nichol G S & Clegg W, *Polyhedron*, 25 (2006) 1043.
9 Srinivasan B R, Shetgaonkar S Y, Sawant J V & Raghavaiah P, *Polyhedron*, 27 (2008) 3299.
10 Starosta W & Leciejewicz J, *Acta Crystallogr*, 66E (2010) m1561.
11 Turner D R, Hatton J S & Batten S R, *Z Anorg Allg Chem*, 635 (2009) 439.
12 Chen S, Hoffmann S, Prots Y, Zhao J T & Kniep R, *Z Anorg Allg Chem*, 636 (2010) 1710.
13 Tran D T, Chu D, Oliver A J & Oliver S R J, *Inorg Chem Commun*, 12 (2009) 351.
14 Borah B M, Dey S K & Das G, *Cryst Growth Des*, 11 (2011) 2773.
15 Dietzel P C, Blom R & Fjellvag H, *Z Anorg Allg Chem*, 635 (2009) 1953.
16 Srinivasan B R, Shetgaonkar S Y & Raghavaiah P, *Polyhedron*, 28 (2009) 2879.
17 Williams C A, Blake A J, Wilson C, Hubberstey P & Schroder M, *Cryst Growth Des*, 8 (2008) 911.
18 Volkringer C, Marrot J, Ferey G & Loiseau T, *Cryst Growth Des*, 8 (2008) 685.
19 Rossin A, Ienco A, Costantino F, Montini T, Credico B D, Caporali M, Gonsalvi L, Fornasiero P & Peruzzini M, *Cryst Growth Des*, 8 (2008) 3302.
20 Srinivasan B R, Shetgaonkar S Y, Näther C & Bensch W, *Polyhedron*, 28 (2009) 534.
21 Fox S, Busching I, Barklage W & Strasdeit H, *Inorg Chem*, 46 (2007) 818.
22 Yusenko K, Fox S, Guni P & Strasdeit H, *Z Anorg Allg Chem*, 634 (2008) 2347.
23 Murugavel R & Korah R, *Inorg Chem*, 46 (2007) 11048 .
24 Ptasiewicz-Bak H & Leciejewicz J, *J Coord Chem*, 56 (2003) 173.
25 Wiesbrock F, Schier A & Schmidbaur H, *Z Naturforsch*, B57 (2002) 251.
26 Dale S H, Elsegood M R J & Kainth S, *Acta Crystallogr*, 59C (2003) m505.
27 Murugavel R, Karambelkar V V & Anantharaman G, *Indian J Chem*, 39A (2000) 843.
28 Srinivasan B R, Shetgaonkar S Y & Raghavaiah P, *Indian J Chem*, 48A (2009) 1662.
29 Morgant G, Angelo J, Desmaele D, Dichi E, Sghaier M, Fraisse B, Retailleau P, Brumas V, Fiallo M M L & Tomas A, *Polyhedron*, 27 (2008) 2097.
30 Srinivasan B R, Sawant J V, Näther C & Bensch W, *J Chem Sci*, 119 (2007) 243.
31 Indrani M, Ramasubramanian R, Fronczek F R, Braga D, Vasanthacharya N Y &. Kumaresan S, *J Chem Sci*, 121 (2009) 413.
32 Srinivasan B R, Shetgaonkar S Y & Näther C, *Z Anorg Allg Chem*, 637 (2011) 130.
33 Shrivastava H N & Speakman J C, *J Chem Soc*, (1961) 1151.
34 Turowska-Tyrk I, Krygowski T M, Gdaniec M, Hafelinger G & Ritter G, *J Mol Struc*, 172 (1988) 401.
35 Prabhakar S, Bhagwat V W, Vijaywargiya V & Poonia N S, *Curr Sci*, 53 (1984) 1287.
36 Srinivasan B R & Sawant S C, *Thermochim Acta*, 402 (2003) 45.
37 Sheldrick G M, *Acta Crystallogr*, 64A (2008) 112.
38 Regulska E, Samsonowicz M, Swislocka R & Lewandowski W, *J Phys Org Chem*, 20 (2007) 93.
39 Srinivasan B R, Shetgaonkar S Y, Saxena M & Näther C, *Indian J Chem*, 51A (2012) 435.
40 Kloskowska M, Chojnacki J, Wojnowski W & Becker B, *Acta Crystallogr*, 62C (2006) m541.
41 Srinivasan B R, Sawant J V & Raghavaiah P, *Indian J Chem*, 45A (2006) 2392.
42 Srinivasan B R, Raghavaiah P & Sawant J V, *Acta Crystallogr*, 63E (2007) m2251.
43 Srinivasan B R, Sawant J V, Sawant S C & Raghavaiah P *J Chem Sci*, 119 (2007) 593.

DOI: 10.1002/zaac.201000214

Preparation, Crystal Structures, and Thermal Studies of Alkaline Earth Nitrocarboxylates

Bikshandarkoil R. Srinivasan,*[a] **Santosh Y. Shetgaonkar,**[a] **and Christian Näther***[b]

Dedicated to Professor Srinivasan Chandrasekaran on the Occasion of His 65th Birthday

Keywords: Coordination compounds; Polymers; Calcium; Magnesium; 4-Nitrobenzoate; Pyrazole

---

Abstract. The preparation, crystal structures, and thermal properties of $[Ca(pyr)_2(4\text{-nba})_2]_n$ (**1**) (pyr = pyrazole; 4-nba = 4-nitrobenzoate) $\{[Ca(H_2O)_2(3\text{-npth})]\cdot H_2O\}_n$ (**2**) (3-npth = 3-nitrophthalate), $[Mg(H_2O)_5(3\text{-npth})]\cdot 2H_2O$ (**3**), and $[Mg(H_2O)_4(2\text{-nba})_2]$ (**4**) (2-nba = 2-nitrobenzoate) are reported. The anhydrous Ca^{II} compound **1** and the diaqua Ca^{II}-3-nitrophthalate monohydrate **2** are one-dimensional coordination polymers containing a hexacoordinate Ca^{II} ion located on a center of inversion in **1** and a heptacoordinated Ca^{II} ion in **2**. In **1**, the 4-nitrobenzoate moiety acts as a μ_2-bridging bidentate ligand, whereas the 3-nitrophthalate anion exhibits a μ_3-bridging pentadentate coordination mode in **2**. The hexacoordinate Mg^{II}-containing compounds **3** and **4** do not contain a $[Mg(H_2O)_6]^{2+}$ unit and the central Mg^{II} ion is coordinated to at least one monodentate carboxylate unit namely the monodentate 3-npth molecule in **3** and two *trans* monodentate 2-nba molecules in **4**. Hydrogen bonding between the lattice water molecules results in the formation of a water dimer in **3**. A comparative study of 17 alkaline earth nitrocarboxylates is described.

Introduction

The study of coordination polymers is a topical research area [1–2]. Compared to the extensive chemistry of coordination polymers based on transition metals [2], the coordination chemistry of group 1 and 2 metal compounds with organic linkers has remained a relatively less explored area. The reluctance in using alkaline earth cations as building blocks for coordination polymers can be attributed to their unpredictable coordination numbers and arrangements as no ligand field stabilization effects govern their bonding. The closed shell s-block metal cations lack intrinsically useful properties like magnetism or variable oxidation states. However, they do have some advantages for application in materials science as they are non toxic, cheap, and generally amenable to aqueous preparation. For these reasons alkaline earth salts are the preferred formulations for a host of commercial materials, including many common pharmaceuticals and colorants. Hence, in the recent years interest in the chemistry of coordination compounds of alkali and alkaline-earth metal cations has been growing [3–8]. In a recent article, *Fromm* reviewed the different ligand and polymer types of s-block compounds [9].

In view of their high affinity for oxygen donors [10], especially water, alkaline earth coordination polymers are normally synthesized in aqueous medium under ambient conditions by reactions between alkaline earth metal sources and multidentate oxygen donor ligands (aromatic carboxylic acids) [7–8]. For compound synthesis many groups have employed hydrothermal reactions, which involve the reactions of metal sources with carboxylic acids in autoclaves under autogenous pressure [11–15]. The metal sources usually employed for product formation in the above reactions are metal carbonates or hydroxides or metal halides/nitrates. As part of our longstanding research interest in the chemistry of alkaline earth carboxylates [16], we have investigated the reactions of alkaline earth metal carbonates with aromatic nitrocarboxylic acids like 4-nitrobenzoic acid (4-nbaH), 2-nitrobenzoic acid (2-nbaH), and 2-carbamoyl-4-nitrobenzoic acid (Scheme 1) in aqueous media and have unraveled a rich chemistry of alkaline earth nitrocarboxylates [17–27].

In the present work, we have investigated the reactions of MCO_3 (M = Mg, Ca) with 3-nitrophthalic acid (3-npthH_2) and 2-nbaH and have synthesized $\{[Ca(H_2O)_2(3\text{-npth})]\cdot H_2O\}_n$ (**2**) (3-npth = 3-nitrophthalate), $[Mg(H_2O)_5(3\text{-npth})]\cdot 2H_2O$ (**3**) and $[Mg(H_2O)_4(2\text{-nba})_2]$ (**4**) (2-nba = 2-nitrobenzoate). A report on the structure of the polymeric Ca^{II} compound based on 3-nitrophthalate **2** has recently appeared [28]. In recent work [22, 23] we have demonstrated that a zero-dimensional compound $[Ca(H_2O)_4(4\text{-nba})_2]$ can be readily transformed into a one-di-

---

* Prof. Dr. B. R. Srinivasan
E-Mail: srini@unigoa.ac.in
* PD Dr. C. Näther
E-Mail: cnaether@ac.uni-kiel.de
[a] Department of Chemistry
Goa University
Goa 403 206, India
[b] Institut für Anorganische Chemie
Christian-Albrechts-Universität Kiel
Max-Eyth Straße 2
24118 Kiel, Germany

Supporting Information for this article is available on the WWW under **http://dx.doi.org/10.1002/zaac.201000214** or from the author.

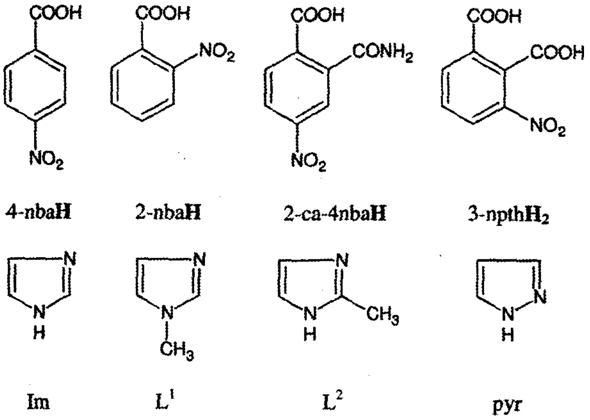

Scheme 1. Nomenclature of ligands relevant to this study.

mensional coordination polymer by reaction with N-donor ligands like N-methylimidazole (L^1) or 2-methylimidazole (L^2) (Scheme 1). In continuation of this, we have structurally characterized a new Ca^{II} coordination polymer $[Ca(pyr)_2(4\text{-nba})_2]_n$ (pyr = pyrazole) (**1**) based on 4-nitrobenzoate. The preparation, crystal structures, spectral and thermal properties of compounds **1**–**4** are described herein.

Results and Discussion

Description of Crystal Structures of 1–4

Compounds **1**, **3**, and **4** crystallize in the centrosymmetric triclinic space group $P\bar{1}$, whereas **2** crystallizes in the centrosymmetric monoclinic space group $P2_1/c$. In compounds **1** and **4** the central metal ion (Ca in **1** and Mg in **4**) is located on a center of inversion, whereas in **2** and **3** all atoms are situated in general positions. Except compound **2**, where the calcium ion is heptacoordinated, the calcium (in **1**) and magnesium ions (in **3** and **4**) are hexacoordinated. The coordination spheres of the central metal ions are $\{CaN_2O_4\}$, $\{CaO_7\}$ in **1** and **2**, and $\{MgO_6\}$ in **3** and **4** (Figure 1). The calculated bond valence sums [29] from the crystallographic data for the central metal ions in **1** to **4** are 2.23, 2.18, 2.10 and 2.11 respectively. The structural parameters of the organic ligands in **1** to **4** are in normal range.

The crystal structure of **1** consists of a central Ca^{II} ion, a terminal pyrazole ligand and a (μ_2-η^1:η^1) bridging 4-nitrobenzoate molecule (Figure 1a). Each Ca^{II} ion is linked to two symmetry related terminal pyrazole molecules and four oxygen atoms of four symmetry related 4-nba anions resulting in a distorted $\{CaN_2O_4\}$ coordination polyhedron around Ca^{II}. The *trans* O–Ca–O and N–Ca–N angles exhibit ideal values, whereas the *cis* O–Ca–O and O–Ca–N angles range from 84.56(4) to 95.44(4)° (Supporting Information Table S1) indicating a distortion of the $\{CaN_2O_4\}$ octahedron. The terminal Ca–N bond length of 2.4886(13) Å is slightly shorter than the reported Ca–N distances 2.5088(14) and 2.5024(13) Å in $[Ca(L^1)(4\text{-nba})_2]_n$ [22] and $[Ca(H_2O)(L^2)(4\text{-nba})_2]_n$ [23]. The (μ_2-η^1:η^1) bridging 4-nba ligand makes a short Ca–O bond at 2.3144(11) Å and is linked to an adjacent calcium atom at a longer distance of 2.3722(11) Å resulting in the formation of an infinite chain structure. The polymeric structure of **1** is based on a dimeric building block (Supporting Information Figure S1). A pair of (μ_2-η^1:η^1) bridging 4-nba ligands link a pair of $\{Ca(pyr)_2\}$ units leading to the formation of a one dimensional polymer extending along the *a* axis with a long Ca···Ca separation of 5.335(1) Å (Figure 2, Supporting Information Figure S2).

A scrutiny of the crystal structure of **1** reveals several weak secondary interactions. The amine hydrogen atom in pyrazole and four hydrogen atoms (two each) from the 4-nba and pyrazole molecules function as hydrogen-donors, whereas the carboxylate and nitro oxygen atoms except O1 function as hydrogen-acceptors resulting in five hydrogen bonds comprising of an intramolecular N–H···O and four intermolecular C–H···O interactions (Table S2). All C–H···O interactions observed in **1** are between a hydrogen donor from either the 4-nba or pyr units in one chain with an oxygen atom in an adjacent chain and can be termed as interchain interactions. Thus, the intermolecular C12–H12···O4 interaction between the pyrazole hydrogen atom and the nitro oxygen atom links two adjacent one dimensional chains (Figure S3) and extends the network.

The structure of **2** consists of a central Ca^{II} ion, an unique 3-npth dianion, two terminal water molecules, and a lattice water molecule (Figure 1b). The central metal ion is heptacoordinated and linked to five oxygen atoms from three symmetry related bridging 3-nitrophthalate anions, two terminal water molecules resulting in a distorted pentagonal bipyramidal $\{CaO_7\}$ polyhedron (Figure S4). The Ca–O bond lengths vary between 2.3310(9) to 2.6301(9) Å, whereas the O–Ca–O angles range from 51.43(3) to 157.73(3)° (Table S1). The 3-npth moiety acts as a bridging pentadentate ligand (Figure S4). The carboxylate group (O3, O4) adjacent to the nitro functionality acts as a bridging bidentate ligand and is linked to a calcium atom by O4 at a distance of 2.3718(9) Å and is bridged to a symmetry related calcium atom through O3 at 2.3669(9) Å resulting in a Ca···Ca separation of 4.860(18) Å. The distant carboxylate ligand (O1, O2) meta to $-NO_2$ group functions as a bridging tridentate ligand with the O1 and O2 atoms linked to a Ca^{II} ion in a bidentate fashion at 2.6301(9) and 2.4516(9) Å, respectively, and the O2 atom is further linked to a symmetry related calcium atom at 2.3504(9) Å with a shorter Ca···Ca separation of 3.902(12) Å. The net result of the pentadentate coordination of the 3-npth ligand is the formation of an infinite chain extending along the *a* axis with alternating Ca···Ca separations of 3.902(5) and 4.860(18) Å, respectively (Figure 2).

Unlike in compound **1**, the nitro group in **2** is not involved in any C–H···O interactions, where neighboring chains are linked by O–H···O bonds involving nitro oxygen atoms and hydrogen atoms of coordinated water molecules. It has to be noted that C–H···O interactions involving the nitro group, which have been reported for many nitrobenzoates [22–27, 30] are not observed in the 3-nitrophthalate compounds **2** and **3**. Compound **2** exhibits only O–H···O interactions (Table S2) involving the hydrogen atoms of coordinated and lattice water

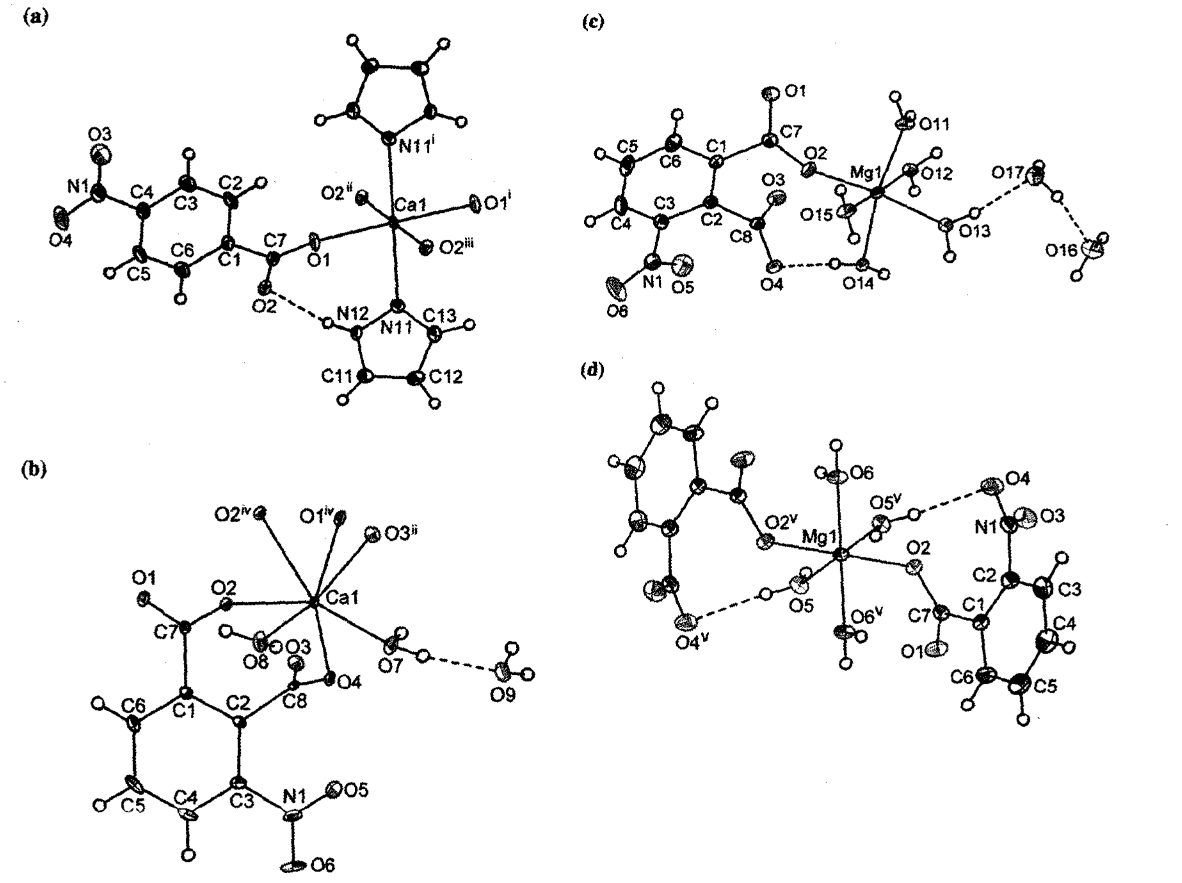

Figure 1. A view of the coordination sphere of the central metal ion in $[Ca(pyr)_2(4\text{-}nba)_2]_n$ (**1**) (a) $\{[Ca(H_2O)_2(3\text{-}npth)]\cdot H_2O\}_n$ (**2**) (b), $[Mg(H_2O)_5(3\text{-}npth)]\cdot 2H_2O$ (**3**) (c) and $[Mg(H_2O)_4(2\text{-}nba)_2]$ (**4**) (d) showing the atom-labeling scheme. Displacement ellipsoids are drawn at the 50 % probability level excepting for the hydrogen atoms, which are shown as circles of arbitrary radius. Intramolecular hydrogen-bonding is shown as broken lines. Symmetry codes: i) $-x+2, -y+1, -z+1$; ii) $-x+1, -y+1, -z+1$; iii) $x+1, y, z$; iv) $-x, -y+1, -z+1$; v) $-x+1, -y+1, -z$.

molecules (hydrogen-donors) and the oxygen atoms of nitro and carboxylate groups and the lattice water molecule (Figure S3 and Figure S5).

The structure of **3** consists of a hexacoordinate Mg^{II} atom coordinated to a monodentate 3-npth ligand, five terminal water molecules, and two lattice water molecules (Figure 1c). It is to be noted that the bonding situation in **3** is different from that normally observed for several known Mg^{II} compounds consisting of an octahedral $[Mg(H_2O)_6]^{2+}$ unit [19, 26, 31–34]. The *trans* O–Mg–O angles deviate from ideal values and range from 169.73(4) to 176.70(5)°, whereas the *cis* O–Mg–O angles range between 84.20(4) and 100.47(5)° (Table S1) indicating a distortion of the $\{MgO_6\}$ octahedron. The Mg–O bond lengths scatter in a very narrow range between 2.0351(11) to 2.1255(8) Å. The npth dianion functions as a monodentate ligand and makes a Mg–O bond at 2.0351(11) Å. The supramolecular structure of **3** is similar to that of **2**, only O–H···O interactions (Table S2) between the hydrogen atoms of coordinated and lattice water molecules and all the oxygen atoms except O2, O11, and O15 are observed. The O17–H13O···O16 bond between the lattice water molecules O16 and O17 results in the formation of a water dimer, which is hydrogen-bonded to six different $[Mg(H_2O)_5(3\text{-}npth)]$ units (Figure S6). The water dimers are linked into an infinite hydrogen-bonded chain along the *a* axis (Figure 3) by the O1 atom of a 3-npth ligand with the aid of O17–H14O···O1 and O16–H12O···O1 interactions.

The structure of **4** consists of a central Mg^{II} ion in a special position, two terminal water molecules and a monodentate 2-nba ligand. The Mg^{II} ion is linked to four symmetry related terminal water molecules, which lie on a square plane and two symmetry related *trans*-monodentate 2-nba ligands complete the hexacoordination around the Mg^{II} ion (Figure 1d). It is interesting to note that **4** is monomeric unlike the 2-nitrobenzoates of calcium [25] and barium [24], which are one-dimensional polymers with the 2-nba ligand acting as a tridentate ligand in the calcium and barium polymers. Compound **4** with Mg and H_2O in a 1:4 ratio and two *trans* 2-nba ligands differs from the related 4-nba compound $[Mg(H_2O)_6](4\text{-}nba)_2\cdot 2H_2O$ [19] and several other Mg^{II} carboxylates with a $[Mg(H_2O)_6]^{2+}$ unit, which is charge balanced by uncoordinated carboxylate ligands [26, 31–34]. The *trans* O–Mg–O angles exhibit ideal values, whereas the *cis* O–Mg–O angles deviate slightly and range from 88.16(4) to 91.84(4)° indicating a slight distortion of the $\{MgO_6\}$ octahedron. The Mg–O bond lengths scatter

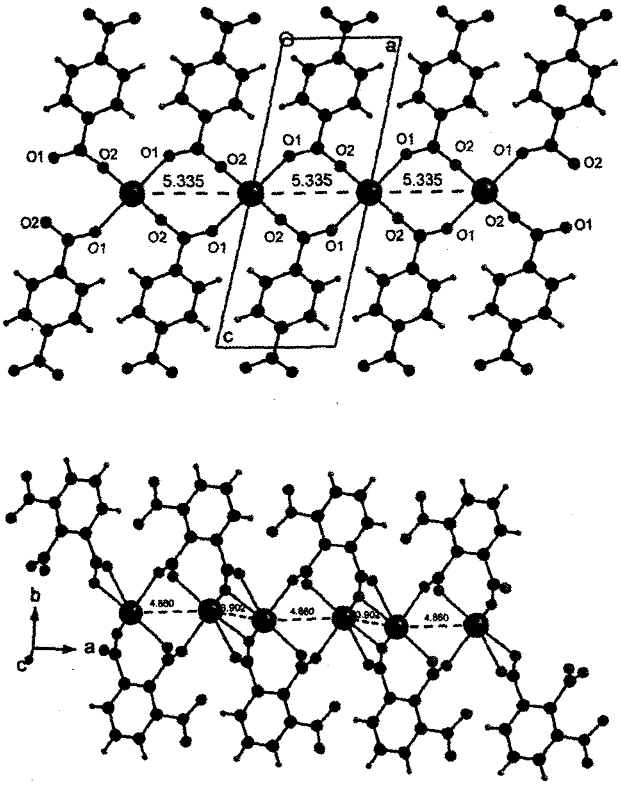

Figure 2. A portion of the 1D polymeric chain extending along the *a* axis in $[Ca(pyr)_2(4\text{-}nba)_2]_n$ (**1**) with a Ca···Ca separation of 5.335 Å (top). A part of the infinite chain extending along the *a* axis in $\{[Ca(H_2O)_2(3\text{-}npth)]\cdot H_2O\}_n$ (**2**) with alternating Ca···Ca distances of 4.860 and. 3.902 Å (bottom). For clarity the terminal pyrazole ligands in **1** and coordinated and lattice waters in **2** are not included and shown in Supporting Information Figure S2.

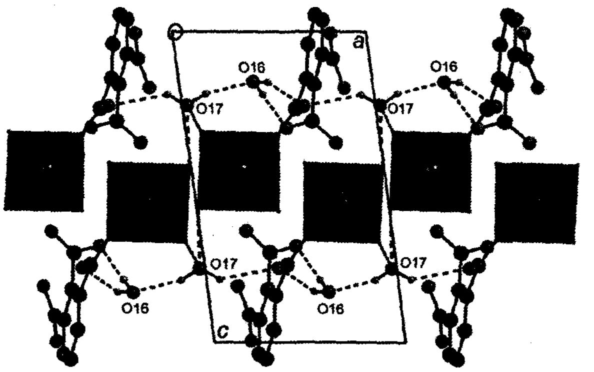

Figure 3. The O1 atom of $[Mg(H_2O)_5(3\text{-}npth)]\cdot 2H_2O$ (**3**) links adjacent water dimers into a hydrogen-bonded chain along the *a* axis. $\{MgO_6\}$ units are represented as open octahedra.

between 2.0638(9) and 2.1045(8) Å (Table S1). The monodentate 2-nba ligand makes a Mg–O bond at 2.1045(8) Å. Compound **4** is involved in two varieties of hydrogen bonds, which includes four O–H···O, and two C–H···O interactions (Table S2). Both the weak intermolecular C–H···O interactions link neutral molecules of **4** into a two dimensional network (Figure 4).

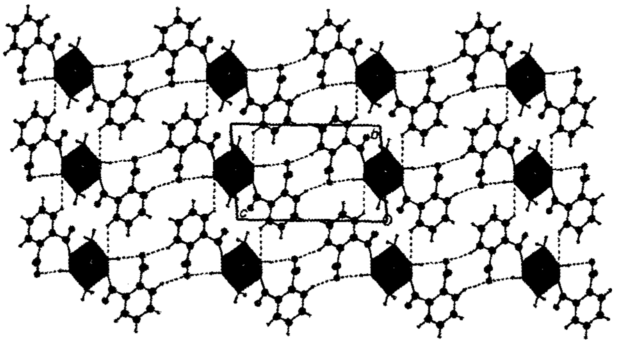

Figure 4. A view of the crystallographic packing of $[Mg(H_2O)_4(2\text{-}nba)_2]$ (**4**) showing the hydrogen-bonding characteristics of the nitro functionality. O–H···O and C–H···O interactions are shown as broken lines. $\{MgO_6\}$ units are represented as open octahedra.

Comparative Study of Alkaline Earth Nitrocarboxylates

The availability of structural data for several alkaline earth nitrocarboxylates [17–27] permits a comparative study, the details of which are described below (Table 1). All known alkaline earth nitrocarboxylates crystallize in centrosymmetric space groups. The Ba^{II} compounds and six Ca^{II} compounds listed in Table 1 are one dimensional coordination polymers, whereas all other compounds except the dimeric $[Mg(H_2O)(L^1)_2(4\text{-}nba)_2]_2$ (L^1 = N-methylimidazole) are monomers. All structurally characterized Mg^{II} nitrocarboxylates are octahedral, whereas the Sr^{II} and Ba^{II} compounds show nonacoordination. The coordination number of Ca^{II} ranges from 6 to 8. In the heavier congeners, the central Sr^{II} or Ba^{II} ion is only surrounded by oxygen donors, whereas for the lighter elements Mg^{II} and Ca^{II}, compounds containing both oxygen and nitrogen donors are known. Nitrogen donor ligands can be incorporated into the metal coordination sphere by reaction of $[Mg(H_2O)_6](4\text{-}nba)_2\cdot 2H_2O$ or $[Ca(H_2O)_4(4\text{-}nba)_2]_n$ with the corresponding N-donor ligand. In the case of Ca^{II}, the incorporation of N-methylimidazole, 2-methylimidazole, or pyrazole results in the formation of a one dimensional polymer. It is interesting to note that the use of pyrazole results in a polymer, wherein the Ca:N ratio is 1:2. The centrosymmetric alkaline earth nitrocarboxylates exhibit a rich supramolecular chemistry. All compounds excepting the anhydrous compounds $[Ca(L^1)(4\text{-}nba)_2]_n$ and $[Ca(pyr)_2(4\text{-}nba)_2]_n$ exhibit O–H···O interactions with the hydrogen atom of coordinated water functioning as hydrogen-donors. In the coordination polymers based on 4-nba, 2-ca-4nba, and 2-nba, the nitro group in one chain is linked to an adjacent chain by C–H···O interactions. However this feature is not observed in the 3-nitrophthalate compounds of calcium.

Synthetic Aspects and Properties

The anhydrous compound $[Ca(pyr)_2(4\text{-}nba)_2]$ (**1**) was synthesized in a two step process, the first step involves the synthesis

Table 1. Comparative structural features of alkaline-earth nitrocarboxylates.

Compound[a)]	C.S.[b)]	Space Group	Nuclearity	H-bonding	Ref
$[Mg(H_2O)_6](4\text{-nba})_2\cdot 2H_2O$	$\{MgO_6\}$	$P\bar{1}$	monomer	O–H···O	[19]
$[Mg(H_2O)_6](2\text{-ca-4nba})_2$	$\{MgO_6\}$	$P2_1/c$	monomer	O–H···O, N–H···O, C–H···O	[26]
$[Mg(H_2O)_5(3\text{-npth})]\cdot 2H_2O$ (**3**)	$\{MgO_6\}$	$P\bar{1}$	monomer	O–H···O	This work
$[Mg(H_2O)_4(2\text{-nba})_2]$ (**4**)	$\{MgO_6\}$	$P\bar{1}$	monomer	O–H···O, C–H···O	This work
$[Ca(H_2O)_4(4\text{-nba})_2]_n$	$\{CaO_7\}$	$P2_1/c$	monomer	O–H···O, C–H···O	[17]
$[Sr(H_2O)_7(4\text{-nba})](4\text{-nba})\cdot 2H_2O$	$\{SrO_9\}$	$P2_1/c$	monomer	O–H···O, C–H···O	[20]
$[Ba(H_2O)_5(4\text{-nba})_2]_n$	$\{BaO_9\}$	$P2_1/c$	polymer	O–H···O, C–H···O	[21]
$[Ba(H_2O)_3(2\text{-nba})_2]_n$	$\{BaO_9\}$	$P\bar{1}$	polymer	O–H···O, C–H···O	[24]
$[Ca(H_2O)_2(2\text{-nba})_2]_n$	$\{CaO_8\}$	$P\bar{1}$	polymer	O–H···O, C–H···O	[25]
$[Ca(H_2O)_2(2\text{-ca-4nba})_2]_n$	$\{CaO_7\}$	$P\bar{1}$	polymer	O–H···O, N–H···O, C–H···O	[27]
$\{[Ca(H_2O)_2(3\text{-npth})]\cdot H_2O\}_n$ (**2**)	$\{CaO_7\}$	$P2_1/c$	polymer	O–H···O	[28], this work
$[Mg(H_2O)_2(Im)_2(4\text{-nba})_2]$	$\{MgO_4N_2\}$	$P\bar{1}$	monomer	O–H···O, N–H···O	[18]
$[Mg(H_2O)(L^1)_2(4\text{-nba})_2]_2$	$\{MgO_4N_2\}$	$P\bar{1}$	dimer	O–H···O	[19]
$[Ca(H_2O)_3(Im)(4\text{-nba})_2]\cdot Im$	$\{CaO_5N\}$	$P2_1/c$	monomer	O–H···O, N–H···O, O–H···N	[18]
$[Ca(L^1)(4\text{-nba})_2]_n$	$\{CaO_5N\}$	$P\bar{1}$	polymer	C–H···O	[22]
$[Ca(H_2O)(L^2)(4\text{-nba})_2]_n$	$\{CaO_6N\}$	$P2_1/n$	polymer	O–H···O, N–H···O, C–H···O	[23]
$[Ca(pyr)_2(4\text{-nba})_2]_n$ (**1**)	$\{CaO_4N_2\}$	$P\bar{1}$	polymer	N–H···O, C–H···O	This work

a) 4-nba = 4-nitrobenzoate; 2-ca-4nba = 2-carbamoyl-4-nitrobenzoate; 3-npth = 3-nitrophthalate; 2-nba = 2-nitrobenzoate; Im = imidazole; L^1 = N-methylimidazole; L^2 = N-methylimidazole; pyr = pyrazole. b) C.S. = Coordination sphere of the central metal ion.

of a monohydrate $[Ca(H_2O)(4\text{-nba})_2]$ by partial dehydration of $[Ca(H_2O)_4(4\text{-nba})_2]$. The reaction of the monohydrate with pyrazole (pyr) afforded the anhydrous compound **1** in good yield. Crystals suitable for X-ray structure analysis were prepared by recrystallizing from an aqueous solution in the presence of excess pyrazole. The mixed ligand compound **1** could also be prepared by a direct reaction of an intimate mixture of $[Ca(H_2O)_4(4\text{-nba})_2]$ with pyr (Supporting Information Scheme S1). The methodology employed for the synthesis of **1** is similar to our recently reported synthesis of $[Ca(Im)(4\text{-nba})_2]$ (Im = imidazole) or $[Ca(L^1)(4\text{-nba})_2]_n$ (L^1 = N-methylimidazole) [22]. It is interesting to note that the use of pyrazole, which is a positional isomer of Im, has resulted in the formation of an anhydrous compound with a Ca:N-donor ligand (pyr) in a 1:2 ratio.

The aqueous compounds **2**–**4** were prepared by reaction of metal carbonate (Ca for **2**; Mg for **3** and **4**) with the corresponding nitrocarboxylic acid in a 1:1 (for **2** and **3**) and 1:2 (for **4**) molar ratio (Supporting Information Scheme S1). Compounds **2** to **4** could also be prepared by reacting an aqueous solution of MCl_2 (M = Ca or Mg) with *in situ* generated sodium salt of the nitrocarboxylic acid namely 3-npthH_2 or 2-nbaH. The $Mg:H_2O$ ratio is 1:7 and 1:4 in **3** and **4**, respectively. From crystal structure analysis, it is evident that compound **3** contains five coordinated and two lattice water molecules. Several known structurally characterized Mg^{II} carboxylates crystallized from aqueous solutions under ambient conditions, contain an octahedral $[Mg(H_2O)_6]^{2+}$ unit, which is charge balanced by the carboxylate moiety [31–34]. In contrast, the central Mg^{II} ion in **3** and **4** contains a monodentate carboxylate unit bonded to the Mg^{II} ion. It is observed that Mg^{II} compounds synthesized under solvothermal conditions contain less water per magnesium atom and in many cases the $Mg:H_2O$ ratio is 1:2 [15]. The composition of the synthesized compounds **1** to **4** was determined based on the analytical data and the metal oxide formed by heating in a furnace at 800 °C. The details of spectral and thermal characteristics of **1** to **4** are given in the Supporting Information.

Conclusions

In this study, the preparation, crystal structures, spectral, and thermal characteristics of $[Ca(pyr)_2(4\text{-nba})_2]_n$ (**1**) $\{[Ca(H_2O)_2(3\text{-npth})]\cdot H_2O\}_n$ (**2**), $[Mg(H_2O)_5(3\text{-npth})]\cdot 2H_2O$ (**3**), and $[Mg(H_2O)_4(2\text{-nba})_2]$ (**4**) are described. The Ca^{II} compounds **1** and **2** exhibit one-dimensional structures, whereas the Mg^{II} compounds **3** and **4** are zero dimensional. The observed trend of a higher dimensionality for larger metal ions is in accordance with literature report [12]. The anhydrous compound **1** containing terminal pyrazole ligands is a new Ca^{II} coordination polymer based on 4-nitrobenzoate. The use of 3-nitrophthalate or 2-nitrobenzoate has resulted in the hexacoordinate Mg^{II} compounds **3** and **4**, which contain five and four molecules of coordinated water respectively. Compound **3** can be considered as a molecular container for a water dimer. The nitrophthalate compounds **2** and **3** do not exhibit any C–H···O interactions and differ from other reported alkaline earth 2- and 4-nitrobenzoates. A comparative study of the known alkaline earth nitrocarboxylates reveals the rich structural chemistry of this group of compounds.

Experimental Section

Materials and Methods: All chemicals used in this study were of reagent grade and were used as received. The known compound $[Ca(H_2O)_4(4\text{-nba})_2]$ was prepared by a reported procedure [17]. All starting materials and reaction products are air stable and hence were prepared under normal laboratory conditions. The 4-nitrobenzoate (4-nba) content of **1** was determined as the insoluble 4-nbaH as described earlier [35]. Details of instrumentation as well as the procedures for the preparation of compounds **1** to **4** and their spectroscopic data are given in Supplementary Material.

Table 2. Crystal data and structure refinement for $[Ca(L^3)_2(4\text{-nba})_2]_n$ (**1**), $\{[Ca(H_2O)_2(3\text{-npth})]\cdot H_2O\}_n$ (**2**), $[Mg(H_2O)_5(3\text{-npth})]\cdot 2H_2O$ (**3**), and $[Mg(H_2O)_4(2\text{-nba})_2]$ (**4**).

	$[Ca(pyr)_2(4\text{-nba})_2]_n$ (**1**)	$\{[Ca(H_2O)_2(3\text{-npth})]\cdot H_2O\}_n$ (**2**)	$[Mg(H_2O)_5(3\text{-npth})]\cdot 2H_2O$ (**3**)	$[Mg(H_2O)_4(2\text{-nba})_2]$ (**4**)
Empirical formula	$C_{20}H_{16}CaN_6O_8$	$C_8H_9CaNO_9$	$C_8H_{17}MgNO_{13}$	$C_{14}H_{16}MgN_2O_{12}$
Formula weight /g·mol^{-1}	508.47	303.24	359.54	428.60
Temperature /K	170(2)	170(2)	170(2)	170(2)
Wavelength /Å	0.71073	0.71073	0.71073	0.71073
Crystal system	Triclinic	Monoclinic	Triclinic	Triclinic
Space group	$P\bar{1}$	$P2_1/c$	$P\bar{1}$	$P\bar{1}$
a /Å	5.3346(5)	6.1289(4)	7.3921(5)	5.2587(5)
b /Å	7.8475(8)	20.9606(11)	8.6642(6)	7.6309(7)
c /Å	13.7756(14)	8.9218(6)	12.0943(9)	11.7095(10)
α /°	96.582(12)	90	76.948(9)	81.745(11)
β /°	99.934(12)	96.006(8)	81.120(8)	78.443(10)
γ /°	107.703(12)	90	82.391(8)	73.797(11)
Volume /Å^3	532.50(9)	1139.85(12)	741.7(9)	440.15(7)
Z	1	4	2	1
Density (calculated) /mg·m^{-3}	1.586	1.767	1.610	1.617
Absorption coefficient /mm^{-1}	0.358	0.596	0.191	0.174
$F(000)$	262	624	376	222
θ range for data collection /°	2.77 to 27.00	2.49 to 28.03	2.43 to 28.06	2.79 to 27.94
Crystal size /mm	0.3 × 0.2 × 0.2	0.2 × 0.1 × 0.1	0.15 × 0.1 × 0.1	0.3 × 0.2 × 0.2
Index ranges	$-6 \le h \le 6$ $-10 \le k \le 10$ $-17 \le l \le 17$	$-8 \le h \le 8$ $-27 \le k \le 27$ $-11 \le l \le 11$	$-9 \le h \le 9$ $-11 \le k \le 11$ $-15 \le l \le 15$	$-6 \le h \le 6$ $-10 \le k \le 10$ $-15 \le l \le 15$
Reflections collected	4537	13362	7767	4989
Independent reflections	2261[R(int) = 0.0327]	2645 [R(int) = 0.0387	3419 [R(int) = 0.0370	2007 [R(int) = 0.0423
Completeness to θ /%	97.4	96.3	95.1	95.2
Refinement method	Full-matrix least-square on F^2			
Data / restraints / parameters	2261 / 0 / 161	2645 / 0 / 173	3419 / 0 / 212	2007 / 0 / 134
Goodness-of-fit on F^2	1.045	1.043	1.043	1.019
Final R indices [$I > 2\sigma(I)$]	$R_1 = 0.0356$, $wR_2 = 0.0916$	$R_1 = 0.0252$, $wR_2 = 0.0653$	$R_1 = 0.0364$, $wR_2 = 0.0967$	$R_1 = 0.0346$, $wR_2 = 0.0931$
R indices (all data)	$R_1 = 0.0439$, $wR_2 = 0.0957$	$R_1 = 0.0292$, $wR_2 = 0.0668$	$R_1 = 0.0457$, $wR_2 = 0.1014$	$R_1 = 0.0427$, $wR_2 = 0.0966$
Extinction coefficient	0.070(12)	0.016(2)	0.062(7)	0.092(16)
Largest diff. peak and hole /e·Å^{-3}	0.380 and –0.433	0.357and –0.314	0.335 and –0.315	0.273 and –0.339
Bond valence sum[a] of central metal	2.23	2.18	2.10	2.11

a) Bond valence sums were determined from the crystallographic data using the software Valist [29].

Crystal Structure Determination: Intensity data for **1**–**4** were collected on an Image Plate Diffraction System (IPDS-1) from STOE using graphite-monochromated Mo-K_α radiation. The structures were solved with direct methods using SHELXS-97 [36] and refinement was done against $|F|^2$ using SHELXL-97 [36]. All non-hydrogen atoms were refined anisotropically. Aromatic hydrogen atoms were introduced on calculated positions and included in the refinement riding on their respective parent atoms. The hydrogen atoms attached to the nitrogen of pyrazole in **1** and the water molecules in **2** to **4** were located in the difference Fourier map but were positioned with idealized geometry and refined using a riding model. Selected crystal refinement results for compounds **1**–**4** are listed in Table 2.

Crystallographic data (excluding structure factors) for the structures reported in this paper have been deposited with the Cambridge Crystallographic Data Centre as supplementary publication no. CCDC-769298 (**1**), CCDC-769299 (**2**), CCDC-769300(**3**), and CCDC-769301 (**4**). Copies of the data can be obtained, free of charge, on application to CCDC, 12 Union Road, Cambridge CB2 1 EZ, UK. (Fax: +44-1223-336033, http://www.ccdc.cam.ac.uk/conts/retrieving.html; E-Mail: deposit@ccdc.cam.ac.uk).

Supporting Information (see footnote on the first page of this article): Additional pictures related to crystal structure, figures of diffused reflectance and infrared spectra, thermograms, details of spectral and thermal characteristics and procedures for the synthesis of **1** to **4** (Figures S1–S10, Scheme S1, Tables S1–S2).

Acknowledgement

The authors thank *Prof. Dr. W. Bensch*, University of Kiel, for permission to use his equipment and helpful discussions. BRS thanks the *University Grants Commission*, (UGC) New Delhi for financial support under the Special Assistance Program.

References

[1] a) C. Janiak, *Dalton Trans.* **2003**, 2781; b) A. Y. Robin, K. M. Fromm, *Coord. Chem. Rev.* **2006**, *250*, 2127.

[2] S. R. Batten, S. M. Neville, D. R. Turner, *Coordination Polymers: Design, Analysis and Application*, RSC Publishing, Cambridge UK, **2009**.

[3] a) M. Dinca, J. R. Long, *J. Am. Chem. Soc.* **2005**, *127*, 9376; b) J. A. Rood, B. C. Noll, K. W. Henderson, *Inorg. Chem.* **2006**, *45*, 5521.

[4] a) K. M. Fromm, E. D. Gueneau, G. Bernardinelli, H. Goesmann, J. Weber, M.-J. Mayor-López, P. Boulet, H. Chermette, *J. Am. Chem. Soc.* **2003**, *125*, 3593; b) K. M. Fromm, E. D. Gueneau, A. Y. Robin, W. Maudez, J. Sague, R. Bergougnant, *Z. Anorg. Allg. Chem.* **2005**, *631*, 1725.

[5] H.-K. Liu, T.-H. Tsao, Y.-T. C.-H. Lin, V. Zima, *CrystEngComm* **2010**, *12*, 1044.

[6] K. M. Fromm, *Chem. Eur. J.* **2001**, *7*, 2236.

[7] a) H.-F. Zhu, Z.-H. Zhang, W.-Y. Sun, T. Okamura, N. Ueyama, *Cryst. Growth Des.* **2005**, *5*, 177; b) Z. Fei, T. J. Geldbach, R. Scopelliti, P. J. Dyson, *Inorg. Chem.* **2006**, *45*, 6331; c) F. Wiesbrock, H. Schimdbaur, *Inorg. Chem.* **2003**, *42*, 7283.

[8] a) R. Murugavel, P. Kumar, M. G. Walawalkar, R. Mathialagan, *Inorg. Chem.* **2007**, *46*, 6828; b) S. Wörl, I. O. Fritsky, D. Hellwinkel, H. Pritzkow, R. Krämer, *Eur. J. Inorg. Chem.* **2005**, 759;

[9] K. M. Fromm, *Coord. Chem. Rev.* **2008**, *252*, 856.

[10] K. M. Fromm, E. D. Gueneau, *Polyhedron* **2004**, *23*, 1479.

[11] a) I. Senkovska, S. Kaskel, *Eur. J. Inorg. Chem.* **2006**, 4564; b) K. C. Kam, K. L. M. Young, A. K. Cheetam, *Cryst. Growth Des.* **2007**, *7*, 1522; c) C. Volkringer, T. Loiseau, G. Férey, J. E. Warren, D. S. Wragg, R. E. Morris, *Solid State Sci.* **2007**, *9*, 455;

[12] E. H. L. Falcao, N. Naraso, R. K. Feller, G. Wu, F. Wudl, A. K. Cheetham, *Inorg. Chem.* **2008**, *47*, 8336.

[13] a) C. A. Williams, A. J. Blake, C. Wilson, P. Hubberstey, M. Schroder, *Cryst. Growth Des.* **2008**, *8*, 911; b) P. C. Dietzel, R. Blom, H. Fjellvag, *Z. Anorg. Allg. Chem.* **2009**, *635*, 1953.

[14] a) M. C. Das, S. K. Ghosh, E. C. Sanudo, P. K. Bharadwaj, *Dalton Trans.* **2009**, 1644; b) Z. Guo, G. Li, L. Zhou, S. Su, Y. Lei, S. Dang, H. Zhang, *Inorg. Chem.* **2009**, *48*, 8069–8071; c) D. T. Tran, D. Chu, A. G. Oliver, S. R. J. Oliver, *Inorg. Chem. Commun.* **2009**, *12*, 351.

[15] a) X.-A. Chen, F.-P. Song, X.-A. Chang, H.-G. Zang, W.-Q. Xiao, *Acta Crystallogr., Sect. E* **2008**, *64*, m863; b) H.-K. Liu, X.-W. Peng, C.-H. Lin, *Acta Crystallogr., Sect. E* **2009**, *65*, m237; c) Y. L. Li, X. Guo, J. X. Wang, Y. C. Wang, *Acta Crystallogr., Sect. E* **2009**, *65*, m772; d) X.-Y. Liu, L.-H. Liu, *Acta Crystallogr., Sect. E* **2010**, *66*, m305.

[16] B. R. Srinivasan, S. C. Sawant, *Thermochim. Acta* **2003**, *402*, 45.

[17] B. R. Srinivasan, J. V. Sawant, P. Raghavaiah, *Indian J. Chem.* **2006**, *45A*, 2392.

[18] B. R. Srinivasan, J. V. Sawant, P. Raghavaiah, *J. Chem. Sci.* **2007**, *119*, 11.

[19] B. R. Srinivasan, J. V. Sawant, C. Näther, W. Bensch, *J. Chem. Sci.* **2007**, *119*, 243.

[20] B. R. Srinivasan, P. Raghavaiah, J. V. Sawant, *Acta Crystallogr., Sect. E* **2007**, *63*, m2251.

[21] B. R. Srinivasan, J. V. Sawant, S. C. Sawant, P. Raghavaiah, *J. Chem. Sci.* **2007**, *119*, 593.

[22] B. R. Srinivasan, S. Y. Shetgaonkar, J. V. Sawant, P. Raghavaiah, *Polyhedron* **2008**, *27*, 3299;

[23] B. R. Srinivasan, S. Y. Shetgaonkar, C. Nather, W. Bensch, *Polyhedron* **2009**, *28*, 534.

[24] B. R. Srinivasan, S. Y. Shetgaonkar, P. Raghavaiah, *J. Chem. Sci.* **2008**, *120*, 249.

[25] B. R. Srinivasan, S. Y. Shetgaonkar, P. Raghavaiah, *Polyhedron* **2009**, *28*, 2879.

[26] B. R. Srinivasan, S. Y. Shetgaonkar, P. Raghavaiah, *Indian J. Chem.* **2009**, *48A*, 1662.

[27] B. R. Srinivasan, S. Y. Shetgaonkar, *J. Coord. Chem.* **2010**, *63*, 3403.

[28] M. L. Guo, *Acta Crystallogr. Sect. C* **2009**, *65*, m395.

[29] Bond valence sums were determined using the software: A. S. Wills, VaList, Program available from www.ccp14.ac.uk.

[30] a) B. R. Srinivasan, J. V. Sawant, P. Raghavaiah, *Indian J. Chem.* **2009**, *48A*, 181; b) B. R. Srinivasan, G. K. Rane, *J. Chem. Sci.* **2009**, *121*, 145.

[31] a) F. Vanhouteghem, A. T. H. Lenstra, P. Schweiss, *Acta Crystallogr., Sect. B* **1987**, *43*, 523; b) B. M. Kariuki, W. Jones, *Acta Crystallogr., Sect. C* **1989**, *45*, 1297; c) C. Castellari, F. Comelli, S. Ottani, *Acta Crystallogr., Sect. C* **1999**, *55*, 1054; d) F. Wiesbrock, A. Schier, H. Schmidbaur, *Z. Naturforsch. B* **2002**, *57*, 251.

[32] a) H. Ptasiewicz-Bak, J. Leciejewicz, *J. Coord. Chem.* **2003**, *56*, 173; b) S. H. Dale, M. R. J. Elsegood, S. Kainth, *Acta Crystallogr., Sect. C* **2003**, *59*, m505; c) J.-G. Zhao, Z.-Y. Zhang, L.-H. Huo, S. Gao, *Acta Crystallogr., Sect. E* **2004**, *60*, m1987.

[33] a) R. Murugavel, V. V. Karambelkar, G. Anantharaman, *Indian J. Chem.* **2000**, *39A*, 843; b) J.-W. Liu, S. Gao, L.-H. Huo, Y. Dong, H. Zhao, *Acta Crystallogr., Sect. E* **2004**, *60*, m845; c) V. H. Rodrigues, A. Matos Beja, J. A. Paixão, M. M. R. Costa, *Z. Kristallogr. NCS.* **2005**, *220*, 620; d) Q. Yang, S. Gao, L.-H. Huo, *Acta Crystallogr., Sect. E* **2005**, *61*, m277.

[34] a) X.-F. Zhang, S. Gao, L.-H. Huo, H. Zhao, *Acta Crystallogr., Sect. E* **2006**, *62*, m2898; b) G. Morgant, J. Angelo, D. Desmaele, E. Dichi, M. Sghaier, B. Fraisse, P. Retailleau, V. Brumas, M. M. L. Fiallo, A. Tomas, *Polyhedron* **2008**, *27*, 2097; c) M. Indrani, R. Ramasubramanian, F. R. Fronczek, D. Braga, N. Y. Vasanthacharya, S. Kumaresan, *J. Chem. Sci.* **2009**, *121*, 413.

[35] B. R. Srinivasan, S. C. Sawant, S. K. Das, *Indian J. Chem.* **2004**, *43A*, 1066.

[36] G. M. Sheldrick, *Acta Crystallogr., Sect. A* **2008**, *64*, 112–122.

Received: May 19, 2010

Journal of Coordination Chemistry
Vol. 64, No. 7, 10 April 2011, 1113–1124

Synthesis and characterization of calcium(II) coordination polymers based on phenylacetic acid§

BIKSHANDARKOIL R. SRINIVASAN*†, SANTOSH Y. SHETGAONKAR† and NARENDRA NATH GHOSH‡

†Department of Chemistry, Goa University, Goa 403206, India
‡Chemistry Group, Birla Institute of Technology and Science – Pilani, Goa Campus, Zuarinagar, Goa 403726, India

(*Received 15 August 2010; in final form 6 January 2011*)

The syntheses, crystal structures, and thermal properties of the coordination polymers $[Ca(H_2O)_2(L_1)_2]\cdot H_2O$ (**1**) (L_1 = 4-methoxyphenylacetate) and $[Ca(H_2O)_2(L_2)_2]\cdot 2H_2O$ (**2**) (L_2 = 2-chlorophenylacetate) are described. **1** and **2** can be dehydrated to the anhydrous $[Ca(L_1)_2]$ (**1a**) or $[Ca(L_2)_2]$ (**2a**), respectively. Compounds **1** and **2** crystallize in the non-centrosymmetric monoclinic space group $P2_1$ and the structures consist of a central Ca(II), two terminal waters, and two crystallographically unique L_1 (or L_2) anions, one of which functions as a chelating bidentate ligand. The second independent L_1 (or L_2) is tetradentate, coordinated in a μ_3-bridging mode leading to the formation of a 1-D coordination polymer. In the infinite chain extending along the *b*-axis, each Ca(II) is eight-coordinate and bonded to two terminal waters and six oxygens from four different L_1 or L_2 ligands.

Keywords: Coordination polymer; Calcium; 4-Methoxyphenylacetate; 2-Chlorophenylacetate

1. Introduction

Coordination polymers (CPs), also known as metal organic frameworks (MOFs), have attracted attention because of their topology and applications in catalysis, adsorption (gas storage), separation, and luminescence [1–3]. Compared to the extensive chemistry of CPs based on transition metals, the coordination chemistry of group 1 and 2 metals with organic linkers is less explored. The reluctance in using alkaline earth cations as building blocks for open framework materials can be attributed to their unpredictable coordination numbers and geometries, as no ligand field stabilization governs their bonding. Although closed shell s-block metal cations lack useful properties like magnetism or variable oxidation states, alkali and alkaline-earth metals are preferred to transition or lanthanide metal ions because many of the s-block cations have the advantage of being non-toxic, cheap, and soluble in aqueous media. The growing interest in coordination chemistry of s-block elements can be evidenced by several

---

*Corresponding author. Email: srini@unigoa.ac.in
§Dedicated to Prof. Dr M. S. Wadia on the occasion of his 74th Birthday.

Journal of Coordination Chemistry
ISSN 0095-8972 print/ISSN 1029-0389 online © 2011 Taylor & Francis
DOI: 10.1080/00958972.2011.562289

recent reports [4–16]. In a recent manuscript, Fromm [17] reviewed the different ligand and polymer types of s-block compounds.

Depending on electronic and steric requirements of the central metal, flexibility, binding modes, and hydrogen-bonding characteristics of the organic ligand, CPs of differing dimensionalities can be constructed. For oxophilic s-block metals, carboxylic acids are useful linkers as the metals can be linked into an extended chain with bridging of the carboxylate. In view of their known affinity for oxygen donors, especially water, s-block metal carboxylates are normally synthesized in aqueous medium by reactions between alkaline earth metal sources and aromatic carboxylic acids under ambient conditions [18–36]. Many groups employ hydrothermal reactions of metal sources with carboxylic acids for compound synthesis [4–13].

As part of our longstanding research interest in the chemistry of alkaline earth carboxylates [32] we have investigated the reactions of alkaline earth metal carbonates with 4-nitrobenzoic acid (4-nbaH) [33–35], 2-nitrobenzoic acid (2-nbaH) [15, 16], and 2-carbamoyl-4-nitrobenzoic acid [36, 37] in aqueous media and have prepared several 1-D CPs [13–16, 34–36]. In this study, we have investigated the reactions of $CaCO_3$ with 4-methoxyphenylacetic acid (L_1-H) and 2-chlorophenylacetic acid (L_2-H) (scheme 1) and have synthesized two new non-centrosymmetric Ca(II) CPs. The carboxylic acid functionality in phenylacetic acid is more flexible than nitrobenzoic acids where the –COOH group is linked to a rigid six-membered ring.

2. Experimental

2.1. *Materials and methods*

All chemicals used in this study were reagent grade and used as received. The starting materials and reaction products are air stable and hence were prepared under normal laboratory conditions. Infrared (IR) spectra of the solid samples diluted with KBr were recorded on a Shimadzu (IR Prestige-21) FT-IR spectrometer from 4000 to 400 cm^{-1}. Diffuse-reflectance spectra were recorded on a Shimadzu UV-2450 double beam spectrophotometer using $BaSO_4$ as reference (100% reflectance). Absorption data were calculated from the reflectance data using the Kubelka–Munk function ($a/S = (1 - R)^2/2R$, where a is the absorption coefficient, R the reflectance, and S the scattering coefficient).

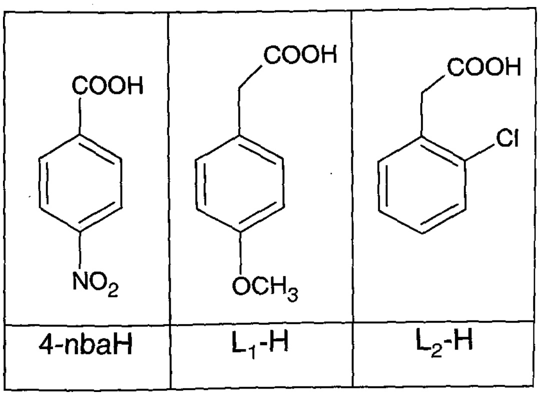

Scheme 1. Nomenclature of ligands relevant to this study.

TG-DTA studies were performed in flowing air in Al_2O_3 crucibles on a STA-409PC simultaneous thermal analyzer from Netzsch. A heating rate of $10\,K\,min^{-1}$ was employed for all measurements. Isothermal weight loss studies were performed in an electric furnace. BET surface area of freshly prepared anhydrous compounds **1a** and **1b** was measured using micromeritics surface area and porosimetry analyzer (Tristar 3000, Norcross, GA) and N_2 gas as adsorbate. X-ray powder patterns were recorded on a Rigaku Miniflex II powder diffractometer using Cu-Kα radiation with a Ni-filter.

2.2. *Preparation of $[Ca(H_2O)_2(L_1)_2]\cdot H_2O$ (1) and $[Ca(H_2O)_2(L_2)_2]\cdot 2H_2O$ (2)*

To a slurry of $CaCO_3$ (0.500 g, 5 mmol) in water (50 mL) was added L_1-H (1.66 g, 10 mmol) and the reaction mixture was heated on a water bath. The insoluble $CaCO_3$ slowly dissolved accompanied by brisk effervescence. Heating was stopped when effervescence ceased resulting in the formation of an almost clear solution. The hot reaction mixture was filtered and left undisturbed for 6–7 days to obtain colorless crystalline needles of **1** in 84% yield; these were filtered, washed with water followed by ether, and dried in air. Use of L_2-H (1.7 g, 10 mmol) in the above reaction instead of L_1-H resulted in the formation of **2** in 70% yield.

Anal. Calcd for $CaC_{18}H_{24}O_9$ (424.46) **1** (%): Ca, 9.44; C, 50.93; H, 5.70; CaO, 13.19. Found (%): Ca, 9.4; C, 50.92; H, 5.79; CaO, 13.28. IR data: 3610 ν(–OH), 3427, 3001, 2961, 2928, 2838, 2050, 1612, 1567 ν_{as}(–COO), 1546, 1512, 1444, 1416, 1401 ν_s(–COO), 1287, 1250 ν_{as}(–COC–), 1201, 1177, 1153, 1105, 1036, 950, 926, 824, 790, 736, 696, 627, 600, 543 cm^{-1}. DTA (in °C): 116 (endo), 375 (exo), 492 (exo).

Anal. Calcd for $CaC_{16}H_{20}Cl_2O_8$ (451.31) **2** (%): Ca, 8.88; C, 42.58; H, 4.47; CaO, 12.42. Found (%): Ca, 8.5; C, 42.5; H, 4.40; CaO, 12.3. IR data: 3636 ν(–OH), 3326, 3062, 1618, 1556 ν_{as}(–COO), 1500, 1452, 1431, 1402 ν_s(–COO), 1292, 1146, 1076, 1031, 939, 842, 733, 706, 695, 659 cm^{-1}. DTA (in °C): 121 (endo), 318 (exo), 588 (exo).

2.3. *Dehydration and rehydration studies*

A powdered sample (0.500 g) of **1** or **2** was heated at 130°C for 15 min. The observed mass losses of 12.65% (for **1**) and 15.57% (for **2**) are in good agreement with the expected values for the formation of the anhydrous compounds $[Ca(L_1)_2]$ **1a** or $[Ca(L_2)_2]$ **2a**.

Anal. Calcd for $CaC_{18}H_{18}O_6$ (370.41) **1a** (%): CaO, 15.14. Found (%): CaO, 15.02. IR data: 3000, 2953, 2934, 2910, 2833, 1551 ν_{as}(–COO), 1512, 1429, 1406 ν_s(–COO), 1300, 1279, 1248, 1177, 1105, 1036, 947, 818, 799, 729, 696 cm^{-1}.

Anal. Calcd for $CaC_{16}H_{12}Cl_2O_4$ (379.25) **2a** (%): CaO, 14.79. Found (%): CaO, 14.63%. IR data: 3066, 1566, 1556 ν_{as}(–COO), 1474, 1425, 1396 ν_s(–COO), 1302, 1269, 1177, 1122, 1053, 1040, 934, 843, 743, 687, 619, 577 cm^{-1}.

2.4. *X-ray crystal structure determination*

Intensity data for **1** and **2** were collected on a Bruker Smart Apex charged coupled device (CCD) diffractometer using graphite-monochromated Mo-Kα radiation.

Table 1. Selected refinement data for $[Ca(H_2O)_2(L_1)_2]\cdot H_2O$ (**1**) and $[Ca(H_2O)_2(L_2)_2]\cdot 2H_2O$ (**2**).

Empirical formula	$[Ca(H_2O)_2(L_1)_2]\cdot H_2O$	$[Ca(H_2O)_2(L_2)_2]\cdot 2H_2O$
Formula weight ($g\,mol^{-1}$)	424.45	451.30
Temperature (K)	293(2)	293(2)
Wavelength (Å)	0.71069	0.71069
Crystal system	Monoclinic	Monoclinic
Space group	$P2_1$	$P2_1$
Unit cell dimensions (Å, °)		
a	9.568(2)	11.669(3)
b	6.6381(16)	6.6737(18)
c	16.165(4)	13.508(4)
β	99.196(4)	105.295(5)
Volume ($Å^3$), Z	1013.5(4), 2	1014.7(5), 2
Calculated density ($Mg\,m^{-3}$)	1.391	1.477
Absorption coefficient (mm^{-1})	0.356	0.612
$F(000)$	448	468
θ range for data collection (°)	2.16–28.33	2.69–28.49
Limiting indices	$-8 \le h \le 12$; $-8 \le k \le 8$; $-21 \le l \le 21$	$-15 \le h \le 13$; $-8 \le k \le 8$; $-17 \le l \le 15$
Reflections collected	6663	6740
Independent reflections	4544 [$R(\mathrm{int}) = 0.0447$]	4597 [$R(\mathrm{int}) = 0.0312$]
Completeness to θ (%)	98.3	97.4
Refinement method	Full-matrix least-squares on F^2	Full-matrix least-squares on F^2
Data/restraints/parameters	4544/1/248	4597/1/244
Goodness-of-fit on F^2	1.103	1.117
Final R indices [$I > 2\sigma(I)$]	$R_1 = 0.0711$, $wR_2 = 0.1840$	$R_1 = 0.0501$, $wR_2 = 0.1140$
R indices (all data)	$R_1 = 0.0989$, $wR_2 = 0.2385$	$R_1 = 0.0763$, $wR_2 = 0.1516$
Flack X parameter	0.00(14)	−0.03(6)
Largest difference peak and hole ($e\,Å^{-3}$)	0.799 and −0.647	0.389 and −0.490

Data integration and reduction were processed with SAINT software [38]. An empirical absorption correction was applied to the collected reflections with the Siemens Area Detector Absorption (SADABS) [38]. Structures were solved with direct methods using SHELXS-97 [39] and refinement was done against F^2 using SHELXL-97 [39]. All non-hydrogen atoms were refined anisotropically. Aromatic hydrogens were introduced in calculated positions and included in the refinement riding on their respective parent atoms. Hydrogen attached to O21 in **1** and an H-atom attached to O22 in **2** could not be located. All other hydrogens of the coordinated and lattice waters were located in the difference Fourier map but were positioned with idealized geometry and refined using a riding model. Selected crystal refinement results for **1** and **2** are summarized in table 1.

3. Results and discussion

3.1. *Synthesis, spectra, and thermal investigations*

In earlier work we demonstrated that crystalline hydrates of metal carboxylates can be prepared in good yields under ambient conditions, by an aqueous reaction of alkaline earth metal carbonate with aromatic carboxylic acids. The generality of this reaction for the preparation of hydrated alkaline earth metal carboxylates can be evidenced by the synthesis of several such compounds [15, 16, 32–37]. In the present work, the same methodology has been employed for the synthesis of **1** and **2**. Thus the aqueous reaction of $CaCO_3$ with the substituted phenylacetic acid L_1-H (or L_2-H) resulted in the formation of **1** (or **2**) in good yield. Compounds **1** and **2** were also prepared in a two-step reaction. In the first step the sodium salt of L_1-**H** or L_2-**H** was generated *in situ* by the reaction of the acids with $NaHCO_3$. In the second step the aqueous solution of the Na-salt was reacted with $CaCl_2$ and the title compounds were then crystallized from the reaction mixture. Both **1** and **2** can be dehydrated to the corresponding anhydrous compounds **1a** or **2a** by heating at 130°C. On reaction with dilute HCl, **1**, **1a**, **2**, and **2a** decompose resulting in the separation of the insoluble L_1-**H** or L_2-**H**. Analytical and thermal data show that **1** and **2** which are differently hydrated contain Ca : carboxylate in a 1 : 2 mole ratio. The X-ray powder diffractograms (figure S1) reveal the crystalline nature of **1** and **2**, and the anhydrous compounds **1a** and **2a**. A comparison of the powder pattern of **1** and **1a** or **2** and **2a** clearly indicates that dehydration of **1** or **2** leads to changes in structure as evidenced by the appearance of new peaks in the diffractogram of the anhydrous compound. On pyrolysis at 800°C, **1** and **2** are converted into calcium oxide as shown by X-ray powder pattern (figure S1). Compound **1** (or **2**) was characterized as a 1-D CP based on single crystal X-ray work. It has been reported [6–10] that use of di or tricarboxylic acids and/or hydrothermal reactions result in the formation of CPs of higher dimensionality, unlike the 1-D polymers obtained in the present work.

Diffuse reflectance spectra of the title compounds are nearly identical to that of the corresponding free acid and the signals at 265 nm can be assigned to intraligand charge transfer of the organic acid. IR spectra of **1** or **2** (figure S2) exhibit several signals in the mid-IR region, indicating the presence of the organic moiety. The intense band at 3610 (in **1**) and 3636 cm^{-1} (in **2**) can be assigned as O–H stretch of water; this signal is not observed in anhydrous **1a** or **2a**. Characteristic signals due to the symmetric and asymmetric stretching of the carboxylate are observed at 1567 and 1401 cm^{-1} (in **1**) and 1556 and 1402 cm^{-1} (in **2**). The N_2 adsorption–desorption isotherms of the anhydrous compounds **1a** or **2a** show very little uptake of N_2, suggesting non-porous nature of **1** and **2**. On heating to 800°C, **1** or **2** can be decomposed to the binary oxide as evidenced by weight loss and the featureless IR spectra of the residues. The thermal profiles of **1** and **2** which exhibit an initial endothermic event at 116 and 121°C, respectively, assignable for the loss of coordinated and lattice water followed by exothermic events at higher temperatures (figure S3) due to the decomposition of the organic linker are in accord with the isothermal weight loss studies.

3.2. *Crystal structure description of* $[Ca(H_2O)_2(L_1)_2]\cdot H_2O$ *(1) and* $[Ca(H_2O)_2(L_2)_2]\cdot 2H_2O$ *(2)*

The polymeric compounds **1** and **2** crystallize in the chiral non-centrosymmetric monoclinic space group $P2_1$ with all atoms situated in general positions. The structures of **1** and **2** consist of a central Ca(II), two terminal waters, and two crystallographically unique (L_1) or (L_2) ligands (figure 1), one of which functions as a chelating bidentate ligand. The second independent L_1 (or L_2) is a tetradentate μ_3-bridging ligand. The geometric parameters of the organic ligands are in the normal range. Compounds **1** and

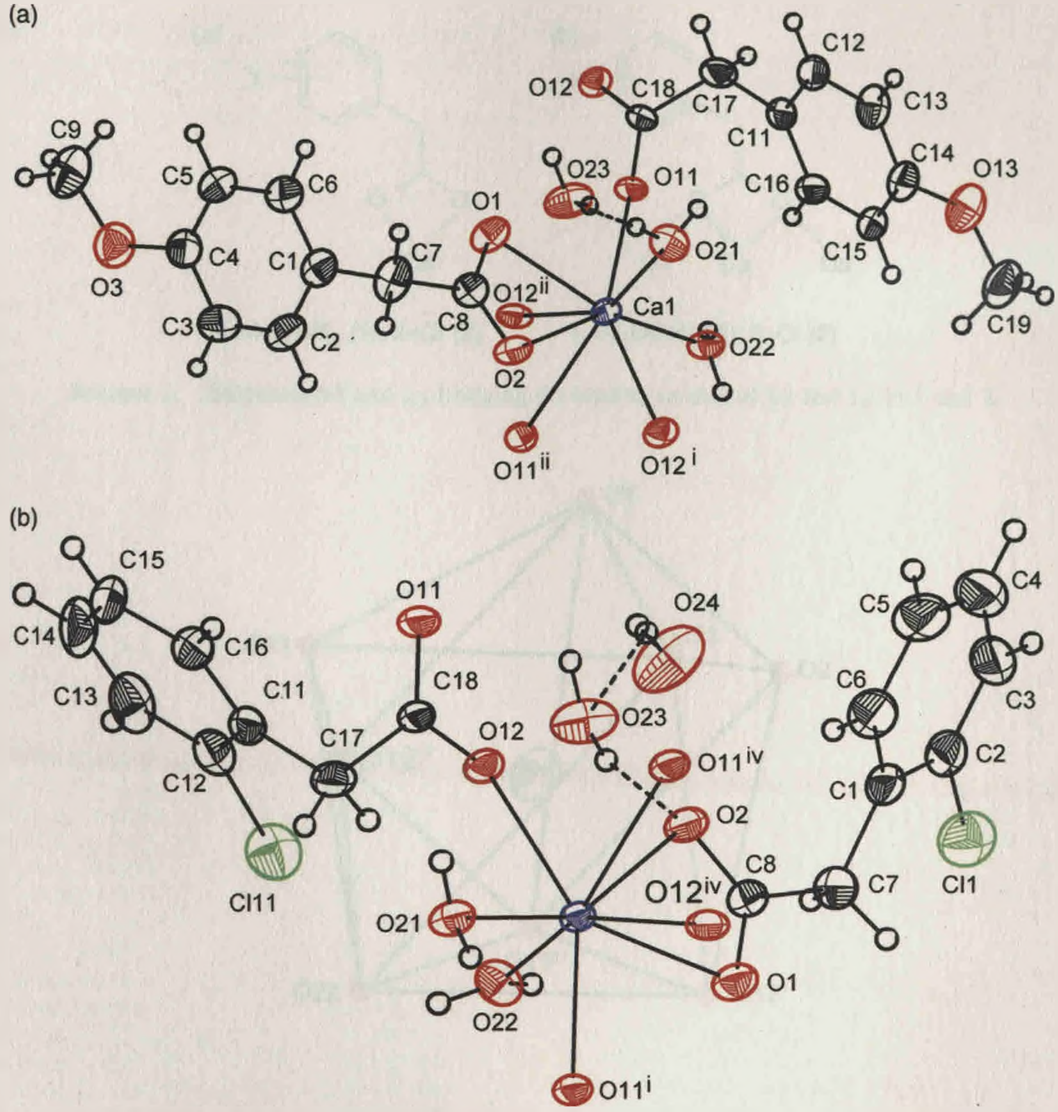

Figure 1. The coordination sphere of Ca(II) in $[Ca(H_2O)_2(L_1)_2] \cdot H_2O$, **1** (a) and $[Ca(H_2O)_2(L_2)_2] \cdot 2H_2O$, **2** (b) showing the atom-labeling scheme. Displacement ellipsoids are drawn at the 50% probability level except for hydrogens, which are shown as circles of arbitrary radius. Intramolecular H-bonding is shown as broken lines. Symmetry codes: (i) $x, y-1, z$; (ii) $-x+1, y-1/2, -z+1$; (iv) $-x+2, y-1/2, -z+1$.

2 are structurally similar in terms of the coordination environment of calcium and the binding modes of the crystallographically unique carboxylates but differ in disposition of the methoxy or chloro substituents with respect to the carboxylate in the aromatic ring (scheme 2) and the number of lattice waters. In **1**, which contains a single lattice water, the $-OCH_3$ group is *trans* to the carboxylate, while in **2**, which has two lattice waters, the –Cl group is *ortho* to the –COO functionality.

In view of similar structures, identical labels namely O1, O2 for the bidentate ligand, O11, O12 for the bridging ligand, and O21, O22 for coordinated waters are used for the oxygens in **1** and **2**. In the crystal structure, each Ca(II) in **1** or **2** is eight coordinate, bonded to two oxygens (O21 and O22) from water and six oxygens from four different L_1 or L_2 ligands resulting in a distorted triangular dodecahedron $\{CaO_8\}$ around Ca (figure 2). Compounds **1** and **2** exhibit a very long Ca–O distance of 2.753(4) and

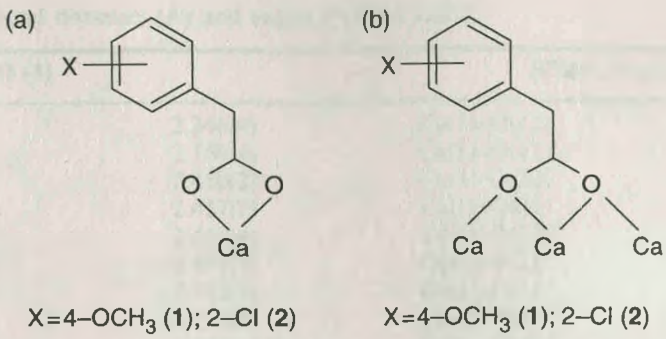

Scheme 2. Bidentate (a) and μ_3-bridging (b) binding modes of L_1 and L_2 in **1** and **2**.

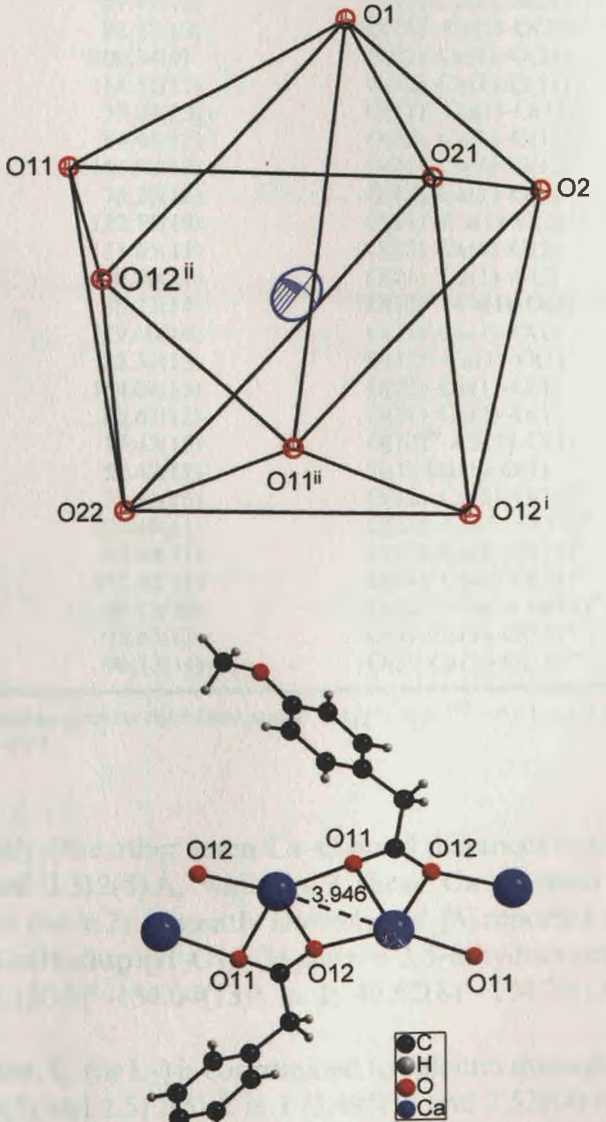

Figure 2. (a) The distorted triangular dodecahedral coordination around Ca(II) in **1**. (b) A pair of μ_3-$\eta^2:\eta^2$ ligands form a tricyclic dicalcium–dicarboxylate unit. Symmetry codes: (i) x, $y-1$, z; (ii) $-x+1$, $y-1/2$, $-z+1$. (For the basic building block of **2** see figure S4.)

Table 2. Selected bond distances (Å) and angles (°) for **1** and **2**.

$[Ca(H_2O)_2(L_1)_2]\cdot H_2O$ (**1**)		$[Ca(H_2O)_2(L_2)_2]\cdot 2H_2O$ (**2**)	
Ca(1)–O(12)$^{\mathrm{i}}$	2.346(4)	Ca(1)–O(12)	2.361(3)
Ca(1)–O(11)	2.358(4)	Ca(1)–O(11)$^{\mathrm{i}}$	2.368(3)
Ca(1)–O(22)	2.410(2)	Ca(1)–O(22)	2.387(3)
Ca(1)–O(21)	2.417(2)	Ca(1)–O(21)	2.415(3)
Ca(1)–O(12)$^{\mathrm{ii}}$	2.454(4)	Ca(1)–O(12)$^{\mathrm{iv}}$	2.460(3)
Ca(1)–O(2)	2.501(5)	Ca(1)–O(2)	2.495(4)
Ca(1)–O(1)	2.512(5)	Ca(1)–O(1)	2.529(4)
Ca(1)–O(11)$^{\mathrm{ii}}$	2.753(4)	Ca(1)–O(11)$^{\mathrm{iv}}$	2.704(3)
Ca(1)–Ca(1)$^{\mathrm{iii}}$	3.9461(11)	Ca(1)–Ca(1)$^{\mathrm{iv}}$	3.9533(11)
O(12)$^{\mathrm{i}}$–Ca(1)–O(11)	145.32(13)	O(12)–Ca(1)–O(11)$^{\mathrm{i}}$	145.61(10)
O(12)$^{\mathrm{i}}$–Ca(1)–O(22)	75.55(14)	O(12)–Ca(1)–O(22)	88.38(14)
O(11)–Ca(1)–O(22)	75.54(13)	O(11)$^{\mathrm{i}}$–Ca(1)–O(22)	83.62(13)
O(12)$^{\mathrm{i}}$–Ca(1)–O(21)	89.11(13)	O(12)–Ca(1)–O(21)	74.80(13)
O(11)–Ca(1)–O(21)	82.77(13)	O(11)$^{\mathrm{i}}$–Ca(1)–O(21)	76.13(13)
O(22)–Ca(1)–O(21)	109.34(9)	O(22)–Ca(1)–O(21)	108.27(10)
O(12)$^{\mathrm{i}}$–Ca(1)–O(12)$^{\mathrm{ii}}$	118.51(11)	O(12)–Ca(1)–O(12)$^{\mathrm{iv}}$	119.22(9)
O(11)–Ca(1)–O(12)$^{\mathrm{ii}}$	77.04(13)	O(11)$^{\mathrm{i}}$–Ca(1)–O(12)$^{\mathrm{iv}}$	76.05(10)
O(22)–Ca(1)–O(12)$^{\mathrm{ii}}$	84.45(12)	O(22)–Ca(1)–O(12)$^{\mathrm{iv}}$	151.94(13)
O(21)–Ca(1)–O(12)$^{\mathrm{ii}}$	151.88(12)	O(21)–Ca(1)–O(12)$^{\mathrm{iv}}$	85.60(11)
O(12)$^{\mathrm{i}}$–Ca(1)–O(2)	78.29(16)	O(12)–Ca(1)–O(2)	79.13(12)
O(11)–Ca(1)–O(2)	132.73(15)	O(11)$^{\mathrm{i}}$–Ca(1)–O(2)	132.23(12)
O(22)–Ca(1)–O(2)	151.65(13)	O(22)–Ca(1)–O(2)	82.20(11)
O(21)–Ca(1)–O(2)	80.80(11)	O(21)–Ca(1)–O(2)	151.43(13)
O(12)$^{\mathrm{ii}}$–Ca(1)–O(2)	98.73(14)	O(12)$^{\mathrm{iv}}$–Ca(1)–O(2)	97.24(12)
O(12)$^{\mathrm{i}}$–Ca(1)–O(1)	129.60(16)	O(12)–Ca(1)–O(1)	130.21(12)
O(11)–Ca(1)–O(1)	82.33(15)	O(11)$^{\mathrm{i}}$–Ca(1)–O(1)	80.94(12)
O(22)–Ca(1)–O(1)	154.04(13)	O(22)–Ca(1)–O(1)	79.10(12)
O(21)–Ca(1)–O(1)	80.67(12)	O(21)–Ca(1)–O(1)	154.79(13)
O(12)$^{\mathrm{ii}}$–Ca(1)–O(1)	77.43(15)	O(12)$^{\mathrm{iv}}$–Ca(1)–O(1)	78.76(12)
O(2)–Ca(1)–O(1)	51.42(11)	O(2)–Ca(1)–O(1)	51.64(8)
O(12)$^{\mathrm{i}}$–Ca(1)–O(11)$^{\mathrm{ii}}$	71.51(13)	O(12)–Ca(1)–O(11)$^{\mathrm{iv}}$	71.58(10)
O(11)–Ca(1)–O(11)$^{\mathrm{ii}}$	124.49(11)	O(11)$^{\mathrm{i}}$–Ca(1)–O(11)$^{\mathrm{iv}}$	123.83(9)
O(22)–Ca(1)–O(11)$^{\mathrm{ii}}$	85.60(11)	O(22)–Ca(1)–O(11)$^{\mathrm{iv}}$	152.08(13)
O(21)–Ca(1)–O(11)$^{\mathrm{ii}}$	152.12(11)	O(21)–Ca(1)–O(11)$^{\mathrm{iv}}$	85.54(11)
O(12)$^{\mathrm{ii}}$–Ca(1)–O(11)$^{\mathrm{ii}}$	49.13(10)	O(12)$^{\mathrm{iv}}$–Ca(1)–O(11)$^{\mathrm{iv}}$	49.62(8)
O(2)–Ca(1)–O(11)$^{\mathrm{ii}}$	75.85(13)	O(2)–Ca(1)–O(11)$^{\mathrm{iv}}$	75.22(11)
O(1)–Ca(1)–O(11)$^{\mathrm{ii}}$	96.13(14)	O(1)–Ca(1)–O(11)$^{\mathrm{iv}}$	98.84(12)

Symmetry transformations used to generate equivalent atoms: $^{(\mathrm{i})}\ x, y-1, z$; $^{(\mathrm{ii})}\ -x+1, y-1/2, -z+1$; $^{(\mathrm{iii})}\ -x+1, y+1/2, -z+1$; $^{(\mathrm{iv})}\ -x+2, y-1/2, -z+1$.

2.704(3) Å, respectively. The other seven Ca–O bond distances in **1** vary in a small range between 2.346(4) and 2.512(5) Å, while in **2** these Ca–O bond lengths range from 2.361(3) to 2.529(4) Å (table 2). Recently Dietzel *et al.* [8] reported a long Ca–O distance of 2.8384(16) Å in $[Ca(H_2dhtp)(H_2O)_2]$ (H_4dhtp = 2,5-dihydroxyterephthalic acid). The O–Ca–O angles (49.13(10)°–154.04(13)° in **1**; 49.62(8)°–154.79(13)° in **2**) scatter in a very wide range.

The first independent L_1 (or L_2) is coordinated to calcium through O1 and O2 with Ca–O distances of 2.501(5) and 2.512(5) Å in **1** (2.495(5) and 2.529(4) Å in **2**), indicating the symmetrical bidentate behavior of this ligand. The second L_1 (or L_2) which binds through O11 and O12 is tetradentate in a μ_3–$\eta^2:\eta^2$ binding mode, resulting in a 1-D CP. Both O11 and O12 are bonded to two Ca(II)s, of which one Ca(II) is common to both. The polymeric structure of **1** and **2** is based on a dimer and can be visualized as follows. A pair of μ_3-bridging L_1 (or L_2) ligands link a pair of $\{Ca(H_2O)_2(L_1)\}$ (or $\{Ca(H_2O)_2(L_2)\}$)

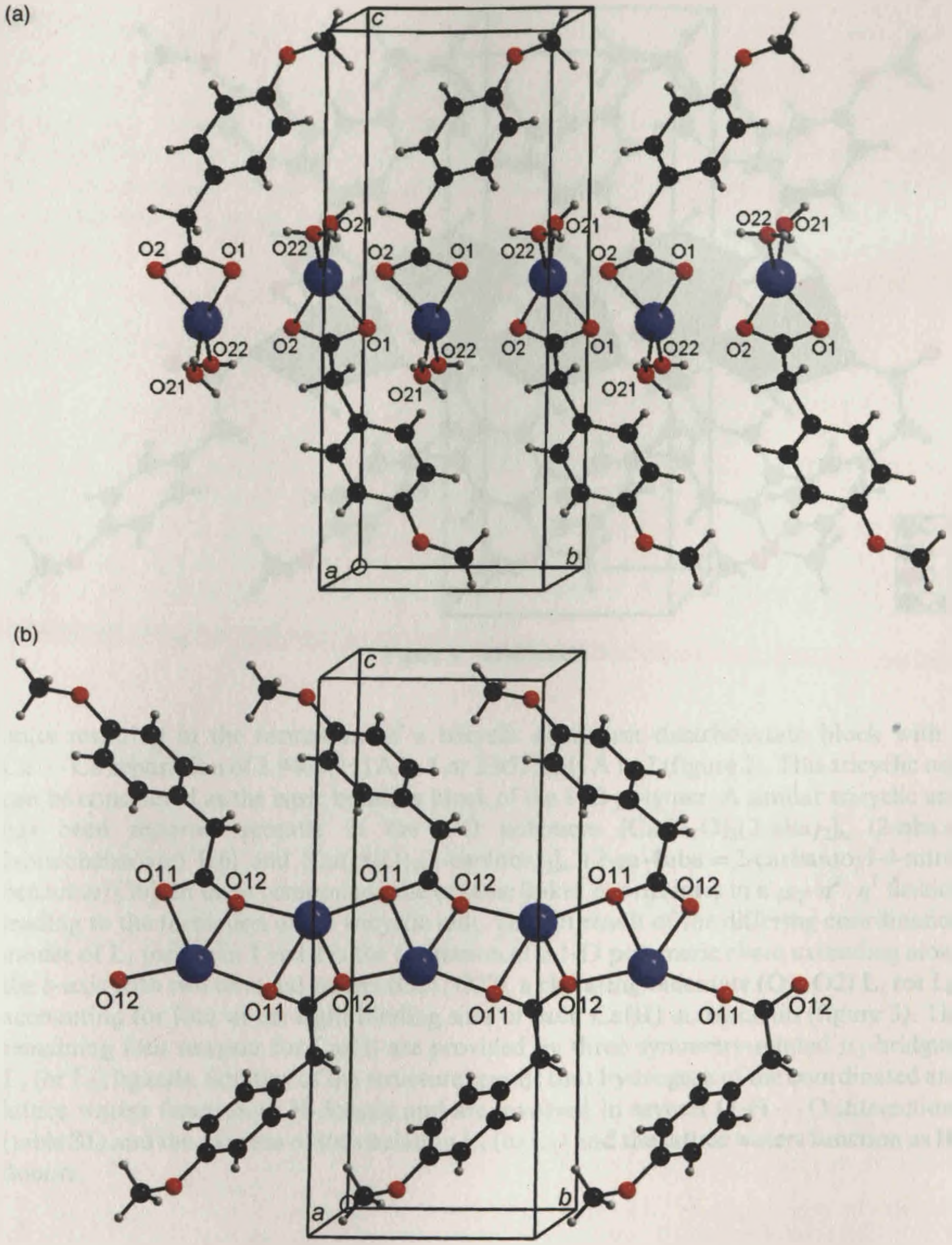

Figure 3. (a) The crystal structure of **1** along the *a*-axis showing only the bidentate L_1 ligand (O1, O2) and the coordinated waters (O21, O22) around Ca(II). (b) A portion of the polymeric chain in **1** extending along the *b*-axis only due to the μ_3-$\eta^2:\eta^2$ bridging binding mode of the L_1 (O11, O12) ligand, showing the linking of each Ca(II) to three different bridging ligands. (c) The crystallographic packing of **1** showing the eight-coordinate Ca(II) due to terminal aqua ligands and the chelating and bridging L_1. The $\{CaO_8\}$ units are represented as polyhedra. (For the crystallographic packing of **2** see figure S5.)

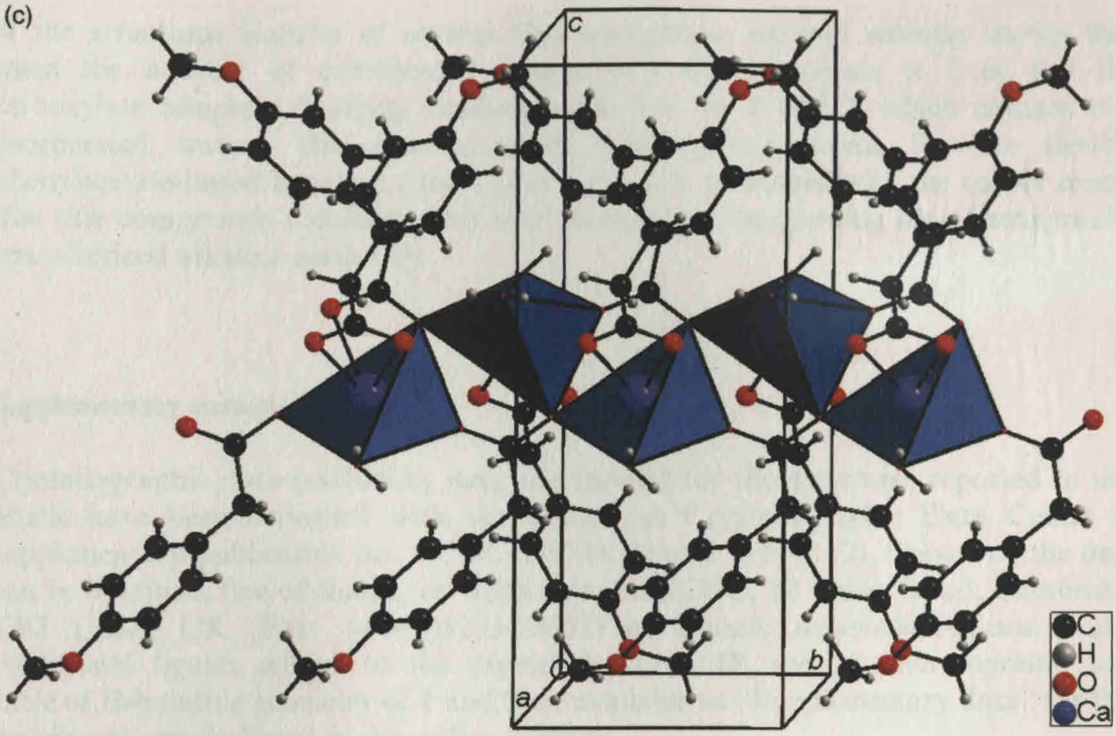

Figure 3. Continued.

units resulting in the formation of a tricyclic dicalcium–dicarboxylate block with a Ca $\cdots$ Ca separation of 3.9461(11) Å in **1** or 3.9533(11) Å in **2** (figure 2). This tricyclic unit can be considered as the basic building block of the 1-D polymer. A similar tricyclic unit has been reported recently in the 1-D polymers $[Ca(H_2O)_2(2\text{-nba})_2]_n$ (2-nba = 2-nitrobenzoate) [16] and $[Ca(H_2O)_2(2\text{-ca-4nba})_2]_n$ (2-ca-4nba = 2-carbamoyl-4-nitrobenzoate) [36]. In these compounds the organic linker coordinates in a μ_2–$\eta^2:\eta^1$ fashion leading to the formation of the tricyclic unit. The net result of the differing coordination modes of L_1 (or L_2) in **1** and **2** is the formation of a 1-D polymeric chain extending along the *b*-axis with two terminal waters (O21, O22), a chelating bidentate (O1, O2) L_1 (or L_2) accounting for four of the eight binding sites of each Ca(II) in the chain (figure 3). The remaining four oxygens for Ca(II) are provided by three symmetry-related μ_3-bridging L_1 (or L_2) ligands. Scrutiny of the structure reveals that hydrogens of the coordinated and lattice waters function as H-donors and are involved in several O–H $\cdots$ O interactions (table S1) and the oxygens of the chelating L_1 (or L_2) and the lattice waters function as H-donors.

4. Conclusions

Ca(II) CPs have been synthesized under hydrothermal conditions and structurally characterized in recent years [6–10]. Organic linkers containing two or more –COOH groups were used for the hydrothermal synthesis. In this work, we describe the synthesis under ambient conditions, structural characterization, and thermal properties of two new Ca(II) CPs, based on flexible monocarboxylic acid linkers. Based on an analysis of the structural features of several Ca-carboxylates, we had recently shown that when the number of coordinated waters in a Ca-carboxylate is 3 or less the carboxylate adopts a bridging binding mode [16]. In **1** and **2**, which contain two coordinated waters, the observation of bridging carboxylate for the flexible phenylacetate-based ligands L_1 (or L_2) in **1** (or **2**) is in accord with the earlier result. The title compounds constitute two new examples to the growing list of structurally characterized alkaline earth CPs.

Supplementary material

Crystallographic data (excluding structure factors) for the structures reported in this article have been deposited with the Cambridge Crystallographic Data Centre as supplementary publication no. CCDC 719744 (**1**) and 719743 (**2**). Copies of the data can be obtained, free of charge, on application to CCDC, 12 Union Road, Cambridge CB2 1 EZ, UK (Fax: +44-(0)1223-336033 or E-mail: deposit@ccdc.cam.ac.uk). Additional figures related to the crystal structure, IR spectra, thermograms, and table of H-bonding geometry of **1** and **2** are available as "Supplementary data" for this article and can be found in the online version.

Acknowledgments

BRS thanks Prof. P.K. Bharadwaj, Department of Chemistry, IIT-Kanpur for the single crystal data. Financial support under the Special Assistance Programme [F.540/25/DRS/2007/(SAP-I)] of University Grants Commission, New Delhi and the Nanomission program (SR/NM/NS-86, 2009) of Department of Science and Technology, New Delhi is gratefully acknowledged.

References

[1] S.R. Batten, S.M. Neville, D. R. Turner. *Coordination Polymers: Design, Analysis and Application*, RSC Publishing, Cambridge UK (2009). For reviews on CP see (a) C. Janiak. *J. Chem. Soc., Dalton Trans.*, 2781 (2003); (b) A.Y. Robin, K.M. Fromm. *Coord. Chem. Rev.*, **250**, 2127 (2006); (c) R. Robson. *J. Chem. Soc., Dalton Trans.*, 5113 (2008).
[2] For recent reviews on MOF see D.J. Tranchemontagne, J.L. Mendoza-Cortes, M. O'Keeffe, O.M. Yaghi. *Chem. Soc. Rev.*, **38**, 1257 (2009); S. Natarajan, P. Mahata. *Chem. Soc. Rev.*, **38**, 2304 (2009).
[3] K. Biradha, A. Ramanan, J.J. Vittal. *Cryst. Growth Des.*, **9**, 2969 (2009) – A perspective on the pros and cons of CP and MOF terminology.
[4] Z. Guo, G. Li, L. Zhou, S. Su, Y. Lei, S. Dang, H. Zhang. *Inorg. Chem.*, **48**, 8069 (2009).
[5] M.C. Das, S.K. Ghosh, E.C. Sanudo, P.K. Bharadwaj. *Dalton Trans.*, 1644 (2009).
[6] C.A. Williams, A.J. Blake, C. Wilson, P. Hubberstey, M. Schroder. *Cryst. Growth Des.*, **8**, 911 (2008).
[7] C. Volkringer, J. Marrot, G. Ferey, T. Loiseau. *Cryst. Growth Des.*, **8**, 685 (2008).
[8] P.C. Dietzel, R. Blom, H. Fjellvag. *Z. Anorg. Allg. Chem.*, **635**, 1953 (2009).
[9] S. Neogi, J.A.R. Navarro, P.K. Bharadwaj. *Cryst. Growth Des.*, **8**, 1554 (2008).
[10] A. Rossin, A. Ienco, F. Costantino, T. Montini, B.D. Credico, M. Caporali, L. Gonsalvi, P. Fornasiero, M. Peruzzini. *Cryst. Growth Des.*, **8**, 3302 (2008).

[11] L.N. Appelhans, M. Kosa, A.V. Radha, P. Simoncic, A. Navrotsky, M. Parrinello, A.K. Cheetham. *J. Am. Chem. Soc.*, **131**, 15375 (2009).
[12] D.T. Tran, D. Chu, A.J. Oliver, S.R.J. Oliver. *Inorg. Chem. Commun.*, **12**, 351 (2009).
[13] B.R. Srinivasan, S.Y. Shetgaonkar, J.V. Sawant, P. Raghavaiah. *Polyhedron*, **27**, 3299 (2008).
[14] B.R. Srinivasan, S.Y. Shetgaonkar, C. Näther, W. Bensch. *Polyhedron*, **28**, 534 (2009).
[15] B.R. Srinivasan, S.Y. Shetgaonkar, P. Raghavaiah. *J. Chem. Sci.*, **120**, 249 (2008).
[16] B.R. Srinivasan, S.Y. Shetgaonkar, P. Raghavaiah. *Polyhedron*, **28**, 2879 (2009).
[17] K.M. Fromm. *Coord. Chem. Rev.*, **252**, 856 (2008).
[18] M. Dan, A.K. Cheetham, C.N.R. Rao. *Inorg. Chem.*, **45**, 8227 (2006).
[19] H.-F. Zhu, Z.-H. Zhang, W.-Y. Sun, T. Okamura, N. Ueyama. *Cryst. Growth Des.*, **5**, 177 (2005).
[20] Z. Fei, T.J. Geldbach, R. Scopelliti, P.J. Dyson. *Inorg. Chem.*, **45**, 6331 (2006).
[21] R.K.B. Nielsen, K.O. Kongshaug, H. Fjellvåg. *Solid State Sci.*, **8**, 1237 (2006).
[22] F. Wiesbrock, H. Schimdbaur. *Inorg. Chem.*, **42**, 7283 (2003).
[23] R. Murugavel, P. Kumar, M.G. Walawalkar, R. Mathialagan. *Inorg. Chem.*, **46**, 6828 (2007).
[24] R. Murugavel, S. Banerjee. *Inorg. Chem. Commun.*, **6**, 810 (2003).
[25] A. Bacchi, M. Carcelli, C. Pelizzi, G. Pelizzi, P. Pelagatti, D. Rogolino, M. Tegoni, C. Viappiani. *Inorg. Chem.*, **42**, 5871 (2003).
[26] S. Fox, I. Büsching, W. Barklage, H. Strasdeit. *Inorg. Chem.*, **46**, 818 (2007).
[27] Q. Shuai, S. Chen, S. Gao. *Inorg Chim. Acta*, **360**, 1381 (2007).
[28] A. Grirrane, A. Pastor, E. Álvarez, R. Moyano, A. Galindo. *Inorg. Chem. Commun.*, **10**, 1125 (2007).
[29] R. Murugavel, V.V. Karambelkar, G. Anantharaman, M.G. Walawalkar. *Inorg. Chem.*, **39**, 1381 (2000).
[30] R. Murugavel, V.V. Karambelkar, G. Anantharaman. *Indian J. Chem.*, **39A**, 843 (2000).
[31] R. Murugavel, K. Baheti, G. Anantharaman. *Inorg. Chem.*, **40**, 6870 (2001).
[32] B.R. Srinivasan, S.C. Sawant. *Thermochim. Acta*, **402**, 45 (2003).
[33] B.R. Srinivasan, J.V. Sawant, P. Raghavaiah. *Indian J. Chem.*, **45A**, 2392 (2006).
[34] B.R. Srinivasan, J.V. Sawant, S.C. Sawant, P. Raghavaiah. *J. Chem. Sci.*, **119**, 593 (2007).
[35] B.R. Srinivasan, S.Y. Shetgaonkar, C. Näther. *Z. Anorg. Allg. Chem.*, **637**, 130 (2011).
[36] B.R. Srinivasan, S.Y. Shetgaonkar. *J. Coord. Chem.*, **63**, 3410 (2010).
[37] B.R. Srinivasan, S.Y. Shetgaonkar, P. Raghavaiah. *Indian J. Chem.*, **48A**, 1662 (2009).
[38] *Bruker SMART V5.630* and *SAINT-PLUS V6.45*, Bruker-Nonius Analytical X-ray Systems Inc., Madison, Wisconsin, USA (2003); *SADABS, Empirical Absorption Correction Program*, Bruker AXS Inc., Madison, Wisconsin, USA (1997).
[39] G.M. Sheldrick. *Acta Crystallogr.*, **64A**, 112 (2008).

Indian Journal of Chemistry
Vol. 49A, November 2010, pp. 1468-1477

Synthesis, characterization and properties of a water-rich calcium(II)-4-nitrobenzoate

Bikshandarkoil R Srinivasan[a,]*, Santosh Y Shetgaonkar[a], Sabeta Kohli[b] & Rajnikant[b]
[a]Department of Chemistry, Goa University, Goa 403 206, India
Email: srini@unigoa.ac.in

[b]X-ray Crystallography Laboratory, Department of Physics, University of Jammu, Jammu Tawi 180 006, India

Received 18 August 2010; revised and accepted 11 October 2010

Solid state reaction of $[Ca(H_2O)_4(4\text{-nba})_2]$ (4-nba = 4-nitrobenzoate) with 2-aminopyridine (2-ap) at 100 °C results in the formation of an anhydrous compound, $[Ca(2\text{-ap})(4\text{-nba})_2]$, while in aqueous solution, the coordination sphere of Ca(II) in $[Ca(H_2O)_4(4\text{-nba})_2]$ reorganises in the presence of 2-ap resulting in the formation of a water-rich Ca(II) compound, $[Ca(H_2O)_6(4\text{-nba})](4\text{-nba})(2\text{-ap})\cdot H_2O$. A comparative study of differently aquated 4-nitrobenzoates of Ca(II) is described.

Keywords: Coordination chemistry, Calcium, Nitrobenzoates, Aminopyridines, Water-rich compounds

IPC Code: Int. Cl.^{9} C07F1/08

Non-toxic and water soluble nature, variable structural chemistry, affinity for O-donor ligands, relevance in biology are some factors responsible for the current interest in the chemistry of *s*-block elements[1]. Of the *s*-block elements, calcium has received considerable attention in terms of development of its structural chemistry. The major structural features of interest are the interactions of calcium with O-donor ligands like water, carboxylate, carbonate, sulfate etc. The importance of the naturally occurring calcium carbonate, calcium sulfate and calcium phosphate is well documented[2] while the hydrates and carboxylates of Ca(II) are biologically relevant. Many research groups[3-6] have analyzed the structural data in the Cambridge Structural Database (CSD) and Protein Data Bank (PDB) crystal structure databases in order to understand the structural chemistry of calcium and identify geometrical features of a general nature. In a pioneering study, Einspahr and Bugg[3] examined the crystal structures of sixty two crystalline hydrates of calcium and showed that calcium-water interactions involve factors that impose significant constraints on the geometries of these compounds. Based on a study of protein crystal structures, Glusker and coworkers[5] reported that calcium has less affinity for water as compared to magnesium. Of the 187 small molecular crystal structures examined by the Glusker group[5], only 16 compounds (8.5 %) had a Ca:water ratio of 1:5 and more. Of these, only one compound had a $Ca:H_2O$ ratio of 1:8, while a 1:6 and 1:7 ratio for Ca:water was observed in six and two compounds respectively. A majority (73 %) of the Ca(II) compounds showed a Ca:water ratio of 1:3 or less, which is indicative of the low affinity of Ca(II) for water. To the best of our knowledge, the structures of the Ca(II) compounds $(ImH)_4[Ca(H_2O)_6][Mo_7O_{24}](Im)\cdot 3H_2O$[7] (Im = imidazole), $[Ca(H_2O)_6(C_{16}H_{12}O_4)]\cdot 2H_2O$[8] ($C_{16}H_{12}O_4$ = meso-2,3-diphenylsuccinate) and $[(H_2O)_6Ca(\mu\text{-Hpdc})Ca(H_2O)_3(Hpdc)_2](Hpdc)\cdot 2H_2O$[8] ($H_2pdc$ = pyridine-3,5-dicarboxylic acid) are the only known examples of Ca(II) containing six coordinated water molecules, after the study by Glusker[5] and coworkers.

In small molecular weight compounds, many of which are normally crystallized from aqueous media, the affinity of Mg(II) for water can be evidenced by the structural characterization of many compounds which contain the octahedral $[Mg(H_2O)_6]^{2+}$ ion[9-13]. In contrast, several Ca(II) compounds prepared from aqueous reactions contain four or less than four coordinated water molecules[13-29] as can be evidenced by the synthesis and characterization of $[Ca(H_2O)_2(4\text{-aba})_2]_n$, $[Ca(H_2O)_3(2\text{-aba})_2]_n$, $[Ca(H_2O)(gly)_2]_n$, $[Ca(H_2O)_2(3\text{-aba})_2]_n$, $[Ca(H_2O)_4(aip)_2]_n$,

$[Ca(H_2O)_3(1,4\text{-bdc})_2]_n$, $[Ca(H_2O)_2(mal)]_n$, $[Ca(H_2O)(OAc)_2]_n$, $[Ca(H_2O)_3(benz)_2]_n$ $[Ca(H_2O)(DMF)(benz)_2]_n$, $[Ca(H_2O)_3(4\text{-fba})_2]_n$, $[Ca(H_2O)_2(2\text{-fba})_2]_n$, $[Ca(H_2O)_3(dipic)_2]_n$, $[Ca(H_2O)_3(3,5\text{-dnsa})_2]_n$, $[Ca(H_2O)_2(2\text{-nba})_2]_n$, $[Ca(H_2O)_2(2\text{-ca-4nba})_2]_n$ and $[Ca(H_2O)_4(4\text{-nba})_2]$ (4-aba = 4-aminobenzoate[13]; 2-aba = 2-aminobenzoate[14]; gly = glycinate[15]; 3-aba = 3-aminobenzoate[16]; aip = 5-aminoisophthalate[17]; 1,4-bdc = benzene-1,4-dicarboxylate[18]; mal = malonate[19]; OAc = acetate[20]; benz = benzoate[21]; DMF = dimethylformamide[22]; fba = fluorobenzoate[23,24]; dipic = dipicolinate[25]; 3,5-dnsa = 3,5-dinitrosalicylate[26]; 2-nba = 2-nitrobenzoate[27]; 2-ca-4nba = 2-carbamoyl-4-nitrobenzoate[28] ; 4-nba = 4-nitrobenzoate[29]). The seven coordinated compound, $[Ca(H_2O)_4(4\text{-nba})_2]$[29], differs from several other Ca-carboxylates in that the 4-nba ligand does not exhibit bridging coordination. We have shown in earlier reports[30-33], that on reaction with N-donor ligands, the zero-dimensional compound $[Ca(H_2O)_4(4\text{-nba})_2]$, can be transformed into mixed ligand Ca(II) compounds containing less or no water as evidenced by the characterization of $[Ca(Im)(H_2O)_3(4\text{-nba})_2]\cdot Im$[30], $[Ca(Im)(4\text{-nba})_2]$[31], $[Ca(N\text{-MeIm})(4\text{-nba})_2]_n$, $[Ca(H_2O)(2\text{-MeIm})(4\text{-nba})_2]_n$ and $[Ca(pyr)_2(4\text{-nba})_2]_n$ (Im = imidazole[30,31]; N-MeIm = N-methylimidazole[31]; 2-MeIm = 2-methylimidazole[32]; pyr = pyrazole[33]).

In this work, we have investigated the solid state and solution reactions of $[Ca(H_2O)_4(4\text{-nba})_2]$ with 2-aminopyridine (2-ap). In aqueous solution, reorganization of the coordination sphere of Ca(II) leading to the formation of an unusual water-rich Ca(II) compound, $[Ca(H_2O)_6(4\text{-nba})](4\text{-nba})(2\text{-ap})\cdot H_2O$, is observed, the details of which are reported herein.

Materials and Methods

All the chemicals used in this study were of reagent grade and were used as received. The starting materials and reaction products were air stable and hence were prepared under normal laboratory conditions. Infrared (IR) spectra of the solid samples diluted with KBr were recorded on a Shimadzu (IR Prestige-21) FT-IR spectrometer in the range 4000-400 cm^{-1}. UV-visible spectra were recorded in water on a Shimadzu UV-2450 double beam spectrophotometer using matched quartz cells. TG-DTA studies were performed in flowing air, in Al_2O_3 crucibles on a STA-409 PC simultaneous thermal analyzer from Netzsch. A heating rate of 10 K min^{-1} was employed for all measurements. Isothermal weight loss studies were performed in an electric furnace.

Modified method for rapid synthesis of $[Ca(H_2O)_4(4\text{-nba})_2]$ (1)

A modified method involving less reaction time is described for the rapid and bulk synthesis of the earlier reported $[Ca(H_2O)_4(4\text{-nba})_2]$[29]. The 4-nbaH (3.34 g, 20 mmol) was taken in water (20 mL) and the slurry was warmed on a water bath to expel dissolved CO_2. A freshly prepared sample of CaO obtained by heating commercial $CaCO_3$ (1 g, 10 mmol) in a muffle furnace at 800 °C for ~30 min, was added to the above slurry. The reaction mixture was stirred well for ~10 min, resulting in the immediate formation of a microcrystalline product. The reaction mixture was cooled to room temperature, filtered and the product was washed well with water, followed by ether and dried. Yield 3.9 g. The infrared spectrum and thermal properties of the product were identical to that of the reported compound[29].

Preparation of $[Ca(2\text{-ap})(4\text{-nba})_2]$ (1-a)

A finely powdered solid mixture of $[Ca(H_2O)_4(4\text{-nba})_2]$ (**1**) (0.445 g, 1 mmol) and 2-aminopyridine (0.094 g, 1 mmol) was heated over a steam bath at 100 °C for 15-20 min., until the entire powder turned light yellow. The mixture was washed with ether and dried under vacuo. The observed weight loss of the product indicated the loss of four molecules of water resulting in the formation of an anhydrous compound (**1-a**). Alternatively (**1-a**) can be also prepared by first heating (**1**) at 100 °C for 15 min. and then adding 2-ap, followed by washing with ether and drying under vacuo. The use of 4-aminopyridine (4-ap) in the above reaction instead of 2-ap resulted in the formation of the monohydrate $[Ca(H_2O)(4\text{-nba})_2]$.

$[Ca(2\text{-ap})(4\text{-nba})_2]$ (**1-a**): (Yield 0.458 g, 98 %); Anal.: Found (calc %) for $CaC_{19}H_{14}N_4O_8$: (466.41) = CaO 12.50 (12.02). IR (KBr cm^{-1}): 3458 (υ_{NH}), 3345 (υ_{NH}), 3082, 1620, 1566 υ_{as}(-COO), 1518 $\upsilon_{as}(-NO_2)$, 1487, 1440, 1416 υ_s(-COO), 1346 $\upsilon_s(-NO_2)$, 1317, 1153, 1107, 1014, 878, 841, 799, 775, 725, 513.

Preparation of $[Ca(H_2O)_6(4\text{-nba})](4\text{-nba})(2\text{-ap})\cdot H_2O$ (2)

A mixture of $[Ca(H_2O)_4(4\text{-nba})_2]$ (**1**) (0.445 g, 1 mmol) and 2-aminopyridine (0.366 g, 4 mmol) was taken in water (~8 mL) and the reaction mixture was heated on a steam bath to obtain a clear yellow solution. The clear reaction mixture was left aside for crystallization. The pale yellow crystalline blocks suitable for structure determination which separated after ~3 h were isolated by filtration, washed with a little ice cold water followed by ether and air dried. The use of stoichiometric amount of 2-ap (1 mmol) also resulted in the formation of a microcrystalline product which analyzed satisfactorily. The use of 4-ap instead of 2-ap in the above reaction under identical conditions resulted in the formation of the starting material (**1**).

$[Ca(H_2O)_6(4\text{-nba})](4\text{-nba})(2\text{-ap})\cdot H_2O$ (**2**): (Yield 0.46 g, 77 %). Anal.: Found(calc.) (%) for $CaC_{19}H_{28}N_4O_{15}$ (592.52) = Ca 6.21 (6.76); C 38.13 (38.51); H 4.21 (4.76); N 8.74 (9.46); CaO 9.69 (9.46). IR (KBr cm^{-1}): 3475 (υ_{OH}), 3443, 3379 (υ_{NH}), 3347, 3217, 1678, 1620, 1572 υ_{as}(-COO), 1518 υ_{as}(-NO_2), 1445, 1422 υ_s(-COO), 1341 υ_s(-NO_2), 1319, 1258, 1155, 1105, 1044, 988, 876, 839, 797, 779, 771, 727, 623, 557, 515. DTA (in °C) : 117 (endo), 238 (endo), 421 (endo), 534 (exo). UV-Vis (λ_{max} in water) = 297 nm. ^{1}HNMR (DMSO-d_6) δ (in ppm): 5.85 (s, 2 H), 6.41 (m, 1 H), 6.40 (m, 1 H), 7.34 (m, 1 H), 7.88 (d, 1 H), 8.11 (d, 2 H), 8.20 (d, 2 H).

X-ray crystal structure determination

A single crystal of the title compound was selected using a Leica polarizing microscope and was used for intensity data-collection on an X'calibur (Oxford Diffraction System) X-ray diffractometer having CCD camera, using graphite-monochromated Mo-K$_\alpha$ radiation. CrysAlis^{Pro} program was used for data collection, reduction and space group determination. All non-hydrogen atoms were refined anisotropically. H atoms attached to the O and N atoms of water and 2-aminopyridine were located in the difference map and were refined isotropically using a riding model. Selected refinement data for (**2**) are listed in Table 1.

Results and Discussion

Synthetic aspects, spectral and thermal studies

The zero-dimensional compound, $[Ca(H_2O)_4(4\text{-nba})_2]$ (**1**) used earlier as a starting material for the synthesis of new Ca(II) coordination polymers[31-33] has been used in this study for the synthesis of new compounds using aminopyridines. We have developed a facile method for the synthesis of $[Ca(H_2O)_4(4\text{-nba})_2]$ in this work. The modified method of preparation involves direct reaction of a slurry of 4-nbaH in water with freshly prepared CaO (Eq. 1). Use of CaO affords the synthesis of (**1**) in high yields in a very short time period, unlike the earlier reported method[29] using $CaCO_3$ where the reaction of commercial $CaCO_3$ with aqueous 4-nbaH as well as crystallization of (**1**) required longer time duration. Thermal behaviour of (**1**) (Eq. 2) to form $[Ca(H_2O)(4\text{-nba})_2]$ with loss of three moles of water (weight loss = 12.16 %) on heating at 100 °C, serves as a sensitive and useful method for the convenient identification of (**1**).

$$CaO + 2\,(4\text{-nbaH}) \xrightarrow{H_2O} [Ca(H_2O)_4(4\text{-nba})_2] \quad \ldots(1)$$

$$[Ca(H_2O)_4(4\text{-nba})_2] \xrightarrow{100\,^{\circ}C} [Ca(H_2O)(4\text{-nba})_2] \ldots(2)$$

In earlier works[31,32] we have shown that N-donor ligands like N-methylimidazole (N-MeIm) or 2-methylimidazole (2-MeIm) can be incorporated into the coordination sphere of Ca(II) by reaction of solid

Table 1 — Selected refinement data for compound **2**

Empirical formula	$C_{19}H_{28}CaN_4O_{15}$
Formula weight (g mol^{-1})	592.52
Temperature (K)	293 (2)
Wavelength (Å)	0.71073
Crystal system/Space group	Triclinic / $P\bar{1}$
Unit cell dimensions	
a (Å)	6.8667(4)
b (Å)	10.1174(4)
c (Å)	19.4741(8)
α (°)	75.700(4)
β (°)	87.453(4)
γ (°)	84.675(4)
Volume (Å^3) / Z	1305.03(11) / 2
Density (calc.) (mg/m^3)	1.508
Abs. coeff. (mm^{-1})	0.321
F (000)	620
Crystal size (mm^3)	0.15 × 0.2 × 0.30
Θ range for data collection (°)	3.15 to 32.35
Completeness to θ (32.35°)	90.0 %
Index ranges	$-10 \le h \le 10$, $-15 \le k \le 15$, $-28 \le l \le 28$
Reflections collected	19968
Independent reflections	8439 [*R*(int) = 0.0201]
Refinement method	Full-matrix least-square on F^2
Data/restraints/parameters	8439 / 0 / 465
Goodness-of-fit on F^2	0.936
Final *R* indices [*I*>2sigma(*I*)]	*R*1 = 0.0373 w*R*2 = 0.0961
R indices (all data)	*R*1 = 0.0556 w*R*2 = 0.1008
Extinction coefficient	0.0060(19)
Largest diff. peak and hole (e. Å^{-3})	0.325 and -0.276

$[Ca(H_2O)_4(4\text{-nba})_2]$ with N-MeIm or 2-MeIm. Further, the same reaction using excess methylimidazoles when performed in minimum quantity of water can give rise to the formation of the same product obtained in the solid state reaction as crystalline material suitable for structure determination. It is to be noted that use of excess N-donor ligand is essential to suppress the hydrolysis of mixed ligand compounds into the starting tetraaqua compound $[Ca(H_2O)_4(4\text{-nba})_2]$. In addition, N-donor ligands which are soluble in water as well as organic solvents are desirable for the synthesis of new mixed ligand compounds of Ca(II) from (**1**). The aminopyridines are both water and organic soluble and hence, were employed for the formation of new compounds in this study by reaction with $[Ca(H_2O)_4(4\text{-nba})_2]$ (**1**) in the solid state or in aqueous solution.

Reaction of a solid 1:1 mixture of (**1**) and 2-aminopyridine at 100 °C resulted in the formation of the anhydrous compound $[Ca(2\text{-ap})(4\text{-nba})_2]$ (**1-a**) in near quantitative yields (Scheme 1). The presence of free or unreacted 2-ap can be easily ruled out as no free 2-ap was recovered on washing of compound (**1-a**) with ether. Alternatively, (**1-a**) was prepared by first heating (**1**) at 100 °C for 15 min to form the reactive monohydrate $[Ca(H_2O)(4\text{-nba})_2]$ and then adding 2-ap. However, under identical conditions, reaction of 4-ap with $[Ca(H_2O)_4(4\text{-nba})_2]$ resulted in the formation of $[Ca(H_2O)(4\text{-nba})_2]$ and unreacted 4-ap which could be separated from the monohydrate by washing with ether in which 4-ap dissolves while the monohydrate remains insoluble. The reaction of $[Ca(H_2O)_4(4\text{-nba})_2]$ (**1**) was investigated in aqueous solution in the presence of excess 2-ap and 4-ap (Ca:aminopyridine = 1:4). With 4-ap, only the starting material $[Ca(H_2O)_4(4\text{-nba})_2]$ could be recovered as evidenced by the IR spectrum and weight loss study of the product at 100 °C. Interestingly, the aqueous reaction of (**1**) with 2-ap resulted in the formation of a crystalline material (**2**) which is quite different from that of the product of the solid state reaction, namely, (**1-a**). The different nature of (**1-a**) and (**2**) can be readily evidenced from the spectral, analytical and thermal data. The crystalline material (**2**) exhibits a weight loss of 16.2 % at 100 °C indicating that was not the starting material (**1**). Further, the large weight loss is indicative of the probable presence of more water in (**2**) than in (**1**). Analytical data of (**2**) reveals a Ca:4-nba:2-ap:water ratio of 1:2:1:7 ratio. The presence of seven moles of water in (**2**) can be accounted for by six coordinated water molecules and a lattice water based on the single crystal data (vide infra). Compound (**2**) can be fully dehydrated by heating at 120 °C leading to the formation of (**1-a**), while (**1-a**) can be converted to (**2**) on exposure to moisture under controlled conditions. Both (**1-a**) and (**2**) can be converted to (**1**) by stirring in excess water (Scheme 1). Such a hydrolysis reaction of mixed ligand Ca(II) complexes has been reported by us earlier[31,32]. Pyrolysis of (**2**) or (**1-a**) results in the formation of calcium oxide. Reaction of (**2**) or (**1-a**) with dilute HCl results in decomposition leading to the quantitative formation of insoluble 4-nbaH, which can be filtered and weighed.

The presence of 4-nba and 2-ap in (**2**) can be readily evidenced from the ^{1}H NMR spectrum, which exhibits characteristic signals of both moieties. The electronic spectrum of (**2**) exhibits a strong absorption at 297 nm and the peak position is the same as that of a dilute aqueous solution of (**1**) containing 2-ap in a Ca:2-ap ratio of 1:1. The observed signal can be attributed to an internal charge transfer of the aromatic 4-nba anion. In addition to a change in profile of the IR spectrum of (**2**) as compared to that of $[Ca(H_2O)_4(4\text{-nba})_2]$ (**1**) in the 3000-3500 cm^{-1} region, additional signals are observed in the spectrum of (**2**) at 1258, 1155, 1044, 988, 876, 779 cm^{-1} indicating the presence of 2-ap in (**2**). A broad and strong absorption in the O-H and N-H region of the IR spectrum with signals centered around 3475 cm^{-1} and 3345 cm^{-1} may be assigned for the O-H and N-H stretching vibrations of water and amine of 2-ap respectively in (**2**). The symmetric and asymmetric stretching vibrations of carboxylate are observed at 1572 and 1421 cm^{-1} respectively, while

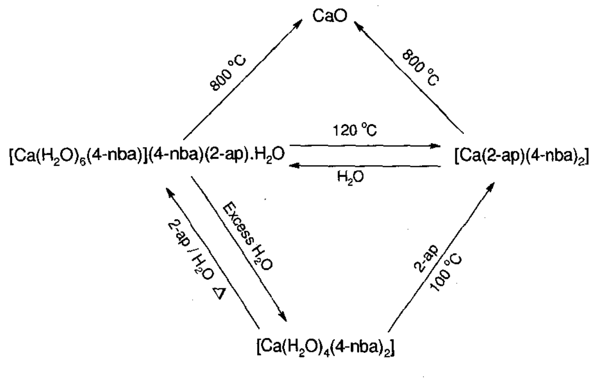

Scheme 1

those of the nitro group are observed at around 1517 and 1341 cm^{-1} respectively.

The TG-DTA thermogram of (**2**) (Fig. 1) exhibits first an endothermic process at 117 °C which is not observed for (**1-a**). The observed weight loss and the profile of the dropping TG curve of (**2**) can be attributed to the loss of the neutral water followed by 2-ap. The profile of the TG curve of (**1-a**) which is initially a straight line parallel to X-axis until about 150 °C drops down, indicating the loss of 2-ap. The exothermic events at temperatures above 400 °C in both compounds can be attributed to the decomposition of 4-nba[31]. In both cases CaO is formed as the final residue. The observed mass loss of 20.6 %, on heating (**2**) at 120 °C is in agreement with the expected value (21.28 %) for the loss of seven moles of water. The formation of CaO as the final residue was further confirmed based on isothermal weight loss studies by heating compounds (**2**) or (**1-a**) at 800 °C in a temperature controlled furnace. Thus the weight loss studies add credence to the thermal behavior of both compounds.

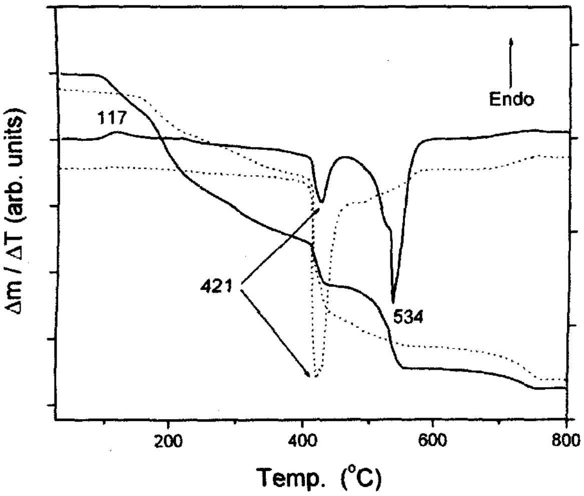

Fig. 1 — TG-DTA thermograms of $[Ca(H_2O)_6(4\text{-nba})](4\text{-nba})(2\text{-ap})\cdot H_2O$ (**2**) (solid line) and $[Ca(4\text{-nba})_2(2\text{-ap})]$ (**1-a**) (dotted line).

Crystal structure of $[Ca(H_2O)_6(4nba)](4\text{-nba})(2\text{-ap})\cdot H_2O$ (2)

The water-rich Ca(II) compound (**2**), crystallizes in the centrosymmetric triclinic space group *P*$\bar{1}$ with all atoms situated in general positions. The crystal structure consists of a $[Ca(H_2O)_6(4nba)]^+$ complex cation, a free 4-nitrobenzoate anion, a solvent 2-aminopyridne (2-ap) and a lattice water (Fig. 2). In the complex cation, the central Ca(II) is seven coordinated and is bonded to six terminal water molecules and a monodentate 4-nitrobenzoate resulting in a distorted pentagonal bipyramidal $\{CaO_7\}$ polyhedron (Fig. 2). The water-rich Ca(II) compound differs from the known structurally characterized Ca(II)-4-nitrobenzoates[29-33] in that the central metal is coordinated to a single 4-nba ligand with the second unique 4-nba remaining uncoordinated. In all other structurally characterized 4-nitrobenzoates of Ca(II), the central metal is bonded to at least two 4-nba anions as in $[Ca(H_2O)_4(4\text{-nba})_2]$[29] or to more than two 4-nba ligands as observed in the one-dimensional polymers[31-33]. The coordination of six water molecules to Ca(II) and the presence of free

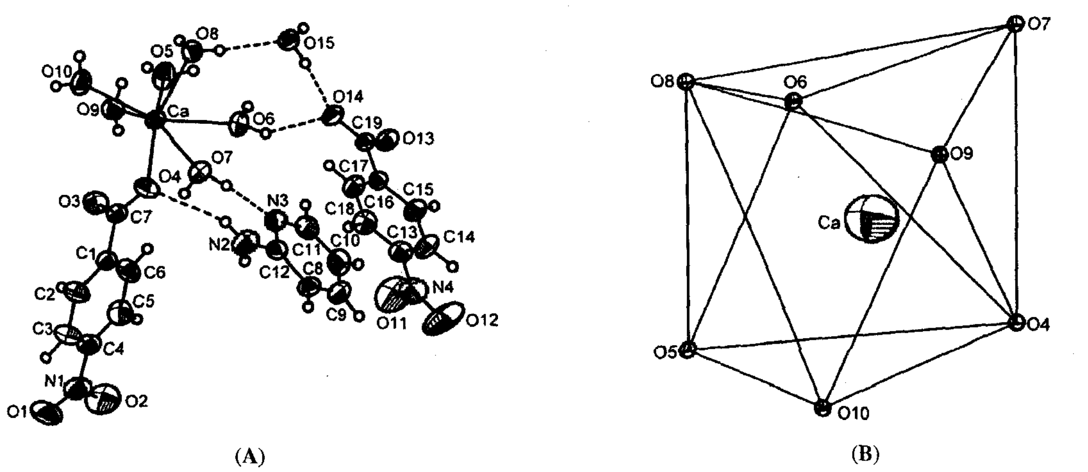

(A) (B)

Fig. 2 — (A) Crystal structure of $[Ca(H_2O)_6(4\text{-nba})](4\text{-nba})(2\text{-ap})\cdot H_2O$ showing the atom labeling scheme. Displacement ellipsoids are drawn at 50% probability level except for the H atoms, which are shown as circles of arbitrary radius. Intramolecular H-bonding is shown as broken lines. (B) The distorted pentagonal bipyramidal $\{CaO_7\}$ coordination polyhedron around Ca.

4-nba in (**2**) clearly indicate the reorganization of the coordination sphere of Ca(II) in $[Ca(H_2O)_4(4nba)_2]$ (**1**) on reaction with 2-ap. The geometric parameters of the coordinated and the free 4-nba and the 2-ap solvent are in the normal range. The Ca-O distances range from 2.3595(9) to 2.5315(10) Å (Table 2) and are in good agreement with reported values for several Ca(II) compounds. The O-Ca-O angles range from 47.91(3) to 159.89(4)°.

Table 2 — Selected bond lengths and bond angles for (**2**)

Bond lengths (Å)			
Ca-O(4)	2.3595(9)	Ca-O(7)	2.4367(9)
Ca-O(8)	2.4379(9)	Ca-O(6)	2.4493(10)
Ca-O(9)	2.5315(10)	Ca-O(10)	2.3900(10)
Ca-O(5)	2.4881(11)		
Bond angles (°)			
O(4)-Ca-O(7)	84.30(3)	O(4)-Ca-O(10)	98.76(4)
O(4)-Ca-O(8)	159.89(4)	O(10)-Ca-O(7)	145.92(4)
O(7)-Ca-O(8)	91.49(3)	O(10)-Ca-O(8)	95.71(4)
O(10)-Ca-O(6)	141.87(4)	O(4)-Ca-O(6)	83.71(3)
O(8)-Ca-O(6)	76.29(3)	O(7)-Ca-O(6)	72.17(4)
O(10)-Ca-O(5)	71.83(4)	O(4)-Ca-O(5)	86.86(4)
O(8)-Ca-O(5)	84.46(4)	O(7)-Ca-O(5)	142.(4)
O(4)-Ca-O(9)	122.74(3)	O(6)-Ca-O(5)	70.32(4)
O(7)-Ca-O(9)	76.31(3)	O(10)-Ca-O(9)	73.59(4)
O(6)-Ca-O(9)	136.14(3)	O(8)-Ca-O(9)	74.83(3)
O(4)-Ca-O(3)	47.91(3)	O(5)-Ca-O(9)	137.31(4)
O(7)-Ca-O(3)	74.70(3)	O(10)-Ca-O(3)	82.33(4)
O(6)-Ca-O(3)	123.11(3)	O(8)-Ca-O(3)	148.99(3)
O(9)-Ca-O(3)	74.96(3)	O(5)-Ca-O(3)	123.36 (4)

A scrutiny of the crystal structure of (**2**) reveals that the $[Ca(H_2O)_6(4nba)]^+$ cation, the free 4-nba anion, lattice water and solvent 2-aminopyridine are involved in four varieties of H-bonding interactions, comprising of thirteen O-H···O, two N-H···O, one O-H···N and four C-H···O bonds (Table 3). The O···H distances ranging from 1.772 to 2.674 Å are accompanied by DHA angles ranging from 125° - 174°. All the H atoms of the coordinated and lattice water molecules, the amino group of 2-ap, H atoms attached to two of the carbon atoms (C2 and C5) of the monodentate 4-nba and H atoms bonded to C8 and C10 of 2-ap function as H-donors. All oxygen atoms of the coordinated and lattice water molecules and the N3 nitrogen atom of 2-ap, function as H-acceptors. The oxygen atom (O1) of the nitro group of coordinated 4-nba is not involved in H-bonding. The O11 and O12 atoms of the nitro group of free 4-nba are involved in weak C-H···O interactions, a feature observed in several metal 4-nitrobenzoates[29-33,36].

The H-acceptor characteristics of the lattice water (O15) results in tetra coordination around O15 (Fig. 3). In addition, O15 functions as H-donor, which results in the lattice water being linked to three different $[Ca(H_2O)_6(4nba)]^+$ cations and a free 4-nba anion. The solvent, 2-aminopyridine, serves to link three different $[Ca(H_2O)_6(4nba)]^+$ cations and a free anion with the aid of two O-H···N, two C-H···O and one N-H···O interaction (Fig. 3). The secondary interactions of 2-ap with the cations and free

Table 3 — Hydrogen-bonding geometry for $[Ca(H_2O)_6(4\text{-}nba)](4\text{-}nba)(2\text{-}ap)\cdot H_2O$ (**2**)

D-H···A	*D*(D-H) (Å)	*D*(H···A) (Å)	*D*(D···A) (Å)	<DHA (°)	Symmetry code
O8-H8B···O15	0.772	2.022	2.785	169	x, y, z
O6-H6A···O14	0.916	2.050	2.826	142	x, y, z
O15-H16A···O14	0.824	1.909	2.713	165	x, y, z
O8-H8A···O13	0.960	1.773	2.713	166	-x+1, -y+1, -z
O9-H9B···O13	0.878	1.958	2.821	167	-x+1, -y+1, -z
O15-H16···O7	0.802	2.014	2.809	172	-x+1, -y+1, -z
O9-H9A···O15	0.881	1.914	2.792	174	x-1, y, z
O7-H7A···O14	0.890	2.023	2.886	163	x-1, y, z
O5-H5A···O3	0.898	1.957	2.846	170	x+1, y, z
O6-H6B···O3	0.835	1.986	2.812	170	x+1, y, z
O5-H5B···O13	0.740	2.167	2.891	166	x, y-1, z
O10-H10A···O8	0.857	2.025	2.873	170	-x+1, -y, -z
O10-H10B···O9	0.805	2.202	2.961	157	-x, -y, -z
N2-H34···O4	0.821	2.399	3.174	158	x, y, z
N2-H33···O2	0.830	2.241	3.057	168	-x, -y, -z+1
O7-H7B···N3	0.911	1.772	2.671	169	x, y, z
C2-H2···O6	0.971	2.666	3.505	145	x-1, y, z
C5-H5···O11	0.997	2.526	3.204	125	x-1, y, z
C8-H8···O12	0.899	2.563	3.397	154	-x+1, -y+1,-z+1
C10-H10···O4	0.915	2.674	3.555	162	x, y+1, z

4-nba appears to be an important factor for the formation of the water-rich compound starting from $[Ca(H_2O)_4(4\text{-nba})_2]$ (**1**) since the reaction of 4-ap with (**1**) does not give rise to any new compound. It is interesting to note that the H-bonding surrounding of 2-ap is identical to that of the lattice water. An analysis of the crystal structure reveals that each seven coordinated Ca(II) complex cation is H-bonded to two symmetry related lattice water molecules, two different 2-ap molecules, five different uncoordinated 4-nba anions and four symmetry related $[Ca(H_2O)_6(4nba)]^+$ ions with the aid of eleven O-H···O bonds, one N-H···O bond, one O-H···N bond and three weak C-H···O interactions (Fig. 4). The free uncoordinated 4-nba anion is linked to a lattice water, a solvent 2-ap and five different complex cations with the aid of seven O···H contacts (Fig. 4). The net result of the several H-bonding interactions in (**2**) is the organization of cations and anions into alternating layers with the lattice water and solvent 2-amino-pyridine serving as links between layers (Fig. 5).

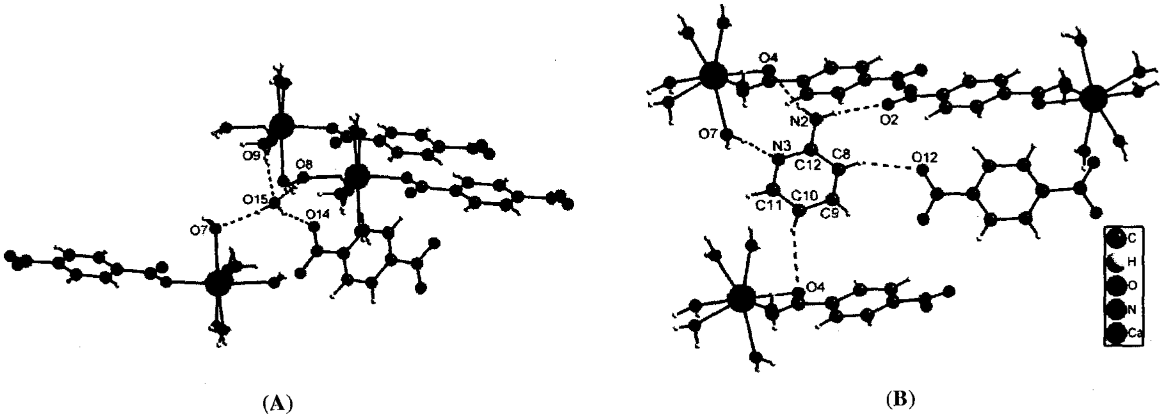

(A) (B)

Fig. 3 — H-bonding surroundings of (A) lattice water (O15) and (B) 2-aminopyridine.

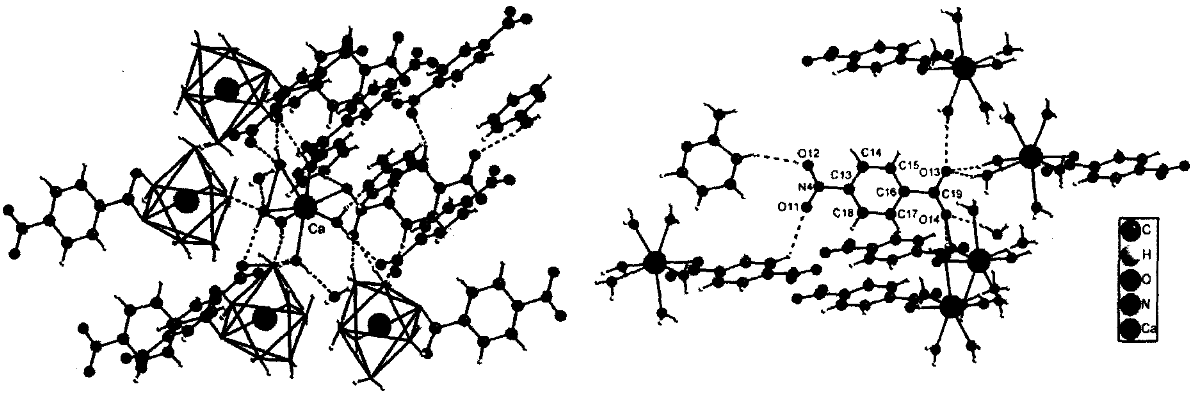

(A) (B)

Fig. 4 — (A) H-bonding surroundings of the $[Ca(H_2O)_6(4nba)]^+$ cation showing the Ca cation bonded to two lattice waters, two 2-ap molecules, five free 4-nba anions and four different cations (open polyhedra). (B) H-bonding surroundings of free uncoordinated 4-nba.

Comparative study of differently hydrated 4-nitrobenzoates of Ca(II)

During the course of our studies on alkaline earth 4-nitrobenzoates[37], we have synthesized and characterized several 4-nitrobenzoates of Ca(II) which differ in their water content (Table 4). The mixed ligand compounds containing both 4-nba and N-donor ligands like Im, N-MeIm, 2-MeIm, pyr, 2-ap (for ligand abbreviation see Table 4) have been prepared starting from the zero-dimensional compound $[Ca(H_2O)_4(4\text{-nba})_2]$. All compounds listed in Table 4 exhibit a 1:2 ratio of Ca:4-nitrobenzoate and the structurally characterized compounds crystallize in

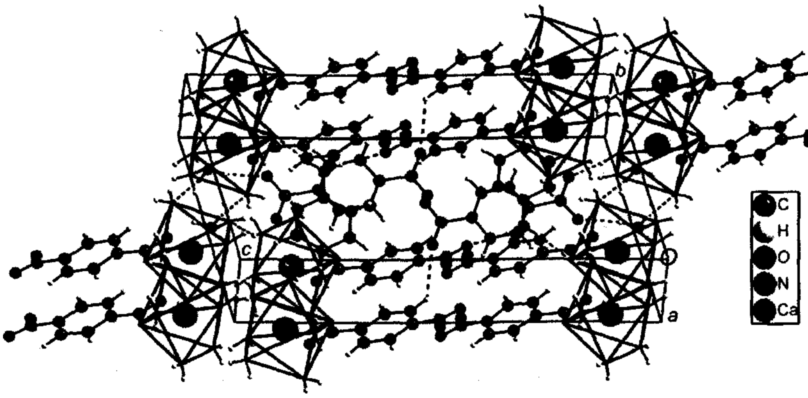

Fig. 5 — A view of the crystallographic packing of $[Ca(H_2O)_6(4\text{-nba})](4\text{-nba})(2\text{-ap})\cdot H_2O$ (**2**). [H-bonding is shown in broken lines. $\{CaO_7\}^+$ units are shown as open polyhedra].

Table 4 — Comparative structural features of some Ca(II) 4-nitrobenzoates[a]

Compound	S. G.	$Ca:H_2O$[b]	Coord. sphere	No. of 4-nba	Binding mode[c]	D	Ref.
$[Ca(H_2O)_4(4\text{-nba})_2]$ (**1**)	$P2_1/c$	1:4	$\{CaO_7\}$	2	(d), (e)	0-D	29
$[Ca(H_2O)_3(Im)(4\text{-nba})_2]\cdot Im$	$P2_1/c$	1:3	$\{CaNO_5\}$	2	(d), (d)	0-D	30
$[Ca(N\text{-MeIm})(4\text{-nba})_2]_n$	$P\bar{1}$	1:0	$\{CaNO_5\}$	5	(a), (b)	1-D	31
$[Ca(pyr)_2(4\text{-nba})_2]_n$	$P\bar{1}$	1:0	$\{CaN_2O_4\}$	4	(a)	1-D	33
$[Ca(H_2O)(2\text{-MeIm})(4\text{-nba})_2]_n$	$P2_1/n$	1:1[d]	$\{CaNO_6\}$	4	(a), (c)	1-D	32
$[Ca(H_2O)_6(4\text{-nba})](4\text{-nba})(2\text{-ap})\cdot H_2O$ (**2**)	$P\bar{1}$	1:6	$\{CaO_7\}$	1	(e), (f)	0-D	This work
$[Ca(4\text{-nba})_2]^\#$	---	1:0	---	---	---	---	29
$[Ca(H_2O)(4\text{-nba})_2]^\#$	---	1:1	---	---	---	---	29, 31
$[Ca(Im)(4\text{-nba})_2]^\#$	---	1:0	---	---	---	---	31
$[Ca(2\text{-ap})(4\text{-nba})_2]^\#$ (**1-a**)	---	1:0	---	---	---	---	This work

[a] All Ca(II) compounds excepting $[Ca(pyr)_2(4\text{-nba})_2]_n$ contain two unique 4-nitrobenzoates;
[b] Only coordinated water molecules are considered;
[c] for the binding mode of 4-nba see Scheme 2;
[d] μ_2-bridging water; # characterized by analytical, spectral and thermal data.

Abbreviations used: S.G. = Space group; Coord sphere = Coordination sphere of Ca; No. of 4-nba = Number of 4-nitrobenzoates linked to each Ca; D = Dimensionality; 4-nba = 4-nitrobenzoate; Im = imidazole; N-MeIm = N-methylimidazole; pyr = pyrazole; 2-MeIm = 2-methylimidazole; 2-ap = 2-aminopyridine.

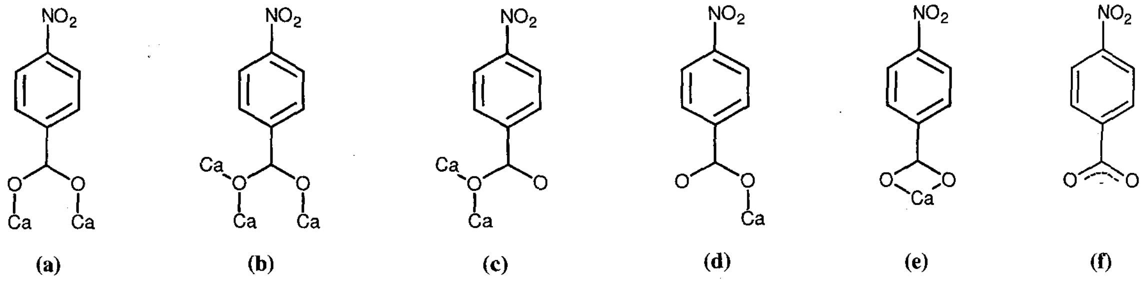

Scheme 2

centrosymmetric space groups. The 4-nba ligand exhibits six different modes of binding in these compounds (Scheme 2). The three different bridging modes of ligation, namely, symmetrical bridging, tridentate bridging and monoatomic bridging are observed in the one-dimensional mixed ligand polymers[31-33], while the monodentate and bidentate modes of ligation and free uncoordinated form are observed in the zero-dimensional compounds. In the polymeric compounds, each Ca(II) is coordinated to oxygen atoms from at least four different 4-nba ligands with five carboxylates surrounding the Ca(II) in the one-dimensional ladder polymer $[Ca(N\text{-}MeIm)(4\text{-}nba)_2]_n$. It is interesting to note that five of the compounds listed in Table 4 are anhydrous (water deficient), while two compounds $[Ca(H_2O)(4\text{-}nba)_2]$ and $[Ca(H_2O)(2\text{-}MeIm)(4\text{-}nba)_2]_n$ exhibit a Ca:water ratio of 1:1. The mixed ligand compounds, $[Ca(H_2O)_3(Im)(4\text{-}nba)_2]\cdot Im$ and $[Ca(H_2O)_4(4\text{-}nba)_2]$, show a Ca:water ratio of 1:3 and 1:4 respectively. The title compound, $[Ca(H_2O)_6(4\text{-}nba)](4\text{-}nba)(2\text{-}ap)\cdot H_2O$, referred to as water-rich Ca(II) 4-nitrobenzoate, contains the maximum water and is unique in that it contains six water molecules coordinated to Ca(II) and a lattice water and a solvent 2-aminopyridine. In the water-rich compound, each Ca(II) is linked to a single 4-nba ligand in a monodentate fashion, while the second unique 4-nba functions as a free anion for charge balance. It is to be noted that compounds which contain less or no water exhibit bridging 4-nba ligation, while compounds with a higher water content exhibit monodentate or bidentate binding modes of 4-nba.

Conclusions

In the present work we have described a simple method of synthesis of the compound $[Ca(H_2O)_4(4\text{-}nba)_2]$ (**1**) which can be used as a convenient source for the synthesis of new mixed ligand compounds of Ca(II) on reaction with N-donor ligands. The reaction of (**1**) with 2-ap resulted in the formation of a water-rich compound (**2**) in aqueous conditions and an anhydrous compound (**1-a**) in a solid state reaction. The water-rich Ca(II) compound, $[Ca(H_2O)_6(4\text{-}nba)](4\text{-}nba)(2\text{-}ap)\cdot H_2O$, is a rare example of a structurally characterized Ca(II) compound containing six coordinated water molecules. A comparative study of differently hydrated Ca(II) 4-nitrobenzoates reveals a rich structural chemistry.

Supplementary Data

Crystallographic data (excluding structure factors) for the structure of $[Ca(H_2O)_6(4\text{-}nba)](4\text{-}nba)(2\text{-}ap)\cdot H_2O$ reported in this paper have been deposited with the Cambridge Crystallographic Data Centre as supplementary publication no. CCDC 793917. Copies of the data can be obtained, free of charge, on application to CCDC, 12 Union Road, Cambridge CB2 1 EZ, UK; Fax: +44-(0)1223-336033; Email: deposit@ccdc.cam.ac.uk

Acknowledgement

BRS thanks University Grants Commission (UGC), New Delhi, for financial support under the Special Assistance Programme F.540/25/DRS/2007/(SAP-I).

References

1 Fromm K M, *Coord Chem Rev*, 252 (2008) 856.

2 Cotton F A, Wilkinson G, Murillo C A & Bochmann M, *Advanced Inorganic Chemistry*, 6th Edn, (Wiley, New York), 1999, Chap. 4, pp. 111-130.

3 Einspahr H & Bugg C E, *Acta Crystallogr*, 36B (1980) 264.

4 Einspahr H & Bugg C E, *Acta Crystallogr*, 37B (1981) 1044.

5 Katz A K, Glusker J P, Beebe S A & Bock C W, *J Am Chem Soc*, 118 (1996) 5752.

6 Murugavel R & Korah R, *Inorg Chem*, 46 (2007) 11048.

7 Gili P, Lorenzo-Luis P A, Mederos A, Arrieta J M, Germain G, Castiñeiras A & Carballo R, *Inorg Chim Acta*, 295 (1999) 106.

8 Morin G, Shang M & Smith B D, *Acta Crystallogr*, 56C (2000) 544; Starosta W, Ptasiewicz-Bak H & Leciejewicz J, *J Coord Chem*, 56 (2003) 33.

9 Srinivasan B R, Shetgaonkar S Y & Raghavaiah P, *Indian J Chem*, 48A (2009) 1662.

10 Dale S H, Elsegood M R J & Kainth S, *Acta Crystallogr*, 59C (2003) m505; Morgant G, Angelo J, Desmaele D, Dichi E, Sghaier M, Fraisse B, Retailleau P, Brumas V, Fiallo M M L, Tomas A, *Polyhedron*, 27 (2008) 2097.

11 Srinivasan B R, Sawant J V, Näther C & Bensch W, *J Chem Sci*, 119 (2007) 243; Srinivasan B R & Sawant S C, *Thermochim Acta*, 402 (2003) 45.

12 Wiesbrock F, Schier A & Schmidbaur H, *Z Naturforsch*, B57 (2002) 251; Srinivasan B R, Sawant S C & Dhuri S N, *Indian J Chem*, 41A (2002) 290.

13 Murugavel R, Karambelkar V V & Anantharaman G, *Indian J Chem*, 39A (2000) 843.

14 Murugavel R, Karambelkar V V, Anantharaman G & Walawalkar M G, *Inorg Chem*, 39 (2000) 1381.

15 Fox S, Busching I, Barklage W & Strasdeit H, *Inorg Chem*, 46 (2007) 818.

16 Murugavel R & Banerjee S, *Inorg Chem Commun*, 6 (2003) 810.

17 Murugavel R, Kumar P, Walawalkar M G & Mathialagan R, *Inorg Chem*, 46 (2007) 6828.

18 Groneman R H & Atwood J L, *Cryst Eng*, 2 (1999) 241.

19 Karipides A, Ault J & Reed A T, *Inorg Chem*, 16 (1977) 3299.

20 van Der Sluis P, Schouten A & Spek A L, *Acta Crystallogr,* 43C (1987) 1922.

21 Senkovska I & Thewalt U, *Acta Crystallogr,* 61C (2005) m448.

22 Yano S, Numata M, Kato M, Motoo S & Nishimura T, *Acta Crystallogr,* 57E (2001) m488.

23 Karipides A, McKinney C & Peiffer K, *Acta Crystallogr,* 44C (1988) 46.

24 Karipides A & Miller C, *J Am Chem Soc,* 106 (1984) 1494.

25 Strahs G & Dickerson R E, *Acta Crystallogr,* 24B (1968) 571.

26 Song W D, Guo X & Zhang C H, *Acta Crystallogr,* 63E (2007) m399.

27 Srinivasan B R, Shetgaonkar S Y & Raghavaiah P, *Polyhedron,* 28 (2009) 2879.

28 Srinivasan B R & Shetgaonkar S Y, *J Coord Chem,* 63 (2010) 3403.

29 Srinivasan B R, Sawant J V & Raghavaiah P, *Indian J Chem,* 45A (2006) 2392.

30 Srinivasan B R, Sawant J V & Raghavaiah P, *J Chem Sci,* 119 (2007) 11.

31 Srinivasan B R, Shetgaonkar S Y, Sawant J V & Raghavaiah P, *Polyhedron,* 27 (2008) 3299.

32 Srinivasan B R, Shetgaonkar S Y, Näther C & Bensch W, *Polyhedron,* 28 (2009) 534.

33 Srinivasan B R, Shetgaonkar S Y & Näther C, *Z Anorg Allg Chem,* 636 (2010) (in press). http://onlinelibrary.wiley.com/doi/10.1002/zaac.201000214/abstract.

34 Sheldrick G M, *Acta Crystallogr,* 64A (2008) 112.

35 Srinivasan B R, Sawant S C & Das S K, *Indian J Chem,* 43A (2004) 1066; Srinivasan B R, Sawant J V & Raghavaiah P, *Indian J Chem,* 48A (2009) 181; Srinivasan B R & Rane G K, *J Chem Sci,* 121 (2009) 145.

36 Srinivasan B R, Sawant J V, Sawant S C & Raghavaiah P *J Chem Sci,* 119 (2007) 593; Srinivasan B R, Raghavaiah P & Sawant J V, *Acta Crystallogr,* 63E (2007) m2251.

Journal of Coordination Chemistry
Vol. 63, No. 19, 10 October 2010, 3403–3412

A calcium(II) coordination polymer showing two different bridging 2-carbamoyl-4-nitrobenzoate coordination modes†

BIKSHANDARKOIL R. SRINIVASAN* and SANTOSH Y. SHETGAONKAR

Department of Chemistry, Goa University, Panaji 403206, Goa, India

(*Received 10 March 2010; in final form 16 June 2010*)

Aqueous reaction of $CaCO_3$ with 2-carbamoyl-4-nitrobenzoic acid (2-ca-4nbaH) results in the formation of a 1-D coordination polymer $[Ca(H_2O)_2(2\text{-ca-4nba})_2]$ (**1**), which crystallizes in the centrosymmetric triclinic space group $P\bar{1}$. The structure consists of a central Ca(II), two coordinated waters, a symmetrical bridging (μ_2-$\eta^1:\eta^1$) 2-ca-4nba, and a tridentate bridging (μ_2-$\eta^2:\eta^1$) 2-ca-4nba. The calcium in **1** is coordinated by two water molecules and five oxygens of four symmetry-related 2-ca-4nba, resulting in a distorted pentagonal bipyramidal $\{CaO_7\}$ polyhedron. Pairs of $\{Ca(H_2O)_2\}$ units are linked into a 1-D coordination polymer extending along the *a*-axis with the aid of pairs of bridging 2-ca-4nba ligands. In the infinite chain, alternating pairs of Ca(II) ions exhibit Ca $\cdots$ Ca separations of 4.124 and 4.855 Å.

Keywords: 2-Carbamoyl-4-nitrobenzoic acid; Coordination polymer; Crystal structure; Symmetrical bridging; Tridentate bridging; Pentagonal bipyramid

1. Introduction

Coordination polymers or metal–organic frameworks (MOFs) have attracted much attention because of their topologies and potential applications in catalysis, adsorption (gas storage), separation, luminescence, etc. [1–3]. Compared to the extensive chemistry of coordination polymers based on transition metals, the coordination chemistry of group 1 and 2 metals with organic linkers is less explored, although there is growing interest in coordination polymers of s-block elements as alkali and/or alkaline earth metal cations are preferred to transition or lanthanide metal ions because they are nontoxic, cheap, and soluble in aqueous media. In a recent article, Fromm [4] reviewed the different ligand and polymer types of the s-block compounds.

Depending on the electronic and steric requirements of the central metal, the flexibility, binding modes, and hydrogen bonding characteristics of the organic linker (ligand), coordination polymers of differing dimensionalities can be constructed. For oxophilic s-block metals, carboxylic acid based ligands are useful for the construction of coordination polymers as the metals can be linked into an extended chain with bridging carboxylate. For the preparation of coordination polymers

---

*Corresponding author. Email: srini@unigoa.ac.in
†Dedicated to Prof. Dr Shashikumar K. Paknikar on the occasion of his 75th birthday.

Journal of Coordination Chemistry
ISSN 0095-8972 print/ISSN 1029-0389 online
DOI: 10.1080/00958972.2010.512955

different synthetic methodologies, namely, aqueous reaction of metal carbonate or hydroxide with the carboxylic acid under ambient conditions [5–12], reaction of aqueous metal chloride or nitrate with the carboxylic acid in the presence of a mild base [13–21], and hydrothermal reaction of metal sources with carboxylic acids [22–30] are employed. Several coordination polymers based on alkaline earth metals have been synthesized and structurally characterized [5–30].

As a part of an ongoing research program, we are investigating coordination chemistry of nitrobenzoates of s-block elements. In an earlier study, we reported synthetic aspects, spectral characteristics, structural features, and thermal properties and have unraveled a rich structural chemistry of the alkaline earth nitrobenzoates [31–38]. In a recent report, we used 2-carbamoyl-4-nitrobenzoic acid (2-ca-4nbaH) in which an amide (H-donor) and a nitro group (H-acceptor) disposed *ortho* and *trans*, respectively, with respect to the carboxylate to form a monomeric Mg(II) carboxylate $[Mg(H_2O)_6](2\text{-ca-4nba})_2$, which exhibits a supramolecular bilayer of 2-carbamoyl-4-nitrobenzoate (2-ca-4nba) anions sandwiched between layers of $[Mg(H_2O)_6]^{2+}$ cations [39]. In continuation of this study, we have synthesized and structurally characterized a 1-D coordination polymer of Ca(II) using 2-ca-4nba as a bridging ligand.

2. Experimental

2.1. *Materials and methods*

All chemicals used in this study were of reagent grade and used as received. The free acid 2-ca-4nbaH was prepared as described earlier [39]. Infrared (IR) spectra were recorded on a Shimadzu (IR Prestige-21) FT-IR spectrometer from 4000 to 400 cm^{-1}. Samples for IR spectra were diluted with KBr in the solid state and the signals referenced to polystyrene bands. UV-Vis diffuse reflectance spectra were obtained using a Shimadzu UV-2450 double beam spectrophotometer using $BaSO_4$ powder as reference (100% reflectance). Absorption data were calculated from the reflectance data using the Kubelka–Munk function ($a/S = (1 - R)^2/2R$, where a is the absorption coefficient, R the reflectance, and S the scattering coefficient). Luminescence spectra of the solid samples were recorded at room temperature (RT) using a Perkin Elmer LS 55 Luminescence spectrophotometer. Isothermal weight loss studies were performed in an electric furnace fitted with a temperature controller. Thermogravimetry–differential thermal analyzer (TG–DTA) measurements were performed in flowing air using a heating rate of 10 K min^{-1} in Al_2O_3 crucibles on a STA-409PC simultaneous thermal analyzer from Netzsch.

2.2. *Preparation of $[Ca(H_2O)_2(2\text{-ca-4nba})_2]$ (1)*

A mixture of 2-ca-4nbaH (0.420 g, 2 mmol) and $CaCO_3$ (0.100 g, 1 mmol) in water (25 mL) was heated on a steam bath for ~2 h until the effervescence ceased completely to obtain a clear pale yellow solution. The hot reaction mixture was filtered and kept undisturbed at RT. Pale yellow crystalline blocks of $[Ca(H_2O)_2(2\text{-ca-4nba})_2]$ (**1**) separated after several days were filtered, washed with a little ice cold water and then by ether, and dried in air. Yield 0.32 g (64%). Crystals obtained in this method were suitable for X-ray structure determination. Compound **1** was also prepared by reacting 2-ca-4nbaH (0.420 g, 2 mmol) with Na_2CO_3 (0.106 g, 1 mmol) at RT in water (25 mL) to obtain the Na salt. To the clear solution thus obtained, $CaCl_2 \cdot 2H_2O$ (0.147 g, 1 mmol) was added. The reaction mixture was filtered and left aside to isolate the product as before in ~75% yield.

Analytical data: Calcd for $CaC_{16}H_{14}N_4O_{12}$, $M = 494.39$ (**1**) (%): C, 38.87; H, 2.85; N, 11.33; and CaO, 11.32. Found (%): C, 38.47; H, 2.79; N, 11.03; and CaO, 11.1. IR data (in cm^{-1}): 3613, 3464, 3358, 3115, 3082, 2843, 2787, 2467, 2251, 2102, 1942, 1827, 1680, 1574, 1512, 1487, 1416, 1358, 1273, 1163, 1149, 1113, 1070, 974, 914, 858, 849, 833, 795, 787, 746, 692, 642, 584, 569, 488, and 447. UV-Vis (diffused reflectance): 294 nm. DTA data (°C): 152 (endo), 297 (endo), 440 (exo), and 557 (exo).

2.3. *X-ray crystal structure determination*

Intensity data for **1** were collected on a Bruker Smart Apex CCD diffractometer (CCD, charged coupled device) using graphite-monochromated Mo-Kα radiation. Data integration and reduction were carried out with SAINT software [40] and an empirical absorption correction was applied to the collected reflections with Siemens Area Detector Absorption (SADABS) [40]. All non-hydrogen atoms were refined anisotropically. Aromatic hydrogens were introduced in calculated positions and included in the refinement riding on their respective carbons. Hydrogens attached to O of water and N of amide were located in the difference map and refined isotropically with restraints for hydrogens attached to O using a riding model. Crystal data of (**1**): $C_{16}H_{14}CaN_4O_{12}$, $M = 494.39\,g\,mol^{-1}$, triclinic, space group $= P\bar{1}$, $\lambda = 0.71073$ Å, $a = 7.8884(16)$ Å, $b = 8.2028(16)$ Å, $c = 15.5763(16)$ Å, $\alpha = 75.15(3)°$, $\beta = 80.71(3)°$, $\gamma = 87.58(3)°$, $V = 961.5(3)$ Å^3, $Z = 2$, $D_{Calcd} = 1.708\,mg\,m^{-3}$, $\mu = 0.406\,mm^{-1}$, $F(000) = 508$, index range $= -9 \leq h \leq 10$, $-10 \leq k \leq 8$, and $-18 \leq l \leq 20$, and completeness to $\theta = 28.35°$ (95.0%). A total of 6349 reflections ($2.57 < \theta < 28.35°$) were collected of which 4556 were unique ($R_{int} = 0.0208$) and used for structure solution. Structure was solved using SHELXS-97 [41] and refined using SHELXL-97 [41] to R_1 (wR_2) $= 0.0615$ (0.1617) for 3231 reflections with ($I > 2\sigma(I)$) using 330 parameters. The highest peak and the deepest hole were observed at -0.694 and $+0.863$ eÅ^{-3}, respectively.

3. Results and discussion

3.1. *Description of crystal structure of 1*

Compound **1** crystallizes in the centrosymmetric triclinic space group $P\bar{1}$ with all atoms situated in general positions. Its structure consists of a central Ca(II), two coordinated water molecules, and two crystallographically independent 2-ca-4nba ligands (figure 1). The Ca(II) is seven coordinate, ligated by two terminal waters and five oxygens of four symmetry-related 2-ca-4-nba ligands, resulting in a distorted pentagonal bipyramidal $\{CaO_7\}$ (figure 1). The geometric parameters of the carboxylates are in the normal range. The O–Ca–O angles scatter in a wide range between 50.46(9)° and 172.13(18)° (table 1). The two terminal waters (O20 and O21) are bonded to calcium with Ca1–O20

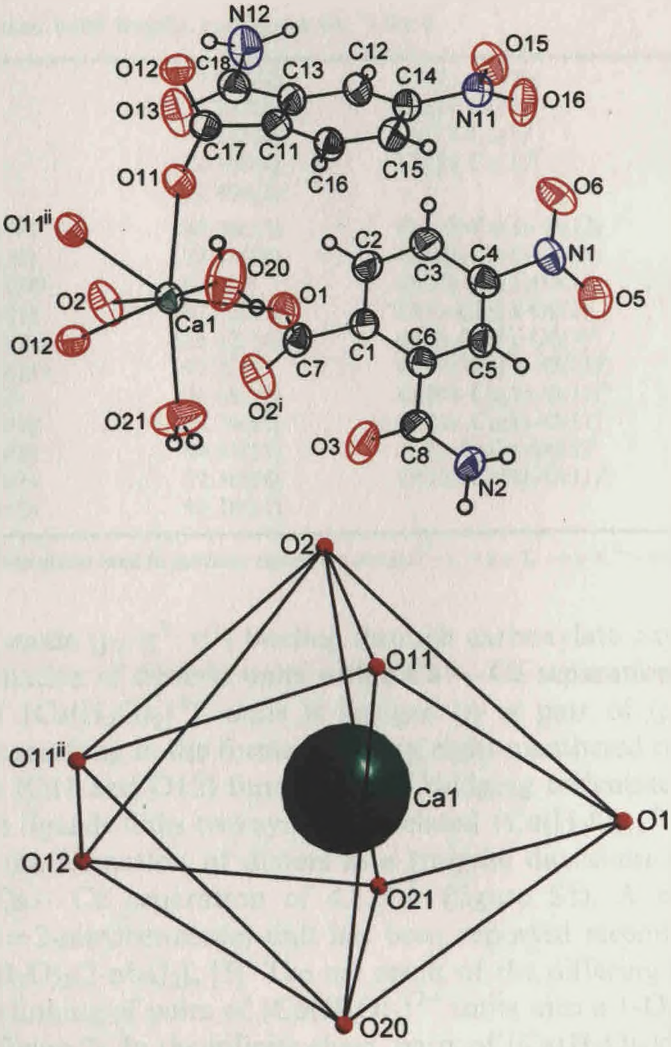

Figure 1. The coordination sphere of Ca(II) in **1** showing the atom-labeling scheme. Displacement ellipsoids are drawn at 50% probability excepting for hydrogens, which are shown as circles of arbitrary radius (top). The distorted pentagonal bipyramidal coordination polyhedron around Ca(II) in **1** (bottom). Symmetry code: ^{i} $-x, -y+1, -z+1$; ^{ii} $-x+1, y+1, -z+1$. Color code: C, black; H, gray; N, blue; O, red; and Ca, green.

and Ca1–O21 distances of 2.351(4) and 2.380(4) Å, respectively. The bidentate 2-ca-4nba is ligated to Ca *via* O1 with a Ca1–O1 distance of 2.400(3) Å and O2 is further bonded to a neighboring Ca(II) at 2.299(3) Å. The tridentate ligand (O11 and O12) bridges two neighboring Ca(II) ions with Ca1–O11 and Ca1–O12 bond lengths of 2.337(3) and 2.467(3) Å, respectively. The O11 is further linked to a symmetry-related Ca(II) at a very long distance of 2.656(3) Å. Recently, Dietzel *et al.* [25] reported a long Ca–O bond of 2.8384(16) Å in $[Ca(H_2dhtp)(H_2O)_2]_n$ (H_4dhtp = 2,5-dihydroxyterephthalic acid).

Compound **1** is a coordination polymer and its structure is based on dinuclear $\{Ca_2(H_2O)_4(2\text{-ca-4nba})_2\}^{2+}$. The crystallographically independent 2-ca-4nba in each formula unit coordinate to Ca(II) differently, namely, a symmetrical bridging mode (μ_2-$\eta^1:\eta^1$) and a tridentate bridging mode (μ_2-$\eta^2:\eta^1$). A pair of 2-ca-4nba ligands related by an inversion center bridges a pair of $\{Ca(H_2O)_2\}^{2+}$ units. The symmetrical

Table 1. Selected bond lengths and angles (Å, °) for **1**.

Ca(1)–O(2)	2.299(3)	Ca(1)–O(12)	2.467(3)
Ca(1)–O(11)	2.337(3)	Ca(1)–O(11)^{ii}	2.656(3)
Ca(1)–O(20)	2.351(4)	Ca(1)–Ca(1)^{i}	4.855
Ca(1)–O(21)	2.380(4)	Ca(1)–Ca(1)^{ii}	4.124
Ca(1)–O(1)	2.400(3)		
O(2)–Ca(1)–O(11)	87.76(13)	O(11)–Ca(1)–O(12)	119.19(10)
O(2)–Ca(1)–O(20)	172.13(18)	O(20)–Ca(1)–O(12)	86.18(15)
O(11)–Ca(1)–O(20)	87.0(2)	O(21)–Ca(1)–O(12)	74.96(13)
O(2)–Ca(1)–O(21)	87.30(19)	O(1)–Ca(1)–O(12)	151.06(11)
O(11)–Ca(1)–O(21)	165.12(14)	O(2)–Ca(1)–O(11)^{ii}	91.83(12)
O(20)–Ca(1)–O(21)	99.2(2)	O(11)–Ca(1)–O(11)^{ii}	68.80(11)
O(2)–Ca(1)–O(1)	100.68(12)	O(20)–Ca(1)–O(11)^{ii}	80.81(15)
O(11)–Ca(1)–O(1)	87.79(11)	O(21)–Ca(1)–O(11)^{ii}	125.39(13)
O(20)–Ca(1)–O(1)	84.97(15)	O(1)–Ca(1)–O(11)^{ii}	153.05(10)
O(21)–Ca(1)–O(1)	79.36(14)	O(12)–Ca(1)–O(11)^{ii}	50.46(9)
O(2)–Ca(1)–O(12)	91.28(11)		

Symmetry transformations used to generate equivalent atoms: ^{i} $-x, -y+1, -z+1$; ^{ii} $-x+1, -y+1, -z+1$.

bridging binding mode (μ_2-$\eta^1:\eta^1$) binding through carboxylate oxygens (O1 and O2) results in the formation of dimeric units with a Ca···Ca separation of 4.855 Å. In the dimer, a pair of $\{Ca(H_2O)_2\}^{2+}$ units is bridged by a pair of (μ_2-$\eta^1:\eta^1$) bridging 2-ca-4nba ligands resulting in the formation of an eight-membered ring (figure S1). The second 2-ca-4nba (O11 and O12) functions as a bridging tridentate ligand (μ_2-$\eta^2:\eta^1$) and a pair of such ligands links two symmetry-related $\{Ca(H_2O)_2\}^{2+}$ units *via* O11 and O12 resulting in the formation of dimers as a tricyclic dicalcium–*bis*(2-ca-4nba) unit with a shorter Ca···Ca separation of 4.124 Å (figure S1). A tricyclic dicalcium–*bis*(2-nba) (2-nba = 2-nitrobenzoate) unit has been reported recently in the polymeric carboxylate $[Ca(H_2O)_2(2\text{-nba})_2]_n$ [5]. The net result of the differing bridging 2-ca-4nba ligands in **1** is the linking of pairs of $\{Ca(H_2O)_2\}^{2+}$ units into a 1-D polymer extending along the *a*-axis (figure 2). In the infinite chain, pairs of $\{Ca(H_2O)_2\}^{2+}$ units are bridged *via* pairs of bridging 2-ca-4nba ligands and alternating pairs of Ca(II) ions exhibit Ca···Ca separations of 4.124 and 4.855 Å. The observed values of Ca···Ca distances are comparable with Ca···Ca distances in coordination polymers based on 4-nitrobenzoate [37, 38].

The structure reveals several H-bonding interactions. All oxygens of the amide, carboxylate, and nitro of 2-ca-4nba except O4 and O15 function as H-bond acceptors. Hydrogens of coordinated water, the amide, and two attached to carbon function as H-donors. Eleven O···H distances ranging from 1.901 to 2.583 Å (table 2) are comprised of four N–H···O, five O–H···O, and two C–H···O interactions. In several structurally characterized nitrobenzoates, oxygen of nitro functions as a H-acceptor and is involved in C–H···O interactions, in addition to O–H···O bonds [35–39, 42, 43]. In **1**, a similar feature is observed. The N2–H2A···O16, C5–H5···O16, and C13–H13···O6 interactions which link adjacent chains (figure 2) are interchain interactions and they extend the H-bonding network.

3.2. *Synthesis, spectroscopy, and thermal studies*

The reaction of $CaCO_3$ with 2-ca-4nbaH in boiling water followed by crystallization resulted in the formation of $[Ca(H_2O)_2(2\text{-ca-4-nba})_2]$ (**1**), containing

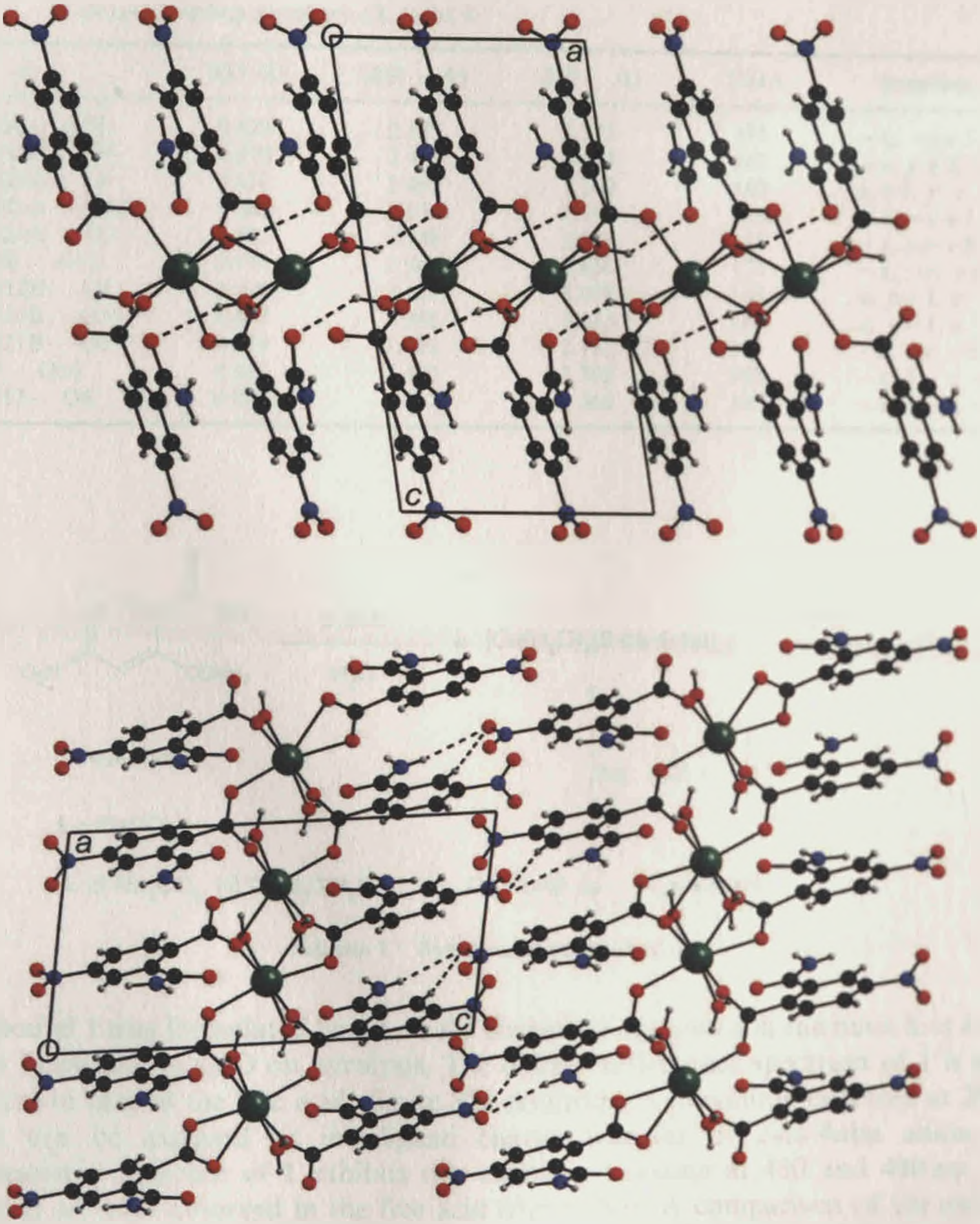

Figure 2. A view along the *b*-axis showing a part of the 1-D chain extending along the *a*-axis due to the bridging 2-ca-4nba in **1**. Intrachain H-bonding is shown by broken lines (top). Two adjacent polymeric chains of **1** in the *ac* crystallographic plane are linked by weak N–H ··· O and C–H ··· O bonds shown in broken lines (bottom). Color code: C, black; H, gray; N, blue; O, red; and Ca, green.

Ca : water : 2-ca-4nba in 1 : 2 : 2 ratio. Reaction of $CaCO_3$ with 4-nitrobenzoic acid (4-nbaH) under identical conditions resulted in the formation of $[Ca(H_2O)_4(4\text{-nba})_2]$ containing Ca : water : 4-nba in a 1 : 4 : 2 ratio [32]. Hence, it appears that the presence of the carbamoyl (amide) group at the 2-position in 2-ca-4nbaH is responsible for the different reactivities. Compound **1** was also prepared by the reaction of the water-soluble Na salt of 2-ca-4nbaH with $CaCl_2$ (scheme 1). Reaction of **1** with dilute HCl results in quantitative formation of the free acid, 2-ca-4nbaH.

Table 2. Hydrogen bonding geometry (Å, °) for **1**.

D–H···A	*d*(D–H)	*d*(H···A)	*d*(D···A)	∠DHA	Symmetry code
N2–H2A···O16	0.821	2.583	3.395	171	$-x, -y+1, -z$
N12–H12A···O5	0.970	2.465	3.412	165	$-x, y+2, -z$
O20–H20A···O3	0.836	2.495	3.192	142	$x+1, y, z$
O21–H21A···O13	0.865	2.530	3.142	128	$-x, -y+1, -z+1$
O21–H21A···O2	0.865	2.538	3.043	118	$-x, -y+1, -z+1$
N2–H2B···O12	0.926	1.965	2.884	171	$-x, -y, -z+1$
N12–H12B···O1	0.928	2.125	3.038	167	$x, y+1, z$
O20–H20B···O13	0.847	1.988	2.813	164	$x, y-1, z$
O21–H21B···O3	0.859	1.901	2.755	173	$-x, -y, -z+1$
C5–H5···O16	0.931	2.400	3.302	163	$-x, 1-y, -z$
C13–H13···O6	0.930	2.537	3.368	149	$-x, 2-y, -z$

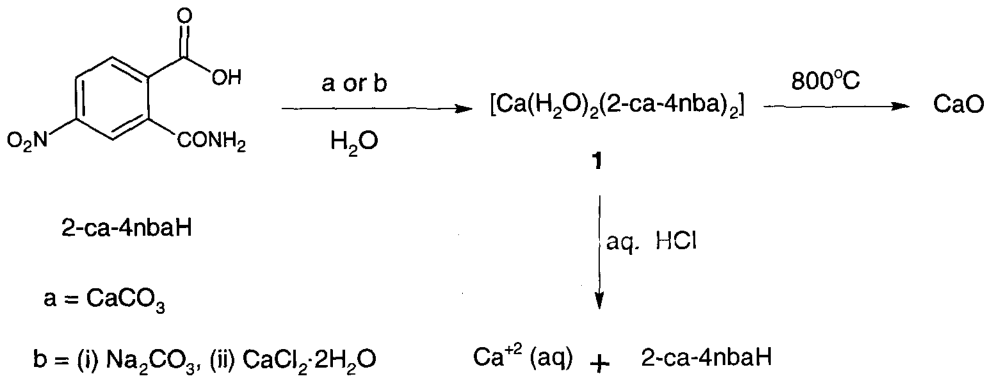

Scheme 1. Synthesis of compound **1**.

Compound **1** was formulated based on the elemental analysis and the mass loss leading to the formation of CaO on pyrolysis. The diffuse reflectance spectrum of **1** is nearly identical to that of the free acid (figure S2) exhibiting a maximum centered at 294 nm which can be assigned as intraligand charge transfer of 2-ca-4nba anion. The luminescence spectrum of **1** exhibits two emission maxima at 450 and 490 nm, both of which are also observed in the free acid (figure S3). A comparison of the emission spectra reveals that the first emission band of the Ca(II) compound is enhanced in intensity.

The IR spectrum of **1** exhibits several signals in the mid IR region, many of which are also observed in the free acid (figure S4), thus indicating the presence of the organic moiety in **1**. The presence of water can be readily inferred from the strong signal at 3613 cm^{-1}. The peak at 3464 cm^{-1} can be assigned for the N–H stretching vibration of the amide functionality, while the band due to the C=O of the amide is observed as a strong signal at 1680 cm^{-1}. Intense bands at 1512 and 1358 cm^{-1} can be assigned to the asymmetric and symmetric stretching vibrations of $-NO_2$. The asymmetric and symmetric stretching vibrations of the carboxylate are strong bands at 1574 and 1416 cm^{-1}, respectively.

The TG–DTA thermogram of **1** (figure 3) exhibits four thermal events. The first endothermic process at 152°C accompanied by a weight loss of 6.0% (expected to be 7.2%) can be assigned to the loss of two coordinated waters. Heating of **1** at 150°C

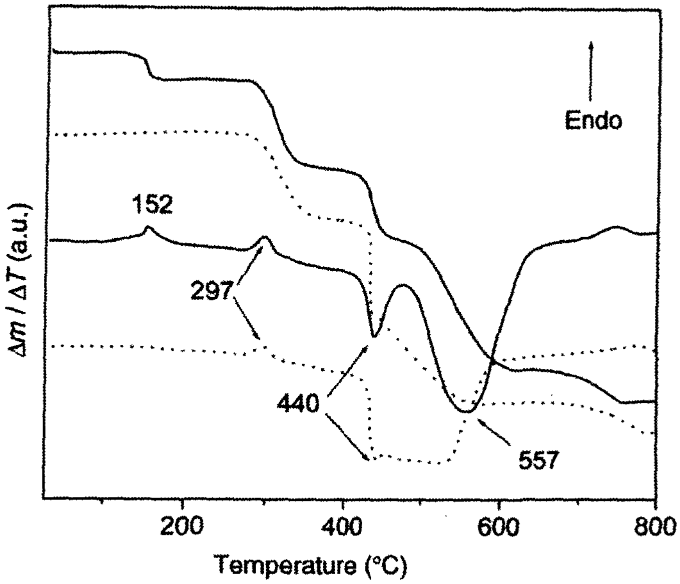

Figure 3. TG–DSC thermogram of **1** (solid line) and the anhydrous compound (dotted lines) obtained by heating **1** at 150°C.

in an oven results in the formation of an anhydrous compound, whose IR spectrum is devoid of the strong O–H signal at 3600 cm^{-1}. The second endothermic signal at 297°C as well as the exothermic events at 440°C and 557°C can be assigned as decomposition of the organic ligand leading to the formation of the oxide residue. Although the exact nature of these ligand decomposition processes cannot be commented upon, in the absence of associated mass spectral data of the emitted fragments, the formation of CaO as the final residue can be inferred as the residue based on mass loss. The complete loss of organics was also evidenced from the featureless IR spectrum of the residue. As expected, the thermogram of the anhydrous product (figure 3) is nearly identical to that of **1** except for the absence of an endothermic signal at around 152°C. Similar results were obtained from the isothermal weight loss studies which add credence to the above observations.

4. Conclusions

Several Ca(II) coordination polymers based on aromatic carboxylic acids have been hydrothermally synthesized and structurally characterized [22–27]. Linkers containing two or more –COOH groups like terephthalic acid, isophthalic acid, 2,5-dihydroxyterephthalic acid, pyrazole-3,5-dicarboxylic acid, pyridine-2,4,6-tricarboxylic acid, etc., were used for synthesis in hydrothermal reactions (table S1). In this study, we have reported on the structural characterization of a 1-D Ca(II) coordination polymer using monocarboxylic 2-ca-4nbaH as the organic linker. The synthesis of the title compound was performed under ambient conditions. The role of the 2-carbamoyl (amide) substituent in 2-ca-4nbaH forming a differently hydrated Ca(II) product can be shown by comparison of the reaction of $CaCO_3$ with 2-ca-4nbaH and (4-nbaH) under identical conditions. Based on the analysis of the structural features of several Ca-carboxylates, we recently showed that when the number of coordinated waters in a Ca-carboxylate is three or less, the carboxylate bridges [5]. The observation of bridging carboxylate for 2-ca-4nba in **1** is in accordance with the earlier result. The coordination polymer **1** reported herein constitutes a new example to the growing list of structurally characterized polymeric alkaline earth coordination compounds.

Supplementary material

CCDC 760722 contains the supplementary crystallographic data for the structure reported in this article. These data can be obtained free of charge *via* http://www.ccdc.cam.ac.uk/conts/retrieving.html or from the Cambridge Crystallographic Data Centre, 12 Union Road, Cambridge CB2 1EZ, UK (Fax: +44-1223-336033; Email: deposit@ccdc.cam.ac.uk). Additional figures related to the crystal structure and diffused reflectance UV-Vis, IR, and luminescence spectra of **1** are available as "Supplementary data" for this article and can be found in the online version.

Acknowledgments

BRS thanks Prof P.K. Bharadwaj, Department of Chemistry, Indian Institute of Technology (IIT), Kanpur for providing the X-ray intensity data of **1**, Dr P. Raghavaiah, School of Chemistry, University of Hyderabad, for facilitating helpful discussions, and Department of Science and Technology (DST), New Delhi, for financing a visit to IIT Kanpur under the DST-SERC Visiting Fellowship.

References

[1] C. Janiak. *J. Chem. Soc., Dalton Trans.*, 2781 (2003).
[2] R. Robson. *J. Chem. Soc., Dalton Trans.*, 5113 (2008). For a recent perspective on the pros and cons of coordination polymer and MOF terminology, see K. Biradha, A. Ramanan, J.J. Vittal. *Cryst. Growth Des.*, **9**, 2969 (2009).
[3] S.R. Batten, S.M. Neville, D.R. Turner. *Coordination Polymers: Design, Analysis and Application*, RSC Publishing, Cambridge, UK (2009).
[4] K.M. Fromm. *Coord. Chem. Rev.*, **252**, 856 (2008).
[5] B.R. Srinivasan, S.Y. Shetgaonkar, P. Raghavaiah. *Polyhedron*, **28**, 2879 (2009).
[6] B.R. Srinivasan, S.Y. Shetgaonkar, P. Raghavaiah. *J. Chem. Sci.*, **120**, 249 (2008).
[7] M. Dan, A.K. Cheetham, C.N.R. Rao. *Inorg. Chem.*, **45**, 8227 (2006).
[8] Z. Fei, T.J. Geldbach, D. Zhao, R. Scopelliti, P.J. Dyson. *Inorg. Chem.*, **44**, 5200 (2005).
[9] H.-F. Zhu, Z.-H. Zhang, W.-Y. Sun, T. Okamura, N. Ueyama. *Cryst. Growth Des.*, **5**, 177 (2005).
[10] S. Fox, I. Büsching, W. Barklage, H. Strasdeit. *Inorg. Chem.*, **46**, 818 (2007).
[11] A. Bacchi, M. Carcelli, C. Pelizzi, G. Pelizzi, P. Pelagatti, D. Rogolino, M. Tegoni, C. Viappiani. *Inorg. Chem.*, **42**, 5871 (2003).
[12] R. Murugavel, P. Kumar, M.G. Walawalkar, R. Mathialagan. *Inorg. Chem.*, **46**, 6828 (2007).
[13] S. Neogi, J.A.R. Navarro, P.K. Bharadwaj. *Cryst. Growth Des.*, **8**, 1554 (2008).
[14] Q. Shuai, S. Chen, S. Gao. *Inorg. Chim. Acta*, **360**, 1381 (2007).
[15] A. Grirrane, A. Pastor, E. Álvarez, R. Moyano, A. Galindo. *Inorg. Chem. Commun.*, **10**, 1125 (2007).
[16] R. Murugavel, V.V. Karambelkar, G. Anantharaman, M.G. Walawalkar. *Inorg. Chem.*, **39**, 1381 (2000).

[17] R. Murugavel, V.V. Karambelkar, G. Anantharaman. *Indian J. Chem.*, **39A**, 843 (2000).
[18] R. Murugavel, K. Baheti, G. Anantharaman. *Inorg. Chem.*, **40**, 6870 (2001).
[19] Y. Yang, G. Jiang, Y.-Z. Li, J. Bai, Y. Pan, X.-Z. You. *Inorg. Chim. Acta*, **359**, 3257 (2006).
[20] D.A. Lenev, K.A. Lyssenko, R.G. Kostyanovsky. *Eur. J. Inorg. Chem.*, 2979 (2003).
[21] I. Senkovska. *Z. Naturforsch.*, **61b**, 1383 (2006).
[22] C.A. Williams, A.J. Blake, C. Wilson, P. Hubberstey, M. Schroder. *Cryst. Growth Des.*, **8**, 911 (2008).
[23] L.-C. Yu, Z.-F. Chen, H. Liang, C.-S. Zhou, Y. Li. *J. Mol. Struct.*, **750**, 35 (2005).
[24] L. Pan, T. Frydel, M.B. Sander, X. Huang, J. Li. *Inorg. Chem.*, **40**, 1271 (2001).
[25] P.C. Dietzel, R. Blom, H. Fjellvag. *Z. Anorg. Allg. Chem.*, **635**, 1953 (2009).
[26] C. Volkringer, T. Loiseau, G. Férey, J.E. Warren, D.S Wragg, R.E. Morris. *Solid State Sci.*, **9**, 455 (2007).
[27] M.C. Das, S.K. Ghosh, E.C. Sanudo, P.K. Bharadwaj. *Dalton Trans.*, 1644 (2009).
[28] Z. Guo, G. Li, L. Zhou, S. Su, Y. Lei, S. Dang, H. Zhang. *Inorg. Chem.*, **48**, 8069 (2009).
[29] I. Senkovska, S. Kaskel. *Eur. J. Inorg. Chem.*, 4564 (2006).
[30] A. Rossin, A. Ienco, F. Costantino, T. Montini, B.D. Credico, M. Caporali, L. Gonsalvi, P. Fornasiero, M. Peruzzini. *Cryst. Growth Des.*, **8**, 3302 (2008).
[31] B.R. Srinivasan, S.C. Sawant. *Thermochim. Acta*, **402**, 45 (2003).
[32] B.R. Srinivasan, J.V. Sawant, P. Raghavaiah. *Indian J. Chem.*, **45A**, 2392 (2006).
[33] B.R. Srinivasan, J.V. Sawant, P. Raghavaiah. *J. Chem. Sci.*, **119**, 11 (2007).
[34] B.R. Srinivasan, J.V. Sawant, C. Näther, W. Bensch. *J. Chem. Sci.*, **119**, 243 (2007).
[35] B.R. Srinivasan, J.V. Sawant, S.C. Sawant, P. Raghavaiah. *J. Chem. Sci.*, **119**, 593 (2007).
[36] B.R. Srinivasan, P. Raghavaiah, J.V. Sawant. *Acta Crystallogr.*, **E63**, m2251 (2007).
[37] B.R. Srinivasan, S.Y. Shetgaonkar, J.V. Sawant, P. Raghavaiah. *Polyhedron*, **27**, 3299 (2008).
[38] B.R. Srinivasan, S.Y. Shetgaonkar, C. Näther, W. Bensch. *Polyhedron*, **28**, 534 (2009).
[39] B.R. Srinivasan, S.Y. Shetgaonkar, P. Raghavaiah. *Indian J. Chem.*, **48A**, 1662 (2009).
[40] (a) *Bruker SMART V5.630 and SAINT-PLUS V6.45*, Bruker-Nonius Analytical X-ray Systems Inc.: Madison, Wisconsin, USA (2003); (b) SADABS. *Empirical Absorption Correction Program*, Bruker AXS Inc., Madison, WI, USA (1997).
[41] G.M. Sheldrick. *Acta Crystallogr.*, **A64**, 112 (2008).
[42] B.R. Srinivasan, J.V. Sawant, P. Raghavaiah. *Indian J. Chem.*, **48A**, 181 (2009).
[43] B.R. Srinivasan, G.K. Rane. *J. Chem. Sci.*, **121**, 145 (2009).

Indian Journal of Chemistry
Vol. 48A, December 2009, pp. 1662-1666

First alkaline earth 2-carbamoyl-4-nitrobenzoate: Synthesis and supramolecular structure

Bikshandarkoil R Srinivasan[a, *], Santosh Y Shetgaonkar[a] & Pallepogu Raghavaiah[b]
[a]Department of Chemistry, Goa University, Goa 403 206, India
[b]School of Chemistry, University of Hyderabad,
Hyderabad 500 046, India
Email: srini@unigoa.ac.in

Received 30 September 2009; accepted 17 November 2009

2-Carbamoyl-4-nitrobenzoic acid (2-ca-4nbaH) has been prepared by alkaline hydrolysis of 4-nitrophthalimide. Aqueous reaction of $MgCO_3$ with 2-ca-4nbaH results in the formation of $[Mg(H_2O)_6](2\text{-ca-4nba})_2$, which crystallizes in the centrosymmetric monoclinic space group $P2_1/c$ with Mg(II) situated on an inversion center. The crystal structure consists of a distorted octahedral hexaaquamagnesium(II) cation and a free uncoordinated 2-ca-4nba anion. The cation and anion are involved in three varieties of H-bonding interactions, resulting in a supramolecular bilayer of 2-ca-4nba anions sandwiched between layers of $[Mg(H_2O)_6]^{2+}$ cations.

Keywords: Coordination chemistry, Magnesium, Crystal structure, Supramolecular bilayer

IPC Code: Int. Cl.^{9} C07F3/02

Chemistry of *s*-block elements is a topical area of research[1-6]. Non-toxic and water soluble nature, variable structural chemistry[6], affinity for O-donor ligands[7], relevance in biology[8] are some factors responsible for the growing interest in the chemistry of *s*-block elements. As part of our longstanding research interest[9,10], we are investigating the coordination chemistry of the amino- (aba) and nitro- (nba) benzoates of *s*-block elements. In earlier work, we have reported the spectral characteristics, structural aspects and thermal properties and have unraveled a rich structural chemistry of alkaline earth nitro-(nba) benzoates[5,11-14]. A comparison of the structural features of alkaline earth nitrobenzoates with those of the aminobenzoates[15-17] reveals that in the case of Mg(II), the compounds contain the $[Mg(H_2O)_6]^{2+}$ unit charge balanced by the corresponding carboxylate anion[14,15,17] while the aminobenzoates of the heavier alkaline earths exhibit M-N (M = Sr or Ba) bonding[16]. In the nitrobenzoates, no metal to N bonding is observed, excepting in $[Ba(H_2O)_3(2\text{-nba})_2]$ which shows coordination of Ba to the nitro oxygen[11]. In terms of secondary interactions, the amino group acts as H-donor while the oxygen atom of the nitro moiety functions as a hard H-bond acceptor leading to novel supramolecular assemblies. It is of interest to investigate the structural aspects of metal-carboxylates, containing both H-acceptor and H-donor groups in the same ligand, in addition to the carboxylate. Herein, we report the synthesis of 2-carbamoyl-4-nitrobenzoic acid (2-ca-4nbaH) (**1**) in which an amide (H-donor) and a nitro group (H-acceptor) are disposed *ortho* and *trans* respectively with respect to the carboxylate group. The presence of such substituents in (**1**) results in an interesting supramolecular architecture in $[Mg(H_2O)_6](2\text{-ca-4nba})_2$ (**2**), which constitutes the first example of a structurally characterized alkaline earth 2-carbmoyl-4-nitrobenzoate.

Experimental

Nitration of phthalimide by a literature method[18] afforded a mixture of the isomeric 3- and 4-nitrophthalimide. After separation from the soluble 3-nitro isomer (minor product), the insoluble 4-nitrophthalimide (10 g, 0.052 mol) was taken in water (50 mL) containing NaOH (2.08 g, 0.052 mol) at room temperature and stirred for 15 min to obtain a clear brown solution. To this, dilute HCl was added in drops (*p*H = 4-5) resulting in the separation of the crude product. The solid was filtered and washed well with water till free of chloride and recrystallized from alcohol to obtain (**1**) in 8 g yield. (m.pt.: 144-145 °C)

UV-vis: λ_{max} = 293 nm (ε = 5210 L mol^{-1} cm^{-1}); IR (cm^{-1}): 3396, 3268, 3219, 3116, 3093, 2872, 2778, 2596, 2480, 1725 υ_{as}(-COO), 1667 υ_{CO}(amide), 1611, 1572 $\upsilon_{as}(-NO_2)$ 1502, 1485, 1441, 1380, 1354 υ_s $(-NO_2)$, 1306, 1267, 1246, 1120, 1068, 977, 910, 861, 807, 777, 737, 685, 643, 620, 547, 429; ^{1}H NMR (DMSO-d_6) δ (in ppm) 7.64 (d, J = 8.4 Hz, H3), 8.20 (dd, J = 2.4 Hz, J = 8.4 Hz, H5), 8.36 (d, J = 2.4 Hz, H6), 8.94 (br s, J = 2.4 Hz, -N-H). For assignment, the numbering for H-atom is same as the crystallographic labeling in Fig. 1.

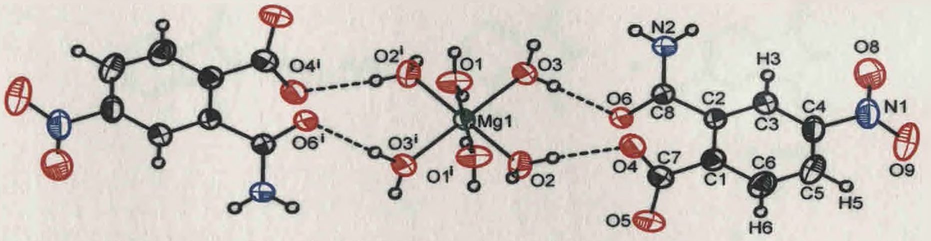

Fig. 1 – Crystal structure of $[Mg(H_2O)_6](2\text{-ca-4nba})_2$ showing the atom-labeling scheme. Displacement ellipsoids are drawn at the 50% probability level except for the H atoms, which are shown as circles of arbitrary radii. Intramolecular H-bonding is shown as dashed lines. [Symmetry code: i) -x+2, -y, -z+1; Selected geometric parameters (Å,°): Mg(1)-O(1), 2.0566(11); Mg(1)-O(2), 2.0626(11); Mg(1)-O(3), 2.0735(11); O(1)-Mg(1)-O(1)^i, 180.0(5); O(2) -Mg(1)-O(2)^i, 180; O(3)^i -Mg(1)-O(3), 180.0(3); O(1)-Mg(1)-O(2), 91.48(5); O(2)-Mg(1)-O(3), 92.13(4); O(1)-Mg(1)-O(3), 94.97(5). O(1)^i–Mg(1)-O(3), 85.03(5); O(2)^i–Mg(1)-O(3), 87.87(4); O(1)^i-Mg(1)-O(2), 88.52(5)].

Compound (**1**) (2.14g, 10mmol) was taken in water (50 mL) and heated on a steam bath till most of the solid dissolved. To the hot reaction mixture, $MgCO_3$ (0.42 g, 5 mmol) was added slowly resulting in brisk effervescence. The heating was continued till effervescence ceased completely to obtain a clear pale yellow solution. The hot reaction mixture was filtered and kept undisturbed at room temperature. Pale yellow crystalline blocks that separated out after 5 days were filtered, washed with ice cold water, followed by ether and dried in air. Yield 1.92 g (69.5%).

Anal.: Calc. for $C_{16}H_{22}N_4MgO_{16}$ (550.67): Mg, 4.41; MgO, 7.32; C, 34.90; H, 4.03; N, 10.17. Found: Mg, 4.33; MgO, 7.21; C, 34.53; H, 4.02; N, 9.57%; UV-vis: 293 nm (ε = 15035 L mol^{-1}cm^{-1}); IR (cm^{-1}): 3568-3215 (br, υ_{OH}), 1680 υ_{as}(-COO), 1643 υ_{CO}(amide), 1612, 1566 υ_{as}(-NO_2), 1516, 1487, 1427, 1395, 1350 υ_s(-NO_2), 1305, 1262, 1149, 1131, 1077, 923, 866, 816, 736, 649, 571, 505.

^{1}H NMR (DMSO-d_6) δ (in ppm) 7.65 (d, J = 8.4 Hz, H3), 8.20 (dd, J = 2.4 Hz, J = 8.4 Hz, H5), 8.4 (d, J = 2.4 Hz, H6), 9.1 (br s, J = 2.4 Hz -N-H); DSC (in °C): 94 (endo), 136 (endo), 245 (endo), 433 (exo), 545 (exo).

Intensity data for (**2**) were collected on a Bruker Smart Apex CCD diffractometer using graphite-monochromated Mo-K$_\alpha$ radiation. Data integration and reduction were processed with SAINT software[19] and an empirical absorption correction was applied to the collected reflections with SADABS[19]. All non-hydrogen atoms were refined anisotropically. Aromatic hydrogens were introduced on calculated positions and included in the refinement riding on their respective carbon atoms. The hydrogen atoms attached to the O and N atoms of water and amide were located in the difference map and were refined isotropically using a riding model. Crystal data of (**2**) $C_{16}H_{22}MgN_4O_{16}$, M = 550.69 g mol^{-1}, monoclinic, space group = $P2_1/c$, λ = 0.71073 Å, a = 15.729(3) Å, b = 7.5571(16) Å, c = 9.982(2) Å, $\alpha = \gamma$ = 90°, β = 100.658(3)°, V = 1166.1(4) Å^3, Z = 2, D_{calc} = 1.568 mg m^{-3}, μ = 0.165 mm^{-1}, F(000) = 572, index range = $-19 \le h \le 19$, $-9 \le k \le 9$, $-12 \le l \le 12$; completeness to theta = 26.02° (99.5%). A total of 11523 reflections ($1.32 < \theta < 26.02°$) were collected of which 2289 were unique (R_{int} = 0.0238) and used for structure solution. Structure was solved using SHELXS-97[20] and refined using SHELXL-97[20] to $R1$ ($wR2$) = 0.0360 (0.0972) for 2070 reflections with ($I > 2\sigma(I)$) using 169 parameters. Highest peak and deepest hole were observed at -0.202 and +0.217 eÅ^{-3} respectively.

Results and discussion

Nitration of phthalimide resulted in the formation of a mixture of isomeric 3- and 4- nitrophthalimides containing the insoluble 4-nitrophthalimide as the major product, which on alkaline hydrolysis followed by acidification afforded the amide substituted acid 2-ca-4nbaH (**1**) (Scheme 1), whose identity was confirmed from spectral data. Aqueous reaction of $MgCO_3$ with (**1**) in a 1:2 ratio followed by crystallization resulted in the formation of X-ray quality blocks of $[Mg(H_2O)_6](2\text{-ca-4nba})_2$ (**2**).

Compound (**2**) was also prepared by the reaction of an aqueous solution of $MgCl_2$ with the Na-salt of 2-ca-4nbaH (**1**). Our synthetic methodology is very similar to the one employed for the synthesis of several Mg(II) carboxylates (Table 1) wherein $MgCO_3$ or $Mg(OH)_2$ is reacted with the carboxylic acid or alternatively the water soluble $MgCl_2$ is reacted with the Na or K salt of the acid generated

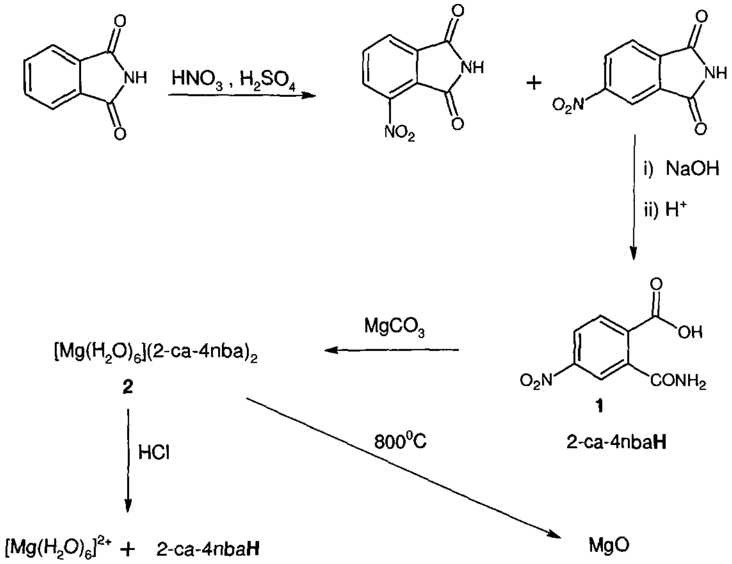

Scheme 1

Table 1 – Synthesis[a] and structural aspects[b] of some Mg(II) carboxylates

Compound	Mg source	Base	Space group	Secondary interaction	Ref.
$[Mg(H_2O)_6](2\text{-ca-4nba})_2$	$MgCO_3$ $MgCl_2$	---- $NaHCO_3$	*P2₁/c*	O-H···O, N-H···O, C-H···O	This work
$[Mg(H_2O)_6](2\text{-aba})_2 \cdot 2H_2O$[c]	$MgCl_2$	KOH	*P2₁/c*	O-H···O, N-H···O	17
$[Mg(H_2O)_6](4\text{-aba})_2 \cdot 2H_2O$	$MgCl_2$	NH_4OH	*Pbca*	O-H···O, N-H···O	15
$[Mg(H_2O)_6](4\text{-nba})_2 \cdot 2H_2O$	$MgCO_3$	----	$P\bar{1}$	O-H···O	14
$[Mg(H_2O)_6](C_7H_4NO_5)_2$	$MgCl_2$	NaOH	$P\bar{1}$	O-H···O	3
$[Mg(H_2O)_4(C_7H_3NO_5)]$[d]	$Mg(OH)_2$	---	$P\bar{1}$	O-H···O	3
$[Mg(H_2O)_6](H_2PMA)_2$	$MgCO_3$	----	*P2/m*	O-H···O	21

[a] In a typical synthesis $MgCO_3$ or $Mg(OH)_2$ is reacted with the acid in aqueous medium. Alternatively $MgCl_2$ can be reacted with the acid in the presence of a base.

[b] All compounds listed in Table are six coordinated and contain a $\{MgO_6\}$ octahedron with Mg(II) situated on an inversion centre.

[c] For an alternate synthesis see Ref. 9

[d] $(C_7H_3NO_5)$ functions as a bidentate ligand binding through a phenolate O and a nitro O.

Abbr.: 2-abaH = 2-aminobenzoic acid; 4-abaH = 4-aminobenzoic acid; 4-nbaH = 4-nitrobenzoic acid; $C_7H_4NO_5$ = 3-hydroxy-4-nitrobenzoate; H_4PMA = benzene-1,2,4,5-tetracarboxylic acid.

in situ by use of NaOH, KOH or $NaHCO_3$[3,14,15,17,21]. In all reactions, a Mg(II) carboxylate product containing a minimum of six moles of water per Mg(II) is obtained. However, with 3-hydroxy-4-nitrobenzoic acid a compound having Mg:H_2O in a 1:4 ratio has been reported using $Mg(OH)_2$ as Mg source[3]. Coordination polymers having one or two moles of water per Mg or no water, are obtained under hydrothermal conditions[1,2]. Reaction of (**2**) with dilute HCl resulted in its decomposition leading to the quantitative formation of 2-ca-4nbaH, while pyrolysis of (**2**) at 800°C resulted in the formation of MgO.

Both compounds analyzed satisfactorily and exhibit identical NMR and UV spectra. The observed chemical shifts in the NMR spectra of the free acid (**1**) and the Mg(II) compound (**2**) are in the normal range and are nearly identical. The strong absorption at 293 nm in the UV spectra of both compounds can be attributed to an internal charge transfer of the aromatic acid. Compound (**2**) exhibits a broad and strong signal centered around 3300 cm^{-1} which can be assigned for the O-H vibration of the coordinated water and the profile of the IR spectrum in this region is different for both compounds. The vibrations of the nitro group are observed around 1560 and 1350 cm^{-1}. The TG-DSC thermogram of (**2**) exhibits three endothermic processes at 94, 136, and 245 °C followed by two exothermic events at 433 and 545 °C respectively. The mass loss of 19 % for the first two processes is in good agreement for the expected

(19.63 %) loss of six water molecules. The third endothermic signal above 200 °C is indicative of a slow decomposition of 2-ca-4nba moiety leading to further decomposition as evidenced by the two exothermic events at 433 and 545 °C. Above this temperature, MgO is formed as a final decomposition product. The formation of MgO as the final residue was further confirmed based on isothermal weight loss studies by heating compound (**2**) at 800 °C in a temperature controlled furnace.

$[Mg(H_2O)_6](2\text{-ca-4nba})_2$ (**2**) crystallizes in the centrosymmetric monoclinic space group $P2_1/c$ and is the first structurally characterized alkaline earth salt of 2-ca-4nbaH. In (**2**) the Mg(II) is located on an inversion center, and the structure consists of an octahedral $[Mg(H_2O)_6]^{2+}$ cation and a 2-ca-4nba anion (Fig 1). The centrosymmetric $[Mg(H_2O)_6]^{2+}$ unit is a well-known structural motif in several Mg(II) compounds (Table 1). The Mg-O bond distances scatter in a narrow range between 2.0566(11) and 2.0735(11) Å and are in agreement with reported values[3,14,15,17,21]. The trans O-Mg-O angles exhibit ideal values, while the cis O-Mg-O angles range between 85.03(5) and 94.97(5)° indicating a slight distortion of the $\{MgO_6\}$ octahedron. The geometric parameters of the anion are in the normal range.

A scrutiny of the crystal structure of (**2**) reveals that the cations and anions are involved in three varieties of H-bonding interactions, comprising six O-H···O, two N-H···O and two C-H···O bonds (Table 2). The O···H distances ranging from 1.915 to 2.677 Å are accompanied by DHA angles ranging from 143 to 178°. An analysis of the crystal structure reveals that each hexacoordinated Mg(II) complex cation is H-bonded to eight different 2-ca-4nba anions via O-H···O interactions (Fig. 2). The H atoms attached to water function as H-donors and the oxygen atoms of the carboxylate (O4, O5) and the amide (O6) function as H-acceptors. In view of the O-H···O interactions the cations always point towards the carboxylate end of the anion and thus play an important role in the supramolecular organization of compound (**2**).

In the 2-ca-4nba anion, all H-atoms excepting H6 act as H-donors and the oxygen atoms of the carboxylate and amide function as H-acceptors. An oxygen (O9) of the nitro group functions as a bifurcated H-acceptor forming a C-H···O bond, a

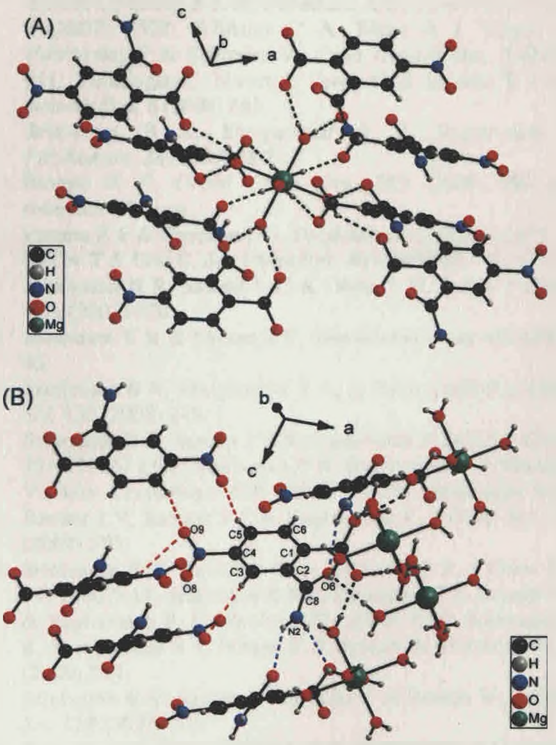

Fig. 2 – (A) View of the surroundings of the $[Mg(H_2O)_6]^{2+}$ cation in (**2**) showing its linking with eight different 2-ca-4nba anions via O-H···O hydrogen bonds. (B) View of the surroundings of the 2-ca-4nba anion in $[Mg(H_2O)_6](2\text{-ca-4nba})_2$ (**2**) showing its linking with four symmetry related $[Mg(H_2O)_6]^{2+}$ cations and five different 2-ca-4nba anions with the aid of three varieties of H-bonding interactions shown as dashed lines.

Table 2—Hydrogen-bonding geometry for $[Mg(H_2O)_6](2\text{-ca-4-nba})_2$ (**2**)

D-H···A	D(D-H) (Å)	D(H···A) (Å)	D(D···A) (Å)	<DHA (°)	Symmetry code
O1-H1O1···O5	0.820	1.950	2.770	178	-x+2, -y+1, -z+1
O1-H2O1···O4	0.820	1.915	2.717	166	-x+2, y-1/2,- z+3/2
O2-H1O2···O4	0.820	2.007	2.826	177	-x+2,-y+1,-z+1
O2-H2O2···O4	0.820	1.992	2.807	172	x, y, z
O3-H1O3···O6	0.820	1.919	2.738	177	x, y, z
O3-H2O3···O5	0.820	2.259	2.99	149	x, -y+1/2, z+1/2
N2-H1N2···O5	0.860	2.118	2.921	155	x, -y+1/2, z+1/2
N2-H2N2···O6	0.860	2.176	2.907	143	x,-y+1/2, z+1/2
C3-H3···O9	0.930	2.677	3.508	149	-x+1, y-1/2, -z+3/2
C5-H5···O9	0.930	2.420	3.321	163	-x+1, -y+2, -z+1

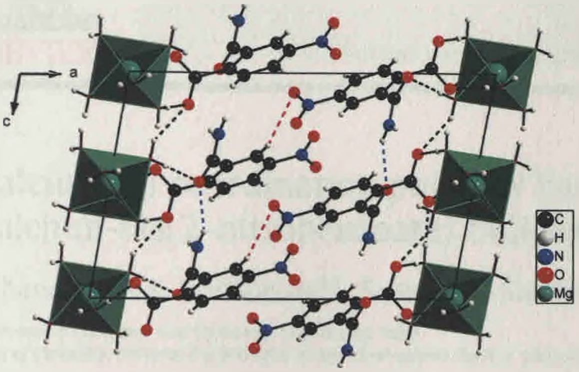

Fig. 3—Crystallographic packing of $[Mg(H_2O)_6](2\text{-ca-4nba})_2$ (**2**) viewed along *b* axis showing the supramolecular bilayer of 2-ca-4nba anions sandwiched between layers of $[Mg(H_2O)_6]^{2+}$ (open polyhedra) cations.

feature observed in several nitrobenzoates[11-14,22]. Each anion is H-bonded to four different $[Mg(H_2O)_6]^{2+}$ cations at the carboxylate end and to five symmetry related anions via O-H···O, N-H···O (amide hydrogen atoms linked to carboxylate oxygen and amide oxygen) and C-H···O interactions (Fig. 2). The intramolecular C-H···O interactions involving nitro oxygen result in a head (nitro) to head (nitro) alignment of anions. Since the cations always point towards the carboxylate oxygen atoms due to the O-H···O interactions, a bilayer of anions sandwiched between layers of $[Mg(H_2O)_6]^{2+}$ cations is formed (Fig. 3). The net result is the organization of cations and anions in the following sequence $[Mg(H_2O)_6]^{2+}$ $(2\text{-ca-4nba})^-$ $(2\text{-ca-4nba})^-$ $[Mg(H_2O)_6]^{2+}$ along *a* axis.

Supplementary data

Crystallographic data (excluding structure factors) for the structure of $[Mg(H_2O)_6](2\text{-ca-4nba})_2$ (**2**) reported herein have been deposited with the Cambridge Crystallographic Data Centre as supplementary publication CCDC 720527. Copies of the data can be obtained, free of charge, on application to CCDC, 12 Union Road, Cambridge CB2 1 EZ, UK. (Fax: +44-(0)1223-336033 or Email: deposit@ccdc.cam.ac.uk). IR and thermal data of compound (**2**) may be obtained from the authors on request.

Acknowledgement

BRS thanks University Grants Commission (UGC), New Delhi for financial support under the Special Assistance Programme. The authors thank Prof. Samar K Das, School of Chemistry, University of Hyderabad for the X-ray data of compound (**2**) and Dr. C Näther, University of Kiel, Kiel, for helpful discussion regarding the structure refinement.

References

1 Das M C, Ghosh S K, Sanudo E C & Bharadwaj P K, *Dalton Trans,* (2009) 1644; Neogi S, Navarro J A R & Bharadwaj P K, *Cryst Growth Des,* 8 (2008) 1554.

2 Guo Z, Li G, Zhou L, Su S, Lei Y, Dang S & Zhang H, *Inorg Chem,* 48 (2009) 8069; Rossin A, Ienco A, Costantino F, Montini T, Credico B D, Caporali M, Gonsalvi L, Fornasiero P & Peruzzini M, *Cryst Growth Des,* 8 (2008) 3302.

3 Morgant G, Angelo J, Desmaele D, Dichi E, Sghaier M, Fraisse B, Retailleau P, Brumas V, Fiallo M M L, Tomas A, *Polyhedron,* 27 (2008) 2097.

4 Kam K C, Young K L M, Cheetham A K, *Cryst Growth Des,* 7 (2007) 1522; Williams C A, Blake A J, Wilson C, Hubberstey P & Schroder M, *Cryst Growth Des,* 8 (2008) 911; Volkringer C, Marrot J, Ferey G & Loiseau T, *Cryst Growth Des,* 8 (2008) 685.

5 Srinivasan B R, Shetgaonkar S Y, Raghavaiah P, *Polyhedron,* 28 (2009) 2879.

6 Fromm K F, *Coord Chem Rev,* 252 (2008) 856 and references therein.

7 Fromm K F & Gueneau E D, *Polyhedron,* 23 (2004) 1479.

8 Dudev T & Lim C, *Acc Chem Res,* 40 (2007) 85.

9 Srinivasan B R, Sawant S C & Dhuri S N, *Indian J Chem,* 41A (2002) 290.

10 Srinivasan B R & Sawant S C, *Thermochim Acta,* 402 (2003) 45.

11 Srinivasan B R, Shetgaonkar S Y, & Raghavaiah P, *J Chem Sci,* 120 (2008) 249.

12 Srinivasan B R, Sawant J V & Raghavaiah P, *Indian J Chem,* 45A (2006) 2392; Srinivasan B R, Raghavaiah P & Sawant J V, *Acta Crystallogr,* 63E (2007) m2251. Srinivasan B R, Sawant J V, Sawant S C & Raghavaiah P *J Chem Sci,* 119 (2007) 593.

13 Srinivasan B R, Sawant J V & Raghavaiah P, *J Chem Sci,* 119 (2007) 11; Srinivasan B R, Shetgaonkar S Y, Sawant J V & Raghavaiah P, *Polyhedron,* 27 (2008) 3299; Srinivasan B R, Shetgaonkar S Y, Näther C & Bensch W, *Polyhedron,* 28 (2009) 534.

14 Srinivasan B R, Sawant J V, Näther C & Bensch W, *J Chem Sci,* 119 (2007) 243.

15 Murugavel R, Karambelkar V V & Anantharaman G, *Indian J Chem,* 39A (2000) 843.

16 Murugavel R, Karambelkar V V, Anantharaman G & Walawalkar M G, *Inorg Chem,* 39 (2000) 1381; Murugavel R and Banerjee S, *Inorg Chem Commun,* 6 (2003) 810; Murugavel R, Kumar P, Walawalkar M G & Mathialagan R, *Inorg Chem,* 46 (2007) 6828.

17 Wiesbrock F, Schier A & Schmidbaur H, Z *Naturforsch,* B57 (2002) 251.

18 Young J G & Onyebuagu W, *J Org Chem,* 55 (1990) 2155.

19 *Bruker SMART V5.630 and SAINT-PLUS V6.45,* (Bruker-Nonius Analytical X-ray Systems Inc.:Madison, Wisconsin, USA) 2003. *SADABS, Empirical absorption correction program,* (Bruker AXS Inc., Madison, Wisconsin, USA) 1997.

20 Sheldrick G M, *Acta Crystallogr,* 64A (2008) 112.

21 Dale S H, Elsegood M R J & Kainth S, *Acta Crystallogr,* 59C (2003) m505.

22 Srinivasan B R, Sawant S C & Das S K, *Indian J Chem,* 43A (2004) 1066; Srinivasan B R, Sawant J V & Raghavaiah P, *Indian J Chem,* 48A (2009) 181; Srinivasan B R & Rane G K, *J Chem Sci,* 121 (2009) 145

Polyhedron 28 (2009) 2879–2886

Contents lists available at ScienceDirect

Polyhedron

journal homepage: www.elsevier.com/locate/poly

A calcium(II) coordination polymer based on a tricyclic dicalcium-bis(2-nitrobenzoate) building block

Bikshandarkoil R. Srinivasan [a,*], Santosh Y. Shetgaonkar [a], Pallepogu Raghavaiah [b]

[a] *Department of Chemistry, Goa University, Goa 403206, India*
[b] *School of Chemistry, National Single Crystal X-ray Diffractometer Facility, University of Hyderabad, Hyderabad 500046, India*

ARTICLE INFO

Article history:
Received 20 April 2009
Accepted 18 June 2009
Available online 7 July 2009

Keywords:
Coordination polymer
Eight coordination
μ_2-η^2:η^1 binding mode
Dicalcium-bis(2-nitrobenzoate)

ABSTRACT

The reaction of $CaCO_3$ with 2-nitrobenzoic acid (2-nbaH) results in the formation of a coordination polymer, $[Ca(2\text{-nba})_2(H_2O)_2]_n$ (**1**) (2-nba = 2-nitrobenzoate), which can be dehydrated to $[Ca(2\text{-nba})_2]$ (**2**). Compound **2** can be rehydrated to **1** on exposure to water vapor. Compounds **1** and **2** were characterized by elemental analysis, IR and UV–Vis spectra, and TG-DSC thermograms. Compound **1** crystallizes in the triclinic space group $P\bar{1}$ and its structure consists of an eight coordinated calcium(II), two terminal aqua ligands and two crystallographically independent 2-nba anions, both of which function as μ_2-η^2:η^1 bridging ligands. Each unique 2-nba ligand is linked to Ca(II) in a bidentate fashion via the carboxylate oxygen atoms and is further linked to a symmetry related Ca(II) via one of the oxygen atoms. A pair of such μ_2-η^2:η^1 2-nba ligands are bridged to two symmetry related Ca(II) ions, resulting in the formation of a tricyclic dicalcium-bis(2-nitrobenzoate) moiety, which constitutes the basic building block of the polymer. In the crystal structure of **1**, alternating pairs of bridging 2-nba ligands link pairs of $\{Ca(H_2O)_2\}^{2+}$ units into a 1-D polymeric chain extending along the *a*-axis. The oxygen atoms of the coordinated water, and the carboxylate and nitro groups of 2-nba are involved in O–H···O and C–H···O interactions.

1. Introduction

The structural chemistry of the alkaline-earth metals, especially calcium, has been an area of considerable research interest for the past several years in view of its biological relevance [1–3]. The structural features of major interest are the interactions of alkaline-earth metals with O-donor ligands [4] like water, carbonate, sulfate, phosphate and especially carboxylate [5,6]. In recent years there has been a growing interest in the synthesis and structural aspects of alkaline-earth carboxylates in order to comprehend the interactions of alkaline-earths with biologically relevant carboxylic acids [7–12] and also to prepare new lightweight s-block based coordination polymeric materials [13–16]. In view of their ready availability, combined with their non-toxic and water soluble nature, the chemistry of the s-block elements is being investigated by several researchers. Recent developments in the chemistry of s-block coordination polymers has been reviewed by Fromm [17] and this work describes an overview on different ligand and polymer types of the s-block compounds.

An analysis of the Cambridge Structural Database (CSD) and Protein Data Bank (PDB) crystal structure databases has been performed by different research groups to identify geometrical features of a general nature that can be useful in understanding the structural chemistry of calcium. In a pioneering study of the crystal structures of 54 calcium-carboxylates, Einspahr and Bugg [18] reported that the Ca ion in all calcium-carboxylates lies near the plane of the carboxylate group and usually binds to several carboxylate groups. The most commonly observed number of carboxylates bound to each Ca was three and the carboxylate groups so bound may be crystallographically independent or symmetry related. It was also noted that the carboxylate groups coordinate to more than one Ca ion, the most common number being two Ca ions. A very recent study based on the analysis of the crystal structures of 131 Ca-carboxylates has shown that the coordination number of calcium ranges from 3 to 10, with octacoordination being the most favored [19]. Due to the larger ionic radius of 106 pm for Ca^{+2}, the carboxylate ligand adopts a bridging binding mode, resulting in the formation of an extended chain structure in many calcium-carboxylates. This property of the carboxylate ligand can be evidenced by the structural characterization of several calcium based coordination polymers [7–12,15–48]. The heptacoordinated Ca compound $[Ca(H_2O)_4(\eta^1\text{-4-nba})(\eta^2\text{-4-nba})]$ (4-nba = 4-nitrobenzoate) reported by us in an earlier work [49] differs from several polymeric Ca-carboxylates in that the 4-nba ligand is not involved in bridging coordination. Instead the 4-nba ligand binds to Ca in a monodentate (η^1) and bidentate (η^2) fashion, accompanied by several O-H···O interactions involving the oxygen atoms of the nitro and carboxylate moieties of 4-nba and the coordinated water. In view of this, it was of interest to

---

* Corresponding author. Tel.: +91 832 6519316; fax: +91 832 2452886.
E-mail addresses: srini@unigoa.ac.in, brsrinivasan@gmail.com (B.R. Srinivasan).

0277-5387/$ - see front matter © 2009 Elsevier Ltd. All rights reserved.
doi:10.1016/j.poly.2009.06.085

investigate the chemistry of Ca with the other isomeric nitrobenzoic acids to understand the role of the nitro substituent in the structural chemistry of calcium-nitrobenzoates. The disposition of the $-NO_2$ substituent, ortho to the –COOH group in 2-nitrobenzoic acid (2-nbaH), results in the formation of a coordination polymer, with the carboxylate moiety of 2-nba (2-nitrobenzoate) functioning as a bridging ligand.

2. Experimental

2.1. Materials and methods

All the chemicals used in this study were of reagent grade and were used as received. The starting materials and reaction products are air stable and hence were prepared under normal laboratory conditions. Infrared (IR) spectra were recorded on a Shimadzu (IR prestige -21) FT-IR spectrometer in the range 4000–400 cm^{-1}. Samples for IR spectra were diluted with solid KBr and the signals referenced to polystyrene bands. UV–Vis diffuse-reflectance spectra were obtained using a Shimadzu UV-2450 double beam spectrophotometer. $BaSO_4$ powder was used as a reference (100% reflectance). Absorption data were calculated from the reflectance data using the Kubelka–Munk function ($a/S = (1 - R)^2/2R$ where a is the absorption coefficient, R the reflectance and S the scattering coefficient). TG-DSC measurements were performed in Al_2O_3 crucibles on a STA-409PC simultaneous thermal analyzer from Netzsch in flowing air. A heating rate of 10 K min^{-1} was employed for all measurements. Acidification of **1** and **2** with a slight excess of dilute HCl resulted in the quantitative formation of the free carboxylic acid (2-nbaH), which was extracted with ether. Evaporation of the ether, followed by drying and weighing, afforded the 2-nbaH content as described earlier [50]. Pyrolysis of **1** and **2** at 800 °C resulted in the quantitative formation of CaO. Isothermal weight loss studies were performed in an electric furnace fitted with a temperature controller. Metal analysis was performed as described earlier [49,51].

2.2. Preparation of $[Ca(H_2O)_2(2\text{-nba})_2]$, 1

A mixture of calcium carbonate (1.0 g, 10 mmol) and 2-nitrobenzoic acid (2-nbaH) (3.34 g, 20 mmol) was taken in water (50 ml) and heated on a steam bath. The insoluble $CaCO_3$ slowly started dissolving, accompanied by brisk effervescence. The heating of the reaction mixture was stopped when there was no more evolution of CO_2. At this stage, the reaction mixture was almost clear. The hot pale yellow solution was filtered and left undisturbed for 9–10 days. The colorless crystalline blocks that separated were filtered, washed thoroughly with ether and dried. Yield: 3.42 g (84%). The crystals obtained in this method were suitable for X-ray studies. **1** can also be prepared starting from $CaCl_2$ as the Ca source. The sodium salt of 2-nba was first generated *in situ* by reacting 2-nbaH (1.67 g, 10 mmol) with $NaHCO_3$ (0.84 g, 10 mmol) in water. Into this, an aqueous solution of $CaCl_2$ (0.555 g, 5 mmol) was added and the reaction mixture was filtered and left aside for crystallization. The crystals that separated after a few days were isolated in 71% yield. The IR spectrum and the DSC thermogram of the product obtained by this method were identical to that of the product obtained using $CaCO_3$ as the Ca source.

Anal. Calc. for $C_{14}H_{12}CaN_2O_{10}$ (408.34): C, 41.18; H, 2.96; N 6.86; Ca, 9.82; 2-nbaH, 81.86; CaO, 13.73. Found: C, 41.10; H, 2.98; N, 6.58; Ca, 9.80; 2-nbaH, 80.35; CaO, 13.70%.

IR (in cm^{-1}): 3649, 3591, 3350, 3078, 2864, 2425, 2000, 1967, 1859, 1626, 1568, 1526, 1485, 1423, 1350, 1306, 1265, 1144, 1076, 968, 870, 851, 795, 789, 746, 702, 650, 430.

UV–Vis (in nm): 250, 350.

DSC (°C): 144 (Endo), 322 (Exo), 354 (Exo), 544 (Exo); residual mass 14.3%.

2.3. Preparation of anhydrous bis(2-nitrobenzoato)calcium(II) 2

A powdered sample of **1** (0.325 g) was heated at 150 °C for 15 min. This resulted in the formation of the anhydrous compound **2**. The observed mass loss of 8.80% is in agreement with the expected value (8.81%) for the loss of two moles of water.

Anal. Calc. for $C_{14}H_8CaN_2O_8$ (372.34): C, 45.17; H, 2.17; N 7.52; Ca, 10.76; 2-nbaH, 89.78; CaO, 15.06. Found: C, 44.53; H, 2.1; N, 7.40; Ca, 10.5; 2-nbaH, 88.15; CaO, 14.80%.

IR (in cm^{-1}): 3074, 2866, 1585, 1566, 1524, 1517, 1485, 1415, 1350, 1308, 1265, 1153, 1078, 961, 864, 847, 785, 737, 700, 648, 432.

DSC (°C): 322 (Exo), 354 (Exo), 544 (Exo); residual mass 14.3%.

2.4. Rehydration studies

The anhydrous compound **2** was prepared from **1** as mentioned above. Equilibration of a powdered sample of **2** over water vapor resulted in the formation of the starting material 1 in near quantitative yield in about a day. The IR spectrum and the DSC thermogram of the rehydrated compound are identical to that of **1**.

2.5. X-ray crystallography

Intensity data for 1 were collected on a Bruker (SMART APEX) CCD diffractometer using graphite-monochromated Mo Kα radiation. The data integration and reduction were carried out using SAINT-PLUS [52] software. An empirical absorption correction was applied to the collected reflections with SADABS [52]. The structure was solved with direct methods using SHELXS-97 [53] and refinement was done against F^2 using SHELXL-97 [53]. All non-hydrogen atoms were refined anisotropically. Aromatic hydrogens were introduced in calculated positions and included in the refinement riding on their respective parent atoms. The hydrogen atoms of the coordinated water molecules were located in the difference map but were not stable on subsequent refinements and hence were fixed at calculated positions by using the DFIX command and later refined isotropically using a riding model. The technical details of data acquisition and selected crystal refinement results for **1** are summarized in Table 1.

3. Results and discussion

3.1. Synthesis and spectroscopy

During the course of our studies on metal-carboxylates [50,54], we have shown that crystalline hydrates of metal-nitrobenzoates can be conveniently prepared in good yields under ambient conditions by an aqueous reaction of an alkali-metal carbonate with 4-nbaH or by the reaction of the *in situ* generated sodium salt of 4-nbaH with a metal halide. The generality of these reactions for the synthesis of hydrated metal-carboxylates can be evidenced by the synthesis of 4-nba compounds of alkaline-earths [49,50,55–57] as well as transition metals [58–60], the synthesis of a polymeric Ba compound [61] containing 2-nba as well as the Ca compound described herein. In the present work, the direct reaction of $CaCO_3$ with 2-nbaH in water resulted in the formation of a crystalline hydrate **1** containing Ca:2-nba:H_2O in a 1:2:2 mole ratio. Compound **1** could also be prepared by reacting an aqueous solution of $CaCl_2$ with in situ generated sodium salt of 2-nbaH. The composition of **1** was arrived at based on elemental analysis, 2-nbaH content

Table 1
Technical details of data acquisition and selected refinement results for **1**.

Empirical formula	$C_{14}H_{12}CaN_2O_{10}$
Formula weight	408.34
T (K)	293(2)
λ (Å)	0.71073
Crystal system	triclinic
Space group	$P\bar{1}$
Unit cell dimensions	
a (Å)	7.7477(10)
b (Å)	10.1953(13)
c (Å)	11.2808(15)
α, (°)	80.851(2)
β (°)	82.233(2)
γ (°)	89.333(2)
V (Å^3)	871.6(2)
Z, D_{calc} (Mg/m^3)	2, 1.556
Absorption coefficient (mm^{-1})	0.418
F (0 0 0)	420
Crystal size (mm^3)	0.38 × 0.32 × 0.20
θ range for data collection (°)	1.85–25.93
Index ranges	$-9 \leqslant h \leqslant 9$, $-11 \leqslant k \leqslant 12$, $-13 \leqslant l \leqslant 13$
Reflections collected/unique	6780/3753 ($R_{int} = 0.0204$)
Completeness to $\theta = 25.93°$	98.4%
Refinement method	full-matrix least-squares on F^2
Data/restraints/parameters	3353/4/260
Goodness-of-fit (GOF) on F^2	1.077
Final R indices [$I > 2\sigma(I)$]	$R_1 = 0.0395$, $wR_2 = 0.0863$
R indices (all data)	$R_1 = 0.0461$, $wR_2 = 0.0896$
Extinction coefficient	0.0040(2)
Largest difference peak and hole (e Å^{-3})	0.215 and −0.202

obtained by acidification and CaO formed on pyrolysis and weight loss studies. Compound **1** can be dehydrated to the anhydrous bis(2-nitrobenzoato)calcium(II) **2** by heating at 150 °C (Scheme 1). The temperature for the dehydration reaction was chosen based on the thermal property (*vide infra*) of **1**. Equilibation of the anhydrous compound **2** in an atmosphere of water vapor resulted in the regeneration of compound **1**. This was confirmed by a comparison of the IR spectrum and the TG-DSC thermogram of the rehydrated product with that of **1**. Both **1** and **2** are decomposed to CaO by heating in a furnace at 800 °C.

The diffuse reflectance spectrum of compound **1**, which absorbs strongly at around 350 nm, is very similar to that of the free acid (Supplementary Fig. 1) and this can be assigned to the intramolecular charge transfer transition of the aromatic 2-nitrobenzoate. In addition **1** also exhibits a signal at around 250 nm, unlike the free acid, and the diffused reflectance spectrum of the anhydrous compound **2** is very similar to that of **1**. The IR spectra of **1** and **2** exhibit several sharp bands in the mid-infrared region, clearly indicating the presence of the organic moiety. The strong signals at 3649 and 3591 cm^{-1} in **1** indicate the presence of water and can be assigned to the O–H stretching vibration. The IR spectrum of **2** is devoid of bands above 3074 cm^{-1}, which is indicative of the anhydrous nature of **2**. Below 3074 cm^{-1}, the IR spectrum is very similar to that of **1**. Although the IR spectra **1** and **2** exhibit absorptions due to the vibrations of the carboxylate and nitro groups, no definite conclusions can be drawn on the exact nature of the binding of the 2-nba ligand based only on infrared data.

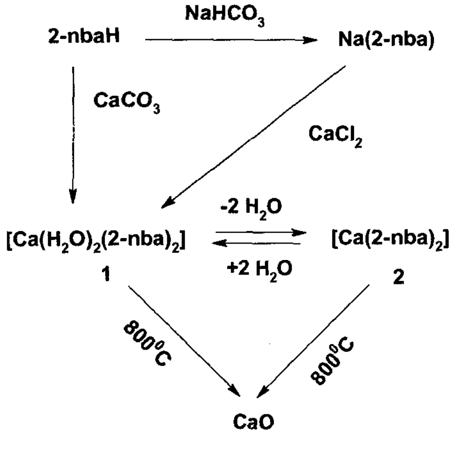

Scheme 1. Synthesis of **1** and **2**.

3.2. Thermal studies

Compound **1** exhibits an endothermic event in its TG-DSC thermogram (Fig. 1) at 144 °C, accompanied by a mass loss of 8.5%. This value is in good agreement with that expected (8.83%) for the loss of two molecules of water. Above this temperature, the thermogram shows only exothermic processes with signals at 322, 354 and 544 °C. The first two closely related exotherms can be attributed to the decomposition of 2-nitrobenzoate. In view of the absence of mass spectral data of the emitted fragments, we do not wish to comment on the exact nature of the decomposition processes at these high temperatures. However it should be noted that the observed residual mass of 14.3% is in good agreement for the formation of CaO. The formation of the oxide phase can also be evidenced by the featureless infrared spectrum of the residue as well as its powder pattern. The residue on exposure to atmosphere shows an increase in weight corresponding to the formation of calcium carbonate. The results of the isothermal weight loss studies at 150 °C and at 800 °C in a furnace add more credence to the TG-DSC data. The TG-DSC thermogram of the anhydrous compound **2** is devoid of the first endothermic signal observed for the dehydration of **1**. A comparison of the TG-DSC thermograms of **1** and **2** (Fig. 1) shows the identical nature of the TG-DSC curve of **2** to that of **1** above 150 °C. The observed residual mass of 13.7% can be accounted for by the formation of CaO.

3.3. Description of the crystal structure of 1

Compound **1** crystallizes in the centrosymmetric triclinic space group $P\bar{1}$ with all atoms situated in general positions. The central metal is eight coordinated and is bonded to two oxygen atoms of

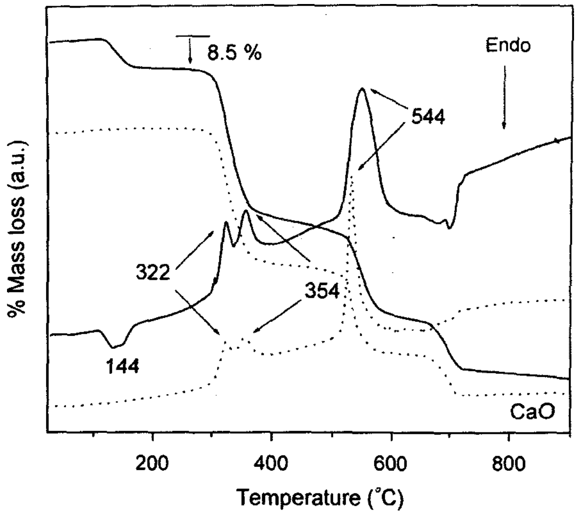

Fig. 1. TG-DSC thermograms of [Ca(2-nba)$_2$(H$_2$O)$_2$]$_n$ **1** (solid line) and [Ca(2-nba)$_2$]$_n$ **2** (dotted lines). (Heating rate 5 K min^{-1}; air atmosphere.)

two terminal aqua ligands and six oxygen atoms from four symmetry related 2-nba anions, resulting in a distorted triangular dodecahedral $\{CaO_8\}$ coordination polyhedron (Fig. 2). The geometric parameters of the 2-nba ligand are in the normal range and are in agreement with reported values [61]. The observed Ca–O bond distances vary between 2.3442(13) and 2.6539(15) Å (Table 2), while the O–Ca–O angles range from 77.32(6)° to 153.76(6)°. These values are comparable with those reported for other Ca(II)-carboxylates [7–12]. The Ca(II) center is linked to the O9 and O10 atoms of the water molecules by bonds of lengths 2.3918(18) and 2.4121(17) Å, respectively.

The structure of compound **1** is a one-dimensional (1-D) polymer and hence it is formulated as $[Ca(2\text{-nba})_2(H_2O)_2]_n$. Each formula unit of **1** contains Ca(II) coordinated to two aqua ligands and two unique 2-nitrobenzoate ligands, both of which function as bridging ligands. The first unique μ_2–η^2:η^1 2-nba ligand (O1, O2) binds to Ca(II) in a bidentate fashion with Ca1–O1 and Ca1–O2 distances of 2.4548(15) and 2.6313(15) Å, respectively. The O2 oxygen is further linked to a symmetry related Ca(II) center at a distance of 2.3498(14) Å, resulting in a Ca···Ca separation of 3.9865(8) Å. A pair of such μ_2–η^2:η^1 2-nba ligands are linked to two Ca(II) ions resulting in the formation of a tricyclic dicalcium-dicarboxylate unit (Fig. 3) which constitutes the basic building block of the coordination polymer. This tricyclic unit differs from the well-known eight membered cyclic dimetal-dicarboxylate unit in several dinuclear carboxylates where (–COO) functions as a μ_2–η^1:η^1 bidentate bridging ligand. The second independent 2-nba ligand (O5, O6) binds to two symmetry related Ca(II) ions in an identical fashion resulting in a tricyclic dicalcium-dicarboxylate unit with a Ca···Ca separation of 3.9967(9) Å (**Supplementary Fig. 2**). The Ca–O bond lengths formed by this ligand are different. With this ligand, a Ca(II) ion is linked to the O5 and O6 oxygen atoms in a bidentate manner (Ca1–O5 2.4213(14); Ca1–O6 2.3442(13) Å) and the O6 atom is further linked to a second Ca(II) ion at 2.6539(15) Å. In the crystal structure of **1** alternating pairs of the two crystallographically independent μ_2–η^2:η^1 2-nba ligands link pairs of $\{Ca(H_2O)_2\}^{2+}$ units into a 1-D polymeric chain extending along the *a*-axis (Fig. 4). As a result, alternating Ca···Ca separations of 3.9865(8) and 3.9967(9) Å are observed in the infinite chain (Fig. 4). These values are in very good agreement with the Ca···Ca separations of 3.8585(7) and 3.8432(3) Å reported for the coordination polymers $[Ca(L^1)(4\text{-nba})_2]_n$ (L^1 = N-methylimidazole)

Table 2
Selected bond distances (Å) for $[Ca(2\text{-nba})_2(H_2O)_2]_n$ **1**.

Ca(1)–O(6)	2.3442(13)	Ca(1)–O(5)	2.4213(14)
Ca(1)–O(2)^{ii}	2.3498(14)	Ca(1)–O(1)	2.4548(15)
Ca(1)–O(9)	2.3918(18)	Ca(1)–O(2)	2.6313(15)
Ca(1)–O(10)	2.4121(17)	Ca(1)–O(6)^{i}	2.6539(15)
Ca(1)–Ca(1)^{ii}	3.9865(8)	Ca(1)–Ca(1)^{i}	3.9967(9)
O(6)–Ca(1)–O(2)^{ii}	148.82(5)	O(5)–Ca(1)–O(1)	88.01(5)
O(6)–Ca(1)–O(9)	77.32(6)	O(6)–Ca(1)–O(2)	128.87(5)
O(2)^{ii}–Ca(1)–O(9)	82.91(6)	O(2)^{ii}–Ca(1)–O(2)	73.82(5)
O(6)–Ca(1)–O(10)	84.37(5)	O(9)–Ca(1)–O(2)	153.76(6)
O(2)^{ii}–Ca(1)–O(10)	77.70(6)	O(10)–Ca(1)–O(2)	82.04(5)
O(9)–Ca(1)–O(10)	104.97(7)	O(5)–Ca(1)–O(2)	75.15(5)
O(6)–Ca(1)–O(5)	124.91(5)	O(1)–Ca(1)–O(2)	50.88(4)
O(2)^{ii}–Ca(1)–O(5)	77.78(5)	O(6)–Ca(1)–O(6)^{i}	73.97(5)
O(9)–Ca(1)–O(5)	88.40(6)	O(2)^{ii}–Ca(1)–O(6)^{i}	124.74(5)
O(10)–Ca(1)–O(5)	150.25(5)	O(9)–Ca(1)–O(6)^{i}	77.23(6)
O(6)–Ca(1)–O(1)	80.89(5)	O(10)–Ca(1)–O(6)^{i}	157.29(5)
O(2)^{ii}–Ca(1)–O(1)	124.69(5)	O(5)–Ca(1)–O(6)^{i}	50.95(4)
O(9)–Ca(1)–O(1)	150.53(5)	O(1)–Ca(1)–O(6)^{i}	77.85(5)
O(10)–Ca(1)–O(1)	92.27(6)	O(2)–Ca(1)–O(6)^{i}	106.15(5)

Symmetry transformations are used to generate equivalent atoms: (i) $-x+1, -y+2, -z$; (ii) $-x+2, -y+2, -z$.

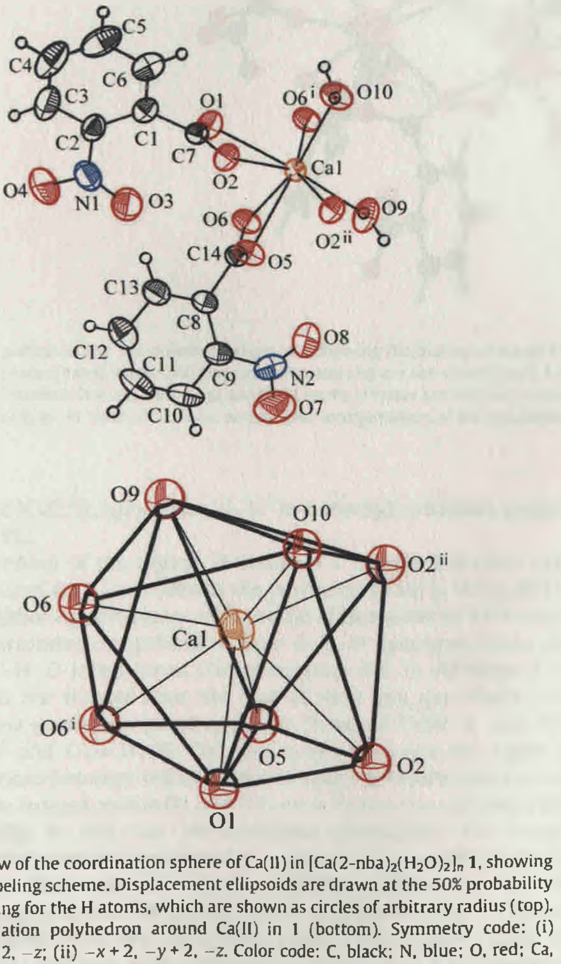

Fig. 2. A view of the coordination sphere of Ca(II) in $[Ca(2\text{-nba})_2(H_2O)_2]_n$ **1**, showing the atom-labeling scheme. Displacement ellipsoids are drawn at the 50% probability level excepting for the H atoms, which are shown as circles of arbitrary radius (top). The coordination polyhedron around Ca(II) in 1 (bottom). Symmetry code: (i) $-x+1, -y+2, -z$; (ii) $-x+2, -y+2, -z$. Color code: C, black; N, blue; O, red; Ca, orange. (For interpretation of the references to color in this figure legend, the reader is referred to the web version of this article.)

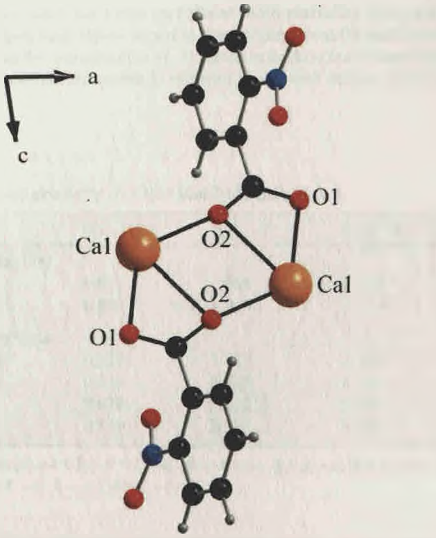

Fig. 3. A view along *b* showing the tricyclic dicalcium-bis(2-nitrobenzoate) unit formed by a pair of μ_2–η^2:η^1 2-nba ligands between two Ca(II) ions. Color code: C, black; H, medium gray; N, blue; O, red; Ca, orange. (For interpretation of the references to color in this figure legend, the reader is referred to the web version of this article.)

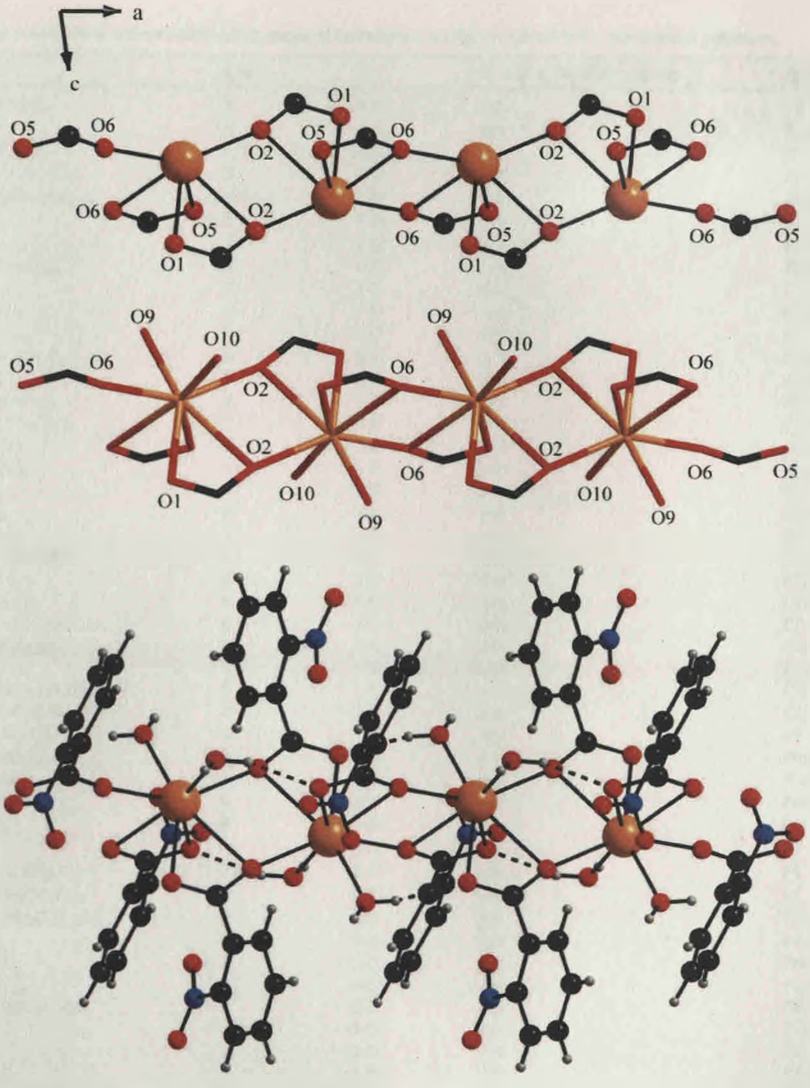

Fig. 4. A portion of the 1-D polymeric chain in **1** showing the linking of tricyclic dicalcium-bis(2-nitrobenzoate) units into an infinite chain extending along the *a*-axis. For clarity the coordinated water molecules and aromatic ring are not shown (top). A wireframe model of the polymeric chain wherein the oxygen atoms O9 and O10 of water are included (middle). The aromatic rings and the H atoms of water are included in the polymeric chain to show the intrachain O–H···O bonds in broken lines. Color code: C, black; H, medium gray; N, blue; O, red; Ca, orange. (For interpretation of the references to color in this figure legend, the reader is referred to the web version of this article.)

[47] and $[Ca(L^2)(H_2O)(4\text{-nba})_2]_n$ (L^2 is 2-methylimidazole), respectively [48].

A scrutiny of the crystal structure of **1** reveals that each eight coordinated Ca(II) complex in the polymeric chain is H-bonded to six neighboring complexes with the aid of two varieties of H-bonding interactions comprising of three O–H···O hydrogen bonds and three C–H···O interactions (Supplementary Fig. 3). All these O···H contacts are shorter than the sum of their van der Waals radii and their geometric parameters are listed in Table 3. The O9–H9···O1^i and O10–H10B···O5^{ii} (for symmetry code see Table 3) interactions between the coordinated water molecules and the carboxylate oxygen atoms O1 and O5 occur within the 1-D polymeric chain (Fig. 4) and thus are intrachain interactions. The oxygen atoms of the nitro group function as H-acceptors and this behavior has been observed in several nitrobenzoates [47–49,55–61]. The nitro oxygen atoms O4 and O7 in one polymeric chain are hydrogen bonded to the H11 and H10A atoms in an adjacent chain via C11–H11···O4^v and O10–H10A···O7^{iii}, and these can be termed as interchain interactions. Likewise the H-bonding between O9 (water) and O1 (carboxylate) with the H atoms of the aromatic ring serve to link parallel chains (Supplementary Fig. 3).

Table 3
Hydrogen-bonding geometry (Å, °) for $[Ca(2\text{-nba})_2(H_2O)_2]_n$ **1**.

D–H···A	d(D–H)	d(H···A)	D(D···A)	<DHA
Intrachain interactions				
O9–H9···O1^i	0.817	1.965	2.769	168
O10–H10B···O5^{ii}	0.832	1.953	2.754	161
Interchain interactions				
O10–H10A···O7^{iii}	0.823	2.257	2.999	150
C3–H3···O9^{iv}	0.930	2.623	3.548	173
C11–H11···O4^v	0.929	2.523	3.404	158
C10–H10···O1^{vi}	0.929	2.539	3.464	174

Symmetry code: (i) $-x+1, -y+2, -z$; (ii) $-x+2, -y+2, -z$; (iii) $x, y+1, z$; (iv) $x, y, 1+z$; (v) $1-x, 1-y, 1-z$; (vi) $x, -1+y, z$.

A comparison of the structure of the recently reported polymeric barium compound of 2-nba, namely $[Ba(H_2O)_3(2\text{-nba})_2]_n$ [61], with that of compound 1 reveals certain similarities and

Table 4
Metal coordination number, number of coordinated waters and binding mode of carboxylate groups in some Ca(II) coordination polymers.

Number	Compound	C.N.	D	Bridging $(RCOO)^-$ present	Space group	Ref.
1	$[Ca(N\text{-}MeIm)(4\text{-}nba)_2]_n$	6	1-D	yes	$P\bar{1}$	[47]
2	$[Ca(Phen)(Sa)_2]_n$	6	1-D	yes	$Pnab$	[19]
3	$[Ca_{1.5}(DEF)(\mu\text{-}BDC)_{1.5}]_n$	6,7	1-D	yes	$I2/a$	[15]
4	$[[Ca(NH_2\text{-}NHCO_2)_2]\cdot H_2O]_n$	8	1-D	yes	$P\bar{1}$	[20]
5	$[Ca(2\text{-}MeIm)(H_2O)(4\text{-}nba)_2]_n$	7	1-D	yes	$P2_1/n$	[48]
6	$[Ca(gly)_2(H_2O)]_n$	8	1-D	yes	$P\bar{1}$	[7]
7	$[Ca(H_2O)(dnSa)]_n$	7	1-D	yes	$P2_1/c$	[21]
8	$[Ca(H_2O)(DMF)(benz)_2]_n$	8	1-D	yes	$P2_1/n$	[22]
9	$[Ca(val)_2(H_2O)]_n$	8	1-D	yes	$C2/c$	[7]
10	$[Ca(H_2O)_2(4\text{-}aba)_2]_n$	8	1-D	yes	$P2_12_12_1$	[8]
11	$[Ca(2\text{-}nba)_2(H_2O)_2]_n$	8	1-D	yes	$P\bar{1}$	this work
12	$[Ca_2(H_2O)_2(OAc)_3(NO_3)]_n$	8	1-D	yes	$Pnma$	[23]
13	$[Ca(H_2O)_2(3\text{-}aba)_2]_n$	8	1-D	yes	$Pbcn$	[11]
14	$[Ca(H_2O)_2(4\text{-}CNbenz)_2]_n$	8	1-D	yes	$P2/n$	[24]
15	$[[Ca(H_2O)_2(Nic)_2]\cdot(H_2O)_3]_n$	7	1-D	yes	$C2/c$	[25]
16	$[Ca(H_2O)_2(2\text{-}OPA)_2]_n$	8	1-D	yes	$Pna2_1$	[26]
17	$[Ca(C_4H_4O_5)_2\cdot 2H_2O]_n$	8	1-D	yes	$C2/c$	[43]
18	$[Ca(leu)_2(H_2O)_3]_n$	8	1-D	yes	$P\bar{1}$	[7]
19	$[Ca(H_2O)_3(bpdc)]_n$	8	1-D	yes	$Ima2$	[46]
20	$[Ca(H_2O)_3(2\text{-}aba)_2]_n$	7	1-D	yes	$Pbcn$	[9]
21	$[[Ca(H_2O)_3(4\text{-}fba)](4\text{-}fba)]_n$	8	1-D	yes	$P2_1/c$	[27]
22	$[[Ca(H_2O)_3(benz)_2]_n$	8	1-D	yes	$P2_1/c$	[28]
23	$[Ca(H_2O)_2(C_8H_5O_3)_2]_n$	8	1-D	yes	$C2/c$	[29]
24	$[[Ca(H_2O)_2(Py\text{-}Thr)_2]\cdot(H_2O)_2]_n$	8	1-D	yes	$C2$	[30]
25	$[Ca(H_2O)_3(C_9H_{11}N_6O_5)_2]_n$	10	1-D	yes	$C2/c$	[31]
26	$[Ca(H_2O)_3(1,4\text{-}bdc)]_n$	8	1-D	yes	$P2_1/c$	[32,33]
27	$[[Ca(H_2O)_2(1,3\text{-}bdc)]_{2.5}\cdot 4\ H_2O]_n$	8	1-D	yes	$C2/c$	[34]
28	$[[Ca_5(1,3\text{-}bdc)_5(H_2O)_9]\cdot 8H_2O]_n$	8	1-D	yes	$C2/c$	[35]
29	$[[Ca(H_2O)]_2(L)(\mu\text{-}H_2O)]_n$	8	1-D	yes	$P\bar{1}$	[36]
30	$[Ca(\mu\text{-}DMF)(\mu\text{-}NDC)]_n$	8	3-D	yes	$Pnma$	[15]
31	$[Ca(\mu\text{-}DEF)(\mu\text{-}TPDC)]_n$	8	3-D	yes	$Pnma$	[15]
32	$[Ca(\mu\text{-}DMF)(\mu\text{-}DADC)]_n$	8	3-D	yes	$Pnma$	[15]
33	$[Ca(HBTC)\cdot 2H_2O]_n$	8	2-D	yes	$P1$	[16]
34	$[Ca(H_2O)(tda)]_n$	8	2-D	yes	$P\bar{1}$	[41]
35	$[Ca_3(H_2O)_8(BTA)_2]_n\cdot 3H_2O$	7,8	2-D	yes	$P\bar{1}$	[42]
36	$[Ca(H_2O)(O_2C)_2C_6H_3CO_2H)]_n$	8	2-D	yes	$P\bar{1}$	[37]
37	$[[Ca(H_2O)_2(DTBB)]0.5C_2H_5OH]_n$	8	2-D	yes	$C2/c$	[10]
38	$[Ca(H_2O)(Hpdc)]_n$	7	3-D	yes	$P2_1/c$	[38]
39	$[Ca_2(A_3Br)]_n\cdot 5H_2O$	6	3-D	yes	$Pnma$	[39]
40	$[Ca(H_2O)(C_{10}H_8O_6)]_n$	8	3-D	yes	$P2_1/c$	[40]
41	$[Ca(H_2O)_3(5\text{-}OH\text{-}BDC)]_n\cdot H_2O$	8	2-D	yes	$P2_1/c$	[44]
42	$[Ca(C_3H_3O_4)_2]_n$	8	3-D	yes	$P2_1/c$	[45]
43	$[Ca(H_2O)(bpdc)]_n$	7	3-D	yes	$P2_1$	[46]
44	$[Ca_2(H_2O)_2(NDC)]_n$	7	3-D	yes	$P2_1/c$	[46]
45	$[[Ca(H_2O)_4(Hpdc)]\cdot H_2O]_n$	8	1-D	yes	$P2_1/c$	[38]
46	$[[Ca(H_2O)_4(Hpdc)]\cdot 2H_2O]_n$	7	1-D	no	$P2_1/n$	[38]
47	$[[Ca(H_2O)_4(AIP)_2](H_2O)]_n$	8	1-D	no	$R\text{-}3$	[12]
48	$[Ca(H_2O)_4(\eta^1\text{-}4\text{-}nba)(\eta^2\text{-}4\text{-}nba)]$	7	0-D	no	$P2_1/c$	[49]

Abbreviations used: C.N. = coordination number; D = dimensionality of polymer; N-MeIm = N-methylimidazole; 4-nba = 4-nitrobenzoate; Phen = 1,10-phenanthroline; Sa = salicylato; BDC – benzene-1,4-dicarboxylate, DEF = N,N-diethylformamide; 2-MeIm = 2-methylimidazole; gly = glycinate; dnSa = 3,5 dinitrosalicylato; DMF = N,N-dimethylformamide; benz = benzoate; val = rac-valinate; 4-aba = 4-aminobenzoate; 2-nba = 2-nitrobenzoate; OAc = acetate; 3-aba = 3-aminobenzoate; 4-CNbenz = 4-cyanobenzoate; *Nic = nicotinate*; OPA = 2-oxo-1,2-dihydropyridine-1-acetate; $C_4H_4O_5$ = malate; leu = rac-leucinate; bpdc = 4,4′-biphenyldicarboxylic acid; 2-aba = 2-aminobenzoate; 4-fba = 4-fluorobenzoate; $C_8H_5O_3$ = 2-formylbenzoate;PY-Thr = N-(6-amino-3,4-dihydro-3-methyl-5-nitroso-4-oxopyrimidin-2-yl) thronato; $C_9H_{11}N_6O_5$ = bis[N-(6-amino-3,4-dihydro-3-methyl-5-*nitroso-4-oxopyrimidine-2-yl) glycylglycinate*; *1,4-bdc* = 1,4-benzenedicarboxylate; 1,3-bdc = 1,3-benzenedicarboxylate; L = 4-(2-nitrophenyl)-3,6-dioxaoctane dioate; NDC – naphthalene 2,6-dicarboxylate; TPDC – 4,5,9,10-tetrahydropyrene-2,7-dicarboxylate; DADC – 5,10-dihydroanthracene-2,7-dicarboxylate; H_3BTC = benzene-1,3,5-tricarboxylic acid; tda = $S(CH_2COO)_2^{2-}$; BTA = 1,3,5-benzenetriacetate; $(O_2C)_2C_6H_3CO_2H$ = trimellitate; DTBB = 2,2′-dithiobis(benzoate); Hpdc = 3,5-pyrazoledicarboxylate; A_3Br = 1,3-biscarboxyethylimidazolium bromide; $C_{10}H_8O_6$ = benzene 1,4-dioxylacetate; 5-OH-BDC = 5-hydroxy isophthalate; $C_3H_3O_4$ = malonate; AIP = 5-aminoisopthalate.

several differences. Both compounds contain alkaline-earth:2-nba in a 1:2 ratio and are 1-D polymers based on dinuclear units. The alkalnei-earth metals in both compounds are linked to four different carboxylate ligands. However the compounds are differently hydrated and Ba adopts a 9 coordination. Of the two crystallographically independent 2-nba ligands in the Ba compound, one ligand binds in a $\mu_2\text{-}\eta^2\text{:}\eta^1$ manner, as observed in the Ca compound, while the other 2-nba ligand functions as a monoatomic bridge between two adjacent Ba ions in the chain with one of the nitro oxygen atoms bonded to one Ba, resulting in a denticity of three for this second 2-nba ligand. This binding mode of the carboxylate moiety in $[Ba(H_2O)_3(2\text{-}nba)_2]_n$ can be designated as $\mu_2\text{-}\eta^1\text{:}\eta^1$. In the 1-D polymeric chain alternating pairs of bivalent metals are bridged by a pair of 2-nba ligands.

In order to understand the role of the nitro group in the structural chemistry of Ca-nitrobenzoates, a comparison of the structural features of the title Ca compound **1** with the related monomeric Ca compound [49] of 4-nba namely $[Ca(H_2O)_4(\eta^1\text{-}4\text{-}nba)(\eta^2\text{-}4\text{-}nba)]$ is made. In the 4-nba compound, containing the nitro group para to the carboxylate functionality, the heptacoordinated Ca(II) is linked to two crystallographically independent 4-nba ligands which coordinate in a monodentate (η^1) and bidentate

(η^2) manner, respectively. In our original report [49] on the structural aspects of [$Ca(H_2O)_4(\eta^1$-4-nba)(η^2-4-nba)] only the O–H···O interactions were described, and the weak C–H···O interactions were not mentioned. A reinvestigation of the structure data reveals that one nitro oxygen atom on each unique 4-nba is involved in a C–H···O interaction at distances of 2.61 and 2.45 Å, accompanied by CHO angles of 158–166°, respectively. Hence the $-NO_2$ group in the 4-nba and 2-nba compounds of Ca, which are differently disposed with respect to the carboxylate in the benzene ring, are very similar in terms of their secondary interactions. However there is a noticeable difference between **1** and [$Ca(H_2O)_4(\eta^1$-4-nba)(η^2-4-nba)] in terms of the number of coordinated waters, which can account for the observed structural variation in these two compounds.

3.4. Comparative study of Ca(II) coordination polymers

In the 4-nba compound [$Ca(H_2O)_4(\eta^1$-4-nba)(η^2-4-nba)], each Ca(II) ion is linked to four oxygen atoms from water, and the monodentate and bidentate coordination of 4-nba results in hepta-coordination around Ca. In contrast, the tridenticity of the two crystallographically independent bridging 2-nba ligands in **1** leads to an eight coordination around Ca in the diaqua compound [Ca(2-nba)$_2(H_2O)_2]_n$ **1**, a feature observed in several calcium-carboxylates [19]. The attainment of a higher coordination number appears to be a key feature in Ca structural chemistry. It is noted that when there are a lesser number of coordinated water molecules in a calcium-carboxylate, the carboxylate ligand prefers to adopt a bridging mode of ligation. The importance of the number of coordinated waters can be evidenced by a comparative study of calcium-carboxylates, several of which are listed in Table 4.

Polymeric Ca-carboxylates of varying dimensionalities, derived from different carboxylic acids, are listed in Table 4. The coordination number of Ca(II) varies from 6 to 10, with eight coordination being observed in the majority of the compounds. It is interesting to note that in all the coordination polymers, excepting the three Ca compounds (entry numbers 45–47) derived from the dicarboxylic acids Hpdc (3,5-pyrazoledicarboxylate) and AIP (5-aminoisophthalate), the number of coordinated water molecules is three or less and in all such compounds the carboxylate ligand exhibits a bridging coordination mode leading to a polymeric chain. In the helical chain compound $[[Ca(H_2O)_4(AIP)_2](H_2O)]_n$, which has four water molecules, the entire AIP ligand acts as a bridge between two symmetry related Ca(II) ions, with each carboxylate showing a bidentate coordination to one Ca(II). In this case, octacoordination around Ca can be achieved without a bridging carboxylate mode of binding. Likewise in $[[Ca(H_2O)_4(Hpdc)]\cdot 2H_2O]_n$, the Hpdc ligand functions as a bridge between two Ca(II) ions with each carboxylate group binding in a monodentate fashion to one Ca. Additionally one of the pyrazole N atoms is also ligated in one of the ligands. It is to be noted that both AIP and Hpdc are ditopic ligands as they contain two carboxylate groups anchored onto a ring, and the ditopicity is responsible for the polymeric structure, without making use of a bridging carboxylate mode in these compounds. It is interesting to note that in the 1-D polymer $[[Ca(H_2O)_4(Hpdc)].H_2O]_n$, synthesized at a more acidic pH, a bridging carboxylate ligation is observed even though the Ca is coordinated to four water molecules. In this case pyrazole N ligation is not observed. From Table 4 it is very clear that when the number of coordinated water molecules is three or less, a bridging carboxylate binding mode is always observed. In Ca(II) compounds derived from mono carboxylic acids like 4-nbaH, for example [$Ca(H_2O)_4(\eta^1$-4-nba)(η^2-4-nba)] (entry number 48 in Table 4) seven coordination around Ca is observed due to the mono and chelating binding modes of the crystallographically independent 4-nba ligands, and this compound exhibits a zero-dimensional structure. When the number of water ligands in this compound is reduced by heating, the 4-nba adopts a bridging binding mode leading to a polymeric structure, as reported by us recently [47,48]. Another noteworthy feature is the tendency for the majority of the compounds to crystallize in centrosymmetric space groups.

4. Conclusions

In the present work we have described the synthesis, spectral and thermal properties and structural characterization of a new Ca(II) coordination polymer based on a tricyclic dicalcium-dicarboxylate building block. A comparative study of several Ca polymers shows that when the number of coordinated water molecules is three or less, in a Ca-carboxylate, the carboxylate ligand adopts a bridging mode of ligation.

Acknowledgement

B.R.S. thanks Prof. Samar K. Das School of Chemistry, University of Hyderabad, for the X-ray intensity data of **1** and the University Grants Commission, (UGC) New Delhi for financial support under the Special Assistance Program (DRS-II).

Appendix A. Supplementary data

CCDC 690437 contains the supplementary crystallographic data for compound 1. These data can be obtained free of charge via http://www.ccdc.cam.ac.uk/conts/retrieving.html, or from the Cambridge Crystallographic Data Centre, 12 Union Road, Cambridge CB2 1EZ, UK; fax: (+44) 1223-336-033; or e-mail: deposit@ccdc.cam.ac.uk.

Supplementary data associated with this article can be found, in the online version, at doi:10.1016/j.poly.2009.06.085.

References

[1] H. Einspahr, C.E. Bugg, Acta Crystallogr., B 36 (1980) 264.
[2] A.K. Katz, J.P. Glusker, S.A. Beebe, C.W. Bock, J. Am. Chem. Soc. 118 (1996) 5752.
[3] X. Shao, B.A. Davletov, R.B. Sutton, T.C. Sudhof, J. Rizo, Science 273 (1996) 248.
[4] K.M. Fromm, E.D. Gueneau, Polyhedron 23 (2004) 1479.
[5] R.C. Mehrotra, R. Bohra, Metal Carboxylates, Academic Press, London, 1983.
[6] F.A. Cotton, G. Wilkinson, C.A. Murillo, M. Bochmann, Advanced Inorganic Chemistry, 6th ed., John Wiley and Sons, Inc., Chichester, 1999.
[7] S. Fox, I. Büsching, W. Barklage, H. Strasdeit, Inorg. Chem. 46 (2007) 818.
[8] R. Murugavel, V.V. Karambelkar, G. Anantharaman, Indian J. Chem. 39A (2000) 843.
[9] R. Murugavel, V.V. Karambelkar, G. Anantharaman, M.G. Walawalkar, Inorg. Chem. 39 (2000) 1381.
[10] R. Murugavel, K. Baheti, G. Anantharaman, Inorg. Chem. 40 (2001) 6870.
[11] R. Murugavel, S. Banerjee, Inorg. Chem. Commun. 6 (2003) 810.
[12] R. Murugavel, P. Kumar, M.G. Walawalkar, R. Mathialagan, Inorg. Chem. 46 (2007) 6828.
[13] M. Dinca, J.R. Long, J. Am. Chem. Soc. 127 (2005) 9376.
[14] J.A. Rood, B.C. Noll, K.W. Henderson, Inorg. Chem. 45 (2006) 5521.
[15] C.A. Williams, A.J. Blake, C. Wilson, P. Hubberstey, M. Schroder, Cryst. Growth Des. 8 (2008) 911.
[16] M.J. Platers, R.A. Howie, A.J. Roberts, Chem. Commun. (1997) 893.
[17] K.M. Fromm, Coord. Chem. Rev. 252 (2008) 856. and references therein.
[18] H. Einspahr, C.E. Bugg, Acta Crystallogr., B 37 (1981) 1044.
[19] R. Murugavel, R. Korah, Inorg. Chem. 46 (2007) 11048.
[20] A. Brainbanti, A.M. Lanfredi, M.A. Pellinghelli, A. Tiripicchio, Chem. Commun. (1970) 377.
[21] W.-D. Song, X.-X. Guo, C.-H. Zhang, Acta Crystallogr., E 63 (2007) m399.
[22] S. Yano, M. Numata, M. Kato, S. Motoo, T. Nishimura, Acta Crystallogr., E 57 (2001) m488.
[23] B.G. Cooksey, L.T. Gibson, A.R. Kennedy, D. Littlejohn, L. Stewart, N.H. Tennent, Acta Crystallogr., C 55 (1999) m324.
[24] R.-X. Yuan, R.-G. Xiong, Z.-F. Chen, X.-Z. You, S.-M. Peng, G.-H. Lee, Inorg. Chem. Commun. 4 (2001) 430.
[25] B.L. Cole, E.M. Holt, Inorg. Chim. Acta 108 (1985) 159.
[26] J.-G. Zhao, S. Gao, Z.-Y. Zhang, L.-H. Huo, H. Zhao, Acta Crystallogr., E 62 (2006) m278.
[27] A. Karipides, C. McKinney, K. Peiffer, Acta Crystallogr., C 44 (1988) 46.

[28] I. Senkovska, U. Thewalt, Acta Crystallogr., C 61 (2005) m448.
[29] M. Odabaşoğlu, O. Büyükgüngör, Acta Crystallogr., E 63 (2007) m712.
[30] M.L.G. Salido, P.A. Mascaros, R.L. Garzon, M.D.G. Valero, J.N. Low, J.F. Gallagher, C. Glidewell, Acta Crystallogr., B 60 (2004) 46.
[31] J.N. Low, P. Arranz, J. Cobo, M.A. Fontecha, M.L. Godino, R. Lopez, D. Cannon, A. Quesada, C. Glidewell, Acta Crystallogr., C 57 (2001) 680.
[32] R.H. Groeneman, J.L. Atwood, Cryst. Eng. 2 (1999) 241.
[33] S.H. Dale, M.R.J. Elsegood, Acta Crystallogr., E 59 (2003) m586.
[34] L.-C. Yu, Z.-F. Chen, H. Liang, C.-S. Zhou, Y. Li, J. Mol. Struct. 750 (2005) 35.
[35] S.H. Dale, M.R.J. Elsegood, Acta Crystallogr., C 59 (2003) m540.
[36] A. Bacchi, M. Carcelli, C. Pelizzi, G. Pelizzi, P. Pelagatti, D. Rogolino, M. Tegoni, C. Viappiani, Inorg. Chem. 42 (2003) 5871.
[37] C. Volkringer, T. Loiseau, G. Férey, J.H. Warren, D.S. Wragg, R.E. Morris, Solid State Sci. 9 (2007) 455.
[38] L. Pan, T. Frydel, M.B. Sander, X. Huang, J. Li, Inorg. Chem. 40 (2001) 1271.
[39] Z. Fei, T.J. Geldbach, R. Scopelliti, P.J. Dyson, Inorg. Chem. 45 (2006) 6331.
[40] Y. Yang, G. Jiang, Y.-Z. Li, J. Bai, Y. Pan, X.-Z. You, Inorg. Chim. Acta 359 (2006) 3257.
[41] A. Grirrane, A. Pastor, E. Álvarez, R. Moyano, A. Galindo, Inorg. Chem. Commun. 10 (2007) 1125.
[42] H.-F. Zhu, Z.-H. Zhang, W.-Y. Sun, T. Okamura, N. Ueyama, Cryst. Growth Des. 5 (2005) 177.
[43] T. Jini, K.V. Saban, G. Varghese, S. Naveen, M.A. Shridhar, J.S. Prasad, J. Alloys Compd. 433 (2007) 211.
[44] Q. Shuai, S. Chen, S. Gao, Inorg. Chim. Acta 360 (2007) 1381.
[45] K. Aliouane, N. Rahahlia, A. Guehria-Laidoudi, S. Dahaoui, C. Lecomte, Acta Crystallogr., E 63 (2007) m1834.
[46] C. Volkringer, J. Marrot, G. Ferey, T. Loiseau, Cryst. Growth Des. 8 (2008) 685.
[47] B.R. Srinivasan, S.Y. Shetgaonkar, J.V. Sawant, P. Raghavaiah, Polyhedron 27 (2008) 3299.
[48] B.R. Srinivasan, S.Y. Shetgaonkar, C. Nather, W. Bensch, Polyhedron 28 (2009) 534.
[49] B.R. Srinivasan, J.V. Sawant, P. Raghavaiah, Indian J. Chem. 45A (2006) 2392.
[50] B.R. Srinivasan, S.C. Sawant, Thermochim. Acta 402 (2003) 45.
[51] B.R. Srinivasan, J.V. Sawant, P. Raghavaiah, J. Chem. Sci. 119 (2007) 11.
[52] Bruker SMART V5.630, SAINT-PLUS V6.45 and SADABS Bruker-Nonius Analytical X-ray Systems Inc., Madison, Wisconsin, USA, 2003.
[53] G.M. Sheldrick, Acta Crystallogr. 64A (2008) 112.
[54] B.R. Srinivasan, S.C. Sawant, S.N. Dhuri, Indian J. Chem. 41A (2002) 290.
[55] B.R. Srinivasan, P. Raghavaiah, J.V. Sawant, Acta Crystallogr. 63E (2007) m2251.
[56] B.R. Srinivasan, J.V. Sawant, C. Näther, W. Bensch, J. Chem. Sci. 119 (2007) 243.
[57] B.R. Srinivasan, J.V. Sawant, S.C. Sawant, P. Raghavaiah, J. Chem. Sci. 119 (2007) 593.
[58] B.R. Srinivasan, S.C. Sawant, S.K. Das, Indian J. Chem. 43A (2004) 1066.
[59] B.R. Srinivasan, G.K. Rane, J. Chem. Sci. 120 (2009) 145.
[60] B.R. Srinivasan, J.V. Sawant, P. Raghavaiah, Indian J. Chem. 48A (2009) 181.
[61] B.R. Srinivasan, S.Y. Shetgaonkar, P. Raghavaiah, J. Chem. Sci. 120 (2008) 249.

Polyhedron 28 (2009) 534–540

Contents lists available at ScienceDirect

Polyhedron

journal homepage: www.elsevier.com/locate/poly

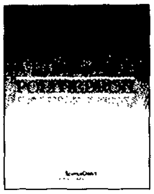

Solid state synthesis and characterization of a triple chain calcium(II) coordination polymer showing two different bridging 4-nitrobenzoate coordination modes

Bikshandarkoil R. Srinivasan[a,*], Santosh Y. Shetgaonkar[a], Christian Näther[b], Wolfgang Bensch[b]

[a] *Department of Chemistry, Goa University, Goa 403 206, India*
[b] *Institut für Anorganische Chemie, Christian-Albrechts Universität Kiel, D-24098 Kiel, Germany*

ARTICLE INFO

Article history:
Received 8 October 2008
Accepted 17 November 2008
Available online 27 December 2008

Keywords:
4-Nitrobenzoate
2-Methylimidazole
Coordination polymer
Pentagonal bipyramid
Monoatomic bridging
Triple chain

ABSTRACT

The solid state reaction of $[Ca(H_2O)_4(\eta^1\text{-4-nba})(\eta^2\text{-4-nba})]$ **1** (4-nba = 4-nitrobenzoate) with 2-methylimidazole (L^2) at 100 °C results in the formation of a Ca(II) coordination polymer $[Ca(H_2O)(L^2)(4\text{-nba})_2]_n$ **2**. Compound **2** was characterized by elemental analysis, spectral and thermal methods, and its structure determined. The coordination polymer **2** crystallizes in the centrosymmetric monoclinic space group $P2_1/n$ with all atoms situated in general positions and its structure consists of a central Ca(II), a monodentate 2-methylimidazole, a bridging water ligand (μ_2-H_2O), a bidentate bridging (μ_2-η^1:η^1) 4-nba ligand and a monoatomic bridging (μ_2-η^2) 4-nba ligand. Each seven-fold coordinated Ca(II) in the title compound is bonded to a nitrogen atom of a terminal 2-methylimidazole (L^2) ligand, two symmetry related water molecules and four symmetry related 4-nba ligands, resulting in a distorted pentagonal bipyramidal $\{CaO_6N\}$ polyhedron. Due to the bridging nature of the aqua and 4-nba ligands [(2-methylimidazole)calcium(II)] units in **2** are linked into a one-dimensional coordination polymer consisting of three chains, all of which propagate along *b*-axis. In the triple chain coordination polymer a Ca···Ca separation of 3.8432(3) Å is observed between neighbouring Ca(II) ions. The oxygen atoms of the carboxylate and nitro functionalities of the 4-nba ligand and the coordinated water are involved in O–H···O, N–H···O and C–H···O interactions. A comparative study of nine alkaline-earth 4-nitrobenzoate compounds is described.

1. Introduction

In recent years metal-organic frameworks (MOFs) or coordination polymers have attracted much attention because of their topology and potential applications in catalysis, adsorption (gas storage), separation, luminescence, magnetism, drug delivery etc [1–9]. Ligands containing carboxylic acid functional groups are attractive candidates for the construction of coordination polymers as metals can be linked into an extended chain with the aid of bridging binding modes of the carboxylate ligand [10,11]. Depending on the electronic and steric requirements of the central metal, the flexibility, binding modes and hydrogen bonding characteristics of the carboxylate ligand, the presence of additional bridging or terminal ligands, coordination polymers of differing dimensionalities (D) namely one (1D)-, two (2D)- and three (3D)-dimensional can be constructed.

Compared to the extensive chemistry of coordination polymers based on transition metals, the coordination chemistry of group 1 and 2 metal compounds with organic ligands is a relatively less explored area. Recently there is a growing interest in the chemistry of the coordination compounds of s-block elements as alkali and/or alkaline-earth metal cations are preferred to transition or lanthanide metal ions because most of the s-block cations have the advantage of being non-toxic, cheap and soluble in aqueous media. The recent work of Fromm [12] provides an overview on different ligand and polymer types of the s-block compounds. In the past decade several MOFs of alkaline earth metals have been synthesized, structurally characterized and their properties investigated [13–48].

For the preparation of coordination polymers different synthetic methodologies have been reported. These include the aqueous reaction of basic metal sources like metal carbonate or hydroxide with the carboxylic acid under ambient conditions [13–26], reaction of aqueous metal chloride or nitrate with the carboxylic acid in the presence of a mild base [27–41], the hydrothermal reaction of metal sources with carboxylic acids in autoclaves under autogeneous pressures [42–48]. Based on a review of the synthetic methods of s-block coordination compounds, it has been noted that microwave and solid state synthesis are scarce for the preparation of alkaline-earth metal-organic frameworks unlike the solution or hydrothermal methods of synthesis, which have been more widely used [12].

---

* Corresponding author. Tel.: +91 832 6519316; fax: +91 832 2451184.
E-mail addresses: srini@unigoa.ac.in, brsrinivasan@gmail.com (B.R. Srinivasan).

0277-5387/$ - see front matter © 2008 Elsevier Ltd. All rights reserved.
doi:10.1016/j.poly.2008.11.022

Recently we reported [49] that the zero-dimensional compound $[Ca(H_2O)_4(\eta^1\text{-4-nba})(\eta^2\text{-4-nba})]$ (4-nba = 4-nitrobenzoate) **1** can be readily transformed into a one-dimensional Ca(II) coordination polymer $[Ca(L^1)(4\text{-nba})_2]_n$ by heating it in the presence of *N*-methylimidazole (L^1) (Scheme 1) demonstrating that thermal reactions can be employed as an useful alternative method for the preparation of new coordination polymers. The loss of coordinated water molecules during the thermal reaction leads to a reorganization of the coordination sphere around Ca(II) resulting in the formation of a polymeric chain compound. In the present work, we have investigated the solid state reaction of compound **1** with 2-methylimidazole (L^2) which is an isomer of L^1 (Scheme 1). It is interesting to note that the reaction of **1** with L^2 at 100 °C results in the formation of a new mixed ligand one-dimensional Ca(II) coordination polymer **2** consisting of three chains.

2. Experimental

2.1. Materials and methods

All the chemicals used in this study were of reagent grade and were used as received. The starting materials and reaction products are air stable and hence were prepared under normal laboratory conditions. The compounds $[Ca(H_2O)_4(\eta^1\text{-4-nba})(\eta^2\text{-4-nba})]$ **1** [50] and $[Ca(H_2O)(4\text{-nba})_2]$ **1a** [49] were prepared as described earlier. Infrared (IR) spectra were recorded on a Shimadzu (IR Prestige-21) FT-IR spectrometer in the range 4000–400 cm^{-1}. The samples for the IR spectra were diluted with KBr in the solid state and the signals referenced to polystyrene bands. UV–Vis diffuse-reflectance spectra were obtained using a Shimadzu UV-2450 double beam spectrophotometer. $BaSO_4$ powder was used as reference (100% reflectance). Absorption data were calculated from the reflectance data using the Kubelka–Munk function ($a/S = (1-R)^2/2R$ where *a* is the absorption coefficient, *R* the reflectance and *S* the scattering coefficient). ^1H NMR spectrum was recorded in DMSO-d_6 on a Bruker 400 MHz FT-NMR spectrometer. Luminescence spectra were recorded at RT using a Perkin–Elmer LS 55 Luminescence spectrophotometer. TG-DSC measurements were performed in flowing air, in Al_2O_3 crucibles on a STA-409PC simultaneous thermal analyzer from Netzsch. A heating rate of 10 K min^{-1} was employed for all measurements. The insoluble 4-nbaH obtained on acid treatment of the complexes was weighed as described earlier [51] and metal analysis was performed titrimetrically following a standard procedure. Isothermal weight loss studies were performed in an electric furnace.

2.2. Preparation of $[Ca(H_2O)(L^2)(4\text{-nba})_2]_n$ 2

A powdered sample of compound **1** (0.444 g, 1 mmol) was mixed well with 2-methylimidazole (L^2) (0.082 g, 1 mmol) and the solid mixture was heated on a steam bath for ~30 min. The hot reaction mixture was cooled, washed well with ether and dried in air to obtain compound **2** as a yellow powder in quantitative yield. Crystals suitable for structure determination were prepared by recrystallizing the powdered sample from hot water (~10 ml) containing L^2 (0.246 g, 3 mmol). The crystalline needles of **2** were washed with cold water followed by alcohol and then dried in air. The infrared spectrum and the DSC thermogram of the crystalline product are identical with that of the yellow powder. **2** can also be prepared by first heating a powdered sample of **1** on a steam bath for ~20 min to obtain the monohydrate $[Ca(H_2O)(4\text{-nba})_2]$. The N-donor ligand ($L^2$) was mixed with this freshly prepared monohydrate and left at 100 °C for 15 min to obtain **2**.

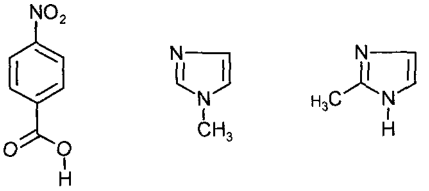

4-nbaH **L¹** **L²**

Scheme 1.

Anal. Calc. for $CaC_{18}H_{16}N_4O_9$ (**2**): Ca 8.48; 4-nbaH 70.75; CaO 11.87; C 45.76; H 3.41; N 11.86. Found: Ca, 8.45; 4-nbaH, 70.30, CaO, 11.81; C, 45.73; H, 3.63; N, 11.8%.

IR data: 3536 (υ_{O-H}), 3264 (υ_{N-H}), 3117, 2204, 1944, 1622, 1591, 1570, 1514, 1487, 1412, 1346, 1323, 1280, 1169, 1148, 1103, 1011, 997, 876, 854, 827, 795, 787, 752, 721, 673, 600, 517, 440 cm^{-1}.

^1H NMR (DMSO-d_6) δ (in ppm): 2.25 (s, 3H); 6.83 (d, 2H); 7.14 (d, 2H); 8.14 (q, 2H); 11.52 (s, H).

DSC data (in °C): 172 (*endo*) 410 (*exo*) 559 (*exo*).

UV–Vis (diffuse reflectance): 251, 330 nm.

2.3. X-ray crystal structure determination

Intensity data for **2** was collected on a STOE Image Plate Diffraction System using graphite-monochromated Mo Kα radiation. The structure was solved with direct methods using SHELXS-97 [52] and refinement was done against F2 using SHELXL-97 [52]. All non-hydrogen atoms were refined anisotropically. Aromatic hydrogens were introduced at their calculated positions and included in the refinement riding on their respective parent atoms. The H atoms of the coordinated water molecule were located in the difference Fourier map and refined with fixed isotropic displacement parameters. The technical details of data acquisition and some selected refinement results are summarized in Table 1.

Table 1

Crystal data and structure refinement for $[Ca(H_2O)(L^2)(4\text{-nba})_2]_n$ **2**.

Empirical formula	$C_{18}H_{16}CaN_4O_9$
Formula weight	472.43 g mol^{-1}
Temperature	220(2) K
Wavelength	0.71073 Å
Crystal system	Monoclinic
Space group	$P2_1/n$
Unit cell dimensions	a = 15.5486(13) Å
	b = 7.0358(4) Å
	c = 18.4282(15) Å
	α = 90°
	β = 98.789(10)°
	γ = 90°
Volume	1992.3(3) $Å^3$
Z	4
D_{calc}	1.575 mg/m^3
Absorption coefficient	0.377 mm^{-1}
$F(000)$	976
Crystal size	0.4 × 0.3 × 0.2 mm^3
Θ range for data collection	2.65–28.09°
Index ranges	$-20 \leqslant h \leqslant 20, -8 \leqslant k \leqslant 9, -24 \leqslant l \leqslant 24$
Reflections collected	18549
Independent reflections	4768 [R_{int} = 0.0334]
Completeness to theta = 28.09°	98.0%
Refinement method	Full-matrix least-squares on F^2
Data/restraints/parameters	4768/0/291
Goodness-of-fit on F^2	1.055
Final R indices [$I > 2\sigma(I)$]	R_1 = 0.0399, wR_2 = 0.1069
R indices (all data)	R_1 = 0.0484, wR_2 = 0.1123
Extinction coefficient	0.027(3)
Largest differences in peak and hole	0.337 and −0.386 e $Å^{-3}$

3. Results and discussion

3.1. Synthesis and spectroscopy

The solid state reaction of an intimate mixture of the tetraaqua compound $[Ca(H_2O)_4(4\text{-nba})_2]$ **1** and 2-methylimidazole (L^2) at 100 °C resulted in the formation of the mixed ligand Ca(II) compound $[Ca(L^2)(H_2O)(4\text{-nba})_2]$ **2** in quantitative yield (Scheme 2). Compound **2** was formulated based on the elemental analysis and the mass loss leading to the formation of CaO on pyrolysis. The use of excess L^2 in the thermal reaction did not result in the formation of new products containing additional N-donor ligands. The mixed ligand compound **2** can also be synthesized in a two step process. The first step involves the synthesis of a monohydrate compound $[Ca(H_2O)(4\text{-nba})_2]$ **1a** by heating **1** at 100 °C. The reaction of L^2 with **1a** at 100 °C afforded the new compound **2**, which is insoluble in all common solvents like water, CH_3CN, CH_2Cl_2, DMF etc. The solid is partially soluble in DMSO and this property was used to study its NMR spectrum, which exhibits the characteristic signals of the organic moieties 4-nba and L^2.

The thermal reaction of **1** was investigated with other N-donor ligands like pyridine (pKa 5.1), benzimidazole (pKa 5.4) and 4-picoline (pKa 6.02). However from these reactions no new product containing N-donor ligand could be obtained. In all these cases the product obtained consisted of a mixture of $[Ca(H_2O)(4\text{-nba})_2]$ and unreacted N-donor ligand. The unreacted ligand could be quantitatively recovered by washing the mixture with ether. The non-incorporation of N-donor ligand can be attributed to the less basic nature of benzimidazole and the pyridine ligands as compared to L^1 (pKa 7.1) or L^2 (pKa 7.75). The N-donor ligands L^1 and L^2 are isomers and differ in terms of the positioning of the methyl substituent. The ligand L^2 employed in this work resulted in the formation of a final product containing a mole of water for each mole of Ca, unlike imidazole or N-methylimidazole (L^1) which yielded anhydrous compounds having molar composition of Ca:4-nba:L^1 1:2:1 [49]. Crystals of **2** suitable for structure determination were prepared by recrystallising compound **1** from an aqueous solution containing L^2. The crystalline nature of **2** (Fig. 1) can be evidenced from the sharp signals in its powder diffractogram. A comparison of the powder pattern of the bulk sample with that of the theoretically calculated pattern from the single crystal data (*vide infra*) reveals the phase purity of the mixed ligand product **2**. The presence of water in **2** is inferred from the strong signal in its infrared spectrum at 3536 cm^{-1}. The signal at 3264 cm^{-1} can be assigned to the $\upsilon_{N\text{-}H}$ (L^2) vibration (Supplementary Fig. 1) of the N-donor ligand. It is to be noted that the profile of the infrared spectra in the region 3500–2800 cm^{-1} of compound **2** is quite different as compared to that of the tetraaqua compound **1** or the monohydrate $[Ca(H_2O)(4\text{-nba})_2]$ **1a**. Compound **2** exhibits several signals in the mid IR region indicating the presence of the organic moieties. The strong signals at 1514 and 1346 cm^{-1} can be assigned to the asymmetric and symmetric stretching vibrations of the $-NO_2$ group of 4-nba while the bands at 1591 and 1570 cm^{-1} are assignable to the asymmetric vibration of the carboxylate group. The signal at 1411 cm^{-1} is assigned for the symmetric vibration of the –COO group. However based only on the infrared data, the exact nature of the binding of the 4-nba ligand cannot be unambiguously determined. In view of the insolubility of **2** in all common solvents the diffuse reflectance spectrum was recorded in the UV–Vis region. The observed signals at 251 and 330 nm in the spectrum can be attributed to the intraligand charge transfer bands of the 4-nba ligand based on a comparison of the reflectance spectra of compounds **2** and **1** (Fig. 2). The luminescence studies of alkaline-earth metal complexes are of considerable importance since the divalent cations Mg and Ca are the most abundant in living cells and play vital roles in many cellular processes [1]. Two emission maxima are observed at around 450 and 490 nm for compound **2**. Interestingly both 4-nbaH and L^2 exhibit emission signals around 450 nm. A scrutiny of the emission spectra reveals that the emission of the Ca(II) compound **2** is reduced as compared to that of the free ligands (Fig. 3). A reduction in the emission intensity has

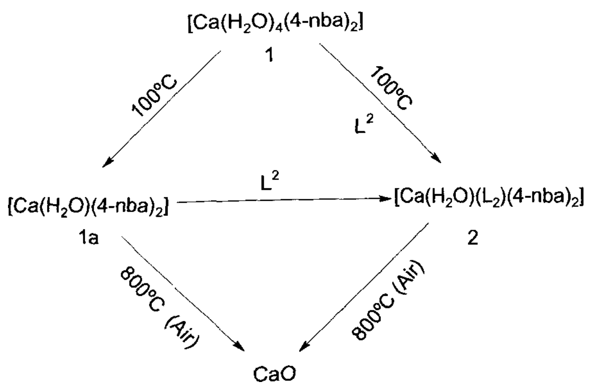

Scheme 2.

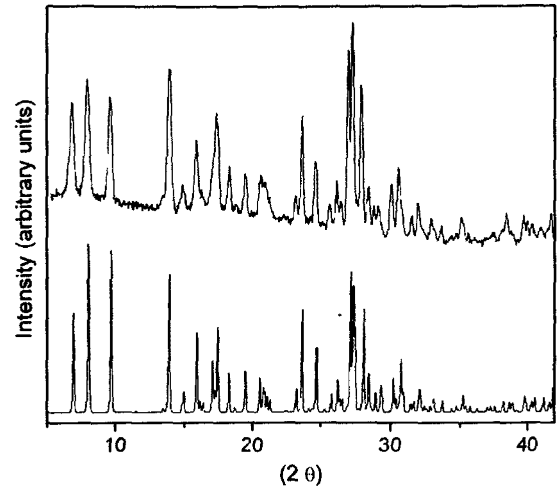

Fig. 1. X-ray powder pattern of a bulk sample of $[Ca(H_2O)(L^2)(4\text{-nba})_2]_n$ **2** (top); theoretical pattern calculated from single crystal data (bottom).

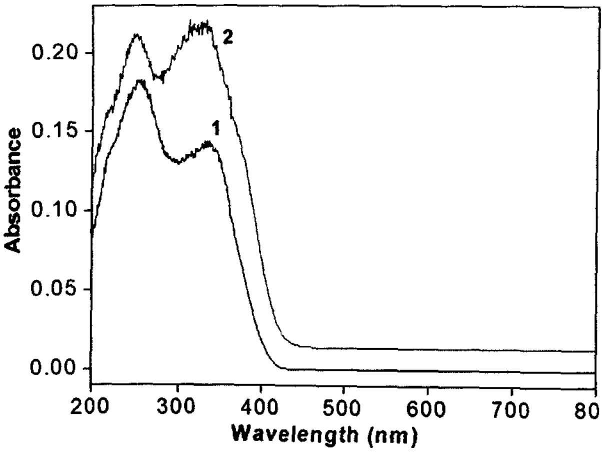

Fig. 2. Diffuse reflectance spectra of **1** and **2**.

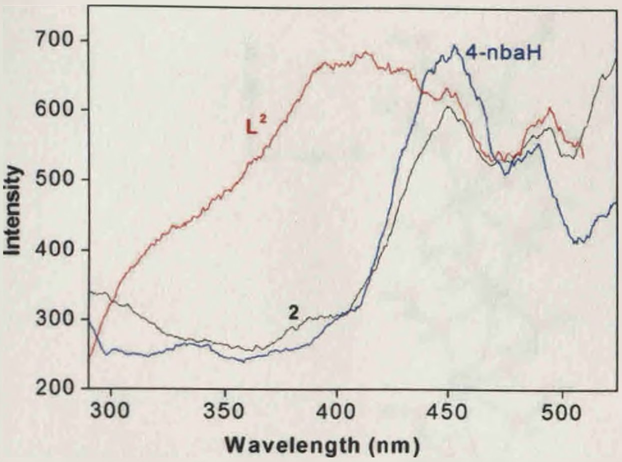

Fig. 3. Luminescence spectra of **2** and free the ligands.

been recently reported for the 1D coordination polymer $[Ca(SA)_2(phen)]_n$ (SA = salicylate; phen = 1,10-phenanthroline) [53].

3.2. Crystal structure description of 2

Compound **2** crystallizes in the centrosymmetric monoclinic space group $P2_1/n$ with all atoms situated in general positions. The structure reveals that **2** is a coordination polymer and can be formulated as $[Ca(H_2O)(L^2)(4\text{-nba})_2]_n$. The structure of *catena*-poly[[(2-methylimidazole)calcium(II)](μ_2-aqua)(μ_2-η^1:η^1-4-nitrobenzoato)(μ_2-η^2-4-nitrobenzoato)] **2** consists of a central Ca(II) ion, a terminal 2-MeIm ligand, a bridging aqua ligand and two crystallographically independent bridging 4-nba ligands (Fig. 4). In the crystal structure, each Ca(II) is bonded to a nitrogen atom of a terminal 2-methylimidazole ligand, two oxygen atoms from two symmetry related aqua ligands and four oxygen atoms from four symmetry related 4-nba ligands resulting in a distorted $\{CaO_6N\}$ pentagonal bipyramidal polyhedron around Ca (Fig. 4). The geometric parameters of the 4-nba anions and 2-MeIm are in the normal range. The O–Ca–O and O–Ca–N angles range from 65.73(3) to 172.63(5)°. The Ca–O distances in **2** range from 2.3100(11)–2.5654(11) Å (Table 2) and are in agreement with literature values [49,50,53]. A Ca–N bond distance of 2.5024(13) Å is observed. The oxidation state of the central metal in compound **2** based on the bond valence sum was found to be 2.139 [54]. The bond valence sum for the precursor calcium compound $[Ca(H_2O)_4(4\text{-nba})_2]$ **1**, the mixed ligand compound $[Ca(H_2O)_3(Im)(4\text{-nba})_2]\cdot Im$ and the 1-D ladder polymer $[Ca(L^1)(4\text{-nba})_2]_n$ are 2.187, 2.27 and 2.177, respectively. It is interesting to note that the bond valence sums are very close to the expected value of 2 for the bivalent metal and the estimated bond valence sums for the coordination polymers **2** and $[Ca(L^1)(4\text{-nba})_2]_n$ are slightly less than those observed for the zero-dimensional calcium compounds.

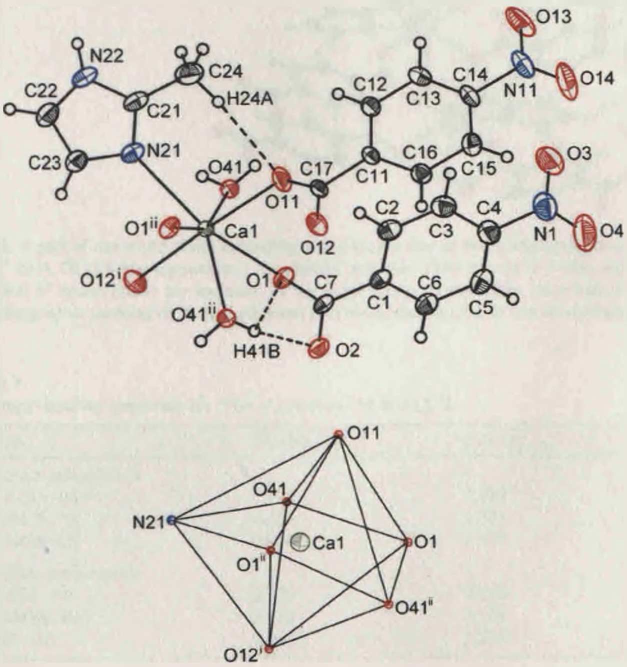

Fig. 4. A view of the coordination sphere of Ca(II) in $[Ca(H_2O)(L^2)(4\text{-nba})_2]_n$ **2**, showing the atom-labeling scheme. Displacement ellipsoids are drawn at the 50% probability level excepting for the H atoms, which are shown as circles of arbitrary radius (top). Intramolecular H-bonding is shown by the broken lines. The distorted pentagonal bipyramidal coordination polyhedron around Ca(II) in **2** (bottom). Symmetry code: (i) $-x+1/2, y-1/2, -z+3/2$; (ii) $-x+1/2, y+1/2, -z+3/2$.

The coordinated water (O41) functions as a μ_2-bridging ligand with the O41 atom linked to two symmetry related Ca(II) ions resulting in the formation of an infinite chain extending along *b*-axis (Supplementary Fig. 2). It is interesting to note that both 4-nitrobenzoates in each formula unit are coordinated to the central Ca(II) in different bridging modes. One of the two unique 4-nba anions in each formula unit is coordinated to two different Ca(II) ions through one of the carboxylate oxygen atoms (O1), which functions as a monoatomic bridge (μ_2-η^2) resulting in an extended chain along *b*-axis (Supplementary Fig. 3). The second independent 4-nba ligand functions as a bridging bidentate ligand (μ_2-η^1:η^1) and is linked to two symmetry related Ca(II) ions via O11 and O12 oxygen atoms. An infinite chain extending along *b*-axis is formed due to this binding mode of 4-nba. Due to the bridging nature of the aqua and 4-nba ligands, [(2-methylimidazole)calcium(II)] units in **2** are linked into a one-dimensional coordination polymer consisting of three chains, all of which propagate along *b*-axis (Fig. 5). In the triple chain coordination polymer a Ca···Ca separation of 3.8432(3) Å is observed between neighbouring Ca(II) ions. This value is comparable with the Ca···Ca distance of 3.8585(7) Å reported for the related compound $[Ca(L^1)(4\text{-nba})_2]_n$ [49] and in several other Ca(II) coordination polymers.

A scrutiny of the structure reveals that the oxygen atoms of the carboxylate and nitro functionalities of the 4-nba ligand and the coordinated water are involved in O–H···O, N–H···O and C–H···O interactions. A total of six H-bonding interactions with H···O dis-

Table 2
Selected bond lengths and bond angle (Å, °) for $[Ca(H_2O)(L^2)(4\text{-nba})_2]_n$ **2**.

Ca(1)–O(11)	2.3100(11)	Ca(1)–O(41)	2.4978(11)
Ca(1)–O(12)^{i}	2.3119(11)	Ca(1)–N(21)	2.5024(13)
Ca(1)–O(1)^{ii}	2.4205(11)	Ca(1)–O(41)^{ii}	2.5654(11)
Ca(1)–O(1)	2.4912(11)	Ca(1)–Ca(1)^{ii}	3.8432(3)
O(11)–Ca(1)–O(12)^{i}	172.63(5)	O(12)^{i}–Ca(1)–N(21)	83.69(5)
O(11)–Ca(1)–O(12)^{ii}	87.00(4)	O(1)^{ii}–Ca(1)–N(21)	77.74(4)
O(12)–Ca(1)–O(1)^{ii}	100.11(4)	O(1)–Ca(1)–N(21)	146.38(4)
O(11)–Ca(1)–O(1)	79.52(4)	O(41)–Ca(1)–N(21)	80.64(4)
O(12)^{i}–Ca(1)–O(1)	93.94(4)	O(11)–Ca(1)–O(41)^{ii}	95.97(4)
O(1)^{ii}–Ca(1)–O(1)	135.28(3)	O(12)^{i}–Ca(1)–O(41)^{ii}	85.31(4)
O(11)–Ca(1)–O(41)	85.80(4)	O(1)^{ii}–Ca(1)–O(41)^{ii}	65.73(3)
O(12)^{i}–Ca(1)–O(41)	88.42(4)	O(1)–Ca(1)–O(41)^{ii}	73.50(4)
O(1)^{ii}–Ca(1)–O(41)	155.67(4)	O(41)–Ca(1)–O(41)^{ii}	138.19(3)
O(1)–Ca(1)–O(41)	65.76(3)	N(21)–Ca(1)–O(41)^{ii}	139.17(4)
O(11)–Ca(1)–N(21)	99.84(5)		

Symmetry transformations used to generate equivalent atoms: $-x+1/2, y-1/2, -z+3/2$; (ii) $-x+1/2, y+1/2, -z+3/2$.

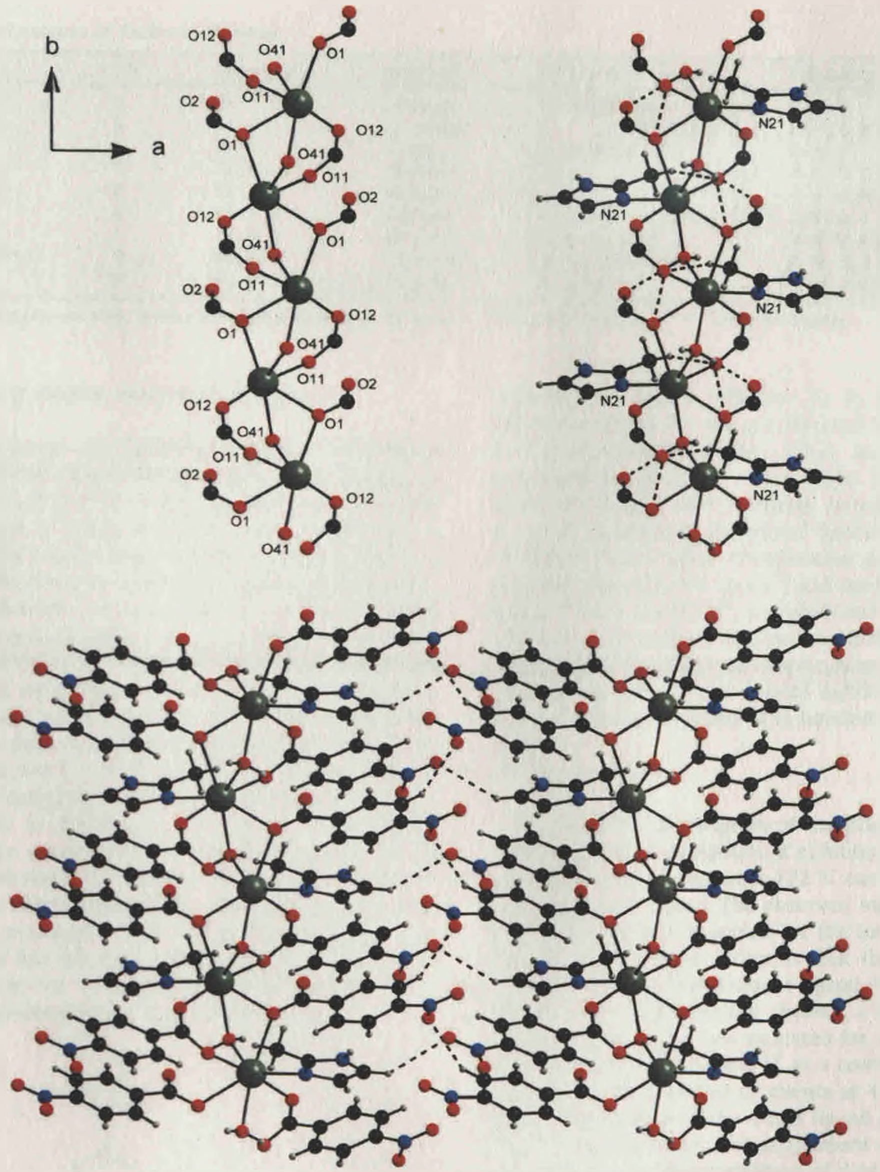

Fig. 5. A part of the triple chain extending along *b*-axis due to the bridging binding modes of the aqua (O41) and the crystallographicaly independent μ_2-η^2 (O1) and μ_2-η^1:η^1 (O11, O12) 4-nba ligands in **2**. For clarity, only the –COO groups of 4-nba and the O atom of water are shown (top right). The H-atoms of the bridging water and the terminal L^2 ligand (N21) are included in the triple chain to show the intrachain H-bonding interactions in broken lines (top left). A view along *c* axis is shown for the crystallographic packing of **2**. Two adjacent polymeric chains of **2** in the *ab* crystallographic plane are linked by weak C–H···O bonds shown in broken lines (bottom).

Table 3
Hydrogen-bonding geometry (Å, °) for $[Ca(H_2O)(L^2)(4\text{-nba})_2]_n$ **2**.

D–H···A	*d*(D–H)	*d*(H···A)	*D*(D···A)	<DHA	Symmetry code
Intrachain interactions					
C24–H24A···O11	0.971	2.411	3.347	162	
O41–H41B···O2	0.820	1.831	2.642	170	$[-x+1/2, y-1/2, -z+3/2]$
O41–H41B···O1	0.820	2.600	3.026	114	$[-x+1/2, y-1/2, -z+3/2]$
Interchain interactions					
N22–H22···O2	0.870	2.012	2.873	170	$[x-1/2, -y+3/2, z-1/2]$
O41–H41A···O13	0.820	2.160	2.972	171	$[-x+1, -y+1, -z+1]$
C5–H5···O3	0.940	2.532	3.398	153	$[-x+3/2, y+1/2, -z+3/2]$

tances ranging from 1.831 to 2.600 Å (Table 3) are observed. These can be classified as intra- and interchain interactions. The C24–H24A···O11, O41–H41B···O2 and O41–H41B···O1 interactions occur within the triple chain 1-D polymer, while the N22–H22···O2, O41–H41A···O13 and C5–H5···O3 interactions serve to link adjacent polymeric chains (Fig. 5).

Table 4
Structural features of 4-nitrobenzoates of alkaline-earth metals.

Compound	C.N.	Space group	Nuclearity	Binding mode of 4-nba	H-bonding	Reference
$[Mg(H_2O)_6](4\text{-nba})_2 \cdot 2H_2O$	6	$P\bar{1}$	Monomer	Uncoordinated	O–H···O	[56]
$[Mg(H_2O)_2(Im)_2(4\text{-nba})_2]$	6	$P\bar{1}$	Monomer	η^1	O–H···O, N–H···O	[55]
$[Mg(H_2O)(L^1)_2(4\text{-nba})_2]_2$	6	$P\bar{1}$	Dimer	η^1, μ_2-η^1:η^1	O–H···O	[56]
$[Ca(H_2O)_4(4\text{-nba})_2]_n$	7	$P2_1/c$	Monomer	η^1, η^2	O–H···O, C–H···O	[50]
$[Ca(H_2O)_3(Im)(4\text{-nba})_2] \cdot Im$	6	$P2_1/c$	Monomer	η^1	O–H···O, N–H···O, O–H···N	[55]
$[Ca(L^1)(4\text{-nba})_2]_n$	6	$P\bar{1}$	Polymer	μ_2-η^1:η^1, μ_3-η^2:η^1	C–H···O	[49]
$[Ca(H_2O)(L^2)(4\text{-nba})_2]_n$	7	$P2_1/n$	Polymer	μ_2-η^1:η^1, μ_2-η^2	O–H···O, C–H···O, N–H···O	This work
$[Sr(H_2O)_7(4\text{-nba})](4\text{-nba}) \cdot 2H_2O$	9	$P2_1/c$	Monomer	η^2, uncoordinated	O–H···O, C–H···O	[57]
$[Ba(H_2O)_5(4\text{-nba})_2]_n$	9	$P2_1/c$	Polymer	η^2, μ_2-η^1:η^1	O–H···O, C–H···O	[58]

Abbreviations: C.N. = coordination number; 4-nba = 4-nitrobenzoate; Im = imidazole; L^1 = N-methylimidazole; L^2 = 2-methylimidazole.

3.3. Comparative study of alkaline-earth 4-nitrobenzoates

The coordination polymer $[Ca(H_2O)(L^2)(4\text{-nba})_2]_n$ **2** described in this work and the reported compounds $[Ca(H_2O)_4(\eta^1\text{-}4\text{-nba})(\eta^2\text{-}4\text{-nba})]$ **1** [50], $[Ca(H_2O)_3(Im)(\eta^1\text{-}4\text{-nba})_2] \cdot Im$ [55], and $[Ca(L^1)(4\text{-nba})_2]_n$ [49] constitute a group of Ca(II) compounds with a 1:2 mol ratio of Ca:4-nba and exhibit different binding modes of the 4-nba ligand. In addition to these 4-nitrobenzoates of Ca(II), five other 4-nba compounds containing Mg, Sr and Ba have been structurally characterized [55–58]. The availability of structural features of several compounds (Table 4) permits a comparative study of the structural chemistry of alkaline-earth 4-nitrobenzoates, the details of which are described below. All the structurally characterized alkaline-earth 4-nitrobenzoates listed in Table 4, exhibit a metal:4-nba ratio of 1:2 and crystallize in centrosymmetric space groups. The nuclearity of the compounds ranges from monomer (five compounds) to dimer (one compound) and polymer (three compounds). The coordination number of the central metal varies from 6 to 9, with the Mg(II) compounds showing hexacoordination. The Sr and Ba compounds exhibit nine coordination while both hexa and hepta coordination are observed in the Ca(II) compounds. In addition to functioning as charge balancing anions for the bivalent metal in all the compounds, 4-nba is bonded to the central metal as a monodentate (η^1) or bidentate or (η^2) or as a bridging (μ-) ligand (Scheme 3). In $[Mg(H_2O)_6](4\text{-nba})_2 \cdot 2H_2O$ the 4-nba anions are not coordinated to the central metal, while in $[Sr(H_2O)_7(4\text{-nba})](4\text{-nba}) \cdot 2H_2O$ one unique 4-nba remains uncoordinated with the other 4-nba functioning as a chelating bidentate ligand. The bridging bidentate binding mode (μ_2-η^1:η^1) is observed in the mixed ligand dimeric Mg(II) compound as well as in the three coordination polymers. The monoatomic bridging binding mode (μ_2-η^2) and the tridentate bridging coordination modes (μ_3-η^2:η^1) are observed in the Ca(II) coordination polymers. Interestingly in the four different Ca(II)-4-nitrobenzoates a total of five different coordination modes of the 4-nba ligand are observed. All the compounds exhibit several H-bonding interactions resulting in different H-bonded networks.

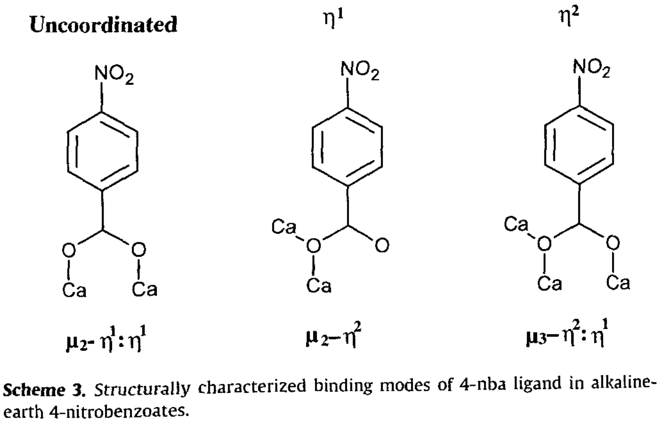

Scheme 3. Structurally characterized binding modes of 4-nba ligand in alkaline-earth 4-nitrobenzoates.

3.4. Thermal studies

The TG–DSC thermogram of compound **2** is depicted in Fig. 6. The DSC curve of compound **2** exhibits three thermal events. The first endothermic process at 172 °C can be assigned to the loss of a neutral water ligand. The observed mass loss of 10.52% is much more than the loss expected for the loss of a mole of water. The drop in the TG curve indicates that the loss of water results in the loss of the neutral N-donor ligand. The isothermal weight loss studies at this temperature showed a mass loss of 13% which is much more than the loss expected for a mole of water and much less than loss due to either L^2 or a combination of two neutral ligands in **2**. The exothermic events at 410 and 559 °C correspond to the degradation of the 4-nba ligand as evidenced by the rapid drop in the TG curve. The assignment of the endothermic signal at 410 °C for the decomposition of 4-nba gains more credence as a similar behaviour has been observed for the related Ca(II) com

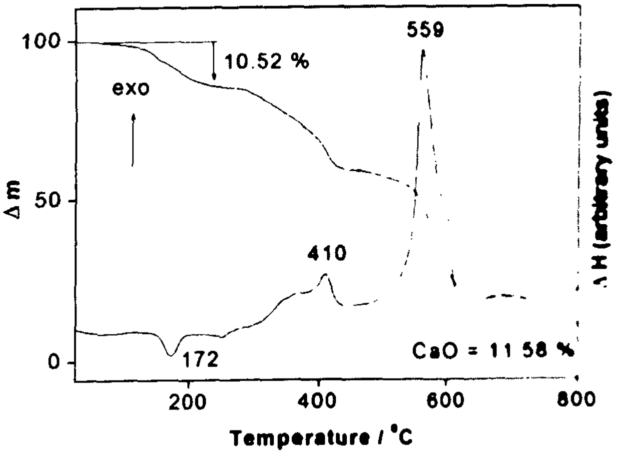

Fig. 6. TG–DSC thermogram of compound 2.

pounds **1** and **1a** [49]. The TG curve above 750 °C is parallel to the temperature axis and observed residue of 11.58% is in very good agreement with the expected value of 11.87% for the formation of CaO. The formation of CaO as the final residue has been confirmed based on the X-ray powder pattern of the residue (Supplementary Fig. 4) as well as isothermal weight loss studies.

4. Conclusions

In summary, we have shown that the zero-dimensional mononuclear tetraaqua Ca(II) compound **1** can be transformed into a phase pure Ca(II) coordination polymer $[Ca(H_2O)(L^2)(4\text{-nba})_2]_n$ **2** by heating it in the presence of 2-methylimidazole (L^2). The key step in this solid state transformation is the formation of an intermediate monohydrate compound followed by incorporation of the N-donor ligand into the coordination sphere of Ca(II) resulting in the formation of a triple stranded coordination polymer. A comparative study of the structural features of nine 4-nitrobenzoate compounds of alkaline-earth metals reveals five different binding modes of the 4-nba ligand all of which are observed in the structurally characterized compounds $[Ca(H_2O)_4(4\text{-nba})_2]_n$ **1** $[Ca(H_2O)_3(Im)(4\text{-nba})_2]\cdot Im$, $[Ca(L^1)(4\text{-nba})_2]_n$ and $[Ca(H_2O)(L^2)(4\text{-nba})_2]_n$ **2**.

Acknowledgements

BRS thanks Miss J.V. Sawant for helpful discussions and Prof. R. Murugavel, Department of Chemistry, IIT-Mumbai for the luminescence spectral data. This work is supported by the Department of Science and Technology, New Delhi under Grant No. SR/S1/IC-41/2003.

Appendix A. Supplementary data

CCDC 688701 contains the supplementary crystallographic data for compound **2**. These data can be obtained free of charge via http://www.ccdc.cam.ac.uk/conts/retrieving.html, or from the Cambridge Crystallographic Data Centre, 12 Union Road, Cambridge CB2 1EZ, UK; fax: (+44) 1223 336 033; or e-mail: deposit@ccdc.cam.ac.uk. Supplementary data associated with this article can be found, in the online version, at doi:10.1016/j.poly.2008.11.022.

References

[1] C. Janiak, J. Chem. Soc. Dalton Trans. 2781 (2003).
[2] M. Eddaoudi, D.B. Moler, H. Li, B. Chen, T.M. Reineke, M. O'Keeffe, O.M. Yaghi, Acc. Chem. Res. 34 (2001) 319.
[3] J. Kim, B. Chen, T.M. Reineke, H. Li, M. Eddaoudi, D.B. Moler, M. O'Keeffe, O.M. Yaghi, J. Am. Chem. Soc. 123 (2001) 8239.
[4] S. Surblé, F. Millange, C. Serre, T. Düren, M. Latroche, S. Bourrelly, P.L. Llewellyn, G. Férey, J. Am. Chem. Soc. 128 (2006) 14889.
[5] H. Dathe, E. Peringer, V. Roberts, A. Jentys, J.A. Lercher, C.R. Chimie 8 (2005) 753.
[6] S.S. Han, W.-Q. Deng, W.A. Goddard, Angew. Chem. Int. Ed. 46 (2007) 6289.
[7] P. Horcajada, C. Serre, M. Vallet-Regi, M. Sebban, F. Taulelle, G. Ferey, Angew. Chem. Int. Ed 45 (2006) 5974.
[8] M. Dinca, J.R. Long, J. Am. Chem. Soc. 127 (2005) 9376.
[9] J.A. Rood, B.C. Noll, K.W. Henderson, Inorg. Chem. 45 (2006) 5521.
[10] R.C. Mehrotra, A. Singh, Prog. Inorg. Chem. 46 (1997) 239.
[11] F.A. Cotton, G. Wilkinson, C.A. Murillo, M. Bochmann, Advanced Inorganic Chemistry, sixth ed., John Wiley & Sons, Inc, Chichester, 1999. p. 487.
[12] K.M. Fromm, Coord. Chem. Rev. 252 (2008) 856. and references therein.
[13] H.-F. Zhu, Z.-H. Zhang, W.-Y. Sun, T. Okamura, N. Ueyama, Crystal Growth Design 5 (2005) 177.
[14] M. Dan, A.K. Cheetham, C.N.R. Rao, Inorg. Chem. 45 (2006) 8227.
[15] Z. Fei, T.J. Geldbach, D. Zhao, R. Scopelliti, P.J. Dyson, Inorg. Chem. 44 (2005) 5200.
[16] B.R. Srinivasan, S.Y. Shetgaonkar, P. Raghavaiah, J. Chem. Sci. 120 (2008) 249
[17] S.H. Dale, M.R.J. Elsegood, Acta Crystallogr. C 59 (2003) m540.
[18] M. Odabaşoğlu, O. Büyükgüngör, Acta Crystallogr. E 63 (2007) m712.
[19] Z. Fei, T.J. Geldbach, R. Scopelliti, P.J. Dyson, Inorg. Chem. 45 (2006) 6331
[20] R.K.B. Nielsen, K.O. Kongshaug, H. Fjellvåg, Solid State Sci. 8 (2006) 1237
[21] K. Aliouane, N. Rahahlia, A.-G. Laidoudi, S. Dahaoui, C. Lecomte, Acta Crystallogr. E63 (2007) m1834.
[22] S. Wörl, I.O. Fritsky, D. Hellwinkel, H. Pritzkow, R. Kramer, Eur. J. Inorg. Chem. (2005) 759.
[23] R. Murugavel, P. Kumar, M.G. Walawalkar, R. Mathialagan, Inorg. Chem. 46 (2007) 6828.
[24] R. Murugavel, S. Banerjee, Inorg. Chem. Commun. 6 (2003) 810
[25] A. Bacchi, M. Carcelli, C. Pelizzi, G. Pelizzi, P. Pelagatti, D. Rogolino, M. Tegoni, C. Viappiani, Inorg. Chem. 42 (2003) 5871.
[26] S. Fox, I. Büsching, W. Barklage, H. Strasdeit, Inorg. Chem. 46 (2007) 818
[27] Q. Shuai, S. Chen, S. Gao, Inorg. Chim. Acta. 360 (2007) 1381.
[28] A. Grirrane, A. Pastor, E. Álvarez, R. Moyano, A. Galindo, Inorg. Chem. Commun. 10 (2007) 1125.
[29] R. Murugavel, V.V. Karambelkar, G. Anantharaman, M.G. Walawalkar, Inorg. Chem. 39 (2000) 1381.
[30] J.-G. Zhao, S. Gao, Z.-Y. Zhang, L.-H. Huo, H. Zhao, Acta Crystallogr. E 62 (2006) m278.
[31] R. Murugavel, V.V. Karambelkar, G. Anantharaman, Indian J. Chem. 39A (2000) 843.
[32] R. Murugavel, K. Baheti, G. Anantharaman, Inorg. Chem. 40 (2001) 6870
[33] Y. Yang, G. Jiang, Y.-Z. Li, J. Bai, Y. Pan, X.-Z. You, Inorg. Chim. Acta 359 (2006) 3257.
[34] L.B. Cole, E.M. Holt, Inorg. Chim. Acta 108 (1985) 159.
[35] D.A. Lenev, K.A. Lyssenko, R.G. Kostyanovsky, Eur. J. Inorg. Chem. (2003) [illegible]
[36] I. Senkovska, U. Thewalt, Acta Crystallogr. C61 (2005) m448.
[37] R.H. Groeneman, J.L. Atwood, Crystal Eng. 2 (1999) 241.
[38] W.-D. Song, X.-X. Guo, C.-H. Zhang, Acta Crystallogr. E 63 (2007) m399
[39] S. Yano, M. Numata, M. Kato, S. Motoo, T. Nishimura, Acta Crystallogr. E 57 (2001) m488.
[40] M.L.G. Salido, P.A. Mascaros, R.L. Garzon, M.D.G. Valero, J.N. Low, J.F. Gallagher, C. Glidewell, Acta Crystallogr. B 60 (2004) 46.
[41] I. Senkovska, Z. Naturforsch. 61b (2006) 1383.
[42] L. Pan, T. Frydel, M.B. Sander, X. Huang, J. Li, Inorg. Chem. 40 (2001) 1271
[43] C.A. Williams, A.J. Blake, C. Wilson, P. Hubberstey, M. Schroder, Crystal Growth Design 8 (2008) 911.
[44] C. Volkringer, T. Loiseau, G. Férey, J.E. Warren, D.S. Wragg, R.E. Morris, Solid State Sci. 9 (2007) 455.
[45] L.-C. Yu, Z.-F. Chen, H. Liang, C.-S. Zhou, Y. Li, J. Mol. Struct. 750 (2005) 35
[46] R.-X. Yuan, R.-G. Xiong, Z.-F. Chen, X.-Z. You, S.-M. Peng, G.-H. Lee, Inorg. Chem. Commun. 4 (2001) 430.
[47] I. Senkovska, S. Kaskel, Eur. J. Inorg. Chem. (2006) 4564.
[48] M.J. Plater, A.J. Roberts, J. Marr, E.E. Lachowski, R.A. Howie, J. Chem. Soc. Dalton Trans. (1998) 797.
[49] B.R. Srinivasan, S.Y. Shetgaonkar, J.V. Sawant, P. Raghavaiah, Polyhedron 27 (2008) 3299.
[50] B.R. Srinivasan, J.V. Sawant, P. Raghavaiah, Indian J. Chem. 45A (2006) 2392
[51] B.R. Srinivasan, S.C. Sawant, Thermochim. Acta 402 (2003) 45
[52] G.M. Sheldrick, Acta Crystallogr. A64 (2008) 112.
[53] R. Murugavel, R. Korah, Inorg. Chem. 46 (2007) 11048.
[54] Bond valence sums were determined using the software Valist. A.S. Wills VaList, Program available from www.ccp14.ac.uk.
[55] B.R. Srinivasan, J.V. Sawant, P. Raghavaiah, J. Chem. Sci. 119 (2007) 11
[56] B.R. Srinivasan, J.V. Sawant, C. Näther, W. Bensch, J. Chem. Sci. 119 (2007) 243.
[57] B.R. Srinivasan, P. Raghavaiah, J.V. Sawant, Acta Crystallogr. E63 (2007) m2251
[58] B.R. Srinivasan, J.V. Sawant, S.C. Sawant, P. Raghavaiah, J. Chem. Sci. 119 (2007) 593.

Polyhedron 27 (2008) 3299–3305

0

ELSEVIER

Contents lists available at ScienceDirect

Polyhedron

journal homepage: www.elsevier.com/locate/poly

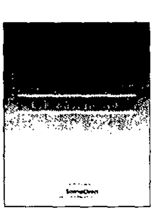

Synthesis, X-ray structure and properties of a calcium(II) coordination polymer showing μ_2-η^1:η^1 and μ_3-η^2:η^1 coordination modes of 4-nitrobenzoate

Bikshandarkoil R. Srinivasan *, Santosh Y. Shetgaonkar, Jyoti V. Sawant, Pallepogu Raghavaiah [1]

Department of Chemistry, Goa University, Panaji, Goa 403 206, India

ARTICLE INFO

Article history:
Received 4 April 2008
Accepted 20 July 2008
Available online 1 September 2008

Keywords:
4-Nitrobenzoate
N-Methylimidazole
Imidazole
Bridging bidentate
Monoatomic bridge
One-dimensional ladder
C–H···O interactions

ABSTRACT

The reaction of the monomeric compound $[Ca(H_2O)_4(\eta^1\text{-4-nba})(\eta^2\text{-4-nba})]$ **1** (4-nba = 4-nitrobenzoate) with *N*-methylimidazole (*N*-MeIm) or imidazole (Im) at 100 °C results in the formation of the anhydrous mixed ligand complexes of composition $[Ca(L)(4\text{-nba})_2]$ (L = *N*-MeIm **2**; L = Im **3**). The compounds were characterized by elemental analysis, IR, UV–Vis and ^{1}H NMR spectra, TG-DSC thermograms, weight loss studies and the structure of **2** was determined by single crystal X-ray crystallography. Compounds **2** and **3** can be transformed into **1** by heating with water. At elevated temperatures all compounds (**1**–**3**) are thermally decomposed to CaO. Compound **2** crystallizes in the centrosymmetric triclinic space group $P\bar{1}$ with all atoms located in general positions. The structure reveals that **2** is a polymer and can be formulated as *catena*-poly[[(*N*-methylimidazole)calcium(II)](μ_2-η^1:η^1-4-nitrobenzoato)(μ_3-η^2:η^1-4-nitrobenzoato)]. The structure of $[[Ca(N\text{-MeIm})](\mu_2\text{-}\eta^1{:}\eta^1\text{-4-nba})(\mu_3\text{-}\eta^2{:}\eta^1\text{-4-nba})]_n$ **2** consists of a central Ca(II) ion, a terminal *N*-MeIm ligand and two crystallographically independent 4-nba ligands. In the crystal structure, each Ca(II) is bonded to a nitrogen atom of *N*-MeIm and five oxygen atoms from five symmetry related 4-nba ligands resulting in a distorted $\{CaO_5N\}$ octahedron. One of the unique 4-nitrobenzoate in each formula unit functions as a bridging bidentate ligand (μ_2-η^1:η^1-4-nba) and is linked to two symmetry related Ca(II) ions leading to the formation of an infinite chain extending along *a* axis with a long Ca···Ca separation of 5.531(1) Å. The second independent 4-nba ligand (μ_3-η^2:η^1-4-nba) is coordinated to three different Ca(II) ions with both the carboxylate oxygen atoms linked to the same infinite chain formed earlier and one of the carboxylate oxygen atoms functions as a monoatomic bridge between two symmetry related Ca(II) ions. This bridge links two chains with a shorter Ca···Ca separation of 3.8585(7) Å resulting in the formation of a one-dimensional ladder structure. The oxygen atoms of the nitro groups are involved in C–H···O interactions. A comparative study of 30 Ca(II) coordination polymers is described.

1. Introduction

The design of coordination polymers employing carboxylic acids as ambidentate and templating ligands with metals providing interesting connectivity is an area of current research [1–3]. Recently several reports have appeared on the synthesis and structural characterization of metal-carboxylate based materials using benzene carboxylic acids [4–11]. The ready availability of benzene based carboxylic acids in pure form, combined with the fact that the carboxylate group is a versatile donor that can bind in a variety of ways [12–14], has contributed to these recent advances in the area of metal–organic frameworks (MOFs). An added advantage of using benzene-based systems is the introduction of potential donor groups like $-NH_2$, –OH, –SH, or another –COOH into the rigid six-membered ring. Further the positioning of these groups can be altered with respect to the carboxylate functionality. The introduction of additional groups affects the acidity of the carboxylic acid, which is useful from a synthetic point of view of metal carboxylates. Substituents present on the benzene ring like $-NO_2$, –F, –Cl, –Br, etc., lack the donor characteristics to form a strong metal–ligand bond. However, the resulting carboxylic acids are stronger acids as compared to benzoic acid and hence can exhibit different reactivity characteristics when treated with metal sources. In addition, substituents like $-NO_2$ can participate in secondary interactions by forming H-acceptor bonds, which can direct the assembly of novel structures. In view of this, we are investigating the synthesis, thermal properties [15] and structure characteristics [16] of metal-4-nitrobenzoate (4-nba) complexes, to prepare new compounds by exploiting the H-bonding characteristics of the $-NO_2$ group.

The structural chemistry of alkaline-earths with carboxylate ligands is an area of current research as evidenced by the several recent reports in literature [17–23]. In our metal carboxylate research programme we have unraveled a rich structural chemistry

---

* Corresponding author. Tel.: +91 832 6519316; fax: +91 832 2451184.
E-mail addresses: brsrinivasan@gmail.com, srini@unigoa.ac.in (B.R. Srinivasan).

[1] Present address: School of Chemistry, University of Hyderabad, Hyderabad 500 046, India.

0277-5387/$ - see front matter © 2008 Elsevier Ltd. All rights reserved.
doi:10.1016/j.poly.2008.07.020

of the 4-nitrobenzoates of the alkaline-earths [24–28]. The triad of compounds $[Mg(H_2O)_6](4\text{-nba})_2 \cdot 2H_2O$, $[Mg(H_2O)_2(Im)_2(\eta^1\text{-4-nba})_2]$ (Im = imidazole) and $[Mg(H_2O)(N\text{-MeIm})_2(\eta^1\text{-4-nba})(\mu_2\text{-}\eta^1{:}\eta^1\text{-4-nba})]_2$ (*N*-MeIm = *N*-methylimidazole) demonstrate a rich and variable chemistry of 4-nitrobenzoates of Mg in terms of the binding modes of 4-nba anions as well as secondary H-bonding interactions. For calcium we reported on the structure and properties of a seven coordinated monomeric complex $[Ca(H_2O)_4(\eta^1\text{-4-nba})(\eta^2\text{-4-nba})]$ **1** [24], which exhibits both mono (η^1) and bidentate (η^2) coordination of 4-nba and $[Ca(H_2O)_3(Im)(\eta^1\text{-4-nba})_2] \cdot Im$ [25] which shows η^1 ligation of 4-nba and contains coordinated as well as free imidazole. In this paper, we present the details of the investigation of the thermal reaction of the seven coordinated Ca compound **1** in the presence of *N*-methylimidazole (*N*-MeIm) and imidazole (Im), resulting in the formation of the anhydrous mixed ligand complexes of composition $[Ca(L)(4\text{-nba})_2]$ (L = *N*-MeIm **2**; L = Im **3**).

2. Experimental

2.1. Materials and methods

All the chemicals used in this study were of reagent grade and were used as received. The starting materials and reaction products are air stable and hence were prepared under normal laboratory conditions. The complex $[Ca(H_2O)_4(\eta^1\text{-4-nba})(\eta^2\text{-4-nba})]$ **1** was prepared as described earlier [24]. Infrared (IR) spectra were recorded on a Shimadzu (IR Prestige-21) FT-IR spectrometer in the range 4000–400 cm^{-1}. The samples for the IR spectra were diluted with KBr in the solid state and the signals referenced to polystyrene bands. Electronic spectra were recorded using matched quartz cells on a Shimadzu (UV-2450) spectrophotometer. ^1H NMR spectra were recorded in DMSO-d_6 on a Bruker 400 MHz FT-NMR spectrometer. TG-DSC measurements were performed in Al_2O_3 crucibles on a STA-409PC simultaneous thermal analyzer from Netzsch in flowing air. A heating rate of 10 K min^{-1} was employed for all measurements. X-ray powder pattern were recorded on a Phillips PW-3710 diffractometer using Cu K_α radiation over 2θ range of 15–75° at a scan rate of 3° min^{-1}. The insoluble 4-nbaH obtained on acid treatment of the complexes was weighed as described earlier [15] and metal analysis was performed titrimetrically following a standard procedure. Isothermal weight loss studies were performed in an electric furnace fitted with a temperature controller.

2.2. Preparation of $[Ca(H_2O)(4\text{-nba})_2]$ **1a**

A powdered sample of **1** (0.444 g) was heated on a steam bath for ~30 min. The heat-treated sample was kept in a desiccator and allowed to cool to room temperature and weighed to obtain **1a**. The observed decrease in weight (12.15%) corresponds to the removal of three moles of water. The yield was quantitative. The compound is insoluble in MeOH, CH_3CN, etc.

Anal. Calc. for $C_{14}H_{10}CaN_2O_9$: Ca, 10.25; 4-nbaH, 85.68; CaO, 14.35. Found: Ca, 10.01; 4-nbaH, 84.8, CaO, 14.0%.

IR data: 3611–3100(br), 3113(s), 2849(w), 1944(w), 1813(w), 1612(s), 1558(s), 1524(m), 1493(sh), 1414(s), 1346(s), 1319(s), 1171(m), 1142(m), 1107(s), 1015(s), 980(s), 880(s), 839(s), 799(s), 725(s), 511(s) cm^{-1}.

DSC data (in °C): 260 (*exo*), 410 (*exo*), 447 (*exo*), 558 (*exo*).

2.3. Preparation of $[Ca(N\text{-MeIm})(4\text{-nba})_2]_n$ **2**

2.3.1. Method 1

N-Methylimidazole (0.082 g, 1 mmol) was added into a freshly prepared sample of **1a** and the reaction mixture was left in a desiccator for ~30 min. The reaction mixture was washed with ether and dried to obtain **2**. Alternatively **2** can also be prepared by directly heating a mixture of a finely powdered sample of **1** (0.45 g, 1 mmol) and *N*-MeIm (0.082 g, 1 mmol) in a steam bath for ~30 min. The hot reaction mixture was cooled and washed well with ether and dried in air. Yield: (quantitative).

Anal. Calc. for $C_{18}CaH_{14}N_4O_8$ (454.43) **2**: Ca, 8.8; 4-nbaH, 73.11; CaO, 12.34; C, 47.53; H, 3.0; N, 12.32. Found: Ca, 8.8; 4-nbaH, 73, CaO, 12.2; C, 47.6; H, 3.03; N, 11.81%.

IR data: 3121(s), 2967(s), 2855(w), 1614(s), 1584(s), 1520(m), 1402(s), 1375(s), 1344(s), 1321(s), 1279(s), 1230(m), 1107(s), 1014(s), 1082(m), 934(s), 878(s), 822(s), 800(s), 752(s), 727(s), 667(s), 621(s), 559(s), 509(s) cm^{-1}.

UV–Vis 274 nm (23775 L mol^{-1} cm^{-1}).

^1H NMR (DMSO-d_6) δ (in ppm): 3.63 (s, 3H); 6.86 (s, 1H); 7.09 (s, 1H); 7.55 (s, 1H); 8.16 (m, 4H).

DSC data (in °C): 188 (*endo*), 412 (*exo*), 558 (*exo*).

2.3.2. Method 2

A powdered sample of **1** (1.78 g, 4 mmol) was heated with *N*-MeIm (1.4 ml, 17 mmol) on a steam bath for ~1 h to obtain a light yellow solid. To this hot mass distilled water (~8 ml) was added and the mixture reheated to obtain a pale yellow solution. The hot solution was quickly filtered and kept aside for crystallization. Fine colorless blocks of crystals suitable for X-ray study, which separated were washed with ether (5 ml) and dried in air. Yield: 60%. The use of reduced amounts of *N*-MeIm in the thermal reaction or excess water for recrystallisation results in the formation of the tetraaqua compound **1** in accordance with its hydration characteristics (*vide infra*). The infrared spectrum and the DSC thermogram of this product is identical with that of the product obtained in the thermal reaction.

2.4. Preparation of $[Ca(Im)(4\text{-nba})_2]$ **3**

Imidazole (0.068 g, 1 mmol) was added into a freshly prepared sample of **1a** and the reaction mixture was left in a desiccator for ~30 min. The reaction mixture was washed with ether and dried to obtain **3**. Alternatively **3** can also be prepared by directly heating a mixture of a finely powdered sample of **1** (0.45 g, 1 mmol) and Im (0.068 g, 1 mmol) in a steam bath for ~30 min. The hot reaction mixture was cooled and was washed well with ether and dried in air. Yield: (quantitative).

Anal. Calc. for $C_{17}CaH_{12}N_4O_8$ **3**: Ca, 9.08; 4-nbaH, 75.88; CaO, 12.73; C, 46.31; H, 2.72; N, 12.71. Found: Ca, 8.9; 4-nbaH, 74.28; CaO, 12.3; C, 45.95; H, 3.13; N, 10.94%.

IR data: 3381(s), 3223(s), 3061(w), 2941(w), 1604(w), 1570(s), 1516(s), 1490(m), 1402(s), 1348(s), 1321(s), 1261(s), 1171(m), 1142(m), 1107(s), 1066(s), 1014(s), 935(s), 918(s), 860(s), 825(s), 802(s), 752(s), 740(s), 723(s), 659(s), 617(s), 497(s), 511(s) cm^{-1}.

^1H NMR (DMSO-d_6) δ (in ppm): 7.00 (s, 2H); 7.63 (s, 1H); 8.13 (m, 4H).

DSC data (in °C): 198 (*endo*), 415 (*exo*), 547 (*exo*).

2.5. Rehydration studies

A powdered sample of **2** (200 mg) was suspended in water (~5 ml) and the reaction mixture left undisturbed overnight. The reaction mixture was filtered and the residue was washed with alcohol followed by ether and dried to obtain **1** in quantitative yields. The formation of **1** is evidenced by its characteristic IR spectrum and DSC thermogram. Alternatively **2** can be transformed to **1** by suspending an amount (200 mg) of **2** in water (5 ml) and heating the solution till dissolution of the solid. The hot solution is cooled to obtain **1** in quantitative yield. The equilibration of a powdered sample of **3** over water vapour, resulted in the formation of the starting compound **1** in quantitative yield in about a day as evidenced by its characteristic IR spectrum and DSC thermogram.

2.6. X-ray crystallography

Intensity data for **2** were collected on a Bruker Smart Apex CCD diffractometer using graphite-monochromated Mo Kα radiation. The data integration and reduction were processed with SAINT software [29]. An empirical absorption correction was applied to the collected reflections with SADABS [30]. The structure was solved with direct methods using SHELXS-97 and refinement was done against F^2 using SHELXL-97 [31]. All non-hydrogen atoms were refined anisotropically. Aromatic hydrogens were introduced on calculated positions and included in the refinement riding on their respective parent atoms. The technical details of data acquisition and some selected refinement results for **2** are listed in Table 1.

3. Results and discussion

3.1. Synthesis and spectroscopy

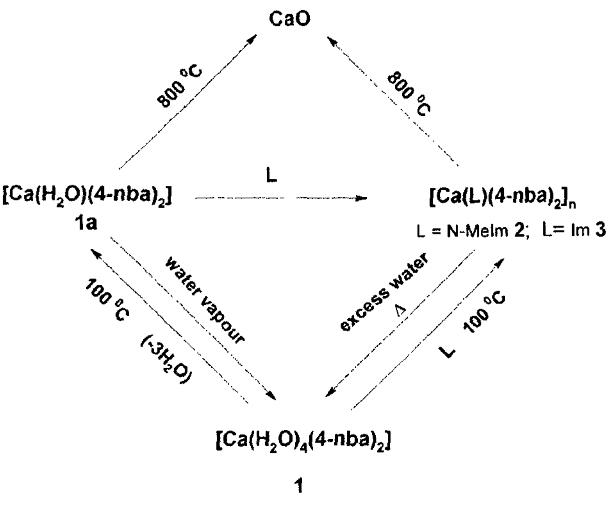

Scheme 1.

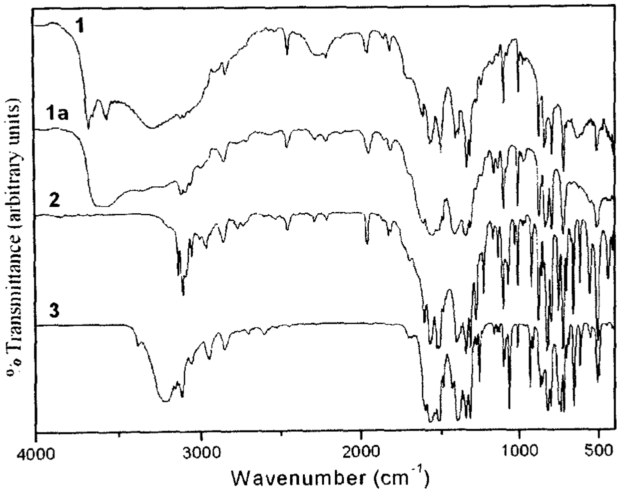

Fig. 1. IR spectra of compounds **1**, **1a**, **2** and **3**.

Table 1
Crystal data and structure refinement for [Ca(*N*-MeIm)(4-nba)$_2$]$_n$ **2**

Empirical formula	$C_{18}H_{14}CaN_4O_8$
Formula weight (g mol^{-1})	454.41
Temperature (K)	293(2)
Wavelength (Å)	0.71073
Crystal system	triclinic
Space group	$P\bar{1}$
Unit cell dimensions	
a (Å)	5.5313(5)
b (Å)	12.7904(12)
c (Å)	14.9226(15)
α (°)	113.08(1)
β (°)	95.72(1)
γ (°)	97.64(1)
Volume (Å^3)	950.11(16)
Z	2
D_{calc} (mg/m^3)	1.588
Absorption coefficient (mm^{-1})	0.388
$F(000)$	468
Crystal size (mm^3)	0.38 × 0.28 × 0.20
Theta range for data collection (°)	1.50–26.0
Index ranges	$-6 \leqslant h \leqslant 6$, $-15 \leqslant k \leqslant 15$, $-18 \leqslant l \leqslant 18$
Reflections collected	9475
Independent reflections (R_{int})	3696 (0.0205)
Completeness to theta = 26.0°	99.3%
Refinement method	full-matrix least-squares on F^2
Data/restraints/parameters	3696/0/285
Goodness-of-fit on F^2	1.057
Final R indices [$I > 2\sigma(I)$]	$R_1 = 0.0348$, $wR_2 = 0.0900$
R indices (all data)	$R_1 = 0.0392$, $wR_2 = 0.0929$
Largest difference in peak and hole (e Å^{-3})	0.338 and −0.235

Heating of a solid sample of the tetrahydrate **1** at 100 °C resulted in the loss of three moles of water leading to the formation of a monohydrate [Ca(H$_2$O)(4-nba)$_2$] **1a** (Scheme 1). The presence of water in **1a** is evidenced by the strong and broad absorption around 3500 cm^{-1} in its infrared spectrum assignable to O–H vibration. It is to be noted that the profile of the O–H signal of compound **1a** is quite different as compared to that of the tetrahydrate compound **1**. In addition the IR signals of the nitro and carboxylate functionalities, which occur between 1300 and 1650 cm^{-1} are broadened in **1a** as compared to the spectrum of **1** (Fig. 1). On exposure to moisture the monohydrate rapidly transforms into the seven coordinated starting material **1**. Interestingly, the reaction of *N*-MeIm or Im with the monohydrate **1a** results in the displacement of water by the N-donor ligands and the formation of anhydrous mixed ligand compounds **2** or **3** having molar composition of Ca:4-nba:*N*-MeIm(Im) 1:2:1 (Scheme 1). The use of excess *N*-MeIm or Im in the thermal reaction did not result in the formation of new products containing additional N-donor ligands. The anhydrous mixed ligand compounds **2** or **3** can also be synthesized in a single step by directly heating a mixture of powdered sample of **1** and *N*-MeIm in a 1:1 mole ratio. The presence of the N-donor ligands in compounds **2** and **3** can be readily confirmed by their NMR spectra which exhibit the characteristic signals of 4-nba, *N*-MeIm or Im. The formation of the anhydrous compounds **2** or **3** is evidenced by their IR spectra, which are devoid of the signals for O–H vibrations of water and is further confirmed by the appearance of additional bands due to the incorporation of the N-donor ligand in its mid IR spectrum (Fig. 1). Compounds **2** and **3** are relatively stable compared to the moisture sensitive monohydrate **1a**. However, both **2** and **3** can be transformed to **1** by suspending them in water overnight or alternatively by heating **2** or **3** in water (Scheme 1). Crystals of **2** suitable for structure determination were prepared by heating a mixture of **1** and excess *N*-MeIm at 100 °C followed by recrystallisation from minimum water. Similar attempts to prepare compound **3** in crystalline form suitable for

X-ray structure determination by solution method always resulted in the formation of the known monomeric compound $[Ca(H_2O)_3(Im)(\eta^1\text{-4-nba})_2]\cdot Im$. The compounds **1a**, **2** and **3** were formulated based on the elemental analysis and the mass loss leading to the formation of CaO on pyrolysis in a Bunsen flame. All the compounds exhibit several signals in the mid IR region indicating the presence of the organic moieties. However, based only on the infrared data the exact nature of the binding of the 4-nba ligand cannot be confirmed. The UV–Vis spectra of all compounds exhibit an absorption in the UV region around 274 nm assignable to the charge transfer of the aromatic 4-nba ligand.

*3.2. Crystal structure description of **2***

Compound **2** crystallises in the triclinic space group $P\bar{1}$ and all atoms are situated in general positions. The structure reveals that **2** is a polymer and can be formulated as *catena*-poly[[(*N*-methylimidazole)calcium(II)](μ_2-η^1:η^1-4-nitrobenzoato)(μ_3-η^2:η^1-4-nitrobenzoato)]. The structure of $[[Ca(N\text{-MeIm})](\mu_2\text{-}\eta^1{:}\eta^1\text{-4-nba})(\mu_3\text{-}\eta^2{:}\eta^1\text{-4-nba})]_n$ **2** consists of a central Ca(II) ion, a terminal *N*-MeIm ligand and two crystallographically independent 4-nba ligands. In the crystal structure, each Ca(II) is bonded to a nitrogen atom of *N*-MeIm and five oxygen atoms from five symmetry related 4-nba ligands resulting in a distorted $\{CaO_5N\}$ octahedron (Fig. 2). The geometric parameters of the 4-nba anions and *N*-MeIm are in the normal range and are comparable with literature values [24–27]. The Ca–O distances in **2** range from 2.2823(12) to 2.4507(11) Å (**Table 2**) and are in agreement with literature values [24,25]. The Ca–N bond is longer at 2.5088(14) Å. The *cis* O–Ca–O and O–Ca–N angles range from 73.71(4)° to 107.39(4)° while the trans O–Ca–O and O–Ca–N angles range from 163.97(4)° to 175.54(4)° indicating a distorted octahedron. It is interesting to note that both 4-nitrobenzoates in each formula unit are coordinated to the central Ca(II) in different bridging modes (Fig. 2). One of the two 4-nba anions in each formula unit functions as a bridging bidentate ligand (μ_2-η^1:η^1-4-nba) (Supplementary data, Fig. 1) and is linked to two symmetry related Ca(II) ions via O5 and O6 atoms resulting in the formation of an infinite chain extending along *a* axis with a Ca⋯Ca separation of 5.531(1) Å. The second independent ligand (μ_3-η^2:η^1-4-nba) is coordinated to three different Ca(II) ions with both the carboxylate oxygen atoms O1 and O2 linked to the same infinite chain formed earlier and one of the carboxylate oxygen atoms (O1) functioning as a monoatomic bridge between two symmetry related Ca(II) ions (Supplementary data, Figs. 2 and 3). This monoatomic bridge serves to link the two infinite chains with a shorter Ca⋯Ca separation of 3.8585(7) Å resulting in the formation of a one-dimensional ladder structure (Fig. 3).

It is to be noted that Ca(II) forms a polymeric compound with 4-nba in the presence of *N*-MeIm unlike Mg(II) which forms a centrosymmetric dimeric complex $[Mg(H_2O)(N\text{-MeIm})_2(\eta^1\text{-4-nba})(\mu_2\text{-}\eta^1{:}\eta^1\text{-4-nba})]_2$ [26]. The coordination polymer **2** and the previously reported monomeric compounds $[Ca(H_2O)_4(\eta^1\text{-4-nba})(\eta^2\text{-4-nba})]$ **1** [24] and $[Ca(H_2O)_3(Im)(\eta^1\text{-4-nba})_2]\cdot Im$ [25] constitute a triad of Ca(II) compounds having Ca:4-nba in a 1:2 mole ratio and showing different binding modes of the 4-nba ligand. In terms of secondary interactions **1** shows only O–H⋯O interactions while the monomeric imidazole compound is involved in three varieties of H-bond-

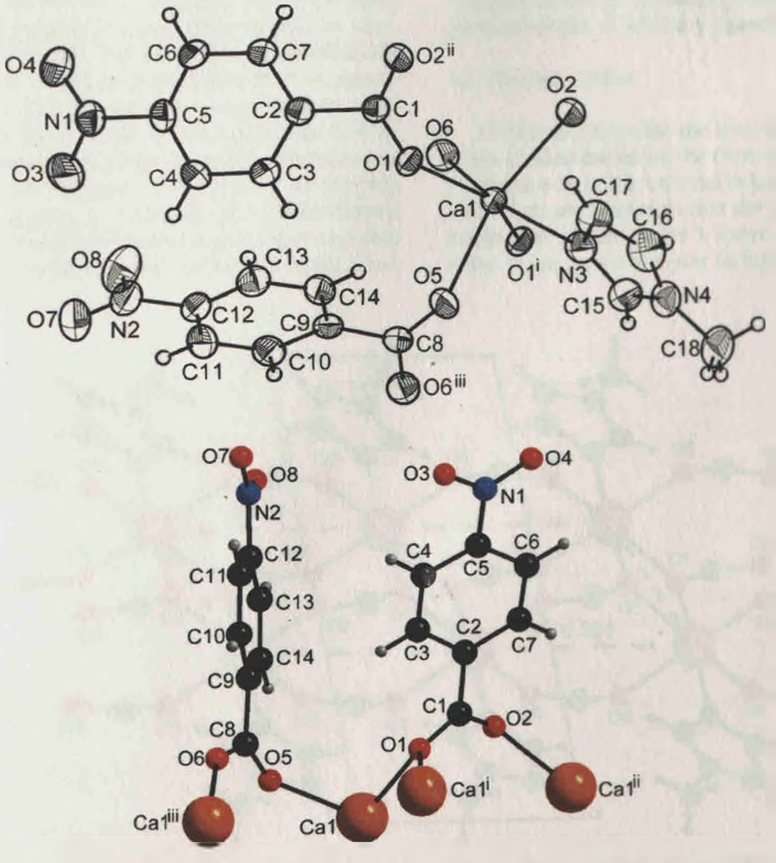

Fig. 2. The coordination sphere of Ca(II) in **2** showing the atom-labeling scheme. Displacement ellipsoids are drawn at the 50% probability level except for the H atoms, which are shown as circles of arbitrary radius (top). The μ_2-η^1:η^1 (O5,O6) and μ_3-η^2:η^1 (O1, O1, O2) bridging binding modes of the 4-nitrobenzoate ligands in **2** (bottom). Symmetry code: (i) $-x+1, -y+1, -z+1$; (ii) $-x+2, -y+1, -z+1$; (iii) $x-1, y, z$.

Table 2
Selected bond lengths (Å) and bond angles (°) for $[Ca(N\text{-}MeIm)(4\text{-}nba)_2]_n$ **2**

Ca(1)–N(3)	2.5088(14)	Ca(1)–O(5)	2.3074(12)
Ca(1)–O(1)	2.3710(11)	Ca(1)–O(6)	2.2823(12)
$Ca(1)^{i}$–O(1)	2.4507(11)	Ca(1)–$Ca(1)^{iii}$	5.531(1)
Ca(1)–O(2)	2.3292(11)	Ca(1)–$Ca(1)^{i}$	3.8585(7)
O(6)–Ca(1)–O(5)	96.22(5)	O(2)–Ca(1)–$O(1)^{i}$	93.23(4)
O(6)–Ca(1)–O(2)	92.78(4)	O(1)–Ca(1)–$O(1)^{i}$	73.71(4)
O(5)–Ca(1)–O(2)	165.10(4)	O(6)–Ca(1)–N(3)	88.01(5)
O(6)–Ca(1)–O(1)	90.60(4)	O(5)–Ca(1)–N(3)	84.47(5)
O(5)–Ca(1)–O(1)	91.47(4)	O(2)–Ca(1)–N(3)	84.00(4)
O(2)–Ca(1)–O(1)	100.31(4)	O(1)–Ca(1)–N(3)	175.54(4)
O(6)–Ca(1)–$O(1)^{i}$	163.97(4)	$O(1)^{i}$–Ca(1)–N(3)	107.39(4)
O(5)–Ca(1)–$O(1)^{i}$	81.25(4)		

Symmetry transformations used to generate equivalent atoms: (i) $-x+1, -y+1, -z+1$, (iii) $x-1, y, z$.

Table 3
Hydrogen-bonding geometry (Å, °) for $[Ca(N\text{-}MeIm)(4\text{-}nba)_2]_n$ **2**

D–H···A	d(D–H)	d(H···A)	D(D···A)	∠DHA
C13–H13···$O8^{iv}$	0.93	2.67	3.456(3)	143
C13–H13···$O4^{v}$	0.93	2.69	3.586(2)	161
C6–H6···$O7^{vi}$	0.93	2.63	3.519(2)	160
C4–H4···$O3^{v}$	0.93	2.62	3.495(2)	157
C18–H18B···$O7^{vii}$	0.93	2.44	3.378(3)	167

Symmetry codes: (iv) $-x+1, -y, -z$, (v) $-x, -y+1, -z$, (vi) $-x+1, y+1, -z$, (vii) $x+1, y, z+1$.

ing interactions namely O–H···O, N–H···O and O–H···N. The absence of coordinated water as well as methylation of the nitrogen atom in N-MeIm in **2** blocks the O–H···O, N–H···O and O–H···N interactions. An analysis of the structure of **2** reveals that the anhydrous compound is involved in only C–H···O interactions (Supplementary data, Fig. 4) with the oxygen atoms of the nitro groups functioning as H-acceptors and the methyl group of imidazole as well as H atoms on the aromatic ring functioning as H-donors. The geometric parameters of these hydrogen bonds are listed in Table 3.

3.3. Comparative study of Ca(II) coordination polymers

A survey of the reported structures of Ca(II) carboxylates reveals that formation of a polymeric chain due to the bridging nature of the carboxylate ligand is a characteristic structural feature of many Ca(II) carboxylates. Several polymeric Ca(II) carboxylates of varying dimensionalities (D) [17–23,32–52] have been reported in the literature many of which are 1-D polymers (Table 4). A comparative study of 30 different Ca(II) 1-D polymers reveals that the coordination number of Ca(II) in these compounds varies from 6 to 10, with eight coordination observed in many cases. Hexacoordination around Ca(II) is observed in compound **2** as well as $[Ca(Sa)_2(Phen)]_n$ and $[Ca(H_2O)_2(C_9H_8NO_4)_2]\cdot 2.5H_2O]_n$ (for abbreviations see Table 4). Of the several Ca(II) coordination polymers reported in the literature using substituted benzene carboxylic acids, compound **2** constitutes the first example of a Ca(II) coordination polymer derived from 4-nba ligand as the two other known Ca(II) compounds of 4-nba are monomeric in nature. A wide range of Ca···Ca distances between 3.612(1) and 9.816(1) Å are observed for the different Ca(II) 1-D polymeric compounds listed in the comparative table. The Ca···Ca separation of 3.8585(7) Å between the chains in the ladder compound is comparable with the Ca–Ca distance of around 4.0 Å observed in several coordination polymers listed in Table 4 while the Ca···Ca separation of 5.531(1) Å across the chains in **2** is relatively longer. A very long Ca···Ca distance of 9.816(1) Å is observed in the one-dimensional polymer $[[Ca(H_2O)_4(AIP)_2](H_2O)]_n$ containing the 5-aminoisophthalate dianion. Interestingly in the related 1-D Ca(II) polymer derived from isophthalic acid which exhibits a triple helix structure, Ca···Ca separations of 3.6402(3) and 3.8705(4) Å are reported. These observations indicate that the Ca···Ca distances across the polymeric chain in the coordination polymers are determined by a combination of several factors, which include the electronic and steric requirements of the central metal, the denticity, flexibility, bridging behavior, H-bonding characteristics of the carboxylate ligand, presence of ancillary ligands, etc.

3.4. Thermal studies

The temperature for the thermal synthesis of compounds **2** and **3** was chosen based on the thermal characteristics of compound **1**. A comparison of the thermal behavior of the tetrahydrate **1** and the monohydrate **1a** reveals that the DSC thermograms of **1a** is identical to that of compound **1** above 100 °C when the tetrahydrate **1** emits three moles of water forming the monohydrate (see Supple-

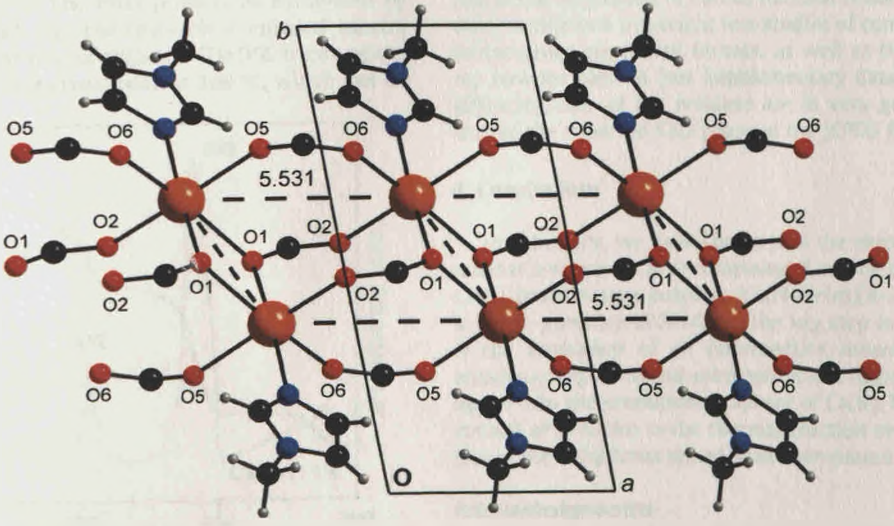

Fig. 3. A view of the bridging bidentate coordination (μ_2-η^1:η^1) of 4-nba through O5 and O6 leading to a one-dimensional polymeric Ca(II) chain extending along *a* with Ca···Ca separation of 5.531(1) Å. The monoatomic bridging mode of O1 in the second 4-nba ligand results in the linking of two infinite chains. In the chains each Ca(II) is bonded to five O atoms and one N atom. For clarity only the carboxylate groups are shown.

Table 4

Ca···Ca distances across the chain in reported one-dimensional (1-D) Ca(II) coordination polymers

Compound	C.N.	Ca···Ca distance (Å)	Reference
$[[Ca(H_2O)_3(4\text{-fba})](4\text{-fba})]_n$	8	3.612(1)	[32]
$[Ca(H_2O)_3(benz)_2]_n$	8	3.6146(4)	[33]
$[Ca(H_2O)_3(1{,}4\text{-bdc})]_n$	8	3.637(2)	[34]
$[[Ca(H_2O)_2(1{,}3\text{-bdc})]_{2.5} \cdot 4H_2O]_n^{*}$	8, 8, 9	3.6402(3), 3.8705(4)	[21]
$[[Ca_5(1{,}3\text{-bdc})_5(H_2O)_9] \cdot 8H_2O]_n$	8, 8, 9	3.659	[35]
$[[Ca(H_2O)]_2(L)(\mu\text{-}H_2O)]_n$	8	3.71	[36]
$[[Ca(NH_2\text{-}NH\text{-}CO_2)_2] \cdot H_2O]_n$	8	3.70, 3.87	[37]
$[Ca(gly)_2 \cdot H_2O]_n$	8	3.749	[22]
$[Ca(N\text{-}MeIm)(4\text{-nba})_2]$	6	3.8585(7), 5.531(1)	This work
$[Ca(H_2O)(dnSa)]_n$	7	3.8665(8), 4.1067(5)	[38]
$[Ca(H_2O)_2(4\text{-aba})_2]_n$	8	3.9047(5)	[39]
$[Ca(H_2O)(DMF)(benz)_2]_n$	8	3.956	[40]
$\{Ca_2(H_2O)_2(Oac)_3(NO_3)\}_n$	8	3.9953(8)	[41]
$[Ca(H_2O)_2(3\text{-aba})_2]_n$	8	4.0034(5)	[42]
$[[Ca(H_2O)_4][Ca(L^1)(H_2O)_2]_2 \cdot 7H_2O]_n$	7	4.008(1)	[43]
$[Ca(leu)_2 \cdot 3H_2O]_n$	8	4.020	[22]
$[Ca(H_2O)_2(4\text{-CNbenz})_2]_n$	8	4.023(15)	[20]
$[Ca(H_2O)[(O_2C)_2C_6H_3CO_2H]]_n^{**}$	8	4.0290(7)	[23]
$[[Ca(H_2O)_2(Nic)_2] \cdot (H_2O)_3]_n$	7	4.055	[44]
$[Ca(H_2O)_2(C_8H_5O_3)_2]_n$	8	4.0651(3)	[45]
$[Ca(H_2O)_2(2\text{-OPA})_2]_n$	8	4.1022	[46]
$[Ca(H_2O)_3(2\text{-aba})_2]_n$	7	4.699(1)	[47]
$[[Ca(Hpdc)(H_2O)_4] \cdot H_2O]_n$	8	4.751(1)	[48]
$[Ca(Sa)_2(Phen)]_n$	6	4.831(1)	[49]
$[Ca(val)_2(H_2O)]_n$	7	6.073	[22]
$[[Ca(PY\text{-}Threonato)_2(H_2O)_2](H_2O)_2]_n$	8	6.404	[50]
$[[Ca(H_2O)_4(Hpdc)] \cdot 2H_2O]_n$	7	6.867(2)	[48]
$[[Ca(H_2O)_2(C_9H_8NO_4)_2] \cdot 2.5H_2O]_n$	6	7.669	[51]
$[Ca(H_2O)_3(C_9H_{11}N_6O_5)_2]_n$	10	7.701	[52]
$[[Ca(H_2O)_4(AIP)_2](H_2O)]_n$	8	9.816(1)	[19]

Abbreviations used: C.N. = coordination number; * *three unique Ca(II) ions.* ** 2-D polymer.

4-fba = 4-fluorobenzoate; benz = benzoate; 1,4-bdc = 1,4-benzenedicarboxylate; 1,3-bdc = 1,3-benzenedicarboxylate; L = 4-(2-nitrophenyl)-3,6-dioxaoctane dioate; $(NH_2\text{–}NH\text{–}CO_2)$ = hydrazine carboxylate; gly = glycinate; dnSa = 3,5-dinitrosalicylato; 4-aba = 4-amino benzoate; DMF = *N,N*-dimethylformamide; OAc = acetate; 3-aba = 3-aminobenzoate; L^1 = 2,2′,2″-nitrilotribenzoate; leu = rac-leucinate; 4-CNbenz = 4-cyanobenzoate; $(O_2C)_2C_6H_3CO_2H$ = 1,2,4-benzenetricarboxylate; Nic = nicotinate; $C_8H_5O_3$ = 2-formylbenzoate; 2-OPA = 2-oxo-1,2-dihydropyridine-1-acetate; 2-aba = 2-aminobenzoate; Hpdc = 3,5-pyrazoledicarboxylate; *Sa = salicylato;* Phen = 1,10-phenanthroline; val = rac-valinate; PY = *N*-(6-amino-3,4-dihydro-3-methyl-5-nitroso-4-oxopyrimidin-2-yl); $C_9H_8NO_4$ = 2-(pyridinium-1-yl)butanedioate $C_9H_{11}N_6O_5$ = bis[*N*-(6-amino-3,4-dihydro-3-methyl-5-nitroso-4-oxopyrimidine-2-yl) glycylglycinate; AIP = 5-aminoisopthalate.

mentary data, Figs. 5 and 6). Both **1** and **1a** decompose at higher temperatures forming CaO as the final product as evidenced by the observed mass loss and also the featureless infrared spectra of the residues indicating the loss of organics. The DSC thermogram of **2** (Fig. 4) exhibits an endothermic peak at 188 °C, which can be attributed to the removal of *N*-methylimidazole and exothermic events above 400 °C assignable to the decomposition of the carboxylate ligand resulting in the formation of CaO. This assignment gains more credence as all the compounds **1**, **1a**, **2** and **3** exhibit the first exothermic event at around 410 °C. The removal of *N*-MeIm leads to further decomposition of **2** as evidenced by a steep drop in the TG curve of **2**. A scrutiny of **2** by isothermal weight loss studies at 185 °C, revealed a weight loss of 21.67% corresponding to the loss of one mole of *N*-MeIm, while further heating to 800 °C resulted in a total mass loss of 88% with 12% residue corresponding to the formation of CaO. However, our efforts to prepare the anhydrous compound $[Ca(4\text{-nba})_2]$ by heating **2** were not successful. The TG-DSC thermogram of **3** exhibits three thermal events at 198, 415 and 547 °C, respectively (Fig. 5). The endothermic signal at 198 °C can be assigned for the loss of the neutral Im ligand. This process appears to be complex and is not well resolved as evidenced by further drop in the TG curve. The exothermic signals at 415 and 547 °C can be attributed to the degradation of the carboxylate moieties leading to the decomposition of **3** to CaO with a residual mass of 12.3%, which is in good agreement with the calculated value. In the absence of associated mass spectral data of the emitted fragments the exact nature of the thermal decomposition taking place above 400 °C cannot be commented upon for both **2** and **3**. The formation of CaO as the final residue can be unambiguously confirmed by weight loss studies of compounds **2** and **3** in a temperature controlled furnace, as well as their characteristic X-ray powder pattern (see Supplementary data, Figs. 7 and 8). The diffractograms of the residues are in very good agreement with that of the reported CaO phase in the JCPDS file No. 37-1497.

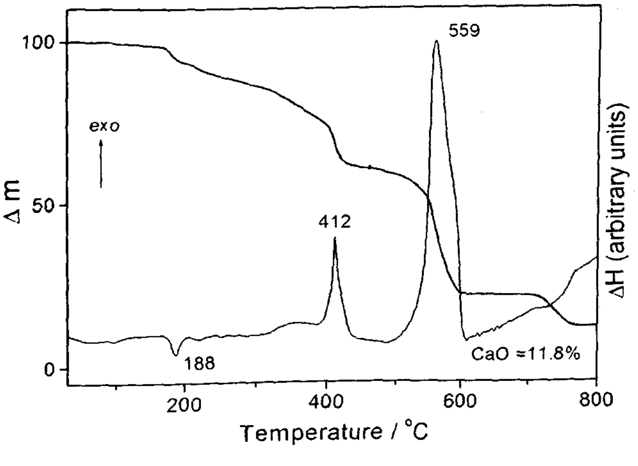

Fig. 4. TG-DSC thermogram of compound **2**.

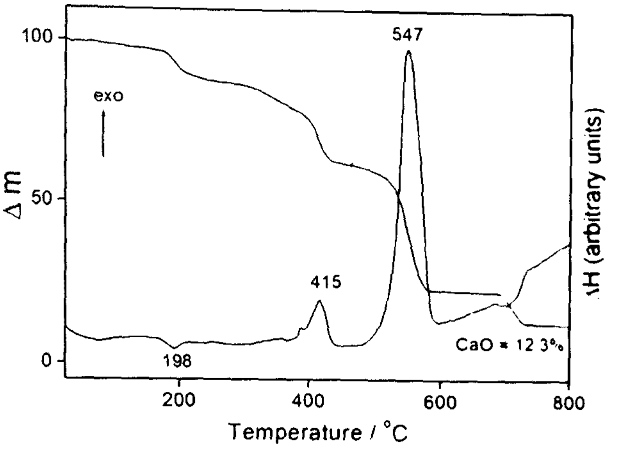

Fig. 5. TG-DSC thermogram of compound **3**.

4. Conclusions

In summary, we have shown that the zero dimensional mononuclear tetraaqua Ca(II) compound **1** can be transformed into the Ca(II) coordination polymer $[Ca(N\text{-}MeIm)(4\text{-nba})_2]_n$ **2** by heating it in the presence of *N*-MeIm. The key step in this transformation is the formation of an intermediate monohydrate compound, which undergoes ligand substitution and incorporation of N donor ligand into the coordination sphere of Ca(II). The use of imidazole instead of *N*-MeIm in the thermal reaction resulted in the formation of the anhydrous mixed ligand compound $[Ca(Im)(4\text{-nba})_2]_n$ **3**

Acknowledgements

B.R.S. thanks Dr. Samar K. Das School of Chemistry, University of Hyderabad, for the X-ray intensity data of compound **2** and the powder diffraction data of the residues. This work is supported by the Department of Science and Technology, New Delhi under Grant No. SR/S1/IC-41/2003.

Appendix A. Supplementary data

CCDC 658462 contains the supplementary crystallographic data for this paper. These data can be obtained free of charge via http://www.ccdc.cam.ac.uk/conts/retrieving.html, or from the Cambridge Crystallographic Data Centre, 12 Union Road, Cambridge CB2 1EZ, UK; fax: (+44) 1223-336-033; or e-mail: deposit@ccdc.cam.ac.uk. Additional figures related to the crystal structure of **2**, comparative DSC thermograms of compounds **1**, **1a**, **2** and **3**, X-ray powder pattern of the residue of compounds **2** and **3** are available. Supplementary data associated with this article can be found, in the online version, at doi:10.1016/j.poly.2008.07.020.

References

[1] C.N.R. Rao, S. Natarajan, R. Vaidhyanathan, Angew. Chem., Int. Ed. 43 (2004) 1466.
[2] M. Eddaoudi, D.B. Moler, H. Li, B. Chen, T M Reineke, M. O'Keeffe, O.M. Yaghi, Acc. Chem. Res. 34 (2001) 319.
[3] J. Kim, B. Chen, T.M. Reineke, H. Li, M. Eddaoudi, D.B. Mole, M. O'Keeffe, O.M. Yaghi, J. Am. Chem. Soc. 123 (2001) 8239.
[4] Y. Li, N. Hao, Y. Lu, E. Wang, Z. Kang, C. Hu, Inorg. Chem. 42 (2003) 3119.
[5] J.L.C. Rowsell, O.M. Yaghi, J. Am. Chem. Soc. 128 (2006) 1304.
[6] S. Surblé, F. Millange, C. Serre, T. Düren, M. Latroche, S. Bourrelly, P.L. Llewellyn, G. Férey, J. Am. Chem. Soc. 128 (2006) 14889.
[7] T.M. Reineke, M. Eddaoudi, M. O'Keeffe, O.M. Yaghi, Angew. Chem., Int. Ed. 38 (1999) 2590.
[8] M.J. Platers, R.A. Howie, A.J. Roberts, Chem. Commun. (1997) 893.
[9] M.J. Plater, A.J. Roberts, J. Marr, E.E. Lachowski, R.A. Howie, J. Chem. Soc., Dalton Trans. (1998) 797.
[10] H. Zhu, Z. Zhang, W. Sun, T. Okamura, N. Ueyama, Cryst. Growth Des. 5 (2005) 177.
[11] C.A. Williams, A.J. Blake, C. Wilson, P. Hubberstey, M. Schroder, Cryst. Growth Des. 8 (2008) 911.
[12] R.C. Mehrotra, R. Bohra, Metal Carboxylates, Academic Press, London, 1983.
[13] R.C. Mehrotra, A. Singh, Prog. Inorg. Chem. 46 (1997) 239.
[14] F.A. Cotton, G. Wilkinson, C.A. Murillo, M. Bochmann, Advanced Inorganic Chemistry, 6th ed., John Wiley & Sons, Inc., Chichester, 1999.
[15] B.R. Srinivasan, S. C Sawant, Thermochim. Acta 402 (2003) 45.
[16] B.R. Srinivasan, S.C. Sawant, S.K. Das, Indian J. Chem. 43A (2004) 1066.
[17] A. Grirrane, A. Pastor, E. Álvarez, R. Moyano, A. Galindo, Inorg. Chem. Commun. 10 (2007) 1125.
[18] Q. Shuai, S. Chen, S. Gao, Inorg. Chim. Acta 360 (2007) 1381.
[19] R. Murugavel, P. Kumar, M.G. Walawalkar, R. Mathialagan, Inorg. Chem. 46 (2007) 6828.
[20] R.-X. Yuan, R.-G. Xiong, Z.-F. Chen, X.-Z. You, S.-M. Peng, G.-H. Lee, Inorg. Chem. Commun. 4 (2001) 430.
[21] L.-C. Yu, Z.-F. Chen, H. Liang, C.-S. Zhou, Y. Li, J. Mol. Struct. 750 (2005) 35.
[22] S. Fox, I. Büsching, W. Barklage, H. Strasdeit, Inorg. Chem. 46 (2007) 818.
[23] C. Volkringer, T. Loiseau, G. Férey, J.E. Warren, D.S. Wragg, R.E. Morris, Solid State Sci. 9 (2007) 455.
[24] B.R. Srinivasan, J.V. Sawant, P. Raghavaiah, Indian J. Chem. 45A (2006) 2392.
[25] B.R. Srinivasan, J.V. Sawant, P. Raghavaiah, J. Chem. Sci. 119 (2007) 11.
[26] B.R. Srinivasan, J.V. Sawant, C. Näther, W. Bensch, J. Chem. Sci. 119 (2007) 243.
[27] B.R. Srinivasan, P. Raghavaiah, J.V. Sawant, Acta Crystallogr., Sect. E 63 (2007) m2251.
[28] B.R. Srinivasan, J.V. Sawant, S. C Sawant, P. Raghavaiah, J. Chem. Sci. 119 (2007) 593.
[29] Bruker SMART V5.630 and SAINT-PLUS V6.45, Bruker-Nonius Analytical X-ray Systems Inc., Madison, WI, USA, 2003.
[30] SADABS, Empirical Absorption Correction Program, Bruker AXS Inc., Madison, WI, USA, 1997.
[31] G.M. Sheldrick, Acta Crystallogr., Sect. A 64 (2008) 112.
[32] A. Karipides, C. Mc Kinney, K. Peiffer, Acta Crystallogr., Sect. C 44 (1988) 46.
[33] I. Senkovska, U. Thewalt, Acta Crystallogr., Sect. C 61 (2005) m448.
[34] R.H. Groeneman, J.L. Atwood, Cryst. Eng. 2 (1999) 241.
[35] S.H. Dale, M.R.J. Elsegood, Acta Crystallogr., Sect. C 59 (2003) m540.
[36] A. Bacchi, M. Carcelli, C. Pelizzi, G. Pelizzi, P. Pelagatti, D. Rogolino, M. Tegoni, C. Viappiani, Inorg. Chem. 42 (2003) 5871.
[37] A. Brainbanti, A.M.M. Lanfredi, M.A. Pellinghelli, A. Tiripicchio, Chem. Commun. (1970) 377.
[38] W.-D. Song, X.-X. Guo, C.-H. Zhang, Acta Crystallogr., Sect. E 63 (2007) m399.
[39] R. Murugavel, V.V. Karambelkar, G. Anantharaman, Indian J. Chem. 39A (2000) 843.
[40] S. Yano, M. Numata, M. Kato, S. Motoo, T. Nishimura, Acta Crystallogr., Sect. E 57 (2001) m488.
[41] B.G. Cooksey, L.T. Gibson, A.R. Kennedy, D. Littlejohn, L. Stewart, N.H. Tennent, Acta Crystallogr., Sect. C 55 (1999) m324.
[42] R. Murugavel, S. Banerjee, Inorg. Chem. Commun. 6 (2003) 810.
[43] S. Wörl, I.O. Fritsky, D. Hellwinkel, H. Pritzkow, R. Krämer, Eur. J. Inorg. Chem. (2005) 759.
[44] B.L. Cole, E.M. Holt, Inorg. Chim. Acta 108 (1985) 159.
[45] M. Odabaşoğlu, O. Büyükgüngör, Acta Crystallogr., Sect. E 63 (2007) m712.
[46] J.-G. Zhao, S. Gao, Z.-Y. Zhang, L.-H. Huo, H. Zhao, Acta Crystallogr., Sect. E 62 (2006) m278.
[47] R. Murugavel, V.V. Karambelkar, G. Anantharaman, M.G. Walawalkar, Inorg. Chem. 39 (2000) 1381.
[48] L. Pan, T. Frydel, M.B. Sander, X. Huang, J. Li, Inorg. Chem. 40 (2001) 1271.
[49] R. Murugavel, R. Korah, Inorg. Chem. 46 (2007) 11048.
[50] M.L.G. Salido, P.A. Mascaros, R.L. Garzon, M.D.G. Valero, J.N. Low, J.F. Gallagher, C. Glidewell, Acta Crystallogr., Sect. B 60 (2004) 46.
[51] D.K. Tian, S.L. Li, J.F. Hou, Acta Crystallogr., Sect. E 62 (2006) m130.
[52] J.N. Low, P. Arranz, J. Cobo, M.A. Fontecha, M.L. Godino, R. Lopez, D. Cannon, A. Quesada, C. Glidewell, Acta Crystallogr., Sect. C 57 (2001) 680.

J. Chem. Sci., Vol. 120, No. 2, March 2008, pp. 249–257. © Indian Academy of Sciences.

A one-dimensional barium(II) coordination polymer with a coordinated nitro group of 2-nitrobenzoate*

BIKSHANDARKOIL R SRINIVASAN[1,#], SANTOSH Y SHETGAONKAR[1] and PALLEPOGU RAGHAVAIAH[1,2]
[1]Department of Chemistry, Goa University, Goa 403 206
[2]School of Chemistry, University of Hyderabad, Hyderabad 500 046
e-mail: srini@unigoa.ac.in

MS received 15 November 2007; accepted 24 January 2008

Abstract. The aqueous reaction of barium carbonate with 2-nitrobenzoic acid (2-nbaH) results in the formation of a one-dimensional coordination polymer, *catena*-poly[[hexa(aqua)dibarium(II)]*bis*[(μ_2-2-nitrobenzoate-O,O,O-NO_2)(μ_2-2-nitrobenzoate-O,O,O′)]] **1**. On heating at 100°C compound **1** is dehydrated to anhydrous barium *bis*(2-nitrobenzoate) **2**. The anhydrous compound can be re-hydrated to **1** on exposure to water vapour. Compounds **1** and **2** were characterized by elemental analysis, IR and UV-Vis spectra, DSC thermograms, weight loss studies and the structure of **1** was determined. **1** and **2** can be thermally decomposed to $BaCO_3$ by heating at 800°C. The polymer $[[Ba(H_2O)_3]_2(\mu_2\text{-2-nba-O,O,O-}NO_2)_2(\mu_2\text{-2-nba-O,O,O}')_2]_n$ **1** crystallizes in the centrosymmetric triclinic space group $P\bar{1}$ and all atoms are located in general positions. The polymeric structure is based on a dimeric unit and consists of three water molecules coordinated to a central Ba(II) and two unique 2-nitrobenzoate (2-nba) anions, one of which (μ_2-2-nba-O,O,O-NO_2) functions as a tridentate ligand and is linked to a Ba(II) through the oxygen atom of the $-NO_2$ group and forms a monoatomic μ_2-carboxylate bridge between two symmetry related Ba(II) ions with a Ba···Ba distance of 4·5726(14) Å. The second unique 2-nba anion (μ_2-2-nba-O,O,O′) also functions as a tridentate ligand with the carboxylate oxygen atoms linked to a Ba(II) ion in a bidentate fashion and one of the carboxylate oxygen atoms forming a monoatomic bridge between two symmetry related Ba(II) ions resulting in a Ba···Ba separation of 4·5406(15) Å. These differing tridentate 2-nba ligands link $\{Ba(H_2O)_3\}$ units into a one-dimensional polymeric chain extending along *b* axis. In the infinite chain each nine coordinated Ba(II) is bonded to three water molecules and further linked to six oxygen atoms of four different 2-nitrobenzoate anions with alternating pairs of Ba(II) ions in the chain bridged by a pair of (μ_2-2-nba-O,O,O-NO_2) and (μ_2-2-nba-O,O,O′) ligands resulting in alternating Ba···Ba distances of 4·5406(15) and 4·5726(14) Å across the chain.

Keywords. Coordination polymer; *catena*-poly[[hexa(aqua)dibarium(II)]*bis*[(μ_2-2-nitrobenzoato-O,O,O-NO_2)(μ_2-2-nitrobenzoato-O,O,O′)]]; nitro ligation; tridentate; monoatomic bridge; nine coordination.

1. Introduction

Although an extensive chemistry of metal carboxylates has been developed[1,2] this field continues to attract the attention of several researchers in view of the importance of metal carboxylates in bioinorganic chemistry, catalysis, porous materials, etc. The use of carboxylic acids as ambidentate and templating ligands for the synthesis of novel coordination polymers, with metals providing interesting connectivity, is an area of topical research.[3,4] A few years ago we initiated a research programme on metal carboxylates[5] and as part of this program we are investigating the synthesis, structural aspects and thermal properties of metal 4-nitrobenzoate (4-nba) complexes.[6–7] The structurally characterized compounds $[Mg(H_2O)_6](4\text{-nba})_2\cdot 2H_2O$, $[Ca(H_2O)_4(4\text{-nba-O})(4\text{-nba-O,O}')]$, $[Sr(H_2O)_7(4\text{-nba-O,O}')](4\text{-nba})\cdot 2H_2O$, $[[Ba(H_2O)_5(4\text{-nba-O,O}')](\mu_2\text{-4-nba-O,O}')]_n$, $[Mg(H_2O)_2(Im)_2(4\text{-nba-O})_2]$ (Im = imidazole), $[Mg(H_2O)(N\text{-MeIm})_2(4\text{-nba-O})(\mu_2\text{-4-nba-O,O}')]_2$ (N-MeIm = N-methylimidazole), and $[Ca(H_2O)_3(Im)(4\text{-nba-O})_2]\cdot Im$, serve to demonstrate the rich structural chemistry of the alkali-earth 4-nitrobenzoates and the versatile ligational behaviour of 4-nba.[8–12] An important structural feature of all these compounds is the H-bonding characteristics of the $-NO_2$ functionality of

---

*Dedicated to Prof. S. K. Paknikar on the occasion of his 73rd birthday. #For correspondence the 4-nba anion with the nitro oxygen atom functioning as a H-bond acceptor and the coordinated or lattice water molecules providing the H-donors. In one-dimensional polymer[12] $[[Ba(H_2O)_5(4\text{-nba-O,O}')](\mu_2\text{-4-nba-O,O}')]_n$ the $-NO_2$ group is involved in several O–H···O and C–H···O interactions with the $-NO_2$ groups in one polymeric chain hydrogen bonded with the coordinated waters and aromatic hydrogen atoms on an adjacent chain. In order to gain more insight on the structure directing influence of the $-NO_2$ group, we have now initiated a systematic study of the structural chemistry of compounds derived from the isomeric 2- and 3-nitrobenzoic acids. The vibrational spectral characteristics of 2- and 3-nitrobenzoates of alkali metals like Li, Na, K, Rb and Cs have been recently reported.[13,14] It is interesting to note that the positioning of the $-NO_2$ functionality ortho to the –COOH group in 2-nitrobenzoic acid (2-nbaH) results in the formation of a polymeric Ba(II) compound **1**, the structure of which contains a nitro group coordinated to Ba(II). The results of these investigations are described in this paper.

2. Experimental

2.1 *Materials and methods*

All the chemicals used in this study were of reagent grade and were used as received. 2-nitrobenzoic acid (2-nbaH) was prepared by the oxidation of 2-nitrobenzaldehyde with 30% H_2O_2 in aqueous methanol. The starting materials and reaction products are air stable and hence were prepared under normal laboratory conditions. The details of the instrumentation used for IR and UV-Vis spectra, DSC and weight loss studies are the same as described in our earlier report.[12] Single crystal X-ray diffraction study was performed at the National single crystal X-ray facility at School of Chemistry, University of Hyderabad.

2.2 *Preparation of* $[[Ba(H_2O)_3]_2(\mu_2\text{-2-nba-O,O,O-NO}_2)_2(\mu_2\text{-2-nba-O,O,O}')_2]_n$ **1**

A mixture of barium carbonate (1·98 g, 10 mmol) and 2-nitrobenzoic acid (2-nbaH) (3·34 g, 20 mmol) was taken in water (50 ml) and heated on a steam bath. The insoluble $BaCO_3$ slowly started dissolving accompanied with brisk effervescence. The heating of the reaction mixture was stopped when there was no more evolution of CO_2. At this stage, the reaction mixture was almost clear. The hot solution was filtered and left undisturbed for 7–8 days. The colourless crystalline blocks that separated were filtered, washed thoroughly with ether and dried. Yield: 4·430 g (85%). The crystals obtained in this method were suitable for X-ray studies. **1** can also be prepared starting from $BaCl_2$ as the Ba source. The sodium salt of 2-nba was first generated *in situ* by reacting 2-nbaH (1·67 g, 10 mmol) with $NaHCO_3$ (0·84 g, 10 mmol) in water. Into this, an aqueous solution of $BaCl_2{\cdot}4H_2O$ (1·221 g, 5 mmol) was added and the reaction mixture was filtered and left aside for crystallization. The crystals that separated after a few days were isolated in 81% yield. The IR spectrum and the DSC thermogram of the product obtained in this method were identical to that of the product obtained using $BaCO_3$ as the Ba source.

Anal. found (calcd.) for $C_{14}H_{14}BaN_2O_{11}$ (523·61): Ba, 25·50 (26·33); 2-nbaH, 62·99 (63·83); C, 31·53 (32·46); H, 2·49 (2·7); N 4·91 (5·41).

IR (in cm^{-1}): 3730–2922 (*br*), 2833 (*w*), 2525 (*w*), 1815 (*w*), 1594 (*s*), 1566 (*s*), 1552 (*s*), 1537 (*m*), 1523 (*s*), 1512 (*s*), 1504 (*m*), 1478 (*s*), 1440 (*s*), 1404 (*s*), 1393 (*s*), 1347 (*s*), 1308 (*s*), 1265 (*w*), 1248 (*w*), 1144 (*w*), 1076 (*w*), 1037 (*w*), 1013 (*w*), 863 (*m*), 841 (*s*), 786 (*s*), 735 (*s*), 702 (*s*), 679 (*w*), 630 (*m*), 513 (*s*), 428 (*s*).

UV-vis: 274 nm ($\varepsilon = 14{,}000\ l\ mol^{-1}\ cm^{-1}$).

DSC (in °C): 88 (*Endo*), 230 (*Endo*), 277 (*Endo*), 338 (*Exo*), 444 (*Exo*).

2.3 *Preparation of barium bis(2-nitrobenzoate)* **2**

A powdered sample of **1** (0·350 g) was heated on a steam bath for 15 min. This resulted in the formation of the anhydrous compound **2**. The observed mass loss of 10·5% is in good agreement with the expected value (10·32%) for the loss of three moles of water.

IR (in cm^{-1}): 3086 (*w*), 3068 (*w*), 3032 (*w*), 2852 (*w*), 1593 (*s*), 1568 (*s*), 1554 (*s*), 1530 (*s*), 1520 (*s*), 1477 (*m*), 1437 (*s*), 1415 (*s*), 1404 (*s*), 1341 (*s*), 1310 (*s*), 1261 (*s*), 1142 (*s*), 1074 (*s*), 1039 (*w*), 964 (*w*), 862 (*s*), 837 (*s*), 775 (*s*), 780 (*s*), 754 (*s*), 702 (*s*), 648 (*s*), 534 (*w*), 630 (*m*), 432 (*s*).

DSC (in °C): 231 (*Endo*), 272 (*Endo*), 336 (*Exo*), 450 (*Exo*).

Table 1. Technical details of data acquisition and selected refinement results for $[[Ba(H_2O)_3]_2(\mu_2\text{-2-nba-O,O,O-NO}_2)_2(\mu_2\text{-2-nba-O,O,O}')_2]_n$ **1**.

Empirical formula	$C_{14}H_{14}BaN_2O_{11}$
Formula weight	523·61 g mol^{-1}
Temperature	293(2) K
Wavelength	0·71073 Å
Crystal system	Triclinic
Space group	$P\bar{1}$
Unit cell dimensions	a = 8·360(3) Å, α = 79·78(6)° b = 8·475(3) Å, β = 85·52(5)° c = 14·077(6) Å, γ = 70·49(5)°
Volume	925·0(6) Å^3
Z	2
Density (calculated)	1·880 mg/m^3
Absorption coefficient	2·209 mm^{-1}
F(000)	512
Crystal size	0·42 × 0·34 × 0·20 mm^3
Theta range for data collection	2·58 to 25·85°
Index ranges	$-10 <= h <= 10$, $-10 <= k <= 10$, $-17 <= l <= 17$
Reflections collected	8554
Independent reflections	3526 [R(int) = 0·0187]
Completeness to theta = 26·06°	98·6%
Refinement method	Full-matrix least-squares on F^2
Data/restraints/parameters	3526/9/271
Goodness-of-fit on F^2	1·113
Final R indices [$I > 2\sigma(I)$]	$R1$ = 0·0227, $wR2$ = 0·0589
R indices (all data)	$R1$ = 0·0230, $wR2$ = 0·0592
Extinction coefficient	0·0040(2)
Largest diff. peak and hole	0·707 and −0·885 eÅ^{-3}

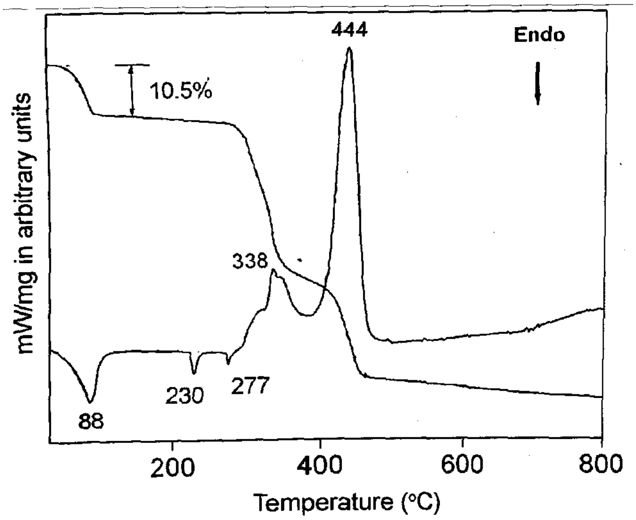

Figure 1. TG-DSC thermogram of $[[Ba(H_2O)_3]_2(\mu_2\text{-2-nba-O,O,O-NO}_2)_2(\mu_2\text{-2-nba-O,O,O}')_2]_n$ **1**. (Heating rate 10 K/min; Air atmosphere).

2.4 *Rehydration studies*

The anhydrous compound **2** was prepared from **1** as mentioned above. Equilibration of a powdered sample of **2** over water vapour resulted in the formation of the starting material **1** in near quantitative yield in about a day. The IR spectra and DSC thermogram of the rehydrated compound is identical to that of **1**.

2.5 *X-ray crystallography*

Intensity data for **1** were collected on a Bruker Smart Apex CCD diffractometer using graphite-monochromated Mo-K_α radiation (λ = 0·71073 Å). The data integration and reduction were processed with SAINT[15] software. An empirical absorption correction was applied to the collected reflections with SADABS.[16] The structure was solved with direct methods using SHELXS-97[17] and refinement was done against F^2 using SHELXL-97.[17] All non-hydrogen atoms were refined anisotropically. Aromatic hydrogens were introduced on calculated positions and included in the refinement riding on their respective parent atoms. The hydrogen atoms of the coordinated water molecules were located in the difference map but were not stable on subsequent refinements and hence were fixed at calculated

Table 2. Selected bond distances (Å) for $[[Ba(H_2O)_3]_2(\mu_2\text{-2-nba-O,O,O-}NO_2)_2(\mu_2\text{-2-nba-O,O,O}')_2]_n$ **1**.

Ba(1)–O(5)	2·703(2)	Ba(1)–O(1)	2·816(2)
Ba(1)–O(11)	2·744(2)	Ba(1)–O(1)^{ii}	2·833(2)
Ba(1)–O(10)	2·767(3)	Ba(1)–O(3)	2·900(2)
Ba(1)–O(6)^{i}	2·777(2)	Ba(1)–O(5)^{i}	2·906(2)
Ba(1)–O(9)	2·807(4)	Ba(1)–Ba(1)^{i}	4·5406(15)
Ba(1)–Ba(1)^{ii}	4·5726(14)		

Symmetry transformations are used to generate equivalent atoms: (i) $-x + 1$, $-y + 1$, $-z + 1$; (ii) $-x + 1$, $-y + 2$, $-z + 1$

positions by using DFIX command and later refined isotropically using a riding model. The technical details of data acquisition and some selected crystal refinement results for **1** are summarized in table 1.

3. Results and discussion

In an earlier study, the neutralization of a 0·1 M $Ba(OH)_2\cdot 8H_2O$ solution by a 0·2 M 2-nbaH solution has been shown to result in the formation of the water soluble barium(II) o-nitrobenzoate trihydrate.[18] In the present work, we have used either $BaCO_3$ or $BaCl_2$ as the Ba(II) source. The aqueous reaction of $BaCO_3$ with 2-nbaH resulted in the formation of the nine coordinated compound $[[Ba(H_2O)_3]_2(\mu_2\text{-2-nba-O,O,O-}NO_2)_2(\mu_2\text{-2-nba-O,O,O}')_2]_n$ **1**. Alternatively, **1** can be prepared by reacting an aqueous $BaCl_2$ with *in situ* generated sodium 2-nba. The observed analytical and spectral characteristics of compound **1** are in good agreement with the previously reported trihydrate.[18] Crystals of **1** were characterized by elemental analysis, infrared and optical spectra, DSC thermogram, and single crystal X-ray structure determination. As the solid state structure of compound **1** (*vide infra*) turned out to be a one-dimensional polymer, the reaction of the water soluble compound **1** was investigated with aqueous sulfate. The reaction of an aqueous solution of **1** with aqueous Na_2SO_4 resulted in the immediate precipitation of $BaSO_4$ in quantitative yield. It cannot be unambiguously stated that the polymeric structure of 1 does not persist in solution, based only on its behaviour towards sulfate. Nevertheless this reaction constitutes a convenient method for the incorporation of 2-nba anions in the place of $(SO_4)^{2-}$ in other metal sulfates. The use of the title compound as a convenient source for delivering 2-nba assumes importance in view of the reported behaviour of 2-nba compounds to exhibit polymorphism.[19]

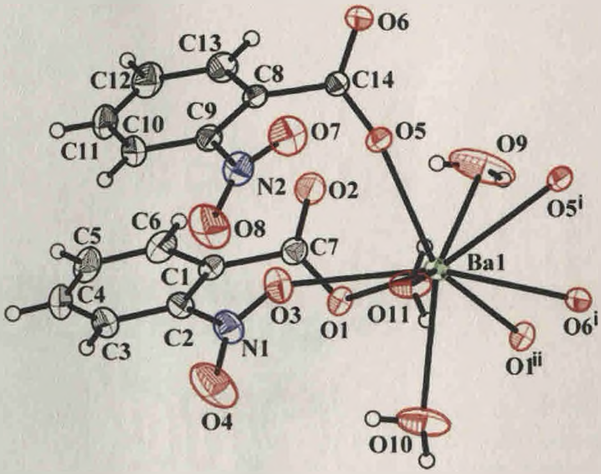

Figure 2. The coordination sphere of Ba(II) in $[[Ba(H_2O)_3]_2(\mu_2\text{-2-nba-O,O,O-}NO_2)_2(\mu_2\text{-2-nba-O,O,O}')_2]_n$ **1** showing the atom-labelling scheme. Displacement ellipsoids are drawn at the 50% probability level except for the H atoms, which are shown as circles of arbitrary radius. Symmetry code: (i) $[-x + 1, -y + 1, -z + 1]$; (ii) $[-x + 1, -y + 2, -z + 1]$.

Heating of **1** on a steam bath results in the formation of the anhydrous barium(II) *bis*(2-nitrobenzoate) **2** while the pyrolysis of **1** or **2** in a Bunsen flame results in the formation of $BaCO_3$. **1** absorbs strongly in the UV region at 274 nm, which can be assigned to the intramolecular charge transfer transition of the aromatic carboxylate. The IR spectra of **1** and **2** (see web version) exhibit several sharp bands in the mid-infrared region, clearly indicating the presence of the organic moiety. The broad and strong signal in the region 3730–2922 cm^{-1} in **1** indicates the presence of water and can be assigned to the O–H stretching vibration. The IR spectrum of **2** is devoid of bands above 3100 cm^{-1}, which is indicative of the anhydrous nature of **2**. The spectrum below 3100 cm^{-1}, is similar to that of **1**. Although the IR spectra **1** and **2** exhibit the absorptions due to the vibrations of the

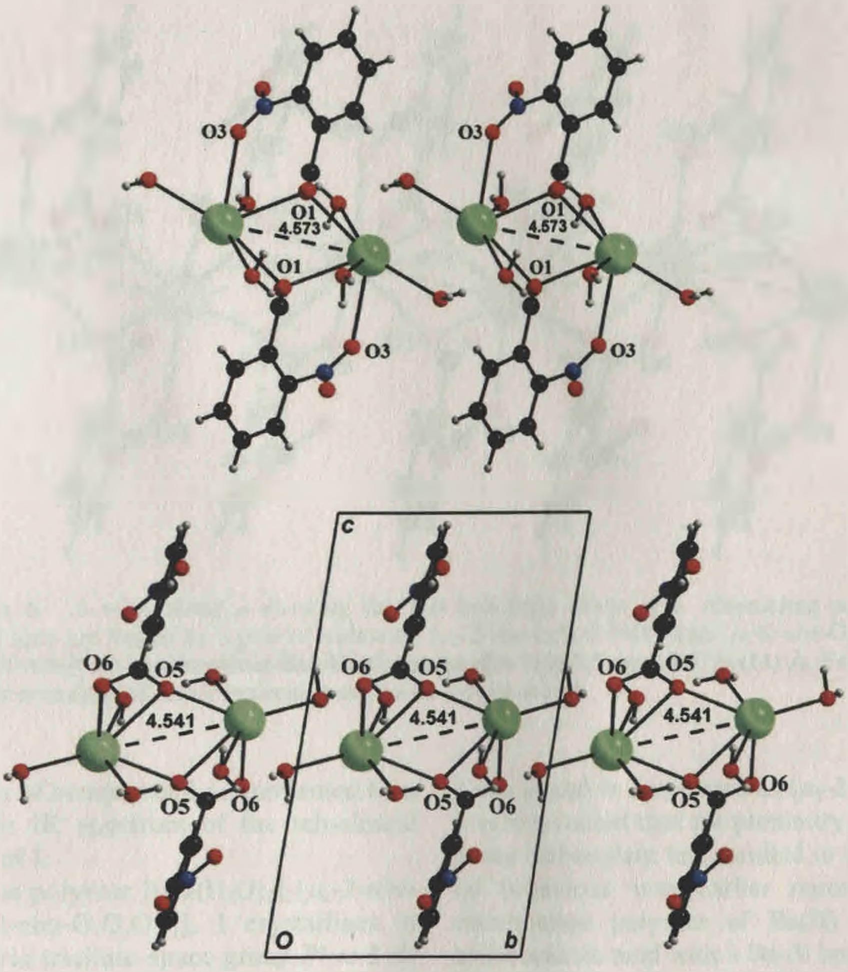

Figure 3. A view along *a* showing the dimeric units of $[Ba(H_2O)_3(\mu_2\text{-2-nba-O,O,O-NO}_2)_2]$ formed by the tridentate ligand (μ_2-2-nba-O,O,O-NO_2). Each Ba(II) is linked to a nitro oxygen O3 and both the Ba(II) are bridged by the carboxylate oxygen O1 (top). A view along *a* of the dimeric units $[Ba(H_2O)_3(\mu_2\text{-2-nba-O,O,O}')_2]$ formed by the tridentate ligand (μ_2-2-nba-O,O,O′). Each Ba(II) is linked to O5 and O6 and both the Ba(II) in the dimer are bridged by the carboxylate oxygen O5 (bottom).

carboxylate and nitro groups, no definite conclusions can be drawn on the nature of the binding of the 2-nba ligand based on infrared data alone.

The TG-DSC thermogram of **1** (figure 1) exhibits an endothermic event at around 88°C accompanied by a mass loss of 10·5% assignable for the removal of three molecules of water. The dehydration process is followed by an endothermic signal at around 230°C, which can be assigned to a phase change. Above this temperature, **1** undergoes a complex decomposition process as evidenced by the strong exothermic events at 338 and 444°C. In the absence of mass spectral data of the emitted fragments no definite conclusions can be drawn on the exact nature of the decomposition processes. The observed residue is in good agreement for the formation of $BaCO_3$. The results of the isothermal weight loss studies at 100°C (steam bath) and at 800°C add credence to the TG-DSC data. As expected, the TG-DSC thermogram of the anhydrous compound **2** (see web version) is devoid of the first endothermic signal observed for the dehydration of **1** and the thermal decomposition pattern of **2** is similar to that of **1** above this temperature, resulting in the formation of $BaCO_3$ residue. Equilibriation of the anhydrous compound **2** in an atmosphere of water vapour results

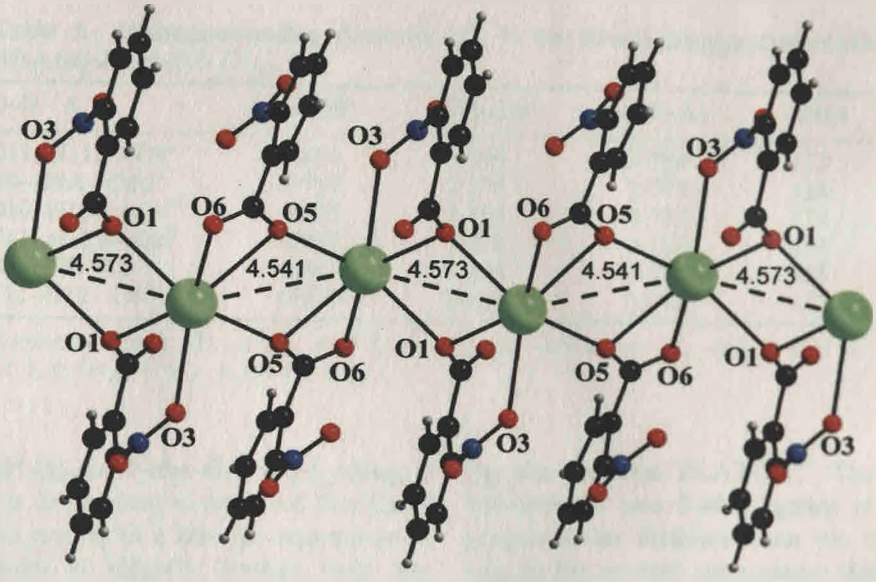

Figure 4. A view along *a* showing the 1-D polymeric chain of **1**. Alternating pairs of Ba(II) ions are linked by a pair of tridentate (μ_2-2-nba-O,O,O-NO_2) and (μ_2-2-nba-O,O,O′) ligands resulting in alternating Ba···Ba distances of 4·5406(15) and 4·5726(14) Å. For clarity, the coordinated water molecules on Ba(II) are not shown.

in the regeneration of compound **1** as confirmed by a comparison of the IR spectrum of the rehydrated product with that of **1**.

The coordination polymer $[[Ba(H_2O)_3]_2(\mu_2\text{-2-nba-O,O,O-}NO_2)_2(\mu_2\text{-2-nba-O,O,O'})_2]_n$ **1** crystallizes in the centrosymmetric triclinic space group P$\bar{1}$ and all atoms are located in general positions. The observed Ba–O bond distances vary between 2·703(2) and 2·906(2) Å (table 2). These values are comparable with those reported for other Ba(II)-carboxylates.[12,20] In the crystal structure, the Ba(II) is nine coordinated and is bonded to three O atoms from the three aqua ligands and six oxygen atoms from four symmetry related 2-nba anions (figure 2). The central metal is linked to the O atoms (O9-O11) of three water molecules and the Ba-O(H_2O) distances range from 2·744(2) to 2·807(4) Å.

The polymeric structure is based on a dimer and each formula unit of **1** contains three coordinated water ligands and two unique 2-nitrobenzoate ligands both of which function as tridentate ligands in different fashion. The first unique 2-nba ligand (O1, O2, O3) functions as a monoatomic bridging ligand, linking two symmetry related Ba(II) ions via O1 with Ba1–O1 bond distances of 2·816(2) and 2·833(2) Å respectively. It is interesting to note that the O3 oxygen of the nitro functionality makes a Ba1–O3 bond at 2·900(2) Å. This unique tridentate 2-nba ligand is designated as (μ_2-2-nba-O,O,O-NO_2). It is to be noted that the proximity of the nitro group to the carboxylate has resulted in this bond. A similar behaviour was earlier reported for the 2D-coordination polymer of Ba(II) derived from 2-aminobenzoic acid with a Ba–N bond at 3·047(4) Å.[20] To the best of our knowledge compound **1** constitutes the first example of a structurally characterized 2-nitrobenzoate showing a coordinated nitro group. The second independent 2-nba ligand (O5, O6) also functions as a tridentate ligand with each Ba(II) linked to O5 and O6 in a bidentate manner (Ba1–O5 2·703(2); Ba1–O6 2·777(2) Å) and the O5 further linked to a symmetry related Ba(II) ion at 2·906(2) Å resulting in a monoatomic bridging mode. However, the nitro oxygen atoms are not at bonding distance to Ba(II) for this ligand. This second tridentate 2-nba ligand is designated as (μ_2-2-nba-O,O,O′). The structure of **1** can be explained as being composed of a pair of $\{Ba(H_2O)_3\}$ units linked via two μ_2-carboxylate bridges by a pair of (μ_2-2-nba-O,O,O-NO_2) ligands leading to a (Ba_2O_2) four-membered ring (figure 3) with a Ba···Ba distance of 4·5726(14) Å resulting in the formation of dimeric units of composition $[Ba(H_2O)_3(\mu_2\text{-2-nba-O,O,O-}NO_2)_2]_2$ along *b* axis. The linking of a pair of $\{Ba(H_2O)_3\}$ units by a pair of tridentate (μ_2-2-nba-O,O,O′) ligands results in the formation of dimeric units of

Table 3. Hydrogen-bonding geometry (Å, °) for $[[Ba(H_2O)_3]_2(\mu_2\text{-2-nba-O,O,O-}NO_2)_2(\mu_2\text{-2-nba-O,O,O}')_2]_n$ **1**.

D–H···A	d(D–H)	d(H···A)	D(D···A)	<DHA
O11–H11A···O9^{i}	0·836	1·949	2·780	173
O9–H9A···O10^{ii}	0·797	2·275	2·775	121
O10–H10A···O6^{iii}	0·857	1·899	2·752	174
O11–H11B···O2^{iv}	0·847	1·870	2·714	175
O9–H9B··O2	0·817	2·429	3·224	165
C12–H12···O8^{v}	0·930	2·689(3)	3·612	172

Symmetry Code: (i) $-x+1$, $-y+1$, $-z+1$; (ii) $-x+1$, $-y+2$, $-z+1$; (iii) $x-1$, $y+1$, z; (iv) $x-1$, y, z; (v) $x+1$, y, z

composition $[Ba(H_2O)_3(\mu_2\text{-2-nba-O,O,O}')_2]_2$ along b axis (figure 3). It is interesting to note that this binding mode of 2-nba results in a Ba···Ba separation of 4·5406(15) Å, which is slightly shorter than the Ba···Ba separation observed earlier for the tridentate 2-nba ligand binding through the nitro oxygen. The extended structure is arrived at by the linking of two $[Ba(H_2O)_3(\mu_2\text{-2-nba-O,O,O-}NO_2)_2]$ units by a pair of (μ_2-2-nba-O,O,O′) ligands. Thus the two different tridentate 2-nba ligands link the $\{Ba(H_2O)_3\}$ units into a one-dimensional polymeric chain extending along b. In the infinite chain, each nine coordinated Ba(II) is bonded to three water molecules and further linked to six oxygen atoms of four different 2-nba anions with alternating pairs of Ba(II) ions in the chain bridged by a pair of (μ_2-2-nba-O,O′,O-NO_2) and (μ_2-2-nba-O,O,O′) ligands resulting in alternating Ba···Ba distances of 4·5406(15) and 4·5726(14) Å across the chain (figure 4).

An analysis of the crystal structure of **1** reveals that each nine coordinated Ba(II) complex in the polymeric chain is H-bonded to neighbouring complexes in the polymeric chain with the aid of two varieties of H-bonding interactions. All the hydrogen atoms attached to the coordinated waters excepting H10B and one hydrogen atom on a benzene ring function as H-donors. Two oxygen atoms from the coordinated water molecules O9 and O10, the free carboxylate oxygen O2 and a coordinated oxygen O6 and the nitro oxygen O8 function as H-acceptors. Thus each Ba(II) complex in **1** is linked to five other complexes with the aid of five O–H···O bonds and a C–H···O interaction (table 3). The C–H···O interaction between the nitro oxygen O8 and an aromatic H serves to link parallel chains resulting in a two-dimensional H-bonded network (see web version).

The short ring interactions and distances between the ring centroids (Cg–Cg) in **1** were analysed by using the program PLATON.[21] The Cg–Cg distance between the two 2-nba ligands is 4·089 Å and the perpendicular distance from the centre of the first ring to the second (interplanar distance) is 3·644 Å accompanied by a dihedral angle of 5·58°. These values indicate that the rings do not overlap and the magnitude of the values is suggestive of no stacking interactions.

The availability of structural information of many Ba(II) coordination polymers of varying dimensionalities derived from several carboxylic acids permits a comparative study of Ba(II) coordination polymers.[22–33] In these compounds the Ba···Ba distance across the polymeric chain varies from 4·069(2) in the three dimensional (3-D) coordination polymer derived from 2,2′-dithiobis(benzoic acid) to 7·467 Å in the 1-D Ba(II) polymer derived from the N-substituted amino acid containing the N-(6-amino-3,4-dihydro-3-methyl-5-nitroso-4-oxopyrimidin-2-yl) group (table 4). In all these compounds, the carboxylate anions function as bridging ligands. The coordination number of Ba(II) varies from 8 to 10 with nine coordination observed in several compounds. In four of the polymers the Ba···Ba separations are shorter than the sum of the van der Waals radii (4·28 Å) indicating weak metal–metal interactions, while in other compounds the observed metal–metal contacts are longer. Interestingly, the observed Ba···Ba distances of 4·5406(15) and 4·5726(14) Å in **1** are much shorter than the Ba···Ba separation of 6·750(1) Å in the related 1-D polymer $[Ba(H_2O)_5(4\text{-nba})_2]_n$ derived from 4-nitrobenzoic acid where the nitro group is disposed *trans* to the carboxylate. It is to be noted that the polymeric complex $[Ba(H_2O)_5(4\text{-nba})_2]_n$ contains two unique 4-nba ligands one of which functions as a bidentate ligand with the other functioning as a bridging bidentate ligand.[12] In the Ba(II) polymer of 4-nba the oxygen atoms of the nitro

Table 4. Ba···Ba distances across the chain in some Ba(II) coordination polymers containing bridging carboxylates.

Compound	C.N.	Ba···Ba distance (Å)*	Dimensionality (*D*) of polymer	Reference
$[\{Ba_2(DTBB)_2(H_2O)_2\}0{\cdot}5H_2O]_n^{\#}$	9, 8, 8	4·069(2)	3-D	22
$[Ba(C_6H_4(COO)_2)]_n$	8	4·123	3-D	23
$[Ba(Hbpdc)_2(H_2O)_2]_n$	9	4·1386(17)	1-D	24
$[Ba_9(CH_3COO)_{14}(ClO_4)_4]_n^{\#}$	8, 9, 9	4·27	3D	25
$[Ba(2\text{-}aba)_2(H_2O)_2]_n$	9	4·32	2-D	20
$[Ba(C_7H_5O_2S)_2(H_2O)_4]_n$	9	4·335	1-D	26
$[Ba(C_8H_5O_3)_2(H_2O)_2]_n$	8	4·4336(3)	1-D	27
$[[Ba(PY\text{-}met)_2(H_2O)_4]{\cdot}3H_2O]_n$	10	4·4451(2)	3-D	28
$[[Ba(H_2O)_3(2\text{-}nba)_2]_2]_n$ **1**	9	4·5406(15) 4·5726(14)	1-D	This work
$[Ba(C_5H_4O_4)_2(H_2O)_4]_n$	9	4·595(4)	2-D	29
$[Ba(1,3\text{-}BDOA)(H_2O)_2]_n$	10	4·755(3)	3-D	30
$[Ba(C_{10}H_{12}N_5O_6)_2(H_2O)_6]_n$	9	6·575(0)	1-D	31
$[Ba(H_2PMA)(H_2O)_5]_n$	9	6·65	2-D	32
$[Ba(H_2O)_5(4\text{-}nba)_2]_n$	9	6·750(1)	1-D	12
$[[Ba(H_2IDC)_2(H_2O)_4]{\cdot}2H_2O]_n$	10	6·765(3)	2-D	33
$[[Ba(PY\text{-}glycinato)_2(H_2O)_5]{\cdot}H_2O]_n$	9	6·916(1)	1-D	28
$[[Ba(PY\text{-}serinato)_2(H_2O)_4]{\cdot}3H_2O]_n$	10	7·139(0)	1-D	28
$[[Ba(PY\text{-}glycilglycinato)_2(H_2O)_2]_n$	8	7·467	2-D	28

Abbreviations used: CN = coordination number; #three unique Ba(II) ions; DTBB = 2,2′-dithiobis(benzoate); $(C_6H_4(COO)_2)]$ = terephthalate; Hbpdc = 2′-carboxybiphenyl-2-carboxylate; 2-aba = 2-aminobenzoate; $(C_7H_5O_2S)$ = thiosalicylate; $(C_8H_5O_3)$ = 2-formylbenzoate; PY = N-(6-amino-3,4-dihydro-3-methyl-5-nitroso-4-oxopyrimidin-2-yl); met = monoanion of methionine; $C_5H_4O_4$ = mesaconate anion; (1,3-BDOA) = *m*-phenylenedioxyacetate; $(C_{10}H_{12}N_5O_6)$ = N-4-amino-1,6-dihydro-1-methyl-5-nitroso-6-oxopyrimidin-2-yl)-(S)-glutamato; (H_4PMA) = pyromellitic acid; 4-nba = 4-nitrobenzoate; H_2IDC = 1H-imidazole-4,5-dicarboxylato monoanion; *For 2-D and 3-D polymers only the shortest Ba···Ba contact is given.

group are not involved in coordination unlike in compound **1**. It is interesting to note that both the oxygen atoms of the nitro functionalities in both the unique 4-nba ligands in $[Ba(H_2O)_5(4\text{-}nba)_2]_n$ are involved in C–H···O interactions unlike in compound **1** where one oxygen atom (O8) of the tridentate (μ_2-2-nba-O,O,O′) ligand is involved in C–H···O bonding. In the Ba(II) coordination polymer derived from 2-aminobenzoic acid the Ba(II) exhibits a Ba–N bond but the coordination polymer is three-dimensional. Hence it appears that the Ba···Ba distances in Ba-carboxylate coordination polymers are probably determined by a combination of several factors, which include the electronic and steric requirements of the central metal, the denticity, flexibility, bridging behaviour and H-bonding characteristics of the carboxylate ligand.

4. Conclusions

In summary, we have described the synthesis, structural characterization and properties of a one-dimensional Ba(II) coordination polymer **1**, containing 2-nba as a bridging ligand. Compound **1** constitutes an example of a structurally characterized 2-nitrobenzoate showing nitro ligation. The observed Ba···Ba distances of 4·5406(15) and 4·5726(14) Å across the chain in the 1-D polymer **1** are much shorter than the Ba···Ba separation of 6·750(1) Å between adjacent metal atoms in the 1-D polymeric Ba(II) compound of 4-nitrobenzoate. The reaction of the title compound with aqueous sulphate constitutes an useful method for the incorporation of 2-nba in lieu of sulphate. Current efforts in our laboratory are directed to exploit this reaction for the synthesis of new 2-nba compounds.

Supplementary material

Illustrations describing the infrared spectra of compounds **1** and **2**, the TG-DSC thermogram of **2** and the crystallographic packing diagram of compound **1** are available on the web version of this paper. Crystallographic data (excluding structure factors) for the structure reported in this paper have been deposited with the Cambridge Crystallographic Data Centre as supplementary publication no. CCDC 666968. Copies of the data can be obtained, free of charge, on application to CCDC, 12 Union Road, Cambridge CB2 1 EZ, UK. (fax: +44-(0)1223-336033 or email: deposit@ccdc.cam.ac.uk).

Acknowledgements

BRS thanks Dr Samar K Das School of Chemistry, University of Hyderabad, for the X-ray intensity data of **1**. This work was supported by the Department of Science and Technology, New Delhi under grant no. SR/S1/IC-41/2003.

References

1. Mehrotra R C and Bohra M 1983 *Metal carboxylates* (Academic Press: London); Mehrotra R C and Singh A 1997 *Prog. Inorg. Chem.* **46** 239
2. Cotton F A, Wilkinson G, Murillo C A and Bochmann M 1999 *Advanced Inorganic Chemistry* (Chichester: John Wiley & Sons, Inc.), 6th edn, p. 487
3. Rao C N R, Natarajan S and Vaidhyanathan R 2004 *Angew. Chem. Int. Ed.* **43** 1466
4. Rowsell J L C and Yaghi O M 2006 *J. Am. Chem. Soc.* **126** 1304
5. Srinivasan B R, Sawant S C and Dhuri S N 2002 *Indian J. Chem.* **A41** 290
6. Srinivasan B R and Sawant S C 2003 *Thermochim. Acta* **402** 45
7. Srinivasan B R, Sawant S C and Das S K 2004 *Indian J. Chem.* **A43** 1066
8. Srinivasan B R, Sawant J V and Raghavaiah P 2007 *J. Chem. Sci.* **119** 11
9. Srinivasan B R, Sawant J V, Näther C and Bensch W 2007 *J. Chem. Sci.* **119** 243
10. Srinivasan B R, Sawant J V and Raghavaiah P 2006 *Indian J. Chem.* **A45** 2392
11. Srinivasan B R, Raghavaiah P and Sawant J V 2007 *Acta Crystallogr.* **E63** m2251
12. Srinivasan B R, Sawant J V, Sawant S C and Raghavaiah P 2007 *J. Chem. Sci.* **119** 593
13. Swisłocka R, Samsonowicz M, Regulska E and Lewandowski W 2007 *J. Mol. Struct.* **834–836** 389
14. Swisłocka R, Oleksinski E, Regulska E, Kalinowska M and Lewandowski W 2007 *J. Mol. Struct.* **834–836** 380
15. Bruker SMART V5.630 and SAINT-PLUS V6.45, Bruker-Nonius Analytical X-ray Systems Inc.: Madison, Wisconsin, USA, 2003
16. SADABS 1997 Empirical absorption correction program, Bruker AXS Inc., Madison, Wisconsin, USA
17. Sheldrick G M 2008 *Acta Crystallogr.* **A64** 112
18. Charbonnier F, Balek V and Bussiere P 1975 *J. Thermal Anal.* 7 373
19. Karmakar A, Sarma R J and Baruah J B 2006 *Eur. J. Inorg. Chem.* 643
20. Murugavel R, Karambelkar V V, Anantharaman G and Walawalkar M G 2000 *Inorg. Chem.* **39** 1381
21. Spek A L 2003 *J. Appl. Cryst.* **36** 7
22. Murugavel R, Baheti K and Anantharaman G 2001 *Inorg. Chem.* **40** 6870
23. Lee B H, Kim C H and Lee S G 2003 *Acta Crystallogr.* **C59** m196
24. Briceno A, Delgado J M and Delgado G D 2002 *Acta Crystallogr.* **E58** m602
25. Dong G, Bing-guang Z, Ke-liang P, Chun-ying D and Qing-jin M 2002 *J. Chem. Soc. Dalton Trans.* 3783
26. Lo S M F, Chui S S Y and Williams I D 1998 *Acta Crystallogr.* **C54** 1846
27. Odabasoglu M and Büyükgüngör O 2006 *Acta Crystallogr.* **E62** m402
28. Salido M L G, Mascaros P A, Garzon R L, Valero M D G, Low J N, Gallagher J F and Glidewell C 2004 *Acta Crystallogr.* **B60** 46
29. Djehni S, Balegroune F, Guehria-Laidoudi A, Dahaoui S and Lecomte C 2007 *Acta Crystallogr.* **C63** m91
30. Gao S, Liu J W, Huo L H and Zhao H 2005 *Acta Crystallogr.* **C61** m348
31. Garzon R L, Leon M D L, Low J N and Glidewell C 2005 *Acta Crystallogr.* **C61** m224
32. Dale S H, Elsegood M R J and Kainth S 2003 *Acta Crystallogr.* **C59** m505
33. Zhang X, Gao S, Huo L H and Zhao H 2005 *Acta Crystallogr.* **E61** m2488